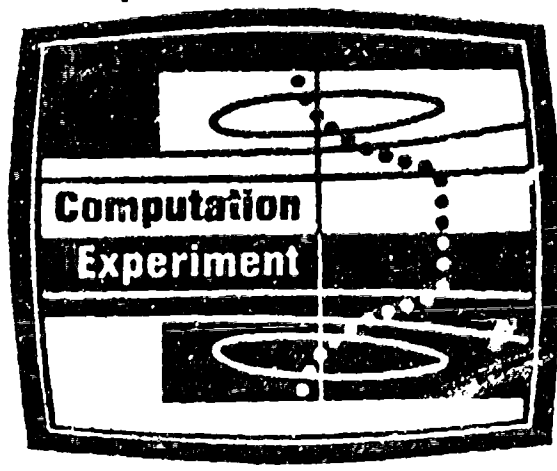


2

AD-A135 569

Complex Turbulent Flows



Volume I

Objectives, Evaluation of Data,
Specifications of Test Cases,
Discussion, and Position Papers

DTIC
RECEIVED
DEC 7 1983
S D

DTIC FILE COPY

Edited by
S. J. Kline,
B. J. Cantwell,
G. M. Lilley

DISTRIBUTION STATEMENT A
Approved for public release;
Distribution Unlimited

83 12 06 097

UNCLASSIFIED

SECURITY CLASSIFICATION OF THIS PAGE (When Data Entered)

REPORT DOCUMENTATION PAGE		READ INSTRUCTIONS BEFORE COMPLETING FORM
1. REPORT NUMBER AFOSR-TR- 83-1001	2. GOVT ACCESSION NO. AD-A135569	3. RECIPIENT'S CATALOG NUMBER
4. THE 1980-81 AFOSR-HTTM-STANFORD CONFERENCE ON COMPLEX TURBULENT FLOWS: COMPARISON OF COMPUTATION AND EXPERIMENT - VOLUME-1		5. TYPE OF REPORT & PERIOD COVERED INTERIM
		6. PERFORMING ORG. REPORT NUMBER
7. AUTHOR(s) S J KLINE. B J CANTWELL G M LILLEY		8. CONTRACT OR GRANT NUMBER(s) F49620-80-C-0027
9. PERFORMING ORGANIZATION NAME AND ADDRESS STANFORD UNIVERSITY MECHANICAL ENGINEERING DEPARTMENT STANFORD, CA 94305		10. PROGRAM ELEMENT, PROJECT, TASK AREA & WORK UNIT NUMBERS 61102F 2307/A1
11. CONTROLLING OFFICE NAME AND ADDRESS AIR FORCE OFFICE OF SCIENTIFIC RESEARCH/NA BOLLING AFB, DC 20332		12. REPORT DATE September 1980
		13. NUMBER OF PAGES 632
14. MONITORING AGENCY NAME & ADDRESS (if different from Controlling Office)		15. SECURITY CLASS. (of this report) Unclassified
		15a. DECLASSIFICATION/DOWNGRADING SCHEDULE
16. DISTRIBUTION STATEMENT (of this Report) Approved for Public Release; Distribution Unlimited.		
17. DISTRIBUTION STATEMENT (of the abstract entered in Block 20, if different from Report)		
18. SUPPLEMENTARY NOTES Proceedings of the 1980-81 AFOSR-HTTM-Stanford Conference on Complex Turbulent Flows: Comparison of Computation and Experiment, Stanford, CA, 3-6 September 1980		
19. KEY WORDS (Continue on reverse side if necessary and identify by block number) COMPLEX TURBULENT FLOWS THREE-DIMENSIONAL FLOW EXPERIMENTAL DATA ATTACHED BOUNDARY LAYERS SEPARATED FLOWS TWO-DIMENSIONAL FLOW		
20. ABSTRACT (Continue on reverse side if necessary and identify by block number) This volume contains the Proceedings of the 1980 Meeting of the 1980-81 AFOSR-HTTM-Stanford Conference on Complex Turbulent Flows: Comparison of Computation and Experiment. The Conference includes two meetings. The first, reported herein, had the goal of establishing a data base of "test cases" for comparison with computations. This volume contains a record of the proceedings of the 1980 meeting and a display of the test cases used in the 1981 meeting for comparison with computations. The main sections of the volume include:		

UNCLASSIFIED

SECURITY CLASSIFICATION OF THIS PAGE (When Data Entered)

(1) Pictorial summary charts providing a compact picture of the nature of the test cases. (2) Introduction: The history and nature of the conference. (3) Three position papers covering: (a) data needs for computational fluid dynamics; (b) some improvements to the theory of uncertainty analysis and the use of that theory for the present Conference; (c) description of Data Library. (4) Description of test cases including: summary; discussion; specifications for computations; output plots for the test cases. (5) Reports of ad-hoc committees on topics of general interest; general discussion; and conclusions. (6) Lists of Participants, Data Evaluators; Index to Flow Cases.

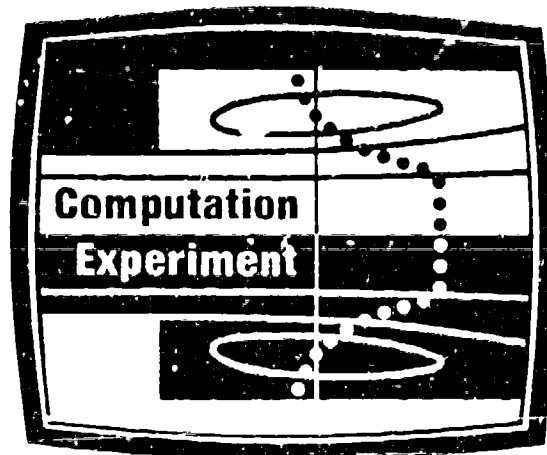
Accession For	
NTIS GRASI	X
DTIC TAB	
Unannounced	
Justification	
By	
Distribution/	
Availability Codes	
Dist	Avail and/or Special
A/1	



UNCLASSIFIED

SECURITY CLASSIFICATION OF THIS PAGE(When Data Entered)

COMPLEX TURBULENT FLOWS



THE 1980-81 AFOSR-HTTM-STANFORD CONFERENCE ON COMPLEX TURBULENT FLOWS:
COMPARISON OF COMPUTATION AND EXPERIMENT

VOLUME 1 -- OBJECTIVES, EVALUATION OF DATA,

SPECIFICATIONS OF TEST CASES,

DISCUSSION AND POSITION PAPERS

Proceedings of the 1980 Conference

Stanford University, Stanford, California

September 3-6, 1980

Edited by S. J. Kline, B. J. Cantwell, and G. M. Lilley

Published and Distributed by
Thermosciences Division
Mechanical Engineering Department
Stanford University
Stanford, California
1981

Approved for public release;
distribution unlimited.

Editors Stephen J. Kline
Mechanical Engineering Department
Stanford University
Stanford, CA 94305, USA

Brian J. Cantwell
Department of Aeronautics and Astronautics
Stanford University
Stanford, CA 94305, USA

Geoffrey M. Lilley
Department of Aeronautics and Astronautics
University of Southampton
Southampton SO9 5NH, England

Production Editor and Conference Secretary:
Ditter Peschke-Koedt
Palo Alto, CA 94301, USA

ISBN.

© 1981 by the Board of Trustees of the Leland Stanford Junior University.

All rights reserved. Printed in the United States of America.

L.C. 81-0908

Stanford, California, USA 94305, 1981.
(First Printing)

ACKNOWLEDGMENTS

The 1980 Conference as a whole is best viewed as a cooperative learning process within the research community. To achieve the aims of the Conference with impartiality, the fullest cooperation of the scientific and engineering communities was sought and generously given. Our special thanks are extended to all the Data Takers, Data Evaluators, Session Chairmen, and Technical Recorders, whose names appear in the List of Participants to the 1980 Conference in this volume. Without their help and participation the Conference could not have been held. The 1980 Conference was attended by approximately 160 invited participants from 14 countries (Australia, Canada, England, France, India, Israel, Japan, Netherlands, Norway, Sweden, Switzerland, United States of America, West Germany, and Yugoslavia).

The principal financial sponsorship for the work of this conference was supplied by the U.S. Air Force Office of Scientific Research under contract AF F49620-80-C-0027 and a predecessor grant. Added support for work on data processing of compressible flow cases was supplied by the NASA Ames Research Center under Grant NAG 2-79. Contributions were also made by the Langley and Lewis Research Centers of NASA, by the U.S. Office of Naval Research and by the National Science Foundation. The specific assistance of Dr. Morris Rubesin and Dr. Dennis Bushnell of NASA with regard to funding is gratefully acknowledged. The steadfast support of Dr. James Wilson of AFOSR was critical to the success of the Conference. When the volume of cases found to be useful grew far beyond the initial estimates, with a resulting and considerable increase in cost, Dr. Wilson spent much effort to organize the concerned government agencies and thereby secure the funds to complete the work. Funds for some special purposes were also supplied from the Heat Transfer and Turbulence Mechanics (HTTM) Program of the Industrial Affiliates Program of the Stanford Thermosciences Division. Funds to cover an overdraft in the base contract were generously supplied by the Stanford School of Engineering.

Special thanks are accorded the Organizing Committee: S. J. Kline (Chairman), P. Bradshaw, B. J. Cantwell, B. E. Launder, E. Reshotko, M. W. Rubesin, and G. Sovran, who worked long and thoughtfully beginning in 1977 on the plans, organization, and personnel problems. The continuing confidence and enthusiasm of the members of this committee were important ingredients in the success of the Conference.

No conference of this sort would have been held without the willing help of the Host Committee, who made all the local arrangements, and the many Stanford graduate students who served as Technical Recorders and Aides (see list on page 607); to all these we add our grateful thanks. Special appreciation is given to Profs. J. P. Johnston and J. H. Ferziger for important assistance in studying data and closing many

special gaps. Professor J. K. Eaton organized the aides and supervised all physical arrangements in a very able fashion. Professors W. C. Reynolds and R. J. Morfat lent the support of the Thermosciences Division and the Department of Mechanical Engineering at important points. Professor M. V. Morkovin acted as a senior advisor on many issues.

The arduous and critical task of recording the data on magnetic tape, organizing the data files and preparing graphs was handled by a cadre of Stanford graduate students under the direction of B. J. Cantwell including: Jalal Ashjaee, Juan Bardina, Bob Carella, Jim McDaniel, Ranga Jayaraman, Charles Narty, Ken Schultz, Tony Strawa, Ram Subbarao, and Jim Tallegiani,

The Conference was fortunate in having the aid of a very able secretarial staff. Particular praise is needed for Ditter Peschcke-Koedt, who was responsible for all typing and for the organization of the paperwork system in a highly independent and responsible fashion. Thanks are also due Barbara Homsy, Ann Ibaraki, Ruth Korb, Diana Thompson and Anne Vollmayer, for various secretarial duties and for their enthusiasm and support.

We are also indebted to Professor S. Honami for his work in producing the pictorial summaries known informally as the "Honami Charts" and to Prof. D. J. Cockrell for special assistance in preparing documents and other matters during the period just before the 1980 Meeting of the Conference.

PREFACE

This volume contains the Proceedings of the 1980 Meeting of the 1980-81 AFOSR-HTTM-Stanford Conference on Complex Turbulent Flows: Comparison of Computation and Experiment. The Conference includes two meetings. The first, reported herein, was held September 3-6, 1980; the goal of this first meeting was the establishment of a data base of "test cases" for comparison with computations. The second meeting, held September 14-19, 1981, compares the output of computations with the test cases. In addition, the Conference has established a data library on magnetic tape in permanent form; the library holds the test cases and certain other flows deemed sufficiently complete and accurate for use in building computer models and testing output in complex turbulent flows. Information on the proceedings or the data library can be obtained from the editors at Department of Mechanical Engineering, Stanford, California, USA 94305.

This volume has two purposes: (i) to record the proceedings of the 1980 meeting; (ii) to display the test cases that will be used in the 1981 meeting for comparison with computations. The volume has six major elements:

1. Pictorial summary charts providing a compact picture of the nature of the test cases.
2. Introduction: The history and nature of the Conference.
3. Three position papers covering: (a) Data needs for computational fluid dynamics; (b) Some improvements to the theory of uncertainty analysis and the use of that theory for the present Conference; (c) Description of Data Library.
4. Description of test cases including: summary; discussion; specifications for computations; output plots for the test cases.
5. Reports of ad-hoc committees on topics of general interest; general discussion; and conclusions.
6. Lists of Participants, Data Evaluators; Index to Flow Cases.

The Introduction, by S. J. Kline, summarizes the history of the Conference including the earlier 1968 AFOSR-IFP-Stanford Conference on Computation of Turbulent Boundary Layers and the 1969 and 1972 NASA Conferences on Compressible Boundary Layers and Free Shear Layers, respectively. The Introduction also discusses the problems that arose which led to the present Conference and the special procedures employed both in the two-year-long preparatory work and in the 1980 meeting of the Conference.

The paper on data needs in computational fluid dynamics is the work of six individuals all deeply involved in the preparatory work, P. Bradshaw, B. J. Cantwell,

J. H. Ferziger, S. J. Kline, M. R. Rubesin, and C. C. Horstman. The first four authors worked on the draft *seriatim* followed by several iterations concerning differences between P. Bradshaw and J. H. Ferziger on questions of numerics and boundary conditions. The final two authors made independent comments on compressible flows which have been consolidated for completeness. It is important to note that some differences regarding the best statement of needs still remains among the authors. Since no paper on this topic seems to have appeared before, the paper should be widely useful, and will hopefully lead, over time, to still further clarifications.

The paper on the data library describes the nature, function and nomenclature of the library; the author B. J. Cantwell has assumed the central responsibility for construction of the library. Sources for distribution of current versions of the library are provided in the paper. Each case on the magnetic tape consists of two or more files of information. File 1 contains a detailed description of the given case. This is followed by one or more files of normalized data. A sample File 1 is included in this paper.

The paper on uncertainty analysis extends and re-opens for discussion an important topic that seems to have been neglected in some circles. In the 1968 meeting the uncertainties in the data are, for the most part, small compared to the uncertainty in computation; thus special considerations of data uncertainty were not needed in 1968. In the 1980-81 Conference, the data uncertainties are frequently significant, and special attention, therefore, had to be focused on estimates of the uncertainties in the data in order that comparisons with computation can be properly interpreted. R. J. Moffat has been one of the few individuals with a sustained interest in the area of uncertainty analysis. In the present paper Moffat contributes important conceptual advances beyond the older standard (of Kline and McClintock). The advances by Moffat are particularly germane to the comparison of data from many laboratories, and thus form a logical portion of the current volume.

The presentations of each test case follow the order and format of the 1980 meeting. When cases were accepted and used for the 1981 meeting, the specifications and output plots are displayed. When a case was not used in the 1981 meeting, only the summary and discussion are presented. The failure to use a given case in the 1981 meeting does not necessarily imply any lack in quality of the data; the final cases for the 1981 meeting were selected not only on the basis of trustworthiness and completeness of the data but also in order to form a reasonably complete set of test cases of manageable size. Some test cases will be stored in the library as usable for future work, but are not employed in the 1981 test cases. The library index will show such flows.

The specifications for computations are not displayed in the form presented in the 1980 meeting where they were given in a variety of written (rather than tabular)

forms. All specifications for computations were converted by the editors to a standard tabular form to provide increased clarity, clear coincidence with plots, and uniformity of presentation. In some instances a few plots requested by data evaluators have been eliminated either because data were lacking (in data file) or to avoid an excessive number of plots. The responsibility for these deletions rests with the Organizing Committee of the Conference.

Because of the large variety of flows and the amount of data processed in a relatively short time, some discrepancies between data files, specifications and plots occurred in the first releases to Computers. At least one Computer group was asked to report such difficulties and errata were issued early in 1981 covering needed changes. These errata have been incorporated into the present volume.

As noted above, the discussion procedures are recorded in the Introduction; they may be of interest in some future meetings. The important differences from the usual procedure is the recordation of differences of opinion as well as agreements in order to focus, not only what is known, but also what still requires further researches.

The reports of ad-hoc committees include discussion by an unusually large gathering of leading experts on topics that, for a variety of reasons, remain vexing to the research community particularly with respect to the reliability of data. Several of these reports should make useful contributions for future data takers.

The pictorial summary charts of the flows appear in two places. A complete set in the numerical order of the flows appears at the end of this section. Separate sectors of the charts are included with each specification. These charts were initially prepared by Professor Shinji Honami, while he was a visitor to the Thermosciences Division of the Mechanical Engineering Department at Stanford in 1979-80. Final editing has been completed by the editors of the volume who assume responsibility for any errors in the final copy.

The conclusions were drawn from notes made during the preparatory phases and the meeting, primarily by S. J. Kline, and by G. M. Lilley. Of particular note in the conclusions is the reference to the "advices to future data takers." The comments by the data evaluators, within each flow class, include a surprisingly large number of remarks indicating difficulties of past data procedures that can and in most cases should be avoided in the future. Hence, they are a rich source for anyone planning future experiments on related flow situations.

Volume I--Objectives, Evaluation of Data, Specifications of Test Cases, Discussion and Position Papers--is presented here. The companion Volumes II and III--Taxonomies, Methods, Conclusions, and Output of Computations will appear roughly a year later. The three volumes should form a relatively complete picture of the state of the art, including both the accomplishments and the remaining difficulties, at the time of publication. Unlike the 1968 Conference, which largely completed a chapter of

research work, the present conference will not complete the needs for either data or computation. However, it should provide potential users with a key to what can be done and an improved picture of remaining needs. It should also provide a clearer direction for future research.

The editors of this volume also want to emphasize that the work is not theirs; it is rather a cooperative effort of a large fraction of the research community, which we have been fortunate to coordinate. The task is and was too large for any one or even a few individuals, and has only been possible through the willing and largely volunteer efforts of the participants. In the 1980 meeting and, hence, in this volume, the critical role has been carried out by the data evaluators whose names appear on each test case. These data evaluators not only assimilated and evaluated the literature, but also performed new functions not understood or requested at the outset. It is largely owing to the efforts of the data evaluators that this volume has become possible.

S. J. Kline
B. J. Cantwell
G. M. Lilley

July 1981

TABLE OF CONTENTS

	<u>Page</u>
Acknowledgments	111
Preface	v
General Committees	xv
Program: 1980 Meeting on Data	xvi
General Nomenclature	xx
Pictorial Summary	xxiii
 INTRODUCTION (S. J. Kline)	 1
 POSITION PAPERS 	
EXPERIMENTAL DATA NEEDS FOR COMPUTATIONAL FLUID DYNAMICS --A POSITION PAPER (P. Bradshaw, B. J. Cantwell, J. H. Ferziger, and S. J. Kline with comments by M. Rubesin and C. Horstman)	23
CONTRIBUTIONS TO THE THEORY OF UNCERTAINTY ANALYSIS FOR SINGLE-SAMPLE EXPERIMENTS (Robert J. Moffat)	40
THE DATA LIBRARY (Brian Cantwell)	57
Discussion of The Data Library	79
 SESSION I 	
Flow 0610, Attached Boundary Layers	
Summary	86
Specifications	83
Flow 0210, Effect of Free-Stream Turbulence on Boundary Layers	
Summary	82
Discussion	91
Specifications	93
Flow 0230, Boundary Layer Flows with Streamwise Curvature	
Summary	94
Discussion	96
Specifications	98
 SESSION II 	
Flow 0240, Turbulent Boundary Layers with Suction or Blowing (Incompressible)	
Flow 8300, Turbulent Boundary Layers with Suction or Blowing (Compressible)	
Summary	112
Discussion	117
Specifications	118
Flow 0330, Free Shear Layer with Streamwise Curvature	
Summary	130
Discussion	133
Specifications	134

Flow 0510, Turbulent Secondary Flows of the First Kind

Summary	139
Discussion	145
Specifications	146

SESSION III

Flow 0250, Three-Dimensional Turbulent Boundary Layer

Summary	162
Discussion	168

Flow 0310, Planar Mixing Layer

Summary	170
Discussion	174
Specifications	176

Flow 0150, Two-Dimensional Channel Flow with Periodic Perturbations

Summary	178
Discussion	180

SESSION IV

Flow 0110, Corner Flow Data Evaluation (Secondary Flow of the Second Kind)

Summary	182
Discussion	188
Specifications	189

Flow 0130, Entry Zone of Round Tube

Summary	213
Discussion	217

NUMERICAL CHECKS (E. Reshotko)

Discussion	218
----------------------	-----

SESSION V

Flow 0410, Evaluation of Bluff-Body, Near-Wake Flows

Summary	220
Discussion	226
Specifications	227

Flow 0440, Two-Dimensional Stalled Airfoil

Summary	234
Discussion	246
Specifications	247

Flow 0140, Diffuser Flows Unseparated; and Flow 0430, Diffuser Flows--Separated

Summary	253
Discussion	258
Specifications	259

	<u>Page</u>
SESSION VI	
Flow 0420, Backward-Facing Step Flow	
Summary	275
Discussion	280
Specifications	281
AN OVERVIEW OF THE PREDICTIVE TEST CASES (J. K. Eaton)	284
Case P1, Flow 0110, Asymmetric Flow in a Square Duct	
Summary	287
Discussion	289
Specifications	290
Case P2, Flow 0420, Backward-Facing Step: Variable Opposite-Wall Angle	
Summary	297
Discussion	299
Specifications	300
Case P3, Flow 0420, Backward-Facing Step: Turned Flow Passage	
Summary	301
Specifications	303
Case P4, Flow 0420, Backward-Facing Step: Variable Area Ratio	
Summary	304
Specifications	305
Case P5, Flow in a Planar Diffuser with Tailpipe	306
Case P6, Shock-Boundary Layer Interaction	310
Discussion	311
Case P7, Transonic Airfoil	312
Discussion	312
Discussion, General Predictive Cases	313
Flow 9000, Flows with Buoyancy Forces	
Summary	314
Discussion	316
Flow 0340, Flows with Swirl	
Summary	317

SESSION VII	
Flow 0360, Wakes of Round Bodies, and Flow 0390, Axisymmetric Boundary Layer with Strong Streamwise and Transverse Curvature	
Summary	327
Discussion	331
Specifications	332
Flow 0380, Wakes of Two-Dimensional Bodies	
Summary	340
Supplement to Summary	346
Specifications	356

	<u>Page</u>
Flow 8500, Compressibility Effects on Free-Shear Layers	
Summary	364
Discussion	366
Specifications	367
Flows 8100/8200, Supersonic Flow over a Flat Plate (Insulated/Cooled Wall)	
Summary	369
Discussion	374
Specifications	375
Flows 8400/8410, Boundary Layers in an Adverse Pressure Gradient in an Axisymmetric Internal Flow/Two-Dimensional Flow	
Summary	378
Supplement to Summary	388
Discussion	393
Specifications	394

SESSION VIII

Flow 0370, Homogeneous Turbulent Flows	
Summary	405
Discussion	411
Pictorial Summary	412
Flow 0260, Turbulent Wall Jet	
Summary	434
Discussion	443
Specifications	444

SESSION IX

Flows 8610, 8630, 8640, Compressible Flows Over Deflected Surfaces	
Summary	458
Discussion	465
Specifications	466
Flow 8680, Axisymmetric Near-Wake Flow (Supersonic)	
Summary	482
Discussion	484

SESSION X

Flows 8650, 8660, 8600, 8690, Shock Wave--Boundary-Layer Interaction Flows	
Summary	486
Discussion	495
Specifications	498

SESSION XI

Flow 8620, Transonic Airfoils	
Summary	523
Discussion	530
Specifications	531

	<u>Page</u>
Flow 8670, Pointed Axisymmetric Bodies at Angle of Attack (Supersonic)	
Summary	543
Discussion	546
Specifications	547
Flow 8310, Variation in C_f/C_{f0} for Blowing/Suction with Mach Number	
Summary	549
Discussion	549

SESSION XII

Transient Flows	
Summary	551
Discussion	551
Flow 0350, Ship Wakes	
Summary	552
Flow 0290, Laminar-Turbulent Transition	
Summary	554
Discussion	554
Flow 0470, Flow Over the Trailing Edge of Blades and Airfoils	
Summary	555
Discussion	558
Specifications	559
Flow 0280, Relaminarizing Flows	
Summary	567
Discussion	571
Specifications	573

SESSION XIII

Ad-Hoc Committee Report on Hot-Wire Anemometry at Low Mach Numbers	583
Ad-Hoc Committee Report on Use of Hot-Wire Anemometers in Compressible Flows	586
Ad-Hoc Committee Report on Free-Shear Layers	588
Ad-Hoc Committee Report on Turbulence Management and Control of Large-Eddy Structure	590
Closing Discussion on Reports from Ad-Hoc Committees	591
Closing Discussion on Sessions I Through XII	592
Report of the Evaluation Committee	595

SESSION XIV

Plans for 1981 and Beyond	596
-------------------------------------	-----

--- # # # ---

	<u>Page</u>
CONCLUSIONS	605
LIST OF PARTICIPANTS	607
GROUP PHOTOGRAPHS A AND B	618
LIST OF DATA EVALUATORS	622
NUMERICAL INDEX OF FLOW CASES AND DATA LIBRARY TAPE	624



B.J. Cantwell



B.E. Launder



S.J. Kline



E. Reshotko



M.W. Rubesin

GENERAL COMMITTEES

Organizing Committee

Stephen Kline, Stanford University, Chairman

Peter Bradshaw, Imperial College, London

Brian Cantwell, Stanford University

Brian Launder, University of Manchester, Manchester

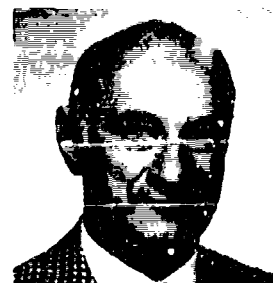
Eli Reshotko, Case-Western Reserve University

Morris Rubesin, NASA-Ames Research Center

Gino Sovran, General Motors Research Laboratories



P. Bradshaw



G. Sovran

Evaluation Committee, 1981 Meeting

H. W. Emmons, Harvard University, Chairman

D. R. Chapman, NASA-Ames and Stanford University

P. G. Hill, University of British Columbia

G. M. Lilley, University of Southampton

Marvin Lubert, General Electric, KAPL

M. V. Morkovin, Illinois Institute of Technology

W. C. Reynolds, Stanford University

P. J. Roache, Consultant

J. Steger, Stanford University

Host Committee at Stanford

Brian Cantwell

John K. Eaton

Joel H. Ferziger

James P. Johnston

Stephen J. Kline

Robert J. Moffat

William C. Reynolds

PROGRAM: 1980 MEETING ON DATA

THE 1980-81 AFOSR-HTTM-STANFORD CONFERENCE ON
COMPLE: TURBULENT FLOWS: COMPARISON OF COMPUTATION AND EXPERIMENT

8:30-8:50 INTRODUCTION: Goals, Framework; and Procedures--S.J. Kline

SESSION I 8:50-10:00 am, Wednesday, September 3, 1980

Chairman: V. C. Patel

Technical Recorders: R. Subbarao, P. Parikh

- 8:50-9:15 (1) The Data Library: Past, Present and Future--B. Cantwell
9:15-9:30 (2) Flow 0210: Effect of Free-Stream Turbulence--P. Bradshaw
9:30-10:00 (3) Flow 0230: Boundary Layer with Streamwise Wall Curvature
--T. Simon/S. Honami

10:00 -10:30 Coffee & Refreshments

SESSION II 10:30-12:00 noon, Wednesday, September 3, 1980

Chairman: B. Launder

Technical Recorders: R. Childs, P. N. Joubert

- 10:30-11:10 (1) Flow 0240: Boundary Layers with Blowing/Suction
--L. C. Squire (E. P. Sutton)
11:10-11:35 (2) Flow 0330: Free Shear Layer with Streamwise Curvature
--P. Bradshaw
11:35-12:00 (3) Flow 0510: Pressure-Driven Secondary Flow--R. B. Dean

12:00 -1:30 Lunch

SESSION III 1:30 -3:00 pm, Wednesday, September 3, 1980

Chairman: J. P. Johnston

Technical Recorders: E. Adams, I. P. Castro

- 1:30-2:10 (1) Flow 0250: Three-Dimensional Boundary Layers--D. Humphreys/
B. van den Berg
2:10-2:35 (2) Flow 0310: Planar Mixing Layer--S. Birch
2:35-3:00 (3) Flow 0150: Channel Flow with Superposed Waves--M. Acharya

3:00-3:30 Refreshments

SESSION IV 3:30-5:00 pm, Wednesday, September 3, 1980

Chairman: W. C. Reynolds

Technical Recorders: A. Cutler, A.K.M.F. Hussain

- 3:30-4:10 (1) Flow 0110: Entry into a Rectangular Duct--F. Gessner
4:10-4:35 (2) Flow 0130: Entry Zone of Round Tube--J. B. Jones
4:35-5:00 (3) Numerical Checks--E. Reshotko

PROGRAM: 1980 MEETING ON DATA

SESSION V 8:30 -10:00 am, Thursday, September 4, 1980

Chairman: A. Roshko

Technical Recorders: A. Strawa, H. L. Moses

- 8:30-8:55 (1) Flow 0410: Circular Cylinder and Related Bluff Bodies
--B. Cantwell
- 8:55-9:20 (2) Flow 0440: Stalled Airfoil--A. Wadcock
- 9:20-10:00 (3) Flows 0140 and 0430:
Diffuser Flows--R. L. Simpson

10:00 -10:30 Coffee and Refreshments

SESSION VI 10:30 -12:00 noon, Thursday, September 4, 1980

Chairman: E. Reshotko

Technical Recorders: R. Westphal, D. J. Cockrell

- 10:30-10:55 (1) Flow 0420: Backward-Facing Step--J. K. Eaton
- 10:55-11:35 (2) Predictive Cases: Organizing Committee
- Discussion of Procedures
 - Specification of Geometries, Initial Conditions
- 11:35-12:00 (3) Report on Flows with Buoyancy Forces--J. Wyngaard
Report on Flows with Swirl--A. Morse

12:00-1:30 Lunch

SESSION VII 1:30-3:15 pm, Thursday, September 4, 1980

Chairman: L. W. Carr

Technical Recorders: B. Afshari, F. A. Dvorak

- 1:30-2:10 (1) Flow 0360 Subsonic Axisymmetric Wake--V. C. Patel
Flow 0390 Boundary Layer with Strong Streamwise and Trans-
verse Curvature--V. C. Patel
- 2:10-2:25 (2) Flow 8500: Spreading Parameter σ for Mixing Layer as a
Function of Mach Number--P. Bradshaw
- 2:25-2:45 (3) Flows 8100 and 8200
Variations in C_f/C_{fo} with M and T_w/T_o
--M. Rubesin/C. Horstman
- 2:45-3:15 (4) Flow 8400 (8401, 8402, 8411)
Compressible Boundary Layers Flows--H. Fernholz
- (5) Case 8403 Compressible Boundary Layer Flow--G. Lilley

3:15-3:30 Refreshments

SESSION VIII 3:30-5:00 pm, Thursday, September 4, 1980

Chairman: J. L. Lumley

Technical Recorders: S. Prorhick, H. Nagib

- 3:30-3:50 (1) Flow 0370: Sheared Homogeneous Turbulence--J. H. Ferziger
- 3:50-4:30 (2) Flow 0260: Wall Jet--B. Launder/W. Rodi
- 4:30-5:00 (3) The Control of Accuracy via Uncertainty Analysis
--R. J. Moffat

PROGRAM: 1980 MEETING ON DATA

SESSION IX 8:30-10:00 am, Friday, September 5, 1980

Chairman: S. Bogdonoff

Technical Recorders: P. Eibeck, T. Morel

- 8:50-9:30 (1) Flow 8610: Transonic Flow over a Bump
--M. Rubesin/C. Horstman
(2) Flow 8630: Two-Dimensional Compression Corner--C. Horstman
(3) Flow 8640: Reattaching Planar Free-Stream Layer (Supersonic)--M. Rubesin/C. Horstman
- 9:30-10:00 (4) Flow 8680: Axisymmetric, Supersonic Near-Wake Flow--A. Favre
- 10:00 -10:30 Coffee & Refreshments

SESSION X 10:30-12:00 noon, Friday, September 5, 1980

Chairman: J. McCroskey

Technical Recorders: R. Strawn, R. So

- 10:30-11:30 (1) Flow 8650: Axisymmetric Shock Impingement (High Supersonic)--M. Rubesin/C. Horstman
(2) Flow 8660: Three-Dimensional Shock Impingement (Supersonic)
--M. Rubesin/C. Horstman
(3) Flow 8600: Impinged Normal Shock Wave, Boundary Layer Interaction at Transonic Speeds
--M. Rubesin/C. Horstman
(4) Flow 8690: Non-Lifting, Transonic Airfoil, Shock-Separated
--M. Rubesin/C. Horstman
- 11:30-12:00 (5) Data Needs for CFD--Discussion of Draft--Participants
- 12:00 -1:30 Lunch

SESSION XI 1:30-3:00 pm, Friday, September 5, 1980

Chairman: P. Bradshaw

Technical Recorders: R. Carella, J. A. C. Humphrey

- 1:30-2:10 (1) Flow 8620: Transonic Airfoils--R. Melnik
- 2:10-2:40 (2) Flow 8670: Pointed Axisymmetric Bodies at Angle of Attack (Supersonic)--D. Peake
- 2:40-3:00 (3) Flow 8300: Variation in C_f/C_{f0} with Blowing
--L. C. Squire (E. P. Sutton)
- 3:00-3:30 Refreshments

SESSION XII 3:30-5:00 pm, Friday, September 5, 1980

Chairman: P. S. Klebanoff

Technical Recorders: M. Lee, J. Gerrard

- 3:30-3:50 (1) Status of Unsteady Boundary Layer Experiments
--An International Review--L. W. Carr
- 3:50-4:00 (2) Flow 0350: Ship Wakes--V. C. Patel
- 4:00-4:10 (3) Flow 0290: Laminar-Turbulent Transition--E. Reshotko
- 4:10-4:30 (4) Flow 0470: Flow over the Trailing Edge of Blades and Airfoils--P. Drescher
- 4:30-5:00 (5) Flow 0280: Relaminarization, Laminar and Retraining Boundary Layers--K. R. Sreenivasan

PROGRAM: 1980 MEETING ON DATA

SESSION XIII 8:30-10:00 am, Saturday, September 6, 1980

Chairman: J. B. Jones

Technical Recorders: R. Westphal, P. Moin

- 8:30-10:00 • Reports from Ad Hoc Committees on Basic Questions;
Revisions of Specifications

10:00 -10:30 Coffee & Refreshments

SESSION XIV 10:30-12:00 noon, Saturday, September 6, 1980

Chairman: G. Sovran

Technical Recorders: R. Jayaraman, G. Lilley

- Plans for 1981 and Beyond--Organizing Committee
- Suggestions from Users, Computers, Experimentalists on Work of 1981 Conference and Data for Library (written comments submitted before session will have first priority).



D. Peschcke-Koedt

GENERAL NOMENCLAURE

Computer	Symbol	Conven- tional	Meaning	S.I. Units
BETA	β		$(dp/dx) \delta^* / \tau_w$	-
DEL	δ_{995}		Boundary-layer thickness to $0.995 U_e$	m
DELS	δ^*		Displacement thickness $= \int_0^\delta (1 - \frac{\rho U}{\rho_e U_e}) dy$	m
ENTH	δ^{**}		Energy thickness $= \int_0^\delta \frac{\rho U}{\rho_e U_e} (1 - \frac{U^2}{U_e^2}) dy$	m
CLTH	Δ		Clauser thickness $= \int_0^\delta \frac{\rho_e U_e - \rho U}{\rho_w U_*} dy$	m
EPSILON	ϵ		Dissipation function	$m^2 \text{ sec}^{-3}$
THETA	θ		Momentum thickness $= \int_0^\delta \frac{\rho U}{\rho_e U_e} (1 - \frac{U}{U_e}) dy$	m
XNU	ν		Kinematic viscosity	$m^2 \text{ sec}^{-1}$
RO	ρ		Density	kg m^{-3}
TAU	τ		Shear stress	N m^{-2}
PHIL	ϕ_L		Left-hand side of momentum integral equation balance	-
PHIR	ϕ_R		Right-hand side of momentum integral equation balance	-
CD	C_D		Drag coefficient	-
CL	C_L		Lift coefficient	-
CF	C_f		Skin-friction coefficient $= \tau_w / (\frac{1}{2} \rho_e U_e^2)$	-
CFE	C_f		C_f as reported by originator	-
CFLT	C_f		C_f according to Ludwig-Tillmann formula	-
CFPT	C_f		Measured using Preston tube	-
CP	C_p		Pressure coefficient	-
G	G		Equilibrium shape factor $= \int_0^\delta (\frac{\rho_e U_e - \rho U^2}{\rho_w U_*}) d(y/\Delta)$	-
H	H		Shape factor $= \delta^* / \theta$	-
HS	H^*		δ^{**} / θ	-
KAY	K		Turbulence kinetic energy $(\overline{u^2} + \overline{v^2} + \overline{w^2})$	-

Computer	Conven- tional	Symbol	Meaning	S.I. Units
LREF	L_{ref}		Reference length	m
XM	M		Mach number	-
XMREF	M_{ref}		Reference Mach number	-
P	p		Pressure	$N\ m^{-2}$
PR	Pr		Prandtl number	-
PREF	P_{ref}		Reference pressure	$N\ m^{-2}$
PIU1	\overline{pu}		Pressure-velocity covariance	-
QREF	q_{ref}		Reference dynamic pressure	$N\ m^{-2}$
RE	Re		Reynolds number based on reference values	-
			$Re = \frac{U_{ref} L_{ref}}{\nu_{ref}}$	-
RDELS	R_{δ^*}		Reynolds number = $U_e \delta^* / \nu$	-
ROIU1	$\overline{\rho u}$		Density-velocity covariance	-
RTHETA	R_{θ}		Reynolds number = $U_e \theta / \nu$	-
ST	St		Stanton number	-
STR	Str		Strouhal number	-
TENTH	t^+		Thermal energy thickness $\frac{\sqrt{C_f/2}}{St} \frac{T_w - T}{(T_w - T_e)}$	m
XS	s		Coordinate tangent to an arc	m
XN	n		Coordinate normal to an arc	m
U	U	}	Mean streamwise velocity	$m\ sec^{-1}$
V	V		Mean transverse velocity	$m\ sec^{-1}$
W	W		Mean spanwise velocity	$m\ sec^{-1}$
UDEF	-		Defect velocity = $(U_e - U)/U_*$	$m\ sec^{-1}$
UE	U_e		Velocity external to boundary layer	$m\ sec^{-1}$
UI	U_{∞}		Free-stream velocity	$m\ sec^{-1}$
UREF	U_{ref}		Reference velocity	$m\ sec^{-1}$
US	U_*		Wall shear velocity = $\sqrt{\tau_w / \rho_w}$	$m\ sec^{-1}$
UPLUS	U^+		U/U_*	-
U2	$\overline{u^2}$	}	Reynolds stress	$m^2\ sec^{-2}$
V2	$\overline{v^2}$		Reynolds stress	$m^2\ sec^{-2}$
W2	$\overline{w^2}$		Reynolds stress	$m^2\ sec^{-2}$
U1V1	\overline{uv}		Reynolds shear stress	$m^2\ sec^{-2}$

Symbol			
Computer	Conven- tional	Meaning	S.I. Units
U1W1	\overline{uw}	Reynolds shear stress	$m^2 \sec^{-2}$
V1W1	\overline{vw}	Reynolds shear stress	$m^2 \sec^{-2}$
UnVm	$\overline{u^n v^m}$	Higher-order velocity covariance	-
X	$\left. \begin{matrix} x \\ y \\ z \end{matrix} \right\}$	Streamwise coordinate	m
Y		Transverse coordinate	m
Z		Spanwise coordinate	m
X	x or s	Streamwise coordinate on curved surface	m
Y	y or n	Direction normal to curved surface	m
Z	z	Spanwise coordinate	m
YPLUS	y^+	yU_\star/ν	-

Subscript "w" denotes wall value.

Subscript "e" denotes conditions external to boundary layer.

$$\phi_L^{(x)} = \frac{U_e^2 \theta}{(U_e^2 \theta)_c} - 1 + \frac{1}{2} \int_{x_0}^x \frac{\delta^*}{\theta_0} d\left(\frac{U_e^2}{(U_e^2)_0}\right).$$

$$\phi_R^{(x)} = \int_{x_0}^x \left(\frac{U_\star}{(U_e)_0}\right)^2 d\left(\frac{x}{\theta_0}\right).$$

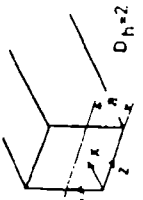
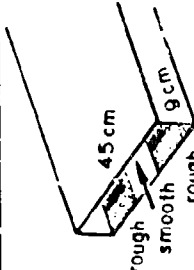
PICTORIAL SUMMARY

The initial version of the pictorial and tabular presentation of all the "Flows" used in the 1981 Conference was prepared by Professor S. Honami. The initial version has been modified and edited for these Proceedings. All the major features of the flows which appear as "Specifications" for the 1981 Conference are included. They are given here in the numerical order of the "Flows." Each individual chart is repeated later within the relevant "Case."




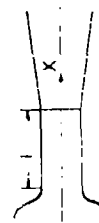
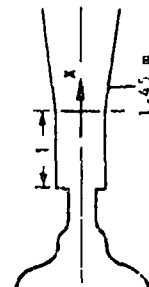
S. Honami G. Lilley

PICTORIAL SUMMARY
Flow 0110. Data Evaluator: F. Gessner. "Corner Flow (Secondary Flow of the Second Kind)."

Case Data Taker	Test Rig Geometry	In/dx or C _p	Number of Stations Measured						Re	Inf- tial Condi- tion	Other Notes
			Mean Velocity		Turbulence Profiles						
			U	V or W	U ²	V ²	W ²	Others			
Case 0111 J. Po E. Lund F. Gessner	 $0 < (x/D_H) < 0.4$	34 sta- tions on walls A and B	17	5	-	-	3 profiles of K UV and VW	1	2.5 $\times 10^5$ (based on bulk velocity and D_H)	sym- metric inlet flow	C _p vs x data for laminar flow (Beavers, Goldstein) included with data file. Goldstein's laminar velocity data also included. Nominally uniform, low turbulence level flow at inlet ($x/D_H = 0$).
Case 0112 J. Rinze	 45 cm rough smooth rough		1		1	1	1	1	1.5 $\times 10^5$ (based on hy- draulic diam and U_{max})	One wall rough with smooth center- and strip	All measurements were made at $x/D_H = 126$. Data include viscous dissipation.

PICTORIAL SUMMARY

Flow 0140. Data Evaluator: R. Simpson. "Diffuser Flows (unseparated)."

Case Data Taker	Test Rig Geometry	$\frac{dp}{dx}$ or C_p	Number of Stations Measured							Re	Initial Condition	Other Notes
			Mean Velocity		Turbulence Profiles				C_f			
			U	V or W	$\overline{u^2}$	$\overline{v^2}$	$\overline{w^2}$	Others				
Case 0141 A. Samuel P. Joubert		$\frac{dp}{dx} > 0$, $\frac{d^2p}{dx^2} > 0$	12	-	6	6	6	6	Float-balance, Preston tube, Clauser plots	1.76×10^6 per m	Turbulence intensity 0.3%	Two-dimensionality was checked.
Case 0142 K. Pozzorini	 1/d = 4.5; Area Ratio 4; Cone Angle 6°	> 0	12	12	12	12	12	12	Clauser plots, Preston tube	2.54×10^5 (based on inlet pipe radius)	Turbulence intensity 0.31%	Conical diffuser --core (low turbulence).
Case 0143 R. Pozzorini	 1/d = 7.25; Area Ratio 4; Cone Angle 6°	> 0	6	6	6	6	6	6	Clauser plots, Preston tube	1.27×10^5 (based on inlet pipe radius)	Turbulence intensity 16%	Conical diffuser --core (high turbulence).

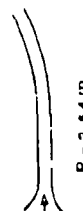

PICTORIAL SUMMARY

Flow 0210. Data Evaluator: P. Bradshaw. "Effect of Free-Stream Turbulence on Boundary Layers."

Case Data Taker	Test Rig Geometry	dp/dx or C _p	Number of Stations Measured						Initial Condi- tion	Other Notes
			Mean Velocity		Turbulence Profiles					
					u ²	uv	Others	C _f		
			V or W							
U										
Case 0211 P. Hancock and others			Smoothed curve of $\frac{dC_f}{C_{f_0}}$ vs $\left(\frac{u'}{U}\right)_e / \left(\frac{U}{\delta} + 2\right)$ given							

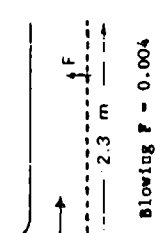
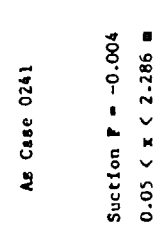
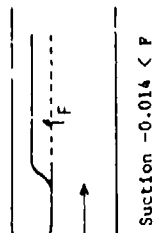
PICTORIAL SUMMARY

Flow 0230. Data Evaluators: T. Simon and S. Konami. "Boundary Layer Flows with Streamwise Curvature."

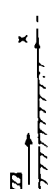
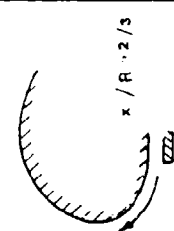

Case Data Taker	Test Rig Geometry	dp/dx or C _p	Number of Stations Measured							Initial Condi- tion	Other Notes
			Mean Velocity		Turbulence Profiles						
			U	V or W	u ²	v ²	uv	Others	C _f		
Case 0231-convex	 R = 2.54 m	12	5	-	5	5	-	5	u ³ -5 uv ² -5 uv ² -5 v ³ -5	5.2 x 10 ⁴ (based on δ at be- ginning of curve)	Hill's Curvature.
Case 0233 J. Gillie & J. Johnson	 R = 0.45 m	24	11	-	12	12	12	12	24 [*]	4.6 x 10 ⁴ (based on δ at be- ginning of curve)	Strong Curvature with Recovery.

* Clauser Plot Method.

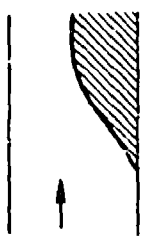
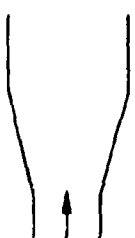
PICTORIAL SUMMARY
Flow 0240. Data Evaluator: L. Squire. "Turbulent Boundary Layers with Suction or Blowing."

Case Data Taker	Test Rig Geometry	dp/dx or C _p	Number of Stations Measured							Inf- tial Condi- tion	Other Notes
			Mean Velocity	Turbulence Profiles					Re		
				U	$\overline{u^2}$	$\overline{v^2}$	\overline{uv}	Others			
Case 0241 P. Andersen W. Kays R. Moffat	 Blowing $P = 0.004$ $0.05 < x < 2.286 \text{ m}$	0	9	-	-	-	-	-	9	6.7×10^5 per m	No turbulence data.
Case 0242 P. Andersen W. Kays R. Moffat	 As Case 0241 Suction $P = -0.004$ $0.05 < x < 2.286 \text{ m}$	Az- verse U_m ~ -0.15	9	-	1	1	1	-	9	6.7×10^5 per m	Turbulence data available at initial station.
Case 0244 A. Favre R. Dumas E. Vercellez M. Coantic	 Suction $-0.014 < P$ $-0.05 < x < 0.4 \text{ m}$	0	1	-	1	1	1	-	-	7.3×10^5 per m	Data available for 4 suction rates: $P = -0.002, -0.0053,$ $-0.0100, -0.0144.$ Velocity and turbulence data restricted to one streamwise station.

PICTORIAL SUMMARY
Flow 0260. Data Evaluators: B. Launder and W. Rodi. "Turbulent Wall Jet."

Case Data Taker	Test Rig Geometry	dp/dx or C_p	Number of Stations Measured							Initial Condi- tion	Other Notes
			Mean Velocity		Turbulence Profiles				C_f		
			U or W	$\overline{u^2}$	$\overline{v^2}$	$\overline{w^2}$	Others				
Case 0261 Various data takers		> 0	Yes	Yes	Yes	Yes	Inter- mit- tency. Razor Triple, blade quad- ruple velocity corre- lations	4×10^3 to 5×10^4		Equilibrium wall jet in adverse pressure gradient.	
Case 0263 D. Guitton B. Newman		-	Yes	Yes	Yes	-	Yes	K	7×10^3 to 5×10^4 (based on slot height)		Self-preserving wall jet on logarithmic spiral surface.
Case 0264 Various Data Takers		-	Yes	-	-	-	-	-	$> 10^4$	Self- simi- lar	3D wall jet in still air on plane surface. No output plots required.

PICTORIAL SUMMARY
Flow 0280. Data Evaluator: K. R. Sreenivasan. "Relaminarizing Flows."

Case Data Taker	Test Rig Geometry	$\frac{dp}{dx}$ or C_p	Number of Stations Measured							Re	Initial Condi- tion	Other Notes
			Mean Velocity	Turbulence Profiles					C_f			
				U or W	$\overline{u^2}$ or $\overline{w^2}$	\overline{uv}	Others					
Case 0281 R. Simpson D. Wallace		-	15	15	-	-	-	-	15	2362 (based on δ^* at inlet)		Boundary layer developing under mild adverse pres- sure gradient upstream of contraction.
Case 0282 J. Laufer; (V. Patel & M. Head)		-	6	5	-	-	-	-	-	1725 (based on radius at di- vergence inlet)	No con- ditions up- stream of di- vergence given	Initial mean velocity data taken from Patel and Head (1969).

xxix

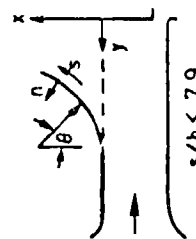
PICTORIAL SUMMARY
Flow 0310. Data Evaluator: S. Birch. "Planar Mixing Layer."

Case Data Taker	Test Rig or Geometry	dp/dx or C_p	Number of Stations Measured							Re	Ini- tial Condi- tion	Other Notes
			Mean Velocity		Turbulence Profiles				C_f			
			U	V or W	$\overline{u^2}$	$\overline{v^2}$	\overline{uv}	Others				
Case 0311 Data combined from several sources.												Initial development of the $u_2 = 0$ plane mixing layer.

L/θ_1 vs x/θ_1

PICTORIAL SUMMARY

Flow 0330. Data Evaluator: P. Bradshaw. "Free-Shear Layer with Streamwise Curvature."

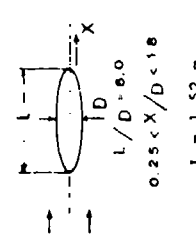
Case Data Taker	Test Rig Geometry	dp/dx or C _p	Number of Stations Measured						Re	Inf- tial Condi- tion	Other Notes
			Mean Velocity	Turbulence Profiles							
				U or W	$\overline{u^2}$ or $\overline{v^2}$	\overline{uv}	Others	C _f			
Case 0331 I. Castro P. Bradshaw			17*	17*	17*	17*	17*	2.5 x 10 ⁵ (based on nozzle opening h)	Turbu- lence level < 0.012	Tabulated data are in a mix of x, y, or r, θ coordinates. Digital processing techniques are used.	

*Results are plotted in semi-curved linear (s,n) coordinates; the n = 0 line being a nominal curved centerline of the mixing layer.

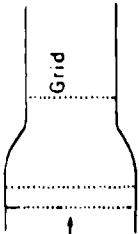
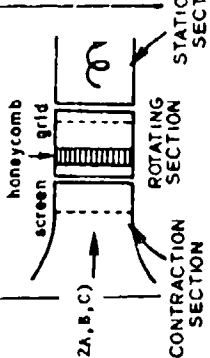
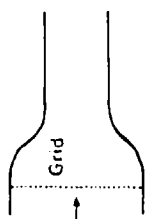
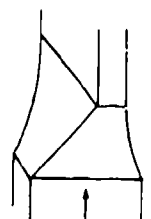
XXX

PICTORIAL SUMMARY

Flow 0360. Data Evaluator: V. Patel. "Wakes of Round Bodies (Axisymmetric Wakes)."

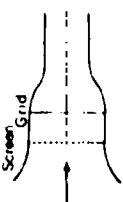
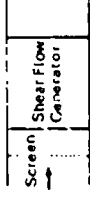
Case Data Taker	Test Rig Geometry	dp/dx or C _p	Number of Stations Measured							Re	Inf- tial Condi- tion	Other Notes
			Mean Velocity		Turbulence Profiles							
			U	V or W	$\overline{u^2}$	$\overline{v^2}$	$\overline{w^2}$	\overline{uv}	Others			
Case 0361 P. Chevray/	 <p>$L/D = 6.0$ $0.25 < x/D < 1.5$ $L = 1.52 \text{ m}$</p>	Negli- gible tunnel block- age effect	12	5	12	12	12	12	-	2.75 $\times 10^6$ (based on L)	Free stream turbu- lence 0.2%	Model 1.52 m long, 0.254 m maximum diam. spheroid. Static pressure distribu- tion across wake is pro- vided. Model surface pressure not measured.

PICTORIAL SUMMARY
Flow 0370. Data Evaluator: J. Perzger. "Homogeneous Turbulent Flows."

Case Data Taker	Test Rig Geometry	dp/dx or C _p	Number of Stations Measured							Re	Initial Condi- tion	Other Notes
			Mean Velocity		Turbulence Profiles							
			U	V or W	$\overline{u^2}$	$\overline{v^2}$	\overline{uv}	Others	C _f			
Case 0371 G. Comte-Bellot S. Corffean		zero	Yes	-	Yes	Yes	-	-	1600 3200 (based on M)	-	Homogeneous isotropic turbulence. Grid 3 cases	
Case 0372 R. Wigeland H. Nagib (0372A,B,C)		-	Yes	-	Yes	Yes	-	-	-	-	Rotating homogeneous turbulence.	
Case 0373 M. Uberoi (0373A,B,C,D) ----- H. Tucker A. Reynolds (0373E)		zero	Yes	-	Yes	Yes	-	-	3710 (based on M)	-	Return to isotropy. Contraction 3 cases.	
Case 0374 A. Townsend (0374A) ----- H. Tucker A. Reynolds (0374B)		-	Yes	-	Yes	Yes	-	-	-	-	Plane strained homo- geneous turbulence.	

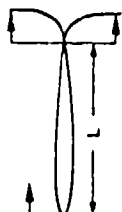

Flow 0370 continued

Flow 0370. Data Evaluator: J. Versiger. "Homogeneous Turbulent Flows." (continued)

Case Data Taker	Test Rig Geometry	dp/dx or C_f	Number of Stations Measured							Inf- tial Condi- tion	Other Notes
			Mean Velocity	Turbulence Profiles					C_f		
				U or W	$\overline{u^2}$	$\overline{v^2}$	$\overline{w^2}$	Others			
Case 0375 J. Tan-atchat (0375A, B, C, D, E)		-	Yes	-	Yes	-	Yes	Spec- trum 8100 cross- covari- ance	-	270 to 8100 (based on W)	Asymmetric strained homogeneous turbulence. Grid 6 cases. Contraction 7 cases.
Case 0376 F. Champagne V. Morris S. Corrain (0376A) V. Morris J. Graham S. Corrain (0376B)		zero	Yes	-	Yes	Yes	Yes	Auto- corre- lation	-	-	Sheared homogeneous turbulence.

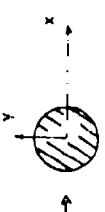
PICTORAL SUMMARY

Flow 0380. Data Evaluator: V. C. Patel. "Wakes of Two-Dimensional Bodies."

Case Data Taker	Test Rig Geometry	dp/dx or C_p	Number of Stations Measured							Re	Initial Condi- tion	Other Notes
			Mean Velocity		Turbulence Profiles							
			U or W	V or W	$\overline{u^2}$	$\overline{v^2}$	$\overline{w^2}$	Others	C_f			
Case 0381 J. Andreopoulos			10		4	4	-	Triple cor- rela- tions	-	6.8 $\times 10^6$ (based on L) < 0.05%	Free- stream turb. < 0.05%	Symmetrical Case. Conditional averages to study the mixing in the central part of wake.
Case 0382 J. Andreopoulos			6		4	4	-	Triple cor- rela- tions	-	6.8 $\times 10^6$ (based on L) < 0.05%	Free- stream turb. < 0.05%	Asymmetrical Case. Conditional averages to study the mixing in the central part of wake.

PICTORIAL SUMMARY

Flow 0410. Data Evaluator: B. Cantwell. "Evaluation of Bluff-Body, Near-Wake Flow."

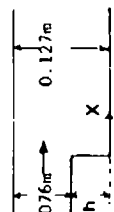
Case Data Taker	Test Rig Geometry	dp/dx or C _p	Number of Stations Measured							Ini- tial Condi- tion	Other Notes
			Mean Velocity	Turbulence Profiles				C _f			
				u or w	u ²	v ²	uv		Others		
Case 0411 B. Cantwell D. Coles	 -3.0 < y/D < 3.0 -0.5 < x/D < 8.0	Mean sur- face pres- sure	Yes*	Yes*	Yes*	-	Yes*	Yes*	Yes*	1.45 x 10 ⁵ (based on cylind- er dia.)	Plying hot-wire data. Large body of data field. Unsteady data included.

Location: y/D = -3.0 + 0.1 (4-1), 1 < 1 < 61; x/D = -0.5 + 0.1 (4-1), 1 < 1 < 86.

*Location: y/D = -3.0 + 0.1 (i-1), 1 ≤ i ≤ 61; x/D = -0.5 + 0.1 (j-1), 1 < j ≤ 86.

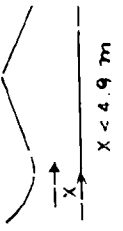
PICTORIAL SUMMARY

Flow 0420. Data Evaluator: J. Eaton and J. Johnston. "Backward-Facing Step Flow."

Case Data Taker	Test Rig Geometry	dp/dx or C _p	Number of Stations Measured								Ini- tial Condi- tion	Other Notes		
			Mean Velocity	Turbulence Profiles				C _f	Reattach- ment length x 10 ⁴ about 7h on h					
				U	V	u ²	v ²			w ²			uv	Others
Case 0421 J. Kim S. Kline J. Johnston	 0.076m 0.127m h X X/h < 16	Wall pres- sure	13	-	6	6	-	6	Inter- mit- tency	6/h = 0.3	Aspect ratio 16. Data inadequate in zones of high turbulence and oscillating flow. Laser data needed. Reattached layer well documented. Pressure on upper and lower walls available.			

PICTORIAL SUMMARY

Flow 0430. Data Evaluator: R. Simpson. "Diffuser Flow (Separated)."

Case Data Taker	Test Rig Geometry	dp/dx or C _p	Number of Stations Measured							Re	Ini- tial Condi- tion	Other Notes
			Mean Velocity		Turbulence Profiles				C _f			
			U	V or W	$\overline{u^2}$	$\overline{v^2}$	\overline{uv}	Others				
Case 0431 R. Simpson Y. Chew B. Shivaprasad		< 0 up- stream of throat	21*	-	21*	11*	6*	11*	Pres- ton tube	1.07 × 10 ⁶ per m	Turbu- lence inten- sity 0.12	Platness, skewness, and fraction of time flow moves downstream is available. Two-dimensionality was checked.
		> 0 down- stream	11†	11†	11†	11†	4†	11†	Spectra Sur- of face hot- wire anemo- meter		Position of an inviscid streamline near the upper wall is given.	


* Hot-wire measurement.

† Laser Doppler measurement.

xxxxiv


PICTORIAL SUMMARY

Flow 0440. Data Evaluator: A. Wadcock. "Two-Dimensional Stalled Airfoil."

Case Data Taker	Test Rig Geometry	dp/dx or C _p	Number of Stations Measured							Re	Ini- tial Condi- tion	Other Notes
			Mean Velocity		Turbulence Profiles				C _f			
			U	V or W	$\overline{u^2}$	$\overline{v^2}$	\overline{uv}	Others				
Case 0441 D. Coles A. Wadcock		Mean sur- face pres- sure	125	125	125	125	-	125	Inter- mit- tency	-	Free stream turb. level < 1.5%	Aspect ratio = 2. Probe interference present for attached boundary layer data--separated zone and wake is interference- free.
	$0.62 \leq x/c \leq 2.00$ $\Delta x/c = 0.0111$											

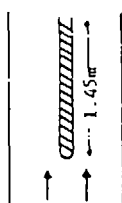

PICTORIAL SUMMARY

Flow 0470. Data Evaluator: P. Drescher. "Flow over the Trailing Edge of Blades and Airfoils."

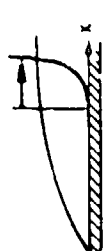
Case Data Taker	Test Rig Geometry	dp/dx or C _p	Number of Stations Measured								Re	M _∞	Other Notes
			Me Velocity		Turbulence F %				C _f				
					U	V or W	U ²	V ²		W ²			
			9	-					7				
Case 0471 P. Viswanath J. Cleary H. Seegmiller C. Horstman	 L = 0.93 m -0.205 < x/L < 0.150	Sur- face and wake pres- sure	9	-	7	7	-	7	-	-	2.4 to 3.7 x 10 ⁷ (based on chord)	0.4 and 0.7	Subsonic trailing edge flow, variable flap angle. Symmetric and unaymmetric cases.

PICTORIAL SUMMARY

Flow 0510. Data Evaluator: R. Dean. "Turbulent Secondary Flows of the First Kind."

Case Data Taker	Test Rig Geometry	dp/dx or C _p	Number of Stations Measured										Re	Ini- tial Condi- tion	Other Notes
			Mean Velocity		Turbulence Profiles				C _f						
			U or V	U ² or V ²	U ² or V ²	U ² or V ²	U ² or V ²	Others							
Case 0511 I. Shabaka	 <p>wing span: 0.127 m wing thickness: 0.051 m</p>	Meas- ured	3	Second- ary flow vectors at 3 sta- tions	3	3	3	3	Inter- mittency and triple pro- ducts, flat- ness factor sta- tions	7	1.15 × 10 ⁵ (based on wing thick- ness)	BL thick- ness at the lead- ing edge was about 0.025 m	Wing-body junction. Calculations should be started downstream of leading edge.		
Case 0512 J. Humphrey	 <p>4.0 × 4.0 cm square cross section</p>	Not recor- ded in bend	U ₀ 7	U _t 2	U ₀ ² 7	U _t ² 2	U _{0t} ² 2	-	-	-	4 × 10 ⁴ (based on duct height)	Nearly fully devel- oped	Curved rectangular duct. Calculations should be started 8.2 duct dia. upstream of bend using Melling's (1975) data.		

PICTORIAL SUMMARY
Flow 0610. Data Evaluator: D. E. Coles. "Attached Boundary Layers ('68 Conference)."

Case Data Taker	Test Rig Geometry	dp/dx or C _p	Number of Stations Measured							Initial Condi- tion	Other Notes
			Mean Velocity		Turbulence Profiles				C _f		
					U or W	$\overline{u^2}$	$\overline{v^2}$	$\overline{w^2}$			
Case 0612 K. Wieghardt		0	23	-	-	-	-	-	-	2.2 x 10 ⁶ per m plots	Data include computed values of boundary layer integral parameters. < 0.25%

PICTORIAL SUMMARY
Flow 8100. Data Evaluators: M. Rubesin and C. Horstman. "Supersonic Flow Over a Flat Plate (Insulated Wall)."

Case Data Taker	Test Rig Geometry	$\frac{dp}{dx}$ or C_p	Number of Stations Measured							Initial Condi- tion	Other Notes
			Mean Velocity		Turbulence Profiles				C_f		
					$\overline{u^2}$	$\overline{v^2}$	$\overline{w^2}$	Others			
			U or W	V or W							
Case 8101 Various data takers										Effect of compressibility on skin friction.	
										C_f/C_{f0} vs. M	

PICTORIAL SUMMARY

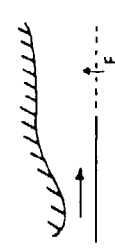
Flow 3200. Data Evaluators: M. Rubesin and C. Horstman. "Supersonic Flow Over a Flat Plate (Cooled Wall)."

Case Data Taker	Test Rig Geometry	dp/dx or C _p	Number of Stations Measured							Re	Ini- tial Condi- tion	Other Notes
			Mean Velocity	Turbulence Profiles								
				V or W	$\overline{u^2}$	$\overline{v^2}$	$\overline{w^2}$	\overline{uv}	Others			
Case 8201 Various data takers												Effect of surface cooling on skin friction.


C_f/C_{f0} vs. T_w/T_0

PICTORIAL SUMMARY

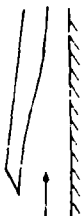
Flow 8300. Data Evaluator: L. Squire. "Turbulent Boundary Layers with Suction or Blowing at Supersonic Speeds."

Case Data Taker	Test Rig Geometry	dp/dx or C _p	Number of Stations Measured						Re	Ini- tial Condi- tion	Other Notes
			Mean Velocity	Turbulence Profiles							
				V or W	$\overline{v^2}$	$\overline{w^2}$	\overline{uv}	Others			
Case 8301 G. Thomas	 Blowing $0.02 < F < 0.0078$ $0 < x < 0.127$ m	< 0	11	-	-	-	-	-	5×10^8 per m	M (2.53 to 2.87)	M, P , H , δ^* vs x data available on file. No turbulence data.

PICTORIAL SUMMARY
Flow 8400. Data Evaluators: M. Rubesin and C. Horstman. "Boundary Layers in an Adverse Pressure Gradient in an Axisymmetric Internal Flow."

Case Data Taker	Test Rig Geometry	dp/dx or C _p	Number of Stations Measured								M _∞	Other Notes
			Mean velocity		Turbulence Profiles					C _f		
					U	V or W	$\overline{u^2}$	$\overline{v^2}$	$\overline{w^2}$			
Case 8403 A. Kuehny C. Horstman M. Acharya		> 0	8	-	8	8	8	8	8	8	1.6 x 10 ⁵ to 4.22 x 10 ⁶ (based on δ ₀)	Axisymmetric. Profile data for 2 pressure gradients. Skin friction data for 6 pressure gradients, each at 4 Reynolds numbers.

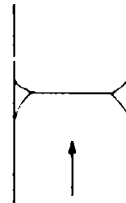
PICTORIAL SUMMARY
Flow 8410. Data Evaluators: M. Rubesin and C. Horstman. "Boundary Layers in an Adverse Pressure Gradient in 2-Dimensional Flow."

Case Data Taker	Test Rig Geometry	dp/dx or C _p	Number of Stations Measured							M _∞	Other Notes
			Mean Velocity	Turbulence Profiles					C _f		
				U or W	$\overline{u^2}$	$\overline{v^2}$	$\overline{w^2}$	Others			
Case 8411 F. Zwarte		> 0	6	-	-	-	-	-	3.5 x 10 ⁴ (based on θ ₀)	4	


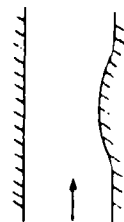
Flow 8500. Data Evaluator: P. Bradshaw. "Compressible Effects on Free Shear Layers."

Case Data Taker	Test Rig Geometry	dp/dx or C _p	Number of Stations Measured							Re	Ini- tial Condi- tion	Other Notes
			Mean Velocity		Turbulence Profiles							
			U	V	u ²	v ²	w ²	uv (other)	C _f			
Case 8501												Shear layer spreading rate vs Mach number.
Various data takers												

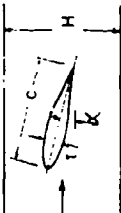

Flow 8600. Data Evaluators: M. Rubesin and C. Horstman. "Impinged Normal Shock Wave-Boundary Layer Interaction at Transonic Speeds."

Case Data Taker	Test Rig Geometry	dp/dx or C _p	Number of Stations Measured						Re	M _∞	Other Notes
			Mean Velocity			Turbulence Profiles					
			U	V or W	$\overline{u^2}$	$\overline{v^2}$	$\overline{w^2}$	Other			
Case 8601 G. Mateer A. Bronh J. Viegas			8	-	-	-	-	8	3x10 ⁵ to 6x10 ⁶ (based on δ ₀)	1.3 - 1.5	Axiymmetric profile data for one test condition. Skin friction data for several test conditions varying M and Re.

PICTORIAL SUMMARY
Flow 8610. Data Evaluators: M. Rubesin and C. Horstman. "Transonic Flow over a Bump."



Case Data Taker	Test Rig Geometry	$\frac{dp}{dx}$ or C_p	Number of Stations Measured							M_∞	Re	Other Notes
			Mean Velocity		Turbulence Profiles				C_f			
			U	V or W	$\overline{u^2}$	$\overline{v^2}$	$\overline{w^2}$	\overline{uv}				
Case 8611 W. Bachalo D. Johnson			12	12	12	12	-	12	-	-	1.4×10^5 (based on δ_0)	Axisymmetric. Complete LDV data.
Case 8612 J. Delery P. Le Duzet			28	28	28	28	-	28	-	-	7×10^4 (based on δ)	M_{shock} 1.37 Complete LDV data. Top wall is important in solving problem.

PICTORIAL SUMMARY
Flow 8620. Data Evaluator: R. E. Melnik: "Transonic Airfoils."

Data Taker	Test Rig Geometry	$\Delta p/dx$ or C_p	Number of Stations Measured							M_∞	Other Notes
			Mean Velocity		Turbulence Profiles				C_f		
			U	V or W	$\overline{u^2}$	$\overline{v^2}$	$\overline{w^2}$	uv			
Case 8621 P. Cook M. McDonald M. Firmin	RAE 2822 Airfoil 	Airfoil upper & lower surface pressure	9	-	-	-	-	-	Modified Law of the Wall chord	5.7 to 6.5 $\times 10^6$ (based on wall chord)	RAE 8x6 ft. transonic tunnel. Data include computed values of boundary-layer integral parameters.
Case 8623 F. Spaid L. Stivers, Jr.	DSMA 523 Airfoil 	Airfoil upper & lower surface pressure	7	-	-	-	-	-	Law of Wall by ρ/ρ_c transformed velocity chord)	2-4 $\times 10^6$ (based on chord)	NASA-Ames 2x2 ft. transonic tunnel.


PICTORIAL SUMMARY

Flow 8630. Data Evaluators: M. Rubesin and C. Horstman. "Compressible Flow over Deflected Surfaces."

Case Data Taker	Test Rig Geometry	$\frac{dp}{dx}$ or C_p	Number of Stations Measured							M_∞	Other Notes
			Mean Velocity		Turbulence Profiles				C_f		
			U	V or W	$\overline{u^2}$	$\overline{v^2}$	\overline{uv}	Others			
Case 8631 G. Settles T. Fitzpatrick S. Bogdonoff		> 0	9	-	-	-	-	M and p/p_∞	Pres- ton tube $\times 10^6$ (based on δ_0)	2.85	$\theta = 8, 16, 20$ and 24° . Wall pressure also available.
Case 8632 J. Dussauge J. Gaviglio		< 0	23	-	2	-	-	\overline{Tu}	Law of wall (based on δ_0)	1.76	Prandtl Meyer expansion. Wall pressure also available.

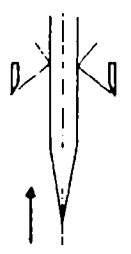
PICTORIAL SUMMARY

Flow 8640. Data Evaluators: M. Rubesin and C. Horstman. "Compressible Flow over Compression Corner with Reattaching Planar Shear Layer."

Case Data Taker	Test Rig Geometry	dp/dx or C_p	Number of Stations Measured							M_∞	Other Notes
			Mean Velocity		Turbulence Profiles				C_f		
			U	V or W	$\overline{u^2}$	$\overline{v^2}$	\overline{uv}	Others			
Case 8641 G. Settles B. Baca D. Williams S. Bogdonoff		> 0	11	-	-	-	-	M_∞ , Pres- ton $\times 10^5$ probe (based on δ_0)	2.8	Combines three problems: Free-shear layer develop- ment, reattachment, and downstream development.	

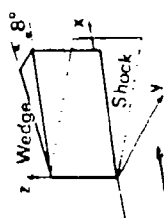
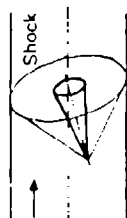
PICTORIAL SUMMARY

Flow 8650. Data Evaluators: M. Rubesin and C. Horstman. "Axisymmetric Shock Impingement (Supersonic)."

Case Data Taker	Test Rig Geometry	dp/dx or C _p	Number of Stations Measured								M _∞	Re	Other Notes		
			Mean Velocity		Turbulence Profiles					C _f					
					U	V or W	— u ²	— v ²	— w ²					— uv	Other
Case 8651 M. Kussey C. Horstman		var- ious	10	-	4	-	-	PT 4	Float- ing ele- ment on δ ₀	3.6 × 10 ⁵ (based on δ ₀)	7.2	Axisymmetric. Two cases - one attached and one separated. Heat transfer measure- ments included.			

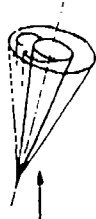
PICTORIAL SUMMARY

Flow 8660. Data Evaluators: M. Rubesin and C. Horstman. "Three-Dimensional Shock Impingement (Supersonic)."

Case Data Taker	Test Rig Geometry	dp/dx or C _p	Number of Stations Measured								M _∞	Re	Other Notes
			Mean Velocity		Turbulence Profiles								
			U	V or W	$\overline{u^2}$	$\overline{v^2}$	$\overline{w^2}$	\overline{uv}	Other	C _f			
Case 8661 D. Peake			5	5*	-	-	-	-	Wall pres- sure	1.5 × 10 ⁵ (based on δ ₀)	2	3D planar shock inter- action. *v known in terms of U and flow angle.	
Case 8663 M. Kussay J. Viegas C. Horstman			5	Flow angle at various sta- tions around cone	5	5	5	5	PT 5	1.0 × 10 ⁶ (based on δ ₀)	2.17	3D curved shock inter- action. Turbulence measurements limited to windward and leeward planes.	


PICTORIAL SUMMARY

Flow 8670. Data Evaluators: D. Peake (D. J. Cockrell). "Pointed Axisymmetric Bodies at Angle of Attack (Supersonic)."

Case Data Taker	Test Rig Geometry	$\frac{dp}{dx}$ or C_p	Number of Stations Measured							Pe	M_∞	Other Notes
			Mean Velocity	Turbulence Profiles				C_f				
				$\frac{U}{V}$ or $\frac{W}{W}$	$\frac{U^2}{V^2}$	$\frac{U^2}{W^2}$	$\frac{uv}{uv}$					
									Others			
Case 8671 W. Rainbird			1	-	-	-	-	Pres- ton to face pres- and sure oil flow on visual- ization length)	2.5 to 3.47 $\times 10^7$ (based on cone length)	1.8	Free-stream turbulence ~ 0.2%. Data at two angles of attack. Measurements at one axial station $x/L = 0.85$.	

PICTORIAL SUMMARY

Flow 8690. Data Evaluators: M. Rubesin and C. Horstman. "Non-lifting, Transonic Airfoil with Shock-Separation."

Case Data Taker	Test Rig Geometry	$\frac{dp}{dx}$ or C_p	Number of Stations Measured								Re	M_∞	Other Notes
			Mean Velocity	Turbulence Profiles				C_f					
				$\frac{U}{V}$ or $\frac{W}{W}$	$\frac{U^2}{V^2}$	$\frac{U^2}{W^2}$	$\frac{U^2}{W^2}$		Others				
Case 8691 J. McDevitt A. Okuno H. Seegmiller			7	7	7	-	7	Surface pres- sure	1.1 $\times 10^7$ (based on chord)	0.785	Circular arc airfoil with large separation.		

INTRODUCTION*

S. J. Kline



I. GOALS OF THE CONFERENCE

The Conference has three related goals:

1. To reach consensus in the research community on trustworthy data sets that can be used as input for modeling of turbulence in complex flows and as the basis for standard "trials" for checking output of computations.
2. The creation of a "data library" on magnetic tape. This library will hold the data selected as trustworthy in standard normalized form. The data will be computer-readable and widely accessible at a moderate fee.
3. Comparison of the output of current methods of computation for turbulent flows for a set of "basic test cases" covering a broad range of flows.

The first objective is the result of the effort of nearly 200 workers during 1979-80 culminating in the 1980 meeting of the Conference. The second objective is an ongoing project that is intended to continue for at least some years. The third objective will be the focus of the 1981 meeting of the Conference.

The word "conference" is somewhat misleading for this project, albeit no better term seems to be available. It is more accurate to think of the project as a several-year research effort by a considerable fraction of the research community aimed at establishing a more solid data base and clarifying both the situation in the data and the state-of-the-art in computation. Such a clarification should be of assistance to both users of computational methods and to the research community in perceiving more clearly what can now be done, and profitable roads to further advances.

It has been my privilege to coordinate these efforts as Chairman of the Organizing Committee. The experience has been educational. The purpose of this introduction is to share some of that education with the readers of this and subsequent volumes dealing with the Conference and the Data Library. It will perhaps be most useful to begin with a brief history. This is followed by a discussion of some current difficulties in turbulence research and fluids engineering. The third and final topic is a

*The sponsorship of the U. S. Air Force Office of Scientific Research under Contract F49620-80-C-0027 and the Industrial Affiliates of the Stanford Thermosciences Division is gratefully acknowledged. Suggestions by Gino Sovran, Brian Launder, Peter Bradshaw, Jim Johnston, Brian Cantwell, Geoffrey Lilley, and John Eaton on an earlier draft led to significant improvements and are also gratefully acknowledged.

description of the Conference and how it plans to ameliorate some of the difficulties described.

II. A BRIEF HISTORY

From the early years of this century until the late 1960s the problem of computing the averaged flow properties of turbulent shear layers was considered a classic unsolved problem. With the advent of wide accessibility to digital computers a number of individuals began to construct codes for solution of shear-layer problems. By the late 1960s, 25 methods had been generated, but there was no consensus that any of them were trustworthy. This lack of consensus was evidenced by the continued efforts to construct new methods, and by the funding of such efforts by governments in several countries.

In order to clarify this situation, a number of individuals, including D. E. Coles, M. V. Morkovin, W. C. Reynolds, G. Sovran and the writer, conceived of the idea of holding a meeting at which as many methods as possible would be tested against carefully standardized and trustworthy data. D. E. Coles, with E. Hirst, assumed the task of standardizing the data. The remainder of the group with assistance from D. J. Cockrell and many others, organized the meeting and coordinated efforts among the research groups. The results are recorded in the two-volume Proceedings of the 1968 AFOSR-IFP-Stanford Conference on Computation of Turbulent Boundary Layers.* The conference was highly structured and involved some unique organizational features that are described by Kline et al. (1969).

The most significant result of the 1968 conference, from the perspective of this volume, is that the result radically altered the common wisdom concerning the ability to compute turbulent shear layers. Before the 1968 Conference, the general belief was that no satisfactory method existed. The excellent report of the Evaluation Committee[†] in the 1968 Conference showed that seven methods were quite satisfactory, within well-defined limits, and that nine more had useful properties for some applications. Another nine were deemed inadequate, and have been for the most part abandoned. As a direct result of the 1968 Conference, the bulk of work on developing programs for attached, incompressible, turbulent boundary layers ceased, and the research community moved on to more complex problems.

*Available for purchase from the Thermosciences Division of the Department of Mechanical Engineering, Stanford University, CA 94305, USA. Price for both volumes, including mailing, \$17.50.

[†]Chaired by H. W. Emmons; see 1968 Proceedings for detail.

Within a few years following 1968, NASA (1969, 1972) organized similar conferences for compressible boundary layers and for free-shear layers. These conferences demonstrated reasonable simulation for compressible boundary layers and the far zones of free-shear layers, but indicated a lack of both data and simulation for the near zone of wakes, jets and mixing layers.

The 1968 Conference had also shown that available methods were successful for attached zones, but generally failed or required ad-hoc "fixes" in regions of detachment. All the methods presented in 1968 failed, qualitatively, in the prediction of a reattached free-shear-layer. Subsequent experiments, particularly that of Kim et al. (1979), have shown that such a reattached layer does not follow the type of correlation used by most methods in 1968. Moreover, all the successful methods in the 1968 "trials" employed the "law" of the wall, indicating a heavy dependence on data correlation and hence a lack of fundamental input in turbulence-closure modeling.

During the 1970s a considerable effort at improving numerical methods and turbulence-closure modeling has been carried out in many research centers around the world. The resulting computational methods have moved beyond the "prediction" of thin shear layers to the computation of entire flow fields, in some cases involving unsteadiness, appreciable zones of separated flow, and other complexities. By the late 1970s, we again find ourselves in a situation where many methods exist, but there is no consensus on what problems they will succeed or which methods have advantages for what flows. Since about 1976, in the words of the old cliché, we have been literally "confused on a higher level." As a result, a number of workers* who had been involved in the 1968 Conference again began to discuss what needed to be done. The 1980-81 Conference grew from those discussions.

Because the 1980-81 Conference concerns "Complex Turbulent Flows," that is, complete flow fields with such complications as shock/boundary-layer interactions, detachment, reattachment of shear layers, large zones of separation, blowing/suction, strong wall-curvature and other phenomena, the task is at once far more complex and far larger than in 1968. In order to understand these tasks, and hence the motivations for the structure of the Conference, it will be useful to give a brief overview of some current difficulties in turbulent flow research, both technical and institutional. One other historical remark is in order before discussion of these difficulties.

Preparatory work for the 1980-81 Conference during 1979 and 1980 has already shown that an important element of the common wisdom does not stand up to detailed examination. At the beginning of the work, every member of the Organizing Committee

*Particularly, M. V. Morkovin, P. Bradshaw, H. W. Emmons, W. C. Reynolds, and the writer.

was concerned with the question, "Are there enough trustworthy data sets of the needed type to form a basis for a conference of the 1968 type on complex turbulent flows?" The Committee believed that if as many as 10 or 15 such sets of data could be identified, a meeting would be well worthwhile. As data evaluations have accumulated, more than 50 cases* have been identified, and something like that many more exist but have not yet been fully evaluated. Moreover, as the work progressed and evaluation reports were circulated for review, workers in various parts of the world volunteered still further data sets; that process is still continuing.

This disclosure of data has obvious benefits, but has also overloaded the finite manpower available for entering the data onto magnetic tape checking, and providing the needed descriptions for each magnetic tape file. As a result, it is the intention of the writer, and Prof. B. J. Cantwell who is supervising the data library work, to continue inputs into the library after 1981 until the backlog of existing data is substantially "caught up". In this work priority has gone to recording the "basic test cases" for the 1981 meeting (see below). After September 1980 priorities were assigned primarily so that the data compilation on magnetic tape provided a balanced set of flow cases and secondarily on a first-come, first-served basis. Further details appear in the section on Organization of the Conference below.

III. SOME DIFFICULTIES IN TURBULENT FLOW RESEARCH

A. Technical Difficulties

1. The complexity and variety of flows

Thin shear layers form a relatively cohesive class of flows. Even when one restricts consideration to one-phase flow of a single, pure Newtonian substance, the totality of complex turbulent flow fields known to exist is quite diverse and far from cohesive. In early research, turbulence was implicitly considered as a single state or condition describable (hopefully) by a few simple models. As data from hot wires became widely available, largely after World War II, it became clear that turbulence is not a single state, but a complex of behaviors that is affected by many parameters. This complexity is well demonstrated by a list of the things that can, and sometimes do, affect the behavior of turbulence. Such a list, collected over some time by the author, is given in Table 1. All the effects of Table 1 are known to be appreciable in some instances; however, there is no guarantee the list is complete. (Every time the author has read the list at a technical meeting someone has commented on still another item--at least thus far.)

*In this volume a "flow" denotes a class of situations usually related to geometries. A "case" is one experimental realization of a flow, or a synthesis of realizations, amalgamated into a single "trial" for computations.

The complexity of turbulent flow fields is also exhibited by the variety of problems or classes of flows that have been considered by the Organizing Committee for the 1980-81 Conference. This list is exhibited as Table 2, which shows the categorization of flow problems for the Conference. These categories are neither unique nor entirely complete. They have been reorganized several times and updated as more information appeared.

Still a third indication of the complexity of turbulent flow fields is given by the variety of levels of modeling that are currently employed for simulation of turbulent flows in computer models. One taxonomy by Kline et al. (1978) is given in Table 3. Most current modeling is at level three in this taxonomy. Level 3 contains a number of subcategories of models from simple mean strain to "many-equation" models. Since both the mean flow and the turbulence can be modeled locally (zone by zone) or globally (uniformly), four combinations of global and local modeling exist. An excellent taxonomy of level 3 models is given by Reynolds (1968). However, the totality of modeling is not confined to level 3; appreciable current efforts exist at all five levels for some problems.

A fourth taxonomy of turbulent flows has been suggested in several papers by Bradshaw (1975). This taxonomy arranges flows according to the type of strains the flow undergoes; it is a very fruitful idea for organizing model assumptions for turbulence closure and suggesting experiments that will give needed model information. A number of such experiments have been provided by Prof. Bradshaw's group, and some are included in Table 2. However, examination of Table 1 shows that categorization via strain type does not include all the effects that we shall ultimately have to be able to model if we are to say that we have adequate models for the computer simulation of all kinds of complex turbulent flows. Table 1 provides a warning for those who would claim too much too early and thereby do disservice to the insightful and continuing efforts of the turbulence research community as a whole.

In 1980, we still lacked a viable method for relating the several taxonomies just discussed. We do not know what methods are best applied to a given flow configuration of Table 2, nor do we know what level of computation will ultimately be needed to model various kinds of strains and effects accurately. As long as that remains the case, we shall not have what is needed for engineering work in complex turbulent flow fields. It is hoped that the 1981 meeting of the Conference will begin to clarify the situation. More discussion on this point appears in the final section.

2. The measurement problem--accuracy control

Measurement of turbulence is inherently difficult. We have lacked instruments to measure some important quantities, for example vorticity, pressure fluctuations,

pressure-strain correlation, local temporary flow reversals,* and some components of the Reynolds stress tensor. Fixed hot-wire data taken at $X/D \leq 5$ behind bluff bodies and in the edges of wakes and jets are far more uncertain than has been generally recognized owing to very large fluctuations (see for example: evaluation by B. J. Cantwell, Flow 0410; Tutu and Chevray, 1975; Coles et al., 1978). Even where we have instruments, the uncertainty in many quantities is high, for example: the rate of dissipation of turbulent energy, Reynolds stresses and higher-order correlations. We have lacked adequate means for calibration of hot-wires for fluctuations (see Young and Kline, 1976). As a result, the N^{th} -order uncertainty (which is discussed in a paper below by R. J. Moffat) has remained relatively high for turbulence data of nearly every kind. It is salutary in this connection to read the remarks of J. B. Jones concerning comparisons of turbulence data in the inlet zone of smooth, round pipe in turbulent Flow 0130, and of J. H. Ferziger on strained homogeneous fields, Flow 0370.

The neophyte worker, moreover, is faced with a lack of unified literature describing instrument techniques. The last attempt at complete coverage of fluid instrumentation seems to be that of R. C. Dean, Jr. (1952). Dean's work was excellent for its time, but is badly in need of updating. Publishers have been unwilling to underwrite or even undertake this task, and no institution seems to assume the responsibility for seeing that such needful technical tasks are carried out. Many engineering schools have never had, or have abandoned, advanced courses in thermal and flow measurements that would provide the student with solid preparation for careful data-taking and reduction.[†] The result is that all too often our data sets are generated by an untrained research-internee supervised solely by a single overworked and over-committed faculty person.

The only known method for reliable control of accuracy is via uncertainty analysis of experiments.[‡] However, the results of the data evaluations show that uncertainty analysis is still not used by many workers. The experienced worker, in a known

*This problem is coming under control via laser anemometry and recent instrument innovations by Westphal et al. (1980) and Owen and Johnston (1980), but there are as yet few data.

[†]The writer is aware of only two sequences of such courses at the graduate level --both at Stanford. He would welcome knowledge of others, and has several times so stated in public meetings.

[‡]The writer is a biased observer on this topic, having written a base paper in the field. However, any other approach leaves significant questions unanswered and fails to provide numerical criteria by which comparisons between data sets or between data and computations can be made quantitative. Similar remarks have been made independently by D. A. Humphreys and B. van den Berg in the evaluation of data for three-dimensional turbulent boundary layers, Flow 0250.

situation, can perhaps produce trustworthy data without formal uncertainty analysis. For a neophyte or a person designing an experiment of a really new type, however, it would seem critical to the production of trustworthy data. For this reason, a separate portion paper on experimental uncertainty has been prepared by R. J. Moffat. Looking to the future, we are fortunate that this paper is a major contribution to several long-standing conceptual problems and also provides a means by which the formal details of uncertainty analysis are made trivial for any experiment employing data reduction in a computer. This paper is strongly recommended to any individual intending to produce data for possible future "trials" of computation or input to turbulence modeling.

B. Institutional Difficulties

No one in the turbulence research community needs to be told that the number of papers has grown in recent years and that with growth has come a compression of both presentation times in meetings and the length of papers acceptable to many journals. This compression of presentation times and paper lengths has direct impact on the data base available for "trials" of computations.

The length requirement of papers in most journals usually prevents discussion of experimental difficulties in adequate detail and in most cases suppresses full publication of data. This means that data must often be read from too-small graphs, and details are sometimes omitted. As a result, data evaluators for the Conference have often had to refer to the originators of data to complete the necessary files. Such a task is not insuperable for a person focusing on evaluation of a single class of flows, but is normally not feasible for computers* who might want to test models against a variety of flows. This need to resort to the originators of data is one reason why a collective effort of the research community has been needed in order to bring the data base into usable form. Moreover, without such a system as the data library now being established, the personal knowledge and files of the individual researchers would have been lost to accurate recapture, over time.

The now-common ten-minute presentation time effectively prevents fully carrying through discussion on points of disagreement in technical meetings. Individual workers may carry out such discussions, but they are no longer part of the publicly accessible record. As Ziman (1968) told us at book length some time ago, what one of us believes is not "science." Information and hypotheses become "science" only when they are subjected to full public discussion and become accepted by the large majority of workers in the relevant field.

*The word "computer" denotes a person doing numerical fluid dynamics, as opposed to a "computer," which denotes hardware for doing numerical calculations.

Still another institutional difficulty has arisen from what one might characterize as the "ten-thousand-card program." Such large programs have not been accessible to review in the older sense of "review" for publication. The typical reviewer can devote a matter of hours, or perhaps days, to a given review. This is grossly insufficient to unravel a large program, even if a printout of the code is provided. This problem compounds with the difficulties of the data base already cited. The usual test for the output of computation has of necessity been comparison with one or more sets of data. Even this is sometimes foregone, but let us assume for this discussion that comparison with a few sets of data is given in a paper that is sent to a reviewer. What is the position of this reviewer? About all he (or she) can do in "reviewing" is to examine the general statements provided about the code and see whether agreement with the data is obtained. It is nearly impossible for the reviewer to penetrate to the implications of the inevitable assumptions made in the turbulence closure and numerics. He (or she) cannot take the time to unravel the code. Moreover, the 1968 experience showed clearly that comparison with as few as three data sets has little meaning in verifying the utility of codes.* Even for the restricted class of flows studied in the 1968 meeting, it became clear that the 16 mandatory flows constituted something like a "minimum" test of viability. Moreover, since the computer rarely has the time to assess data sets, it is altogether possible that untrustworthy data will be employed; see remarks of Owen and Johnson (1980).

This combination of difficulties was known to the Organizing Committee for the Conference in principle when the planning began in 1978. Experience gained since that time has tended in nearly every instance to reinforce the significance of these problems. Data that evaluations showed were wrong by half an order of magnitude have been used as input to models in some cases. Questions and requests for further information have had to be referred by data evaluators to the originators of the data in many instances where the published record was not sufficient. Many deficiencies in both planning and detailed execution of experiments have come to light that could have been avoided had the experience available in the research community on provision for accuracy and on the difficulties of laboratory control of fluid flow been brought to bear in a timely manner.

The Conference was designed to ameliorate some of these difficulties, and thus hopefully to improve matters in the future. The steps taken are described in the next section.

*This difficulty is also revealed and emphasized by the questions of managing engineers responsible for utilizing computational codes. In a number of instances, such managers have expressed to the writer perplexity concerning how to judge codes offered to them by consulting firms which create numerical codes.

IV. ORGANIZATION OF THE CONFERENCE

Some, but not all, of the difficulties recited in the previous section could be significantly reduced by three accomplishments:

1. Provision of a trustworthy data base backed by consensus of the research community on its reliability and on its possible difficulties. To be fully effective, this data base needs to be computer-readable and widely accessible.
2. Clarification of data needs for constructing and checking computer models including: types of new or improved data required; data standards; the methodology for quantitative comparison of data and computation accounting for residual uncertainty in the data. To be fully effective, this knowledge needs to be implemented via thorough review processes.
3. The public comparison of the standard "trials" with at least a large number of different kinds of computer simulations in order to test several questions:
 - a. Does an adequate "closure" model exist that can be utilized in feasible running times, or, on the contrary, will it be necessary for engineering computation to utilize distinct "fine-tuned" models that are "tailored" to specific problems or to classes of problems in order to obtain reliable results of engineering accuracy?
 - b. What kinds of turbulence-closure models and numerics are more/less successful, and in what classes of flows?
 - c. What are the limits, if any, for successful computer simulation of complex turbulent flows in one-phase Newtonian substances in 1981?

Initially, the Organizing Committee, reasoning from the 1968 experience, thought that it might be possible to establish the data base in a suitable closed form. As work progressed, it became clear that both improved data and data of new kinds are still needed. As a result, the concept of a data library as a separate, ongoing function evolved. Agreements have been made with two organizations in Europe to hold the tapes produced for the data library. The addresses of these organizations and cost information are given in the Data Library paper, page 58. Similar arrangements in other parts of the world will be considered. However, all inquiries about the "Tape," including its acquisition, should be sent to Prof. B. J. Cantwell, Dept. of Aeronautics and Astronautics, Stanford University, Stanford, CA 94305.

Procedures were instituted to insure against the inclusion of data on review by only one worker, that is, to create consensus on the data base. Each data evaluation was reviewed by a committee of three to five other workers,* and in most instances this resulted in significant revisions and improvements. In addition, as each final

* A few evaluations were received too late for prior review, and were instead discussed in the 1980 meeting.

evaluation report and its summary, plus a "specification for computations," was received at Stanford, it was sent to at least two other attendants of the 1980 meeting for review and possible comment. As in the 1968 Conference, the attendants were asked in advance to agree to assist with the work as a condition for attendance, and almost without exception that agreement has been honored to the extent requested by the Organizing Committee. Also, as in 1968, procedures to drive discussion to full completion were employed; such completion need not imply agreement; disagreements were also focused and recorded as the basis for further investigations. These meeting procedures were recorded in an advice to Session Chairmen and are bound into this volume as an Appendix to this paper.

In addition to the procedures of the preceding paragraph, one member of the Organizing Committee acted as a liaison person for each flow evaluation in order to coordinate information and assist in formation of standards. Initially, the Organizing Committee was not able to provide detailed standards for the data evaluators, since the character of the various flows is so diverse. Only general guidance was given the data evaluators. The most critical task, that of formulating a data base, is thus the result of the efforts of the data evaluators. Their task was made even more difficult by the fact that the shape of the work process was evolved as information accumulated, and the evaluators were only later asked to formulate summaries (for publication) and specifications (for trial computations). The field owes a considerable debt to the arduous and insightful work of these experts on the various flow classes.

These procedures do not guarantee infallibility; science as a process is not infallible. When it comes to establishing matters of truth, however, the full public discussion of science is much better than any other known method. The public discussion of science is the best we have, and it is at least an order of magnitude better than the assessment by individual data takers with respect to their own output. Even a cursory review of the full data evaluations for this Conference and the comments on them shows this clearly. For this reason and also to make them available to future "data takers," the full evaluation reports are being held in file at Stanford and can be obtained without charge by writing the Thermosciences Division, Department of Mechanical Engineering, Stanford, CA, USA 94305. Some will be published in serials accepting long articles or condensed for journals; one already has been (Eaton and Johnston, 1980); another (Launder and Rodi) has been accepted for publication.

A different lesson also emerged from study of the data evaluations as they were formulated over time. Initially, the common wisdom suggested that tests of computations should be concerned with detailed comparison with single flow fields of high complexity, for example the data of Cantwell and Coles (Flow 0410). However, it became clear from discussions with computers and the results of the data evaluators that at least two other types of comparisons are important. The first is limits on

physical behavior, for example: the cessation of turbulence production when a flow passes through a lower critical Reynolds number (Flow 0280); or the reduction to similarity solutions for asymptotic flows, as in a mixing layer or tube flow (Flows 0110, 0130, 0260). Finally, the use of composites of data on first-order results over a wide range of parameters is an important check, for two reasons. First, testing over a range verifies turbulence models independently from "tuning" processes involved in setting up particular flows. Second, the use of composite data incurs estimates of N^{th} -order uncertainty in the sense defined in the paper in this volume by R. J. Moffat, and thus avoids the difficulties of "one-lab" experiments. These three kinds of checks are all in addition to checks on mathematical consistency as emphasized by a number of workers, for example Coleman Donaldson and John Lumley.

As in 1968, the Evaluation Committee for study of the comparison of the data with the computations will be chaired by Prof. H. W. Emmons of Harvard University. After input from the 1980 meeting and the Organizing Committee, the methods of assessment are the responsibility of Prof. Emmons and his committee. They are left so in order to provide assessment independent from the organizers, data takers, and computers, and because they cannot be properly realized until the results are themselves in hand.

A problem that was foreseen but not initially understood was the question of how to review codes. In 1968 every program utilized was checked by graduate students at Stanford to insure completeness and repeatability. Given the size of current codes and the time required to adapt them to specific problems, such a procedure is not feasible. Moreover, the basic problem of how to "review" codes needed some form of answer. The Organizing Committee dealt with this problem by designing a questionnaire that we hope will assist in this problem. The questionnaire will appear in the Proceedings for the 1981 meeting. It is worth noting that it took six revisions to create this questionnaire. It was only after it was found that new language had to be invented to properly describe the hierarchical structure often used in computations that an apparently usable questionnaire was derived. The Organizing Committee hopes that the questionnaire will assist in reviews of codes by journals and industrial personnel.

These steps will hopefully relieve some of the problems that currently exist in computational fluid dynamics. However, several problems mentioned in the prior section lie outside the scope of work on the Conference and remain unanswered. In particular, the lack of adequate description of experimental uncertainty and the lack of experimental control it implies remain continuing problems. They are well evidenced by the data scatter in the evaluations.

Another problem that lies beyond the scope of the Conference is the need for an adequate treatise on experimental methods that will assist the data-taker in avoiding known pitfalls in mensuration.

Still another remaining problem is the matter of oversight in what are intended to be record experiments as the basis for possible future "trials" of computer output. The nature of data needed for this use is significantly different from the needs for past uses of data. These new needs have been little discussed and hence are the subject of a separate paper in this volume. These new needs, the lack of an up-to-date treatise and the paucity of formal courses in aerodynamic measurements, all speak to the need for increased oversight in planning experiments beyond faculty persons working alone (or with untrained assistants) who are contractually obligated to produce results on a short time-table. How this may be accomplished is not clear at this time. A start in this direction has recently been made by two sets of monitors for government bureaus,* and these examples may serve as at least a partial model.

Finally, the 1980-81 Conference will differ from the 1968 Conference in an important regard that needs to be clearly stated. In 1968 the timing was fortunate. The state of the art was such that the 1968 Conference essentially finished one stage of work and led to another by showing that the problem was essentially solved. No such outcome can be expected from the 1980-81 Conference. The data will not be complete. More flows will need to be added to the library. Data are needed on additional classes of flows; improved data are needed in many. Nor is it reasonable to expect that computational methods will be finished. Computational fluid dynamics is a young and rapidly improving field. The most that can be expected is the beginning of a broad, trustworthy data base and a snapshot of the state of the art that will aid assessments of utility for industrial "consumers" of programs and provide us with a better guide to profitable avenues for further researches. Finally, it needs to be remembered that the class of flows covered in the current data library, and hence the basic test cases for the 1981 meeting, are not yet universal, as a comparison of Tables 1 and 2 shows. It must follow that even a successful model for a large number of basic test cases will not yet be verified as "universal." Moreover, an almost unblemished record of past failures in extrapolation of turbulence models to new classes of flows should warn us against easy assumptions concerning generality.

*M. Rubesin and J. Marvin of NASA-Ames and J. McCroskey and L. W. Carr of Air Mobility Command, Moffett Field, CA.

TABLE 1
SOME EFFECTS THAT CAN INFLUENCE CHARACTERISTICS OF TURBULENCE

A. Nature of Fluid

1. Viscosity (i.e., Reynolds number)
2. Constitutive (e.g., polymers)
3. Energy release (e.g., chemical reactions)
4. Surface tension (e.g., oil-slick calming)
5. Cryogenic effects
6. Multiphase fluid (several subcases)

B. Nature of Outer Flow

7. $\partial p / \partial x$, $\partial p / \partial z$
8. Free-stream fluctuations (noise, turbulence)
9. High Mach number (hypersonic)

C. Wall Effects

10. Blowing/suction
11. Roughness
12. Compliant walls
13. Moving wall

D. Body Forces

14. Coriolis
15. Centrifugal
16. Density gradients
17. EHD, MHD
18. Wall curvature: convex, concave (could be placed in type E)
19. Curvature in free-shear layers (could be placed in type E)

E. Strain and Interaction Effects

20. Shear rate and type
21. Dilatation; transverse stretching/compression
22. Turbulence-turbulence interactions
23. Downstream effects of transitions

TABLE 2
FLOW NUMBERS AND CASES*

("Flow" denotes a geometry or class of related geometries; "Case" denotes a recommended realization of a given geometry.)

Flow Number	Description	Evaluator
<u>Group I -- Numerical Checks</u>		
	Potential flow in 90° corner	
	Howarth flow (solution by Briley)	
	Axisymmetric jet flow (solution in Rosenhead)	
	Flow in square cavity with a moving lid	
<u>Group IIa -- Flow Category - Incompressible</u>		
0110	Corner flow (secondary flow of the second kind) .	F.B. Gessner
0130	Entry zone of round tube	J.B. Jones
0140	Diffuser flows (unseparated)	R. Simpson
0150	Two-dimensional channel flow with periodic perturbations	M. Acharya
0210	Effect of free-stream turbulence on boundary layers	P. Bradshaw
0230	Boundary-layer flows with streamwise curvature .	T.W. Simon/S. Honami
0240	Turbulent boundary layers with suction or blowing	L.C. Squire
0250	Three-dimensional turbulent boundary layers	D.A. Humphreys/ B. van den Berg
0260	Turbulent wall jet	B.E. Launder/W. Rodi
0280	Relaminarizing flows	K.R. Sreenivasan
0290	Laminar-turbulent transition	E. Reshotko
0310	Planar mixing layer	S. Birch
0330	Free shear layer with streamwise curvature . . .	P. Bradshaw
0340	Flows with swirl	A.P. Morse
0350	Ship wakes	V.C. Patel
0360	Wakes of round bodies	V.C. Patel
0370	Homogeneous turbulent flows	J.H. Ferziger
0380	Wakes of two-dimensional bodies	V.C. Patel
0390	Axisymmetric boundary layer with strong streamwise and transverse curvature	V.C. Patel
0410	Evaluation of bluff-body, near-wake flows . . .	B. Cantwell
0420	Backward-facing step flow	J.K. Eaton/J.P. Johnston
0430	Diffuser flow (separated)	R. Simpson
0440	Two-dimensional stalled airfoil	A.J. Wadcock
0470	Flow over the trailing edge of blades and airfoils	P. Drescher
0510	Turbulent secondary flows of the first kind . . .	R.B. Dean
0610	Attached boundary layers - ('68 Conference) . . .	D.E. Coles

(Table 2 cont.)

*As a result of the 1980 Meeting a number of changes were made in the Test Cases. The original form is preserved here as part of the Proceedings. Please see comments on each case and the Proceedings of the 1981 Meeting for the final list of Test Cases used in the 1981 Meeting.

Table 2 cont.

Flow Number	Description	Evaluator
<u>Group IIb -- Flow Category - Compressible</u>		
8100	Supersonic flow over a flat plate (insulated wall)	M.W. Rubesin/ C.C. Horstman
8200	Supersonic flow over a flat plate (cooled wall) .	MWR/CCH
8300	Turbulent boundary layers with suction or blowing at supersonic speeds	L.C. Squire
8310	Variation in C_f/C_{f0} for blowing/suction with Mach Number	L.C. Squire
8400	Boundary layers in an adverse pressure gradient in an axisymmetric internal flow	MWR/CCH
8410	Boundary layers in an adverse pressure gradient in 2-dimensional flow	MWR/CCH
8500	Compressibility effects on free shear layers . .	P. Bradshaw
8600	Impinged normal shock wave-boundary layer interaction at transonic speeds	MWR/CCH
8610	Transonic flow over a bump	MWR/CCH
8620	Transonic airfoils	R.E. Melnik
8630	Compressible flow over deflected surfaces . . .	MWR/CCH
8640	Compressible flow over compression corner with reattaching planar shear layer	MWR/CCH
8650	Axisymmetric shock impingement (supersonic) . .	MWR/CCH
8660	Three-dimensional shock impingement (supersonic).	MWR/CCH
8670	Pointed axisymmetric bodies at angle of attack (supersonic)	D. Peake (D.J. Cockrell)
8680	Axisymmetric near wake (supersonic)	A. Favre
8690	Nonlifting, transonic airfoil with shock separation	MWR/CCH
9000	Flows with buoyancy forces	J.C. Wyngard

Group III -- Some Flows Warranting Further Study

1. Full details of several blunt bodies including wakes: (buildings, bumps, ...)
2. Radial wall jet flows
3. Wall jets impinging at angles to surface
4. Unsteady mean flows (report presented by L. Carr)
5. "Momentum-less" wakes
6. Jets in cross and counter flow
7. Two-dimensional separated flows (airfoil flaps)
8. "Low" Reynolds number boundary layers
9. Rough wall cases
10. Airfoil cases other than transonic

Comments on Group III Flows

Data on several flows in this group were called to the attention of the Organizing Committee too late to provide evaluation or a suitable "Evaluator" was not found for most of these flows. Hence they remain for future possible "evaluation" and inclusion in the data library.

(Table 2 cont.)

Table 2 cont.

TEST CASE NUMBERS

Conference Reference Number	Library Case Number	Description	Data Evaluator	Data Taker
<u>Group A - Entry Cases: Predictive</u>				
P1	0113	Asymmetric flow in square duct	Org. Comm.	Description by J.Eaton
P2 Central Case with Case E2	0422	Backward-facing step: variable opposite-wall angle	"	"
P3	0423	Backward-facing step: turned flow passage	"	"
P4	0424	Backward-facing step: variable area ratio	"	Description by S.Kline
<u>Group B.I - Simple Cases: Incompressible</u>				
S1	0612	On the turbulent friction layer for rising pressure	D.Coles	K.Wieghardt
S2	0141	Increasingly adverse pressure gradient flow	R.Simpson	A.Samuel/ P.Joubert
S8	0371	Isotropic turbulence	J.Ferziger	G.Comte-Bellot/ S.Corrain
S9	0372A, B,C	Rotating turbulence	"	R.Wigeland/ H.Nagib
S10	0373A, B,C,D 0373E	Return to isotropy "	" "	M.Uberoi H.Tucker/ A.Reynolds
S11	0374A 0374B	Plane strain "	" "	A.Townsend H.Tucker/ A.Reynolds
S12	0375A, B,C,D,E	Axisymmetric strain	"	J.Tan-atichat
S13	0376A,B	Sheared turbulence	"	F.Champagne et al. V.Harris et al.

(Table 2 cont.)

Table 2 cont.

Conference Reference Number	Library Case Number	Description	Data Evaluator	Data Taker
<u>Group B.II - Simple Cases: Compressible</u>				
S3	8101	Correlation: C_f/C_{fo} versus M -- insulated plate	M.Rubessin/ C.Horstman	Various
S4	8201	Correlation: C_f/C_{fo} versus T_w/T_{aw} -- constant M	M.Rubessin/ C.Horstman	Various
S5	8403	Pressure gradient and Reynolds number effects on compressible turbulent boundary layers in supersonic flow	M.Rubessin/ C.Horstman (G.Lilley)	M.Kussoy/ C.Horstman/ M.Acharya
S6	8411	Boundary layer in adverse pressure gradient	M.Rubessin/ C.Horstman (G.Lilley)	F.Zwarts
S7	8501	Compressibility effects on free-shear layers	P.Bradshaw	Various
S14	8632	Turbulent boundary-layer/expansion interaction at supersonic speed	M.Rubessin/ C.Horstman	J.Dussauge/ J.Caviglio
<u>Group C - Entry Cases: Incompressible</u>				
E1 Central Case	0331	The turbulence structure of a highly curved mixing layer	P.Bradshaw	I.Castro P.Bradshaw
E2 Central Case with Case P2	0421	Flow over a backward-facing step	J.Eaton/ J.Johnston	J.Kim/S.Kline/ J.Johnston
E3	0142	Six-degree conical diffuser flow, low-core turbulence	R.Simpson	R.Pozzorini
E4	0143	Six-degree conical diffuser flow high-core turbulence	R.Simpson	R.Pozzorini
E5	0211	Effect of free-stream turbulence	P.Bradshaw	P.Hancock/ P.Bradshaw
E6	0231	Turb. boundary layers on surfaces of mild longitudinal curvature (convex)	T.Simon/ S.Honami	P.Hoffman/ P.Bradshaw
E7	0232	Turb. boundary layers on surfaces of mild longitudinal curvature (concave)	T.Simon/ S.Honami	P.Hoffman/ P.Bradshaw
E8	0233	Turb. boundary layer on a convex, curved surface	T.Simon/ S.Honami	J.Gillis/ J.Johnston
E9	0241	Zero pressure gradient, constant, injection	L.Squire	P.Andersen/ W.Kays/R.Moffat

(Table 2 cont.)

Table 2 cont.

Conference Reference Number	Library Case Number	Description	Data Evaluator	Data Taker
E10	0242	Adverse pressure gradient with constant suction	L.Squire	P.Andersen/ W.Kays/R.Moffat
E11	0244	Zero pressure gradient with constant (high) suction	L.Squire	A.Favre et al.
E12	0411	A flying hot-wire study of the turbulent near-wake of a circular cylinder at a Reynolds number of 140,000	B.Cantwell	B.Cantwell/ D.Coles
E13	0441	Flying hot-wire study of 2-dimensional turbulent separation of an NACA 4412 airfoil at maximum lift	A.Wadcock	A.Wadcock/ D.Coles
E14	0511	Turbulent flow in an idealized wing-body junction	R.B.Dean	I.Shabaka
E15	0512	Turbulent flow in a curved duct of square cross-section	R.B.Dean	J.Humphrey
E22A	0111	Developing flow in a square duct	F.Gessner	J.Po/E.Lund F.Gessner
E22B	0112	Secondary currents in the turbulent flow through a straight conduit	F.Gessner	J.Hinze
E23	0261	Turbulent wall jet data (equilibrium wall jet)	B.Launder/W.Rodi	Various
E24	0263	Turbulent wall jet data (self-preserving on log-spiral)	B.Launder/ W.Rodi	D.Guitton/ B.Newman
E25	0264	Turbulent wall jet data (3-dimensional on plane surface)	B.Launder/W.Rodi	Various
E26A	0281	Relaminarizing boundary layer	K.Sreenivasan	R.Simpson/ D.Wallace
E26B	0282	Relaminarizing tube flow	K.Sreenivasan	J.Laufer/
E27	0311	Planar mixing layer developing from turbulent wall boundary layers	S.Birch	Various
E28	0361	The turbulent wake of a body of revolution	V.C.Patel	R.Chevray
E29	0381	Measurements of interacting turbulent shear layers in the near wake of an airfoil (symmetric)	V.C.Patel	J.Andreopoulos

(Table 2 cont.)

Table 2 cont.

Conference Reference Number	Library Case Number	Description	Data Evaluator	Data Taker
E30	0382	Measurements of interacting turbulent shear layers in the near wake of an airfoil (asymmetric)	V.C.Patel	J.Andreopoulos
E31	0471	Trailing edge flows at high Reynolds number	P.Drescher	P.Viswanath et al.
E40	0431	Separating adverse pressure gradient flow	R.Sirpson	R.Simpson et al.
<u>Group D - Entry Cases: Compressible</u>				
E16 Central Case	8621	Aerofoil RAE 2822--pressure distribution, boundary layer and wake measurements	R.Meinik	P.Cook et al.
E17 Central Case	8631	Attached and separated compression corner flow fields in high Reynolds number supersonic flow	M.Rubesin/ C.Horstman	G.Settles et al.
E18	8301	Favorable pressure gradient at supersonic speeds with injection	L.Squire	G.Thomas
E19	8661	Three-dimensional swept shock/turbulent boundary layer interaction	M.Rubesin/ C.Horstman	D.Peake
E20	8691	Non-lifting transonic airfoil, shock-separated flow	M.Rubesin/ C.Horstman	J.McDevitt et al.
E32	8601	Normal shock wave/turb. boundary-layer interaction at transonic speeds	M.Rubesin/ C.Horstman	G.Mateer et al.
E33	8611	Transonic turbulent boundary layer separation on an axisymmetric bump	M.Rubesin/ C.Horstman	W.Bachalo/ D.Johnson
E34	8612	Transonic flow over two-dimensional bump, $M = 1.37$	M.Rubesin/ C.Horstman	J.Delery P.Le Dizet
E35	8623	Supercritical airfoil boundary layer measurements	R.Meinik	F.Spaid/ L.Stivers
E36	8651	Hypersonic shock wave turbulent boundary-layer interaction--with and without separation	M.Rubesin/ C.Horstman	M.Kussoy/ C.Horstman
E37	8663	Investigation of three-dimensional shock separated turb. boundary layer	M.Rubesin/ C.Horstman	M.Kussoy et al.
E38	8671	Pointed axisymmetric bodies at angle of attack (supersonic)	D.Peake	W.Rainbird
E39	8641	Reattaching planar free-shear layer (supersonic)	M.Rubesin/ C.Horstman	G.Settles et al.

TABLE 3
TAXONOMY FOR MODELING OF TURBULENT FLOWS WITH A VARIETY OF LEVELS

Level	Examples	Comments
1. Nondimensional correlations of data.	f versus Re for pipe flow; C_p^* as a function of geometry for straight-walled diffusers; C_p versus Re for flow normal to cylinders, over spheres, etc.	Slow, expensive, accretive; high reliability within carefully defined class of flow situation.
2. Zonal models.	(a) Conventional boundary-layer theory for attached flows, matched to external flow via δ^* . (b) Hyper-boundary-layer viscid-inviscid zonal models, for strong interactions such as detaching flows.	The major class of engineering solutions currently. Advancing rapidly, good promise for many more classes of practical solutions and design tools by 1988. Computing costs well within engineering feasibility. A number of research groups currently active.
3. Numerical solutions for Reynolds equations (time-averaged Navier-Stokes equations).	A number of codes now exist. Can be used for part of flow and matched to external flow like 2b or over entire field.	Also advancing rapidly. To date methods don't appear to extrapolate well; as in Class 2 need to be fitted to specific classes of flows.
4. Large eddy simulation with subgrid closure.	Current research--few solutions yet available.	Computing costs still relatively high. Outcome highly dependent on further advances in large computers.
5. Complete solutions to Navier-Stokes equations.	(a) Analytic. A dozen or so closed solutions (for very simple cases) exist as the results of 150 years' work. (b) Numerical. Only the very simplest cases, which have few applications, so far accessible via numerical methods.	New solutions likely to be scarce, slow; restricted to laminar flows. All but these simplest cases at very modest Reynolds numbers still too large for existing computers; progress dependent on rate of growth of computers and decrease in computing costs.

REFERENCES

- Bradshaw, P., (1975). "Complex Turbulent Flows, JFE, 97, p. 146.
- Coles, D. E., and E. A. Hirst, (1969). "Proceedings Computation of Turbulent Boundary Layers--1968 AFOSR-IFP-Stanford Conference," Vol. II. Compiled Data.
- Coles, D. E., B. J. Cantwell, and A. J. Wadcock, (1978). "The Flying Hot Wire and Related Instrumentation," NASA-CR 3066.
- Dean, R. C., Jr., (ed.), 1952. Aerodynamics Measurement, MIT Press, (out of print).
- Eaton, J. K., and J. P. Johnston, (1980). "A Review of Research on Subsonic Turbulent Flow Reattachment," AIAA (Preprint) 80-1438.
- Kim, J., S. J. Kline, and J. P. Johnston, (1979). "Investigation of a Reattaching Turbulent Shear Layer: Flow over a Backward-Facing Step," ASME Symposium on Flow in Primary Non-Rotating Passages in Turbomachines.
- Kline, S. J., M. V. Morkovin, G. Sovran, and D. J. Cockrell, (1969). "Proceedings Computation of Turbulent Boundary Layers--1968 AFOSR-IFP-Stanford Conference," Vol. I., Methods, Predictions, Evaluations and Flow Structure.
- Kline, S. J., M. V. Morkovin, and H. K. Moffat, (1969). "Report on the 1968 AFOSR-IFP-Stanford Conference on Computation of Turbulent Boundary Layers," JFM 36, pp. 481-484.
- Kline, S. J., J. H. Ferziger, and J. P. Johnston, (1978). Opinion: "The Calculation of Turbulent Shear Flows: Status and Ten-Year Outlook," JFE 100, 1, pp. 3-5.
- NASA, (1969). "Compressible Turbulent Boundary Layers," NASA-SP-216.
- NASA, (1972). Free Turbulent Shear Flows, Vol. 5. Conference Proceedings, NASA SP-321.
- Owen, F. K., and D. A. Johnson, (1980). "Separated Skin Friction Measurement -- Source of Error, an Assessment and Elimination," AIAA-80-1409.
- Reynolds, W. C., (1968). "A Morphology of Prediction Methods," Proceedings of the 1968 AFOSR-IFP-Stanford Conference on Computation of Turbulent Boundary Layers, Vol. I, pp. 1-15.
- Tutu, N., and R. Chevray, (1975). "Cross-Wire Anemometry in High Intensity Turbulence," JFM, 71, pp. 785-800.
- Westphal, R. V., J. K. Eaton, and J. P. Johnston, (1980). "A New Probe for Measurement of Velocity and Wall Shear Stress in Unsteady, Reversing Flow," 1980 Winter Annual Meeting, ASME Symposium Proc., "Measurement and Heat Transfer Processes in Recirculating Flows," HTD-13.
- Young, M. F., and S. J. Kline, (1976). "Calibration of Hot Wires and Hot Films for Velocity Fluctuations," Report TMC-3, Dept. of Mechanical Engineering, Stanford University.
- Zizian, J., (1968). Public Knowledge: The Social Dimensions of Science, Cambridge University Press.

Appendix

THE OPERATION OF SESSIONS--THE ROLE OF EVALUATORS, SESSION CHAIRMEN AND TECHNICAL RECORDERS: 1980 Meeting on Data

Goals of Sessions:

1. Reach consensus on flows within the Basic Test Cases and as many other flows as time and available evaluations allow.
2. Complete discussions by the end of the Meeting.

Each flow case will be presented by the Data Evaluator. The Evaluator will be asked to cover the following points:

- (i) Selection criteria
- (ii) Flows selected
- (iii) Specific computations (zones and output) for each selected flow
- (iv) Advices for future data takers: Data needs, cautions, checks, etc.

A number of attendees, in addition to the review committee, will have been asked to study each evaluation and prepare comments. These comments when offered will take priority in discussions. (Review Committee comments will have already been taken into account by the Data Evaluators.)

Each session will be about 90 minutes in length and will typically cover three flows. All sessions will be recorded on tape. Each session will have two "Technical Recorders" to assist the Chairman.

In the evening following a given session, a committee on that session will convene to complete the discussion and clarify points under question. Normally this committee will include the Session Chairman, Evaluator, Review Committee Chairman, Technical Recorders, and a few others. The task of this committee will be to produce a succinct, clear record of the significant points of the session--in general, this will not be a verbatim transcript.

The tapes will not be transcribed; this is an enormous but seldom valuable task. Rather, the operators of the tape machines will be instructed to create a footage log showing where various persons speak in order to provide access for checking remarks where needed.

Given these resources, the Chairman's task will be to moderate the discussion and be sure that points are completed and accurately reduced to writing by the Recorders. It is nearly always important in this process to keep asking questions of the persons expressing positions until full clarity is reached, and then have the recorder read back the statement for concurrence by the worker concerned; the process should be iterated to closure. As noted above in this packet, consensus as used herein implies not only agreements, but also sharply focused disagreements with the name(s) of each individual holding a given position stated. The iterative process just mentioned is particularly important in registering and focusing disagreements about specific ideas or matters of fact.

The Conference will provide sufficient secretarial assistance so that the typed version of the output from the committee on each session can be produced and posted by the end of lunch on the following day. Individuals will be asked to approve (by initialing) or alternatively comment in writing to the Session Chairman by the evening of that day.

EXPERIMENTAL DATA NEEDS FOR COMPUTATIONAL FLUID

DYNAMICS--A POSITION PAPER*

P. Bradshaw, B. J. Cantwell, J. H. Ferziger, and S. J. Kline,
with Comments on Compressible Flows
by M. Rubesin and C. Horstman



Joel Ferziger

Peter Bradshaw

1. INTRODUCTION

This position paper is intended to provide a starting point for clearer delineation of the interaction between experimental data and computational fluid dynamics. This interaction is central to the present Conference and to effective progress in both experimental and computational fluid dynamics. At the same time, the interaction appears to have been neglected in the recent past, compared to efforts in each area separately. For this reason, a draft of this paper was distributed for comment to a number of attendees prior to the 1980 meeting of the Conference, and time was allocated to its discussion during the meeting.

2. BACKGROUND--NEEDS IN GENERAL

For the past decade a brisk discussion, has continued on the ultimate roles of experiments and computation in fluid dynamics. Certain general conclusions can now be drawn on the likely roles of experimental data and computation for at least the remainder of the century.

There seems to be little question that a role for both computations and experiments will exist. Computation has become, and will doubtless remain, a powerful "third force" in fluid mechanics, strongly augmenting the older methods of experiment and analytical mathematics.

On the other hand, even optimistic estimates of the growth in size and reduction in cost/flop[†] of large digital computers make it unlikely that the complete governing differential equations of viscous flow, undamaged by any kind of averaging procedure, will be solved in feasible machine times for complex turbulent flows at high Reynolds numbers in this century. Since engineering applications usually involve complex turbulent flows at high Reynolds numbers, experimental data will still be needed for at least four purposes: (i) as an engineering tool for the development and testing of hardware; (ii) as input for "modeling" of approximate methods for computing complex turbulent flows; (iii) for checking the output of computations; and (iv) to increase

*Comments on an earlier draft by C. Sovran and B. E. Launder are gratefully acknowledged.

[†]Floating-point arithmetic operation.

understanding of fluid motions. To be correctly perceived, the remarks of the paragraph need to be carefully qualified.

There is no longer doubt that some important results can be obtained from fully time-dependent computations (such as large-eddy simulations) for turbulent flows that cannot be obtained from experiments--at least with the instruments available in 1980. This is already evident in such examples as computations of: the pressure-strain correlation; new, important details of instability in laminar-turbulent transition beyond the linear range; and the dynamics of turbulence production near solid boundaries. In 1980, important results of such types are still relatively new; however, one expects to see many more of them in the next decade. (See also final paragraph of this section.)

In recognizing these important advances, one must at the same time be conscious of the limitations of machine size and cost. In particular, the present and projected costs make it feasible to run the largest types of programs* only when important scientific results can be obtained once and for all, or where economics, legal conditions, or performance demands, make the problem of overriding importance to a large corporate or governmental institution.† Projections of larger machines and reduced costs per (mega)flop suggest that: (i) machines capable of this kind of computation will remain rare, restricted to very large institutions owing to large first costs; and (ii) the costs per run will remain so large that the most powerful approaches are unlikely to become the methods of most‡ day-to-day engineering computation within the twentieth century.

The remarks to this point suggest two foundations for the discussion that follows. First, a need for approximate (specifically, time-averaged) methods of computation of turbulent flows at high Reynolds numbers will continue to exist. It follows that we will continue to need a data base to build simulation models and to substantiate approximations. The nature of the required data base is, however, strongly affected by the specific needs of computation--both for forming models and for checking output for various classes of flows. The requirements for this data base forms a central question of this paper, and for the conference as a whole. Second, it is

*For example, large-eddy simulations or models employing transport equations for Reynolds stresses in closure approximations.

†For example, computation of flow in piston engines relating to creation of pollutants, the design of critical elements of turbomachinery affecting aircraft performance.

‡D. R. Chapman (1980, and personal communication) suggests that design of some critical turbomachinery elements by these methods may occur within the 1990s owing to: (i) low Reynolds numbers in some cases; (ii) relatively simple geometries; and (iii) high cost and difficulty of adequate performance testing.

already evident that computations can both supplement and aid in interpreting experimental results. There is accordingly an inverse question: "What can be learned from computations that will aid design of experiments, supplement experimental data and/or advise on the nature of useful experiments?" Some applications of large-eddy simulation to results not obtainable by experiment have already been suggested. The adaptive-wall wind-tunnel is an example of the use of computation to aid experiment; such tunnels are particularly important for transonic flows and for some classes of complex flows (for example separated flows) at all Mach numbers. Computation can often be an important aid to understanding data. Two instructive, recent examples of such applications have kindly been supplied by F. A. Dvorak of Analytical Methods Incorporated and are attached as Appendix 1.

These examples of the importance of data to good numerical fluid dynamics and of computation to improvements of experiments are by no means exhaustive. They are sufficient, however, to illustrate forcibly the importance of using experiment and computation to augment each other iteratively, as the effective way to increase knowledge and improve engineering design methods. We make this remark specifically to emphasize that while the focus in this paper is on data needs, there is no intention to imply a preference for experiment or for computation. On the contrary, since neither will prosper best alone, the intention there is to help clarify means for effective interaction between experiment and computation.

3. SPECIFIC NEEDS IN EXPERIMENTATION

In order to consider specific needs clearly, it is helpful to consider three types of experiments, depending on the results desired.

- a. Data on quantities of direct importance for engineering design.
- b. Data that will be useful in either construction or checking models for practical simulation of complex turbulent flows at high Reynolds number.
- c. Information that improves understanding of underlying physics of fluid motions.

This paper is primarily devoted to the discussion of category (b). The data needed for category (b) has some characteristics that differ markedly from those of categories (a) or (c).

The first distinctive characteristic is the need for initial and/or boundary data complete enough to specify a test case. In many computational methods, not only mean velocity data but also Reynolds stresses (and perhaps triple-products and dissipation rate) need to be specified over the initial surface. Experimenters need to take data with this in mind, that is, to choose at least one possible "initiating surface"

and document the flow at that surface with as much thoroughness as is feasible. Presumably the 1981 portion of this conference will make the precise needs clearer by providing a "catalog" of what inputs are needed for various successful computation methods.

A word of caution concerning the measurements of flow both at the initial surface and elsewhere is needed. A well-documented experiment needs to record not only the mean flow and fluctuation quantities but also the presence or absence of such phenomena as: (i) gross unsteadiness; (ii) vortex shedding; (iii) stationary (or meandering) vortex structures; (iv) the presence (or absence) of shock patterns and their steadiness; (v) the existence of more than one flow pattern periodically or aperiodically; and (vi) any other "unexpected" flow behavior in the situation under study. This implies the use of flow visualization and/or unaveraged and un-Fourier-analyzed, conditionally sampled rake data. Phenomena of this sort may not be part of the "turbulence field," but may nevertheless affect it to first order.* Moreover such information is essential to identify zones where particularly accurate time calculations or spatial resolution are necessary in the computations if one is to obtain a correct evolution of the dynamics of the flow field. The information is also essential if one is to distinguish gross unsteadiness from turbulence, and thereby obtain appropriate understanding, or to sort data from one flow mode from that of another (see Appendix I for example).

Geoffrey Lilley has made a similar point in a different way. In commenting on an earlier draft of this paper, Lilley noted that turbulence production can be written as an integral of quantities of the form $\vec{q} \times \vec{\omega}$, where \vec{q} is the fluctuating velocity and $\vec{\omega}$ the fluctuating vorticity vector. It follows that one must document the components of velocity and their derivatives not only in the direction normal to the surface chosen for initiating computations but also the velocity components and their derivatives lying in the initiating surface unless the flow at the initiating surface is clearly known to be wholly irrotational.

The second characteristic of experimental data for category (b) is the need for profile measurements of the mean flow and, if possible, turbulence quantities as well. Third-order correlations are useful but generally have lower priority. Measurements of dissipation are useful, but seldom can be made accurate enough for use in computations.

The nature of fluid measurements and the subtleties of fluid motions are such that the question of experimental uncertainty must have a prominent role. Even in "simple" geometries of the most common sort, the data scatter among various

*Emphasis on this point and most of the language of this paragraph were kindly supplied by Dennis Bushnell of NASA-Langley Research Center.

experiments is generally larger than most workers would expect. See, for example, the report by J. B. Jones on the entry region of a round tube (Flow 0130). For this reason, a separate discussion on the analysis of uncertainty is given in the position paper by R. J. Moffat in this volume. Proper understanding of such analysis is important to the comparison of data sets from different test rigs, to comparison of data to computation, and to the formulation of acceptance/rejection criteria for data sets.

An example illustrating this point arose in the preliminary work of data evaluation for this Conference. In commenting on the data evaluation of Launder and Rodi on wall jets, R. L. Simpson noted that it has been conventional to attribute unbalances in the right- and left-hand sides of the momentum-integral equation to "three-dimensionality," but that this attribution has no validity when the unbalance is less than the total experimental uncertainty in the difference between the two summed quantities. Since the experimental uncertainty in this difference is usually large, Simpson's point has considerable significance.

In experiments of category (b), it is better to do one experiment with extreme thoroughness, including redundant measurements and more than one type of instrument, than to provide a variety of experiments that might be more instructive for category (c) information. In planning an experiment for category (b), uncertainty analysis is the strongest single tool available for control of outcomes. The primary argument raised against use of uncertainty analysis is the time and trouble required. However, as the paper by R. J. Moffat shows, the use of uncertainty analysis in design of experiments is critical, and, once that is done, the added work needed to estimate the accuracy of each output result is essentially trivial when data are reduced by computer program. Routine, careful use of uncertainty analysis would go a long way toward facilitating comparisons between experimental results and computation, and is strongly recommended. (See also remarks of B. Cantwell on requirements for future accessions to the data library.)

In addition to deciding what measurements are to be made (to be discussed in more detail below), the experimenter must choose the range of variables, the spacing of data, and the accuracy of the measurements. In most cases he will use the widest range which his experiments will cover and which there is time to explore, and the highest Reynolds number for which his test rig is capable of producing results of the required accuracy. In experiments involving advanced and expensive data analysis, the experimenter may be forced to measure only "enough points for a smooth curve." (He should remember that for many purposes streamwise derivatives of measured quantities are needed, and enough profiles should be taken to permit this.) These semi-trivial statements simply imply that the range and density, and to some extent the accuracy, of the measurements are determined by the experimenter's budget of time and money. Cheap experiments may be useful in some cases, but experiments which are poorly

planned or that have to be skipped for lack of time and money are often useless, and may even play a negative, time-consuming role in data evaluations. Far more important than what is measured is whether the results are trustworthy. Redundancy checks, calibration chains, closure checks using fundamental principles, tunnel documentation, documentation of test configurations and procedures, and fully reported uncertainty of the data from a careful analysis all tend toward creation of this trustworthiness. Wherever possible, the turbulence experimenter should record the fluctuating signals from his hot wires, or if possible his laser velocimeter, so that the data can be re-analyzed in later years if more complicated statistics become of interest or if queries arise about the data.

A further problem regarding trustworthiness is that of "one-lab" data. Experience with many flows evaluated for this conference suggests the very real hazards of relying on a data set from one lab and one apparatus. Not only are residual uncertainties higher for "one-lab" data, but also, far more often than not, comparison of data from several test rigs raises fundamental questions that need resolution by further experimentation. (See for example data evaluations of J. K. Eaton and J. P. Johnston, J. B. Jones, and S. Birch.) This remark has particular force in cases such as: (i) laminar-turbulent transition; (ii) near-zone of free-shear layers; and (iii) separated flows, and other flows which are sensitive to variation of the spectrum of incoming disturbances.

A special situation arises in data involving very high levels of fluctuations and/or rapid local flow reversals, as in zones of incipient detachment. The remarks of Cantwell (1980), Eaton and Johnston (1980), Owen and Johnson (1980), and Simpson (1980) should be consulted for any flow possibly involving these kinds of situations. As all these authors show nearly all older data are inadequate, and only relatively recent laser data, time-of-flight probe data, or flying hot-wire data^{*} have the potential for producing trustworthy data for such flows (in terms of instrumentation available in 1980.) Consequently, there is a need for more category (b) data in these situations.

In general, the scatter in turbulence data is much higher than in mean flow data. In some cases good mean flow data exist, but the turbulence data do not form a consistent band of data (see for example the evaluation of J. B. Jones on Flow 0130). Part of this difficulty is probably owing to the failure to calibrate hot-wires for fluctuations and/or for a suitable value of the yaw constant. A procedure

^{*}The earliest clear recognition of this problem seems to have been by D. E. Coles and co-workers at Cal-Tech, circa 1972. Their solution of the flying hot-wire is adequate but quite difficult to implement compared to laser or time-of-flight probe measurements.

for such calibration is provided in Report TMC-3 of the Mechanical Engineering Department of Stanford University (available on request).

A case of special difficulty in documentation is flows involving instabilities, as in the early zone of free-shear layers and laminar-turbulent transition. The report of E. Reshotko and M. V. Morkovin on laminar-turbulent transition records that no case is yet sufficiently well documented to make a reliable basis for computation possible. Such cases form an area where discussions between computers and data takers will be of particular importance in establishing trustworthy data. (A working committee in the 1980 meeting has made a more detailed report on the question. See report on Session XIII below.)

Another area warranting special care is the documentation of shock waves in compressible flows. Observers need to note not only the mean position, but also the frequency and amplitude of shock motions,* and whether shocks are present all the time or intermittently. Careful measurement of the upstream and downstream conditions of the shocks including turbulence measurements are needed for improving modeling and checking output (see also summary of Rubesin/Horstman Flow 8650 ...).

Considerable questions concerning the reduction of the output of hot-wires for fluctuations in transonic and supersonic regions also exist. A special report of a working committee from the 1980 meeting will expand on this topic. (See reports in the Session XIII below.)

Most of the remarks of this section can be summarized by noting that experiments are useful for category (b) of this paper only when they are documented extremely thoroughly, where the word "documented" is used in both of two senses. In the first sense, documented implies measurements of the flow field that provide a complete picture of the real physics of the flow, with a statement of the uncertainty involved on each output point. It is important to realize that estimates of uncertainty at given odds need themselves not be of high accuracy in order to provide a quantitative basis for comparison of experiments and computations. For example, it is irrelevant whether the uncertainty on a given result is 18% or 20%, but it is critical to know reliably whether it is of the order of 20% or 2%. Documentation in the second sense means reporting sufficient information so that the reader is convinced that the data are trustworthy and is supplied with sufficient information, especially initial conditions, so that a suitable test case for comparison with computation can be constructed. In a number of cases used in the 1980-81 Conference, written documentation was not sufficient for this purpose and data takers had to be consulted in order to establish sufficient information for the formation of trial cases.

*Cases of truly steady shock location seem to be extremely rare, perhaps non-existent.

It is the lack of documentation in these two senses that has made the bulk of past data less than adequate for use as trial cases for checking current computational methods and for interacting effectively with computations in the attempt to advance knowledge and improve engineering methods.

Collectively we have the ability to do far better in the future, it remains to see if we will utilize it. (In this connection see also remarks in the Introduction to this volume concerning oversight and planning of experiments.)

4. BOUNDARY CONDITIONS (INCLUDING INITIAL CONDITIONS)

An experimental investigation of any fluid flow problem, which can later be used for comparison with computed output, must ensure that a complete and accurate specification of the flow field is made, measured, and recorded. This requirement must be satisfied to meet the needs of all computers, even if this means some redundancy in data for certain computers. Formally, the boundary-condition information required depends not on the flow but on the equations to be solved. It is important that sufficient data be given at all boundaries to allow mass and momentum balances to be constructed.

It is useful to consider the following flows:

- a. In "thin shear layer" flows, i.e., having small $d\delta/dx$ and negligible $\partial p/\partial y$, the equations are essentially parabolic, and the needs are as follows:
 - (i) Profiles of all variables except V are required at all inflow surfaces. The minimum requirement is for the velocity U (and W) and the shearing stress τ_{xy} (and τ_{xz}).
 - (ii) The external velocity $U_e(x,z)$ or pressure $p(x,z)$ is required and implies the boundary condition as y tends to infinity.
 - (iii) Boundary conditions at a solid surface, unless stated otherwise, are the usual no-slip conditions. If there is significant surface blowing, suction, or wall roughness, this should be specified as accurately as possible.
 - (iv) The shape of the solid surface must be accurately given.
 - (v) The V -component far from a free shear layer is determined by conditions outside the shear layer and must therefore be specified.
- b. In "slender shear layers" (e.g., streamwise corners, non-circular ducts, etc.), the initial conditions should include all Reynolds stresses. All three mean velocity components should be accurately measured so as to define the streamwise vorticity.

Boundary conditions for 3-D obstacles in 2-D boundary layers will generally be given upstream of the obstacle and will be as in (a) above.

In 3-D cases, such as swept wings, initial data are needed on all "inflow surfaces" across which fluid enters the domain; for example, to compute the flow on the outboard portion of the wing, data are needed on the inboard boundary of the domain, because boundary-layer fluid flows outboard. See also the remarks by Humphreys and van den Berg in the full data evaluation on Flow 0250; they are particularly thorough on three-dimensional boundary layer documentation.

- c. Two-dimensional elliptic flows can almost all be chosen to begin and end with thin shear layers (e.g., flow over a backstep). Computers will usually assume extrapolation conditions at the downstream boundary (i.e., $\partial/\partial x = 0$ for all mean quantities). The experiments should provide data indicating whether this approximation is accurate.

Flows which are genuinely elliptic at the downstream boundary can cause difficulty (an example is a diffuser with a screen at exit). No harm is done if the boundary conditions in the data are over-specified, because a well-posed calculation method will accept only a "sufficient" set; this presumes the uncertainties in the data are not so large that significantly different results arise from different choices for boundary conditions.

Inviscid-flow boundary conditions (e.g., for airfoil calculations) should pose no problem. Usually, uniform flow at infinity will be assumed. In some cases like backstep flows, the upper-wall geometry needs to be specified. The boundary-layer displacement thickness on the upper wall may not be negligible and, if not, should be given.

5. RESULTS TO BE USED IN CHECKING OUTPUT OF COMPUTATION

The results need not include all computed quantities. For example, many calculation methods yield values for the turbulent-energy-dissipation rate; however, there are no direct measurements of this quantity of sufficient accuracy for checking calculations, and hence one does not expect a check. As already indicated, detailed mean-flow measurements are a minimum requirement, and they should include an estimate of the departure of any "two-dimensional" flow from that ideal state. The criteria employed in various cases for ensuring two-dimensionality is exhibited later in this volume. In principle, the static pressure can be deduced from the mean velocity field, but in flows other than thin shear layers it is desirable to have static pressure measurements within the flow. Unfortunately, it is in such flows--notably separated flows--that static-pressure probes are least accurate and most likely to disturb the flow.

It is highly desirable to have measurements of all Reynolds stresses whose gradients affect the mean flow. This is especially true when the acceleration is dominated

by pressure gradient, for mean-flow predictions in such regions can be made by the inviscid equations; consequently, the mean-flow quantities are an insufficient test of the turbulence model. Most flows with significant Reynolds-stress gradients are shear layers, in which shear stress is the most important of the Reynolds stresses. In three-dimensional flows it has components $-\overline{p u v}$ and $-\overline{p v w}$; the latter quantity is usually difficult to measure, appearing in hot-wire measurements as the small difference of two large quantities.

Many modern calculation methods use models based on the exact Reynolds-stress transport equations. The right-hand sides of these equations contain mean triple products as well as Reynolds stresses; they also contain viscous terms and pressure-velocity correlations which are effectively unmeasurable; the major unmeasurable terms can be deduced as the differences of the other terms. (Quantities found as differences are particularly liable to large experimental uncertainties, and are therefore particularly in need of presentation of the carefully estimated uncertainty values.) Triple-product measurements may therefore be necessary for the deduction of dissipation and the pressure-strain "redistribution" term as the "difference" terms in the relevant transport equations, as well as being of intrinsic interest as the dominant parts of the turbulent transport terms.

Transport equations for higher-order quantities, such as dissipation and triple products, are used in some calculation methods, but the exact transport equations contain high-order derivatives of velocity fluctuations and unmeasurable pressure-fluctuation terms. Unless new measurement techniques appear, it is not realistic to discuss data needs for this application.

Conditional-sampling measurements, in contrast, are available in much greater variety than can be used explicitly in Reynolds-averaged calculation methods. Little progress has been made in developing calculation methods based on conditional sampling concepts. The main value of conditional-sampling measurements thus far has been in providing qualitative inspiration for turbulence models. However, an interchange between large-eddy simulation computations and more detailed structural information appears to be beginning. See Section 6 regarding Large-Eddy Simulation data needs.

Unsteady flow measurements must be made by some form of conditional sampling; in periodic flows phase-averages are used, while in a periodic flow true ensemble averages are necessary. There is room for ingenuity in this area. Digital recording techniques are usually helpful in such cases. Relatively few data of any sort are yet available for unsteady flow. A report on the state of data in unsteady flows by L. W. Carr was presented to the 1980 meeting (see Session XII).

6. DATA NEEDS FOR LARGE-EDDY-SIMULATION MODELS

Large-eddy simulation (LES) is limited in 1980 to geometrically simple flows. Free-shear layers and channels are the most difficult flows yet attempted. More difficult flows will be attempted as time goes on and computers increase in power. For these reasons, the data needs are restricted to relatively simple flows; but, because the method operates at a higher level of detail than do time-average methods, LES requires more detailed data.

Since LES explicitly computes the behavior of at least one realization of the large eddies, it would benefit considerably from detailed data on the nature of the large eddies in a flow. In particular, it is the one method that requires spectral data; these data need not be very accurate in the small scales (high wavenumbers), but should include at least two decades of reliable spectral information. We recommend that this information be routinely reported for simple flows; lack of such data has made some experiments impossible to simulate without many assumptions as to the initial spectra. This information should ideally be available for each of the velocity components, and data on the spectra of the products of the components would also be useful.

In the past, a number of experimenters have reported energy spectra which are quite useful and several averages of higher-order products of the velocity fluctuations. The latter have proven of less value because the small-scale contributions to them are often quite large. Since the spectral resolution of LES methods is limited, it has been impossible to make comparisons with these data on higher-order products. It would be more useful for LES modelers if the experimenters low-pass-filtered their signals (with carefully documented filters) before computing the higher-order products. Since the bandwidth available to the computer may not be known to the experimenter, it is suggested that this be done with several different filter widths so that the computer can obtain what he needs by interpolation. Since other uses may have different requirements, it is desirable to retain unfiltered data, where possible, when dealing with experiments intended for category (b) of this paper.

7. NEED FOR ADDITIONAL DATA -- CONCLUSIONS

There is clearly a continuing need for good data both on old and new flows. In the case of flows already tabulated in this volume, new experiments are needed in several instances, as a result of questions raised by comparison of existing cases. Some examples include: the effects of curvature of the free-shear layer on properties of reattaching flows; data in zones of detachment and reattachment; and the effects of entry conditions on "overshoot" in pipe and duct flows. Improved data are needed for: transition; relaminarization; and complex wakes. The comments of the individual evaluators of various flows should be consulted for other cases. For each summary in

this volume, a detailed report (usually much longer) exists that has undergone scrutiny by several workers other than the original evaluator. These longer reports can be obtained from the Thermosciences Division, Dept. of Mechanical Engineering, Stanford University, Stanford, CA 94305, at least until publication in an open journal occurs, as it will in some cases. These evaluations typically contain many comments that should prove important in planning experiments for flows of any given class of related flow-fields.

For new flow cases, it is also important to consider likely next steps in modeling. Current instances of need appear to be: (i) flows with body forces; (ii) protruberances in boundary layers (e.g.: roughness elements, wing-body or blade-hub junctions, wind flow over buildings); and (iii) flow around bluff bodies.

For all flows, good data imply not only adherence to the general suggestions of this paper but also that: (i) data-taking be carried forward, or closely supervised, by an experienced person, if at all possible; (ii) considerable independent advisory or supervisory activity occur during all stages: planning, data-taking, and evaluation. Clear understanding of the pitfalls in various experiments is not accumulated quickly. B. E. Launder and W. Rodi remark in the evaluation of Flow 0260:

Overall the most successful studies have been those undertaken in laboratories that have made a large scale effort evolving over a decade or more. This emphasizes how crucial design and experimental techniques have been to obtaining really useful data. Certainly before anyone embarks on further studies of the wall jet, he (or she) should read through the collected reports from Professor Newman's group at McGill (those of Fekete, Guitton, Gartshore, Irwin, etc.)* to brief himself on the problems that arise and the way that skill can overcome them.

How much can be recaptured from the reports and how much of this experience remains unwritten is always a question. This question supplies still another reason why outside advisory review can be critical in performance of successful experiments for category (b). Strong periodic scrutiny by at least a few able, experienced workers from outside the institution holding the grant or contract would seem highly desirable (even though it has not been past practice). Such an outside body could also be of important service by assuming responsibility for planned replication of experiments in an orderly way.

*Special expertise of this sort on other flows exists in other research groups; the example is not isolated.

8. RECOMMENDATIONS FOR FUTURE DATA TAKERS IN COMPRESSIBLE FLOWS*

When an experiment is designed, care must be taken that the flow field is well defined. All boundary conditions must be specified or shown not to be important; this is especially critical for transonic flows. The establishment of an upstream equilibrium boundary layer is also important. Experiments should also be designed to test a particular aspect of turbulence modeling when possible.

Improvements in the operation and interpretation of the data from laser-doppler and hot-wire anemometers in recent years make it possible to consider these instruments for gathering data of turbulence parameters upon which turbulence model improvements can be made. The relatively small models associated with supersonic wind tunnels utilized for studies of fluid mechanics suggests that measurements within boundary layers can be performed with greater spatial resolution when these boundary layers occur on the wind-tunnel walls. Redundant measurements of both mean and fluctuating quantities are also recommended. Pitot tubes should be used to obtain near-wall data where LDV measurements are suspect. Continuing efforts should be made to obtain more accurate surface skin-friction measurements.

REFERENCES

- Cantwell, B. J. 1980, Evaluation of Flow 0410 for this conference, and NASA CR 3066 (1978).
- Chapman, D. R. (1980), "Trends and Pacing Items in Computational Aerodynamics" (Invited paper for 7th International Conference on Numerical Methods in Fluid Dynamics, Stanford University, June 23-27).
- Coles, D. E., B. J. Cantwell and A. J. Wadcock (1978), "The Flying Hot-Wire and Related Instrumentation," NASA CR-3066.
- Eaton, J. K., and J. P. Johnston (1980), Evaluation of Flow 0420 for this conference.
- Owen, F. K. and D. A. Johnson (1980), "Separated Skin Friction Measurement--Source of Error, an Assessment and Elimination," AIAA-80-1409.
- Simpson, R. L. (1980), Evaluation of Flow 0430 for this conference.

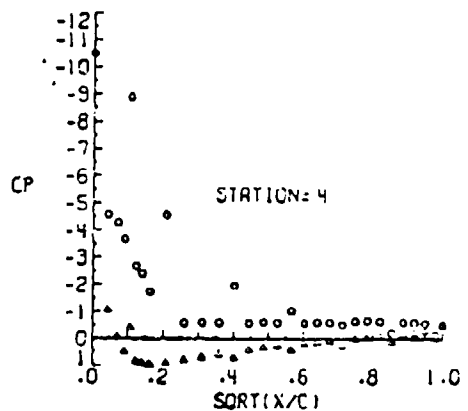
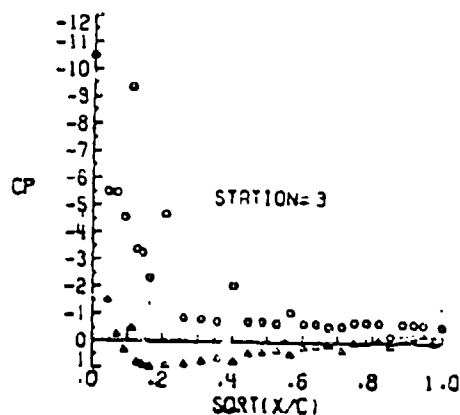
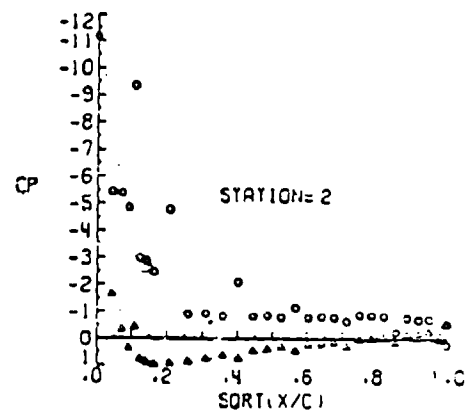
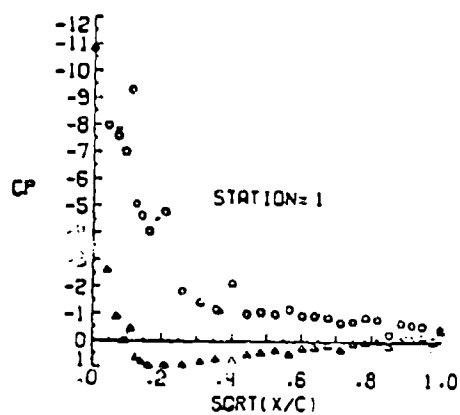
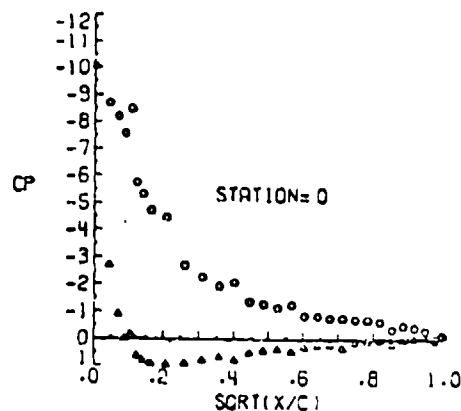
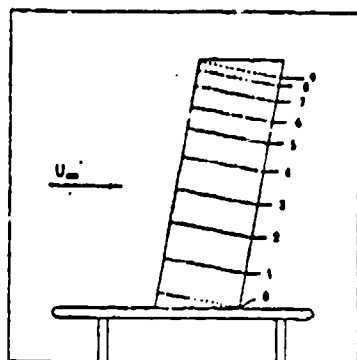
*These remarks were prepared separately by M. Rubesin and C. Horstman for compressible flows, and hence overlap in part remarks above. The remarks have nevertheless been left intact for completeness and as an independent opinion.

APPENDIX 1

(From letter by F. A. Dvorak to S. J. Kline, dated 15 August 1980)

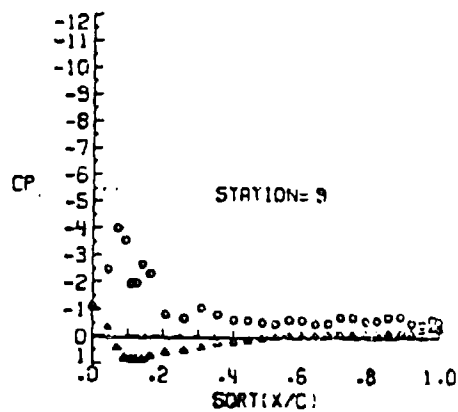
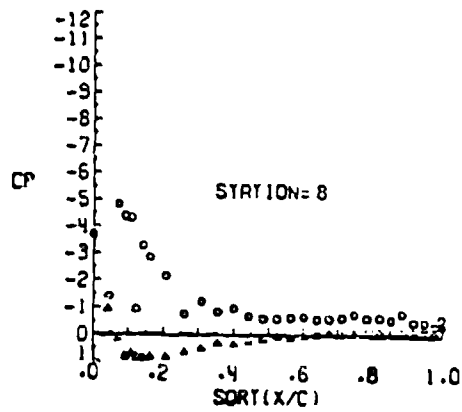
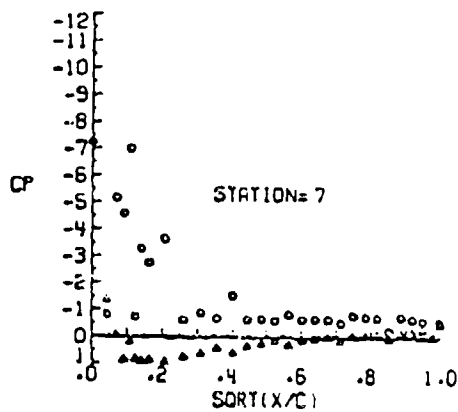
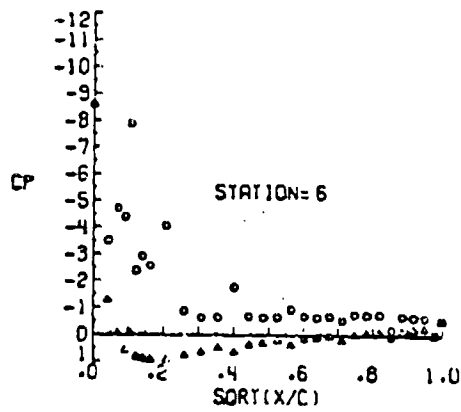
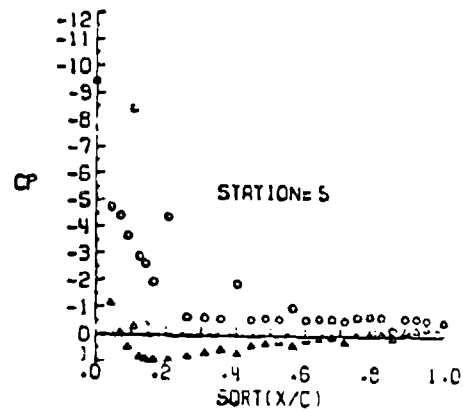
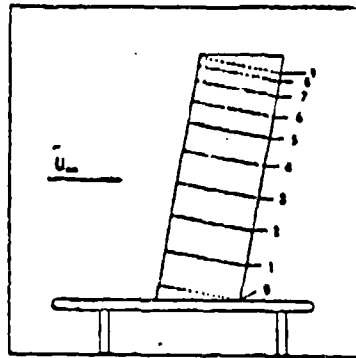
Two examples provide substantive proof that the computations cannot only help in the interpretation of experimental data, but can also save a proposed experiment from disaster. In the first instance, an experiment was conducted by NASA-Langley on a swept semispan wing of aspect ratio 6 at 21° angle of attack. The measured pressure distributions at a series of spanwise stations are shown on Figure 1. Malfunctioning scanivalves were blamed for the large amount of scatter, and the experimental results were discarded. Because of a scarcity of high angle-of-attack three-dimensional pressure data for comparison with theory, the experimental results were retrieved and compared with a recently developed three-dimensional separation model. Comparisons at several spanwise stations, two of which are shown in Figures 2 and 3, indicating that the experimental results were better behaved than previously thought. Furthermore, when the attached flow calculations were plotted on the same figures, it was realized that at least part of the time the wing was experiencing fully attached flow. It is apparent that the wing was experiencing an intermittent separation with reattachment during the scani-valve cycle. The experimental data have since been retrieved by NASA-Langley and is being fully documented.

In the second instance, a comprehensive wind-tunnel test was planned for an 80% of full-scale helicopter fuselage model in the NASA-Langley 14 x 22 foot VSTOL tunnel. The purpose of the test was two-fold: to validate an aerodynamic analysis method, and to investigate ways to reduce configuration drag. In order to have an "unbiased" test of the computational procedure, all analysis was performed in advance of the test. A large splitter plate was planned for use in deflecting the floor boundary layer from the model. Consequently, this was modeled in the analysis as were the tunnel walls, floor and ceiling, in order that tunnel-blockage effects would be accounted for. The wind-tunnel model frontal area was 15% of the working section area. Computed pressure, streamline and boundary layer distributions on the model suggested that the flow on the rear part of the fuselage would be greatly distorted and totally unrepresentative of the flow in free air. Further calculations suggested that the splitter plate should be discarded and the tunnel boundary layer be removed upstream of the model. Following these suggestions, the subsequent test data were in excellent agreement with the theory.



$Q = 51.68$ $\alpha = 21.38$ $SWEET = 9.72$

Figure 1.



$Q = 51.69$ $\alpha = 21.38$ $SHEEP = 9.72$

Figure 2.

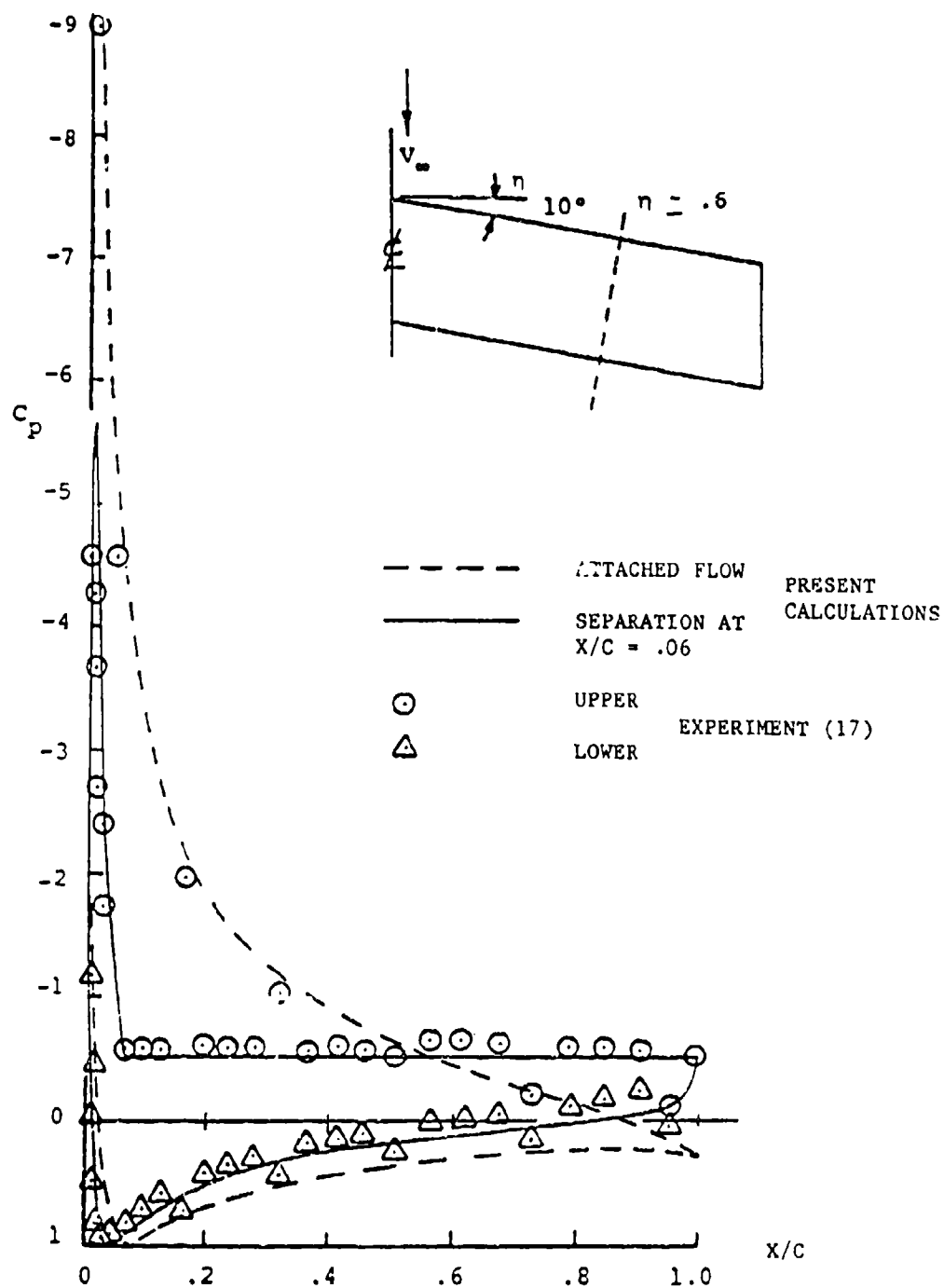


Figure 3.



CONTRIBUTIONS TO THE THEORY OF
UNCERTAINTY ANALYSIS FOR SINGLE-SAMPLE EXPERIMENTS

Robert J. Moffat^{*}

INTRODUCTION

When two "good" experiments differ, how can the significance of the difference be assessed? When a "good" theory and a "good" experiment differ, how much difference can be overlooked before one must conclude that a disagreement exists? There is little hope of quantitatively answering questions such as these until the research community accepts responsibility for documenting the uncertainty in both experimental and computational work.

There is a growing awareness of the need for such analyses. Both the International Standards Organization [1] and the American Society of Mechanical Engineers [2] are developing standards for the description of uncertainties in fluid flow measurements. The U.S. Air Force [3] and JANNAP [4] have adopted guidelines for reporting uncertainties in the performance testing of gas turbines and liquid propellant rockets, respectively. It seems only a matter of time before technical societies and contracting agencies will require such documentation as a regular adjunct to research studies.

The techniques addressed in the above references were developed specifically to suit the needs of industrial performance testing--basically post-hoc operations. The experiment is presumed to have been conducted, one or more sets of data are available, the average results have been computed. The remaining problem: assign a value to the uncertainty interval surrounding each of the calculated results, a single estimator which accounts for both "fixed errors" and random errors." The "fixed error" or "bias" in an experiment is frequently evaluated by an opinion poll, querying those with experience as to the probable magnitude and sign of the fixed errors. There is some disagreement in the current international literature concerning the proper way to combine the "guesstimates" of fixed errors with the recorded uncertainties in the data. Regardless of the combinatorial scheme used, the principal end use of these uncertainty analyses is in reporting: describing the uncertainty in the reported result. The four references cited outline the theory and illustrate some of the differences of opinion.

^{*}Dept. of Mech. Engr., Stanford University, Stanford, California 94305.

The present paper takes a different view of experimental work and of the role of uncertainty analysis. Uncertainty analysis is viewed as one of the principal tools with which a researcher can construct an experiment of provable validity. As such, uncertainty analysis finds its most important use during the planning, development, and shakedown phases of the experiment, not the reporting phase.

An experiment is regarded as a system, composed of an apparatus, its instrumentation, and a data-interpretation program. The entire system is viewed as an instrument designed to obtain certain data, and this instrument requires calibration. The calibration may be based on one of the basic principles of engineering (i.e., a conservation law) or a data set of accepted validity (a baseline data set). In either case, the experimental result will seldom agree exactly with the expected result. This is where uncertainty analysis comes in--to provide a quantitative means for assessing the significance of the difference. If the achieved result differs significantly from the expected result (i.e., differs from it by more than the uncertainty estimate), then the experimental system is deemed to require further improvement before being qualified. If the achieved result lies inside the uncertainty interval, then the experimental system is "qualified," and can be put "on-line" for the production of new data.

Further benefit can be derived from uncertainty analysis after the system has been qualified for data taking. During the conduct of the experiment, the results will probably display scatter (i.e., random variations) about the mean result, from trial to trial. The scatter can be predicted using uncertainty analysis and compared to measured scatter. If measured scatter exceeds the predicted scatter, then the experiment is not being well controlled and needs to be re-examined.

The two uses mentioned above require different estimates of the uncertainty interval. In the first example, an external reference (the baseline data set, or the conservation laws) is used; hence the uncertainties in the instrument calibrations must be acknowledged. In the second case, only repeatability is involved, not accuracy, and the uncertainties in the instrument calibrations should not be included. The point to be emphasized is that different estimates of uncertainty are needed for different purposes. Later in this paper a classification of these types and their uses is discussed.

A word of caution is in order, at this point, directed to those readers who are familiar with either the NBS method or the Air Force method (both described in Ref. 3). Those methods, and their derivatives, use the term "bias" error to designate a class of fixed errors present in an experiment, and treat the bias errors differently from the random errors, called "precision" errors. The "bias errors" include all effects whose values will not change during the course of the experiment, such as instrument calibration defects, or fixed environmental errors (such as the radiation

error of a temperature sensor) whose magnitudes have not been accounted for by a "best estimate." The bias errors are kept separate from the precision errors throughout the calculation of uncertainty until the last step, and are viewed as "non-statistical" in nature. The present approach differs from this in a fundamental way. It is assumed here that every acknowledged "fixed error" is accounted for, using the best available estimate of its value, and that the remaining defect of knowledge is solely due to the uncertainty in the corrections--equally likely to be positive or negative, and coming from a Gaussian distribution of possibilities: a state described as being "zero-centered" in the following paragraphs. The hypothesis that the experiment is "zero-centered" is then tested by comparing the achieved results with the expected results. If the achieved and expected values agree within the predicted scatter, then there is no visible evidence of residual error in the experiment: it is "zero-centered." On the other hand, if the achieved result differs from the expected result by significantly more than the expected scatter, this indicates that the experiment is not yet "zero-centered": there remains an unrecognized error somewhere in the experiment, and diagnostic studies are required. As a consequence of this approach, the final experimental result should not contain any significant bias error--only precision error--and the question of how to combine bias and precision need never be addressed. The present method of experiment development is well suited to research-type experiments, where the experiments are relatively simple to evaluate and repeat. Under such conditions there is no need to tolerate "bias errors"--once they are recognized, they should be corrected. Large-scale engine tests, however, with which the general literature is concerned, may well have to put up with these estimated errors and continue to treat them separately.

In the following analysis, it is presumed that each data set is processed independently; there is no averaging. Each data set is, therefore, a true single-sample experiment.

The uncertainties in data can be propagated into the calculated result either by a Worst Case combination or a Constant Odds combination. The latter is emphasized here.

The mathematics of single-sample uncertainty propagation were described by Kline and McClintock [5] and have been practiced widely, if sparsely, since then. The present paper builds upon that work, adding three elements to the structure:

- The concept of Replication Levels, to distinguish the treatment of scatter on repeated trials from differences of results between independent experiments.
- The concept of the Zero-Centered Experiment, having no residual fixed errors.
- A technique for executing uncertainty analysis on computer-based data-reduction programs which requires only a small amount of programming to obtain an uncertainty analysis on even the most complex program.

The mathematics will be reviewed, and then the new elements discussed, along with some examples of the use of uncertainty analysis.

THE PHYSICAL PROBLEM

Real processes are often affected by more variables than experimenters wish to acknowledge. Most data-gathering experiments are designed as "partial derivatives" of some process with respect to one variable at a time, holding all other aspects ostensibly constant; but rarely are the background conditions truly constant. Rarely is a test conducted as a true "partial derivative." Often there are secondary variables, not observed and not controlled, which are varying randomly during the course of the experiment. Such background variables can cause changes in the result of an experiment, even if all of the acknowledged independent variables are held steady.

The appearance of unexpectedly large scatter in experimental results is one warning of the presence of such uncontrolled or unobserved variables.

THE BASIC MATHEMATICAL FORMS

It is assumed that each data bit will be described either as in Eq. (1a) or (1b) below, with an assignment of the best estimate, \bar{x}_1 , the estimated uncertainty interval, δx_1 or $\delta x_1/x_1$, and the associated confidence level or odds.

Absolute Uncertainty:

$$x_1 = \bar{x}_1 \pm \delta x_1 \quad (20/1) \quad (1a)$$

Best Estimate	Uncertainty Interval	Odds
------------------	-------------------------	------

Relative Uncertainty:

$$x_1 = \bar{x}_1 \pm \delta x_1/x_1 \quad (20/1) \quad (1b)$$

Best Estimate	Uncertainty Interval	Odds
------------------	-------------------------	------

Consider a result R, calculated from a set of values of the x_i . One must choose the method of combining the uncertainties. As a consequence of the uncertainty in each of the x_i , there will be an uncertainty in R. Two logical options exist: worst case combination and constant odds. The combinatorial form for each is shown below:

Worst Case:

$$\delta R = \left| \frac{\partial R}{\partial x_1} \delta x_1 \right| + \left| \frac{\partial R}{\partial x_2} \delta x_2 \right| + \dots + \left| \frac{\partial R}{\partial x_N} \delta x_N \right| \quad (2)$$

Constant Odds:

$$\delta R = \left\{ \left(\frac{\partial R}{\partial x_1} \delta x_1 \right)^2 + \left(\frac{\partial R}{\partial x_2} \delta x_2 \right)^2 + \dots + \left(\frac{\partial R}{\partial x_N} \delta x_N \right)^2 \right\}^{1/2} \quad (3)$$

Kline and McClintock (5) have shown that Eq. (3) assesses the uncertainty with good accuracy for most functions of engineering importance. There are three restrictions:

- Each of the x_i must be an independent variable.
- Each of the x_i must be from a Gaussian distribution.*
- The odds must be the same for each δx_i statement.

As a consequence of Eq. (3), if the uncertainty intervals for each of the x_i are stated for 20/1 odds, the calculated value of δR will also be appropriate for 20/1 odds.

For most single-sample experiments, the δx_i are estimated by the observer. The third restriction, therefore, serves mainly to guide estimation. As to the second restriction, it seems acceptable to presume that most instruments produce repeated values with a Gaussian distribution, but there is little proof of this point for modern instruments.

The choice between Worst Case combination and Constant Odds is usually made based upon the consequences of being wrong. There are a few situations in which the penalty for failure is extreme, and where Worst Case combination would be recommended; but, for most situations, the Constant Odds method is preferred, and yields a more useful result.

When the result is calculated as a product string, it is particularly easy to assess the relative uncertainty:

If
$$R = x_1^a x_2^b x_3^c \dots,$$

then
$$\frac{\delta R}{R} = \left\{ \left(a \frac{\delta x_1}{x_1} \right)^2 + \left(b \frac{\delta x_2}{x_2} \right)^2 + \dots \right\}^{1/2} \quad (4)$$

Equations (3) and (4) are the basic working equations of uncertainty analysis. They pose no particular difficulty in evaluation, providing that information is available as to the values of the δx_i . This proviso points to the critical problem of uncertainty analysis: identifying the appropriate values for the δx_i . The next section will address this problem, and introduce the concept of "replication levels" of the experiment, as a way of classifying the δx_i .

*If the δx_i^2 are taken to be variances, Eqn. (3) holds without the need for a Gaussian-distributed population. Equation (3) is an adequate approximation for any reasonable underlying distribution so long as the δx_i are independent (not cross-correlated).

REPLICATION LEVELS

The Root-Sum-Square combinatorial scheme is generally accepted as the appropriate way to combine uncertainties at constant odds (1,2,3,4). There is, however, some disagreement as to how to deal with "fixed errors" and "random errors" in the same experiment. This disagreement arises from a desire, on the part of some testing laboratories, to present one number, which describes both types of error.

The disagreement can be obviated if one lets the end uses of an uncertainty analysis guide the selection of uncertainty interval. One use of uncertainty analysis is to evaluate the significance of the scatter in repeated trials with the same apparatus and the same instrumentation. In such an application, the instrument calibrations play no role, since they do not change during the conduct of the experiment. Replication of the experiment, at that level, does not involve the instrument calibrations. On the other hand, if one wishes to compare the results of one experiment with another, conducted in a different laboratory, then the uncertainty in instrument calibrations must be considered. If, at this point, one imagines an ensemble average over two or more experiments, each conducted with a different set of instruments, then this higher-ordered replication involves instruments having different calibrations, and will usually show a larger scatter--an ensemble average over several experiments, and its larger uncertainty interval, is the replication level which must be considered in comparing with work at another laboratory. In both cases, it is assumed that the experiment has been "zero-centered," i.e., that all recognizable sources of error have been corrected for by the best available estimate, so that only uncertainties remain. As has been mentioned earlier, this state can be approached using uncertainty analysis to guide the development of the experiment.

It will be apparent, on reflection, that the present viewpoint has rendered unnecessary a treatment of the question of how to combine "fixed errors" and "random errors." The concept of different levels of replication, according to the end use of the analysis, establishes different ensemble averages to which each realization of the experiment simultaneously belongs: one concerned with scatter on repeated trials, and one concerned with absolute accuracy. There is further utility in defining a third replication level for purposes of experiment planning: this level involves only the instrument capabilities.

Three orders of replication level are defined in the following paragraphs, numbered according to the additional degrees of freedom which the conceptual ensemble average adds to the experiment.

Zeroth Order is described by the following conditions: time itself is frozen; the display of each instrument is considered to be invariant under replication; the only component of uncertainty at this order is the interpolation uncertainty, i.e.,

the inability of independent human observers to assign the same numerical value to the displayed x_1 .

The values of uncertainty at this level are often assigned as "one-half the smallest scale division" or some similar rule of thumb. This order of uncertainty is denoted $\delta x_{1,0}$.

First Order: At this order, time is the only variable; with the experiment running, the display for each instrument is assumed to vary stochastically about a stationary mean, x_1 . The First Order uncertainty interval includes the timewise variation of the display and its interpolation uncertainty. The value of uncertainty at this order is denoted $\delta x_{1,1}$ and is usually larger than $\delta x_{1,0}$ for any real process. No changes in instruments are considered at this level.

The value of $\delta x_{1,1}$ can be estimated from a set of repeated observations of the value of x_1 within the apparatus operating at its set point. The set of readings should be made during steady-state operation or should be adjusted for any monotonic trend in the mean during the observation period. The intent is to arrive at a valid estimate of the standard deviation of the population of possible values of x_1 from which future (single-sample) experimental observations will be taken. A diagnostic sample of 20 elements allows a confident estimation. For a Gaussian distribution, the standard deviation of a sample of 20 elements, S_{20} , is within 5% of the standard deviation of the population ($S_{20} \approx 0.96\sigma$ according to Thomas [6]). The value $\delta x_{1,1}$ should be taken as 2σ , or $2.083 S_{20}$, if odds of 20/1 are desired.

It is important to note that the requirement for 20 diagnostic observations of each x_1 is not synonymous with taking 20 repeated runs on each set point of an experiment. The diagnostic observations of x_1 may be taken very rapidly, and should be done at least once during the testing program for each point, or a few points spanning the experimental range. The principal limiting factor is that the period of observation be representative of steady operation.

Just as statisticians frequently permit the use of "pooled variance," so experimenters frequently will pool their observations on an apparatus--relying upon prior experience and a brief period of observation to assign the values of the $\delta x_{1,1}$. It is probably not justified, in terms of the effort required, to do a full statistically valid work-up of each $\delta x_{1,1}$. The basic method has a sound, statistically valid basis, and small errors in the estimates of the $\delta x_{1,1}$ will not defeat the objective. If the labor involved in a "rigorous" treatment is so formidable that the entire effort is abandoned, then more is lost than if good judgment had been used to execute a reasonably accurate analysis.

Nth Order: At this order time and the instrument identities are considered to be variables. For each conceptual replication, each instrument is considered to have been replaced by another of the same type. This makes "instrument identity" a

variable, and introduces the uncertainty due to the calibration of the instrument used. The N^{th} order uncertainty, $\delta x_{1,N}$, is always larger than the First Order uncertainty.

It will be shown in the last section of this paper that, for single sample situations:

$$\delta x_{1,N} = \{(\delta x_{1,\text{cal}})^2 + (\delta x_{1,1})^2\}^{1/2} \quad (5)$$

where

$\delta x_{1,\text{cal}}$ = the 2σ value for the ensemble average of calibrations of instruments of this type,

$\delta x_{1,1}$ = the 2σ value for the stochastic uncertainties observed on repeated observations.

There is an immediate and very practical difficulty with executing N^{th} Order uncertainty analysis: manufacturers of instruments do not describe the uncertainties in their products in the appropriate terms. It is necessary for the experimenter to assign the calibration uncertainty, based on whatever evidence can be assembled.

In critical situations, one can call for a detailed calibration of each instrument (i.e., the generation of a complete output-input response surface). This has the effect of identifying the individual instrument, to within the uncertainty interval of the standard instrument used in the calibration. If that uncertainty interval is less than about 1/3 or 1/4 of the stochastic uncertainty in the reading, $\delta x_{1,1}$, then the instrument calibration can be regarded as "certain." A complete data-reduction program, one which includes detailed calibration curves for every instrument, could then revert to a First-Order estimator and be subject only to First Order uncertainties.

Each replication level (Zeroth, First, and N^{th}) yields a different estimator of the experimental uncertainty (δR_0 , δR_1 , and δR_N). These have different uses, and quite properly have different values.

Uses of the Uncertainty Estimators of Various Orders

For every use, the principal feature is the same: iteration between the experiment and the uncertainty analysis to improve the control of the experiment. The uncertainty analysis allows the researcher to anticipate the scatter in the experiment, at different replication levels, based on present understanding of the system. Comparison of the achieved result with the expected result then gives either a check or a warning. If the achieved results contain no more deviation than predicted, a check of control is indicated. If the achieved results contain more than the predicted deviation, this constitutes a warning that the experiment contains some uncontrolled or unobserved element which is causing significant error; the experimenter can then take steps to correct the situation.

In the following paragraphs, the principal uses of each replication level will be discussed.

Zeroth Order. The calculated value δR_0 represents the minimum uncertainty in R which could be obtained. If the process were entirely steady, the results of repeated trials would lie within $\pm \delta R_0$ of their mean, approximately 95% of the time. No real experiment could do better than δR_0 . The Zeroth Order replication concept is mainly used as a planning tool, as one criterion for accepting a proposed set of instruments as being sufficiently readable for a planned experiment. If the desired result cannot be achieved with sufficient precision at Zeroth Order, then it cannot be achieved at all, and a different experimental approach should be selected.

Once an experiment has been put "on-line," if repeated trials display scatter which is significantly larger than $\pm \delta R_0$, this is evidence that there is significant unsteadiness in the process. The unsteadiness may be concealed, since it may be occurring in an unobserved variable. When this situation occurs, the observed instruments will be steady during each observation period, but the dependent variables will assume different values on repeated trials, even though the independent variables are held constant. If the standard deviation of the results is significantly larger than $1/2 \delta R_0$, then one must suspect a hidden variable. Unsteadiness in this sense includes lack of repeatability in start-up or reset control.

First Order: The calculated value of δR_1 , the First Order uncertainty, estimates the scatter in R which may be expected on repeated trials with the apparatus at hand, considering its documented timewise unsteadiness. The standard deviations of repeated trials would be equal to $1/2 \delta R_1$ if the data reduction program were sufficiently complete to acknowledge each physical mechanism which affected R . If the standard deviation of repeated trials is significantly larger than $1/2 \delta R_1$, then the process being observed is sensitive to variables which are not being accounted for in the data reduction program. Such an occurrence is a warning to the experimenter that diagnostic tests and development work on the test facility, control procedures, or data-reduction program are necessary.

As an example, suppose that the momentum thickness of a boundary layer was being calculated based only on velocity measurements—not accounting for density variations within the boundary layer which might be caused by small variations of wall temperature (reflecting, in turn, changes in ambient temperature during the conduct of the experiment). Actual results on successive trials would include not only the stochastic uncertainties inherent in measuring velocity and position, but also the "unrecorded" effects due to the density differences. As a consequence, the actual results would display a standard deviation greater than the predicted value of $1/2 \delta R_1$. This would be the warning that some mechanism was acting which was not being accounted for.

The First Order uncertainty interval is chiefly useful during the debugging phase of an experiment, when the test system is being developed. It is the principal quantitative tool for deciding when the experiment is sufficiently repeatable, that is, well controlled.

When the standard deviation on repeated trials is significantly larger than expected, based on the First Order uncertainty predicted, this is a warning that unobserved variables are affecting the outcome of the experiment. Diagnostic tests should then be conducted to identify the mechanism involved and to acknowledge that mechanism in the data-reduction program.

When the standard deviation of repeated trials is acceptably close to the First Order uncertainty prediction, then there is no further evidence of difficulty: the repeatability phase of development of the experiment can be considered complete.

It is important that the First Order intervals for the δx_i be set as small as can be justified by observations on the actual apparatus. If the $\delta x_{i,1}$ are taken larger than necessary then δR_1 will be too large, and the diagnostic development may be terminated while the experiment is still incompletely described by its data-reduction program. If, on the other hand, the δx_i are set unrealistically low, then a check on repeatability may never be achieved. Appropriate values for the $\delta x_{i,1}$ are thus the critical problem of experimental control.

Nth Order: The calculated value of δR_N , the Nth Order uncertainty, estimates the scatter in R which could be expected with the apparatus at hand if, for each observation, every instrument were exchanged for another unit of the same type. This estimates the effect upon R of the (unknown) calibrations of each instrument, in addition to the First Order component. The Nth Order calculations allows studies from one experiment to be compared with those from another ostensibly similar one, or with "true" values.

If the results from two different (but nominally identical) experiments disagree significantly, compared with their Nth Order uncertainty intervals, then either: (i) the two experiments are actually studying different situations; or (ii) at least one of the experiments is in error. Condition (i) might be generated, for example, by unmeasured differences in initial conditions in a free-shear layer.

The Nth Order uncertainty calculation must be used wherever the absolute accuracy of the experiment is to be discussed. First Order will suffice to describe scatter on repeated trials, and will help in developing an experiment, but Nth Order must be invoked whenever one experiment is to be compared with another, with computation analysis, or with the "truth."

It frequently occurs that inclusion of all of the instrument calibration uncertainties yields such a large value for δR_N that the experiment seems doomed from the beginning. In such cases, the only recourse is to reduce the Nth Order uncertainty

intervals by detailed calibrations of the most critical instruments. An important implication of Eq. (3) is that the uncertainties with large effect on the output are easy to identify, and should receive the most attention. At each stage of improvement, any term smaller than 1/4 of the largest term can usually be ignored. The same remark applies to calibration uncertainty as indicated by Eq. (5).

When the predicted uncertainty interval δR_N has been reduced to an acceptable value, then the experiment may be tested against some known "true" values. If the experiment returns the "true" value within $\pm \delta R_N$, it may be considered qualified for data production. If not, then further development is indicated. There are few "true" values known. The principal sources of "truth" are those described as Basic Principles:

$$\begin{aligned} \text{The Rate of Creation of Energy} &= 0 \\ \text{The Rate of Creation of } +x \text{ Momentum} &= g_c \sum F_{+x} \\ \text{The Rate of Creation of Mass} &= 0 \\ \text{The Rate of Creation of Entropy} &\geq \int \frac{dq}{T} \end{aligned}$$

Execution of a mass, momentum or energy balance on an apparatus, without knowledge of the expected N^{th} Order uncertainty, is an essentially useless enterprise. To reach any conclusions, one must have the ability to assess the significance of the difference between the observed value and the expected value. The N^{th} Order uncertainty analysis provides that ability.

In the absence of an applicable Basic Principle, one is frequently forced to use a secondary check: a baseline experiment. A baseline experiment is a data set which has so well stood the test of time that its validity is accepted by most workers in the field. Knowledge of the N^{th} Order uncertainty intervals for both experiments is necessary before the significance of any difference between the observed and expected values of R can be assessed.

DEVELOPMENT OF A ZERO-CENTERED EXPERIMENT

Industrial performance testing is faced with the problem of combining "fixed errors" and "random errors" in the uncertainty descriptions, because there is no opportunity to revise the experiment structure to remove the fixed errors. In industrial testing, results may be allowed to retain residual bias such that even the mean of many repeated trials (an N^{th} Order replication) might still be in error.

Many research experiments can be refined using instrument calibrations, and diagnostic tests, such as energy balances, etc., and N^{th} Order uncertainty analysis until the experimental value agrees with the true value within the expected uncertainty. In such cases, the experiment can be considered to be substantially free of fixed error. Such an ideal state can be called a Zero-Centered experiment.

The goal of most research is to conduct Zero Centered experiments.

UNCERTAINTY ANALYSIS ON COMPUTER-BASED DATA-REDUCTION PROGRAMS

It is impractical to execute an uncertainty analysis analytically for any but relatively simple cases. Complex data-reduction programs may involve many corrections to the data and use implicit forms or table look-ups or numerical integration within the program. In such cases, the uncertainty-analysis program might be larger than the main program--certainly an unacceptable burden on the experimenter.

It is a simple matter, however, to do uncertainty analysis on any computer-based data-reduction program, no matter how complex, if the estimates of the δx_i are provided as data for the program in addition to the usual data. If the main program is regarded as a subroutine, it can be called by a Jitter Program, which sequentially indexes each input bit and computes the resulting contribution to the uncertainty in R. A Jitter Program need not be very complex, since it simply controls the main data-reduction program. To illustrate this, a typical Jitter Program is shown in Fig. 1. This example was written for a hand calculator, a TI-59, to illustrate the compactness of the Jitter Program approach, but the flow diagram would be the same for any computer or calculator. Even this simple hand-calculator can handle a data-reduction program involving up to ten variables. The central argument is that:

$$\frac{\partial R}{\partial x_i} \approx \lim_{\Delta x_i \rightarrow 0} \left(\frac{R_{x_i + \Delta x_i} - R_{x_i}}{\Delta x_i} \right) \quad (6)$$

In operation, the program first calculates the best estimate, R_0 , using the input data provided. Then the first variable, x_1 , is indexed by a small amount, ϵx_1 , and a new value, R_1 , calculated. Using the difference $(R_1 - R_0)$, and the value of ϵx_1 , the value of $\partial R / \partial x_1$ is calculated, and the contribution to δx_1 is found from $(\partial R / \partial x_1)(\delta x_1)$ using the value of δx_1 provided. Either forward or central difference estimators of $\partial R / \partial x_1$ may be used. This process is repeated for each variable, and the contributions squared and accumulated.

The values of the ϵx_i may be taken arbitrarily small, in which case the best estimate of the true value of the $\partial R / \partial x_i$ will be found, as in the case illustrated in Fig. 1. On the other hand, it is often justified to use $\epsilon x_i = \delta x_i$.

Once the Jitter Program has been installed, it is a simple matter to obtain the Sensitivity Coefficients, the individual contributions to the overall uncertainty, and the relative and absolute uncertainties in the results.

x_1 -Sensitivity Coefficient	$\Delta = \partial R / \partial x_1$
x_1 -Contribution	$\Delta = (\partial R / \partial x_1) \delta x_1$
Relative Uncertainty	$= \delta R / R$
Absolute Uncertainty	$= \delta R$

Such a program need only be devised once and can then be incorporated in each data-reduction program as a routine addition. Graphics output with error bars and warning flags triggered by high uncertainty values are obvious extensions of this capability. They advise the user that the experiment has moved into a region of variables producing unacceptable output uncertainty (as often occurs at some point). Without this procedure such regions are easily overlooked.

DEFINING THE N^{th} ORDER UNCERTAINTY IN A MEASUREMENT

The intent of the N^{th} Order uncertainty estimator is to account for both the uncertainty of the calibration and the stochastic uncertainty due to unsteadiness.

Consider the reading of a single instrument. It is presumed to fluctuate, over some observation period, about a mean value which may or may not be correct. The reading can be described as a function of time, as:

$$x_j = x^* F_j f(t) \quad (7)$$

where

- x^* = the "true" value, presumed constant,
- F_j = a calibration factor of the instrument, so defined that $\bar{x} = x^* F_j$, where \bar{x} is the mean value of a large number of observations with the j^{th} instrument,
- $f(t)$ = a temporal instability function, having a time average value of unity,
- x_j = The time-varying indication of the j^{th} instrument.

Consider now a single observation of the j^{th} instrument--the i^{th} observation:

$$x_{i,j} = x^* F_j f(i) \quad (8)$$

where $f(i)$ = the value of $f(t)$ at the instant of the i^{th} observation.

The relative uncertainty in $x_{i,j}$ can be written formally as:

$$\frac{\delta x_{i,j}}{x_{i,j}} = \left(\left(\frac{\delta F_j}{F_j} \right)^2 + \left(\frac{\delta f(i)}{f(i)} \right)^2 \right)^{1/2} \quad (9)$$

It remains to show that this form has physical significance, and utility.

The functions F_j and $f(t)$ can each be regarded as having a mean value which is 1.000, with normal distributions about this mean. Let δF_j and $\delta f(t)$ equal twice the standard deviations of these functions. It can be safely assumed that instrument manufacturers describe the mean calibration of their instruments as well as possible, and that there is a normal distribution of the individual calibrations around the mean. It is also apparent that the observer will make every effort to record the mean value of a fluctuating sequence of values, so that $\bar{f}(t)$, an average, will have a value of 1.00.

If these assumptions are correct, then δF_j stands for the uncertainty in calibration of the individual instrument used, and $\delta f(i)$ stands for the temporal component of the recording uncertainty.

Equation (9) thus accounts for the overall uncertainty in a single observation from a single instrument.

Rearranging and interpreting the terms shows the basis for the current treatment of the N^{th} Order uncertainty estimate for single-sample experiments:

$$\delta x_{1,j} = \left\{ \left(x_{1,j} \frac{\delta F_j}{F_j} \right)^2 + \left(x_{1,j} \frac{df(1)}{f(1)} \right)^2 \right\}^{1/2} \quad (10)$$

where $x_{1,j} \frac{\delta F_j}{F_j}$ = the uncertainty in the value of $x_{1,j}$ caused by the uncertainty in calibration $\delta F_j/F_j$; i.e., $\delta x_{1,\text{cal}}$.

and $x_{1,j} \frac{df(1)}{f(1)}$ = the uncertainty in the value of $x_{1,j}$ caused by the uncertainty in the temporal instability term; i.e., $\delta x_{1,1}$.

This can be written as:

$$\delta x_{1,j} = \left\{ (\delta x_{1,\text{cal}})^2 + (\delta x_{1,1})^2 \right\}^{1/2} \quad (11)$$

Once again, it must be emphasized that $\delta x_{1,\text{cal}}$ is hard to identify. Most manufacturers are reluctant to describe their product in such terms, and frequently the experimenter must simply estimate this term, based upon experience or, at best, a few hints in the manufacturers' literature. As already suggested, use of such estimates is better than total lack of uncertainty analysis.

Applications for the Comparison of Experiment and Computation

Ideally, all the experiments used as the basis for model formation and comparison to computation would have well-established values of δR_N . In reality, this is not the case for most existing data sets, partly because of the difficulty of doing the analysis for complex experimental programs. Given the methods of this paper, well-established values of δR_N become feasible for future "record" experiments and are strongly recommended as a criterion for acceptance of such future "record" data.

When well-established values of δR_N are known, assessment of the degree of agreement between data sets and between experiment and computation becomes both easier and more clear-cut. Two data sets "agree" when the data do not differ by more than the root-sum-square of the δR_N for the two experiments. The δR_N will in general be different for the two experiments, owing to different instruments and reduction programs; but when the two are roughly the same, disagreements larger than $1.4 \delta R_N$ indicate some difference in experiments, or uncontrolled variable. When one δR_N is significantly larger than the other, disagreement beyond the larger value is the relevant test. These remarks apply point by point wherever the δR_N are known. For points where agreement is found, one can conclude that the results are consistent, and that the presumed correct value does not differ from the mean by more than the root-sum-square δR_N for the two data sets.

When there are more than two data sets, the same principle can be extended. If, in a group of seven data sets, all the data lie within the uncertainty band found from the square-root of the sum-squares of the δR_N for all the sets, then a correlation band has been established. If two or three of the sets have smaller δR_N than the others, and agree with each other within that uncertainty, a tighter correlation band can be formed.

Comparisons of computation with experiments could proceed on the assumption that differences between computation and experiment that exceed the value of δR_N for the data are attributable to approximations in either the model or the numerical procedure.

When only partial or rough estimates of the δR_N are known, the principles remain the same, but it becomes necessary to use judgment case by case.

Another use for the methodology of this paper is in application of criteria for evaluating data sets. As noted above, the data can be tested against known theory, as for example a check of the right- and left-hand side of the momentum integral equation for shear layers. Since the measurement of some of the terms in the momentum equation typically have large uncertainties, it would be easy to conclude that the flows were three-dimensional, when in fact they were not. Specifically, disagreement by an amount less than the value of δR_N must be regarded as agreement, even though the disagreement might look large. The methodology of this paper can be applied to make such judgments both more specific and more meaningful than has been possible in the past.

CONCLUSION

Uncertainty analysis is a powerful diagnostic tool, useful during the planning and developmental phases of an experiment. Uncertainty analysis is also essential to rational evaluation of data sets, to comparison of one data set with another, and to checking computations against data.

Three conceptual levels of replication can be defined: Zeroth, First, and Nth Order. These levels of replication admit of different sources of uncertainty:

Zeroth Order:

- Includes only interpolation uncertainty.
- Useful chiefly during preliminary planning.

First Order:

- Includes unsteadiness effects, as well as interpolation.
- Useful during the developmental phases of an experiment, to assess the significance of scatter and to determine when "control" of the experiment has been achieved.

Nth Order:

- Includes instrument calibration uncertainty, as well as unsteadiness and interpolation.
- Useful for reporting results and assessing the significance of differences between results from different experiments and between computation and experiment.

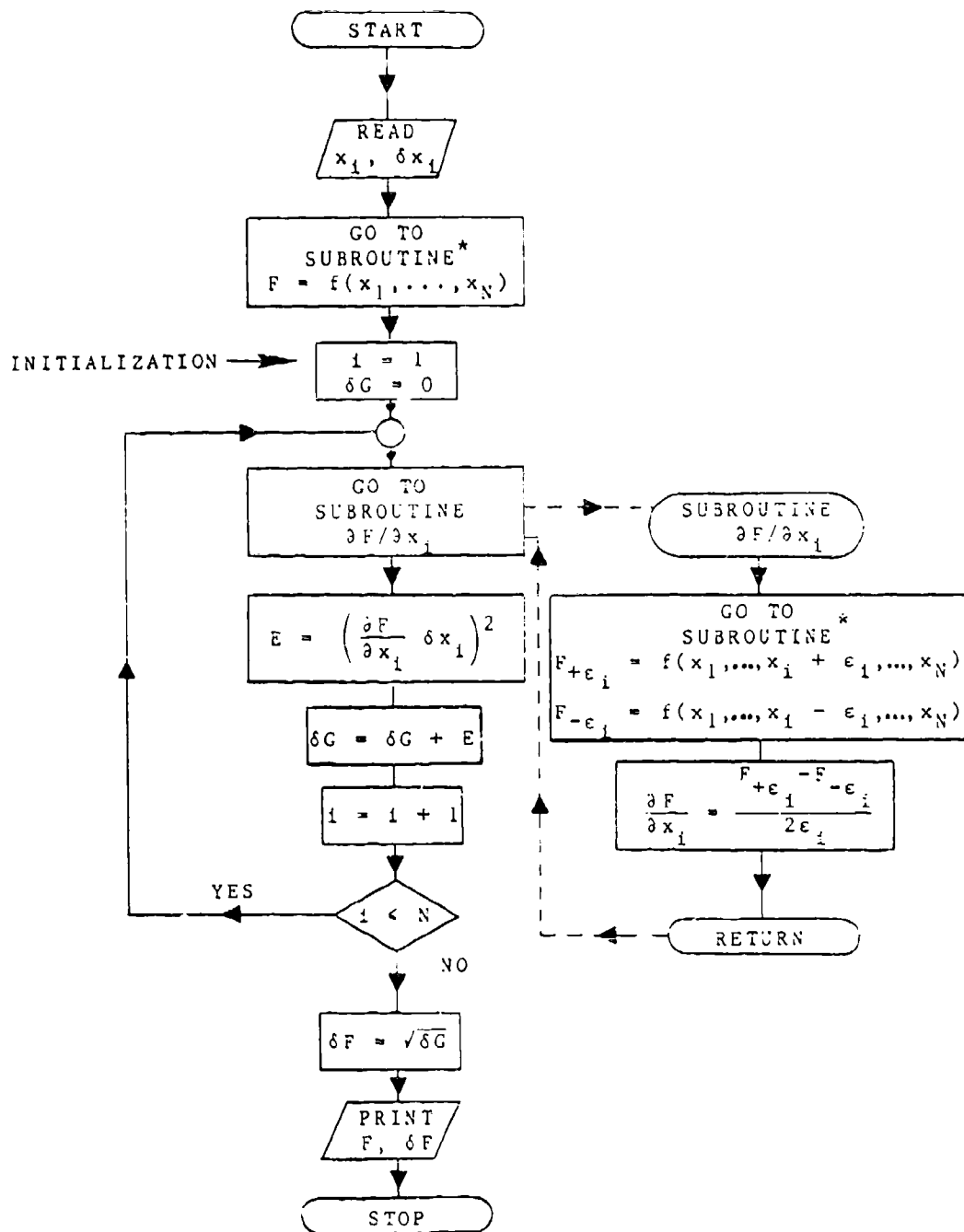
The basic combinatorial equation is the Root-Sum-Square:

$$\delta R = \left[\left(\frac{\partial R}{\partial x_1} \delta x_1 \right)^2 + \left(\frac{\partial R}{\partial x_2} \delta x_2 \right)^2 \dots \left(\frac{\partial R}{\partial x_N} \delta x_N \right)^2 \right]^{1/2}$$

The process is easily adapted to computer-based data reduction programs. A sequential jitter package can be written in standard form which uses the existing data reduction program to execute the uncertainty analysis, obviating the need for a separate analysis. The additional computing time is usually not excessive.

REFERENCES

1. International Organization for Standardization (ISO) Standard ISO-5168, "Measurement of Fluid Flow - Estimation of Uncertainty of a Flow Rate Measurement," ISO 5168-1978(e), p. 8.
2. ASME Committee MFFCC SCI, "Fluid Flow Measurement Uncertainty--Draft of 26 March, 1980," American Society of Mechanical Engineers, Codes and Standard Department, p. 14.
3. USAF AEDC-TR-73-5, "Handbook on Uncertainty in Gas-Turbine Measurements," AD 755356.
4. JANNAF, "ICRPG Handbook for Estimating the Uncertainty in Measurements Made with Liquid Propellant Rocket Engine Systems," CPIA Publication 180, AD 851127.
5. S. J. Kline and F. A. McClintock, "Describing Uncertainties in Single-Sample Experiments," Mechanical Engineering, Jan. 1953.
6. Thomas, H. A., in Marks Mechanical Engineers Handbook, Sixth Edition, Ch. 17, p. 26, McGraw-Hill Book Co. (1964 printing, ed. T. Baumeister).



*Existing data-reduction routine
for calculating parameter F.

Fig. 1. Flow diagram for jitter program.

THE DATA LIBRARY

Brian Cantwell^{*}



I. INTRODUCTION

One of the major tasks of the 1980 conference is the creation of a library of recommended flows. The library consists of experimental data from a variety of flows which has been organized, formatted and placed onto magnetic tape. Although the data covers a broad range, from many sources with many geometries, using many techniques for data taking and data reduction, an attempt has been made to achieve uniformity, consistency and completeness in the information which has been placed onto tape. The task has been largely an organizational one and often considerable ingenuity has been required to organize data sets to follow a common format.

The data as accepted by the 1980 conference have not been enhanced or altered in any way. Use of the data to compute stress profiles, pressures, skin-friction coefficients, thicknesses or any other quantity not explicitly provided by the evaluator has been left to the computer. Moreover, no smoothing or interpolation algorithms have been applied to the data.

At the very least, the data library is intended to provide computers with easy access to data which are also accessible in other forms. Ultimately, the library will be more than a mere convenience. It represents a growing string of useful data in one format gathered in one place, and, like any organized juxtaposition of useful facts, it can be a source of inspiration and new ideas. The data library contains only data sets that have been reviewed by a number of workers among whom there is consensus that they represent as good data as are available in the given class of flow, and about which reservations and uncertainty in the results are stated insofar as they are known. Only data sets that are sufficiently complete that a computational "trial" can be constructed are included. Data sets cover information that bears on both creating models for computer simulation and for checking output from computation. Data can also be used as input to engineering procedures. In many instances, the completion of the data files have required procurement of added information and clarification of questions by the original "data-takers." Data sets this complete would thus be hard for individual computers to accumulate.

During the work of establishing the library and writing "specifications" for computational trials in 1979 and 1980, a considerable amount was learned concerning

^{*}Department of Aero. and Astro., Stanford University, Stanford, CA 94305.

standards and requirements for data intended to be used as the basis for computer models or computational trials. These requirements have been incorporated into guidelines for future additions to the library (see Section VI below).

The data library is not viewed as "cast in concrete"; rather it is intended as a current collection that will be improved over time. The procedures for future improvements are also described below.

II. HOW TO GET THE TAPE

The data tape (hereafter referred to as Library I) will be available from one of the following three locations:

American users write to:

AFOSR-STANFORD DATA LIBRARY
c/o Brian Cantwell
371 Durand Building
Stanford University
Stanford, CA 94305

European users write to

DFVLR
c/o H. U. Meier
Forschungsbereich Strömungsmechanik
Institut für Experimentelle Strömungsmechanik
Bunsenstrasse 10, 3400 Göttingen, Germany
Telephone (05 51) 70 91; Telex 6 839

or

Netherlands National Aerospace Laboratory
c/o Mr. F. J. Hoorema
P. O. Box 153
8300 AD Emmeloord, The Netherlands
Telephone 05274-2828

Prices will vary from one agency to another and from time to time, but in general the cost should be less than \$200.00.

III. READING THE TAPE

Library I has been created by an IBM system 370 computer. It contains only formatted data. The tape is a 2400-ft, 9-track, phase-encoded odd-parity, unlabeled tape written at a density of 1600 bits per inch according to EBCDIC code. The record format is fixed and blocked; record length = 80 bytes; 100 records per block; blocksize = 8000 bytes. The appropriate job control statements for reading the tape using an IBM system are:

```
//GO.FT23F001 DD UNIT = T1600, VOL = SER = (LIBRARY I),  
// DISP = (OLD,KEEP),DCB = (RECFM = FB,LREC = 80,BLKSIZE = 8000,DEN = 3)  
// LABEL = (1,NL)
```

The key quantity in the above control statements is the DCB parameter which designates the exact form of the data on the tape. For a more detailed discussion of the DCB parameter, see Appendix I.

IV. FILE 1

Each case on the magnetic tape consists of two or more files of information. File 1 contains a detailed description of the given case. This is followed by one or more files of normalized data. A sample File 1 for Case 8631 is included as Appendix II. File 1 contains 11 sections broken down as follows.

- 1) Flow title: This includes the name of the author(s) who originally created the data along with the flow case number and a brief descriptive title consistent with the descriptor for the flow class used in the 1980-81 AFOSR-HTTM-Stanford Conference on Complex Turbulent Flows.
- 2) Revision date: This refers to the date of the most recent revision of File 1.
- 3) Evaluator: The name and address of the evaluator who is responsible for recommending the data set to the 1980-81 conference.
- 4) Experiment location and date: This item gives the institution and, where possible, the apparatus where the data set was created. The date is an approximate time when the measurements were actually made. The purpose of providing this information is to give the computer an idea of the age of the data vis-a-vis measurement capabilities of the time.
- 5) Abstract of the experiment: This is a brief description of the experiment along with any peculiarities of the work which may be of importance in deciding how to make use of the data.
- 6) References: Several references are usually included. Along with the reference which contains the raw data, any references to instrumentation techniques used are usually included.
- 7) Instrumentation: A brief description of the methods and equipment used to take the data.
- 8) Experimental parameters: This is a listing of numerical values of important constants of the experiment, including such things as tunnel dimensions, free stream velocity, Mach number, etc.
- 9) Measured variables: This section is a list of all of the measured or inferred variables of the experiment. The list also serves as nomenclature for data found in files 2 on.

- 10) Measurement uncertainty: This is a summary of measurement uncertainties as provided by the evaluator.
- 11) Tape organization: This is the key item in File 1. It contains a detailed description of all of the tape files for the given case. It also contains a short sample program which can be used to read and write a file. All data are in dimensionless, normalized form. That is, any variable is first nondimensionalized by the appropriate parameter of the experiment (for example, a power of the free stream velocity). Maximum and minimum values (X_{\max} and X_{\min}) of the dimensionless variable are determined for the given file. These are used to normalize each data point, $X_{\text{dimensionless}}$, as follows:

$$X_{\text{normalized}} = \frac{X_{\text{dimensionless}} - X_{\min}}{X_{\max} - X_{\min}}$$

X_{\max} and X_{\min} are written in "E" format as the first several records at the head of the file. The remaining records of the file are written as normalized data in the range 0 to 1.0. Each tape record is written as a card image (hence record length = 80 bytes in the DCB parameter). To provide data compression and to permit the maximum number of variables to be written into an 80-byte length, it was found useful in many cases to integerize the normalized data before they were written onto the tape. In these cases, $X_{\text{normalized}}$ was multiplied by 10,000 and rounded up or down to the nearest integer to produce $IX_{\text{normalized}}$. In these cases the normalized data were written onto tape as integers in the range from 0 to 10,000. All null data were written as 2.0 or in the case of integerized data as 20,000. In any case, item 11 contains a detailed description of how the data for that particular case were normalized and integerized. In addition to the above information, item 11 contains a description of each file, including number of records, contents per the nomenclature in item 9, format (usually E13.6 or I6) and comments.

V. NOMENCLATURE

Although each case is self-contained, with its own nomenclature listed in item 9 of each File 1, we have also tried, as far as possible, to retain a common nomenclature for all cases (see general nomenclature). It is essentially an extended version of the nomenclature found in Coles and Hirst.*

*Coles, D. E., and E. Hirst, Proceedings of the 1968 AFOSR-IFP-Stanford Conference on Computation of Turbulent Boundary Layers, Vol. II.

VI. FUTURE ADDITIONS TO THE DATA LIBRARY

Additions to Library I will continue up to November 1, 1981, at which time the tape will be submitted to the holding organizations. Future editions of the tape library will be issued as appropriate. Present plans are to continue to update the library for an indefinite period of time beyond October 1, 1982. If it can be continued, the library can become an important part of world-wide efforts to compute turbulent flows. It will be both a service and a responsibility, for the library cannot continue without the generous efforts of evaluators throughout the fluid mechanics community who may be called upon to assess the suitability of new data sets. Here it can be noted that eventually the library will also be of use to experimentalists who wish to search the literature on a particular flow looking for common effects or correlations in the data; for this purpose the full evaluation reports will also be useful (see Introduction in this volume).

Future additions to the library must meet conditions similar to those evolved for the 1980-81 conference as follows:*

- 1) Evaluation and review by at least two experts not associated with the data taking.
- 2) The results of the data evaluation should include an explicit statement of the criteria employed in selecting the data.
- 3) The data should be completely documented, including:
 - (a) A complete list of references containing the data.
 - (b) A detailed uncertainty analysis. This should include a description of the method used, sufficient to make the analysis reproducible by a person knowledgeable in the state of the art.
 - (c) A 3- to 5-page summary of the data suitable for publication.
 - (d) A suggested form for item 11 of File 1 (tape organization) which can be used to guide the tape processing operation.
 - (e) Specification of a computational trial (see examples in this volume).
 - (f) A complete list giving the values of reference lengths, velocities, and pressures used to normalize the data. All numbers should be expressed in SI units (kilogram/meter/second, pressure in pascals N/m^2).
 - (g) A complete list giving the numerical range for each experimental variable.

*[Ed.: The conditions for adding cases to the Data Library are still under consideration and a final set of rules has not yet been established. Investigators wishing to submit data for consideration should write for further information to Brian Cantwell at the address given on page 58.]

- (h) A complete list of all variables used in the experiment, along with a specification of the coordinates used. The nomenclature listed above should be used where possible.
- (i) A drawing of the experimental set-up would be very helpful.
- 4) Data in machine readable form are preferred (tape, cards, disc, etc.). However, plots and lists can also be accommodated. If the data are submitted as lists or plots, they should be provided in a form suitable for a published volume of the meeting. Axes should be labeled and lists should be headed using the general nomenclature.

VII. THE CONTENTS OF LIBRARY I

An index to the tape is included at the end of this volume (pages 624 to 632). The index lists the flow cases numerically and gives the contents of Library I by number of files and relative file numbers for each case in cols. 4-5. A similar index is also included as the very first file on the tape.

VIII. ACKNOWLEDGMENT

I would like to express thanks to the many people who helped create Library I, especially the students who carried out the difficult task of processing data sets. Most of the thanks goes to Tony Strawa and Ram Subbarao who processed the bulk of the data. Several data sets were processed by Jim McDaniel, Ranga Jayaraman and Bob Carella. More recently the data processing has been carried on by Jim Taleghani, Ken Schultz, and Charles Narty. While sometimes tedious and frustrating, the work was always educational; they were often forced to seek out and read original references before they could proceed. Without their energy and enthusiasm, the data library would not have been possible.

APPENDIX I
Rangarajan Jayaraman

SIMPLIFIED GUIDE TO THE DCB PARAMETER

RECFM, LRECL and BLKSIZE subparameters of DCB parameters in DD JCL statements

The DCB parameter in a DD statement can be a source of confusion to many programmers. This is a brief and simplified writeup on RECFM, LRECL, and BLKSIZE subparameters in DCB. For more detailed information, consult IBM Fortran and JCL manuals. All "lengths" in this writeup are in units of bytes.

Input/Output Terminology

Input/Output (I/O) is performed by READ/WRITE statements in Fortran. An I/O controlled by a FORMAT statement is a "formatted I/O." If there is no FORMAT statement associated with an I/O, then it is an "unformatted I/O." The list of variables to be transferred by an I/O statement is called the "I/O list." An I/O list defines an "actual record." A FORMAT statement defines a "Fortran record." A "block" of records is a number (≥ 1) of Fortran records grouped together. A number of blocks grouped together to form a meaningful set is a "data set." The number used in referring to a data set is its "data set reference number." If records 1 through n-1 are to be accessed before record n can be accessed in a data set, then it is a "sequential access data set." A data set is a "direct access data set" if records in it can be accessed randomly. Direct access data sets can only reside on disks. Data sets on tapes are necessarily sequential access data sets.

RECFM

The "record format" of the data set refers to the physical layout of records within it. The following are a subset of all possible record formats.

- F - fixed length records
- V - variable length records
- FB - fixed length records grouped in blocks
- VB - variable length records grouped in blocks
- U - undefined (none of above)

Data sets referred to by unformatted I/O can only be under the variable length category. Direct access data sets can only be fixed and unblocked.

LRECL and BLKSIZE

Associated with each formatted I/O statement are two lengths: "actual record length" determined by the I/O list and "Fortran record length" determined by the corresponding format statement. The "logical record length" or LRECL parameter is related to the Fortran record length. Data transfer from/to an I/O device takes place

in so called "blocks" and the maximum "block size" or BLKSIZE is dependent on the device/computer combination. The computer comes in here because data are written first in a segment of memory with the same size as BLKSIZE; when it is "full," it is transferred as a block to the device. Thus BLKSIZE is also the size of the "buffer" in the computer memory. The parameter LRECL and BLKSIZE convey to the computer information regarding Fortran record length and buffer size. The record format determines what is specified and how.

<u>RECFM</u>	<u>LRECL</u>	<u>BLKSIZE</u>
F	not specified	maximum Fortran length LRECL +4
V	maximum Fortran length +4	LRECL +4
FB	maximum Fortran length	$N * LRECL, n = \text{integer} \geq 1$
VB	maximum Fortran length +4	$4 + n * LRECL, n = \text{integer} \geq 1$
U	not specified	maximum Fortran length

Notes: The BLKSIZE chosen in FB and VB should reflect the compromise between reduction of number of accesses to the device and the increase in buffer size, reducing core available for program use. Different FORMAT statements with possibly different FORTRAN record lengths can refer to the same data set. The longest of the Fortran record lengths associated with a data set as its "maximum Fortran length".

The physical organization of data in the device is as shown in Fig. 1. Blocks of data are separated by so-called "inter-block gaps," to provide synchronization, to enable start/stops, and to provide the required latency.

The actual record length can be less than, equal to or greater than maximum Fortran length. The way actual data are written into the buffer and the way the buffer is transferred onto the device depends on the record format. Fig. 2 illustrates the various cases. All data processed onto tape for the 1980 Conference use DCB=(RECFM=FB, LRECL=80, BLKSIZE=8000, DEN=3).

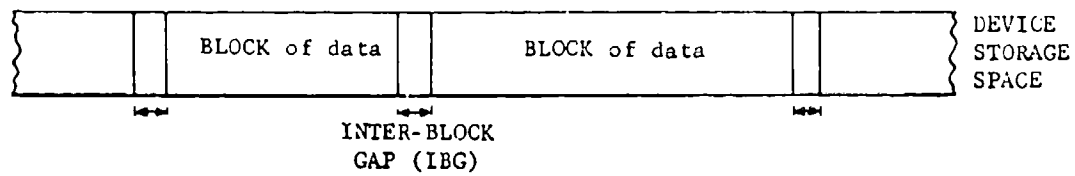


Figure 1

LR - Logical Record

BD - Block Descriptor
Word (4 bytes)

AR - Actual Record

SD - Segment D

B - Buffer or Block

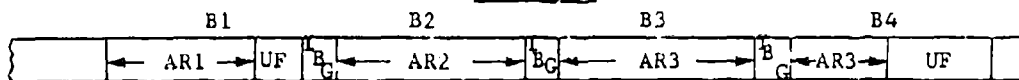
UF - Blanks

RECFM = F

IN CORE

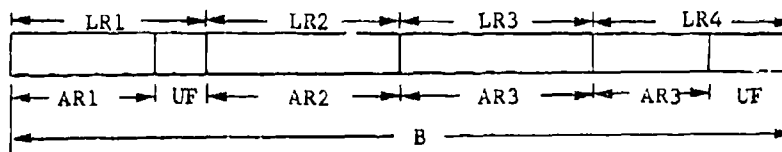


IN DEVICE



RECFM = FB

IN CORE



IN DEVICE

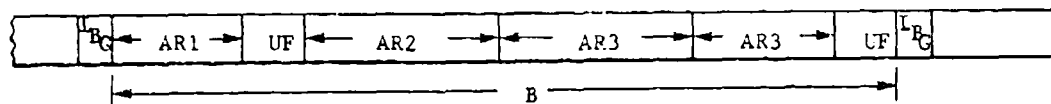
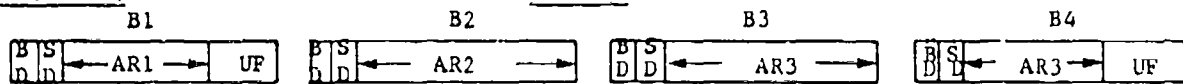
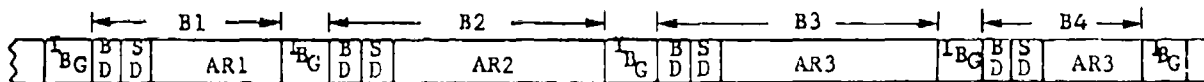


Figure 2 (cont.)

RECFM = V

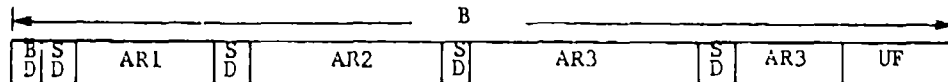


IN DEVICE



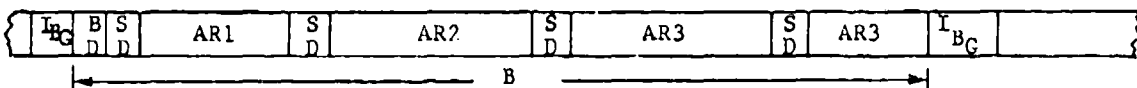
RECFM = VB

IN CORE



B is considered "full" if $UF < LRECL$
and next block is started

IN DEVICE



RECFM = U

IN CORE



IN DEVICE

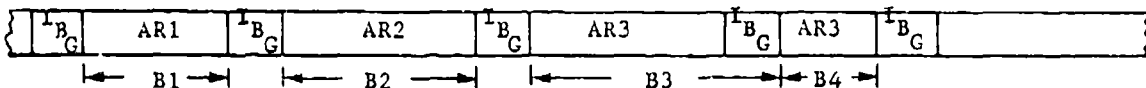


Figure 2 (end)

APPENDIX II. Sample File 1

1. FLOW TITLE: CASE 8631; SETTLES, G. S., FITZPATRICK, T. J. AND BOGDONOFF, S. M.; "ATTACHED AND SEPARATED COMPRESSION CORNER FLOWFIELDS IN HIGH REYNOLDS NUMBER SUPERSONIC FLOW",
2. REVISION DATE: NOVEMBER 18, 1980
3. EVALUATORS: RUBESIN, M. W. AND HORSTMAN, C. C., NASA AMES RESEARCH CENTER, MOFFETT FIELD, MOUNTAIN VIEW, CA 94035
4. EXPERIMENT LOCATION AND DATE: GAS DYNAMICS LABORATORY, FORRESTAL CAMPUS, PRINCETON UNIVERSITY, PRINCETON, NJ 08544

5. ABSTRACT OF EXPERIMENT:

THESE RESULTS FOLLOW AN EXTENSIVE STUDY OF SHOCK WAVE / TURBULENT BOUNDARY LAYER INTERACTIONS AT TWO-DIMENSIONAL COMPRESSION CORNERS. THE CORNER MODELS WERE MOUNTED ON THE FLOOR OF THE PRINCETON UNIVERSITY 0.2 X 0.2 M HIGH REYNOLDS NUMBER SUPERSONIC BLOWDOWN WIND TUNNEL. THE TEST MACH NUMBER WAS 2.8 TO 2.9, AND THE FREE-STREAM UNIT REYNOLDS NUMBER WAS $6.3E+07/M$. FLOWFIELD DATA ARE PRESENTED HERE FOR COMPRESSION CORNER ANGLES OF $\alpha=8$ DEGREES (CASE A), 16 DEGREES (CASE B), 20 DEGREES (CASE C), AND 24 DEGREES (CASE D). CASE A IS A FULLY ATTACHED FLOW, WHILE CASE B IS NEAR INCIPIENT SEPARATION. CASES C AND D BOTH INVOLVE SEPARATED FLOW AT THE CORNER LOCATION. SURFACE AND FLOWFIELD MEASUREMENTS ARE GIVEN AT SELECTED STATIONS THROUGHOUT EACH INTERACTION. FINALLY, ADDITIONAL DATA SETS (CASES E-H) INCLUDE WALL PRESSURE MEASUREMENTS AND SEPARATION AND REATTACHMENT LOCATIONS FOR THE 20 DEGREES COMPRESSION CORNER OVER A REYNOLDS NUMBER RANGE, BASED ON INCOMING BOUNDARY LAYER THICKNESS, OF $0.8E+06$ TO $7.6E+06$.

THE X COORDINATE IS DEFINED IN THE STREAMWISE DIRECTION ALONG THE SURFACE OF THE WIND TUNNEL WALL AND THE COMPRESSION RAMP. THE ORIGIN OF X IS AT THE COMPRESSION CORNER; THUS, ALL LOCATIONS UPSTREAM OF THE CORNER BEAR NEGATIVE X-VALUES, WHILE ALL THOSE ON THE RAMP BEAR POSITIVE VALUES. THE Y COORDINATE IS ZERO ON THE TEST SURFACE AND POSITIVE ABOVE IT, AND IS ORIENTED WITH RESPECT TO THE TEST SURFACE ACCORDING TO THE TABLE GIVEN BELOW.

CASE	X RANGE	Y ORIENTATION
A	LESS THAN OR	VERTICAL
	EQUAL TO 0.0254 M	
	GREATER THAN	
B	0.0254 M	NORMAL TO RAMP SURFACE
	LESS THAN 0.0 M	
	GREATER THAN OR	
C	EQUAL TO 0.0 M	NORMAL TO RAMP SURFACE
	LESS THAN OR	
	EQUAL TO 0.0127 M	
D	GREATER THAN	VERTICAL
	0.0127 M	
	LESS THAN OR	
	EQUAL TO 0.0102 M	NORMAL TO RAMP SURFACE
	GREATER THAN	
	0.0102 M	

6. REFERENCES:

1. SETTLES, G. S. "AN EXPERIMENTAL STUDY OF COMPRESSIBLE TURBULENT BOUNDARY LAYER SEPARATION AT HIGH REYNOLDS NUMBER,"

PH.D. DISSERTATION, AFROSPACE AND MECHANICAL SCIENCES DEPARTMENT, PRINCETON UNIVERSITY, PRINCETON, NJ, SEPTEMBER 1975.

2. SETTLES, G. S., BOGDONOFF, S. M. AND VAS, I. E., "INCIPIENT SEPARATION OF A SUPERSONIC TURBULENT BOUNDARY LAYER AT HIGH REYNOLDS NUMBERS," AIAA JOURNAL, VOL. 14, JANUARY 1976, PP. 50-56.

3. SETTLES, G. S., VAS, I. E., AND BOGDONOFF, S. M., "DETAILS OF A SHOCK-SEPARATED TURBULENT BOUNDARY LAYER AT A COMPRESSION CORNER," AIAA JOURNAL, VOL. 14, DECEMBER 1976, PP. 1709-1715.

4. HORSTMAN, C. C., SETTLES, G. S., VAS, I. E., BOGDONOFF, S. M. AND HUNG, C. M., "REYNOLDS NUMBER EFFECTS ON SHOCK-WAVE TURBULENT BOUNDARY LAYER INTERACTIONS," AIAA JOURNAL, VOL. 15, AUGUST 1977, PP. 1152-1158.

5. SETTLES, G. S., FITZPATRICK, T. J. AND BOGDONOFF, S. M., "DETAILED STUDY OF ATTACHED AND SEPARATED COMPRESSION CORNER FLOWFIELDS IN HIGH REYNOLDS NUMBER SUPERSONIC FLOW," AIAA JOURNAL, VOL. 17, JUNE 1979, PP. 579-585.

7. INSTRUMENTATION:

WALL STATIC PRESSURE DISTRIBUTIONS WERE SENSED THROUGH ORIFICES INSTALLED IN THE COMPRESSION CORNER MODELS. SKIN FRICTION WAS ESTIMATED BY PRESTON TUBE MEASUREMENTS. SEPARATION AND REATTACHMENT LOCATIONS WERE FOUND FROM SURFACE STREAK METHODS AND WERE CONFIRMED BY THE OTHER MEASUREMENTS. MEAN FLOW PROFILES WERE OBTAINED FROM SURVEYS OF PITOT PRESSURE, STATIC PRESSURE, AND TOTAL TEMPERATURE.

8. EXPERIMENTAL PARAMETERS:

IN ALL CASES THE INFINITY CONDITIONS ARE DEFINED IN TERMS OF BOUNDARY LAYER EDGE AT $X = -0.5$ M (THE INCOMING TURBULENT BOUNDARY LAYER AND FREE STREAM JUST BEFORE THE BEGINNING OF THE INTERACTION). FLOWFIELD PROFILES FOR CASES A-D ARE GIVEN BELOW.

TEST CONDITIONS	CASE A	CASE B	CASE C	CASE D	COMMENTS
XMINF	2.87	2.85	2.79	2.84	MACH NUMBER
ALPHA (DEG.)	8.0	16.0	20.0	24.0	CORNER ANGLE
REINF/M	6.3E+07	6.3E+07	6.3E+07	6.3E+07	UNIT REYNOLDS NO.
TTOT (DEG. K)	280	258	258	262	TOTAL TEMP.
TW (DEG. K)	291	282	274	276	WALL TEMP.
TINF (DEG. K)	106	102	101	100	STATIC TEMP.
UINF (M/S)	592	576	562	569	VELOCITY
PIKF (N/M**2)	2.3E+04	2.4E+04	2.6E+04	2.4E+04	STATIC PRES.
DELINF (M)	0.026	0.026	0.025	0.023	B. L. THICK.
DELSINF (M)	0.0067	0.0063	0.0066	0.0061	DISP. THICK.
THETAINF (M)	0.0013	0.0013	0.0013	0.0012	MOM. THICK.
L (M)	1.98	1.98	1.98	1.98	DIST. FROM. COMP. CORNER TO NOZZLE THREAT

FLOWFIELD PROFILES ARE ALSO GIVEN BELOW FOR THE ADDITIONAL CASES E-H.

TEST CONDITIONS	CASE E	CASE F	CASE G	CASE H
XMINF	2.95	2.96	2.90	2.88
ALPHA (DEG.)	20.0	20.0	20.0	20.0
REINF/M	6.3E+07	3.1E+08	3.1E+08	3.1E+08
TTOT (DEG. K)	272	268	275	277
TW (DEG. K)	286	281	289	291

TINF (DEG. K)	99	97	103	104
UINF (M/S)	589	585	589	589
PINF (N/M**2)	2.1E+04	9.8E+04	1.1E+05	1.1E+05
DELINF (M)	0.012	0.011	0.018	0.025
DELSINF (M)	0.0033	0.0025	0.0046	0.0061
THETAINF (M)	0.0006	0.0004	0.0008	0.0011
L (M)	1.07	1.07	1.98	2.88

9. MEASURED VARIABLES:
 X - STREAMWISE COORDINATE (M)
 PW - WALL PRESSURE (N/M**2)
 CFINF - FRICTION COEFFICIENT BASED ON INFINITY CONDITION
 DENSITY AND VELOCITY
 XS - SEPARATION DISTANCE (M)
 XR - REATTACHMENT DISTANCE (M)
 Y - TRANSVERSE COORDINATE (M)
 XM - MACH NUMBER
 P - PRESSURE (N/M**2)
 U - MEAN STREAMWISE VELOCITY (M/S)
 REINF - REYNOLDS NUMBER BASED ON DELINF AND UINF

10. MEASUREMENT UNCERTAINTY:
 PW=+ OR - 2%
 CFINF=+ OR - 15%
 U=+ OR - 5%
 P=+ OR - 4%
 M=+ OR - 3%

11. TAPE ORGANIZATION:
 THE TAPE IS A 2400 FOOT, 9 TRACK, ODD PARITY, PHASE
 ENCODED, UNLABELLED TAPE WRITTEN AT A DENSITY OF 1600 BITS
 PER INCH ACCORDING TO EBCDIC CODE. THE RECORD FORMAT IS
 FIXED AND BLOCKED; RECORD LENGTH=80 BYTES; 100 RECORDS PER
 BLOCK; BLOCKSIZE=8000 BYTES.

NORMALIZED DATA ARE CREATED FROM MEASURED DATA AS FOLLOWS:

$$XNORM = (X - XMIN) / (XMAX - XMIN)$$

 NORMALIZED VALUES ARE INTEGERIZED BY MULTIPLYING BY 10000
 AND ROUNDING UP OR DOWN TO THE NEAREST INTEGER

$$IXNORM = XNORM * 10000$$

 THUS EACH NORMALIZED AND INTEGERIZED DATUM IS WRITTEN ONTO
 TAPE AS A NUMBER BETWEEN 0 AND 10000. ALL NULL DATA
 ARE WRITTEN AS 20000. THE EQUATION DESCRIBING THE
 RELATION BETWEEN ACTUAL DATA AND THE NORMALIZED DATA
 ON TAPE IS

$$X = XMIN + (((XMAX - XMIN) * IXNORM) / 10000)$$

 WHERE X, XMAX AND XMIN ARE REAL AND IXNORM IS AN INTEGER.

FILE #	NREC	CONTENTS	FORMAT	COMMENTS
1		TEXT FILE		CONTAINS ITEMS 1-11 OF THIS WRITE-UP
2	49	X, PW/PINF	2E13.6	CASE A
		X, PW/PINF	2E13.6	RECORD 1 MAXIMUM VALUES
		X, PW/PINF	2I6	RECORD 2 MINIMUM VALUES
				RECORDS 3-49 NORMALIZED VALUES
3	49	X, PW/PINF	2E13.6	CASE B
				RECORD 1 MAXIMUM VALUES

		X, PW/PINF X, PW/PINF	2E13.6 2I6	RECORD 2 MINIMUM VALUES RECORDS 3-49 NORMALIZED VALUES
4	49	X, PW/PINF X, PW/PINF X, PW/PINF	2E13.6 2E13.6 2I6	CASE C RECORD 1 MAXIMUM VALUES RECORD 2 MINIMUM VALUES RECORDS 3-49 NORMALIZED VALUES
5	49	X, PW/PINF X, PW/PINF X, PW/PINF	2E13.6 2E13.6 2I6	CASE D RECORD 1 MAXIMUM VALUES RECORD 2 MINIMUM VALUES RECORDS 3-49 NORMALIZED VALUES
6	49	X, PW/PINF X, PW/PINF X, PW/PINF	2E13.6 2E13.6 2I6	CASE E RECORD 1 MAXIMUM VALUES RECORD 2 MINIMUM VALUES RECORDS 3-49 NORMALIZED VALUES
7	49	X, PW/PINF X, PW/PINF X, PW/PINF	2E13.6 2E13.6 2I6	CASE F RECORD 1 MAXIMUM VALUES RECORD 2 MINIMUM VALUES RECORDS 3-49 NORMALIZED VALUES
8	49	X, PW/PINF X, PW/PINF X, PW/PINF	2E13.6 2E13.6 2I6	CASE G RECORD 1 MAXIMUM VALUES RECORD 2 MINIMUM VALUES RECORDS 3-49 NORMALIZED VALUES
9	49	X, PW/PINF X, PW/PINF X, PW/PINF	2E13.6 2E13.6 2I6	CASE H RECORD 1 MAXIMUM VALUES RECORD 2 MINIMUM VALUES RECORDS 3-49 NORMALIZED VALUES
10	29	X, CFINF X, CFINF X, CFINF	2E13.6 2E13.6 2I6	CASE A RECORD 1 MAXIMUM VALUES RECORD 2 MINIMUM VALUES RECORDS 3-29 NORMALIZED VALUES
11	21	X, CFINF X, CFINF X, CFINF	2E13.6 2E13.6 2I6	CASE B RECORD 1 MAXIMUM VALUES RECORD 2 MINIMUM VALUES RECORDS 3-21 NORMALIZED VALUES
12	23	X, CFINF X, CFINF X, CFINF	2E13.6 2E13.6 2I6	CASE C RECORD 1 MAXIMUM VALUES RECORD 2 MINIMUM VALUES RECORDS 3-23 NORMALIZED VALUES
13	20	X, CFINF	2E13.6	CASE D RECORD 1 MAXIMUM VALUES

		X,CFINF X,CFINF	2E13.6 2I6	RECORD 2 MINIMUM VALUES RECORDS 3-20 NORMALIZED VALUES
14	6	XS,XR XS,XR XS,XR	2E13.6 2E13.6 2I6	CASES C-H RECORD 1 MAXIMUM VALUES RECORD 2 MINIMUM VALUES RECORDS 3-8 NORMALIZED VALUES
15	44	Y,XM,P/PINF, U/UINF Y,XM,P/PINF, U/UINF Y,XM,P/PINF, U/UINF	4E13.6 4E13.6 4I6	CASE A STATION 11,X=-0.0254 M RECORD 1 MAXIMUM VALUES RECORD 2 MINIMUM VALUES RECORD 3-44 NORMALIZED VALUES
16	41	Y,XM,P/PINF, U/UINF Y,XM,P/PINF, U/UINF Y,XM,P/PINF, U/UINF	4E13.6 4E13.6 4I6	CASE A STATION 24,X=0.0 M RECORD 1 MAXIMUM VALUES RECORD 2 MINIMUM VALUES RECORD 3-41 NORMALIZED VALUES
17	35	Y,XM,P/PINF, U/UINF Y,XM,P/PINF, U/UINF Y,XM,P/PINF, U/UINF	4E13.6 4E13.6 4I6	CASE A STATION 29,X=0.0025 M RECORD 1 MAXIMUM VALUES RECORD 2 MINIMUM VALUES RECORD 3-35 NORMALIZED VALUES
18	40	Y,XM,P/PINF, U/UINF Y,XM,P/PINF, U/UINF Y,XM,P/PINF, U/UINF	4E13.6 4E13.6 4I6	CASE A STATION 31,X=0.0051 M RECORD 1 MAXIMUM VALUES RECORD 2 MINIMUM VALUES RECORD 3-40 NORMALIZED VALUES
19	41	Y,XM,P/PINF, U/UINF Y,XM,P/PINF, U/UINF Y,XM,P/PINF, U/UINF	4E13.6 4E13.6 4I6	CASE A STATION 33,X=0.0102 M RECORD 1 MAXIMUM VALUES RECORD 2 MINIMUM VALUES RECORD 3-41 NORMALIZED VALUES

20	34		CASE A STATION 39, X=0.0254 M
		Y, XM, P/PINF, U/UINF	4E13.6 RECORD 1 MAXIMUM VALUES
		Y, XM, P/PINF, U/UINF	4E13.6 RECORD 2 MINIMUM VALUES
		Y, XM, P/PINF, U/UINF	4I6 RECORD 3-34 NORMALIZED VALUES
21	35		CASE A STATION 47, X=0.0457 M
		Y, XM, P/PINF, U/UINF	4E13.6 RECORD 1 MAXIMUM VALUES
		Y, XM, P/PINF, U/UINF	4E13.6 RECORD 2 MINIMUM VALUES
		Y, XM, P/PINF, U/UINF	4I6 RECORD 3-35 NORMALIZED VALUES
22	41		CASE A STATION 52, X=0.0660 M
		Y, XM, P/PINF, U/UINF	4E13.6 RECORD 1 MAXIMUM VALUES
		Y, XM, P/PINF, U/UINF	4E13.6 RECORD 2 MINIMUM VALUES
		Y, XM, P/PINF, U/UINF	4I6 RECORD 3-41 NORMALIZED VALUES
23	40		CASE A STATION 69, X=0.1372 M
		Y, XM, P/PINF, U/UINF	4E13.6 RECORD 1 MAXIMUM VALUES
		Y, XM, P/PINF, U/UINF	4E13.6 RECORD 2 MINIMUM VALUES
		Y, XM, P/PINF, U/UINF	4I6 RECORD 3-40 NORMALIZED VALUES
24	41		CASE B STATION 5, X=-0.0381 M
		Y, XM, P/PINF, U/UINF	4E13.6 RECORD 1 MAXIMUM VALUES
		Y, XM, P/PINF, U/UINF	4E13.6 RECORD 2 MINIMUM VALUES
		Y, XM, P/PINF, U/UINF	4I6 RECORD 3-41 NORMALIZED VALUES
25	41		CASE B STATION 17, X=-0.0127 M
		Y, XM, P/PINF, U/UINF	4E13.6 RECORD 1 MAXIMUM VALUES
		Y, XM, P/PINF, U/UINF	4E13.6 RECORD 2 MINIMUM VALUES
		Y, XM, P/PINF, U/UINF	4I6 RECORD 3-41 NORMALIZED VALUES

26	41		CASE B STATION 25, X=-0.0064 M
		Y, XM, P/PINF, U/UINF	4E13.6 RECORD 1 MAXIMUM VALUES
		Y, XM, P/PINF, U/UINF	4E13.6 RECORD 2 MINIMUM VALUES
		Y, XM, P/PINF, U/UINF	4I6 RECORD 3-41 NORMALIZED VALUES
27	42		CASE B STATION 33, X=0.0 M
		Y, XM, P/PINF, U/UINF	4E13.6 RECORD 1 MAXIMUM VALUES
		Y, XM, P/PINF, U/UINF	4E13.6 RECORD 2 MINIMUM VALUES
		Y, XM, P/PINF, U/UINF	4I6 RECORD 3-42 NORMALIZED VALUES
28	42		CASE B STATION 41, X=0.0064 M
		Y, XM, P/PINF, U/UINF	4E13.6 RECORD 1 MAXIMUM VALUES
		Y, XM, P/PINF, U/UINF	4E13.6 RECORD 2 MINIMUM VALUES
		Y, XM, P/PINF, U/UINF	4I6 RECORD 3-42 NORMALIZED VALUES
29	41		CASE B STATION 53, X=0.0191 M
		Y, XM, P/PINF, U/UINF	4E13.6 RECORD 1 MAXIMUM VALUES
		Y, XM, P/PINF, U/UINF	4E13.6 RECORD 2 MINIMUM VALUES
		Y, XM, P/PINF, U/UINF	4I6 RECORD 3-41 NORMALIZED VALUES
30	38		CASE B STATION 61, X=0.0381 M
		Y, XM, P/PINF, U/UINF	4E13.6 RECORD 1 MAXIMUM VALUES
		Y, XM, P/PINF, U/UINF	4E13.6 RECORD 2 MINIMUM VALUES
		Y, XM, P/PINF, U/UINF	4I6 RECORD 3-38 NORMALIZED VALUES
31	44		CASE B STATION 73, X=0.0762 M
		Y, XM, P/PINF, U/UINF	4E13.6 RECORD 1 MAXIMUM VALUES
		Y, XM, P/PINF, U/UINF	4E13.6 RECORD 2 MINIMUM VALUES
		Y, XM, P/PINF, U/UINF	4I6 RECORD 3-44 NORMALIZED VALUES

32	45		CASE B STATION 83, X=0.1397 M
		Y, XM, P/PINF, U/UINF	4E13.6 RECORD 1 MAXIMUM VALUES
		Y, XM, P/PINF, U/UINF	4E13.6 RECORD 2 MINIMUM VALUES
		Y, XM, P/PINF, U/UINF	4I6 RECORD 3-45 NORMALIZED VALUES
33	46		CASE C STATION 14, X=-0.0381 M
		Y, XM, P/PINF, U/UINF	4E13.6 RECORD 1 MAXIMUM VALUES
		Y, XM, P/PINF, U/UINF	4E13.6 RECORD 2 MINIMUM VALUES
		Y, XM, P/PINF, U/UINF	4I6 RECORD 3-40 NORMALIZED VALUES
34	47		CASE C STATION 36, X=-0.0111 M
		Y, XM, P/PINF, U/UINF	4E13.6 RECORD 1 MAXIMUM VALUES
		Y, XM, P/PINF, U/UINF	4E13.6 RECORD 2 MINIMUM VALUES
		Y, XM, P/PINF, U/UINF	4I6 RECORD 3-47 NORMALIZED VALUES
35	37		CASE C STATION 50, X=0.0 M
		Y, XM, P/PINF, U/UINF	4E13.6 RECORD 1 MAXIMUM VALUES
		Y, XM, P/PINF, U/UINF	4E13.6 RECORD 2 MINIMUM VALUES
		Y, XM, P/PINF, U/UINF	4I6 RECORD 3-37 NORMALIZED VALUES
36	30		CASE C STATION 55, X=0.0004 M
		Y, XM, P/PINF, U/UINF	4E13.6 RECORD 1 MAXIMUM VALUES
		Y, XM, P/PINF, U/UINF	4E13.6 RECORD 2 MINIMUM VALUES
		Y, XM, P/PINF, U/UINF	4I6 RECORD 3-30 NORMALIZED VALUES
37	25		CASE C STATION 66, X=0.0127 M
		Y, XM, P/PINF, U/UINF	4E13.6 RECORD 1 MAXIMUM VALUES
		Y, XM, P/PINF, U/UINF	4E13.6 RECORD 2 MINIMUM VALUES
		Y, XM, P/PINF, U/UINF	4I6 RECORD 3-25 NORMALIZED VALUES

38	39		CASE C STATION 70, X=0.0254 M
		Y, XM, P/PINF, U/UINF	4E13.6 RECORD 1 MAXIMUM VALUES
		Y, XM, P/PINF, U/UINF	4E13.6 RECORD 2 MINIMUM VALUES
		Y, XM, P/PINF, U/UINF	4I6 RECORD 3-39 NORMALIZED VALUES
39	38		CASE C STATION 75, X=0.0413 M
		Y, XM, P/PINF, U/UINF	4E13.6 RECORD 1 MAXIMUM VALUES
		Y, XM, P/PINF, U/UINF	4E13.6 RECORD 2 MINIMUM VALUES
		Y, XM, P/PINF, U/UINF	4I6 RECORD 3-38 NORMALIZED VALUES
40	41		CASE C STATION 86, X=0.0762 M
		Y, XM, P/PINF, U/UINF	4E13.6 RECORD 1 MAXIMUM VALUES
		Y, XM, P/PINF, U/UINF	4E13.6 RECORD 2 MINIMUM VALUES
		Y, XM, P/PINF, U/UINF	4I6 RECORD 3-41 NORMALIZED VALUES
41	47		CASE C STATION 94, X=0.1143 M
		Y, XM, P/PINF, U/UINF	4E13.6 RECORD 1 MAXIMUM VALUES
		Y, XM, P/PINF, U/UINF	4E13.6 RECORD 2 MINIMUM VALUES
		Y, XM, P/PINF, U/UINF	4I6 RECORD 3-47 NORMALIZED VALUES
42	49		CASE D STATION 2, X=-0.0635 M
		Y, XM, P/PINF, U/UINF	4E13.6 RECORD 1 MAXIMUM VALUES
		Y, XM, P/PINF, U/UINF	4E13.6 RECORD 2 MINIMUM VALUES
		Y, XM, P/PINF, U/UINF	4I6 RECORD 3-49 NORMALIZED VALUES
43	48		CASE D STATION 10, X=-0.0305 M
		Y, XM, P/PINF, U/UINF	4E13.6 RECORD 1 MAXIMUM VALUES
		Y, XM, P/PINF, U/UINF	4E13.6 RECORD 2 MINIMUM VALUES
		Y, XM, P/PINF, U/UINF	4I6 RECORD 3-48 NORMALIZED VALUES

44	41		CASE D STATION 18, X=-0.0102 M
		Y, XM, P/PINF, U/UINF	4E13.6 RECORD 1 MAXIMUM VALUES
		Y, XM, P/PINF, U/UINF	4E13.6 RECORD 2 MINIMUM VALUES
		Y, XM, P/PINF, U/UINF	4I6 RECORD 3-41 NORMALIZED VALUES
45	48		CASE D STATION 22, X=0.0 M
		Y, XM, P/PINF, U/UINF	4E13.6 RECORD 1 MAXIMUM VALUES
		Y, XM, P/PINF, U/UINF	4E13.6 RECORD 2 MINIMUM VALUES
		Y, XM, P/PINF, U/UINF	4I6 RECORD 3-48 NORMALIZED VALUES
46	39		CASE D STATION 26, X=0.0102 M
		Y, XM, P/PINF, U/UINF	4E13.6 RECORD 1 MAXIMUM VALUES
		Y, XM, P/PINF, U/UINF	4E13.6 RECORD 2 MINIMUM VALUES
		Y, XM, P/PINF, U/UINF	4I6 RECORD 3-39 NORMALIZED VALUES
47	46		CASE D STATION 33, X=0.0305 M
		Y, XM, P/PINF, U/UINF	4E13.6 RECORD 1 MAXIMUM VALUES
		Y, XM, P/PINF, U/UINF	4E13.6 RECORD 2 MINIMUM VALUES
		Y, XM, P/PINF, U/UINF	4I6 RECORD 3-46 NORMALIZED VALUES
48	47		CASE D STATION 39, X=0.0610 M
		Y, XM, P/PINF, U/UINF	4E13.6 RECORD 1 MAXIMUM VALUES
		Y, XM, P/PINF, U/UINF	4E13.6 RECORD 2 MINIMUM VALUES
		Y, XM, P/PINF, U/UINF	4I6 RECORD 3-47 NORMALIZED VALUES
49	47		CASE D STATION 47, X=0.1016 M
		Y, XM, P/PINF, U/UINF	4E13.6 RECORD 1 MAXIMUM VALUES
		Y, XM, P/PINF, U/UINF	4E13.6 RECORD 2 MINIMUM VALUES
		Y, XM, P/PINF, U/UINF	4I6 RECORD 3-47 NORMALIZED VALUES

Y, XM, P/PINF,		
U/UINF	4E13.6	RECORD 1 MAXIMUM VALUES
Y, XM, P/PINF,		
U/UINF	4E13.6	RECORD 2 MINIMUM VALUES
Y, XM, P/PINF,		
U/UINF	4I6	RECORD 3-48 NORMALIZED VALUES

A SAMPLE PROGRAM FOR READING AND PRINTING FILE 2 IS SHOWN BELOW. THE JCL IS FOR THE THE STANFORD CIT FACILITY. CHECK WITH YOUR OWN COMPUTER FACILITY FOR THE EXACT JCL NEEDED.

```
//TAPE JOB SETTLES
/*SETUP TAPE1, INPUT=(LIBRARY NUMBER ASSIGNED TO TAPE)
// EXEC FORTCG
//FORT.SYSIN DD *
C READ FILE 2 OFF THE TAPE AND PRINT THE MAXIMAS AND
C MINIMAS OF ALL THE VARIABLES AS WELL AS THE NORMALIZED
C AND INTEGERIZED VALUES OF ALL THE VARIABLES
  INTEGER X(47),PW(47)
  READ(23,30) XMX,PWMX
  READ(23,30) XMN,PWMN
C SET N=THE NUMBER OF RECORDS IN THE FILE MINUS 2
  N=49-2
  DO 10 I=1,N
10  READ(23,40) X(I),PW(I)
    WRITE(6,50) XMX,PWMX
    WRITE(6,50) XMN,PWMN
  DO 20 I=1,N
20  WRITE(6,60) X(I),PW(I)
30  FORMAT(2E13.6)
40  FORMAT(2I6)
50  FORMAT(1X,2E13.6)
60  FORMAT(1X,2I6)
  STOP
  END
//GO.FT23F001 DD UNIT=TI600.VOL=SER=(TAPE,LIBRARY),
// DISP=(OLD,KEEP),DCP=(RECFM=FB,LREC=80,BLKSIZE=8000,
// DEN=3),LABEL=(2,NL)
//
```

DISCUSSION

The Data Library

- P. Bradshaw (Imperial College): What code was on the tape, P.E. or N.R.Z?
- B. Cantwell: Phrase encoded--P.E.
- W. C. Reynolds (Stanford University): Inevitably, as all these computers start working with these data there will be things found that need to be fixed. What provisions are made for disseminating this information?
- B. Cantwell: A list of tape users will be kept and updated information will be mailed out to all users as errata.
- S. J. Kline: At the end of the 1980 meeting various computational groups will be asked to assume one flow and compute it very early to see if some troubles show up to prevent other groups having similar problems. [Ed.: This has been done.]
- G. Sovran (General Motors Research Labs.): Please indicate where these tapes will be stored.
- B. Cantwell: Initially all mailings to computers will be from Stanford. Later the tapes will be available from three sources listed on page 58 [this volume].
- G. Mellor (Princeton): There will be about six months between the availability of the data tapes and the deadline for submission of predictions, which is a very short period of time. The end result will suffer because of this short time period.
- B. Cantwell: The first tape will become available on November 30, 1980. An updated version with a few more cases will come out on January 31, 1981. In the meantime the test cases are also available in the literature.
- S. J. Kline: If this time period is too short, we shall discuss postponing the 1981 meeting.
- W. C. Reynolds: Will the 1968 Conference flows be included?
- B. Cantwell: We have included three cases and hope to include more later.
- V. C. Patel (University of Iowa): Are there any others who feel that the time period allowed for computation is too short?
- (About half a dozen thought so.)
- G. Sovran: Let this be one of the topics for discussion in the open forum in Session XIV.

At the evening discussion B. Cantwell, R. So, V. C. Patel and J. Hunt discussed the criteria for selection of types of flows. It was felt that certain important classes of flows were omitted. It was further felt that a discussion of the types of flows to be added to the data library should be discussed in the open forum in Session XIV.

SESSION I

Chairman: V. C. Patel

Technical Recorders:

R. Subbarao
P. Parikh



Flow 0610

Flow 0210

Flow 0230

PREVIOUS PAGE
IS BLANK



ATTACHED BOUNDARY LAYERS

Flow 0610

Cases 0611, 0612, 0613

Evaluator: D. E. Coles*

SUMMARY

Certain test cases were selected from the 1968 Conference. These were:

Case 0611. Attached Boundary Layer (Tillman, Ledge Flow)

Case 0612. Attached Boundary Layer (Wieghardt, Flat Plate Flow)

Case 0613. Attached Boundary Layer (Bradshaw $\alpha = -0.255$)

However, after discussion at the 1980 meeting, only Case 0612 was selected as a test case for the 1981 meeting.

*California Institute of Technology, Pasadena, CA 91125

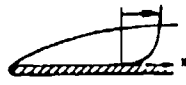
SPECIFICATIONS FOR COMPUTATION

SIMPLE CASE/INCOMPRESSIBLE

Case #0612; Data Evaluator: D. E. Coles (1968)

Data Taker: K. Wieghardt

PICTORIAL SUMMARY
Flow 0410. Data Evaluator: D. E. Coles. "Attached Boundary Layers ('68 Conference)."

Case Data Taker	Test Rig Geometry	dp/dx or C _p	Number of Stations Measured							C _f	Re	Initial Condition	Other Notes
			Mean Velocity		Turbulence Profiles								
			U	V or W	$\overline{u^2}$	$\overline{v^2}$	$\overline{w^2}$	\overline{uv}	Others				
Case 0612 K. Wieghardt		0	23	-	-	-	-	-	-	Eleven plots	2.2 x 10 ⁶ per m	Turbu- lence intensity < 0.25%	Data include computed values of boundary layer integral parameters.

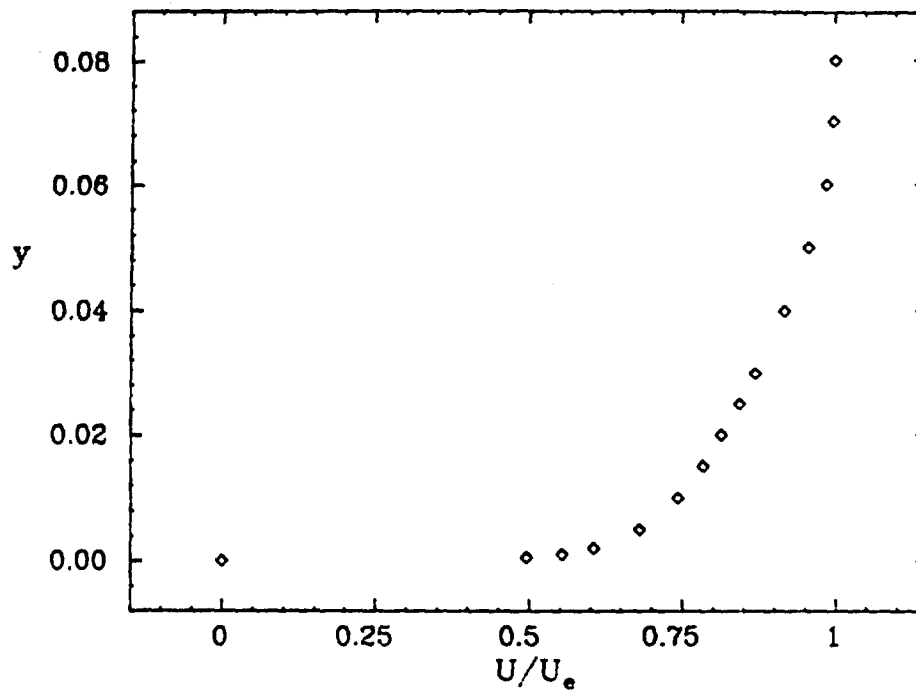
Plot	Ordinate	Abcissa	Range/Position	Comments
1	y	U/U _e	x = 4.987 m	One profile only.
2	C _f	x	0.087 ≤ x ≤ 4.987 m	
3	H	x	0.087 ≤ x ≤ 4.987 m	

Special Instructions, General Comments:

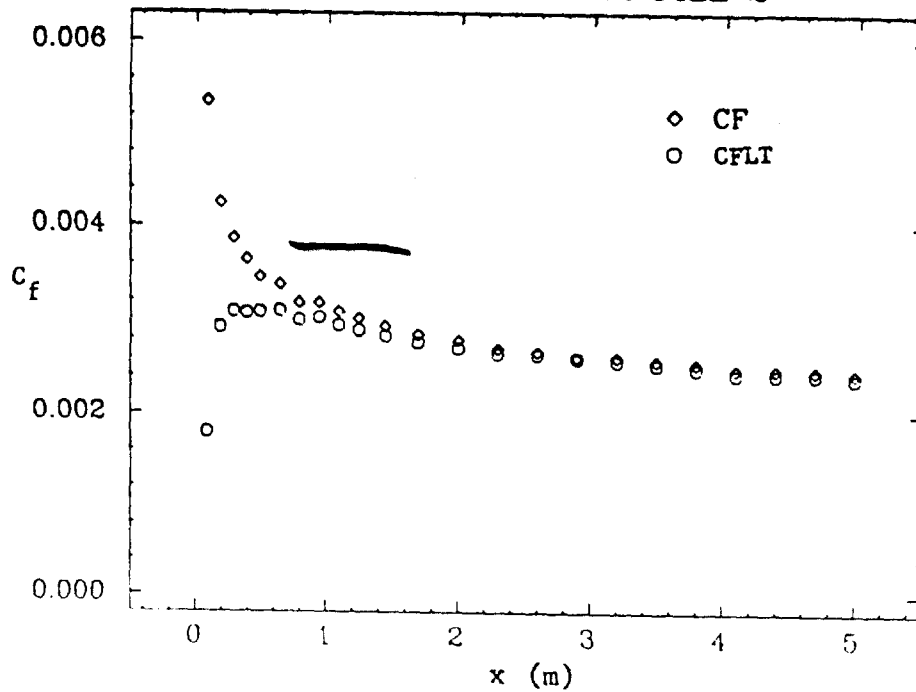
This is a check flow to tie to 1968 results, and assure simple shear layers are modeled adequately.

Starting conditions can be laminar or turbulent. Please report what is used.

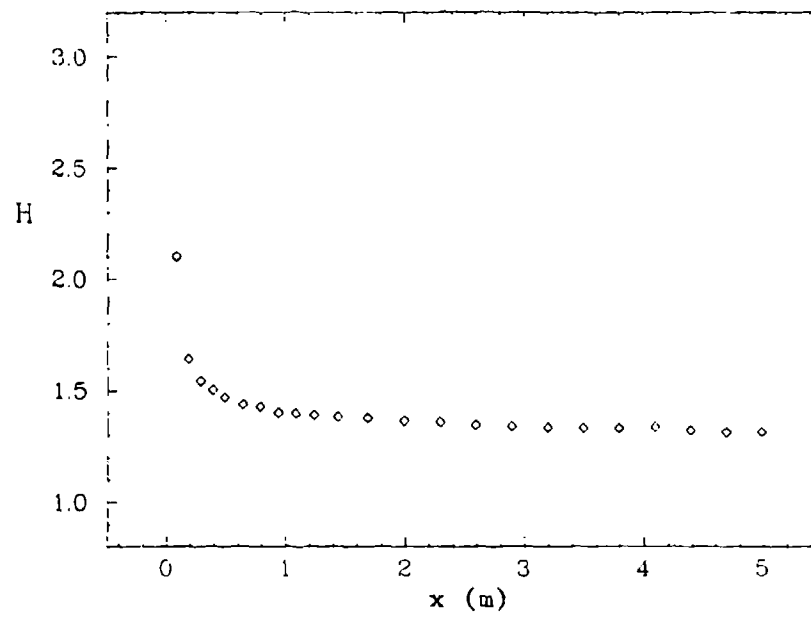
PLOT 1 CASE 0612 FILE 25



PLOT 2 CASE 0612 FILE 2



PLOT 3 CASE 0612 FILE 2



EFFECT OF FREE-STREAM TURBULENCE ON BOUNDARY LAYERS

Flow 0210

Case 0211

Evaluator: P. Bradshaw^{*}

SUMMARY

SELECTION CRITERIA AND FLOWS SELECTED

This report is based on the Ph.D. thesis of the evaluator's student, Hancock (1980). Since previous data, reviewed by Hancock, are incomplete or in some ways unsatisfactory, the available data are presented as a correlation for the variation of skin-friction coefficient in constant-pressure boundary layers with the intensity and length scale of free-stream turbulence, based on Hancock's results and on previous work.

It is intuitively obvious, and also seems to be true, that the effect of free-stream turbulence is felt mainly by the outer layer of the boundary layer. Although some investigators have just assumed without discussion that the logarithmic law still applies in its usual form, this assumption has led to self-consistent results (skin-friction values deduced from logarithmic law or Preston tube reading seem to agree well with independent checks) and can therefore be accepted. Boundary layers with high turbulence level in the outer layer still have recognizable log-law regions. Also, pressure gradients do not influence turbulence structure directly, and most calculation methods are able to predict the effects of pressure gradient on simple boundary layers with adequate accuracy, so that it probably follows that a physically well-founded allowance for free-stream turbulence effects that is adequate in boundary layers in zero pressure gradient will also perform satisfactorily in boundary layers with arbitrary pressure gradient. Alas, the point is almost an academic one at present, because most of the experimental data refer to boundary layers without pressure gradients despite the practical importance of pressure gradients.

Nearly all investigators have used biplane square-mesh grid turbulence which is well known to be slightly but consistently anisotropic (the longitudinal mean-square component being about 1.2 times the lateral components). At large enough distances from the grid for the turbulence to have become approximately homogeneous in the cross-sectional plane, the turbulence can be specified by the longitudinal component intensity (say) and one length scale. In cases where free-stream turbulence spectra

^{*}Imperial College, Prince Consort Road, London, SW7 2BY, England.

have not been measured, it is possible to deduce the dissipation length parameter from the decay rate of the turbulence. Other length scales, where available, can be related to this simple dissipation length parameter, and the latter is therefore the most straightforward basis of comparison between all cases. A few sets of measurements have been made in other kinds of free-stream turbulence. One example is the series of measurements made by Huffman et al. (1972) behind parallel bar grids; far enough downstream, the turbulence in this case seems to be fairly close in its effects to that produced by conventional square mesh grids. A few measurements of free-stream turbulence in turbomachinery have also been made. The "turbulence" consists partly of ordered unsteadiness, with frequencies related to the speed of rotation of the machine, and partly of truly random, but probably anisotropic, turbulence. It does not seem reasonable to synthesize any test cases from the turbomachinery data.

Providing that the logarithmic law is unaltered by moderate intensity of free-stream turbulence, the usual wall-plus-wake similarity analysis suggests that the effect of free-stream turbulence can be correlated as a variation in the wake parameter Π with $(\overline{u_e^2})^{1/2}$ in the form

$$\Pi = f[(\overline{u_e^2})^{1/2}/U_\star, L/\delta]$$

where L is the streamwise length scale (L_e^u) of the free-stream turbulence. If Π changes linearly with $(\overline{u_e^2})^{1/2}/U_\star$, a few lines of algebra given by Bradshaw (1974) show that the skin-friction coefficient varies linearly with $(\overline{u_e^2})^{1/2}/U_e$ at given $U_\star\delta/\nu$. This form of correlation for the effect on surface shear stress is commonly used, and it is useful to observe that its apparent incompatibility with the inner and outer layer analysis, in which U_\star , not U_e , is the correct velocity scale, is spurious. In the above analysis Π is implicitly defined in terms of the extrapolated log-law velocity at $y = \delta$, and considerations of change in wake shape due to free-stream turbulence need not enter. It is found in fact that the wake-profile shape changes considerably, and that neither the traditional cosine curve nor the more elaborate cubic fit originally due to Finley et al. (see Moses, 1963) adequately represents the profiles at high free-stream turbulence intensity. Since the wake profile shape is difficult to define, the simplest way of correlating free-stream-turbulence effects is in terms of skin-friction coefficient as a function of $(\overline{u_e^2})^{1/2}/U_e$ and of L/δ times the skin friction at the same momentum-thickness Reynolds number (for convenience) in a constant-pressure boundary layer without free-stream turbulence. In practice the dependence on Re_τ that should enter this equation is negligible, at least for Reynolds numbers greater than the upper limit of about 5000 for significant viscous effects in the outer layer. Thus $C_f/C_{f0} = (\overline{u_e^2})^{1/2}/U_e, L/\delta$ as shown in Fig. 1.

ADVICE FOR FUTURE DATA TAKERS

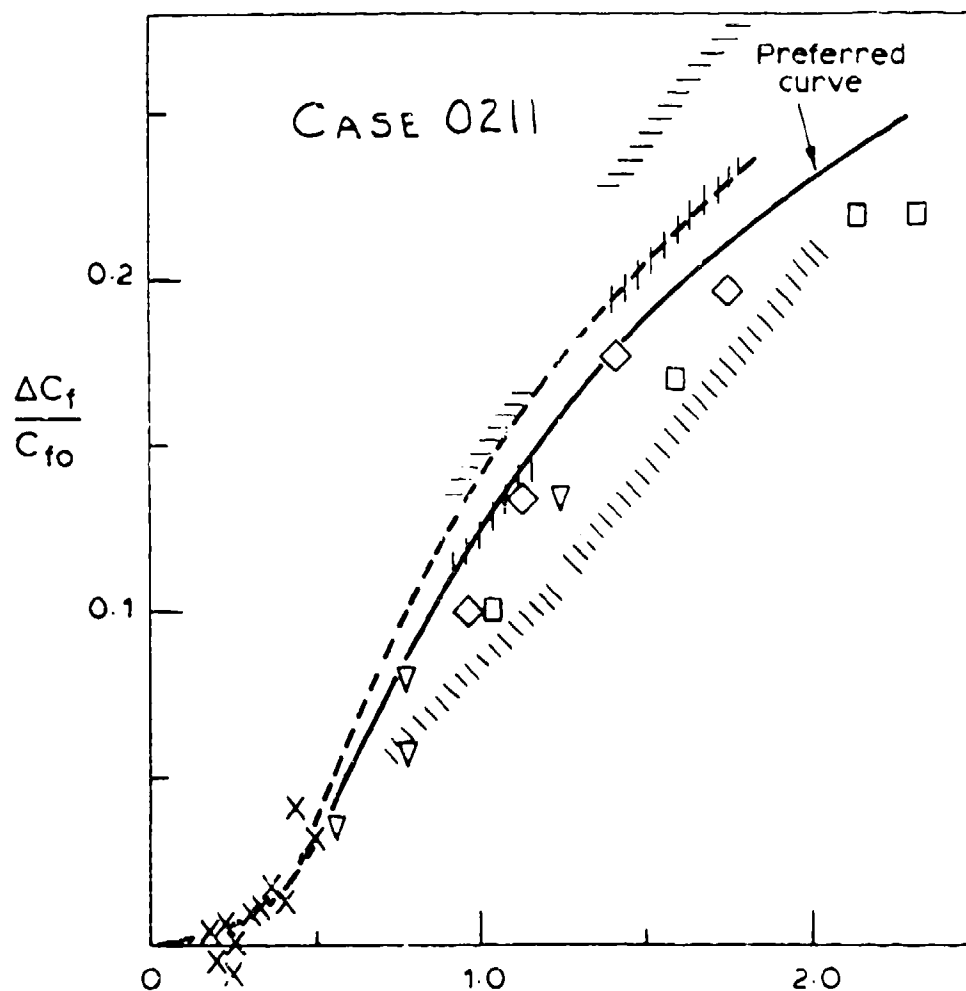
The assumption that grid turbulence can be characterized by one length scale and one velocity scale, inherent in nearly all previous work, is crude; however, it is equivalent to current turbulence-modeling assumptions, and although the free-stream turbulence should be carefully documented in the experiment it should not be necessary to use more elaborate data correlations at present. Experiments with arbitrarily anisotropic free-stream turbulence are not likely to be of practical use, but more work is needed to explore and classify the disturbance field in axial turbomachines and its effect on blade and annulus boundary layers.

Further exploration of the effect of free-stream length scale or spectra is needed. The rms intensity $(\overline{u_e^2})^{1/2}$ varies with distance x from the grid as $x^{-1/2}$, approximately, while the length scale L varies as $x^{1/2}$, approximately. The boundary-layer thickness δ varies as $(x - x_0)^{4/5}$, approximately, where x_0 is the position of the leading edge. x_0/M must exceed about 5 if the turbulence is to be adequately homogeneous by the time it reaches the first measuring station, which must be far enough downstream of the leading edge for the momentum-thickness Reynolds number Re_δ to exceed about 2000 so as to avoid severe viscous effects in the outer layer. These facts mean that, (1) it is difficult to achieve rms intensities of much more than $0.05 U_e$ at any measuring station, and (2) since δ grows faster than L , both L/δ and $(\overline{u_e^2})^{1/2}/U_e$ decrease with increasing x . The tendency for intensity and length scale to vary together is so strong that all published data except Hancock's lie very close to a single line in the $(\overline{u_e^2})^{1/2}/U_e, L/\delta$ plane. Thus it is very difficult to extract information about the effect of length scale from previous data. Even after recognizing this constraint Hancock had some difficulty in covering a reasonable area in the intensity/length-scale plane.

Since the free-stream turbulence intensity inevitably decreases with the distance down the boundary layer, while the length scale just as inevitably increases, each calculation provides a trajectory in Fig. 1; the initial portion of the calculation (where the profiles are settling down from the assumed starting condition) will be spurious, and probably easily seen to be so. The correlation in Fig. 1 is empirical; a residual effect of length scale may appear in the calculations, in which case runs should be done with more values of L/δ to document effect.

REFERENCES

- Bradshaw, P., (1974). "Effect of free-stream turbulence on turbulent shear layers," Report 74-10, Dept. of Aeronaut., Imperial College, London.
- Charnay, G., G. Comte-Bellot, and J. Mathieu (1971). "Development of a turbulent boundary layer on a flat plate in an external turbulent flow," AGARD Conf. Proc. No. 93.
- Dean, R. B. (1976). "A single formula for the complete velocity profile in a turbulent boundary layer," J. Fluids Engr., 98, 723.
- Evans, R. L. (1972). "Free stream turbulence effects on the turbulent boundary layer," Dept. of Engineering, University of Cambridge, Report CUED/A Turbo/TR41.
- Finley, P. J., K. C. Phoe, and C. J. Poh (1966). "Velocity measurements in a thin turbulent water layer," Houille Blanche, 21, 713.
- Green, J. E. (1972). "On the influence of free stream turbulence on a turbulent boundary layer as it relates to wind tunnel testing at subsonic speeds," RAE Technical Report 72201.
- Hancock, P. E. (1980). "The effect of free-stream turbulence on turbulent boundary layers," Ph.D. thesis, Imperial College, London. Available on microfiche from Dept. of Aeronaut., Imperial College, London, SW7 2BY.
- Huffman, G. D., D. R. Zimmerman, and V. A. Bennett (1972). "The effect of free-stream turbulence level on turbulent boundary-layer behavior," AGARD Conf. Proc., 164.
- Meider, H. U. (1976). "The response of turbulent boundary layers to small turbulence levels in the external free stream," DFVLR Report IB 251-76 A.17.
- Meier, H. U., and H. P. Kreplin (1980). "Influence of free-stream turbulence on boundary-layer development," J. AIAA, 18, 11.
- Moses, H. (1963). "Gas turbine lab report," Massachusetts Institute of Technology.
- Robertson, J. M., and C. F. Holt (1972). "Stream turbulence effects on the turbulent boundary layer," Proc. ASCE, 98, 1093.



- Hancock (1980)
- Robertson and Holt (1972)
- x Meier (1976)
- △ Evans (1972)
- ◇ Huffman et al. (preferred) ; corrected using Meier's results
- ||| Green's analysis of Huffman et al.
- ||| Analysis of Huffman et al. following Green
- ||| Charnay et al. (1971)--Bradshaw's (1974) analysis employed

Figure 1. Correlation of $\Delta C_f / C_{f0}$, where C_{f0} is value with $u_e^2 = 0$ and same Re_δ .

DISCUSSION

Flow 0210

J. Hunt: I have two points to make:

1. In your specification for a discussion of the problem, you said that the skin friction is the only important parameter to be considered for evaluating the effects of the free-stream turbulence. However, there are several other turbulence quantities which should be used for a more complete comparison. For example, one of the effects of free-stream turbulence is to amplify the turbulence within the boundary layer. I am wondering whether the data are of such a sort that some such comparison is possible.

2. In your suggestions for specifications for computations you suggest the initial ratio of length scales to boundary-layer thickness should be 1, 2, and 5. If it is as large as 5, the turbulence outside the boundary layer will be affected by the presence of the wall and you will have an outer damped region where the turbulence in the normal direction is reduced. So it would be a artificial calculation to start with uniform turbulence at the initial point where the turbulence outside the boundary layer is feeling the presence of the wall.

P. Bradshaw: There are no adequate measurements to make more detailed comparisons than those suggested here. The free-stream turbulence, if it has a large scale, will indeed be affected by the presence of the wall. The conditions to be specified for the computers are farther away from the edge of the boundary layer. I think it would be worthwhile to include this point in a revised specification for computation. The effect of the interaction between large eddies of free-stream turbulence outside the boundary layer and the boundary layer itself will fall out of a calculation carried to a point far away from the wall.

G. Lilley: It is possible that the constants in the law of the wall change due to the anisotropy of the free-stream turbulence.

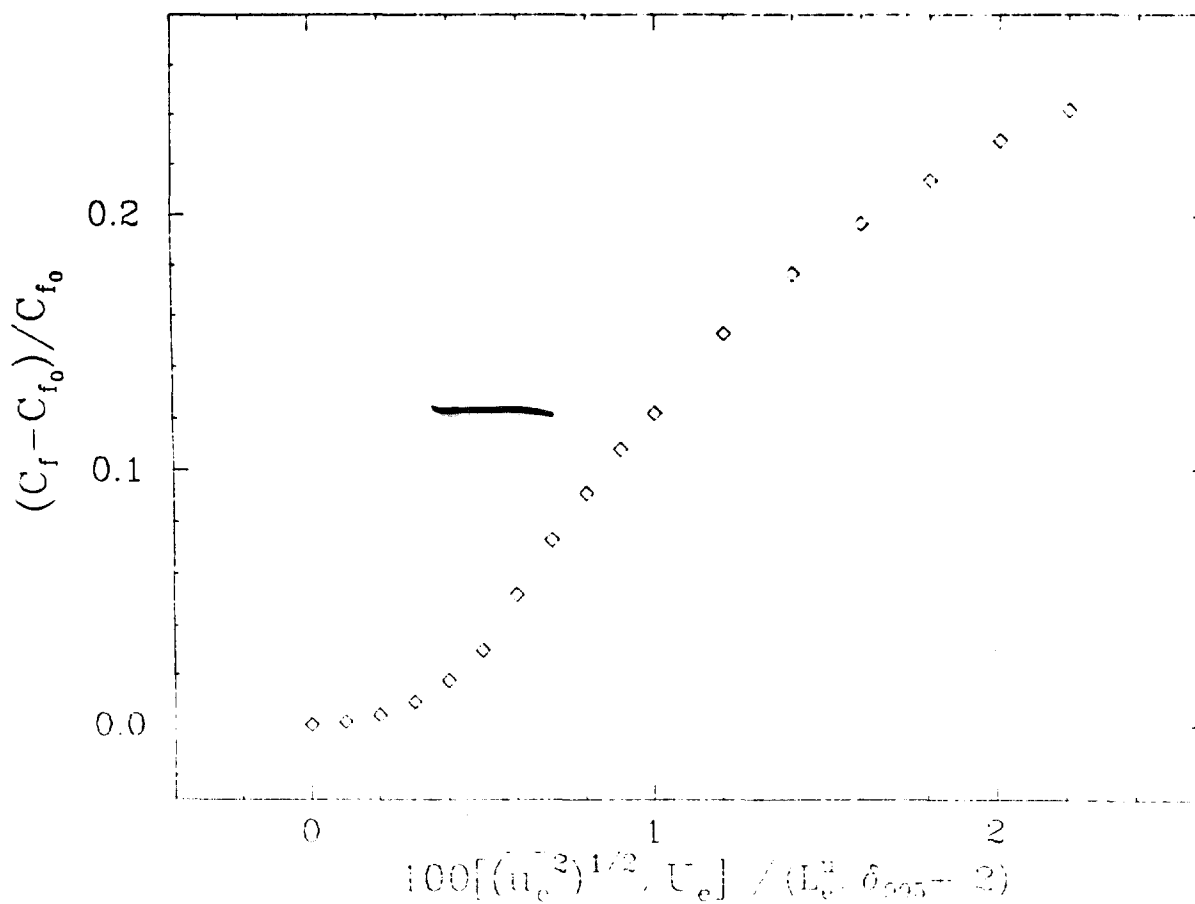
P. Bradshaw: I think this is rather unlikely, because the law of the wall is incredibly insensitive to what is happening in the outer part of an ordinary boundary layer in the absence of free-stream turbulence. I cannot imagine the constants changing in any of the cases we have chosen.

P. S. Klebanoff: Free-stream turbulence upstream of a plate may be different from data alongside a plate. Data should therefore also include turbulence intensity as a scale in the stream approaching the plate.

M. V. Morkovin: Could you say to what extent the data are insensitive to the transition effects as opposed to free-stream turbulence effects.

- P. Bradshaw: We tried to avoid low Reynolds number data. Most of the data is at R_θ greater than 2000, and comparisons of skin friction are presented at the same value of R_θ .
- F. Champagne: You mentioned that you would like to characterize free-stream turbulence by its intensity and dissipation rate. I would like to define the free-stream turbulence using power spectra of some of the components of turbulence.
- P. Bradshaw: Most of the available data involved measurements of the u' component and its free stream decay; hence all you can get out is the dissipation length parameter.

PLOT 1 CASE 0211 FILE 2



SPECIFICATIONS FOR COMPUTATION

ENTRY CASE/INCOMPRESSIBLE

Case #0211; Data Evaluator: P. Bradshaw

Data Takers: P. E. Hancock and others

PICTORIAL SUMMARY

Flow 0210. Data Evaluator: P. Bradshaw. "Effect of Free-Stream Turbulence on Boundary Layers."

Case Data Taker	Test Rig Geometry	dp/dx or C _p	Number of Stations Measured								C _f	Re	Initial Condition	Other Notes
			Mean Velocity		Turbulence Profiles									
			U	V or W	$\overline{u^2}$	$\overline{v^2}$	$\overline{w^2}$	\overline{uv}	Others					
Case 0211 P. Hancock and others			Smoothed curve of $\frac{C_f}{C_{f_0}} \approx (\frac{L_e^u}{995}) / (\frac{L_e^u}{995} + 2)$ given											

Plot	Ordinate	Abcissa	Range/Position	Comments
1	$\frac{C_f - C_{f0}}{C_{f0}}$	$\frac{(\overline{u_e^2})^{1/2}}{U_e} \times 100$ $\frac{L_e^u}{995} + 2$	$0 < \frac{(\overline{u_e^2})^2}{U_e^2} \times 100$ $\frac{L_e^u}{995} + 2 < 2.5$	Use $Re > 5000$ to avoid low Re effects. Notation: C_{f0} = value of C_f where $\overline{u_e^2} = 0$. $L_e^u = (\overline{u_e^2})^{3/2} / (2\epsilon/3)$

Special Instruction:

It is suggested that calculations should be started with isotropic free-stream turbulence with rms component intensities of 10, 5, 2 and 1%, with initial ratio of length scale to boundary-layer thickness of 1, 2, and 5 in each case. However, computers should use their judgment to provide enough runs to envelope the skin-friction curve, and it will be of particular interest to see whether methods reproduce the apparent quadratic behavior of the curve for small turbulence intensity. The empirical correlation for length-scale effect implied by Fig. 1 does not necessarily apply to this region; see Meier and Kreplin (1980). Whatever length scale is used in the calculation method, it should be possible to deduce it from the dissipation length parameter $L_e^u \equiv (\overline{u_e^2})^{3/2} / (2\epsilon/3)$. If free-stream turbulence development is not calculable with the method employed, assume that length scale is independent of x (actually varies with x 0.4 power of distance from grid) or deduce $d\overline{u_e^2}/dx$ from implied ϵ . Note that constraint of solid surface alters free-stream turbulence at y values up to 2 or 3 times L_e^u (whatever the value of L/δ). Thus the "free-stream" value should be specified at $y > 2L_e^u$ if the calculation method is expected to reproduce this constraint, even qualitatively.

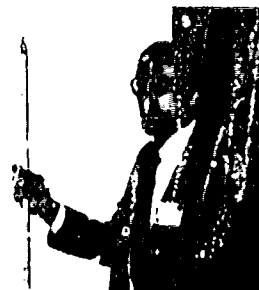
BOUNDARY LAYER FLOWS WITH STREAMWISE CURVATURE



S. Honami^{*}

Flow 0230

Cases 0231, 0232, 0233



T. W. Simon[†]

Evaluators:

SUMMARY

Data sets for incompressible, two-dimensional boundary layer flows with streamwise curvature have been evaluated for their suitability as test cases for comparison with computational results. This report summarizes that data evaluation. More details may be found in the Preliminary and Final Evaluation Reports.

SELECTION CRITERIA

The following criteria were applied to the available data sets to help select the test cases.

The flow must be incompressible and two-dimensional. Two-dimensionality is easily destroyed when the cross-stream pressure gradient accelerates end-wall boundary-layer fluid, resulting in large-scale secondary flow of the first kind. The data must show that the effect of this inevitable secondary flow is minimal.

As a baseline check on the turbulence data, shear-stress profiles taken on a flat wall upstream of curvature must match accepted flat-plate profiles.

Since the data are to be used to evaluate prediction models for turbulent flow, it was decided that mean-flow data, alone, were not sufficient. The test cases must have, at least, the $\overline{u^2}$, $\overline{v^2}$, and \overline{uv} components of the Reynolds stress tensor.

The simpler curved-wall cases were given higher priority than cases with curvature plus other competing effects, e.g., lateral divergence.

Cases which showed the response of the flow to the withdrawal of curvature as well as the introduction of curvature were favored over those with only the introduction of or only the recovery from curvature.

[†]University of Minnesota, Mech. Eng. Dept., Minneapolis, 55455; formerly Stanford University.

^{*}The Science University of Tokyo, Mech. Eng. Dept., Kaguravaka, Shinjuku-Ku, Tokyo, 162, Japan; on leave at Stanford University, 1979-80.

Cases where the curved-wall section was long enough to assess the response of the flow to the introduction of curvature were favored over those with very short curved sections which showed more the response to an "impulse" of curvature.

Concave curvature can result in the establishment of Taylor-Görtler longitudinally roll cells, making the flow locally three-dimensional. Cases where the influence of the roll cells was large (that were otherwise acceptable) were labeled "Advanced Test Cases." These advanced cases have been entered in the data library for future use, but were not recommended for this conference.

SELECTED DATA SETS

Of the many categories of flows being modeled in this conference, the curved-wall flow category seems to be one of the most thoroughly documented. In order to have a reasonably small number of entries, we adopted the highly restrictive criteria discussed above. Five test cases were chosen for this category. These cases followed a common pattern: boundary layers were first developed on flat pre-plates. The flow was then introduced to either concavely or convexly curved walls, followed, in some cases, by flat recovery walls. In all cases the boundary layers on the convex and concave walls did not merge. In all cases there were minimal secondary flow effects; and, except for the formation of weak Taylor-Görtler roll cells on the concave walls, the boundary layers were sufficiently two-dimensional. The test cases are:

Case 0231. Convex: P. H. Hoffmann and P. Bradshaw (1978)

In this case, a boundary layer was grown on a flat wall, then introduced to a convexly curved wall of 2.54 m radius, giving a ratio of δ_{995}/R of 0.01. This indicates weaker curvature than the other boundary-layer cases. There was no recovery.

Case 0232. Concave: P. H. Hoffmann and P. Bradshaw (1978)

This case is for the opposite wall (concave) to Case 0231. The radius of curvature was 2.667 m. Instabilities associated with concave curvature resulted in the formation of weak longitudinal roll cells (Taylor-Görtler vortices) just off the concave wall. This resulted in regular spanwise variations of all quantities. Data were taken near the spanwise location of minimum skin friction with respect to these weak vortices.

Case 0233. J. C. Gillis and J. P. Johnston (1980)

In this case, a boundary layer was grown on a flat wall, then was introduced to a convexly curved wall of 0.45 m radius of curvature, giving a ratio of δ_{995}/R of 0.10. This indicates strong curvature. Downstream of the bend was a flat-wall recovery section.

Case 0234. Hunt, I. A., and P. N. Joubert (1979)

In this case, boundary layers were grown on the two walls of a curved channel which had a radius of curvature (to the channel centerline) of 6.35 m and a nominal channel depth, D, of 6.35 cm. The two boundary layers initially were independent, and began to merge about 40% of the test section length. At the end of the test section, the flow was essentially fully developed. There was no recovery.

Case 0235. Smits, A. J., S. T. B. Young, and P. Bradshaw (1978)

In this case, a boundary layer was grown on a flat wall, then introduced to a convexly curved wall of 12.7 cm radius of curvature, giving a ratio of δ_{995}/R of 0.17. The turning angle of the bend was 30°. This represents a strong "impulse" of curvature. Downstream of the bend was a flat-wall recovery section. No data were taken within the curved region.

REFERENCES

- Gillis, J. C., and J. P. Johnston (1980). "Turbulent boundary layer on a convex curved surface," Rep. HMT No. 31, Dept. of Mech. Eng., Stanford University.
- Hoffman, P. H., and P. Bradshaw (1978). "Turbulent boundary layer on surfaces of mild longitudinal curvature," Imperial College Aero. Rep. 78-04 (submitted to JFM for publication).
- Hunt, I. A., and P. N. Joubert (1979). "Effects of small streamwise curvature on turbulent duct flows," JFM, 91:4, 633-659.
- Smits, A. J., S. T. B. Young, and P. Bradshaw (1978). "The effect of short regions of high surface curvature on turbulent boundary layers," JFM, 94:2, 209-242.

DISCUSSION

Flow 0230

D. Bushnell:

1. Did you consider cases where the curvature might oscillate like the sinusoidal wavy wall?
2. What was your criterion for "small" Taylor-Görtler vortices--small in turbulence or small in its effect on the mean flow momentum equation?

T. Simon: No, we did not look at wavy wall cases. We were looking for simple curvature cases and cases that showed the direct effect of curvature on turbulent structure.

On the concave wall it becomes difficult to evaluate secondary flows by way of the integral momentum equation. What we were looking for was information of the spanwise variations of mean and turbulence quantities. In the evaluation, the variation in skin friction was kept down to about $\pm 5\%$. Where Taylor-Görtler vortices were considered large they were treated as advanced test cases.

- G. Mellor: The So and Mellor concave case is too complicated and has large Taylor-Görtler cells and should be considered an advanced test case. However, the convex case is simpler, and there is enough time to develop a quasi-equilibrium boundary layer.
- T. Simon: The So and Mellor convex case is very similar to the Gillis and Johnston case. However, the Gillis and Johnston case has both sustained curvature and recovery region data, making it the favored choice.
- G. Mellor: Are you sure that the 90-degree bend (of the Gillis and Johnston case) is enough to establish a quasi-equilibrium boundary layer?
- T. Simon: We see that the shear-stress profile and the profiles of the fluctuating quantities develop into what looks like an asymptotic condition within about the first 15 to 30 degrees of the bend. However, the mean velocity profiles continue to evolve even up to 150 degrees.
- D. Wilcox: For computational purposes, does your term "weak Taylor-Görtler vortices" mean that you consider these calculable with a two-dimensional method?
- T. Simon: With a two-dimensional boundary layer method, you will be computing the mean by modeling the additional mixing due to the presence of the Taylor-Görtler vortices.
- J. McCroskey: What are your criteria for certifying these flows as two-dimensional?
- T. Simon: The integral momentum balance. This method compared well with flow-angle measurements made by experimenters.
- R. Narasimha: Was any consideration given to the methods used for measurement of skin friction? What were the uncertainties involved? As there is evidence that classical wall similarity is not valid at large curvatures, Preston tubes and Clauser plots may not be valid.*
- T. Simon: The skin friction was usually measured by using the Clauser plot technique. Though at first questionable, this technique is now accepted for cases of mild curvature, as in these test cases. It does break down near the beginning of the curvature where the boundary layer is still not in equilibrium.†

Following the meeting it was commented on that for Cases 0231/0232, the velocities deduced from pitot-static and pitot/wall-static probes differ by about 10%. As in Case 0141 these differences appear to be real. [Ed.: We have queried this with Prof. Bradshaw.]

*See Evaluation Report. For most of these cases, the uncertainty information was not given.

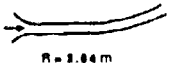
†[Ed.: In the Gillis-Johnston flow, Case 0233, extrapolating uv measurements to the wall agree with the Clauser repeat value of τ_w to within a few percent for all sections beyond about 20° of turn.]

SPECIFICATIONS FOR COMPUTATION
ENTRY CASE/INCOMPRESSIBLE

Case #0231; Data Evaluators: T. Simon and S. Honami
Data Takers: P. H. Hoffman and P. Bradshaw (Convex)

PICTORIAL SUMMARY

Flow 0230. Data Evaluators: T. Simon and S. Honami. "Boundary Layer Flows with Streamwise Curvature."

Case Data Taker	Test Rig Geometry	dp/dx or C _p	Number of Stations Measured										C _f	Re	Initial Condi- tion	Other Notes
			Mean Velocity		Turbulence Profiles											
			U	V or W	u ²	v ²	w ²	uv	Others							
Case 0231-convex Case 0232-concave P. Hoffman & P. Bradshaw	 R = 2.84 m	12	5	-	5	5	-	5	u ² -5 u ² v-5 uv ² -5 v ³ -5	5*	5.2 = 10 ⁴ (based on δ at be- ginning of curve)	6/R = 0.01	Mild Curvature.			

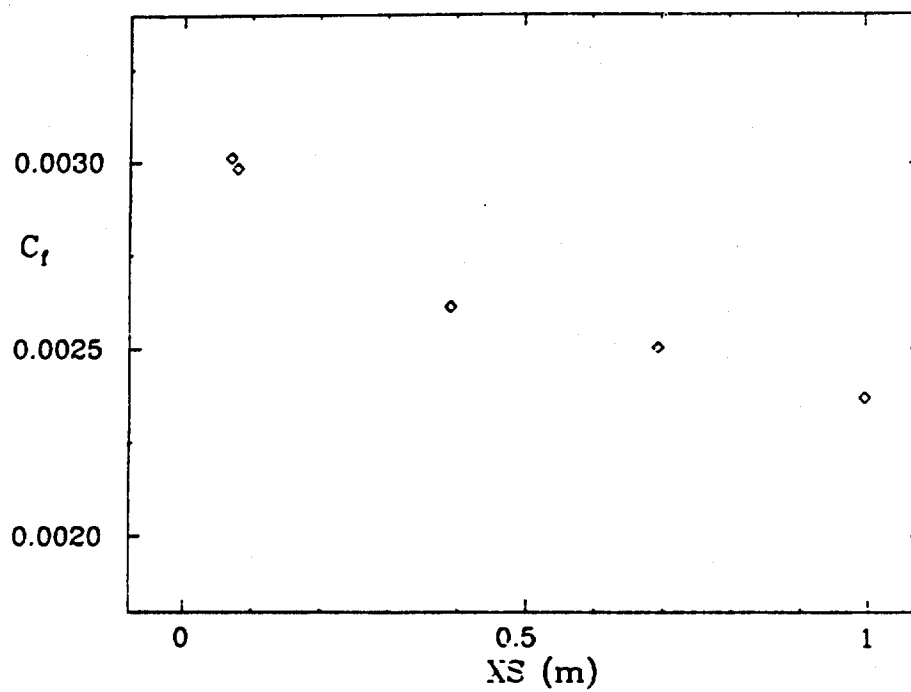
*Clauser Plot Method.

Plot	Ordinate	Abcissa	Range/Position	Comments
1	C _f	XS	0 < XS < 1.0 m	XS = streamwise distance on wall. Curved section begins at XS = 0.
2	θ	XS	-0.2 < XS < 1.0 m	Curved section begins at XS = 0.
3	H	XS	-0.2 < XS < 1.0 m	Curved section begins at XS = 0.
4	y/ δ	U/U _{pot}	at XS = 0.076, 0.685, and 0.99 m	U _{pot} = velocity of potential flow at given location.
5	y/ δ	$\overline{v^2}/U_{pw}^2$	XS = 0.076, 0.685, and 0.99 m	U _{pw} = velocity of potential flow on curved surface at wall.
6	y/ δ	\overline{uv}/U_{pw}^2	XS = 0.076, 0.685, and 0.99 m	

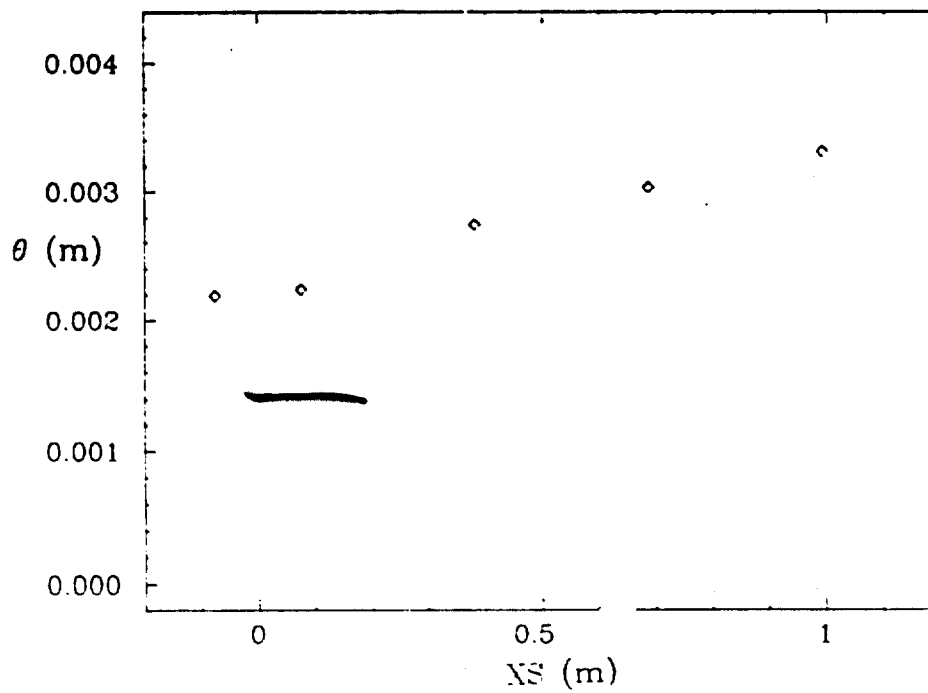
Special Instructions:

1. Begin computations upstream of curve as indicated.
2. Mean and turbulence profiles at XS = -0.076 m can be used to start, or matched for start further upstream. If matched, show values used at start XS = -0.076 m.
3. C_p from data file can be used to compute U_{pw}.
4. Provide a tabulation or curve of output for δ vs XS.

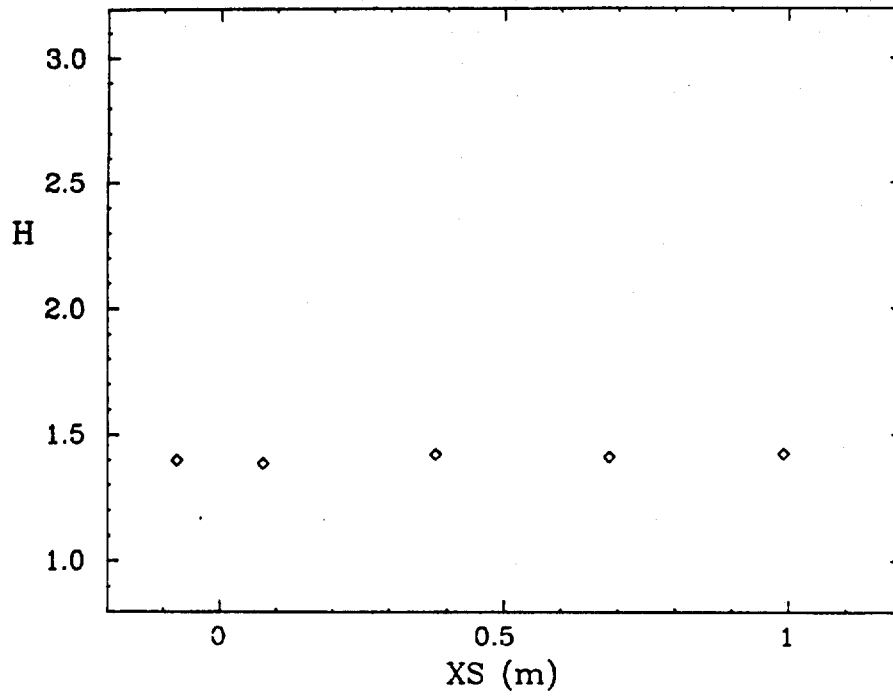
PLOT 1 CASE 0231 FILE 4



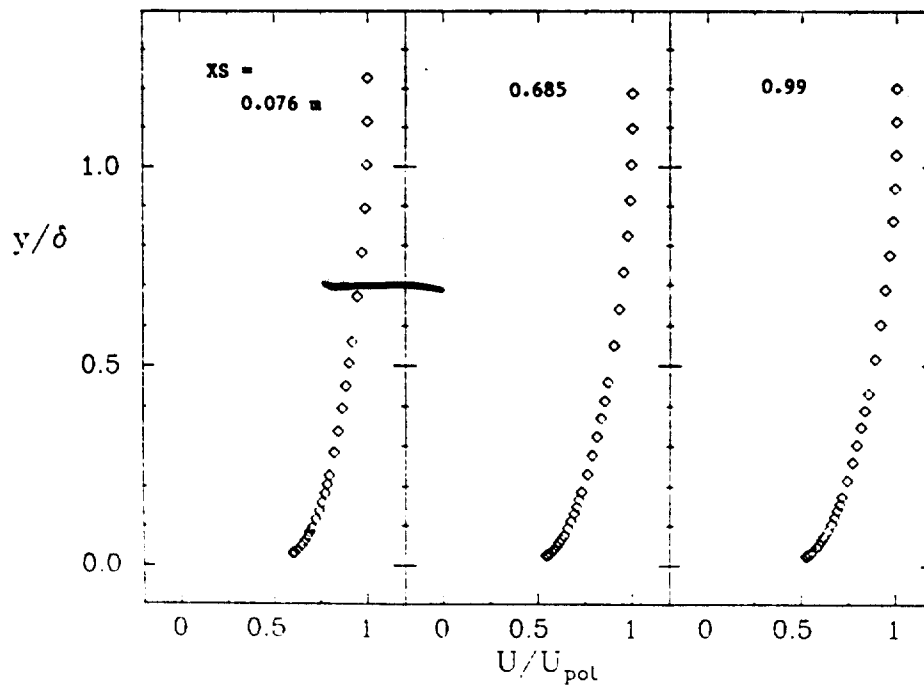
PLOT 2 CASE 0231 FILE 6



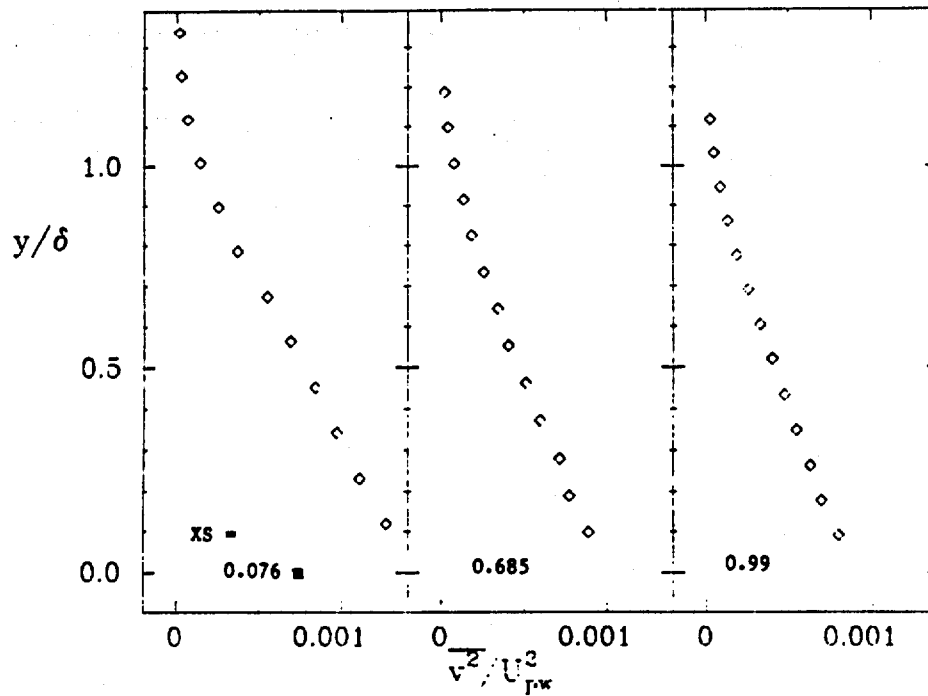
PLOT 3 CASE 0231 FILE 6



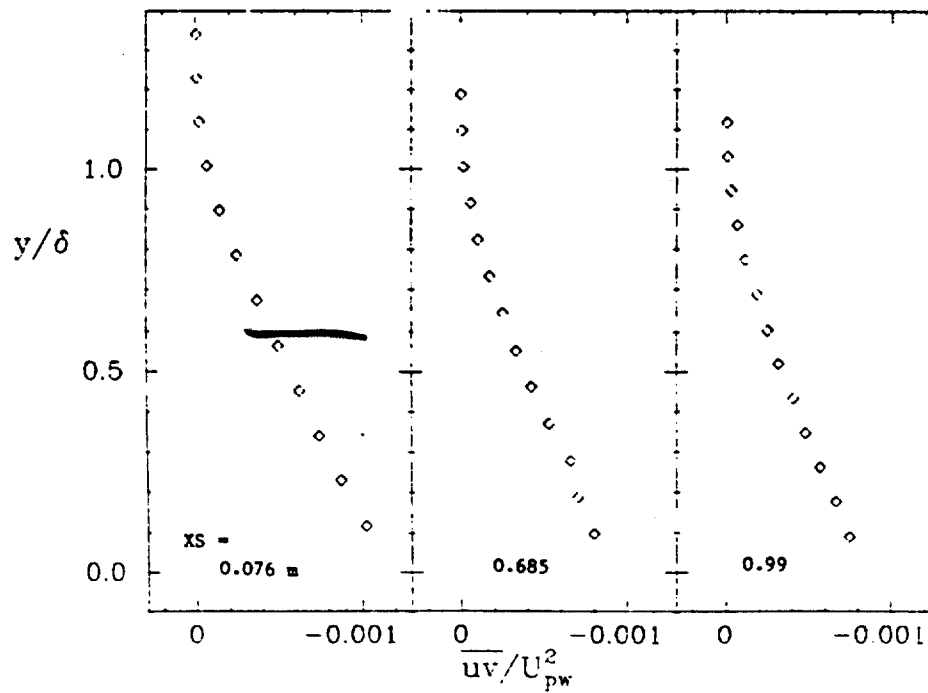
PLOT 4 CASE 0231 FILE 8.11,12



PLOT 5 CASE 0231 FILE 13,14,15,16



PLOT 6 CASE 0231 FILE 13,15,16



SPECIFICATIONS FOR COMPUTATION

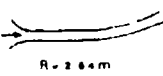
ENTRY CASE/INCOMPRESSIBLE

Case #0232; Data Evaluators: T. Simon and S. Honami.

Data Takers: P. H. Hoffman and P. Bradshaw (Concave)

PICTORIAL SUMMARY

Flow 0232. Data Evaluators: T. Simon and S. Honami. "Boundary Layer Flows with Streamline Curvature."

Case Data Taker	Test Rig Geometry	dy/dx or C _p	Number of Stations Measured										C _f	Re	Initial Condition	Other Notes
			Mean Velocity		Turbulence Profiles											
			U	V or W	u'	v'	w'	uv	Others							
Case 0231-convex Case 0232-concave P. Hoffmann & P. Bradshaw	 R = 2.64 m	12	5	-	5	5	-	5	u' ² -5 u'v'-5 uv ² -5 v ² -5	5 ^a	5.2 x 10 ⁵ (based on δ at be- ginning of curve)	0/R = 0.02	Mild Curvature.			

^aClauser Plot Method.

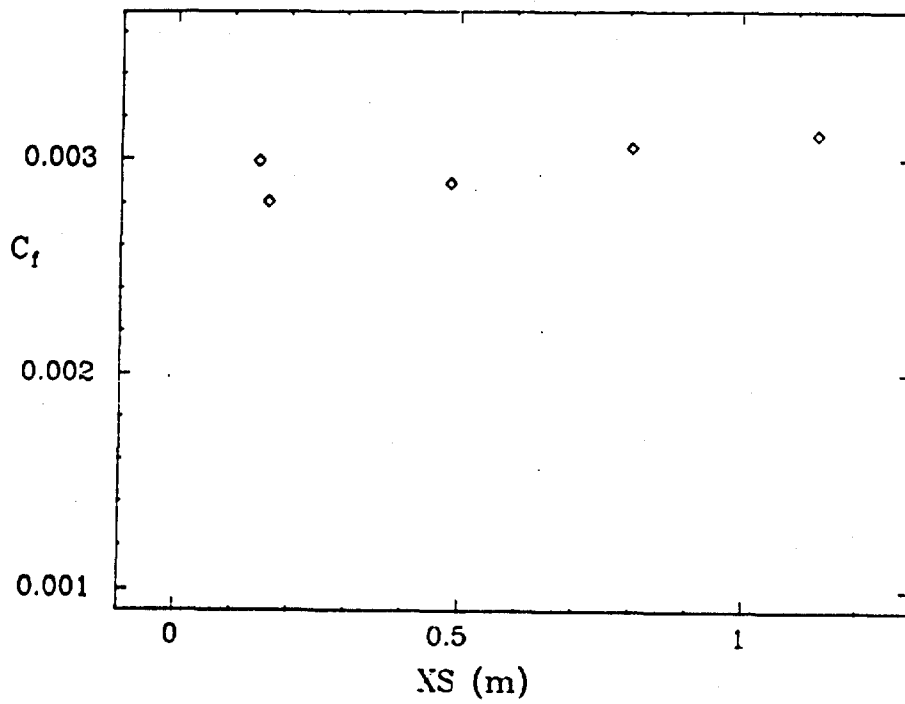
^a Clauser Plot Method.

Plot	Ordinate	Abcissa	Range/Position	Comments
1	C _f	XS	0 < XS < 1.2 m	XS = streamwise distance on wall. Curved section begins at XS = 0.
2	θ	XS	-0.2 < XS < 1.2 m	Curved section begins at XS = 0.
3	h	XS	-0.2 < XS < 1.2 m	Curved section begins at XS = 0.
4	y/δ	U/U _{pot}	XS = 0.16, 0.803, 1.123 m	U _{pot} = velocity of potential flow at given location.
5	y/δ	$\sqrt{2}/U_{pw}^2$	XS = 0.16, 0.803, 1.123 m	U _{pw} = velocity of potential flow on curved surface at wall.
6	y/δ	\overline{uv}/U_{pw}^2	XS = 0.16, 0.803, 1.123 m	

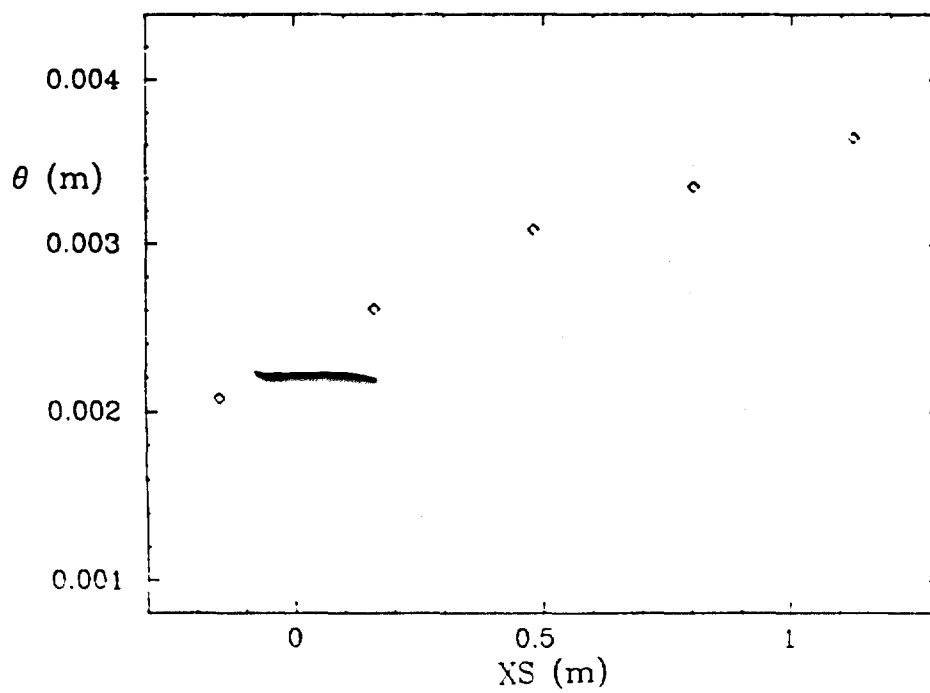
Special Instructions:

1. Begin computations upstream of curve as indicated.
2. Mean and turbulence profiles at XS = -0.152 m can be used to start, or matched for start further upstream. If matched, show values used at XS = -0.152 m.
3. C_p data from file can be used to compute U_{pw}.
4. Provide a tabulation or curve of output for δ vs XS.

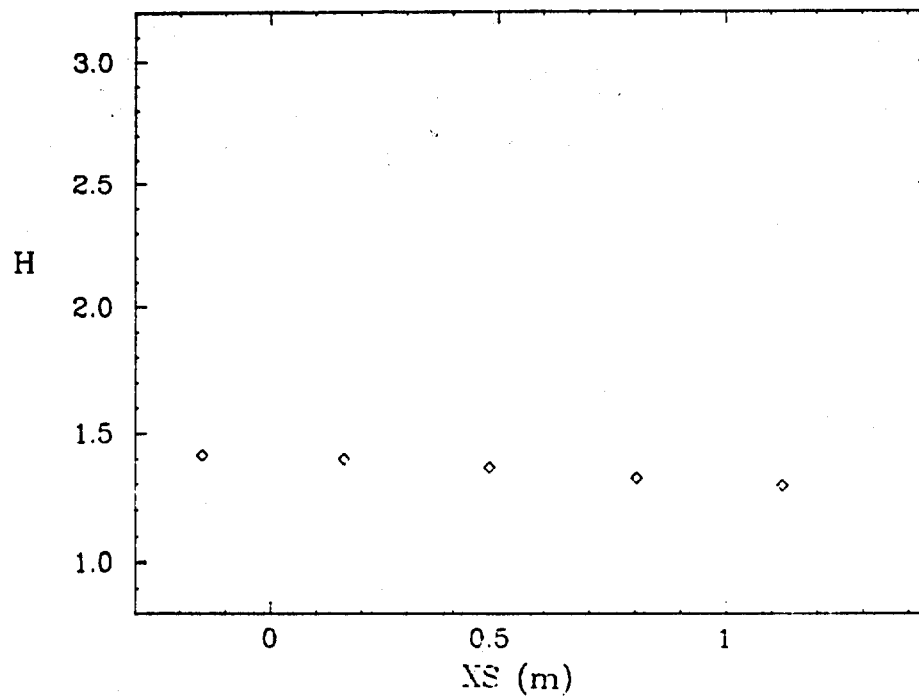
PLOT 1 CASE 0232 FILE 5



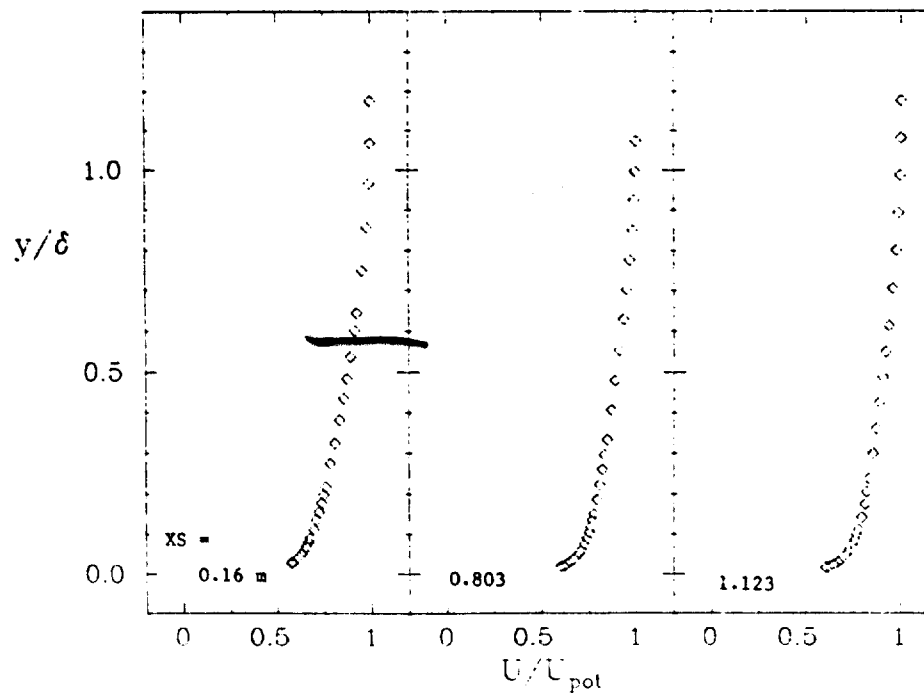
PLOT 2 CASE 0232 FILE 7



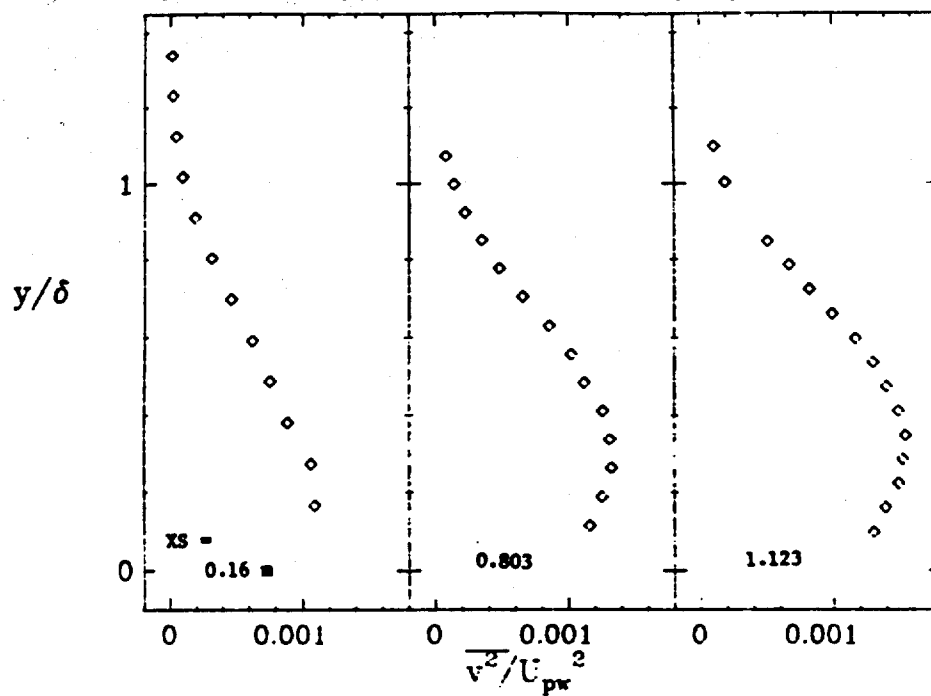
PLOT 3 CASE 0232 FILE 7



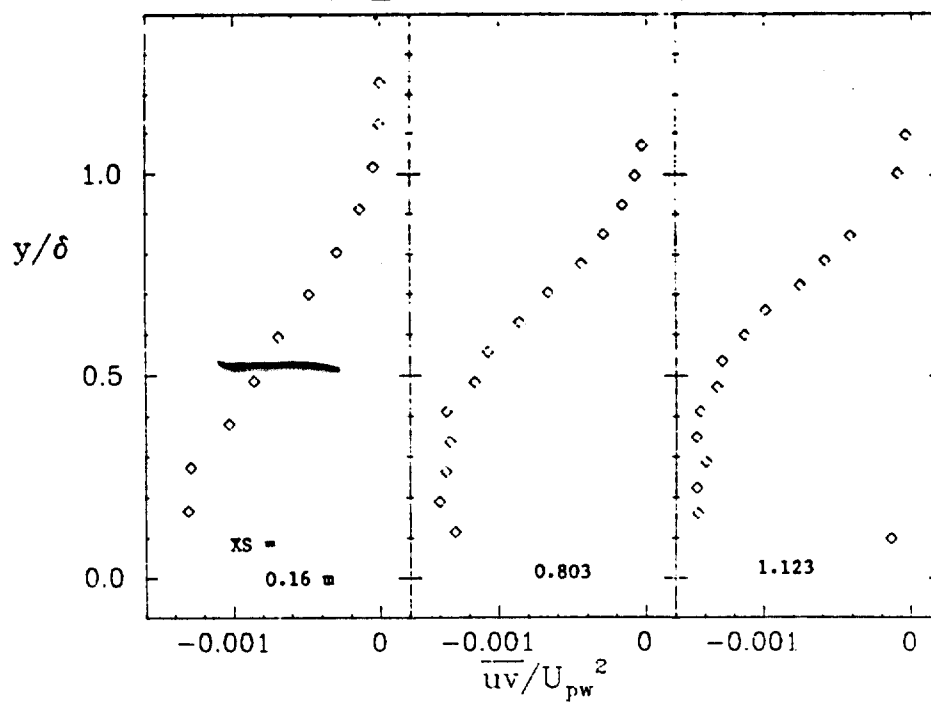
PLOT 4 CASE 0232 FILES 18,20,21



PLOT 5 CASE 0232 FILES 23,25,26



PLOT 6 CASE 0232 FILES 23,25,26



SPECIFICATIONS FOR COMPUTATION


ENTRY CASE/INCOMPRESSIBLE

Case #0233; Data Evaluators: T. Simon and S. Honami

Data Takers: J. Gillis and J. P. Johnston

PICTORIAL SUMMARY

Flow 0230. Data Evaluators: T. Simon and S. Honami. "Boundary Layer flows with Streamwise Curvature."

Case Date Taker	Test Rig Geometry	Ap/dx or C _p	Number of Stations Measured								C _f	Re	Initial Condi- tion	Other Notes
			Mean Velocity		Turbulence Profiles									
			U	V or W	$\overline{u^2}$	$\overline{v^2}$	$\overline{w^2}$	\overline{uv}	Others					
Case 0233 J. Gilite & J. Johnston	 R = 0.48 m	24	11	-	12	12	12	12		24 ^a	4.6 × 10 ⁴ (based on δ at be- ginning of curve)	0.10	Strong Curvature with Recovery.	

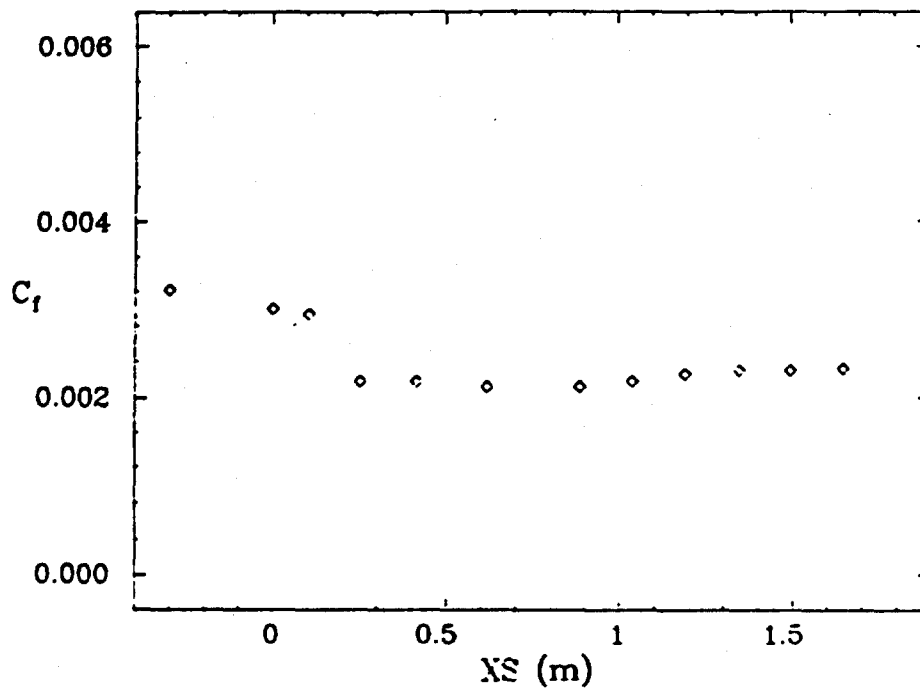
^a Clauser Plot Method.

Plot	Ordinate	Abscissa	Range/Position	Comments
1	C_f	XS	$-0.3 < XS < 1.7$ m	
2	H	XS	$-0.3 < XS < 1.7$ m	
3	y/δ	U/U_{pw}	XS = 0.104, 0.415, 0.885, and 1.647 m	
4	y/δ	$\overline{u^2}/U_{pw}^2$	XS = 0.104, 0.415, 0.885, and 1.647 m	
5	y/δ	$\overline{v^2}/U_{pw}^2$	XS = 0.104, 0.415, 0.885, 1.647 m	
6	y/δ	$\overline{w^2}/U_{pw}^2$	XS = 0.104, 0.415, 0.885, 1.647 m	
7	y/δ	\overline{uv}/U_{pw}^2	XS = 0.104, 0.415, 0.885, 1.647 m	

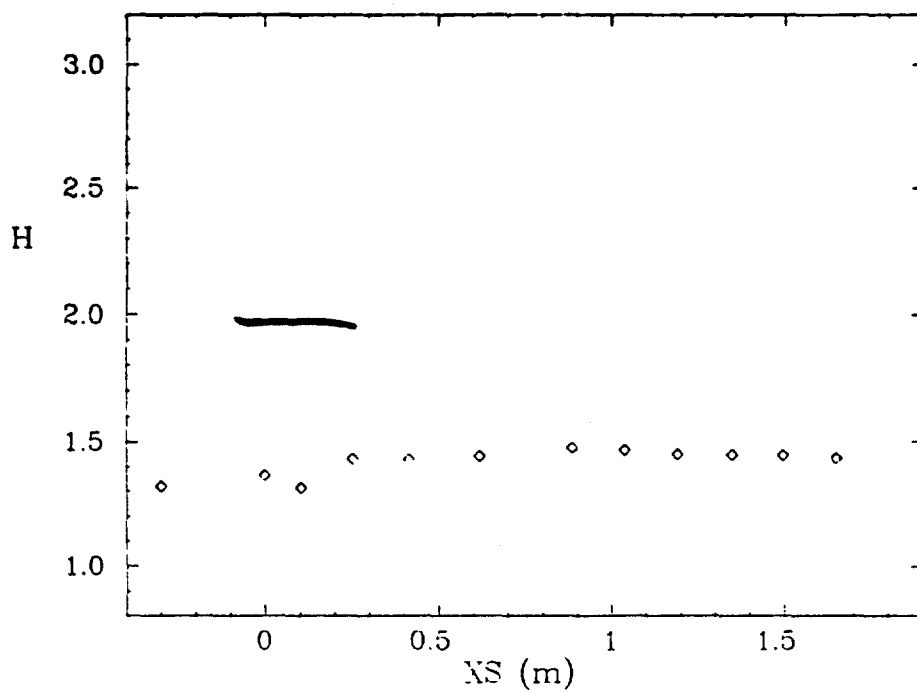
Special Instruction:

- Provide a tabulation or curve of output for δ vs XS.

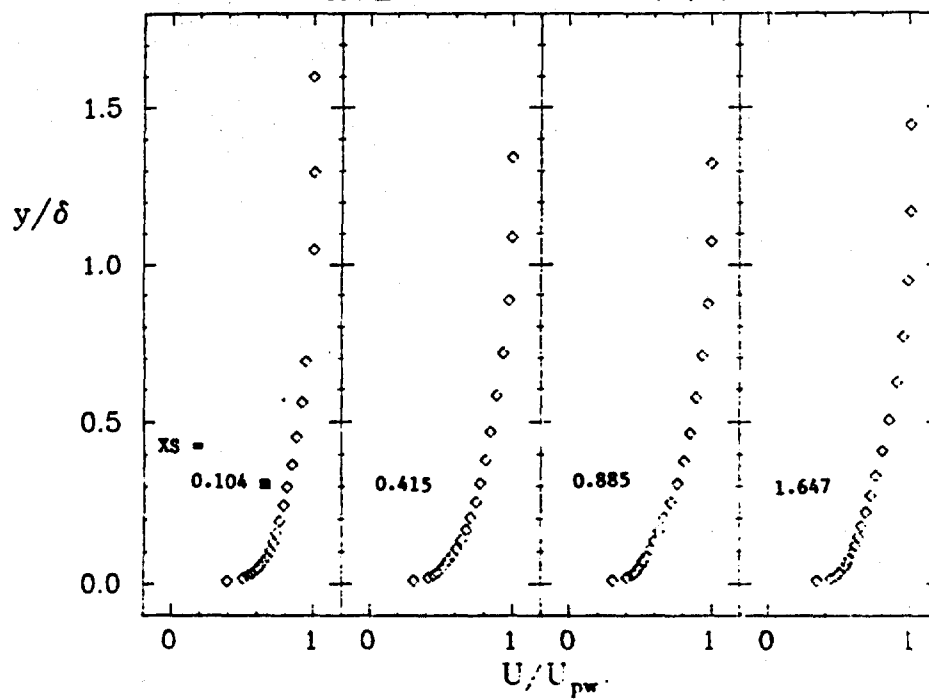
PLOT 1 CASE 0233 FILE 3



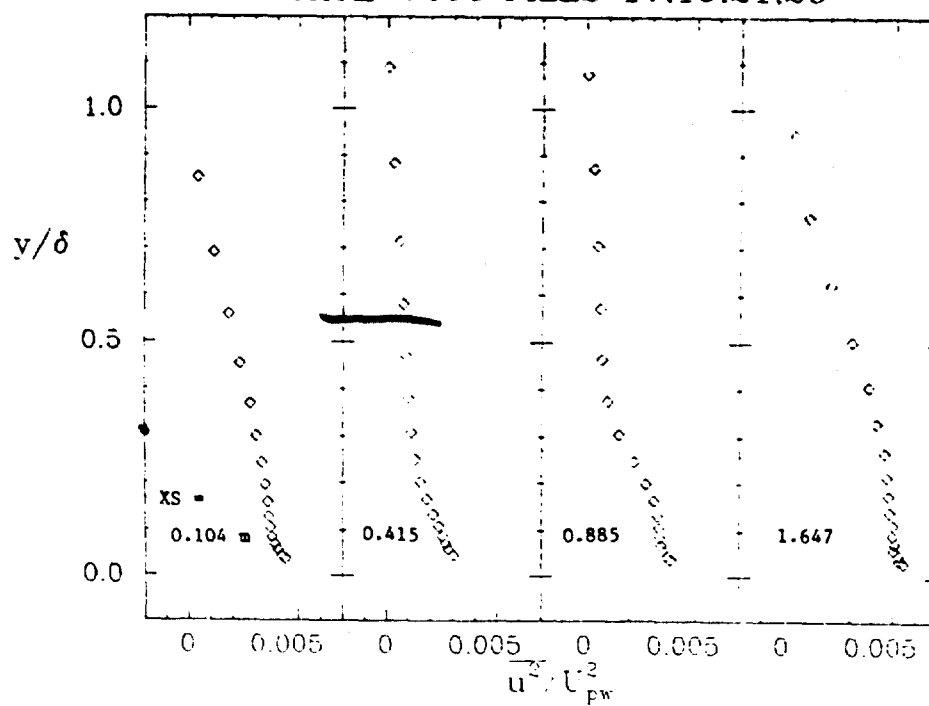
PLOT 2 CASE 0233 FILE 3



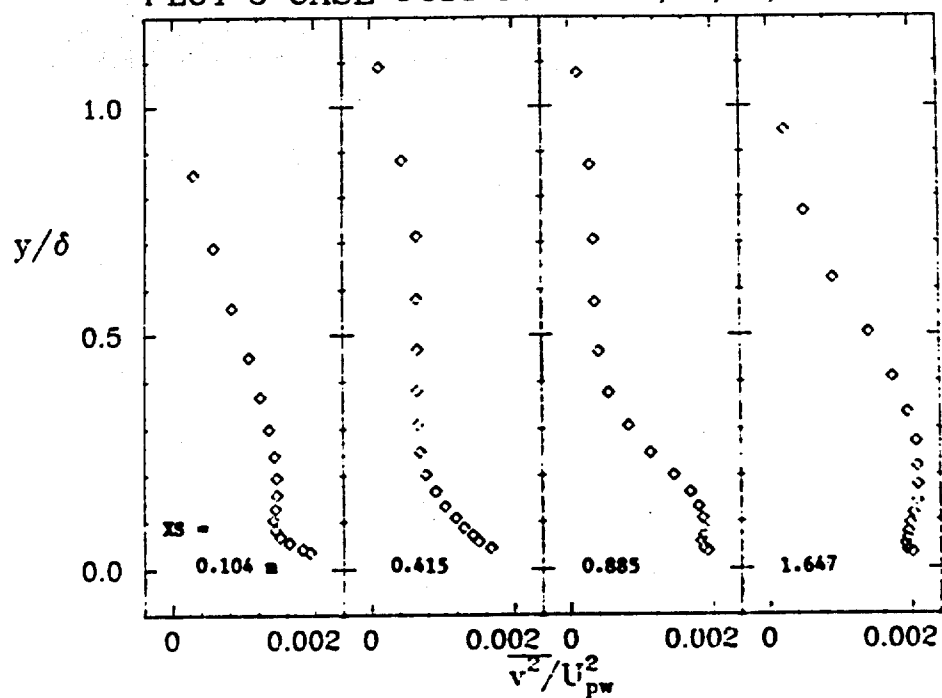
PLOT 3 CASE 0233 FILES 5,7,9,14



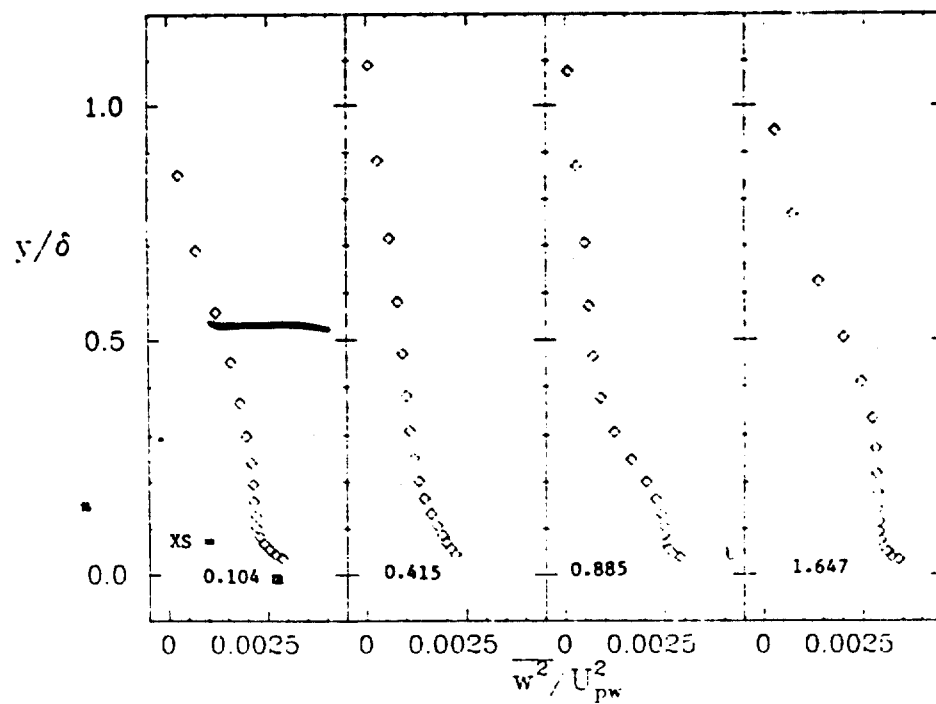
PLOT 4 CASE 0233 FILES 17.19.21.26



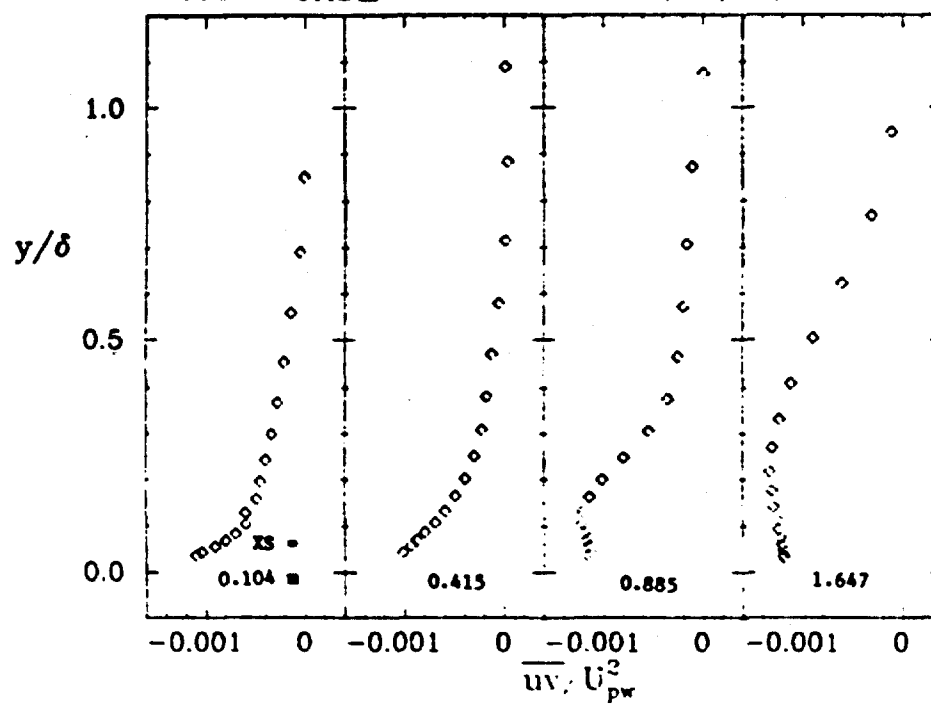
PLOT 5 CASE 0233 FILES 17,19,21,26



PLOT 6 CASE 0233 FILES 17,19,21,26



PLOT 7 CASE 0233 FILES 17,19,21,26



SESSION II

Chairman: B. Launder

Technical Recorders:

R. Childs
P. N. Joubert



Flow 0240

Flow 8300

Flow 0330

Flow 0510

TURBULENT BOUNDARY LAYERS WITH SUCTION OR BLOWING (INCOMPRESSIBLE)

Flow 0240

Cases 0241, 0242, 0244

TURBULENT BOUNDARY LAYERS WITH SUCTION OR BLOWING (COMPRESSIBLE)

Flow 8300

Case 8301

Evaluator: L. C. Squire*



(presented by
E. P. Sutton*)

SUMMARY

There have been numerous experimental studies of turbulent boundary layers with suction or blowing through the surface and many of these data sets are available in numerical form in reports or theses. In order to reduce this mass of data to manageable form it was decided to restrict the evaluation to measurements made on surfaces in which the holes, or pores, through which the fluid is blown or sucked are small relative to the boundary-layer thickness and are so close together that the velocity normal to the surface (V) may be assumed constant locally. That is, the surface is essentially homogeneous and the flow through the surface is a good approximation to the mathematical boundary condition of specified normal velocity at the surface. This restriction allows us to consider flows in which the mass flow rate through the surface varies along that surface, i.e., $V = V(x)$. It also allows consideration of flows in which there is a step change in the mass flow rate at a particular position (i.e., $V = 0$ for $x < X$ and $V = \text{constant}$ for $x > X$). However, it excludes blowing, or suction, through discrete holes or slots. This restriction was made since it was felt that such flows would require very careful consideration before it was possible to specify suitable boundary conditions and test results. In fact the present evaluator regards these flows as more suitable to a conference on very complex turbulent flows. It should also be noted that experiments with foreign gas injection and experiments which concentrate on heat transfer aspects of injection have not been considered.

Even within this restricted class of flows there is a large amount of data. In fact over 200 boundary-layer developments with blowing or suction through porous surfaces have been reported in the literature and for many of these developments full tables of measured profiles are available. In addition to flows in zero pressure gradient a wide range of pressure-gradient conditions have been studied, both at low speeds and at supersonic speeds, and in many cases the mass flow rate through the

*Cambridge University, Cambridge, CB2 1PZ, England.

surface varies along the surface. Some of the experimental studies appear to cover the same blowing (or suction) and pressure-gradient conditions, but this does not imply that the results are directly comparable since in many cases the state of the boundary layer upstream of the region of injection differs in the various experiments.

In the cases in which a direct comparison is possible a number of discrepancies were apparent, particularly in the quoted skin-friction coefficients. In considering these discrepancies it should be noted that most experimenters obtained the skin friction from some form of the momentum integral equation. The use of this equation, in whatever guise it is used, tends to be inaccurate especially at the higher blowing rates. Thus some of the differences in the quoted skin friction may be due to the form of analysis used, rather than to genuine differences in the actual flow conditions. In particular it has been found that some of the discrepancies could be removed by using a consistent form of curve fitting in the analysis of the experimental results. In spite of this many of the data sets have had to be rejected because of the lack of redundant measurements, and hence the impossibility of checking the overall two-dimensionality of the flow.

Redundant measurements were made in the later experiments at Stanford by Andersen, Kays, and Moffat (1972). Basically these workers measured both mean flow and turbulent shear stress through the boundary layer at various stations, and then used the mean-flow velocities in the integrated equations of motion to extrapolate the measured shear stress away from the wall to the skin friction at the wall. Of course, this method is still limited by the accuracy of the hot-wire measurements of the shear stress, but it was found that the skin-friction coefficients so obtained were in good agreement with those obtained from a momentum balance. The agreement was particularly good for flows with moderate blowing rates in zero pressure gradients. Andersen et al. (1972) and Orlando et al. (1974) also studied a set of boundary-layer developments with injection or suction with pressure gradients chosen to give equilibrium conditions along the layer. In general the overall results from these layers were in good agreement with the results for equilibrium layers on solid surfaces as measured by other workers. All these layers were checked for two-dimensionality, and it was found that the best layer was one with suction and an adverse gradient. This layer was chosen for a test case together with one of Andersen's layers with injection in zero pressure gradient. This latter layer corresponds to a relatively moderate blowing rate of $F = 0.004$ ($F \equiv \rho_w V_w / \rho_e U_e$) since unfortunately none of the layers with $F > 0.004$ appears to be two-dimensional. In particular the momentum balance applied to the flow with $F = 0.008$ gave significant negative skin-friction coefficients.

A wide range of experimental results is also available for layers with suction and blowing in favorable pressure gradients, but unfortunately none of these tests provides an independent measurement of skin friction. However, the results of Loyd et

al. (1970) and of Julien et al. (1969) were obtained in the same tunnel as used by Andersen; the fluid-flow measurements were made in parallel with extensive heat-transfer measurements that showed an excellent overall energy balance. Thus these developments might provide further test cases if needed.

An interesting set of results for high suction rates in zero pressure gradient were obtained by Favre et al. (1966). A full check on the reliability of these flows is not possible since full velocity profiles are not available. However, the original report does quote skin-friction values as obtained by two methods and the agreement between the two sets of values is excellent. The tests included measurements of turbulence quantities at one station for suction rates up to $F = -0.014$. It is suggested that these measurements form a simple data set in which the predicted values of, \overline{uv} , $(\overline{u^2})^{1/2}$, and $(\overline{v^2})^{1/2}$ are compared with the measured values for several suction rates.

So far the tests considered have been made in low-speed flows so that the effects of compressibility can be ignored. The present evaluator and his students have made an extensive study of turbulent boundary layers with air injection at supersonic speeds. A critical study of the results from this program has shown that the boundary layers generated in the $M = 2.5$ nozzle are closely two-dimensional in that the skin-friction coefficients on solid surfaces are in close agreement with skin-friction balance measurements made in the same Mach number and Reynolds number ranges by other workers in a variety of test sections. Thomas (1974) used this nozzle to study layers with slight favorable pressure gradients for various injection rates. He also used the razor-blade technique to measure skin-friction coefficients on a solid surface for the same pressure gradients and the measured values gave good agreement with the overall momentum balance. Thus one of these layers is suggested as a test case. However, in spite of the care taken to eliminate spurious wave systems in the pressure gradients some weak waves are still present, and these waves affect one or two of the measured velocity profiles.

As a result of this evaluation the following test cases have been recommended.

- Case 0241. A flow with zero pressure gradient and constant injection ($F = 0.004$) as measured by Andersen, Kays, and Moffat (1972).
- Case 0242. A flow with an adverse pressure gradient ($U_e = x^{-0.15}$) and constant suction ($F = -0.004$) as measured by Andersen, Kays, and Moffat (1972).
- Case 0244. Flows with high suction rates ($-0.014 < F$) in zero pressure gradient as measured by Favre, Dumas, Verollet, and Coantic (1966).

Case 8301. A flow with favorable pressure gradient at supersonic speeds
($2.53 < M < 2.87$) and variable blowing ($0.002 < F < 0.0028$)
as measured by Thomas (1974).

Together these four data sets cover blowing and suction, favorable and adverse pressure gradients, the effect of compressibility and of a step change in suction rate. Also some of the flows include measurements of turbulent quantities. Thus together they would appear to cover the main features of layers with suction or blowing and hence to provide a full test of the various calculation methods.

In completing this evaluation the main obstacle in choosing test cases and in assessing the accuracy of the results has been the lack of direct methods of measuring skin friction. Recently a number of workers (Schetz and Nerney, 1977; Derzhin et al., 1967; Voisinnet, 1979) have developed floating-element balances to measure skin friction on porous surfaces with blowing through the pores. Although these balances show considerable promise there are still a number of problems to be overcome before they can be used in routine tests. However, the results obtained so far do indicate a strong interaction between blowing and surface roughness. From these results it would appear that some of the discrepancies mentioned above may be associated with the different types of porous surfaces used in the various experiments. Thus in future experiments with blowing and suction it is recommended that experimenters take great care to specify the nature of their surface, both in terms of pore size and distribution and in overall roughness characteristics. In this connection it should be pointed out that it is believed that the data sets suggested above are not influenced by the nature of the porous surface.

Finally the evaluator would like to thank workers who have supplied original data and have answered his many questions. He would also like to emphasize that the fact that a particular flow is not included in the data sets does not imply that measurements are considered inaccurate. In fact there are many other sets of measurements which could form useful test cases if needed, and these results have been of considerable value in choosing the test cases mentioned above.

REFERENCES

- Audersen, P. S., W. M. Kays, and R. J. Moffat (1972). "The turbulent boundary layer on a porous plate; an experimental study of the fluid mechanics for adverse pressure gradients," Technical Report No. 15, Dept. of Mech. Eng., Thermosciences Division, Stanford University, Stanford, California.
- Dershin, H., C. A. Leonard, and W. H. Gallaher (1967). "Direct measurements of skin friction on a porous flat plate with mass injection," AIAA Journal, 5, 1934-1939.
- Favre, A., R. Dumas, E. Verollet, and M. Coantic (1966). "Couche limite turbulente sur paroi poreuse avec aspiration," Travaux de l'I.M.S.T. LA No. 130 au C.N.R.S., J. de Mécanique, 5, 3-28.
- Julien, H. L., W. M. Kays, and R. J. Moffat (1969). "The turbulent boundary layer on a porous plate: experimental study of the effects of a favorable pressure gradient," Technical Report No. 4, Dept. of Mech. Eng., Thermosciences Division, Stanford University, Stanford, California.
- Loyd, R. J., R. J. Moffat, and W. M. Kays (1970). "The turbulent boundary layer on a porous plate: an experimental study of the fluid dynamics with strong favorable pressure gradients and blowing," Technical Report No. 13, Dept. of Mech. Eng., Thermosciences Division, Stanford University, Stanford, California.
- Orlando, A. F., R. J. Moffat, and W. M. Kays (1974). "Turbulent transport of heat and momentum in a turbulent boundary layer subject to deceleration, suction and variable wall temperature," Technical Report No. 17, Dept. of Mech. Eng., Thermosciences Division, Stanford University, Stanford, California.
- Schetz, J. A., and B. Nerney (1977). "Turbulent boundary layers with injection and surface roughness," AIAA Journal, 15, 1288-1294.
- Thomas, G. D. (1974). "Compressible turbulent boundary layers with combined air injection and pressure gradient," Aero Res. Council. R & M, 3779.
- Voisinot, R. L. P. (1979). "Combined influence of roughness and mass transfer on turbulent skin friction at Mach 2.9," AIAA Paper 79-0003.

DISCUSSION

Flows 0240/8300

The proposed test cases and the summary report were accepted with the following observations:

1. Prof. Hanjalic, who has made computations of Case 0242 (adverse pressure gradient with suction), believed that the measured \overline{uv} profile near the end of the porous section was inconsistent with those farther upstream because it implied a sudden increase in shear stress.
2. It was felt that the test cases, because they considered only rather moderate levels of blowing, effectively provided only a test of the modeling of the very near-wall region of the flow (i.e., the viscous and "buffer" layer). If computers adopt a bilogarithmic near-wall matching in the calculations, the success in predicting C_f will depend predominantly on the choice made for the dependence of the additive constant in the bi-log law on V_w^+ .
3. In examining the variations in skin friction from flow to flow, several of the review committee felt that there was perhaps an overemphasis on C_f measurements. There is generally good consistency between different experiments on velocity profiles, even at higher blowing rates than have been recommended. Consideration could therefore be given to including, as an additional (or alternative) case, a boundary layer with strong blowing: just the development of mean velocity (not the wall shear stress) would be required of computers.
4. Regarding future data, it was noted that the R_θ for the present test cases were rather modest, a feature that caused some difficulty in starting computations. To separate low Reynolds number effects from those strictly attributable to transpiration, any future measurements could hopefully be made with a substantial impermeable section before blowing or suction began in order to permit the attainment of higher starting Reynolds numbers. (On the other hand, a turbulence model that could accommodate low Reynolds number influences without blowing ought also to be able to handle them in a transpired boundary layer.)

SPECIFICATIONS FOR COMPUTATION

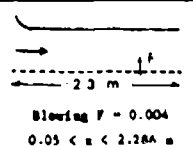
ENTRY CASE/INCOMPRESSIBLE

Case #0241; Data Evaluator: L. C. Squire

Data Takers: P. S. Andersen, W. M. Kays, and R. J. Moffat ($\partial p / \partial x > 0$), ($F = -0.004$)

PICTORIAL SUMMARY

Flow 0240. Data Evaluator: L. Squire. "Turbulent Boundary Layers with Suction or Blowing."

Case Data Taker	Test Rig Geometry	dp/dx or C _p	Number of Stations Measured							C _f	Re	Initial Condi- tion	Other Notes
			Mean Velocity		Turbulence Profiles								
			U	V or W	$\overline{u^2}$	$\overline{v^2}$	$\overline{w^2}$	\overline{uv}	Others				
Case 0241 P. Andersen W. Kays R. Moffat		0	9	-	-	-	-	-	-	9	6.7 × 10 ⁵ per m	M=0	No turbulence data.

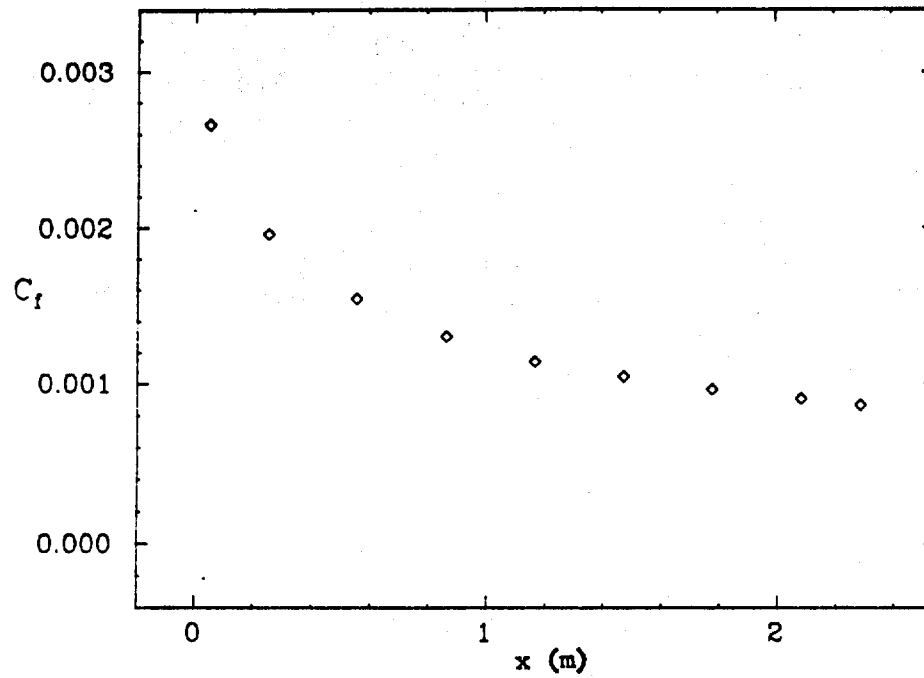
Plot	Ordinate	Abscissa	Range/Position	Comments
1	C_f	x	$0.0508 \leq x \leq 2.286 \text{ m}$	
2	u	x	$0.0508 \leq x \leq 2.286 \text{ m}$	
3	δ^*	x	$0.0508 \leq x \leq 2.286 \text{ m}$	
4	y	U/U_e	at $x = 0.5588,$ $1.1684, 1.778,$ 2.286 m	

Special Instruction:

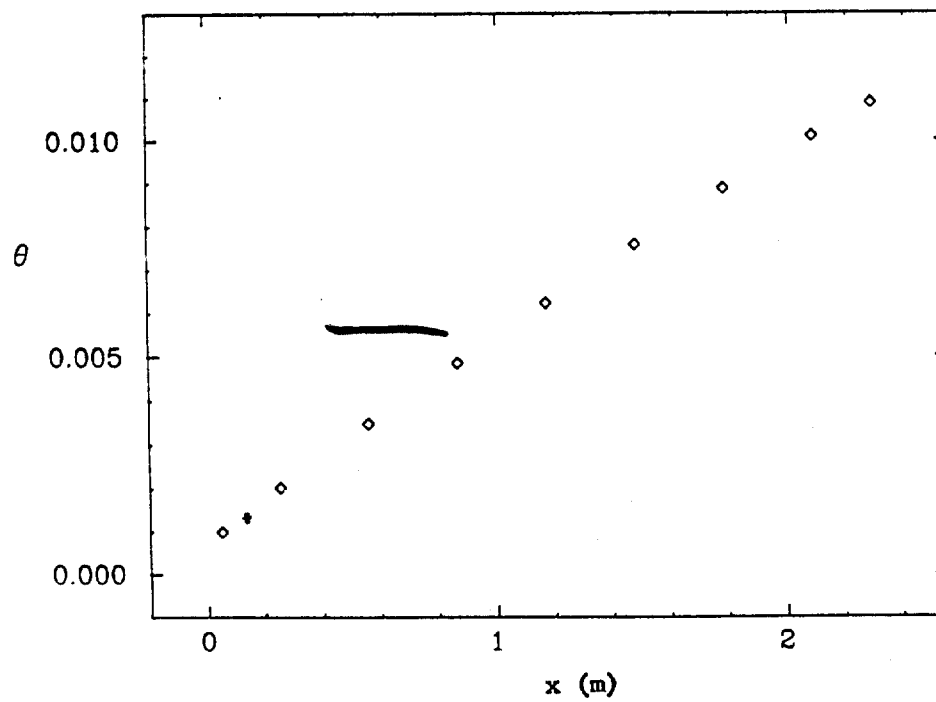
Definition of Special Symbol:

$$F \triangleq \frac{\rho_w V}{\rho_e U_e}$$

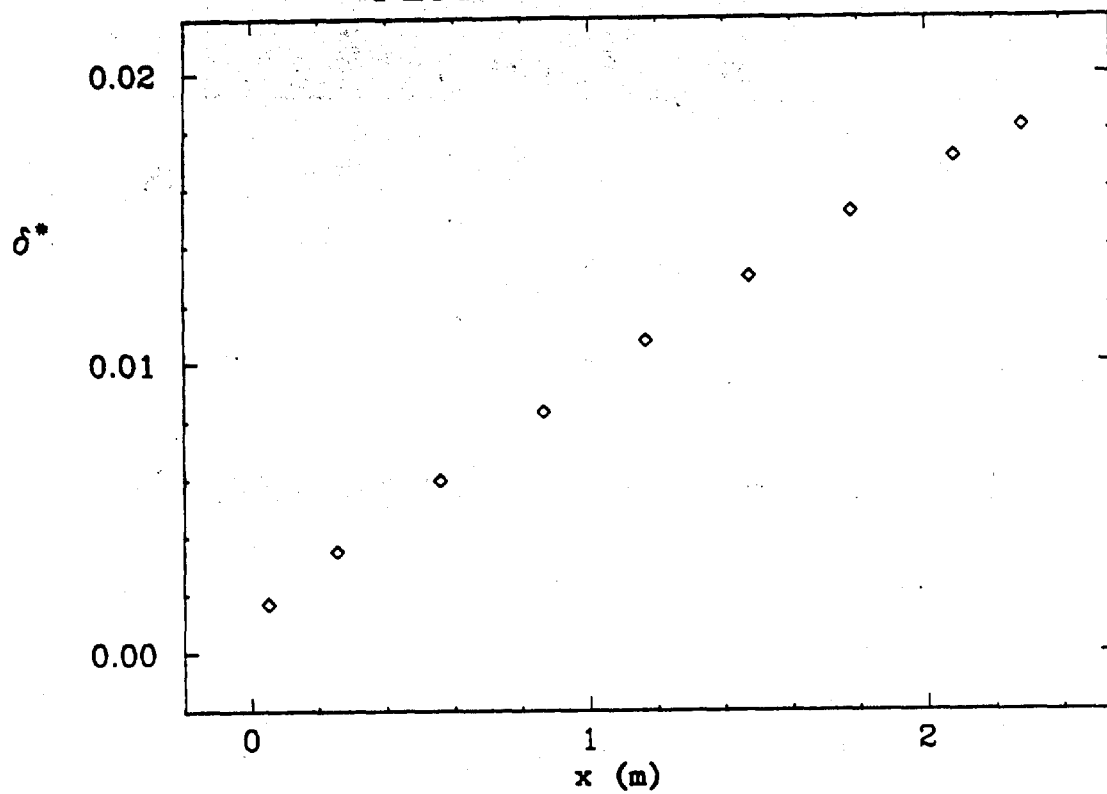
PLOT 1 CASE 0241 FILE 2



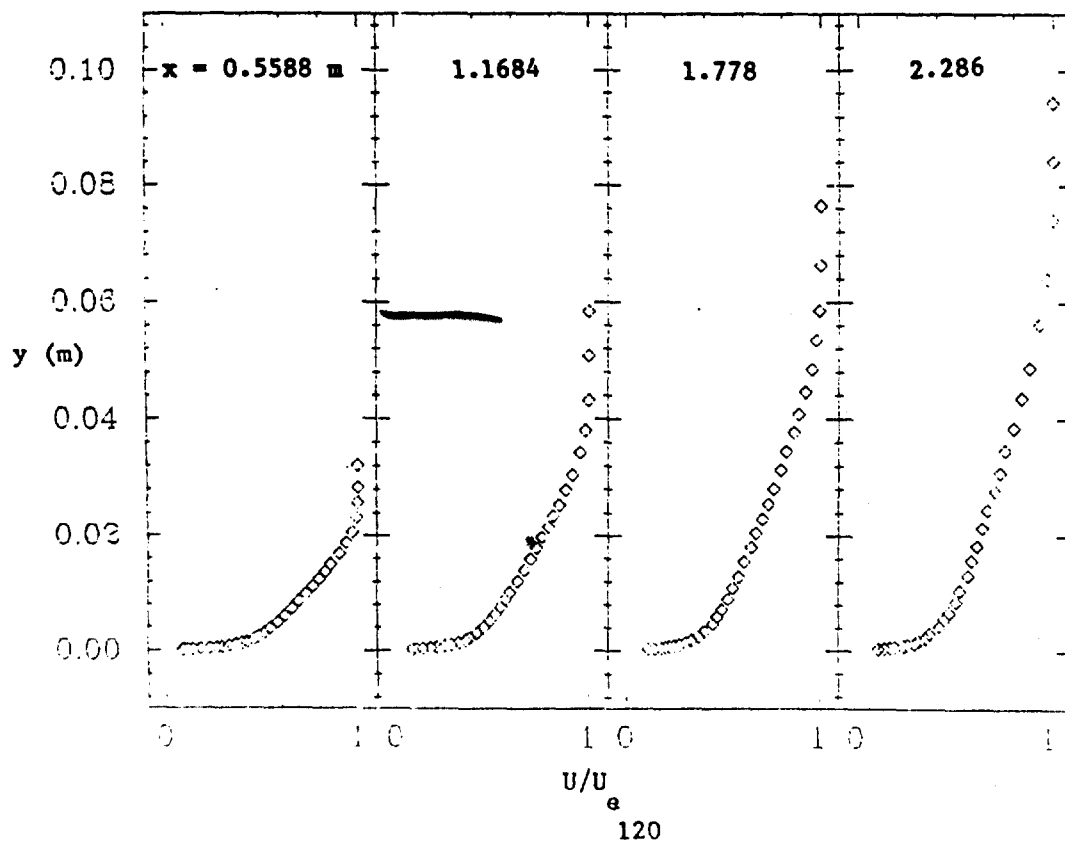
PLOT 2 CASE 0241 FILE 2



PLOT 3 CASE 0241 FILE 2



PLOT 4 CASE 0241 FILES 5,7,9,11



SPECIFICATIONS FOR COMPUTATION

ENTRY CASE/INCOMPRESSIBLE

Case #0242; Data Evaluator: L. C. Squire

Data Takers: P. S. Andersen, W. M. Kays, and R. J. Moffat ($\partial p / \partial x = 0$), ($F = -0.004$)

PICTORIAL SUMMARY

Flow 0240. Data Evaluator: L. Squire. "Turbulent Boundary Layers with Suction or Blowing."

Case Data Taker	Test Rig Geometry	dp/dx or C _p	Number of Stations Measured								C _f	Re	Ini- tial Condi- tion	Other notes
			Mean Velocity		Turbulence Profiles									
			U	V or W	$\overline{u^2}$	$\overline{v^2}$	$\overline{w^2}$	\overline{uv}	Others					
Case 0242 P. Andersen W. Kays R. Moffat	As Case 0241 Suction F = -0.004 0.05 < x < 2.286 m	Ad- verse U _m x ^{-0.15}		9	-	1	1	1	-	9	6.7 × 10 ⁵ per m	0	Turbulence data available at initial station.	

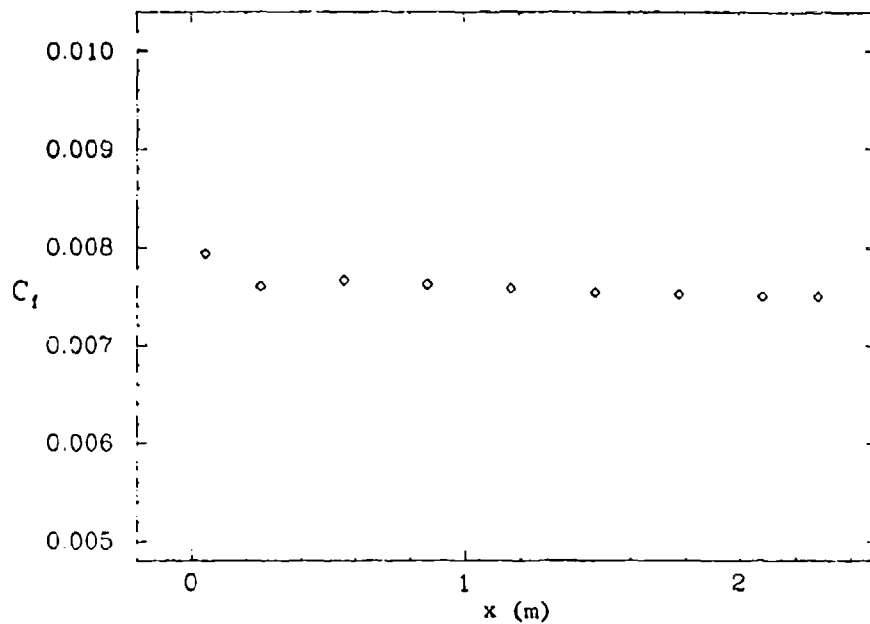
Plot	Ordinate	Abscissa	Range/Position	Comments
1	C_f	x	$0.5588 \leq x \leq 2.286$ m	
2	θ	x	$0.5588 \leq x \leq 2.286$ m	
3	δ^*	x	$0.5588 \leq x \leq 2.286$ m	
4	y	U/U_e	at $x = 0.5588,$ 1.1684, 1.778, 2.286 m	

Special Instruction:

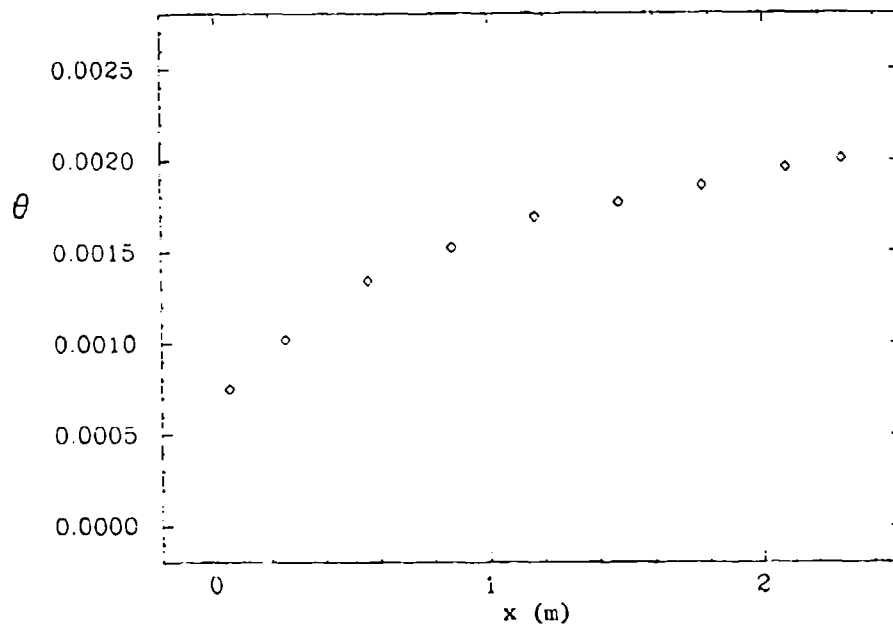
Definition of Special Symbol:

$$F = \frac{\rho}{\rho_e} \frac{V}{U_e} \frac{W}{W_e}$$

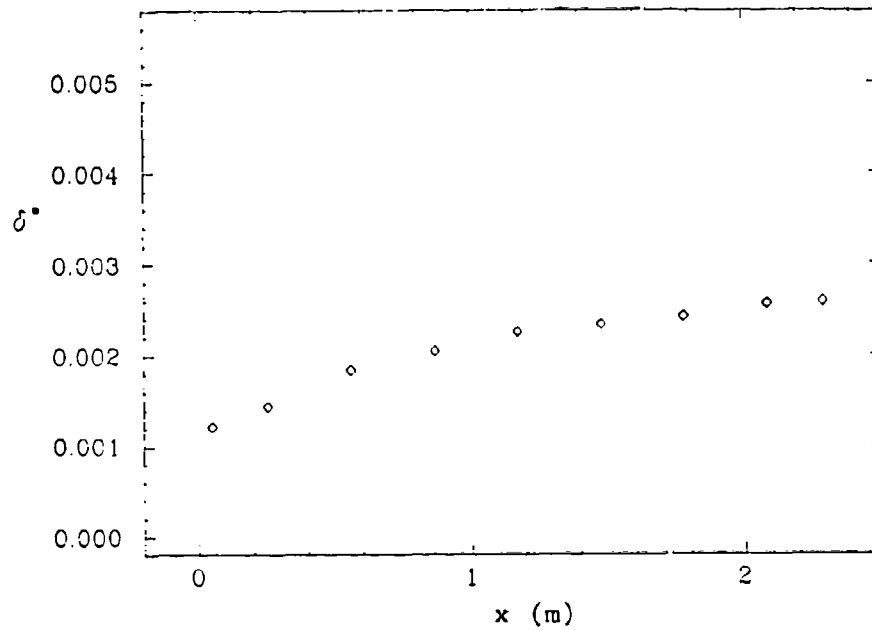
PLOT 1 CASE 0242 FILE 2



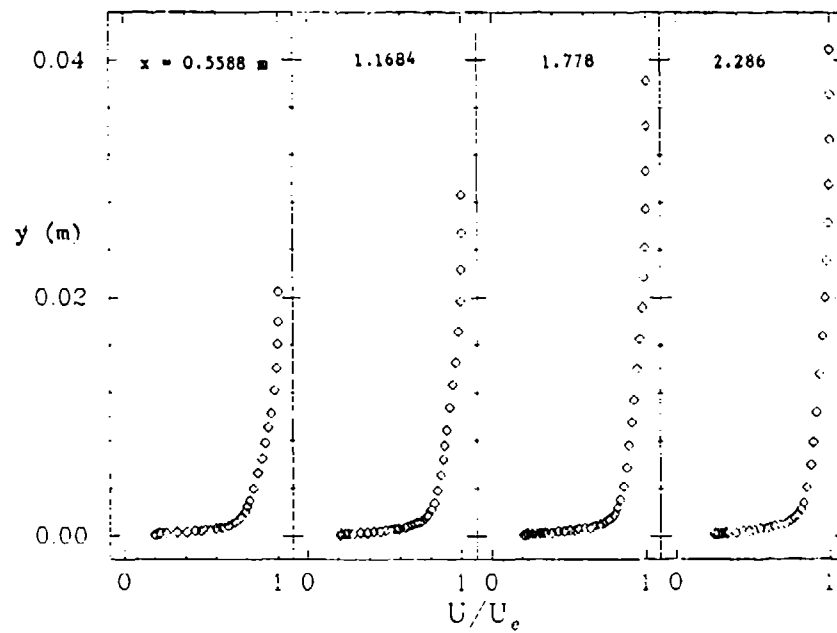
PLOT 2 CASE 0242 FILE 2



PLOT 3 CASE 0242 FILE 2



PLOT 4 CASE 0242 FILES 5,7,9,11



SPECIFICATIONS FOR COMPUTATION

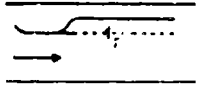
ENTRY CASE/INCOMPRESSIBLE

Case #0244; Data Evaluator: L. C. Squire

Data Takers: A. Favre, R. Dumas, E. Verollet, M. Coantic

PICTORIAL SUMMARY

Flow 0240. Data Evaluator: L. Squire. "Turbulent Boundary Layers with Suction or Blowing."

Case Data Taker	Test Rig Geometry	dp/dx or C_p	Number of Stations Measured								C_f	Re	Ini- tial Condi- tion	Other Notes
			Mean Velocity		Turbulence Profiles									
			U	V or W	$\overline{u^2}$	$\overline{v^2}$	$\overline{w^2}$	\overline{uv}	Others					
Case 0244 A. Favre R. Dumas E. Verollet M. Coantic	 Suction $-0.014 < F$ $-0.05 < x < 0.4$ m	0	1	-	1	1	-	1	-		7.5×10^5 per m	0	Data available for 4 suction rates: $F = -0.002, -0.0053, -0.0100, -0.0144$. Velocity and turbulence data restricted to one streamwise station.	

Plot	Ordinate	Abscissa	Range/Position	Comments
1	y	U/U_e	$x = 400$ mm $0 \leq y \leq \delta_{995}$	$F = 0; -0.0142.$
2	y	$(\overline{u^2})^{1/2}/U_e$	$x = 400$ mm $0 \leq y \leq \delta_{995}$	$F = 0; -0.002; -0.0053;$ $-0.0099; -0.0144.$
3	y	$(\overline{v^2})^{1/2}/U_e$	$x = 400$ mm $0 \leq y \leq \delta_{995}$	$F = 0; -0.002; -0.0053;$ $-0.0099; -0.0144.$
4	y	$-2(\overline{uv})/U_e^2$	$x = 400$ mm $0 \leq y \leq \delta_{995}$	$F = 0; -0.002; -0.0053;$ $-0.0099; -0.0144.$

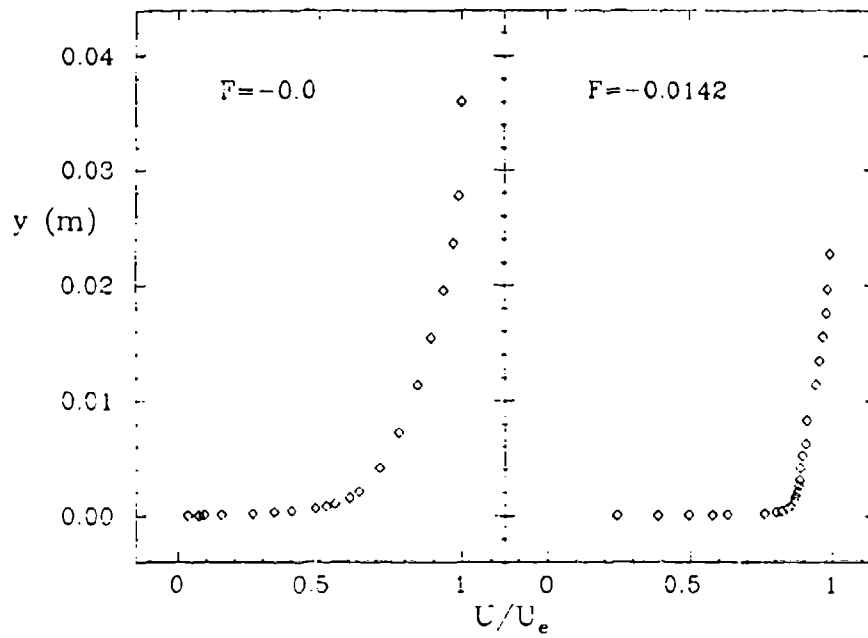
Special Instruction:

- 4 plots for 5 suction rates.
- Start computations at $x = -0.05$ m; use or match initial conditions at this station given in File 1.

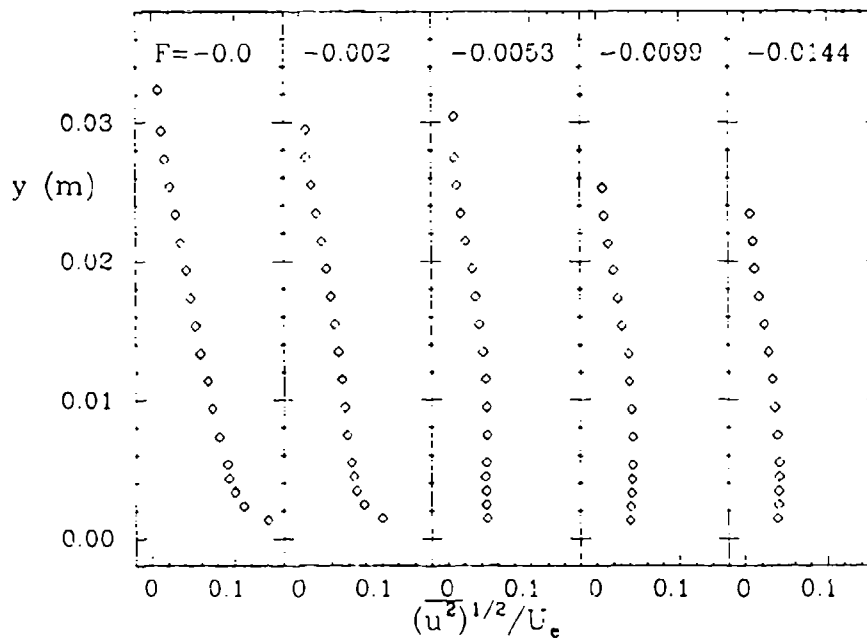
Definition of Special Symbol:

$$F \triangleq \frac{\rho_w V_w}{\rho_e U_e}$$

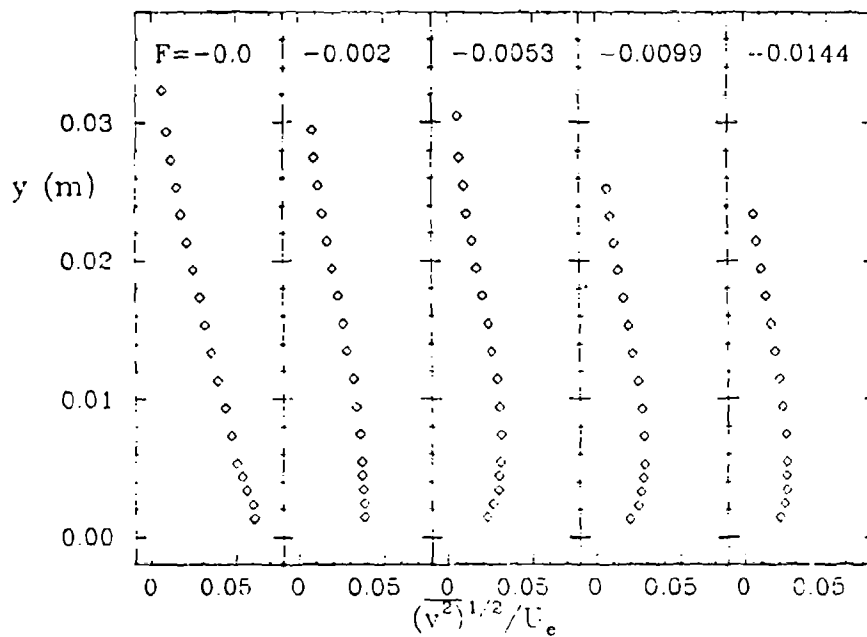
PLOT 1 CASE 0244 FILES 8,9



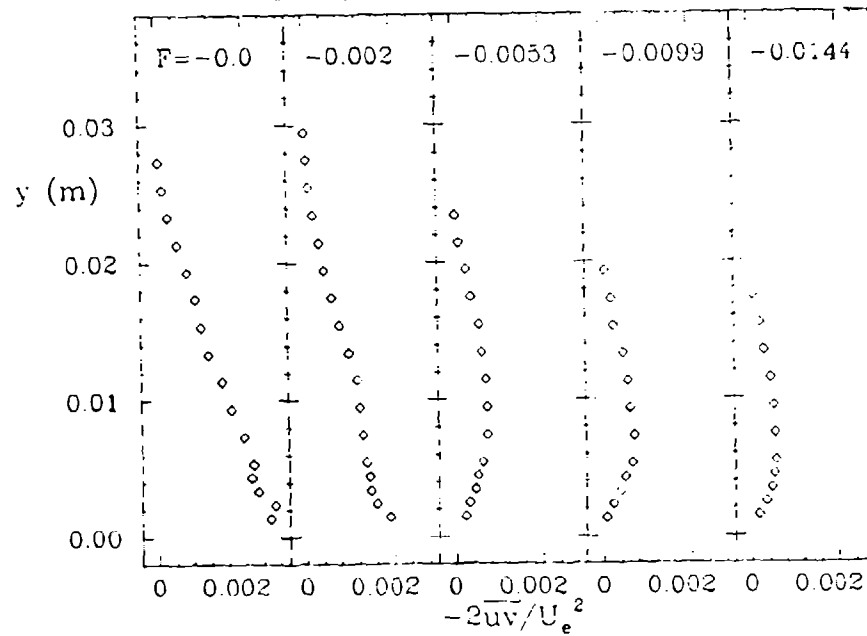
PLOT 2 CASE 0244 FILES 3-7



PLOT 3 CASE 0244 FILES 3-7



PLOT 4 CASE 0244 FILES 3-7



SPECIFICATIONS FOR COMPUTATION

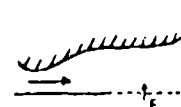
ENTRY CASE/INCOMPRESSIBLE

Case #8301; Data Evaluator: L. C. Squire

Data Taker: G. D. Thomas

PICTORIAL SUMMARY

Flow #300. Data Evaluator: L. Squire. "Turbulent Boundary Layers with Suction or Blowing at Supersonic Speeds."

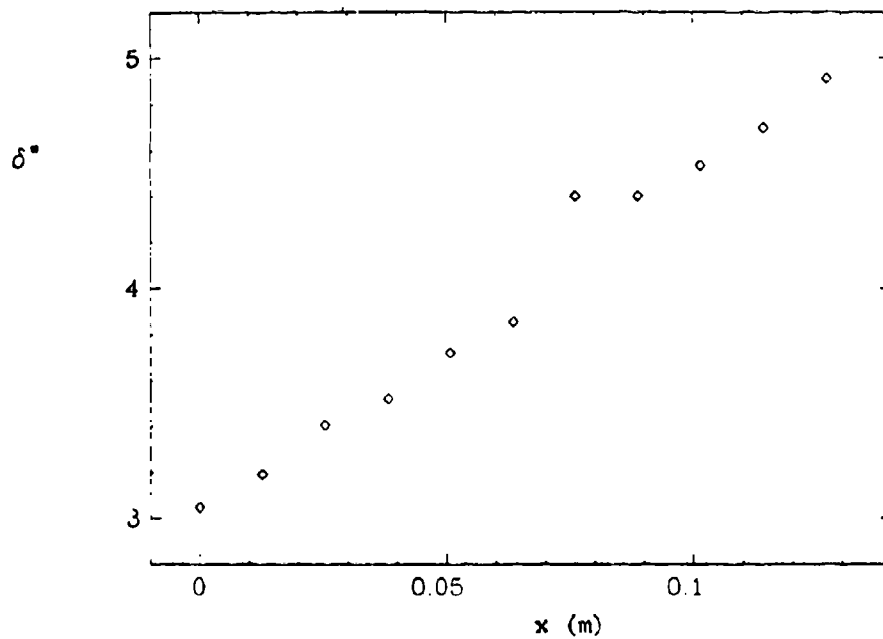
Case Data Taker	Test Rig Geometry	dp/dx or C _p	Number of Stations Measured								C _f	Re	Initial Condition	Other Notes
			Mean Velocity		Turbulence Profiles									
			U	V or W	$\overline{u^2}$	$\overline{v^2}$	$\overline{w^2}$	\overline{uv}	Others					
Case #301 G. Thomas	 Blowing $0.02 < \gamma < 0.0028$ $0 < x < 0.127$ m	< 0	11	-	-	-	-	-	-	-	5×10^6 per m	M (2.53 to 2.87)	M, P, θ , δ^* vs x data available on file. No turbulence data.	

Plot	Ordinate	Abcissa	Range/Position	Comments
1	δ^*	x	$0 \leq x \leq 0.127$ m	Take δ^* as 0.003 m at x = 0. ("false" origin).
2	θ	x	$0 \leq x \leq 0.127$ m	Take θ as 0.0006 m at x = 0. ("false" origin).
3	y	U/U _e	at x = 0.0381, 0.0762, 0.127 m	

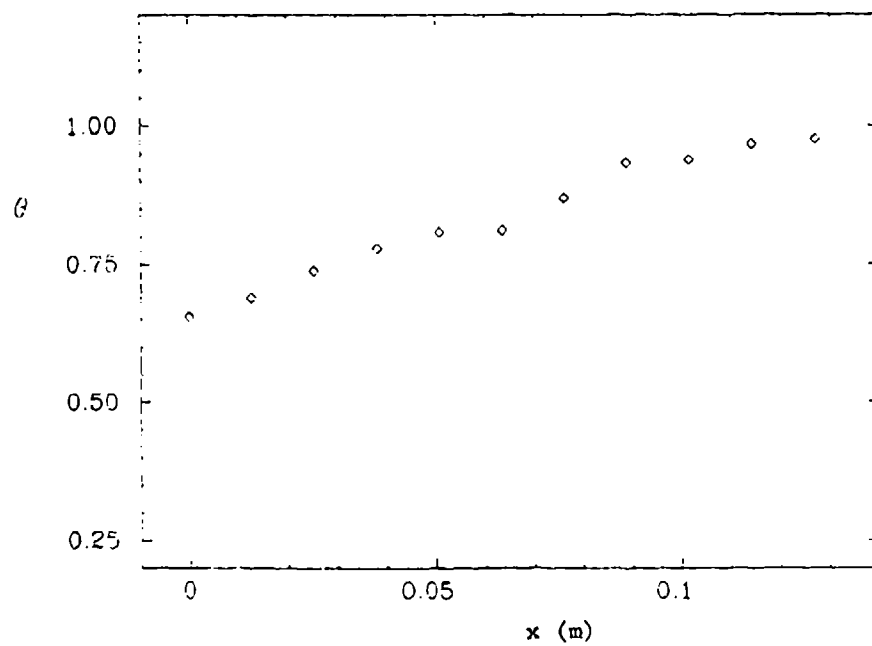
Special Instruction:

None.

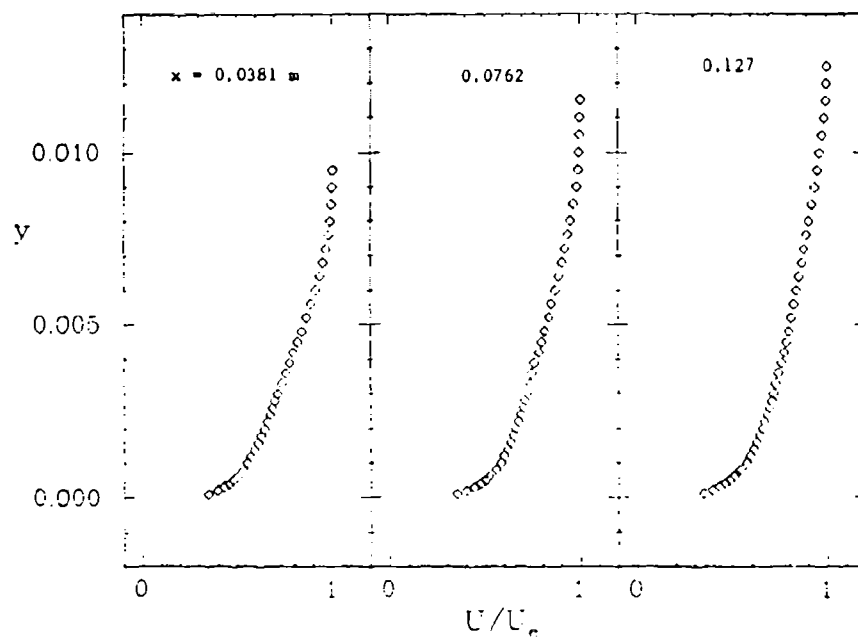
PLOT 1 CASE 8301 FILE 2



PLOT 2 CASE 8301 FILE 2



PLOT 3 CASE 8301 FILE 3



FREE SHEAR LAYER WITH STREAMWISE CURVATURE

Flow 0330

Case 0331

Evaluator: P. Bradshaw*

SUMMARY

SELECTION CRITERIA

This is a one-lab experiment (Castro, 1973; Castro and Bradshaw, 1976). The alternative experiment, by Wyngasrd et al. (1968) contains measurements at one station only, and the turbulent-energy-balance results are dubious. Hot-wire errors due to high turbulence intensity should be no worse than in a plane mixing layer, Flow 0310. In the region of maximum shear stress, uncertainty estimates are as follows: $\overline{u^2}$, $\pm 10\%$; \overline{uv} , $\pm 15\%$; triple products, $\pm 20\%$.

FLOW SELECTED

Castro and Bradshaw took some trouble to present their results in a sufficiently complete form to be usable for test cases, and Gibson and Rodi (1980) have successfully used the data. The only serious drawback to the use of the data is the need to analyze the flow in curvilinear coordinates. In Castro and Bradshaw (1976) the main results are plotted in semi-curvilinear (s,n) coordinates, the $n = 0$ line being a nominal curved centerline of the layer, the $s = \text{constant}$ line being perpendicular to this centerline. For this meeting, data are presented as in Castro (1973), with respect to polar coordinates for the curved portion and rectangular Cartesian coordinates for the straight portion further downstream. Figure 1 shows the flow geometry and quantitative details are given in the data file.

ADVICE FOR FUTURE DATA TAKERS

The experiment presented no special difficulties and since it was effectively a comparison between plane and curved layers the absolute accuracy of hot-wire measurements in highly turbulent flows was not too serious a question. A companion experiment on an unstably curved mixing layer would be valuable and could be set up as the initial region of a wall jet on a convex surface ("Coanda nozzle"). Boundary-layer control might be needed on the nozzle wall.

Since the pressure difference across the shear layer was considerable, it should strictly be computed by using a Navier Stokes code: if the pressure field is input to the calculations, it will be advisable to assume it to be atmospheric at the outer

*Imperial College, Prince Consort Road, London, SW7 2BY, England.

edge of the mixing layer, with $\partial p / \partial n = \rho U^2 / R$, where R is the local radius of curvature of streamline; the radius of the "reference streamline" in the inviscid flow on the high velocity side of the mixing layer will not be an adequate value for R . Calculations of this flow, using an assumed pressure variation, have already been made by Gibson and Rodi (J. Fluid Mech., in press). Neither in the Navier Stokes calculation nor in a "thin shear layer" calculation should the pressure on the reference streamline be used as a boundary condition: this would inevitably lead to the predictions of pressure variations in the "still air" on the low velocity side. The rate of volume flow through the "boundary-layer bleed" in the corner between the floor and the backplate can be taken as $U_{ref} \times 0.04$ m per unit span; the displacement thickness of the boundary layer on the floor and on the backplate can be neglected.

In addition to the coordinates specified, computers may care to examine plots of the results in the $(s, n/\delta)$ plane used by Castro and Bradshaw; this shows up departures from self-preservation immediately. Note that in Castro and Bradshaw's plots, all quantities are resolved with respect to a nominal but plausible centerline of the shear layer so that uv , for instance, has slightly different numerical values to those in the present coordinate system which has been chosen for geometrical convenience rather than physical significance.

REFERENCES

- Castro, I. P. (1973). "A highly distorted turbulent free shear layer." Ph.D. thesis, available on microfiche from Aeronautics Department, Imperial College, London, SW7 2BY.
- Castro, I. P., and P. Bradshaw (1976). "The turbulence structure of a highly curved mixing layer," J. Fluid Mech., **73**, 265.
- Gibson, M. M. (1979). "Prediction of curved free shear layers with a Reynolds stress model of turbulence." Presented at 2nd Symposium on Turbulent Shear Flows, Imperial College, p. 2.6. Also, M. M. Gibson and W. Rodi, J. Fluid Mech. (in press).
- Wyngaard, J. C., H. Tennekes, J. L. Lumley, and D. P. Margolis (1968). "Structure of turbulence in a curved mixing layer." Phys. Fluids, **11**, 1291.

CASTRO / BRADSHAW CASE 0331

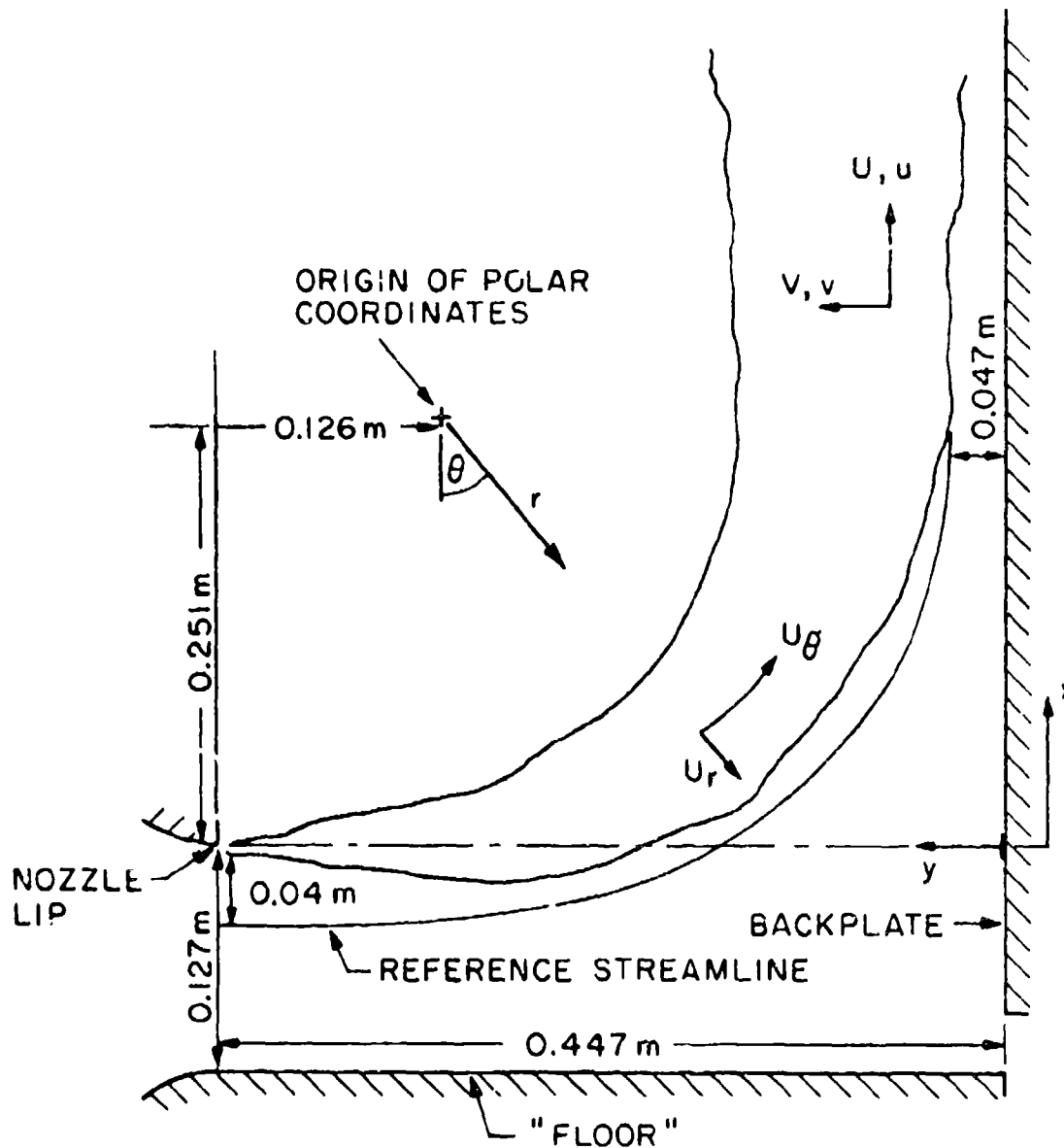


Figure 1. Curved mixing layer geometry.

DISCUSSION

Flow 0330

The experimental data were accepted as providing a valuable test case. Questions and discussion centered on whether the "reference streamline" provided an adequate internal boundary condition for computations made with an elliptic treatment.

The conclusion was that persons providing elliptic analyses would probably prefer to extend the calculation domain to include the region between the reference streamline and the boundary walls (Fig. 1). Accurate data of the mass outflow rate between the backplate and the flow would thus be required;* the evaluator agreed to include this information in the specification.[†]

The committee endorsed the suggestion that computers who tackled this flow should if possible also examine the mixing layer without curvature.

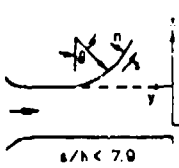
*An incorrect specification would mainly show up as spurious y-displacement of the mixing layer.

[†][Ed.: The specification has been modified to allow one suggested form of computation.]

SPECIFICATIONS FOR COMPUTATION
CENTRAL, ENTRY CASE/INCOMPRESSIBLE
Case #0331; Data Evaluator: P. Bradshaw
Data Taker: I. P. Castro

PICTORIAL SUMMARY

Flow 0330. Data Evaluator: P. Bradshaw. "Free-Shear Layer with Streamline Curvature."

Case Date Taker	Test Rig Geometry	dp/ds or C _p	Number of Stations Measured							C _f	Re	Ini- tial Condi- tion	Other Notes
			Mean Velocity		Turbulence Profiles								
			U	V or W	$\overline{u^2}$	$\overline{v^2}$	$\overline{w^2}$	\overline{uv}	Others				
Case 0331 I. Castro P. Bradshaw			17*	17*	17*	17*	17*	17*	$\overline{u^2}$ $\overline{v^2}$ $\overline{w^2}$ \overline{uv} $\overline{u^2v}$, $\overline{uv^2}$ Tertiary tendency	2.5 x 10 ⁵ (based on nozzle opening h)	Turbu- lence level <0.011	Tabulated data are in a mix of x, y, or r, θ coordinates. Digital processing techniques are used.	

*Results are plotted in semi-circumlinear (s,n) coordinates; the n = 0 line being a nominal curved centerline of the mixing layer.

Plot	Ordinate	Abscissa	Range/Position	Comments
1	r	U_θ/U_{ref}	$0 \leq r \leq r_{max}$	For $\theta = 0, 30, 60, 90$.
2	r	$-\overline{u_\theta u_r}/U_{ref}^2$	$0 \leq r \leq r_{max}$	For $\theta = 0, 30, 60, 90$.
3	r	$\overline{u_\theta^2}/U_{ref}^2$	$0 \leq r \leq r_{max}$	For $\theta = 0, 30, 60, 90$.
4	y	U/U_{ref}	$0 \leq y \leq 0.225$ m	For x = 0.352, 0.556, 0.708 m.
5	y	\overline{uv}/U_{ref}^2	$0 \leq y \leq 0.225$ m	For x = 0.352, 0.556, 0.708 m.
6	y	$\overline{v^2}/U_{ref}^2$	$0 \leq y \leq 0.225$ m	For x = 0.352, 0.556, 0.708 m.
7	y	$\overline{uv^2}/U_{ref}^3$	$0 \leq y \leq 0.225$ m	For x = 0.352, 0.556, 0.708 m.

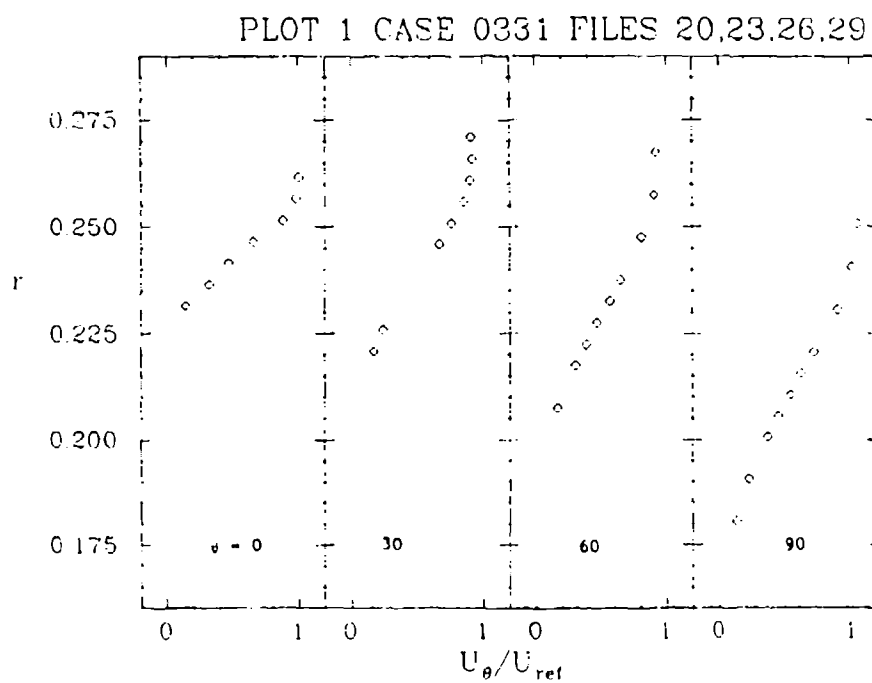
Special Instructions:

- Note that two coordinate systems are used: in curved section (Plots 1, 2, 3) given by θ ; in straight recovery section by x (Plots 4, 5, 6); see sketch in Summary above; plot in straight section runs leftward.
- U_{ref} is nominal speed at nozzle exit.

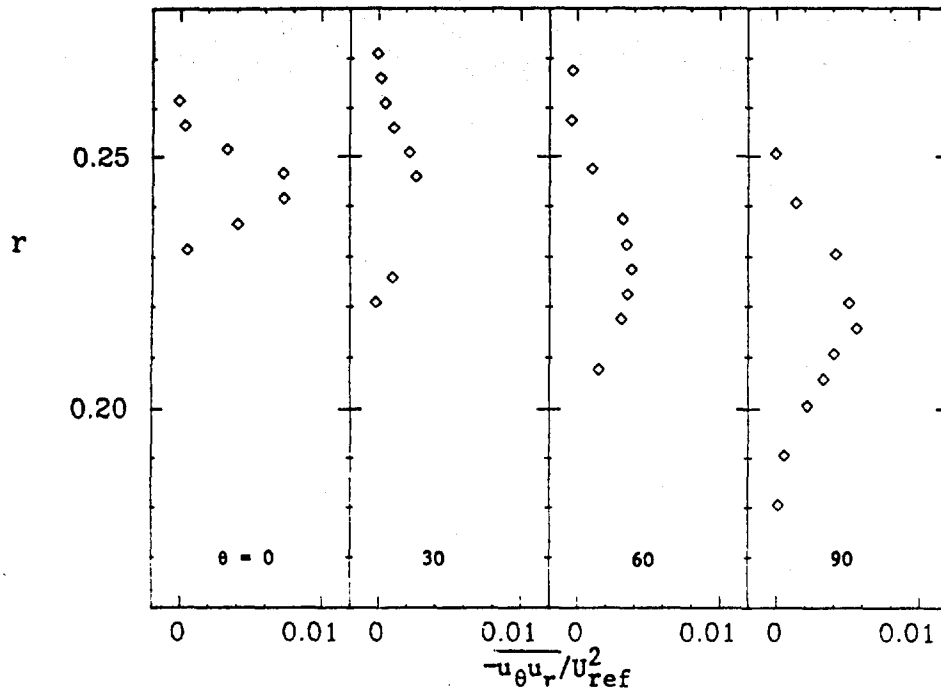
Definitions of Special Symbols:

- n distance normal to nominal curved centerline of shear layer
- R radius of curvature of a mean streamline
- r polar coordinate: see Fig. 1
- s distance along shear-layer centerline from nozzle lip
- x distance along the backplate measured positive (upward) from an origin level with nozzle upper lip

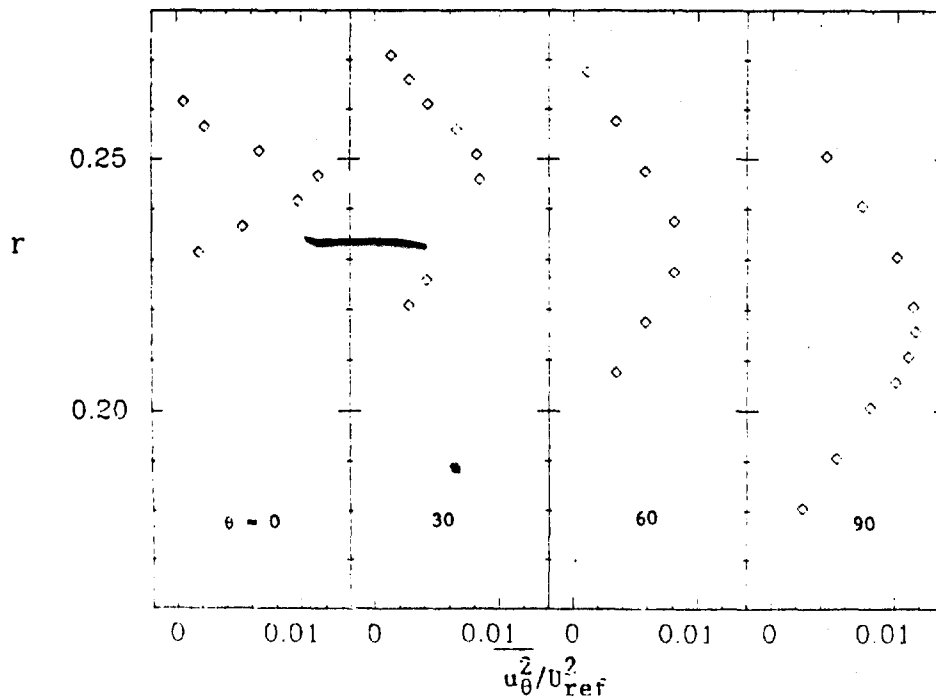
y distance from the backplate measured positive, leftward (horizontal)
 z coordinate normal to x and y
 U_{ref} reference velocity (nominal nozzle exit speed)
 θ polar coordinate: see Fig. 1
 $U_r, U_\theta, U, V, u, v$: see Fig. 1



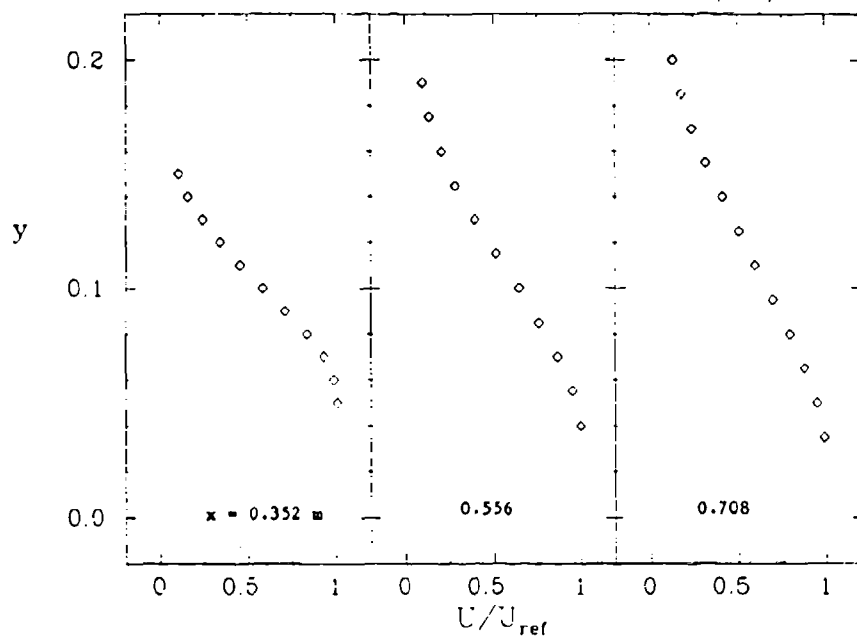
PLOT 2 CASE 0331 FILES 20,23,26,29



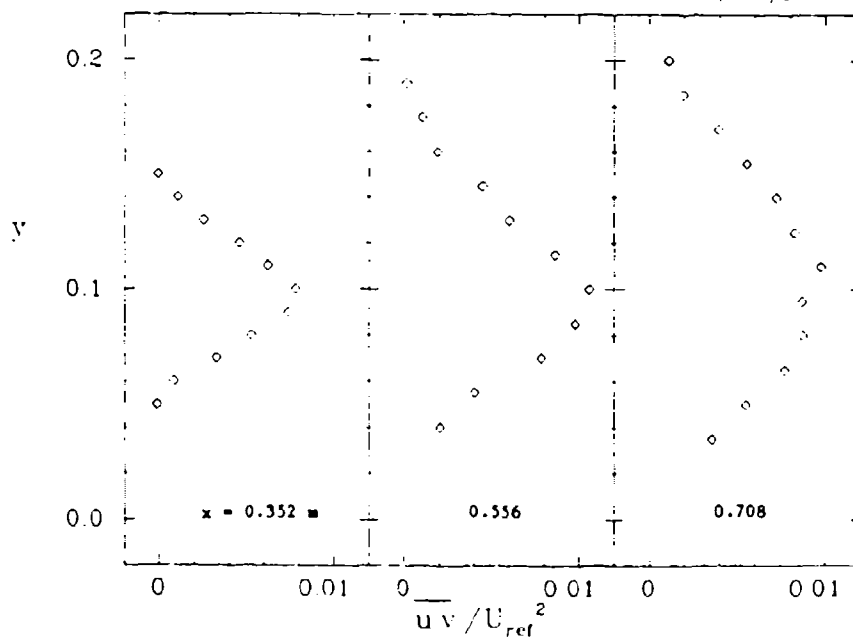
PLOT 3 CASE 0331 FILES 20,23,26,29



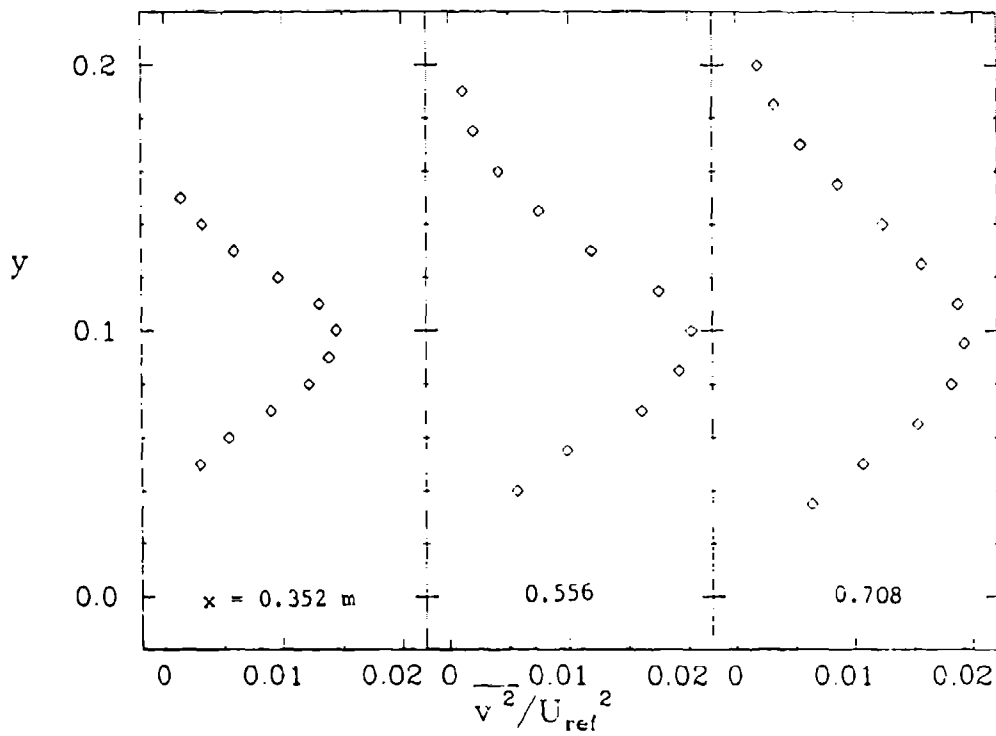
PLOT 4 CASE 0331 FILES 31,33,35



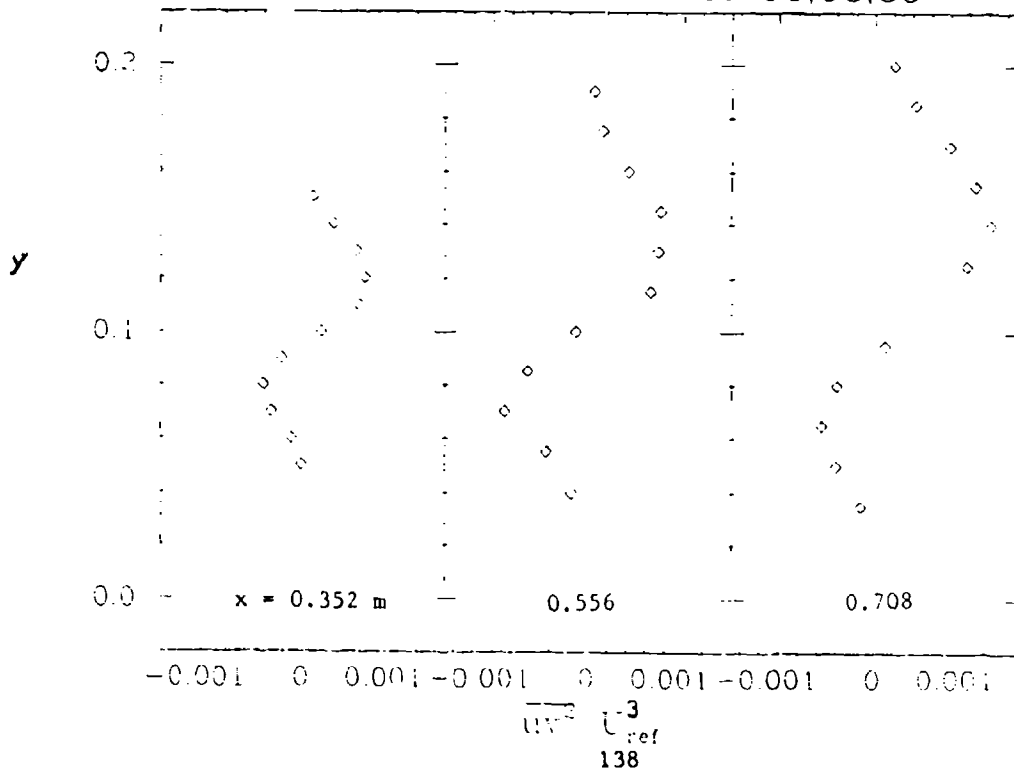
PLOT 5 CASE 0331 FILES 31,33,35



PLOT 6 CASE 0331 FILES 31,33,35



PLOT 7 CASE 0331 FILES 31,33,35



TURBULENT SECONDARY FLOWS OF THE FIRST KIND

Flow 0510

Case 0511, 0512, 0513

Evaluator: R. B. Dean*



SUMMARY

INTRODUCTION

In flows exposed to lateral curvature of the potential flow outside the boundary layer, as in a curved duct for example, the pressure field induces a time mean flow in a plane perpendicular to the main flow direction. Prandtl (1952) defined this as a secondary flow of the first kind, while secondary flows of the second kind are true turbulence phenomena produced by the time-averaged action of anisotropic inhomogeneous turbulence, as for example in a straight rectangular duct. Cebeci and Bradshaw (1977) have suggested that the two flow types should be described as "skew-induced secondary flows" and "stress-induced secondary flows," respectively.

This evaluation of experimental data is concerned only with secondary flows of the first kind, and data have been sought for the following types of flow:

Nozzles

Curved ducts of arbitrary cross-section

S-shaped ducts of arbitrary cross-section

Surface-mounted bodies

Wing-body junctions

Turbomachinery

A large number of experiments have been carried out in these flows during the last fifty years, and a considerable number of references (totaling several hundred) were reviewed. In addition, twenty individuals at universities and research laboratories around the world were consulted, and their advice on availability of data, and whether it would be suitable, has been extremely useful in reaching the conclusions drawn from this survey.

CRITERIA OF SELECTION

The main objective was to locate references which contained turbulence data, as well as mean-flow measurements, in sufficient quality and quantity to form test cases. In view of the complexity of this class of secondary flows, the majority of the pre-1970 papers and reports were found to contain mean-flow data only. These were

* Atkins Research & Development, Woodcote Grove, Ashley Road, Epsom, Surrey, KT18 5BW, England.

therefore discarded as data sources, but many were clearly of a high standard and have been used in the development of very useful calculation methods for the design of turbine cascades in turbomachinery, for example.

Ideally, suitable references would contain total and/or static pressure distributions and profiles of wall shear stress, mean velocities, turbulence intensities, Reynolds stresses, triple products and intermittency. However, it soon became clear that the minimum requirement of both mean-flow data and Reynolds-stress measurements would be met in only a few cases.

Documentation of data was also an important criterion. It is essential to have details of reference lengths, velocities and pressures used to normalize the data, as well as the author's interpretation of the uncertainty in the measured quantities. In addition, a check was made to confirm that \overline{uv} extrapolated to the wall agreed with wall shear stress measured by other means.

As a result of applying these criteria to the large number of references reviewed, only three emerged as possibilities for test cases. These were the wing-body junction by Shabaka (1979), the curved square duct by Humphrey (1977), and the same curved square duct of Taylor et al. (1980) but with a thin inlet boundary layer.

Case 0511. Wing-Body Junction (Shabaka, 1979)

Shabaka carried out detailed hot-wire measurements in the corner of an idealized wing-body junction (Fig. 1). The wing was fixed to the floor of a 0.762×0.127 m (30"x5") wind tunnel, which simulated the body surface and spanned the full 0.127 m (5") height of the tunnel. The wing had a semi-elliptical leading edge 0.1524 m (6") long followed by a section of constant thickness 0.0508 m (2") and a blunt trailing edge. Nine measuring stations were located upstream of the wing leading edge and nine downstream. All tests were carried out in air at a nominal tunnel speed of 33 m/s (100 ft/sec) and a Reynolds number of 1.1×10^5 (based on wing thickness). Considerable care was taken in obtaining the hot-wire data and anemometer outputs were recorded on analog tape and later transcribed to digital tape for processing, including linearization, on the main Imperial College computer. The turbulence measurements included all triple products, flatness factor, and intermittency. The cross-wire determination of the tunnel main shear stress ($-\overline{uv}$) and the wing main shear stress ($-\overline{uw}$) asymptoted reasonably well to the Preston-tube data measured on the respective surfaces.

The results show that the lateral skewing of the streamlines in the tunnel-floor boundary layer, caused by the wing leading edge, induces streamwise vorticity in the corner flow. It is also found that the ratio between the shear stress and the turbulent kinetic energy is constant over most of the flow, except close to the corner junction.

Adequate initial profiles for a calculation beginning upstream of the leading edge can be inferred from the measurements downstream of the leading edge but at a large distance from the wing. However, it is not recommended that computations should start upstream of the leading edge, as errors in the quasi-inviscid calculations around the leading edge could well jeopardize the vortex-decay predictions which are of primary interest in this test case. Instead, it is suggested that calculations should be started at the second measuring station downstream of the leading edge. The measured pressure distribution $p(x)$ may be used, or it could be calculated one-dimensionally by treating half the tunnel cross-section as a duct. It would be reasonable to assume that the displacement thickness everywhere on the tunnel walls is equal to that measured on the tunnel floor at the maximum distance from the wing.

Further work on the wing-body junction should consider the effect of streamwise pressure gradient on the corner flow. In most practical applications (e.g., turbomachinery), the pressure fields have a significant effect in intensifying or attenuating vortex strength. More information on these effects would help in understanding the wake interaction in cascades which gives rise to "end-wall cross-flow" and leads to reduced performance in gas turbines and similar multi-bladed turbomachinery.

Case 0512. Curved Square Duct (Humphrey, 1977)

Humphrey used laser-Doppler velocimetry to measure mean-flow and turbulence quantities in a duct of square cross-section (0.04×0.04 m) with a 90° bend (Fig. 2). Water was employed as the fluid medium at a bulk average velocity of 0.89 m/s and a Reynolds number of 4.0×10^4 .

Considerable care was taken to set up the experiment. All known sources of error in the laser-Doppler system were considered. This employed a fringe mode forward-scatter optical configuration with a frequency-tracking signal-processing system. This choice of instrumentation was based on the successful use of frequency trackers by Durst et al. (1976) in water flows, where signals are essentially continuous with high signal-to-noise ratios.

Measurements of U_x , U_θ , U_r , $\overline{u_x^2}$, $\overline{u_\theta^2}$, $\overline{u_r^2}$, $\overline{u_\theta u_r}$ were obtained at four stations around the 90° bend, but wall-shear-stress data are absent. No comparison is therefore possible with extrapolations of Reynolds-stress data to the wall.

A major shortcoming is the fact that the inlet straight-length tangent to the bend was only 45 hydraulic diameters. As pointed out by F. Gessner, the flow would definitely not have been fully developed at the entrance to the bend $\theta = 0^\circ$ (see Gessner et al., 1979), and was influenced by the bend itself. This latter influence would probably be much less significant at $x/D_h = -2.5$, but Humphrey's measurements at this station are limited to U_x and $\overline{u_x^2}$. In fact, he did not measure distributions of $U_z(r,z)$, $\overline{u_z^2}(r,z)$, $\overline{u_\theta u_z}(r,z)$, and $\overline{u_r u_z}(r,z)$ at any station, so the starting

conditions for "k-ε" and higher-order closure models cannot be specified satisfactorily.

A solution to this impasse, already suggested by F. Gessner, is to employ A. Melling's (1975) data at 36.8 duct diameters downstream of the square duct inlet. This very nearly coincides with Humphrey's position of $x/D_h = -8.2$, and Gessner states that the two sets of data agree quite well at a comparable Reynolds number. This comparison was not presented by Humphrey in his thesis. Melling's results include all three mean-velocity components and five of the six components of the Reynolds stress ($\overline{v'w'}$ excluded).*

Humphrey's measurements provide a clear demonstration of secondary flow of the first kind arising through an imbalance between centrifugal force and radial pressure gradient at the side walls of the bend. This motion is responsible for strong cross-stream convection of Reynolds stress, while stress-driven secondary flow of the second kind was probably negligible in the bend. The result is for high kinetic energy-containing fluid to be driven from the outer-radius wall towards the inner-radius wall. Similarly, stabilized flow with a lower level of kinetic energy of turbulence at the inner-radius wall is convected by the secondary motion into the core region of the flow and towards the outer-radius wall.

Further work on the flow in the curved duct should include measurements of the z component velocities U_z , $\overline{u_z^2}$, and $\overline{u_\theta u_z}$ in the upstream tangent, as well as in the bend. Also needed are wall-pressure data so that reliable values of skin friction can be determined. From the point of view of engineering applications, the flow field downstream of the bend is of equal importance, and measurements throughout a length of at least 40 hydraulic diameters would help in understanding how the flow recovers from the effects of the bend.

Case 0513. Curved Square Duct with Thin Inlet Boundary Layers (Taylor et al., 1980)

Taylor et al. (1980) have carried out a further series of experiments in the same duct (Fig. 2) as Humphrey (1977) using similar LDV measurement techniques. The quantities recorded were U_x , U_y , U_z , U_θ , U_r , $\overline{u_x^2}$, $\overline{u_y^2}$, $\overline{u_\theta^2}$, $\overline{u_r^2}$, $\overline{y_z^2}$, $\overline{u_x u_y}$, $\overline{u_\theta u_r}$, $\overline{u_x u_z}$ at most of the stations $x/h = +0.25, +2.5$. Water was employed as the fluid medium at a bulk average velocity of 1.00 m/s and the Reynolds number was 4.0×10^4 .

The experiment has clearly been carried out with considerable attention to accuracy and detail and the data are well tabulated in a convenient form for use as a Test Case. However, the boundary layers at the inlet to the bend were (deliberately) thin, being only 15% of the hydraulic diameter. The ratio of shear-layer thickness to radius of curvature in the bend is therefore much less than for Humphrey's (1977) flow

*The suggestion by F. Gessner to use A. Melling's data has been adopted by the Organizing Committee; see Specification.

in which the inlet conditions were nearly fully developed. The strength of the secondary flow and its effects will be much less in the experiment of Taylor et al. and, in view of this and the fact that Humphrey's data are considered satisfactory for use as a Test Case, it is concluded that the Taylor et al. data will not be required as an additional Test Case in the class of flows. Specifications of computations have therefore not been presented.

REFERENCES

- Cebeci, T., and P. Bradshaw (1977). Momentum Transfer in Boundary Layers, Hemisphere Publishing Corporation, McGraw Hill Book Co., New York.
- Durst, F., A. Melling, and J. H. Whitelaw (1976). Principles and Practice of Laser-Doppler Anemometry, Academic Press, New York.
- Gessner, F. B., J. K. Po, and A. F. Emery (1979). "Measurements of developing turbulent flow in a square duct," Turbulent Shear Flows (edited by Durst et al.), Springer-Verlag, New York.
- Humphrey, J. A. C. (1977). "Flow in ducts with curvature and roughness," Ph.D. thesis, University of London.
- Melling, A. (1975). "Investigation of flow in non-circular ducts and other configurations by laser-Doppler anemometry," Ph.D. thesis, University of London.
- Prandtl, L. (1952). Essentials of Fluid Dynamics, Blackie, London.
- Shabaka, I. M. M. A. (1979). "Turbulent flow in an idealised wing-body junction," Ph.D. thesis, University of London.
- Taylor, A. M. K. P., J. H. Whitelaw, and M. Yianneskio (1980). "Measurements of laminar and turbulent flow in a curved duct with thin inlet boundary layers," NASA Contract Rep. NASW-3258.

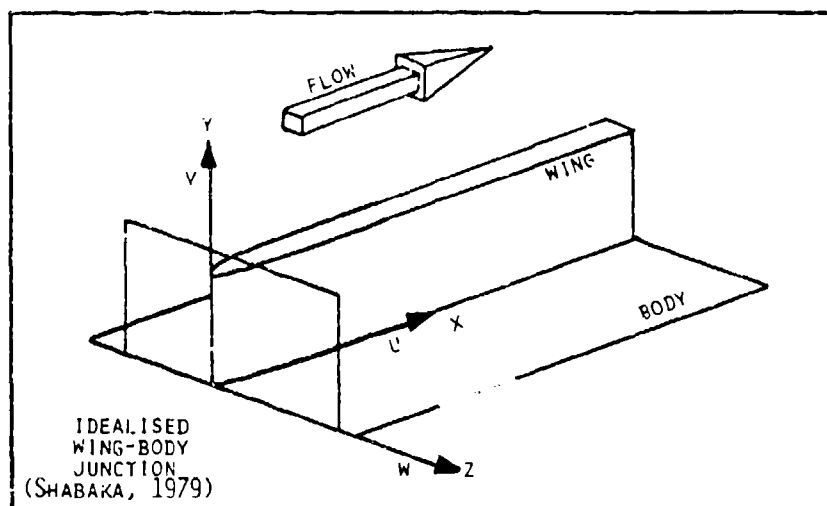


Figure 1. Secondary flow of the first kind due to a body in contact with a surface.

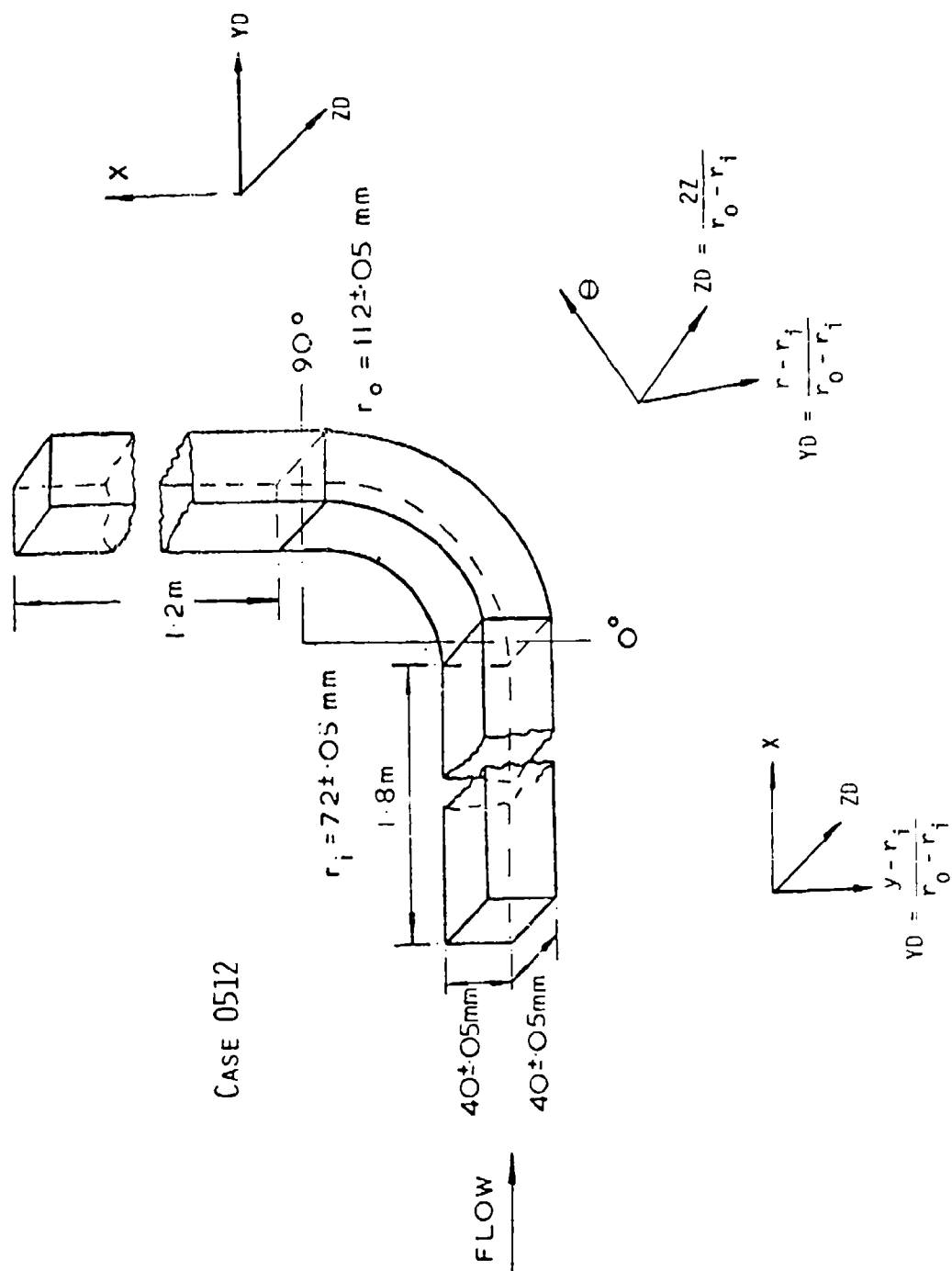


Figure 2. Experimental geometry of 90° bend with tangents.

DISCUSSION

Flow 0510

The two very different flows considered here are discussed separately.

Concerning the idealized wing-body junction, there was some feeling that computations should begin upstream of the junction, thereby testing how well the calculation methods managed to capture the horseshoe vortex formed at the wing root. On further consideration of this possibility, the majority view was that, because of the huge computational effort required (a fully three-dimensional elliptic calculation), it would be unwise to prescribe starting conditions upstream of the wing. Computers wishing to demonstrate predictive prowess at handling the largely inviscid bending of the vortex lines around the wing can always do so. There was a suspicion voiced by several discussers that the three-dimensional parabolic flow as presented by the evaluator would not pose a very severe test of turbulence models because the swirl underwent little decay over the test section length. In responding to this suggestion, Peter Bradshaw (who had supervised the experiment) acknowledged that the accumulation (as distinct from the distribution of streamwise vorticity) was little affected by Reynolds stresses. There were, however, other aspects of the measurements that would be very challenging, such as substantial regions where the effective viscosities were negative: also the streamwise vorticity is not confined to a simple "vortex core" as one might think.

Concerning the flow in the 90° bend, there was agreement that Melling's data at $36.8D$ (corresponding to $-8.2D$ in this flow) be used as starting conditions in order to provide initial conditions for all Reynolds stresses. The mean flow development in the bend was, however, expected to be largely pressure dominated and uninfluenced by turbulent stresses, an expectation confirmed by J.A.C. Humphrey, who had obtained flow predictions that were largely independent of whether or not turbulent stresses were included.

It was recommended that the test-case specifications should prescribe that computations be extended into the straight section following the 90° bend, since fully elliptic computations for laminar flow (Taylor et al., 1980) suggest that strong variations in pressure over the cross-section remain at the 90° station.

SPECIFICATIONS FOR COMPUTATION

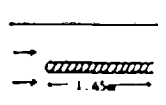
ENTRY CASE/INCOMPRESSIBLE

Case #0511; Data Evaluator: R. B. Dean

Data Taker: I. Shabaka

PICTORIAL SUMMARY

Flow 0510. Data Evaluator: R. Dean. "Turbulent Secondary Flows of the First Kind."

Case Data Taker	Test Rig Geometry	dp/dx or C _p	Number of Stations Measured										Initial Condition	Other Notes
			Mean Velocity		Turbulence Profiles						C _f	Re		
			U	V or W	$\overline{u^2}$	$\overline{v^2}$	$\overline{w^2}$	\overline{uv}	Others					
Case 0511 I. Shabaka	 wing span: 0.127 m wing thickness: 0.031 m	Meas- ured	3	Second- ary flow vectors at 3 sta- tions	3	3	3	3	Inter- mittency and triple pro- ducts, flat- ness factor 3 sta- tions	7	1.1×10^5 (based on wing thick- ness)	BL thick- ness at the lead- ing edge was about 0.025 m	Wing-body junction. Calculations should be started downstream of leading edge.	

Plot	Ordinate	Abscissa	Range/Position	Comments
1	C _f	z	0 < z < 0.08 m	Tunnel wall C _f at x = 0.6858 m.
2	C _f	z	0 < z < 0.03 m	Tunnel wall C _f at x = 1.2954 m.
3	C _f	y	0 < y < 0.08 m	Wing C _f at x = 0.6858 m.
4	C _f	y	0 < y < 0.08 m	Wing C _f at x = 1.2954 m.
5	y	U/U _e	0 < y < 0.05 m	x = 0.6443 m, z = 0.005025, 0.01003, 0.02337, 0.04338 m.
6	y	V/U _e	0 < y < 0.05 m	x = 0.6443 m, z = 0.005025, 0.01003, 0.02337, 0.04338 m.
7	y	W/U _e	0 < y < 0.05 m	x = 0.6443 m, z = 0.005025, 0.01003, 0.02337, 0.04338 m.
8	y	$-\overline{uv}/U_e^2$	0 < y < 0.05 m	x = 0.6443 m, z = 0.005025, 0.01003, 0.02337, 0.04338 m.
9	y	$-\overline{vw}/U_e^2$	0 < y < 0.05 m	x = 0.6443 m, z = 0.005025, 0.01003, 0.02337, 0.04338 m.
10	y	U/U _e	0 < y < 0.05 m	x = 1.254 m, z = 0.005025, 0.01003, 0.02337, 0.04338 m.
11	y	V/U _e	0 < y < 0.05 m	x = 1.254 m, z = 0.005025, 0.01003, 0.02337, 0.04338 m.
12	y	W/U _e	0 < y < 0.05 m	x = 1.254 m, z = 0.005025, 0.01003, 0.02337, 0.04338 m.

Plot	Ordinate	Abscissa	Range/Position	Comments
13	y	$-\overline{uv}/U_e^2$	$0 < y < 0.05 \text{ m}$	$x = 1.254 \text{ m}, z = 0.005025, 0.01003, 0.02337, 0.04338 \text{ m}.$
14	y	$-\overline{vw}/U_e^2$	$0 < y < 0.05 \text{ m}$	$x = 1.254 \text{ m}, z = 0.005025, 0.01003, 0.02337, 0.04338 \text{ m}.$

Special Instructions:

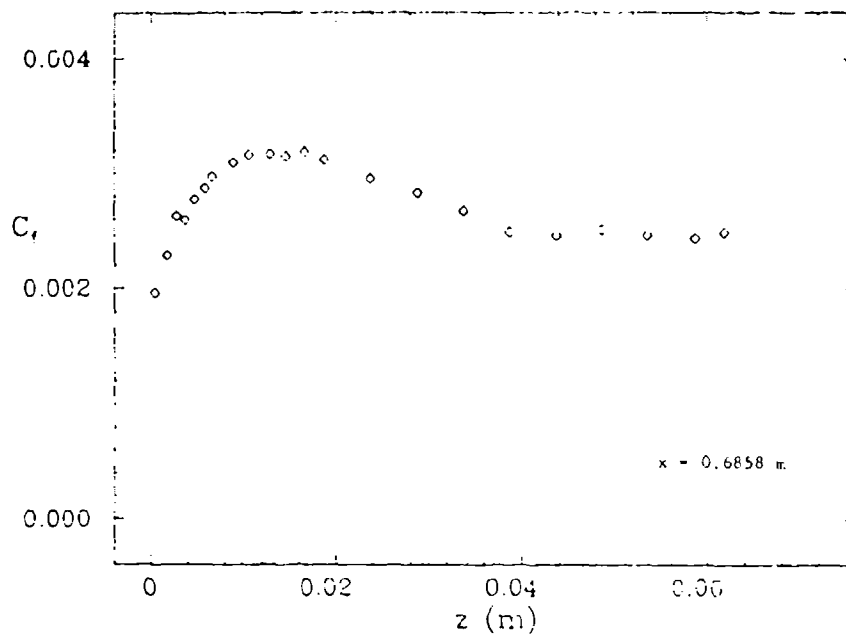
It is suggested that calculations should be started at Station 2 of Table 1 below, which is sufficiently far downstream of the leading edge on the parallel-sided part of the wing. Table 1 gives the positions of all measurement planes used for recording data from static pressure taps, pitot tubes, Preston tubes, single hot wires and cross-wires. It is noted that the wing is offset by 2" from the tunnel centerline, but the asymmetric effects in a 30"-wide tunnel will be small near the leading edge and insignificant farther downstream at Station 2. This allows a one-dimensional treatment of the pressure field outside the shear layer in two possible ways:

1. Use the measured $p(x)$, which is assumed constant outside the shear layer at a given cross-section.
2. Calculate $p(x)$ one-dimensionally by treating half the tunnel cross-section as a duct. The skew-induced secondary flow on the plane walls of the two-dimensional contraction is unlikely to cause any significant disturbance to the boundary layer on the 5"-high sidewalls. It would therefore be sufficient to assume that the displacement thickness everywhere on the tunnel walls is equal to that measured on the tunnel floor at the maximum distance from the wing.

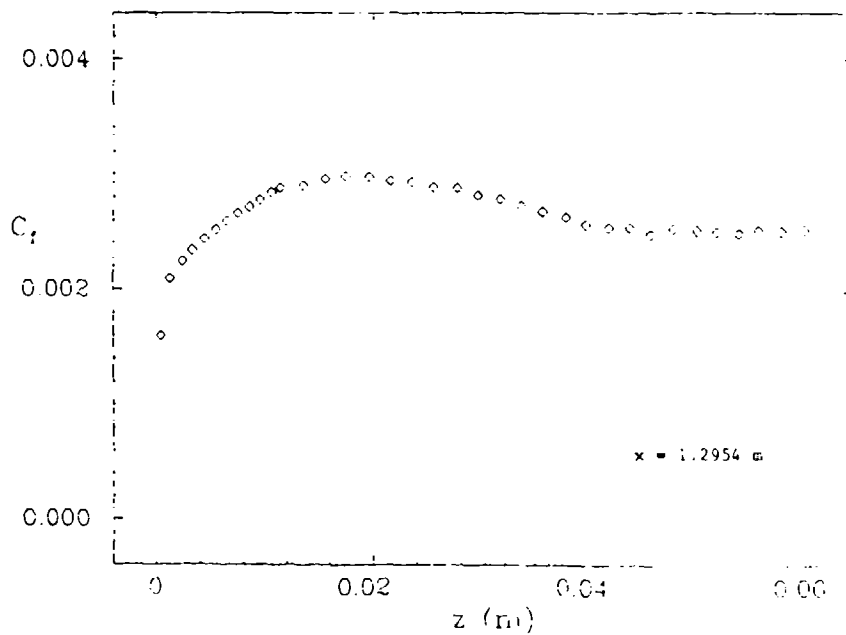
Table 1
Axial Positions of Measurement Stations
(Distances are measured in mm relative to the wing leading edge)

Station No.	Disc center and static-pressure tapings	Pitot-tube measurement planes	Preston-tube measurement planes	Single-wire (U-wire) measurement planes	Cross-wire (X-wire) measurement planes
-9	-1,295.4				
-8	-1,143.0				
-7	-990.6		-1,043.6		
-6	-838.2				
-5	-685.8		-738.8		
-4	-533.4		-586.0		
-3	-381.0		-434.0		
-2	-228.6		-281.6		
-1	-76.2		-129.2	-137.2	
1	76.2	34.66	23.2	15.2	
2	228.6	187.06	175.6	167.6	156.6
3	381.0	339.46	328.0	320.0	
4	533.4	491.86	480.4		
5	685.8	644.26	632.8	624.8	613.8
6	838.2				
7	990.6	949.06	937.6	929.6	
8	1,143.0				
9	1,295.4	1,253.86	1,242.4	1,234.3	1,223.4

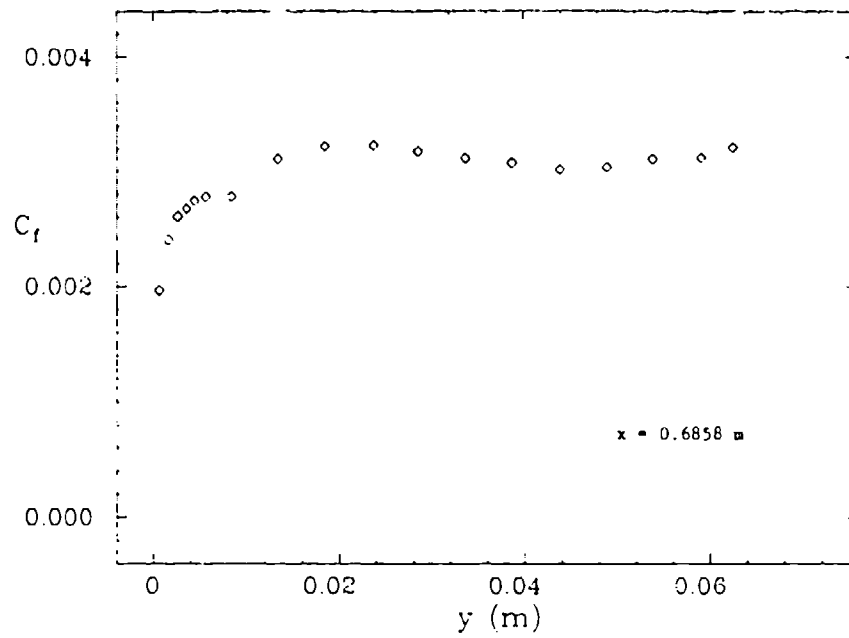
PLOT 1 CASE 0511 FILE 61



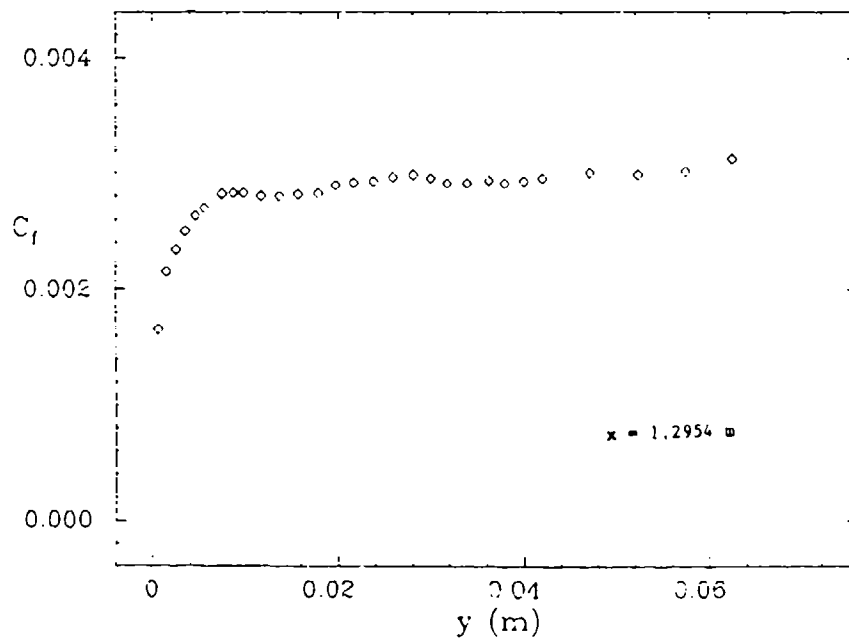
PLOT 2 CASE 0511 FILE 63



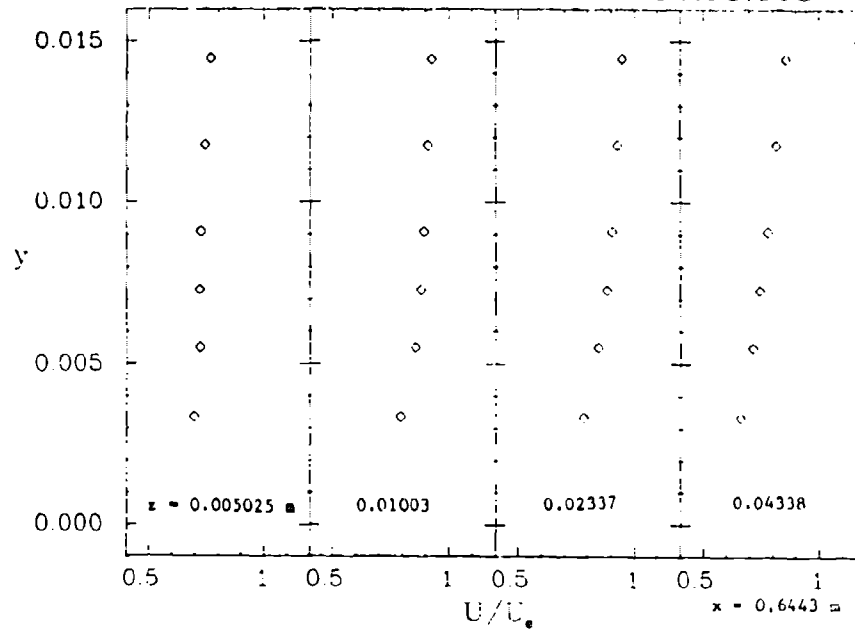
PLOT 3 CASE 0511 FILE 61



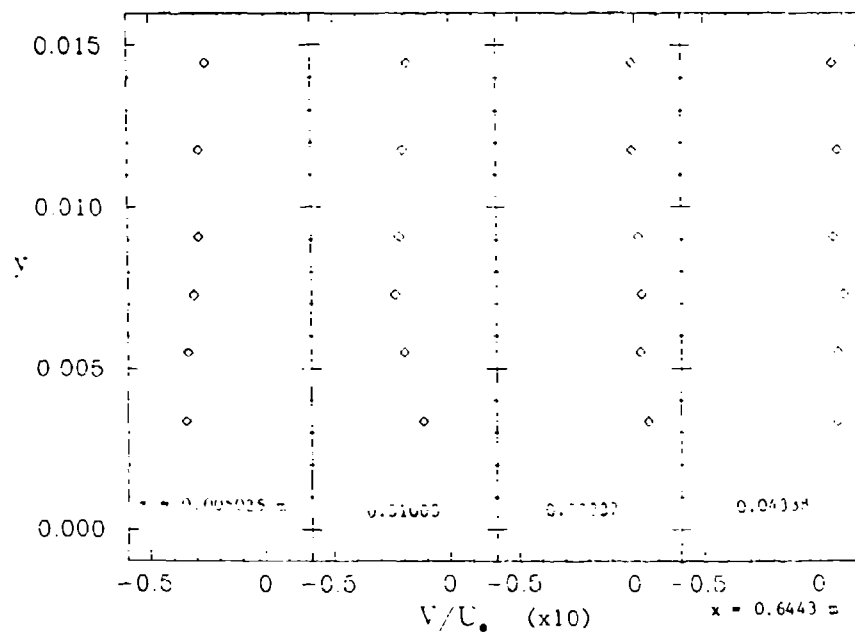
PLOT 4 CASE 0511 FILE 63

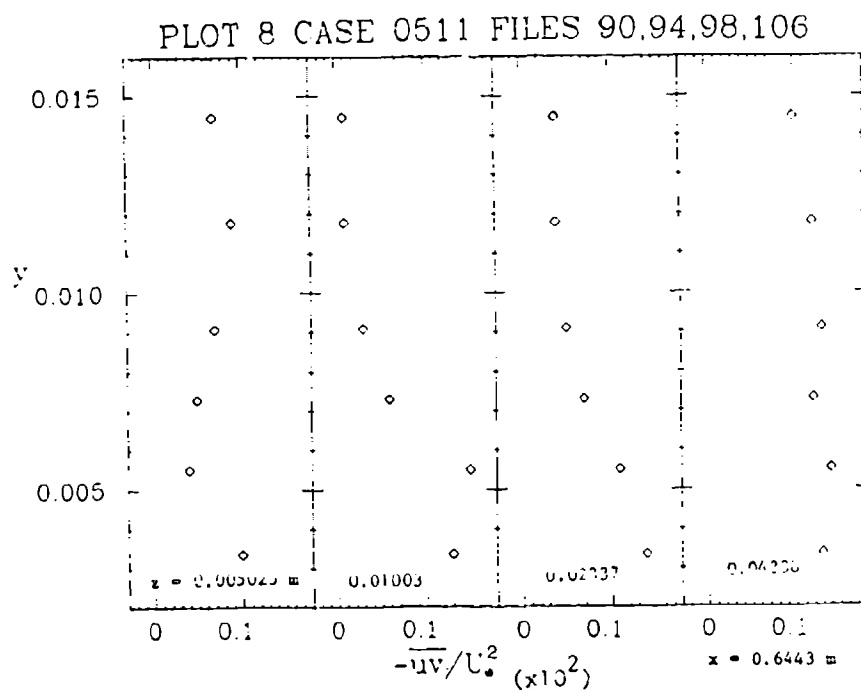
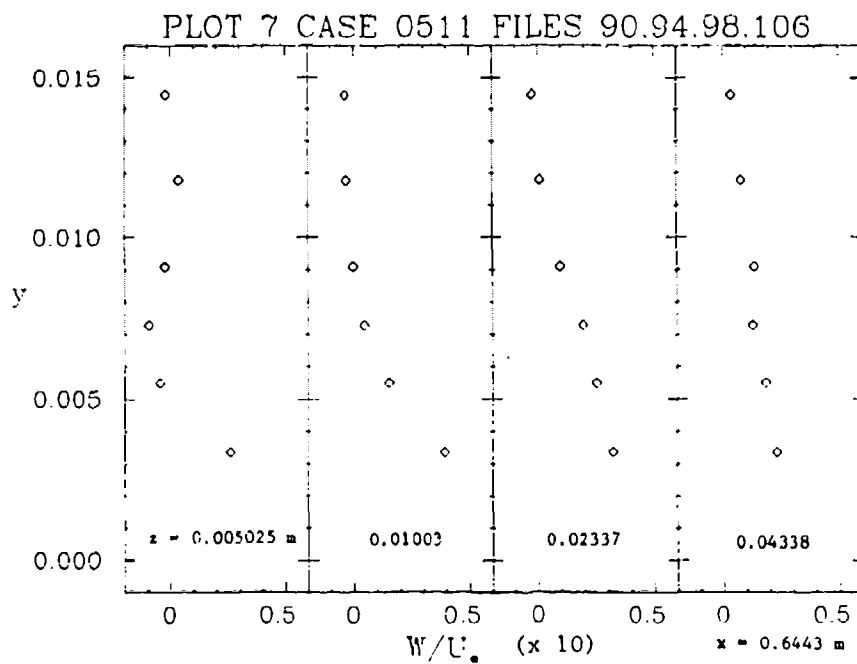


PLOT 5 CASE 0511 FILES 90,94,98,106

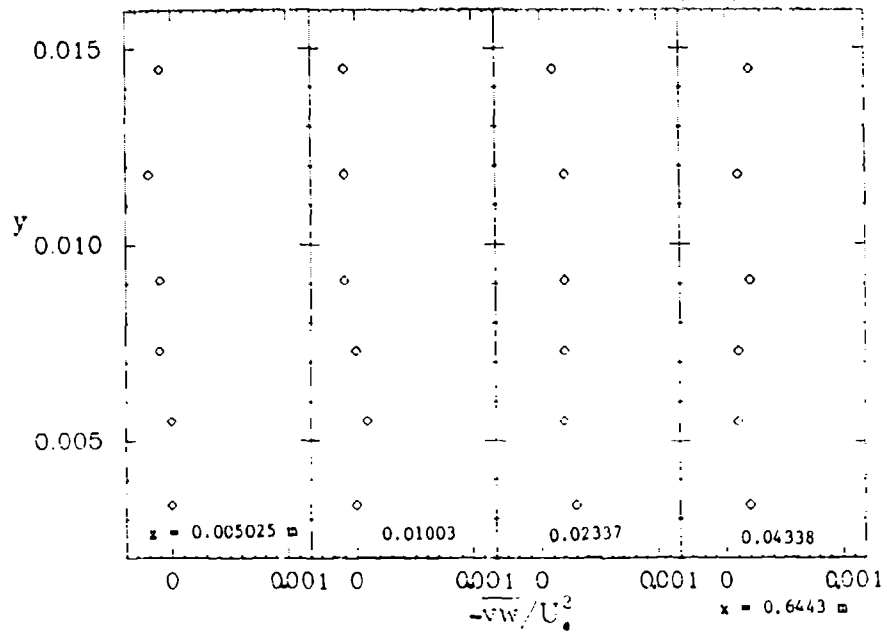


PLOT 6 CASE 0511 FILES 90,94,98,106

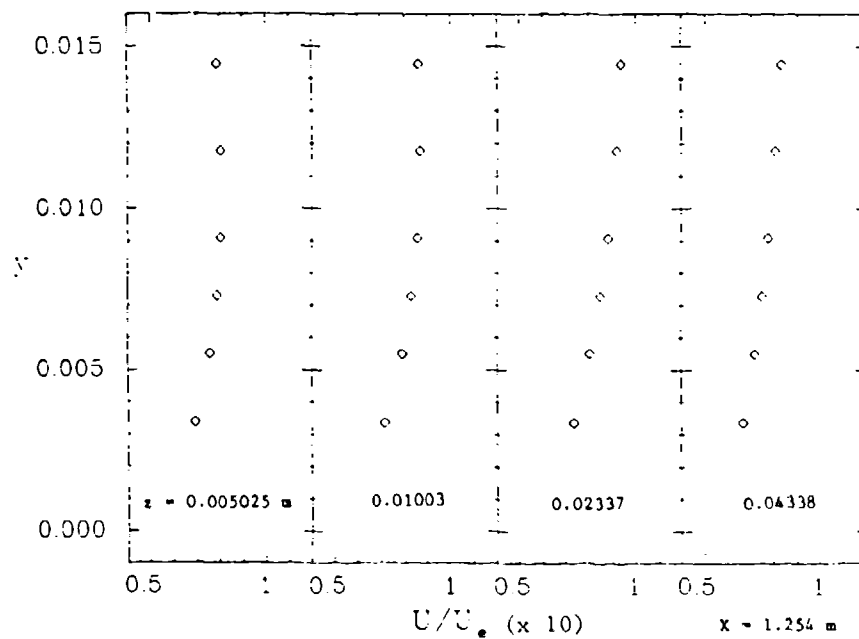




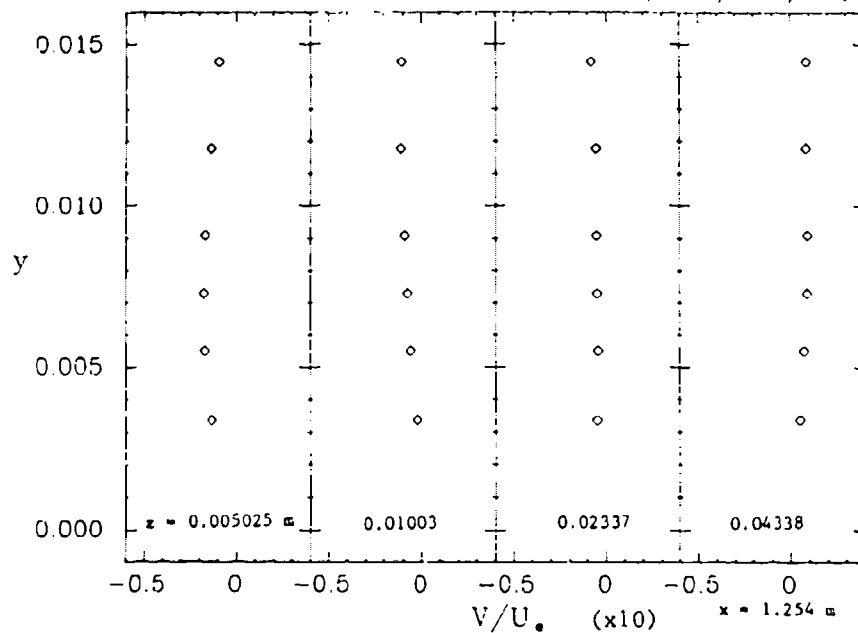
PLOT 9 CASE 0511 FILES 90,94,98,106



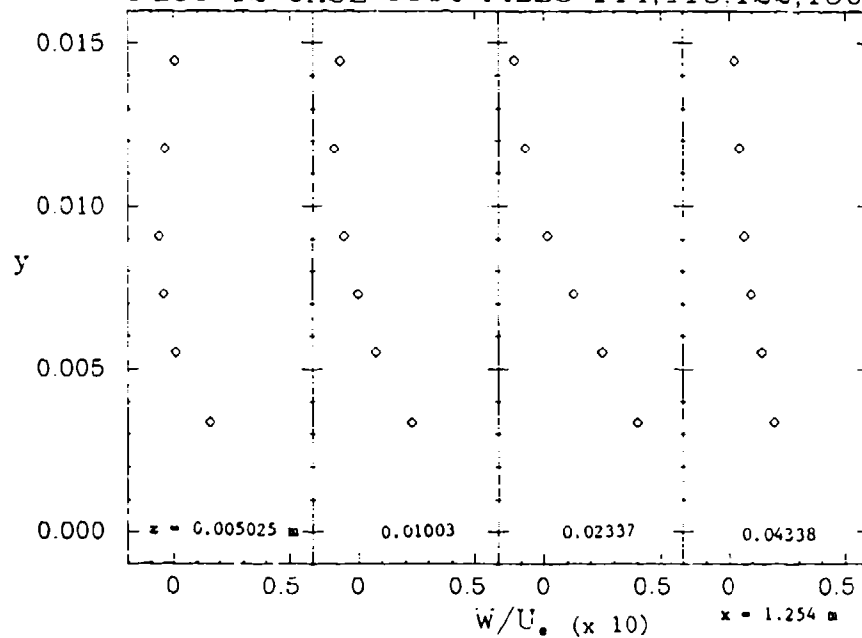
PLOT 10 CASE 0511 FILES 114,118,122,130



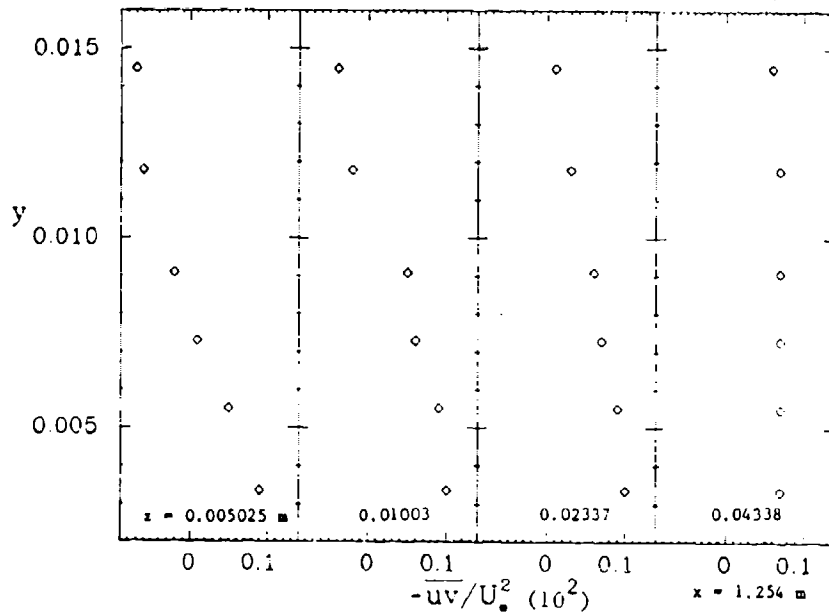
PLOT 11 CASE 0511 FILES 114,118,122,130



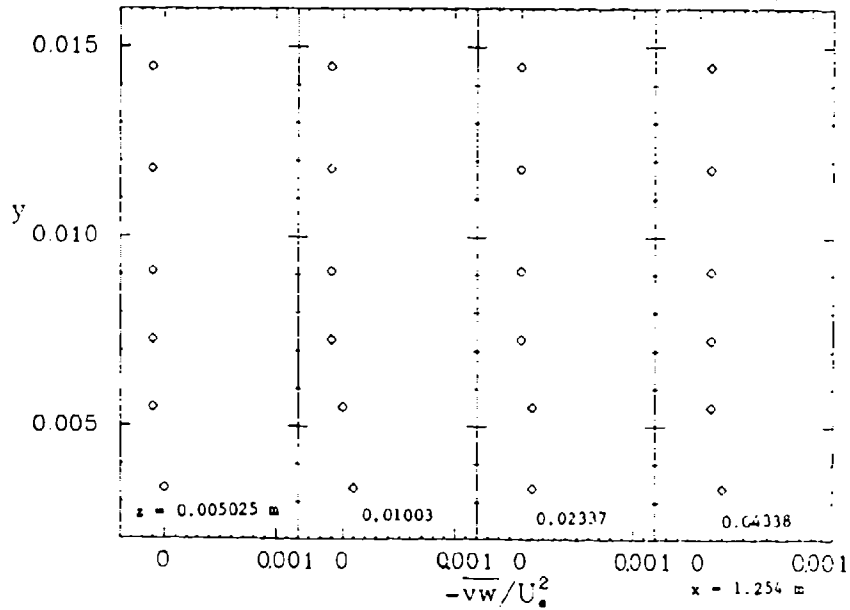
PLOT 12 CASE 0511 FILES 114,118,122,130



PLOT 13 CASE 0511 FILES 114,118,122,130



PLOT 14 CASE 0511 FILES 114,118,122,130



SPECIFICATIONS FOR COMPUTATION


ENTRY CASE/INCOMPRESSIBLE

Case #0512; Data Evaluator: R. B. Dean

Data Taker: J. A. C. Humphrey

PICTORIAL SUMMARY

Flow 0510. Data Evaluator: R. Dean. "Turbulent Secondary Flows of the First Kind."

Case Data Taker	Test Rig Geometry	dp/dx or C _p	Number of Stations Measured										Re	Initial Condi- tion	Other Notes
			Mean Velocity		Turbulence Profiles						C _f				
			U	V or W	$\overline{u^2}$	$\overline{v^2}$	$\overline{w^2}$	\overline{uv}	Others						
Case 0512 J. Humphrey	 4.0 x 4.0 cm square cross section	Not recorded in band	U _θ 7	U _r 2	$\overline{u_θ^2}$ 7	$\overline{u_r^2}$ 2	-	$\overline{u_θ u_r}$ 2	-	-	-	4 x 10 ⁴ (based on duct height)	Nearly fully developed	Curved rectangular duct. Calculation should be started 8.2 duct dia. upstream of bend using Melling's (1975) data.	

Plot	Ordinate	Abscissa	Range/Position	Comments
1	YD	ZD	$0 \leq YD \leq 1$ $-1.0 \leq ZD \leq 0$	Contours of $U_θ/U_{ref}$ at $θ = 0°$. Contour values 1.30, 1.20, 1.10, 1.0.
2	YD	ZD	$0 \leq YD \leq 1$ $-1.0 \leq ZD \leq 0$	Contours of $U_θ/U_{ref}$ at $θ = 45°$. Contour values 1.28, 1.20, 1.10 0.95.
3	YD	ZD	$0 \leq YD \leq 1$ $-1.0 \leq ZD \leq 0$	Contours of $U_θ/U_{ref}$ at $θ = 71°$. Contour values 1.20, 1.18, 1.15, 1.10.
4	YD	ZD	$0 \leq YD \leq 1$ $-1.0 \leq ZD \leq 0$	Contours of $U_θ/U_{ref}$ at $θ = 90°$. Contour values 1.25, 1.23, 1.20, 1.10.
5	YD	ZD	$0 \leq YD \leq 1$ $-1.0 \leq ZD \leq 0$	Contours of U_r/U_{ref} at $θ = 0°$. Contour values -0.55, -0.60, -0.65, -0.75.
6	YD	ZD	$0 \leq YD \leq 1$ $-1.0 \leq ZD \leq 0$	Contours of U_r/U_{ref} at $θ = 90°$. Contour values 0.28, 0.22, 0.12, -0.08.
7	YD	ZD	$0 \leq YD \leq 1$ $-1.0 \leq ZD \leq 0$	Contours of $\overline{u_θ u_r}/U_{ref}^2$ at $θ = 0°$. Contour values 0.0005, 0, 0.001, 0.002.
8	YD	ZD	$0 \leq YD \leq 1$ $-1.0 \leq ZD \leq 0$	Contours of $\overline{u_θ u_r}/U_{ref}^2$ at $θ = 90°$. Contour values -0.0005, 0.002, 0.003, 0.0045.

Special Instructions:

This test case considers the flow in a rectangular duct of square cross-section with a 90° bend (Fig. 2). Water was employed as the fluid medium at a bulk average velocity of 0.89 m/s, and the Reynolds number was 4.0×10^4 .

Calculation should be started at $x/D_h = -8.2$, i.e., 8.2 duct diameters upstream of the entrance to the 90° bend at $\theta = 0^\circ$. At this station, profiles of mean velocity U_x , U_y , U_z and stresses

$$\overline{uv}, \overline{uw}, \overline{u^2}, \overline{v^2}, \overline{w^2}$$

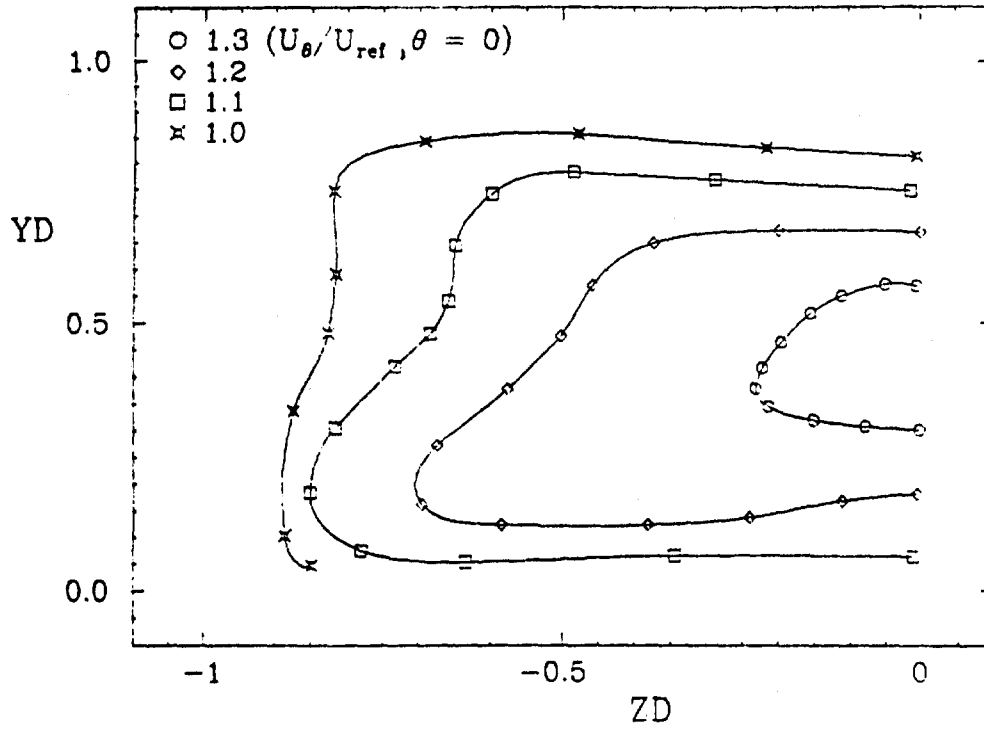
are available from the data bank, together with details of the local pressure gradient and skin friction.

A plane of symmetry along the centerline of the bend from $\theta = 0^\circ$ to 90° may be assumed and predictions made for one-half of each plane at $\theta = 0^\circ, 45^\circ, 71^\circ, 90^\circ$.

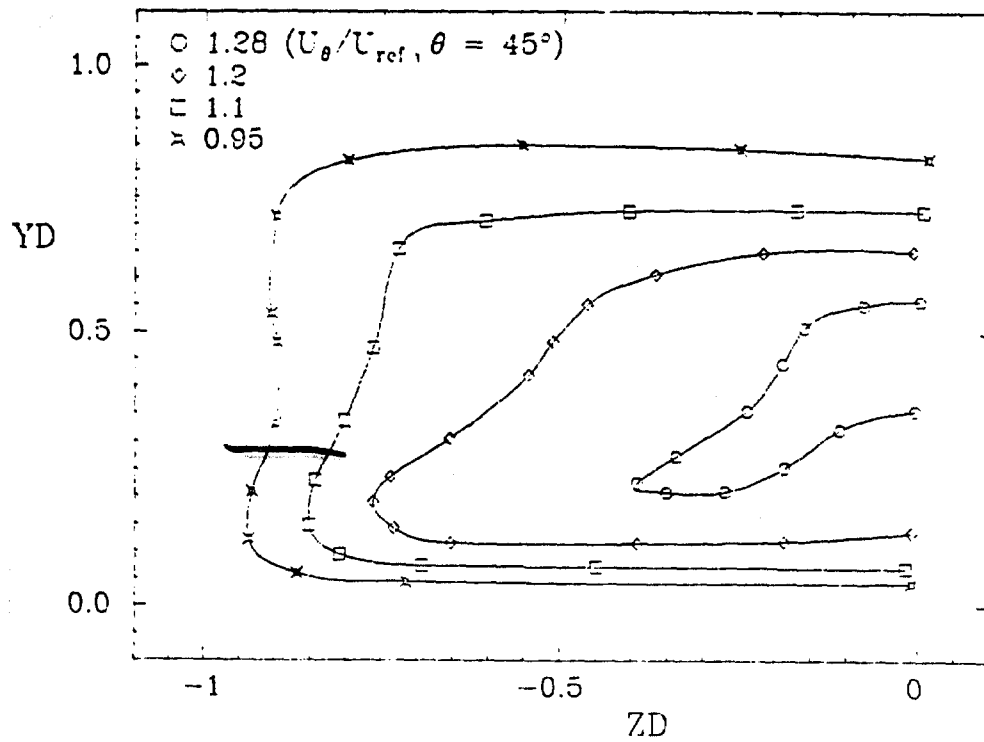
It must be noted that the additional upstream information data of Melling can materially affect computations. There are two sets of Melling's data; one set has been adjusted to satisfy the two-dimensional continuity equation in the cross-flow plane. It remains an open question, at present, which data set more closely represents the true physical situation.

YD and ZD are defined in Fig. 2.

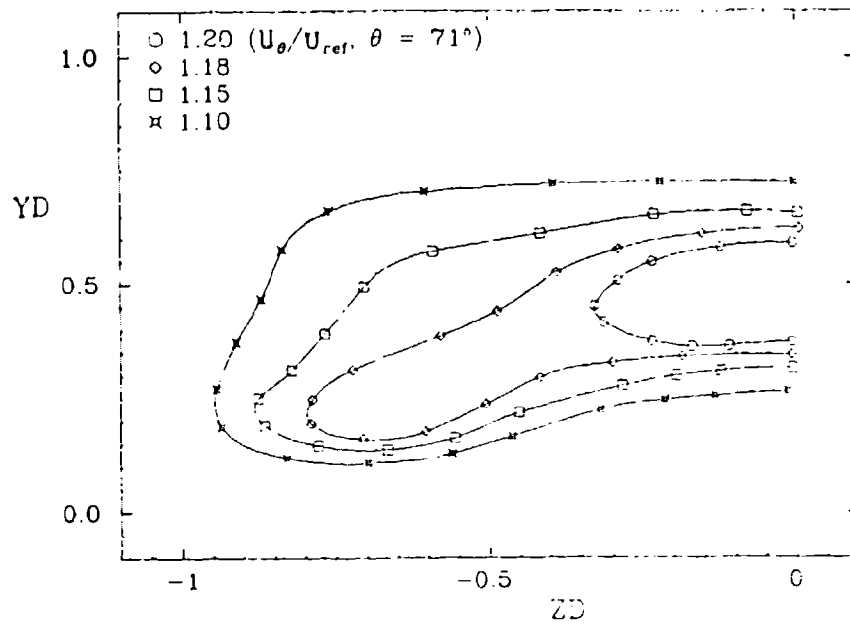
PLOT 1 CASE 0512 FILE 8



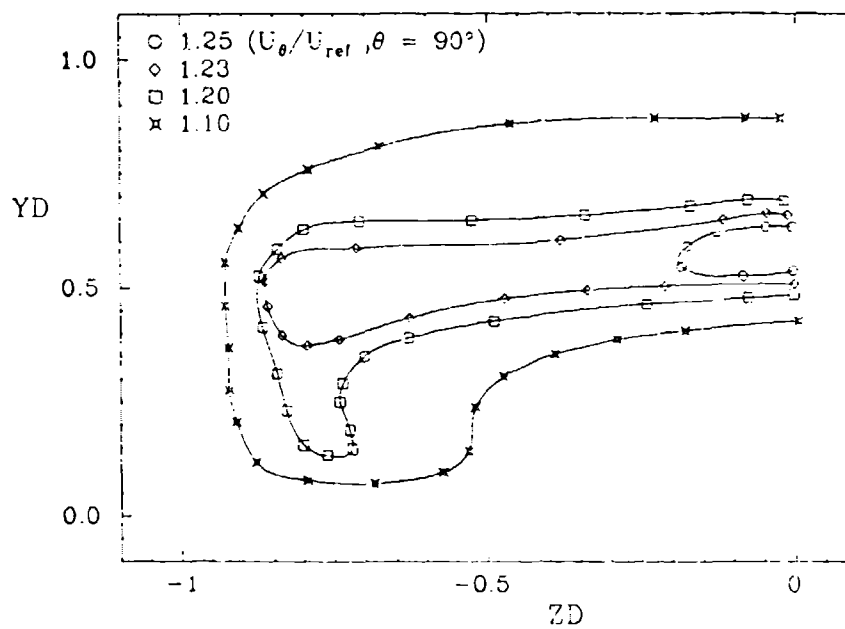
PLOT 2 CASE 0512 FILE 13



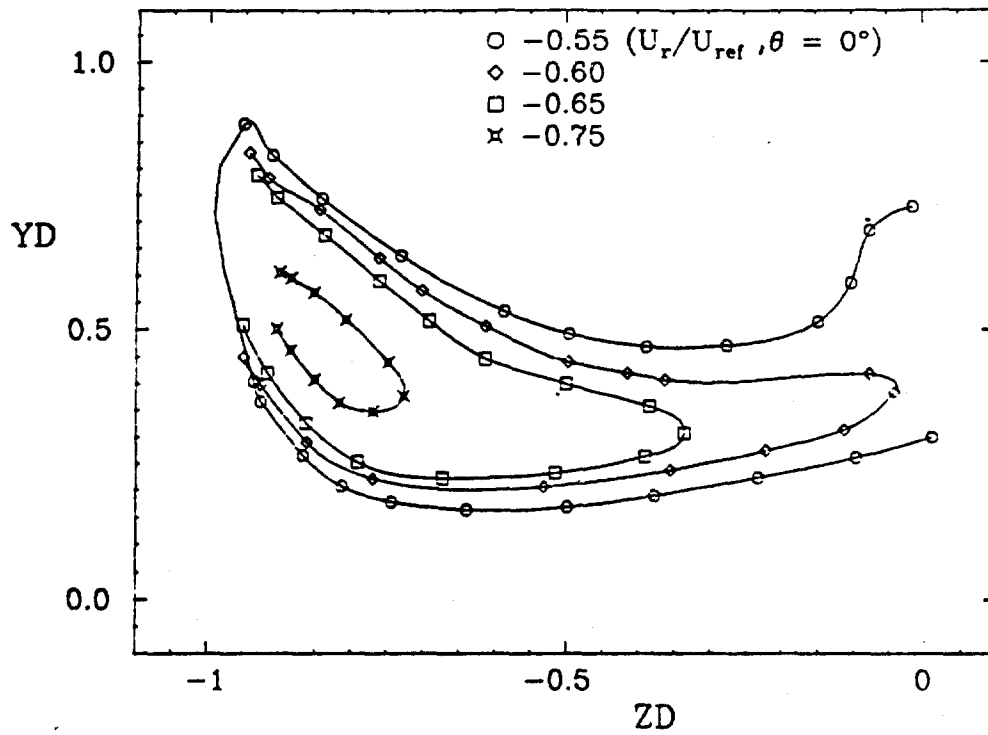
PLOT 3 CASE 0512 FILE 15



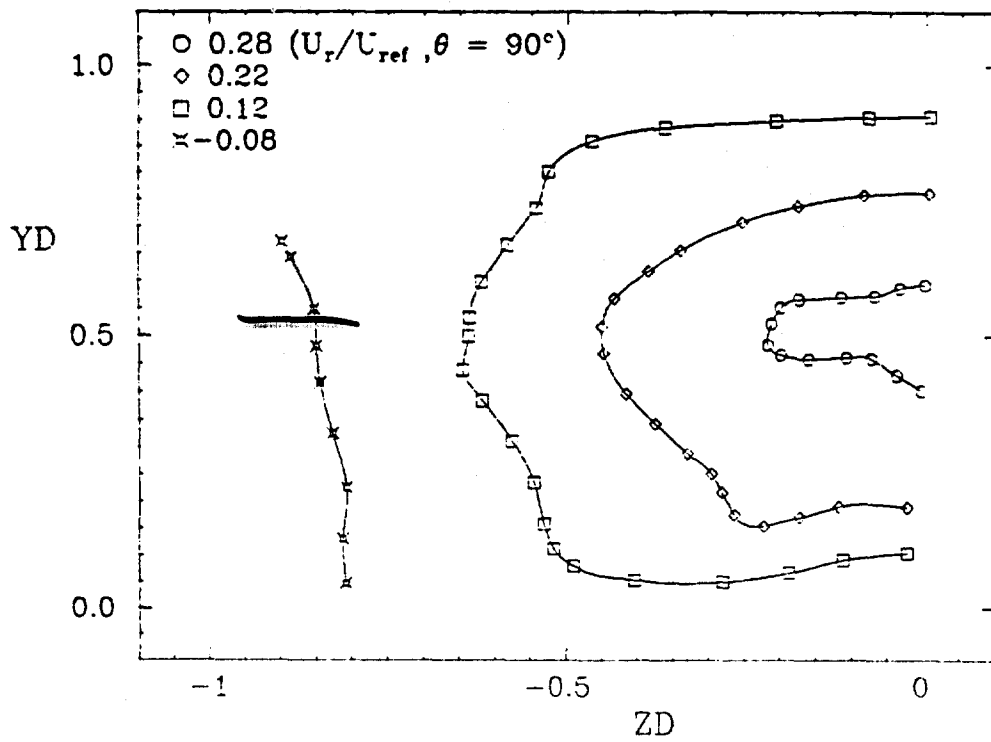
PLOT 4 CASE 0512 FILE 17



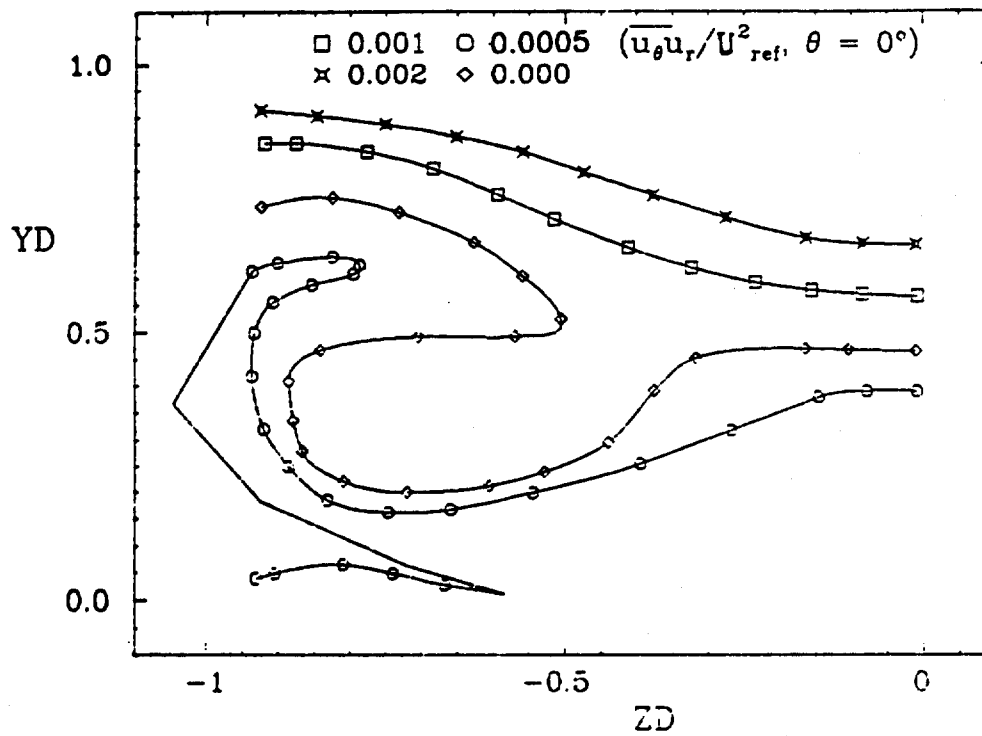
PLOT 5 CASE 0512 FILE 10



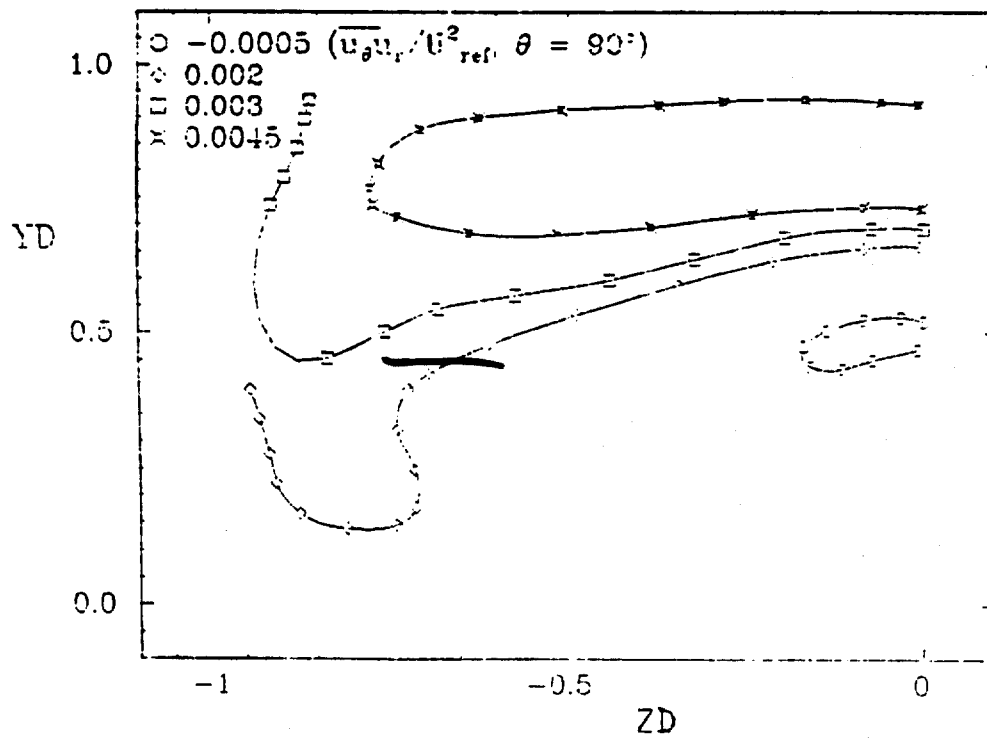
PLOT 6 CASE 0512 FILE 19



PLOT 7 CASE 0512 FILE 12



PLOT 8 CASE 0512 FILE 21



SESSION III

Chairman: J. P. Johnston

Technical Recorders:

A. Strawa
I. P. Castro



Flow 0250

Flow 0310

Flow 0150



THREE-DIMENSIONAL TURBULENT BOUNDARY LAYER

Flow 0250

Evaluators: D. A. Humphreys^{*} and B. van den Berg[†]



SUMMARY

Of the 16 cases potentially suitable for testing three-dimensional turbulent boundary-layer calculation methods, four can be recommended immediately. A further three might also be adopted, but with the rider that they are believed to be deficient in at least one essential respect. Of the rest, some will undoubtedly prove useful as test cases but cannot be recommended at present, either because they lack important measurements, which could still be performed, or because satisfactory flow quality has not been demonstrated. All 16 of the cases are expected to provide information for modeling the turbulence.

INTRODUCTION

The report describes, in condensed form, the results of a survey of three-dimensional turbulent boundary-layer experiments made with the purpose of identifying which of them could serve to test calculation methods. From the outset the survey was limited to cases in which Reynolds stresses were measured. This was because there is in general no simple relation connecting the turbulence and the mean velocity field in boundary layers and calculations must allow for this.

The experimental results are being collected from their originators and filed in computer-digestible form. Up to now, 13 cases have been received but three more are expected. It was decided not to recommend as test cases at this stage experiments where there has been no opportunity to examine the data in detail.

Table 1 lists all cases under evaluation. Note that a six-character alphanumeric label has been given to each data set, made up from the names of the principal authors and the date of the earliest major source publication.

The work has taken two directions. First, the instrumentation and measurement procedures were studied. This was in order to extract fundamental clues relating to experimental uncertainty but was also an attempt to understand which techniques should or should not be employed in a new experiment being planned today. Secondly, a series of criteria was drawn up and applied to each case. The criteria arrived at are given in the next section. Some of the main points to be noted for each case are discussed

^{*}The Aeronautical Research Institute of Sweden, Bromma, Sweden.

[†]National Aerospace Laboratory, Emmeloord, The Netherlands.

in the section after that and finally, relying mostly on the selection criteria, the cases are put in suitability groups according to all evidence to hand. It should be emphasized, however, that the opinions expressed here could be modified if further information becomes available.

TABLE 1. Cases Evaluated

Test Case	Label	First Major Publication
0251	BEEL72	van den Berg and Elsenaar (1972)
0252	BIME70 BRTE69 COPA79	Bissonnette (1970) Bradshaw and Terrell (1969) Pailhas (1979)
0253	DEFE77 EASA79 FEVA78 GRHI78 JOHN70 LALO74	Dechow (1977) East and Sawyer (1979) Fernholz and Vagt (1978) de Grande and Hirsch (1978) Johnston (1970) Larsson (1974)
0254	LOHM73 MUKR79 PIDU74 PIEZ75 SWGL78 ZIMM75	Lohmann (1973) Müller and Krause (1979) Pierce and Duerson (1974) Pierce and Ezekwe (1975) Swamy, Gowda, Lakshminath (1978) Zimmerman (1975)

EVALUATION CRITERIA

An experiment may be viewed on three levels, the whole flow in context, the characteristics of the particular realization and the detailed results. In its role as a possible test of calculation methods for three-dimensional turbulent flow, the boundary layer should be

sufficiently three-dimensional, and
adequately eventful in all aspects.

For calculations to be possible and worth doing, the experiment must provide

a full set of dynamic similarity parameters,
closely spaced initial and boundary conditions, and
enough additional results to verify computations.

Before conclusions can be drawn from the comparison between calculation and experiment, it should be demonstrated for the experiment that

flow symmetry assumptions are reasonable,
the turbulence structure is normal,
the momentum equations balance, and
the measurements are reliable and compatible.

The onus is on the originators of an experiment to show that their results are of good quality. Where quantitative reliability and internal compatibility checks are

possible but have not been done, it has been concluded that flow quality has not been demonstrated.

REMARKS ON THE EXPERIMENTS

Case 0251

In (BEEL72) pressure gradients were induced by a body suspended above the flat test surface. Quasi-two-dimensional conditions were achieved within the region of influence of the initial line and the momentum balance has been shown to be good. The flow is long in terms of the initial boundary-layer thickness.

Case 0252/0254

Both (BIME70) and (LOHM73) are realizations of the axisymmetric (quasi-two-dimensional) boundary layer on a cylinder whose afterbody is rotating about its axis. They differ in the afterbody rotation rates, though. Wall pressure was measured in neither case but was probably approximately constant. The momentum equations have been shown to hold except at two of seven measuring stations in (BIME70). There are no "redundant" measurements in (BIME70) for internal compatibility checks.

Maximum cross-flow angle in (BRTE69), a nominally quasi-two-dimensional boundary layer relaxing after removal of pressure gradient, is only 8° in the test region, which is considered marginal. An integral momentum balance has been carried out for this case by Wheeler and Johnston (1972). Agreement was not wholly satisfactory and it was suggested that the external flow was not sufficiently quasi-two-dimensional. No compatibility checks have been carried out.

(COPA79) is the three-dimensional turbulent boundary layer of a lifting wing. An unfortunate deficiency with this case is that the initial line turbulence was not measured. This is important because transition occurred over a leading-edge bubble. Momentum balance could be tested but has not been. Reynolds shear stresses do not extrapolate simply to corresponding wall shear stresses but may be compatible if due allowance for pressure gradient is made.

Case 0253 (see DEFE77)

Two of the cases reviewed are nominally, in separate regions, both quasi-two-dimensional and fully three-dimensional boundary-layer flows. (DEFE77) is the boundary layer approaching a symmetrical obstacle on a flat plate and (PIEZ75) is the boundary layer generated on a flat plate by a jet blowing against a perpendicular back wall. The most serious shortcoming of (DEFE77) is that no momentum balance has been done, nor would it in fact be very easy to do one, because of inconveniently located measuring stations. However, the data set does appear to be reliable as far as has been determined. The symmetry plane boundary layer can be calculated in isolation but only one station is available to verify such calculations. The case can be treated

also as a fully three-dimensional boundary layer with free side lines. (PIEZ75), on the other hand, suffers principally from a too sparsely defined pressure field and very high levels of turbulence in the external flow. Momentum balances and internal compatibility of results have not been demonstrated for (PIEZ75).

(EASA79), flow against a 45° swept step mounted on a flat plate, very nearly reproduces (JOHN70) in all flow-defining respects, but there are puzzling differences in the resulting boundary layers. It must be stated, however, that (EASA79) was set up not principally to provide a test case but to investigate the performance of a new measuring technique (double-split film probe) and the originators regard the experiment as not having been completed. Both cases are very short, less than about six initial boundary-layer thicknesses. In order to calculate them it would be necessary to assume quasi-two-dimensional flow, which has not been demonstrated satisfactorily for either experiment. No momentum balances have been carried out for (EASA79). They have for (JOHN70), as shown by Humphreys (1980) but the results were not entirely convincing.

(FEVA78) is the boundary layer flowing along a circular cylinder against a skew-mounted back plate. Momentum balances have not been done but the data set is complete enough to do so. The flow is not quasi-two-dimensional in principle and cannot strictly be treated as such in practice, but unfortunately it varies little in the transverse direction over most of the test region. This means that by supplying initial conditions along all inflow boundaries as demanded by the Influence Principle, the whole boundary layer is specified to a high degree, so that there is apparently not much scope for differences to arise in subsequent calculations.

Comments on the evaluation of (GRHI78), (LALO74) and (SWGL78) are held over at this stage because for various reasons no data have been received yet from the originators of these experiments. (GRHI78) is the boundary layer on the flat floor of a curved duct, (LALO74) on a model ship hull measured in a wind tunnel, and (SWGL78) on a swept flat plate at incidence. All three are believed to represent potentially useful test cases, although the small cross-flows of (SWGL78) make it marginal in the present context.

(MUKR79) is the three-dimensional boundary layer formed on a flat surface by mounting a deflecting wall to one side of the measuring region and by the action of adverse pressure gradients produced by a body suspended above the test surface. The boundary layer was very strongly affected by a large transition trip and the initial line turbulence shows some unusual features possibly as a result. Pressures were measured at the outer edge of the boundary layer only and as the adverse pressure gradients were relatively large it is believed that pressure variation through the boundary layer should have been investigated. Momentum balance has not been demonstrated. Skin-friction values obtained with a Preston tube and with a Clauser method

are compatible but cannot easily be compared with Reynolds stresses extrapolated to the wall because of the large pressure gradients.

The boundary layer on the flat floor of a duct also provides (PIDU74) but the geometry is different from (GRHI78). (PIDU74) was carried out in 1968 and is believed to be the earliest attempt to measure the full Reynolds stress tensor. It was not intended as a test for calculation methods. The flow must be regarded as fully three-dimensional but the results, along one line only, are unfortunately insufficient to define it for calculations.

(ZIMM75) is the boundary layer on a swept flat plate at nominally constant pressure. The integral momentum equations have been shown to hold and reliability and internal compatibility tests showed acceptable results. However, the flow has features which are not understood. The turbulence level outside the boundary layer was very high and within the boundary-layer turbulence profiles are convected downstream almost without change, while cross-stream differences are large. As the cross-flow angle was $4\text{--}1/2^\circ$ at most, this case should perhaps be seen as a disturbed two-dimensional boundary layer.

The four cases which best satisfy the criteria are (BEEL72), (BIME70), (DEFE77), and (LOHM73), which are, respectively, Cases 0251, 0252, 0253, and 0254.* These, it is felt, can provide good test cases for three-dimensional turbulent boundary-layer calculation methods. Three more cases can probably be used too but they appear to have limitations. The cases are (BRTE69) in which the cross-flow is rather small and the essential quasi-two-dimensional condition is in doubt. (FEVA78), which has to be treated as fully three-dimensional, but which does not show very much transverse variation, and (MUKR79), which is believed to have been adversely affected by the transition device.

CONCLUSIONS

A survey of all known three-dimensional turbulent boundary-layer experiments, which include Reynolds-stress measurements, has indicated that at least four exist which should provide satisfactory tests of calculation methods, and that at least three more may be acceptable for this purpose but are thought to be defective in some way.

*[Ed.: It is regretted that these four test cases could not be used for the 1981 meeting. Dr. Humphreys is arranging for the results of predictions on three-dimensional boundaries to be presented at a forthcoming conference--IUTAM Berlin 1982. The data are, however, in the Data Library for Cases 0251, 0252, 0253, and 0254.]

REFERENCES

- Bissonnette, L. R. (1970). "An experimental study of the development of a three-dimensional turbulent boundary layer under rapidly changing rate of strain," Dissertation, Princeton University.
- Bradshaw, P., and M. G. Terrell (1969). "The response of a turbulent boundary layer on an 'infinite' swept wing to the sudden removal of pressure gradient," NFL Aero Report 1305.
- Dechow, R. (1977). "Mittlere Geschwindigkeit und Reynoldsscher Spannungstensor in der drei-dimensionalen turbulenten Wandgrenzschicht vor einem stehenden Zylinder," Dissertation, University of Karlsruhe.
- de Grande, G., and Ch. Hirsch (1978). "Three-dimensional incompressible turbulent boundary layers," VUB-STR-8, Vrije University, Brüssel.
- East, L. F., and W. G. Sawyer (1979). "Measurements of the turbulence ahead of a 45° swept step using a double split-film probe," RAE TR 76136.
- Fernholz, H. H., and J.-D. Vagt (1978). "Measurements in an axisymmetric turbulent boundary layer with weak and strong three-dimensional disturbances," Structure and Mechanisms of Turbulence, Vol. I, Berlin, pp. 222-234.
- Humphreys, D. A. (1980). "Terms in the equations of motion for Johnston's step flow," Aero. Res. Inst. Sweden (FFA), Tech. Note AU-1379, Beräkningsbesked 1 (to appear).
- Johnston, J. P. (1970). "Measurements in a three-dimensional turbulent boundary layer induced by a swept forward-facing step," J. Fluid Mech., 42:4, 823-844.
- Larsson, L. (1974). "Boundary layers of ships. Part III. An experimental investigation of the turbulent boundary layer on a ship model," Swedish State Shipbuilding Experimental Tank (SSPA), Report No. 46.
- Lohmann, R. P. (1973). "The response of a developed turbulent boundary layer to local transverse surface motion," Dissertation, University of Connecticut.
- Müller, U., and E. Krause (1979). "Measurements of mean velocities and Reynolds stresses in an incompressible three-dimensional turbulent boundary layer," 2nd Symp. Turbulent Shear Flows, Imperial College, London, pp. 15.36-15.41.
- Pailhas, G. (1979). "Couche limite et sillage turbulents tridimensionnels. Champ moyen--Tensions de Reynolds," Diss. Conservatoire National des Arts et Métiers, Centre Régional Associé de Toulouse.
- Pierce, F. J., and S. H. Duerson (1974). "Measurements of the Reynolds stress tensor in a three-dimensional turbulent boundary layer," Virginia Polytech. Inst. and State University, VPI-E-74-4.
- Pierce, F. J., and C. I. Ezekwe (1975). "Turbulent stress tensors in a three-dimensional boundary layer," Virginia Polytech. Inst. and State University, VPI-E-75-1.
- Swamy, N. V. Ch., B. H. L. Gowda, and V. R. Lakshminath (1978). "Turbulence measurements in the three-dimensional boundary layer on a yawed flat plate at incidence," Z. Flügwiss. Weltraumforsch., 2:1, 15-22.

van den Berg, B., and A. Elsenaar (1972). "Measurements in a three-dimensional incompressible turbulent boundary layer in an adverse pressure gradient under infinite swept wing conditions," NLR TR 72092 U (draft).

Wheeler, A. J., and J. P. Johnston (1972). "Three-dimensional turbulent boundary layers--Data sets for two-space coordinate flows," Thermosci. Div., Dept. of Mech. Eng., Stanford University, Rep. MD-32.

Zimmerman, D. R. (1975). "An experimental investigation of a three-dimensional turbulent boundary layer," Dissertation, Purdue University.

DISCUSSION

Flow 0250

1. The evening discussion concentrated on the adequacy of the few suggested test cases and on the selection criteria and their application. With regard to selection criteria, in daytime discussions between the Chairman and other interested parties, the point was made that a number of other excellent data sets are available, although they do not contain turbulence measurements and therefore did not meet the evaluators' selection criteria. In the evening discussion, the consensus was that these criteria were reasonable for the purposes of the 1981 meeting, although they might not be for a specialist meeting on this topic.
2. There was some disagreement over whether flows in which reversals of cross-flow direction occur should be included as test cases and whether such flows would require a respecification of the necessary side boundary conditions. The evaluators felt that no respecification is required for such cases. However, there is, in any case, no suitable data set satisfying the selected criteria, so it was agreed that these disagreements were not currently important.
3. Pierce commented that some doubt remains about the validity of using two- or three-dimensional log-like laws to infer wall-shear stress in strongly three-dimensional flows.
4. There was much discussion about the accuracy of hot-wire measurements, particularly in three-dimensional flows. Perry and Müller both felt that, unless independent evaluation of the uncertainties in the turbulence data for the four suggested flows were made, they should not automatically be included as test cases. Johnston suggested that, in addition to the error estimates of the original authors being quoted, the evaluators should make some personal judgments about the adequacy of those estimates. The evaluators noted that it is not really possible to verify uncertainty estimates of the originators. There was general agreement that redundant measurements are especially useful in these flows in their role as accuracy checks, and, in particular, van den Berg stated that he relied on them as much as on the standard momentum balance checks.

5. Joubert expressed the opinion that unless hot wires are calibrated dynamically, any measurements made in regions where total turbulence intensity (q'/Q) exceeds about 10% should be questioned. Also, where possible, redundant measurements should be obtained in a given apparatus with two different classes of instrument, e.g., hot-wire and LDV. The evaluators comment (see above) that their criteria emphasize the need for redundant data. In regard to the question of dynamic hot-wire calibration, the Chairman notes that there are other opinions on this subject. Some feel, for example, that, as long as q'/Q does not exceed 25 to 30%, calibration in a similar turbulent flow with known characteristics (e.g., fully developed pipe flow) should suffice.



PLANAR MIXING LAYER

Flow 0310

Case 0311

Evaluator: S. Birch*

SUMMARY

SELECTION CRITERIA AND FLOWS SELECTED

The reported variation in the spreading rate of a nominally fully developed, incompressible, single-stream mixing layer has been a major source of concern in recent years. There now appears to be sufficient data available, however, to conclude that an isolated mixing layer does reach a unique (within the uncertainty of the data) asymptotic spreading rate, if the Reynolds number is sufficiently high and that much of the earlier confusion was due to an underestimate of the sensitivity of mixing layers to initial and boundary condition.

The present reviewer's estimate for the spreading rate of a fully developed mixing layer is given approximately by

$$\frac{dL}{dx} = 0.115 \frac{U_1 - U_2}{U_1 + U_2} \quad (1)$$

where U_1 and U_2 are the velocities on the high and low velocity sides of the layer and L is the width defined to be the distance between the points at which U equals $0.316(U_1 - U_2) + U_2$ and $0.949(U_1 - U_2) + U_2$.

In the limit, as the velocities in the two streams become equal, a planar wake is formed. Since, for practical purposes, the velocity defect on the wake centerline persists indefinitely, the zero spreading rate predicted by Eq. (1) is not achievable in practice; but the local spreading rate does approach zero with increasing downstream distance.

The spreading rate of the approximately self-similar region of a planar wake is generally quoted in terms of the velocity half-width $Y_{1/2}$ and is given approximately by (where $U_o = U_e - U_{CL}$)

$$\frac{U_e}{U_o} \frac{dY_{1/2}}{dx} = 0.098 \quad (2)$$

Since in the far wake $U_o \ll U_e$, we can rewrite this in a form equivalent to Eq. (1) as

$$\frac{1}{\lambda} \frac{dL}{dx} = 0.242 = \frac{2U_e}{U_o} \frac{dL}{dx} \quad (3)$$

*Boeing Military Airplane Co., P. O. Box 3999, Seattle, WA 98124.

where λ is defined as

$$\lambda = \frac{1}{2} \frac{U_o}{U_e} = \frac{U_e - U_{CL}}{U_e + U_{CL}}; \quad U_{CL} = \text{centerline velocity} \quad (4)$$

Comparing this with Eq. (1), we see that the spreading rate of the half-wake is almost twice that of a mixing layer.

The developing region of a mixing layer is less well understood. For calculation purposes one would like a flow with well-defined initial conditions and sufficient turbulence measurements--particularly shear-stress measurements--to characterize the main features of the flow. The data should cover the complete developing region and extend into the fully developed region of the flow, since it is difficult to assess the accuracy and consistency of the data unless the fully developed region is included. Until we have a better understanding of the sensitivity of the flow to initial conditions, a fully developed turbulent wall boundary layer is probably a better starting condition than a laminar boundary layer, because of the sensitivity of the latter flow to external disturbances.

No totally satisfactory data set that satisfies all the above criteria appears to be available at present. Four single-stream mixing layers, all developing from turbulent wall boundary layers, are listed in Table 1 (Gartshore, 1965; Foss, 1977; and two flows from Husain and Hussain, 1979). The normalized data for these flows are plotted in Fig. 1. All four sets of data appear to collapse to a single curve when normalized by the corresponding momentum thickness of the boundary layer at the separation point. The spreading rate at the farthest downstream station appears to be close to the asymptotic value.

The axisymmetric mixing-layer data extend downstream to a distance of about four nozzle diameters where transverse curvature effects are no longer negligible. These effects, however, appear to lead to no noticeable change in the shape of the mean velocity spreading rate curve. The variation in Re_θ for these four flows is too small to justify a conclusion that the normalized data are totally independent of Reynolds number; but the plot does suggest that Reynolds number effects are probably fairly small.

ADVICE FOR FUTURE DATA TAKERS

The planar mixing layer poses a number of difficulties that, if not completely unique to this flow, are at least particularly troublesome in this flow geometry. The most important of these is probably the persistent effects of initial conditions and the resulting difficulty in achieving a truly self-similar flow. If the objective is to obtain a fully developed flow in the minimum distance, the boundary layer at the separation point should be laminar. A low value of Re_θ is probably also helpful.

As an estimate of the distance required for a single-stream flow to become fully developed, Bradshaw's (1966) suggestion of $7 \times 10^5 \nu/U_1$ or 1000δ still appears to be the most useful. This distance increases with velocity ratio; but, for two stream mixing layers, there appears to be a stronger dependence on the detailed initial conditions. Tripping the boundary layer before the separation point will typically extend the development distance by at least a factor of two.

Although the best data from planar mixing-layer studies agree very well with data from the quasi-planar region in the near field of axisymmetric jets, the incidences of anomalous or apparently anomalous behavior are encountered more frequently in planar mixing-layer studies. This suggests that particular care should be taken when using this flow geometry.

REFERENCES

- Bradshaw, P. (1966). "The effect of initial conditions on the development of a free shear layer," J. Fluid Mech., 26, Part 2, 225-236.
- Foss, J. F. (1977). "The effect of the laminar/turbulent boundary layer states on the development of a plane mixing layer," Proc. Symposium on Turbulent Shear Flows, April 18-20, pp. 11.33-11.42.
- Gartshore, I. S. (1965). "The streamwise development of two-dimensional wall jets and other two-dimensional turbulent shear flows," Ph.D. Thesis, McGill University, Montreal.
- Husain, Z. D., and Hussain, A. K. M. F. (1979). "Axisymmetric Mixing Layer: influence of the initial and boundary conditions," AIAA Jou., 17(1), 48-55.

TABLE 1
Summary of Data in Mixing-Layer (Fig. 1)

Author	Vel., m/sec	θ_1 , cm	$Re_\theta \times 10^3$	Comments
Gartshore (1965)	19.6	0.079	1.04	Plane mixing layer
Foss (1977)	18.3	0.081	1.07	Plane mixing layer with end plate
Husain and Hussain (1979)	30.0	0.0706	1.45	12.7-cm diam. nozzle without end plate
Husain and Hussain (1979)	30.0	0.0632	1.29	12.7-cm diam. nozzle with end plate

All flows are developing from nominally fully developed wall boundary layers.

θ_1 = momentum thickness of wall boundary layer at the separation point.

L = width of mixing layer: defined as the distance between the points at which $U = \sqrt{0.9} U_1$ and $\sqrt{0.1} U_1$.

Asymptotic spreading rate approx. = 0.115.

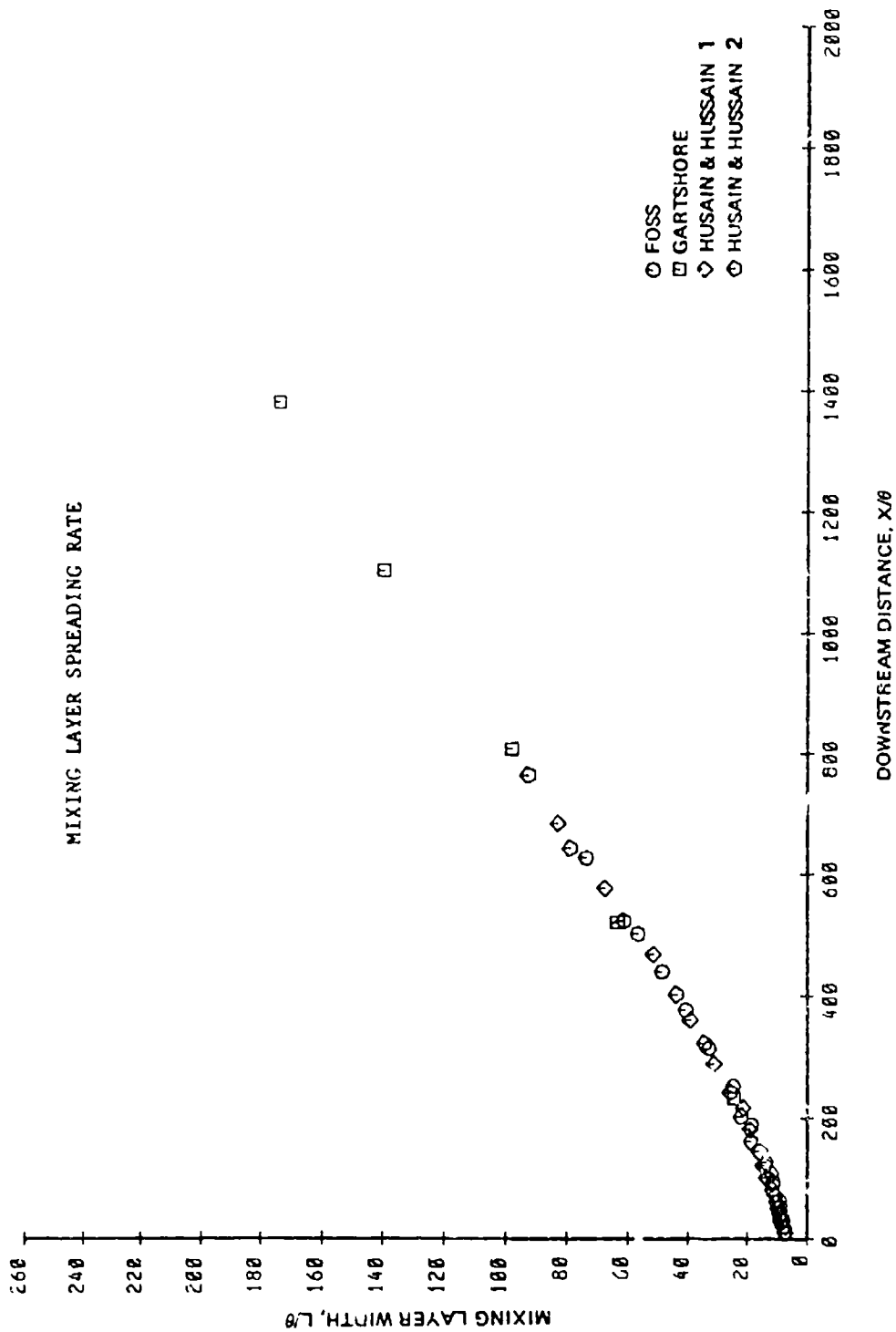


Figure 1. Mixing layer developing from turbulent wall boundary layer.

DISCUSSION

Flow 0310

1. The major point to emerge from the discussion, which was initiated by M. Morkovin, was that the influence of initial conditions was not at all clear. For example, R. Luxton pointed out that sound affected the flow, and I. Wygnanski noted that a simple distinction between "laminar" and "turbulent" initial boundary layers is not sufficient. S. Birch essentially agreed with all these remarks, and it was decided that the problem was of sufficient importance to the computers to warrant a more extended discussion (see Ad-Hoc Committee report No. 3).
2. There were two minor points raised which were clarified in floor discussion, later during the day, or at the evening committee meeting. In response to a query from W. Reynolds, S. Birch confirmed that his θ was that of the separating boundary layer (in a single-stream mixing layer). P. Saffman pointed out that, in elliptic calculations of this flow whilst the physics are well posed, the mathematics may not be, unless the outlet boundary conditions are properly specified.
3. Finally, S. Birch disagreed with I. Wygnanski over his definition of mixing-layer width, which the latter felt concealed much of the scatter in the published data. After the 1980 meeting the following comments were received from A. Hussain:
 - A. Asymptotic mixing layer: Only in the experiment of Hussain and Kleis (1980) is it conclusively demonstrated that a universal plane mixing layer does exist, both with laminar and fully developed turbulent exit boundary layers.
 - B. Region of self-preservation: Since self-preservation is only attained at $x > 1000 \theta$, the value of dL/dx is found to exceed 0.115, the value suggested by the evaluator. However, the value of dL/dx obtained by Hussain and Kleis (1980) was 0.11. In an axisymmetric mixing layer it was found that $dL/dx = 0.116$ for an initially laminar boundary layer and 0.139 for an initially turbulent flow. When the initial boundary layer was laminar, the shear-layer evolution was independent of Re_θ , but noticeably dependent on the initial fluctuation level and its spectral content.
 - C. Dependence on the end-plate: It has been found by Husain and Hussain (1979) that the single-stream free mixing layer is independent of the presence or otherwise of an end-plate.
 - D. Initial shear-stress measurement: The initial conditions that are meaningful are namely $U(y)$, $\overline{u^2}(y)$, and ϕ_u . Measurements of $\overline{v^2}$ and UV present difficulties due to the finite lateral extent of hot-wire or LDV instrumentation.

- E. Role of initial conditions: In incompressible free turbulent flows it has been found that the integral measures of the single-stream mixing layer asymptotic flow are a unique function of the initial conditions. These are classified as (i) laminar, (ii) nominally laminar, (iii) highly disturbed, and (iv) fully turbulent.
- F. Appropriate trips: In most previous experimental studies trip wires have rarely produced fully developed turbulent flow at exit. Experience of this author is that effective trips should be placed $100 \delta^*$ upstream of lip, have a height equal to the displacement thickness, and have spanwise notches spaced a displacement thickness apart.
- G. Initial fluctuation: The spectral content of the initial fluctuations is important because of its influence on the instability of an initially laminar shear layer. An initially fully turbulent boundary layer has strong fluctuations and is uninfluenced by the typical low-level free-stream fluctuations. However, a fully turbulent shear layer may itself become unstable and roll up further downstream (Clark and Hussain, 1979).
- H. Distortion by shear tone: Any invasive measurements of the initial shear layer almost always induce a shear tone (Hussain and Zaman, 1978), and this leads to misleading data on initial conditions. [Ed.: This is a summary of much longer discussion notes submitted by Dr. A. K. M. F. Hussain. Although these comments are important with respect to data on mixing layers it is not considered they require the specification for Case 0311 to be modified.]

SPECIFICATIONS FOR COMPUTATION

ENTRY CASE/INCOMPRESSIBLE

Case #0311; Data Evaluator: S. Birch

Data Taker: Four sets; see specification

PICTORIAL SUMMARY

Flow 0310. Data Evaluator: S. Birch. "Planar Mixing Layer."

Case Data Taker	Test Rig Geometry	dp/dx or C _p	Number of Stations Measured							Initial Condition	Other Notes
			Mean Velocity		Turbulence Profiles						
			U	V	$\overline{u^2}$	$\overline{v^2}$	$\overline{w^2}$	\overline{uv}	Others		
Case 0311			L/θ ₁ vs x/θ ₁								Initial development of the U ₂ = 0 plane mixing layer.
Data combined from several sources.											

Plot	Ordinate	Abscissa	Range/Position	Comments
1	L/θ ₁	x/θ ₁	0 ≤ x/θ ₁ ≤ at 1 at 2000	For single-stream mixing layer, continue to fully developed con- dition, but at least x/θ ₁ = 2000.

Special Instruction:

1. θ₁ = momentum thickness at separation point.
2. Take R_{θ₁} as 1210.
3. Report asymptotic spreading rate dL/dx found for Plot 1 as a number.
4. Experimental data (Husain and Hussain, 1979) for the mean velocity and the axial component of the turbulence are provided for the wall boundary layer at the initial station. Other quantities needed to start the calculation should be obtained by assuming that the boundary layer is fully developed. All quantities used to start the calculation should be reported.

Special Symbols

L = width for a mixing layer between the point at which U = U₂ is

$$\sqrt{0.1}(U_1 - U_2) \text{ and } \sqrt{0.9}(U_1 - U_2);$$

U₁ = value of U on the high-speed side of a mixing layer;

U₂ = value of U on the low-speed side of a mixing layer;

x = downstream distance;

y = cross-stream distance;

$$\lambda = \frac{U_1 - U_2}{U_1 + U_2}.$$

Figure 1 is a scatter plot showing the relationship between the normalized vertical coordinate L/θ_i (Y-axis) and the normalized horizontal coordinate x/θ_i (X-axis). The Y-axis ranges from 0 to 200, and the X-axis ranges from 0 to 2000. Data points are plotted for four different studies: FOSS (diamonds), GARTSHORE (squares), HUSSAIN 1 (crosses), and HUSSAIN 2 (circles). The data points generally follow a linear trend, starting near the origin and extending to approximately $(1400, 175)$.

TWO-DIMENSIONAL CHANNEL FLOW WITH PERIODIC PERTURBATIONS



Flow 0150

Cases 0151, 0152

Evaluator: M. Acharya*

SUMMARY

The following criteria were used in the selection of test cases:

1. The turbulent flow should be two-dimensional (planar or axisymmetric) and fully developed.
2. The imposed periodic disturbance should not cause flow separation.
3. Measurements of periodic quantities should include phase- as well as amplitude-information.
4. Measurements of the perturbation stress field are desirable.
5. Data should satisfy requirements of accuracy and repeatability, and enough information should be available to serve as a basis for computations.

Based on the foregoing, the following two cases were selected.

Case 0151. Hussain-Reynolds Experiment (1970).

The experiments were conducted in a high-aspect-ratio air channel in which fully developed two-dimensional turbulent flow could be obtained.

Nearly plane wave disturbances were introduced in the test section with the help of electromagnetically driven ribbons. These introduced additional periodic velocities and pressure in the turbulent flow. Hot-wire instrumentation and conditional sampling techniques were used to measure the mean, fluctuating, and periodic components of the streamwise velocity.

Most of the data were obtained for a Reynolds number of 13,800, based on channel half-width and centerline velocity. The amplitudes and phases of the streamwise perturbation velocity \tilde{u} at different streamwise locations in the flow for symmetric disturbances were documented for four oscillation frequencies, 25, 50, 75, and 100 Hz. The perturbation Reynolds stresses and the transverse perturbation velocity \tilde{v} were not measured.

The data show that the perturbation velocities are small compared to the mean, and decay almost exponentially in the streamwise direction. The decay rate increases and wave length decreases with increasing frequency.

*Brown, Boveri Ltd., CH-5405 Baden-Datwil, Switzerland.

Case 0152. Acharya-Reynolds Experiment (1975).

The experiments were conducted in the same flow channel used by Hussain and Reynolds, modified to produce controlled periodic oscillations in the test section. The perturbation velocity had a slug-flow character, constant over most of the flow, with a Stokes layer developing in the wall regions. As in the case of Hussain and Reynolds, hot-wire instrumentation and conditional sampling techniques were used to measure the mean, fluctuating, and periodic components of the streamwise velocity. In addition, the mean and perturbation Reynolds stresses were also measured. These data were also obtained for a Reynolds number of 13,800 based on channel half-width and centerline velocity. The amplitudes and phases of the perturbation velocities and the perturbation Reynolds stresses were measured for two oscillation amplitudes at an oscillation frequency of 24 Hz, and for one (the higher) oscillation amplitude at 40 Hz. Only data for the higher oscillation amplitude are reported here.

The uncertainty estimates gave 5% on magnitude and 4° on phase for most flow quantities other than the perturbation Reynolds stresses, which were 10% and 15°, respectively.

Other comments: There is a lack of data of this kind for unsteady turbulent flows; more experiments would be welcome. It is recommended that future measurements also include data on higher harmonics.

REFERENCES

- Acharya, M., and W. C. Reynolds (1975). "Measurements and predictions of a fully developed turbulent channel flow with imposed controlled oscillations," Tech. Rept. TF-8, Thermosciences Div., Dept. of Mech. Eng., Stanford University.
- Hussain, A. K. M. F., and W. C. Reynolds (1970). "The mechanics of a perturbation wave in turbulent shear flow," Tech. Rept. FM-6, Thermosciences Div., Dept. of Mech. Eng., Stanford University.

DISCUSSION

Flow 0150

The discussion of this flow was flavored by the fact that the general topic of unsteady flows will be discussed in Session XII by L. Carr.*

In response to queries by A. Smits and A. Perry, W. Reynolds pointed out that in the two experiments evaluated the only significant source of "jitter" on the velocity waveforms was the turbulence and is therefore part of the problem to be solved by the predictors.

There was some discussion concerning the presence of higher harmonics in the data which resulted in a final consensus that these were not important, since they were of low amplitude compared to the fundamental, which was itself of small amplitude. In view of the latter fact, it was also agreed that computers would have the option of either using a full, time-dependent method or a method based on the small-amplitude, linearized equations for the ensemble-averaged results.

Several discussers mentioned other flows that should have been considered in this class. For example, B. Ramaprian mentioned his own high-amplitude perturbations of a pipe flow and two other similar experiments. In the evening discussion, the general feeling was that the evaluated cases are important enough to be recommended for consideration as test cases, but first an independent evaluator should be asked to review the data and, second, a third test case of the high-amplitude, pipe-flow variety should be evaluated and included as a test case if possible.

B. Ramaprian expressed the opinion that the recommended data sets were not suitable as test cases because the modulation amplitude (1% and 4% of mean flow speed) was too small to enable most predictive schemes to distinguish the effects of unsteadiness. This opinion was not unanimously held by all people present at the evening discussion.

*[Ed.: The participants at this conference concluded that Flow 0150 should be withdrawn as a test case for 1981 since there are advantages in treating unsteady flows as a separate class from the majority of steady flows treated in the 1981 Conference. This recommendation has been carried out. However, the data remain in the Data Library.]

SESSION IV

Chairman: W. C. Reynolds
(for W. M. Kays)

Technical Recorders:

A. Cutler
A. K. M. F. Hussain



Flow 0110

Flow 0130

Numerical Checks

G. Mellor

F. Gessner



CORNER FLOW (SECONDARY FLOW OF THE SECOND KIND)

Flow 0110

Cases 0111, 0112

Evaluator: F. B. Gessner*

SUMMARY

INTRODUCTION

This report summarizes the results of a data survey related to turbulent flow along a streamwise corner in which secondary flows are induced by virtue of Reynolds-stress gradients acting in the corner region (secondary flow of the second kind). In all, over ninety sources of data were located, and approximately seventy of these were surveyed. The results of this survey are presented in a preliminary report (Gessner, 1979) in which various data sets are rated with respect to both accuracy and suitability for comparison with numerical predictions. The data sets considered in that survey were categorized within six major categories, namely:

1. Turbulent flow in constant-area rectangular ducts
2. Turbulent flow in other constant-area, non-circular ducts
3. Transitional flow in constant-area, non-circular ducts
4. Zero- and variable-pressure gradient turbulent corner flows (interior)
5. Zero- and variable-pressure gradient turbulent corner flows (exterior)
6. Turbulent corner flows with heat transfer.

In Categories 1, 2, and 6, several data sets were rated as being suitable for comparison purposes, while those in the other categories were either unsuitable or only marginally acceptable. In reviewing the report, the Organizing Committee has recommended that attention be confined to data sets within Category 1 (flow in constant-area rectangular ducts) for the purposes of this conference. Accordingly, this summary shall concentrate on data sets which have been selected for inclusion in the final report.

SELECTED DATA SETS

Ten data sets in Category 1 on smooth-wall ducts are regarded as suitable (in part or in total) for comparison with numerical results. Four of these concern fully developed flow in a smooth-walled, square duct: Hoagland (1960); Leutheusser (1961); Brundrett (1963); and Launder and Ying (1971). Six concern developing flow in the

*Mech. Eng. Dept., University of Washington, Seattle, WA 98195.

same geometric configuration: Melling (1975); Po (1975); Lund (1977); Gessner et al. (1979); and Gessner and Emery (1979). In order to compare numerical predictions with the most comprehensive set of data available for square-duct flow (at a given Reynolds number to minimize computational costs), it was considered desirable that the data encompass measurements in three zones: the near-entrance region; the shear-layer-interaction region after the wall boundary layers have merged; and at a location where the mean flow is nominally fully developed. The data should also provide a fairly complete characterization of the flow in terms of primary- and secondary-flow velocity profiles, local wall-shear-stress distributions, and Reynolds-stress distributions. It was also considered essential that inlet flow conditions should be well posed and that the flow should be relatively symmetric about corner and wall bisectors for all levels of flow development. The only available data sets which meet these criteria are those reported by Po (1975), Lund (1977), and Gessner et al. (1979), and Gessner and Emery (1979). All these results are based on measurements in the same experimental facility at a bulk Reynolds number of 2.5×10^5 .

In performing the hot-wire measurements reported in these four studies, each probe was calibrated in the potential core of a free jet before and after measurements at a given test station in order to determine the intercept value of the mean bridge voltage (for data-reduction purposes). Each inclined wire probe was also calibrated in fully developed, turbulent pipe-flow before and after each set of measurements in order to determine the tangential cooling factor for that particular wire (again, for the purpose of reducing hot-wire data taken in the duct). Details of the calibration procedures are described by Po (1975). The consistency of the Reynolds stress measurements was investigated by comparing distributions of $\overline{u^2}$, $\overline{v^2}$, $\overline{w^2}$, and \overline{uv} measured by various investigators along the corner and wall bisectors of a square duct and along the plane of symmetry of high-aspect-ratio ducts. It was found that the results obtained by Po (1975) are consistent with those reported by Melling (1975) and Dean (1974) at other Reynolds numbers in that normalized values of each stress component exhibit a consistent decrease with an increase in Reynolds number. As a further check, one may refer to the Reynolds-stress transport-equation balances reported by Gessner et al. (1979) which provide indirect confirmation of the overall accuracy of both the primary-flow-velocity profile (mean-velocity gradient) and Reynolds-stress measurements by Po. The secondary-flow-velocity data selected for comparison purposes are the profiles reported by Gessner and Emery (1979) which are based on multiple measurements (two or more data sets for each profile) using a relatively accurate single-wire rotation technique. (Flow angles in low-intensity flows can be determined to within $\pm 0.05^\circ$ by this technique). The local wall-shear-stress measurements made by Lund (1977) are considered to be suitable for comparison purposes because of the careful calibration and measurement techniques employed. (Measurements were made with

three different-diameter Preston tubes at each point after the probes were calibrated in fully developed turbulent pipe flow). The near-wall data reported by Lund (1977) and more recent data obtained by Eppich (1980) using the same calibration techniques described above have also been analyzed in order to provide additional information on observed near-wall behavior. These results are summarized in the "Specification for Computations" (Flow 0110). Tabulated data based on the results of Po (1975), Lund (1977), Gessner et al. (1979), and Gessner and Emery (1979) are presented in the final report (Gessner, 1980).

The above selected data sets are all based on measurements in a smooth-walled, square duct. In order to explore the predictive capabilities of a particular code more fully, the Organizing Committee has recommended that flow in a duct with combined smooth-rough wall conditions also be considered. The experimental data generated by Hinze (1973) constitute an acceptable data set for this purpose. In that study measurements were made in the fully developed region of a 5:1 aspect-ratio duct with one wall selectively roughened. More recent studies by Fujita (1978) and Humphrey (1977) have provided additional data on flow in square ducts with artificially roughened walls. The measurements by Fujita include primary flow in a square duct with six different wall-roughness conditions (one wall smooth, three walls rough, etc.). No turbulence data are included, however, which limits the comparisons that can be made with this data set.

The data of Humphrey (1977) include both mean-flow and Reynolds-stress distributions in the entrance region of a square duct with one wall selectively roughened by means of equally spaced, transverse ribs. This particular flow situation is exceedingly complex, however, and not believed amenable to analysis within the present state-of-the-art. For example, because the rib height relative to the duct width is relatively large, the local flow structure at a cross-section between adjacent ribs varies markedly from that in the cross-section above either rib. Furthermore, at a given streamwise location, the coefficients which appear in the law-of-the-wall must vary in the spanwise direction in order to model near-wall velocity-profile behavior properly. These points are discussed in more detail in Gessner (1980).

For the present, it will suffice to note that only the data of Hinze (1973) constitute a reasonably complete data set for a combined smooth-rough wall duct flow which can be compared with predictions based on currently available turbulence models. The selection of this particular data set is justified also on the basis of consistency in the measurements and the care that was exercised in performing the experiments. Lines of constant axial mean velocity in the duct cross-section are symmetric about the midplane and, on the plane of symmetry, transverse mean-velocity and turbulent shear-stress profiles measured on three separate occasions are in good agreement. The dissipation-rate data in the plane of symmetry appear to be accurate, inasmuch as

profiles based on assumed isotropy at three different levels follow a common distribution. The overall data which are available for this test case include lines of constant axial mean velocity in the duct cross-section, and complete mean-velocity, Reynolds-stress, and dissipation-rate data in the plane of symmetry. These results are employed in the "Specifications for Computations, Case 0112." Tabulated data are available in Cessner (1980).*

ADVICE FOR FUTURE DATA TAKERS

The afore-mentioned selected studies provide a reasonably complete picture of developing turbulent flow in a square duct and fully developed flow in a rectangular duct with selectively roughened walls. In acquiring data in these types of flow with a relatively short, slant-wire probe ($200 \leq l/d \leq 400$), it is advisable to calibrate the probe in fully developed turbulent pipe flow before and after each set of measurements in order to prescribe a proper value for the tangential cooling factor when data are reduced. This set of measurements can also serve as a check on the accuracy of the over-all hot-wire anemometer system. Analysis of local wall-shear and turbulent-shear-stress data taken in the near-wall region of a smooth duct can also serve as a further check on the measurements, in that a well-defined constant stress layer $[(\overline{uv})^2 + (\overline{uw})^2]^{1/2}/U_*^2 \approx 1$ should still exist in the presence of weak to moderate secondary flows.

The need presently exists for additional corner-flow data which can provide a more stringent test of three-dimensional predictive codes. These data include global data referred to adverse-pressure-gradient flow conditions when the flow is detached locally in the corner region but remains attached elsewhere. More comprehensive data referred to the near-wall structure of the flow are also needed. In particular, near-wall data in ducts with various types of wall roughness for zero, favorable, and adverse-pressure-gradient flow conditions would be desirable. This information is particularly important if the effects of the prescribed turbulence model are to be isolated from the influence of the specified wall functions when comparisons between predictions and measurements are made.

*[Ed.: These data have been put on tape and are accessible in machine-readable form; see paper on Data Library by B. J. Cantwell.]

REFERENCES

- Beavers, G. S., E. M. Sparrow, and R. A. Magnuson (1970). "Experiments on hydrodynamically developing flow in rectangular ducts of arbitrary aspect ratio," IJHMT, 13, 689-702.
- Brundrett, E. (1963). "The production and diffusion of vorticity in channel flow," Report UT Mech E TP6302, Mech. Eng. Dept., University of Toronto (see also J. Fluid Mech., 19, Part 3, 375-394, 1964).
- Dean, R. B. (1974). "An experimental investigation of shear layer interaction in ducts and diffusers," Ph.D. Thesis, University of London.
- Emery, A. F., P. K. Neighbors, and F. B. Gessner (1980). "The numerical prediction of developing turbulent flow and heat transfer in a square duct, J. Heat Transfer, Trans. ASME, 102, 51-57.
- Eppich, H. M. (1980). "Development of a pressure-strain model for turbulent flow along a streamwise corner," M.S. Thesis, Mech. Eng. Dept., University of Washington (in preparation).
- Fujita, H. (1978). "Turbulent flows in square ducts consisting of smooth and rough wall planes," Research Report of the Faculty of Engineering, Vol. 3, Mie University, pp. 11-15.
- Gessner, F. B. (1979). "Corner flow data evaluation," Preliminary Report, Mech. Eng. Dept., University of Washington.
- Gessner, F. B. (1980). "Corner flow data evaluation," Final Report, Mech. Eng. Dept., University of Washington.
- Gessner, F. B., J. K. Po, and A. F. Emery (1979). "Measurements of developing turbulent flow in a square duct," Turbulent Shear Flows, Vol. I, F. Durst et al., eds., Springer-Verlag, New York, pp. 119-136.
- Gessner, F. B., and A. F. Emery (1979). "The numerical prediction of developing turbulent flow in rectangular ducts," Symposium on Turbulent Shear Flows, Vol. II, Imperial College, London, pp. 17.1-17.6.
- Goldstein, R. J., and D. K. Kreid (1967). "Measurement of laminar flow development in a square duct using a laser-Doppler flowmeter," ASME, J. Appl. Mech., 34, 813-818.
- Hinze, J. O. (1971). "Experimental investigations on secondary currents in the turbulent flow through a straight conduit," Report WTHD 27, Laboratory for Aero- and Hydrodynamics, Delft University of Technology (also available as NBS No. N73-14279).
- Hinze, J. O. (1973). "Experimental investigation on secondary currents in the turbulent flow through a straight conduit," Appl. Sci. Res., 28, 453-465.
- Hoagland, L. C. (1960). "Fully developed turbulent flow in straight rectangular ducts--secondary flow, its cause and effect on the primary flow," Ph.D. Thesis, Mech. Eng. Dept., M.I.T.
- Humphrey, J. A. C. (1977). "Flow in ducts with curvature and roughness," Ph.D. Thesis, University of London (see also Symposium on Turbulent Shear Flows, Vol. II, Imperial College, London, 1979, pp. 17.7-17.12).

- Launders, B. E., and W. M. Ying (1971). "Fully developed turbulent flow in ducts of square cross section," Report TM/TN/A/11, Mech. Eng. Dept., Imperial College of Science and Technology, London (see also J. Fluid Mech., 54, Part 2, 289-295, 1972).
- Leutheusser, H. J. (1961). "The effect of cross-section geometry upon the resistance to flow in conduits," Ph.D. Thesis, Mech. Eng. Dept., University of Toronto (see also J. ASCE, Hydraulics Div., 89(HY3), 1-19, 1963).
- Lund, E. G. (1977). "Mean flow and turbulence characteristics in the near corner region of a square duct," M.S. Thesis, Mech. Eng. Dept., University of Washington.
- Melling, A. (1975). "Investigation of flow in non-circular ducts and other configurations by laser Doppler anemometry," Ph.D. Thesis, University of London (see also J. Fluid Mech., 78, Part 2, 289-315, 1976).
- Po, J. K. (1975). "Developing turbulent flow in the entrance region of a square duct," M.S. Thesis, Mech. Eng. Dept., University of Washington.

DISCUSSION

FLOW 0110

1. The main criticism of the flow specifications was whether it was desirable for conditions to be specified along the first mesh line adjacent to the wall. Empirical wall functions were to be given to do this, which involved changing the wall-function constants from those applicable to the flat-plate boundary layer.
2. The argument for this approach was that it was more economical in computing time than having many grid points very close to the wall, particularly if the method were to be extended to other types of three-dimensional flows, and so, from the engineering point of view, more useful. The counter argument was that, if a method is to be truly predictive, the computation should start at the wall itself; and if a modified law of the wall and wall functions are required to get to the first mesh line adjacent to the wall, such relationships should not be specific to the case in hand.*
3. The consensus was that F. Gessner's wall-function constants may be used by computers as a guide but cannot specifically be used in an algorithm unless the algorithm uses the same constants from case to case.
4. It was suggested by D. Wilcox that use of a systematic perturbation analysis upon the flat-plate wall function might be used to get around this problem. The question arose as to how k should be regarded, whether as a true turbulence kinetic energy or simply as a turbulence velocity scale used merely as a calculation convenience, and computers are asked to say how they regard k if they use a k - ϵ model.

*[Ed.: Gessner has modified the specification to reflect this recommendation.]

SPECIFICATIONS FOR COMPUTATION

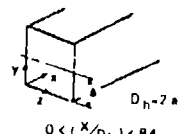
ENTRY CASE/INCOMPRESSIBLE

Case #0111; Data Evaluator: F. B. Gessner

Data Takers: J. Po (and others)

PICTORIAL SUMMARY

Flow 0110. Data Evaluator: F. Gessner. "Corner Flow (Secondary Flow of the Second Kind)."

Case Data Taker	Test Rig Geometry	dp/dx or C _p	Number of Stations Measured							C _f	Re	Initial Condi- tion	Other Notes
			Mean Velocity		Turbulence Profiles								
			U	V or W	$\overline{u^2}$	$\overline{v^2}$	$\overline{w^2}$	\overline{uv}	Others				
Case 0111 J. Po S. Lund F. Gessner	 D _h =2a 0 < x/D _h < 84	34 sta- tions on walls A and B	17	5	-	-	-	3 UV and VW	3 pro- files of K	1	2.5 × 10 ⁵ (based on bulk velocity and U _b)	sym- metric inlet flow	C _p vs x data for laminar flow (Beavers, Goldstein) included with data file. Goldstein's laminar velocity data also included. Nominally uniform, low turbulence level flow at inlet (x/D _h = 0).

Plot	Ordinate	Abscissa	Range/Position	Comments
1	C _p	x/D _h	$0 \leq x/D_h \leq 90$	Axial static pressure distribution
2	U/U _b	x/D _h	$0 \leq x/D_h \leq 90$	4 curves at y/a = 0.02, 0.04, 0.06, 0.10.
3	U/U _b	x/D _h	$0 \leq x/D_h \leq 90$	4 curves at y/a = 0.2, 0.4, 0.6, 1.0.
4	U/U _b	x/D _h	$0 \leq x/D_h \leq 90$	4 curves at y'/a' = 0.02, 0.04, 0.06, 0.10.
5	U/U _b	x/D _h	$0 \leq x/D_h \leq 90$	4 curves at y'/a' = 0.2, 0.4, 0.6, 1.0.
6	V/U _b	y/a	$0 \leq y/a \leq 1$	2 curves at x/D _h = 40, 84.
7	V'/U _b	y'/a'	$0 \leq y'/a' \leq 1$	2 curves at x/D _h = 40, 84.
8	τ_w/τ_w	y/a	$0 \leq y/a \leq 1$	Wall shear stress profile at x/D _h = 84.
9	y/a	z/a	$0 \leq y/a \leq 1$ $0 \leq z/a \leq 1$ x/D _h = 8	5 contours for U/U _c = 0.7, 0.8, 0.85, 0.9, 0.95. See comment 4b; use of symmetry along corner bisector permissible.
10	y/a	z/a	$0 \leq y/a \leq 1$ $0 \leq z/a \leq 1$ x/D _h = 16	5 contours for U/U _c = 0.7, 0.8, 0.85, 0.9, 0.95.

Plot	Ordinate	Abcissa	Range/Position	Comments
11	y/a	z/a	$0 \leq y/a \leq 1$ $0 \leq z/a \leq 1$ $x/D_h = 24$	5 contours for $U/U_c = 0.7$, 0.8, 0.85, 0.9, 0.95.
12	y/a	z/a	$0 \leq y/a \leq 1$ $0 \leq z/a \leq 1$ $x/D_h = 40$	5 contours for $U/U_c = 0.7$, 0.8, 0.85, 0.9, 0.95.
13	y/a	z/a	$0 \leq y/a \leq 1$ $0 \leq z/a \leq 1$ $x/D_h = 84$	5 contours for $U/U_c = 0.7$, 0.8, 0.85, 0.9, 0.95.
14	y/a	z/a	$0 \leq y/a \leq 1$ $0 \leq z/a \leq 1$ $x/D_h = 24$	6 contours for $-\overline{uv}/U_b^2 = 2$, 4, 6, 8, 12, 16 (all $\times 10^4$).
15	y/a	z/a	$0 \leq y/a \leq 1$ $0 \leq z/a \leq 1$ $x/D_h = 24$	7 contours for $K/U_b^2 = 10, 20$, 30, 40, 50, 60, 70 (all $\times 10^4$).
16	y/a	z/a	$0 \leq y/a \leq 1$ $0 \leq z/a \leq 1$ $x/D_h = 40$	7 contours for $-\overline{uv}/U_b^2 = 2$, 4, 6, 8, 12, 16, 20 (all $\times 10^4$).
17	y/a	z/a	$0 \leq y/a \leq 1$ $0 \leq z/a \leq 1$ $x/D_h = 40$	7 contours for $K/U_b^2 = 20, 30$, 40, 50, 60, 70, 80 (all $\times 10^4$).
18	y/a	z/a	$0 \leq y/a \leq 1$ $0 \leq z/a \leq 1$ $x/D_h = 84$	10 contours for $-\overline{uv}/U_b^2 = -3$, -2, -1, 0, 2, 4, 6, 8, 12, 16 (all $\times 10^4$).
19	y/a	z/a	$0 \leq y/a \leq 1$ $0 \leq z/a \leq 1$ $x/D_h = 84$	6 contours for $K/U_b^2 = 20, 30$, 40, 50, 60, 70 (all $\times 10^4$).

Special Instructions:

1. For notation see Fig. 1 below. Note that two coordinates are used.

2. General Features

This test case is concerned with turbulent flow in a constant-area square duct which develops ideally from a zero-turbulence level, uniform mean flow at the duct inlet ($U = U_b$, $V = W = 0$), as shown in Fig. 1. The bulk Reynolds number may be

regarded as being sufficiently high to initiate turbulent boundary-layer development at the duct inlet ($x/D_h = 0$). A unique feature of this flow is the streamwise development of two secondary-flow cells in each quadrant which are centered about the corner bisector (the dashed-line distributions in Fig. 1). These cells correspond to a flow pattern formed by the vector sum of the transverse mean-velocity components (V and W) which can be regarded as being superimposed upon the primary mean flow. The formation of these cells is the direct result of Reynolds-stress gradients acting in the corner region which are not present in two-dimensional boundary-layer flows.

3. Optional Laminar Flow Predictions

In order to aid the development of an appropriate predictive code, it is recommended that initial comparisons be made with data obtained under laminar flow conditions. Two data sets suitable for this purpose include axial static-pressure profiles measured by Beavers et al. (1970) and mean-velocity profiles measured by Goldstein and Kreid (1967) for developing laminar flow in a square duct. These data are available in tabulated form (Gessner, 1980).^{*} Separate plots should be made in accordance with the listings below:

Plot	Variables	Range	Scale
1. Axial static	C_p (ordinate) $(x/D_h)/Re_b$ (abscissa)	0 to 6 0 to 8×10^{-2}	1 cm = 0.5 1 cm = 5×10^{-3}
2. Axial centerline velocity distribution	U_o/U_b (ordinate) $(x/D_h)/Re_b$ (abscissa)	1 to 2.2 0 to 18×10^{-2}	1 cm = 0.1 1 cm = 1×10^{-2}
3. Wall bisector velocity profiles [†]	U/U_b (ordinate) y/a (abscissa)	0.4 to 2.4 0 to 1	1 cm = 0.2 1 cm = 0.1
4. Corner bisector velocity profiles [†]	U/U_b (ordinate) y'/a' (abscissa)	0.4 to 2.4 0 to 1	1 cm = 0.2 1 cm = 0.1

Turbulent Flow Predictions

4. a. Specification of Boundary Conditions

In order to compute local flow development from an initially uniform state ($x/D_h = 0$) to a location where the mean flow is nominally fully developed ($x/D_h = 84$), it is expedient to use empirical wall functions to minimize computational times. For two-dimensional predictive codes which employ the $K-\epsilon$ model,

^{*}[Ed.: The computation of the laminar case is optional; plots are not supplied.]

[†]Comparisons are to be made with profiles measured at $(x/D_h)/Re_b = 0.0075$, 0.020, and 0.15 (fully developed flow).

the following conditions are often specified along the first mesh line adjacent to a bounding wall namely

$$\frac{U}{U_*} = \frac{1}{\kappa} \ln \frac{yU_*}{\nu} + C \quad (1)$$

$$\frac{K}{U_*^2} = \frac{1}{C_\mu^{1/2}} \quad (2)$$

$$\frac{\epsilon y}{U_*^3} = \frac{1}{\kappa_1} \quad (3)$$

where κ , κ_1 , C , and C_μ are prescribed constants with $\kappa \equiv \kappa_1$ for two-dimensional flows. In the past, some computers have made K- ϵ type predictions of developing turbulent flow in a square duct by applying Eqs. (1)-(3) in a given transverse plane along the first mesh line (say, $y = \text{constant}$) between the corner bisector ($z = y$) and the wall bisector ($z = a$) at each streamwise location. The purpose of this section is to note that although Eq. (1) is fitted well by near-wall data, K/U_*^2 and $\epsilon y/U_*^3$ vary in the near-wall region, so that Eqs. (2) and (3) do not appear to be satisfied when C_μ and κ_1 are prescribed as constants.

At the Reynolds number of interest (2.5×10^5) and at a streamwise location where the mean flow is nominally fully developed ($x/D_h \sim 84$), data obtained by Lund (1977) show that Eq. (1) is a good approximation at all z -locations within the interval $0.01 \leq z/a \leq 1.0$ (with $\kappa = 0.40$ and $C = 5.2$), provided that y^+ lies between 40 and 200 ($0.01 \leq y/a \leq 0.04$). In the y^+ interval between 200 and 500 ($0.04 \leq y/a \leq 0.1$), the law-of-the-wall is still a good approximation, although profiles in this region exhibit slight wake-like behavior. Within this same overall region, however, recent measurements by Eppich (1980) show that consistent variations in K/U_*^2 occur and that apparent variations in $\epsilon y/U_*^3$ exist when the dissipation rate is modeled by equating it to the turbulence kinetic-energy production rate. These variations are summarized in the table below:

Variable	y/a	y^+	z/a					
			0.02	0.05	0.10	0.20	0.60	1.00
$\left(\frac{K}{U_*^2}\right)^{-2}$	0.02	~ 100	0.081	0.075	0.069	0.066	0.059	0.051
	0.05	~ 250	-	0.095	0.090	0.073	0.068	0.058
	0.10	~ 500	-	-	0.115	0.106	0.084	0.064
$\left(\frac{\epsilon y}{U_*^3}\right)^{-1}$	0.02	~ 100	0.40	0.31	0.34	0.37	0.41	0.41
	0.05	~ 250	-	0.31	0.32	0.31	0.38	0.37
	0.10	~ 500	-	-	0.43	0.37	0.40	0.39

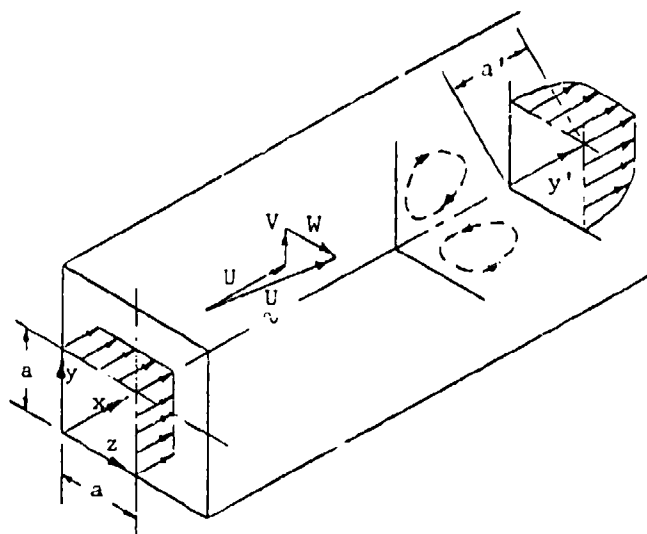
The trends exhibited by the $(K/U_*^2)^{-2}$ values in the above table are also present when $Re_b = 1.2 \times 10^5$ (Eppich, 1980), which lends support to the observed decrease in values between the corner and wall bisectors when y is fixed, or at a given z -location as the wall is approached. The observed spanwise variations in $(\epsilon y/U_*^3)^{-1}$ at a given y -location also exist at this lower Reynolds number.

On the basis of these results, it appears that prescribed constant values for C_μ and κ_1 in Eqs. (2) and (3) are not in accord with reality. If predictions based on constant values of C_μ and κ_1 are made, discrepancies between predictions and experiment in the near-wall region may be due primarily to improperly specified wall functions, rather than deficiencies in the $K-\epsilon$ model itself. If this model is employed, transverse gradients of U , K , and ϵ may be set equal to zero on lines of symmetry ($y/a = 1$ and $z/a = 1$) without reservation. The proper starting conditions consists of letting $U = U_b$, $V = W = 0$, and $K = \epsilon = 0$ at $x/D_h = 0$.

b. Flow in an Octant: Plots 9 through 22

Because $\overline{UV}(y_1, z_1) = \overline{UW}$, ($y = z_1$, $z = y_1$) by virtue of image reflection about the corner bisector, isocontours of \overline{UV} in the region $0 \leq y/a \leq 1$, $0 \leq z/a \leq 1$ completely define the primary shear-stress field. Although global information on the secondary flow field in the developing flow region is not available from the present measurements, it is recommended that the plotting of predicted results include secondary-flow velocity vectors plotted in the octant of the flow at various streamwise locations. [The computations of Emery et al. (1980) show that only a single cell should develop in each octant.]

The isocontour plots are intended to compare predicted and measured results in: (i) a region where the wall boundary layers have not yet merged ($x/D_h = 8, 16, 24$); (ii) in the shear-layer interaction region where the axial centerline velocity peaks ($x/D_h = 40$); and (iii) at a location where the mean flow is nominally fully developed ($x/D_h = 84$).



Duct Dimensions

$a = 12.7 \text{ cm (5.000 in.)}$

$(x/D_h)_{\max} = 84$

Operating Conditions

$U_b = 15.2 \text{ mps (50.0 fps)}$

$Re_b = 2.5 \times 10^5$

Symbol Definitions

a = duct half width

a' = diagonal half width ($a' = \sqrt{2} a$)

C_p = pressure coefficient

$$(C_p \equiv [P(0) - P]/(1/2 \rho U_b^2))$$

D_h = duct hydraulic diameter ($D_h \equiv 2a$)

K = turbulence kinetic energy

P = mean static pressure

$P(0)$ = mean static pressure at $x = 0$

Re_b = bulk Reynolds number

$$(Re_b \equiv U_b D_h / \nu)$$

u, v, w = fluctuating velocity components in x -, y -, and z -directions, respectively

U, V, W = mean velocity components in x -, y -, and z -directions, respectively

U_b = bulk velocity

U_c = axial centerline velocity

U_\star = friction velocity ($U_\star = \sqrt{\tau_w / \rho}$)

V' = mean velocity component in y' -direction

x, y, z = cartesian coordinates

y' = diagonal coordinate

y^+ = dimensionless coordinate
($y^+ \equiv y U_\star / \nu$)

ϵ = dissipation rate

ν = kinematic viscosity

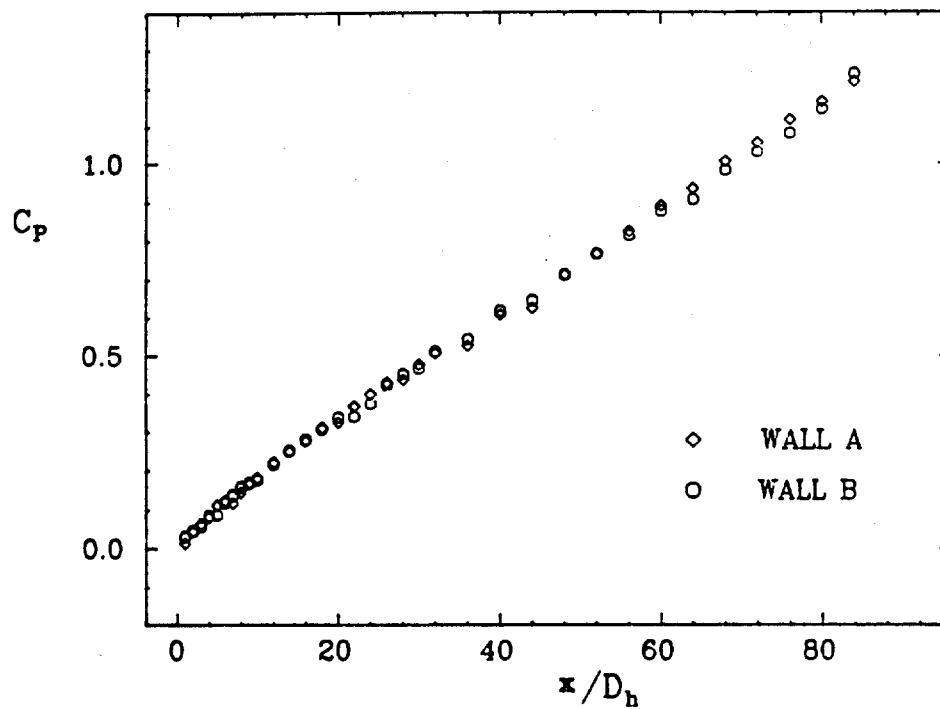
ρ = fluid density

τ_w = local wall shear stress

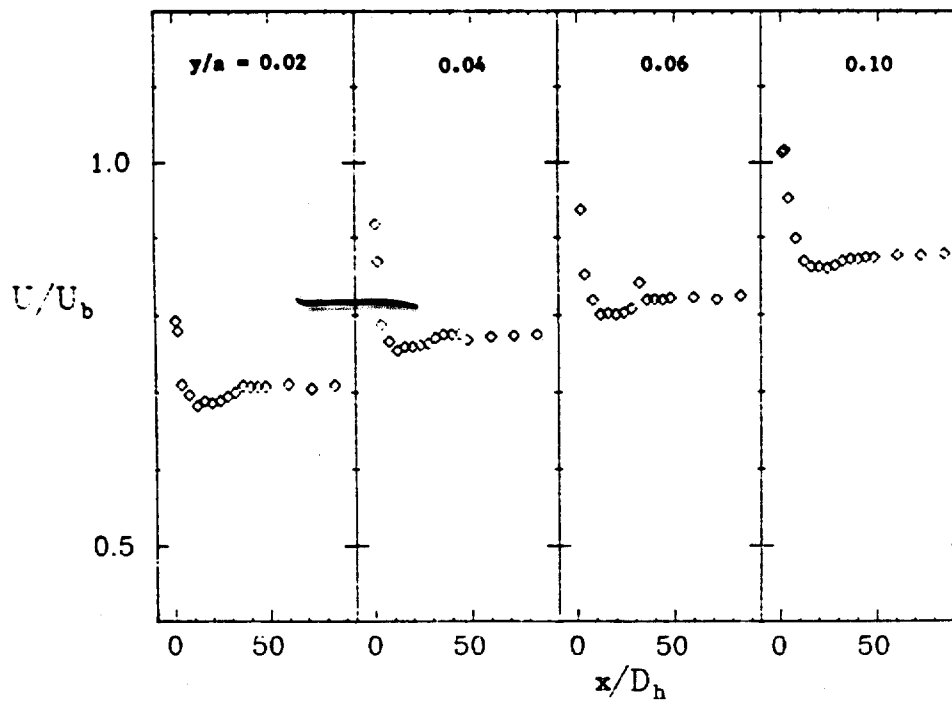
$\bar{\tau}_w$ = spanwise averaged value of τ_w

Figure 1. Duct dimensions, operating conditions, and symbol definitions, Case 0111.

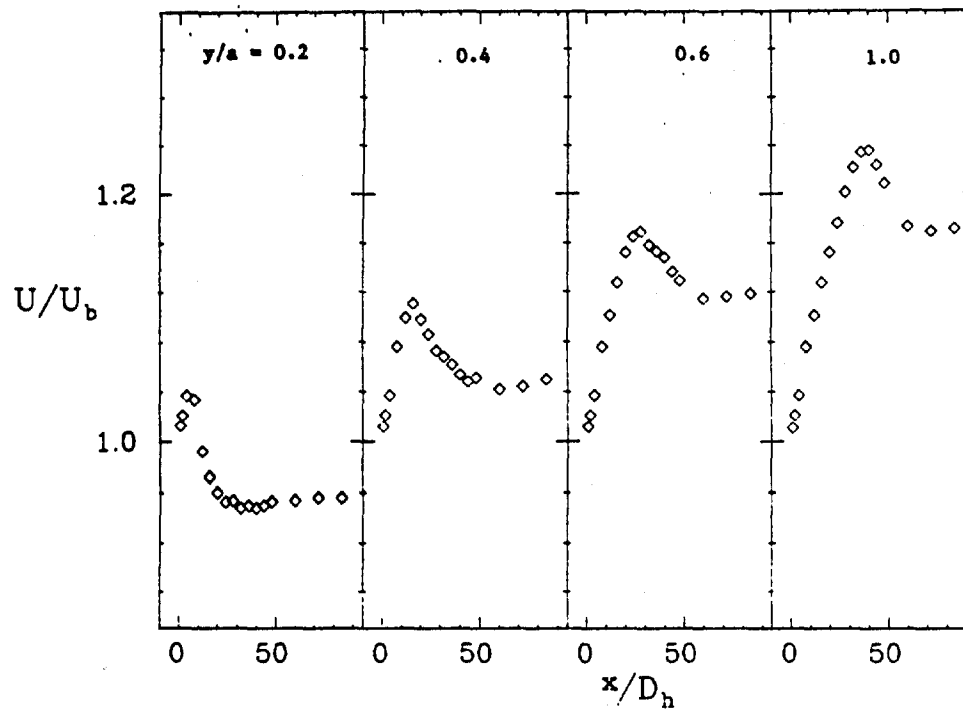
PLOT 1 CASE 0111 FILE 7



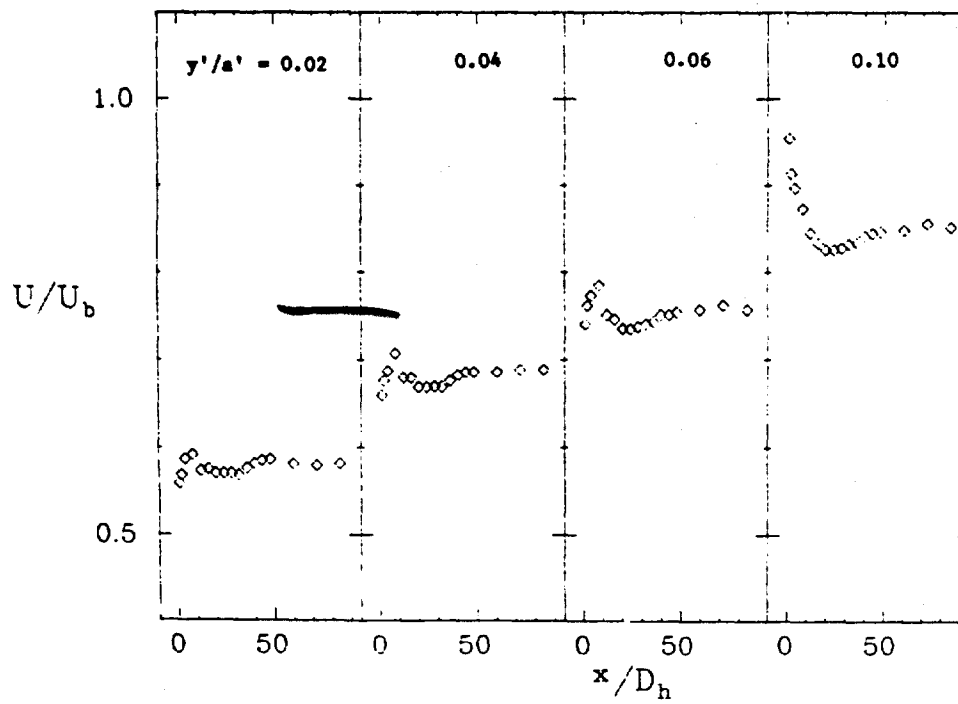
PLOT 2 CASE 0111 FILE 8



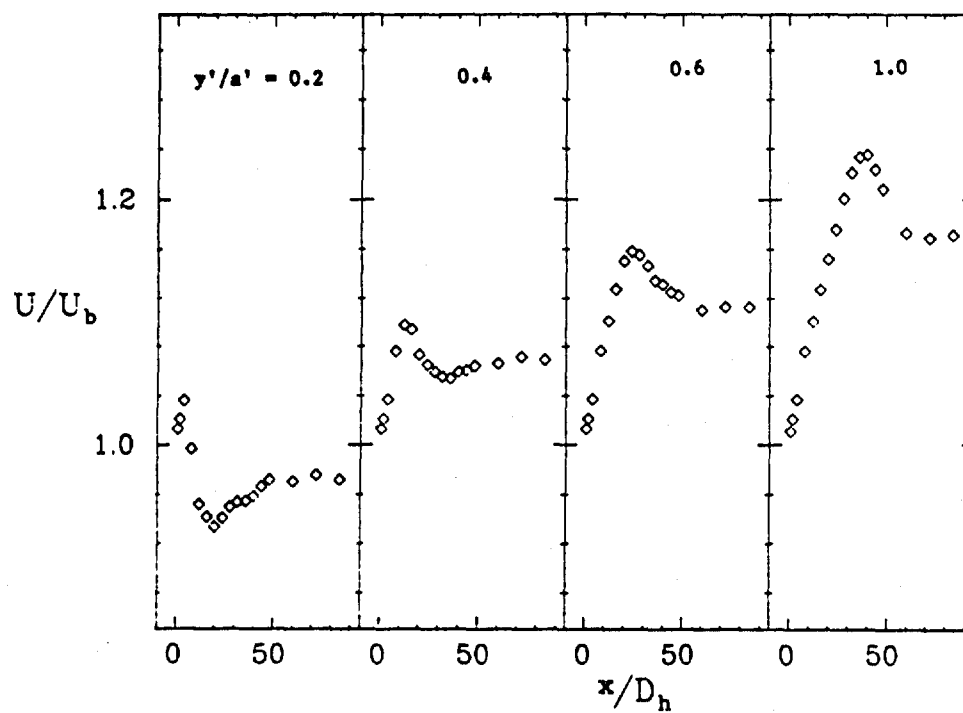
PLOT 3 CASE 0111 FILE 8



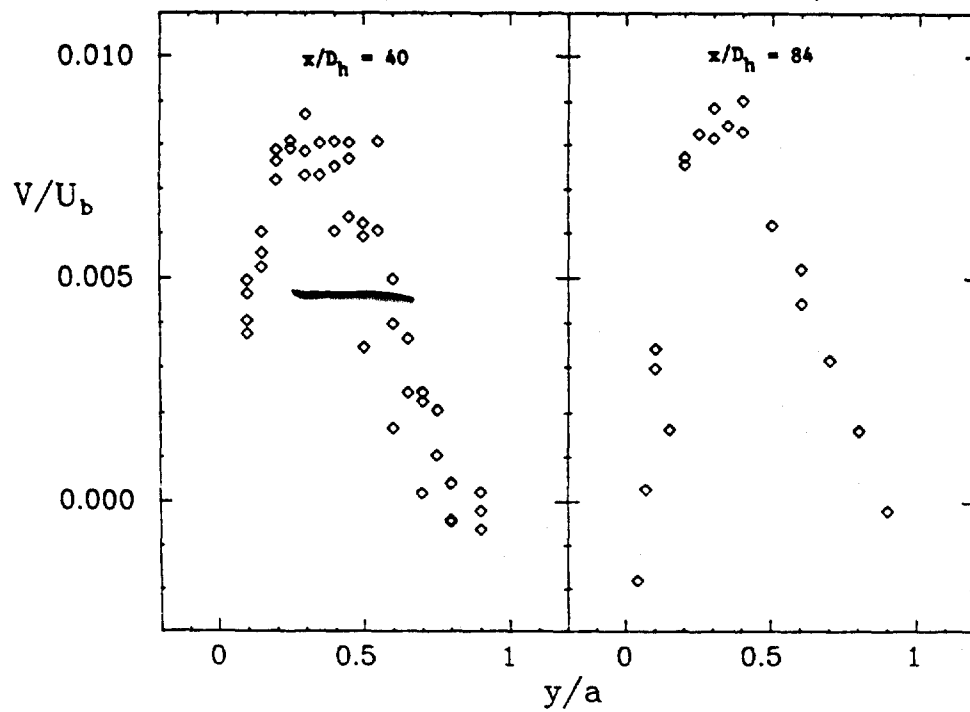
PLOT 4 CASE 0111 FILE 9



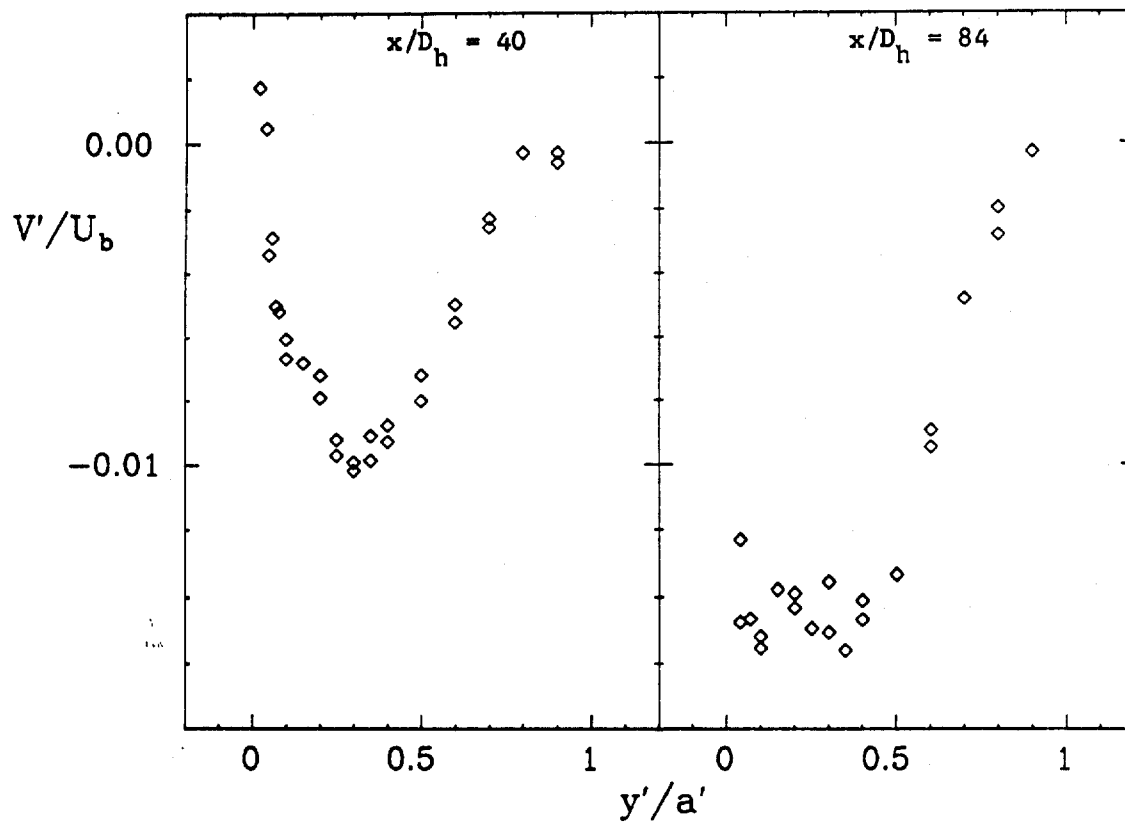
PLOT 5 CASE 0111 FILE 9



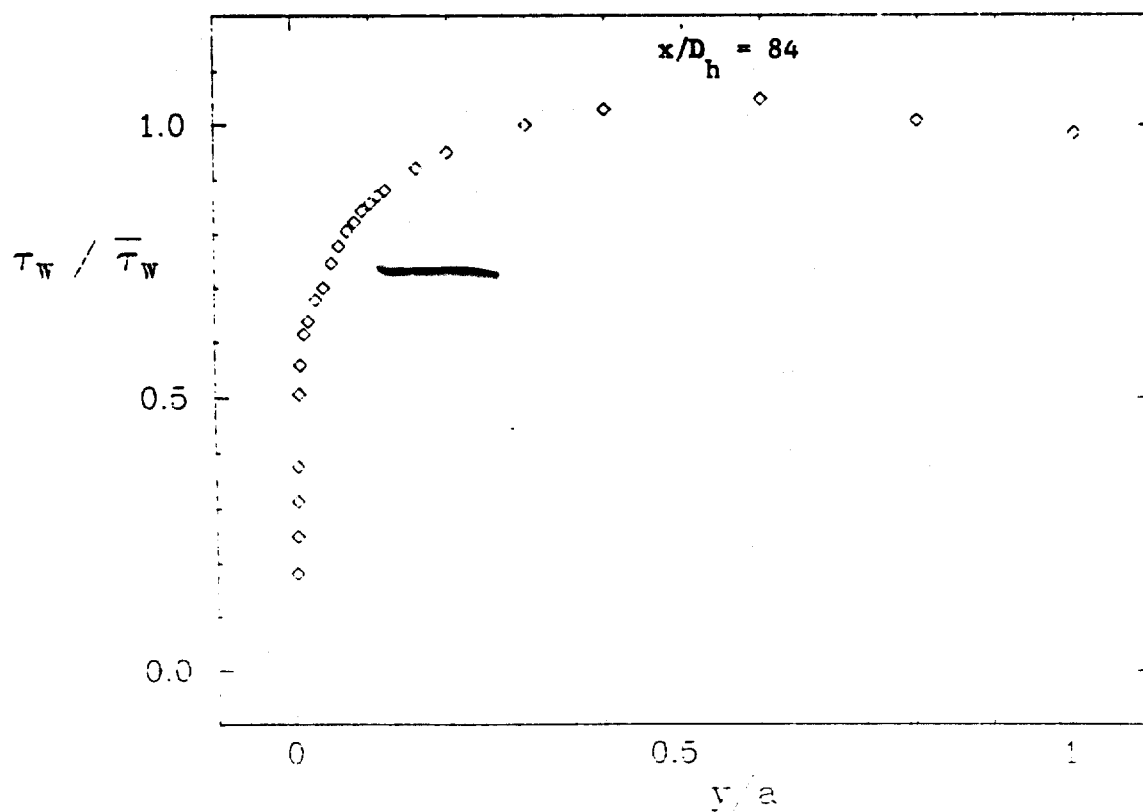
PLOT 6 CASE 0111 FILES 10,12



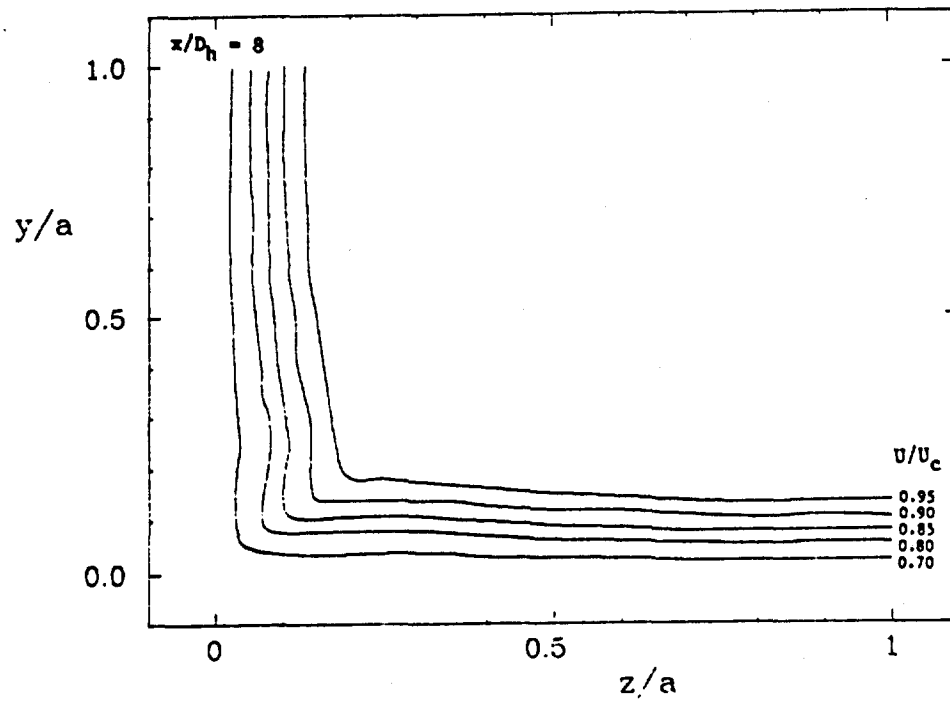
PLOT 7 CASE 0111 FILES 11,12



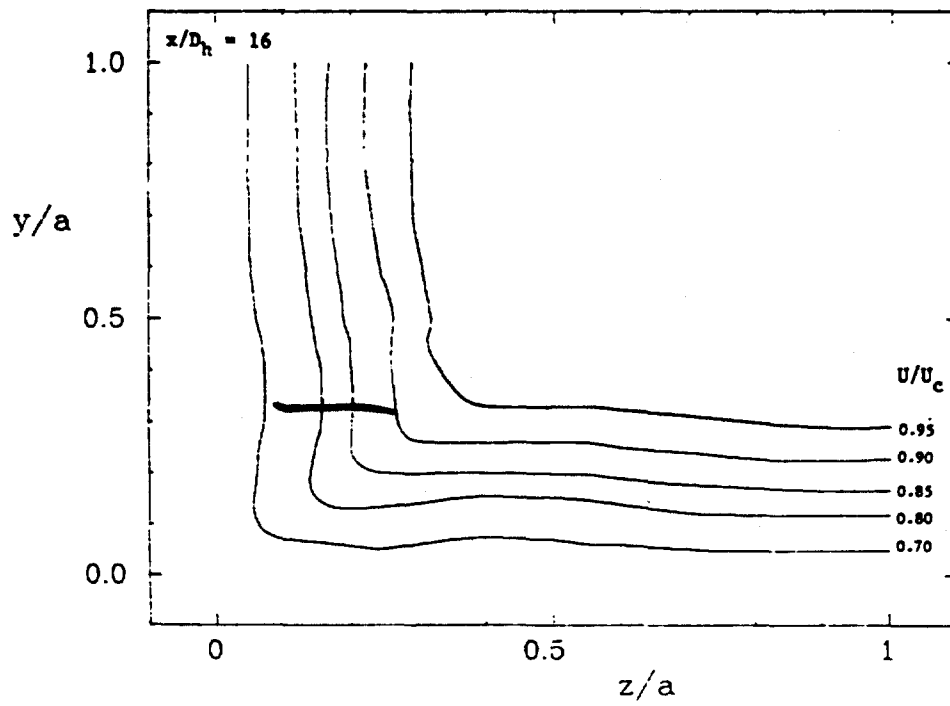
PLOT 8 CASE 0111 FILE 13



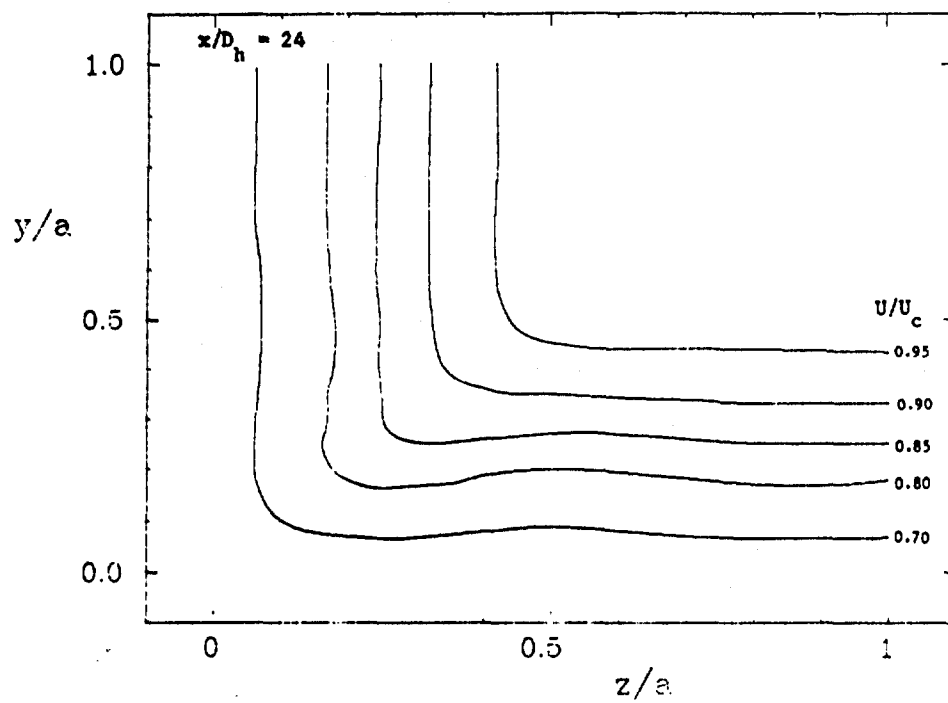
PLOT 9 CASE 0111 FILE 14



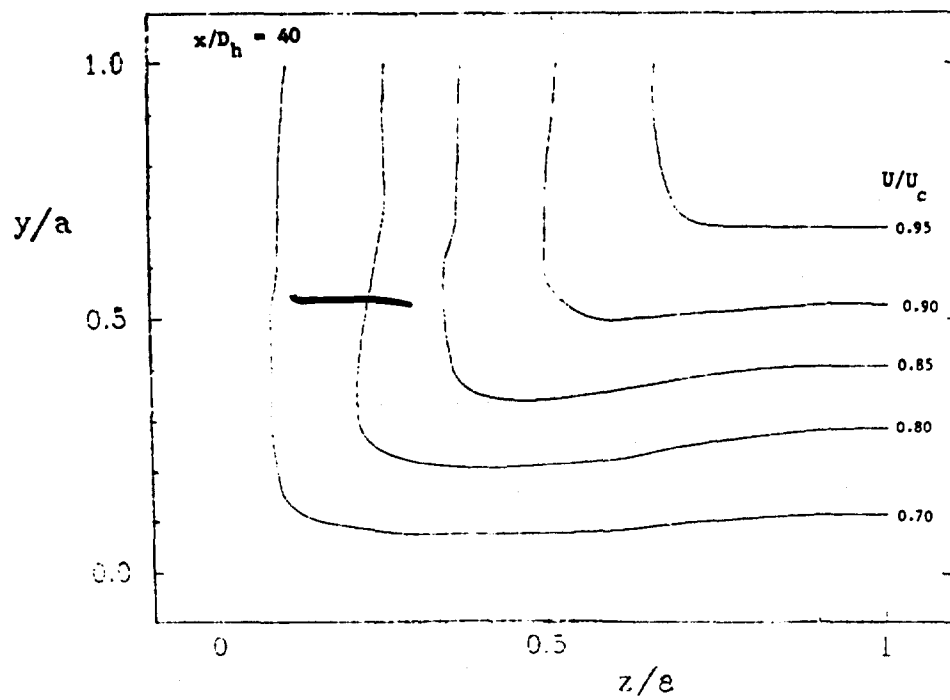
PLOT 10 CASE 0111 FILE 15



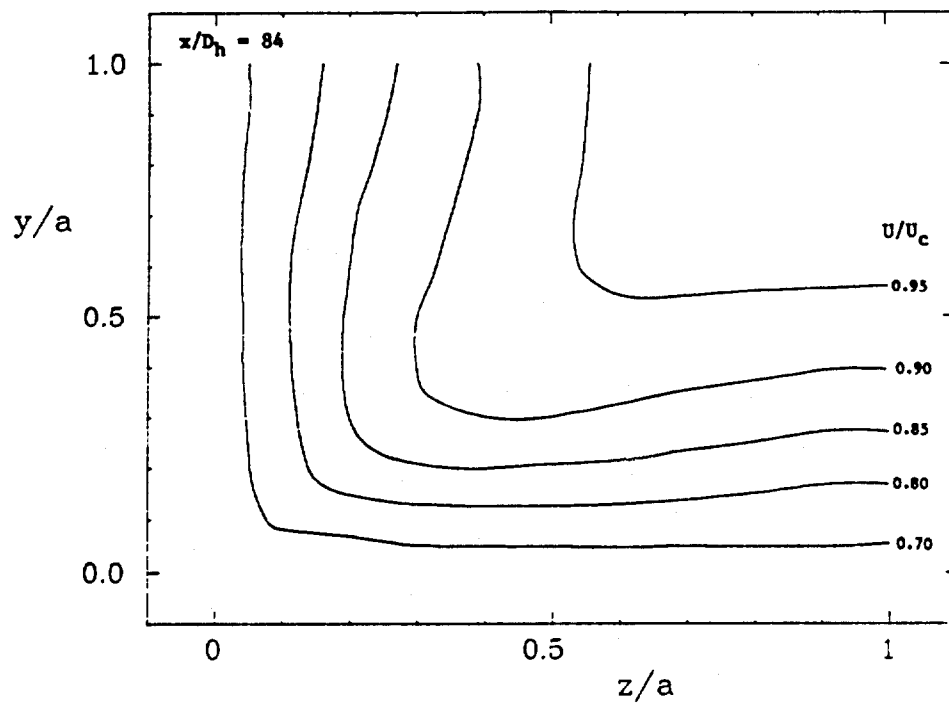
PLOT 11 CASE 0111 FILE 16



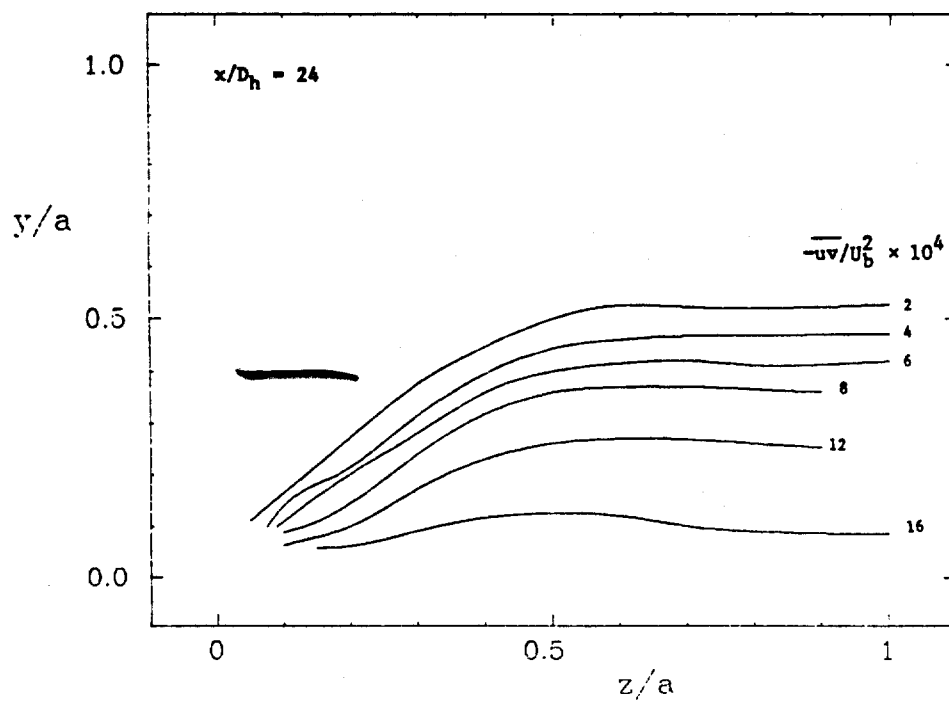
PLOT 12 CASE 0111 FILE 17



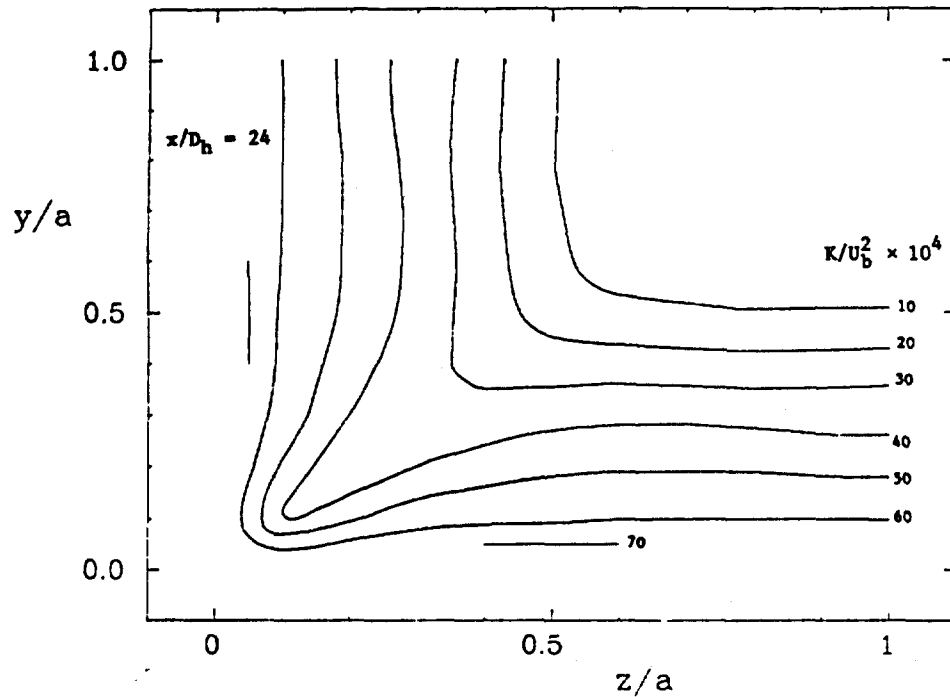
PLOT 13 CASE 0111 FILE 18



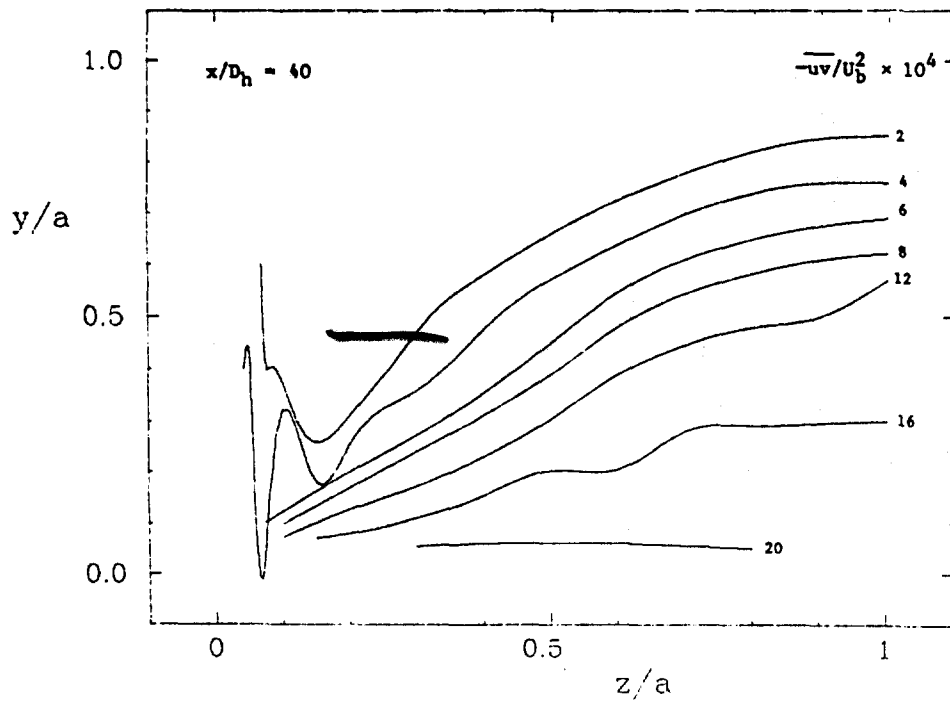
PLOT 14 CASE 0111 FILE 19



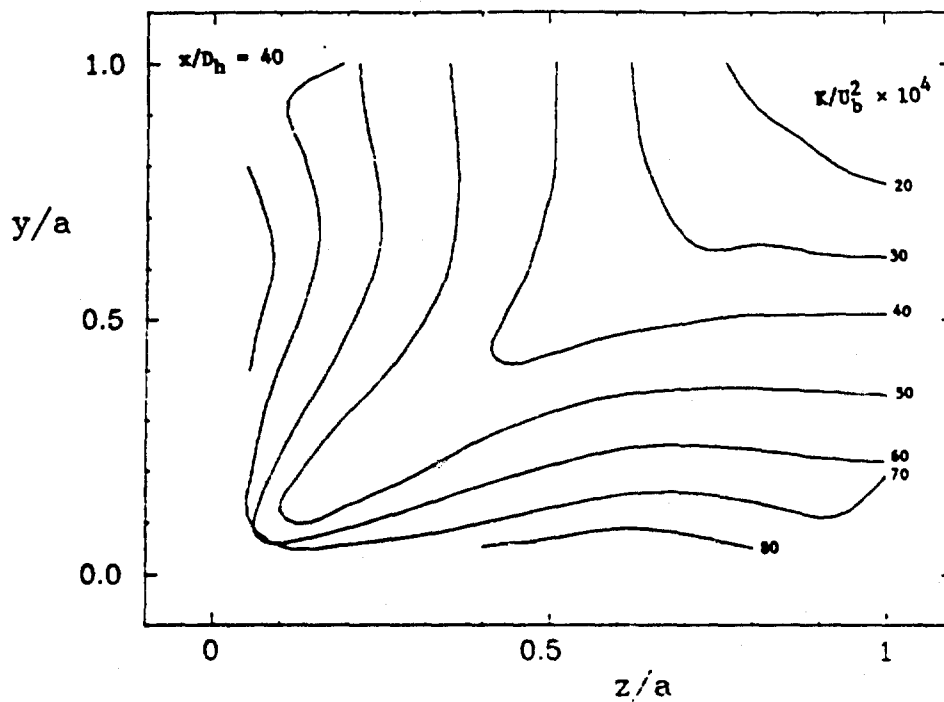
PLOT 15 CASE 0111 FILES 20,21



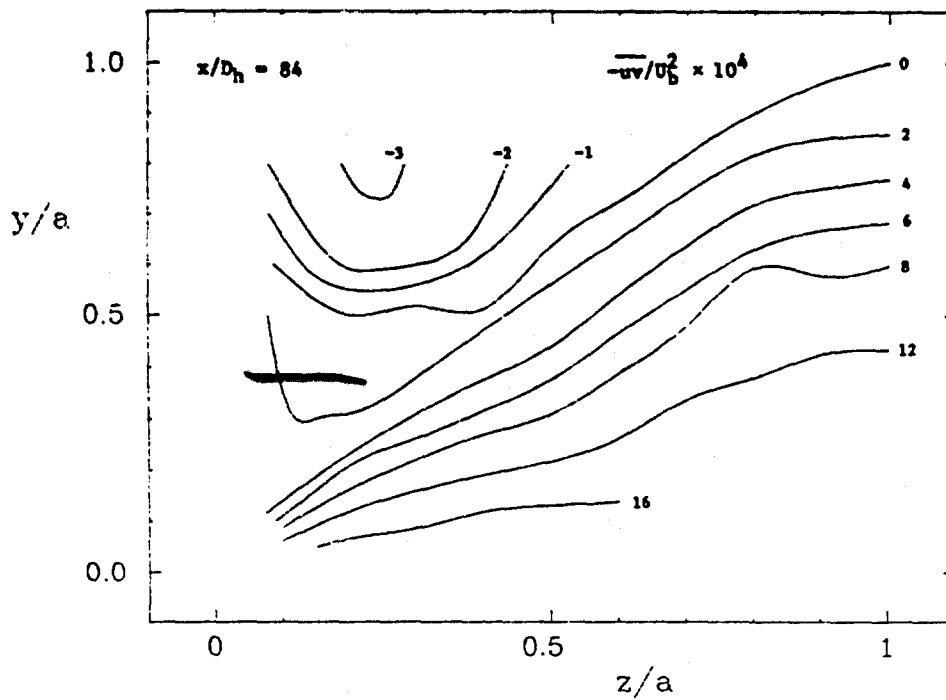
PLOT 16 CASE 0111 FILES 22,23



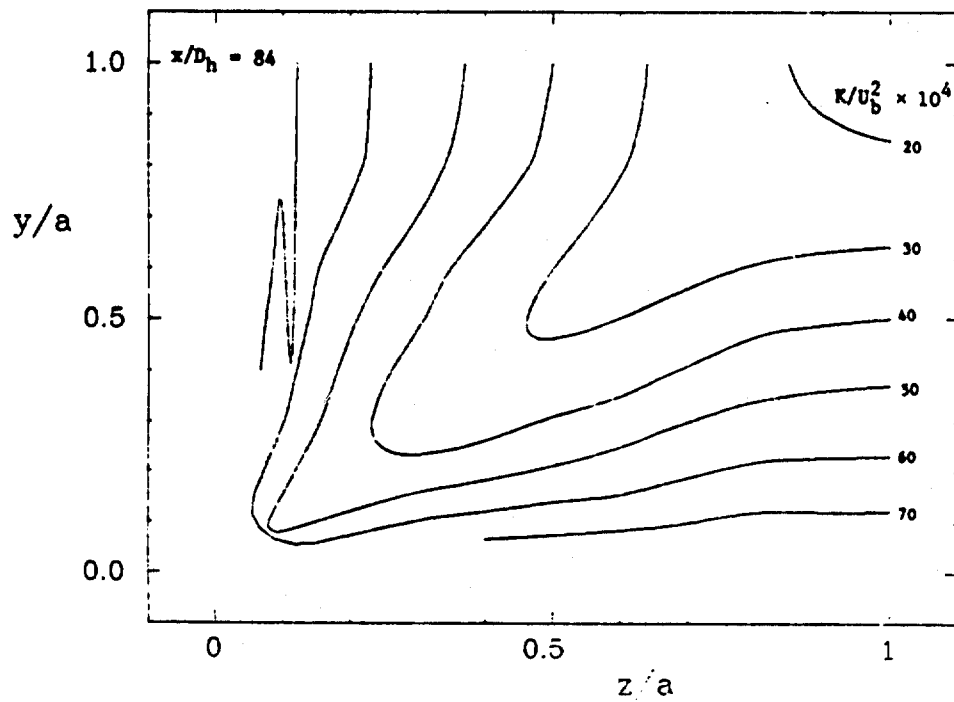
PLOT 17 CASE 0111 FILES 24,25



PLOT 18 CASE 0111 FILES 26,27



PLOT 19 CASE 0111 FILE 28



SPECIFICATIONS FOR COMPUTATION

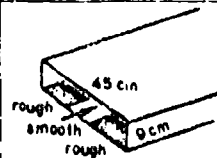
ENTRY CASE/INCOMPRESSIBLE

Case #0112; Data Evaluator: F. R. Gessner

Data Taker: J. Hinze

PICTORIAL SUMMARY

Flow 0110. Data Evaluator: F. Gessner. "Corner Flow (Secondary Flow of the Second Kind)."

Case Data Taker	Test Rig Geometry	$\frac{dp}{dx}$ $\frac{cc}{L}$	Number of Stations Measured								C_f	Re	Initial Condition	Other Notes
			Mean Velocity		Turbulence Profiles									
			U	V or W	$\overline{u^2}$	$\overline{v^2}$	$\overline{w^2}$	\overline{uv}	Others					
Case 0112 J. Hinze			1		1	1	1	1		1	1.5×10^5 (based on hy- draulic diam and U_{max})	One wall rough with smooth center- strip	All measurements were made at $x/D_h = 126$. Data include viscous dissipation.	

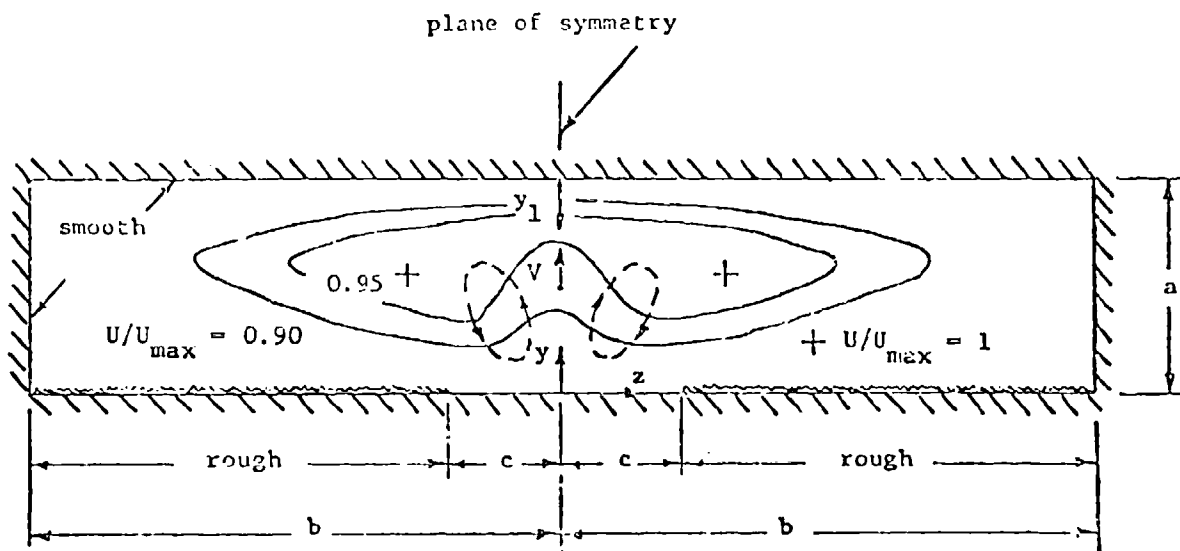
Plot	Ordinate	Abcissa	Range/Position	Comments
1	y/a	z/a	$0 \leq z/a \leq 2.45$ $0 \leq y/a \leq 1$	5 contours for $U/U_{max} = 0.70, 0.80, 0.85, 0.90, 0.95$.
2	y/a	$U/U_{max,0}$	$0 \leq y/a \leq 1$	$z = 0$; $a = 0.092$ m.
3	yU_*/ν y_1U_{1*}/ν	U/U_* U_1/U_{1*}	$20 \leq yU_*/\nu \leq 500$ $30 \leq y_1U_{1*}/\nu \leq 1500$	$z = 0$ $z = 0$ } y, y_1 are defined on Fig. 2 below.
4	y/a	$V/U_{max,0}$	$0 \leq y/a \leq 1$	$z = 0$; $U_{max,0} = 14.4$ m/s.
5	y/a	$(\overline{u^2})^{1/2}/U_{max,0}$	$0 \leq y/a \leq 1$	$z = 0$.
6	y/a	$(\overline{v^2})^{1/2}/U_{max,0}$	$0 \leq y/a \leq 1$	$z = 0$.
7	y/a	$(\overline{w^2})^{1/2}/U_{max,0}$	$0 \leq y/a \leq 1$	$z = 0$.
8	y/a	$-\overline{uv}/U_{max,0}^2$	$0 \leq y/a \leq 1$	$z = 0$.
9	y/a	ϵ (m ² /sec ³)	$0 \leq y/a \leq 1$	$z = 0$.

Special Instructions:

- For notation, see Fig. 2 below; note use of two sets of coordinates.
- All data at $x/D_h = 126$.
- Show on plot for $-\overline{uv}/U_{max,0}^2$ calculated values of U_*^2 at $y/a = 0$ and calculated value of U_{1*}^2 at $y/a = 1$.

5. General Features

This test provides data corresponding to flow in a constant-area rectangular duct with a peripherally non-uniform wall-roughness condition. The roughness elements were plastic grains having average roughness height of 0.004 m. Other pertinent data which define the duct configuration and operating conditions of this study are shown in Fig. 2 below. Inasmuch as all measurements were made at $x/D_h = 126$, where x is measured from the duct entrance, the flow can be regarded as fully developed and independent of inlet flow conditions. The non-uniform wall roughness condition along the lower wall ($y = 0$) gives rise to a fairly strong secondary flow directed away from the wall near the plane of symmetry ($z = 0$). This transverse mean flow appears in the form of two secondary-flow cells in the central portion of the duct (the dashed line distributions in Fig. 2) which distort lines of constant axial mean velocity, as shown in the figure. As a result of this distortion, the maximum velocity does not occur in the plane of symmetry, but instead at the two locations shown in Fig. 2. The data which are available for purposes of comparison include the global variation of lines of constant axial mean velocity, and mean flow and turbulence data along the plane of symmetry. The data also include local friction velocities measured with a Preston tube in the plane of symmetry ($U_{*} = 0.56$ m/s at $y = 0$ and $U_{1*} = 0.69$ m/s at $y_1 = 0$). These data are reported and discussed in two publications by Hinze (1971, 1973).



Duct Dimensions

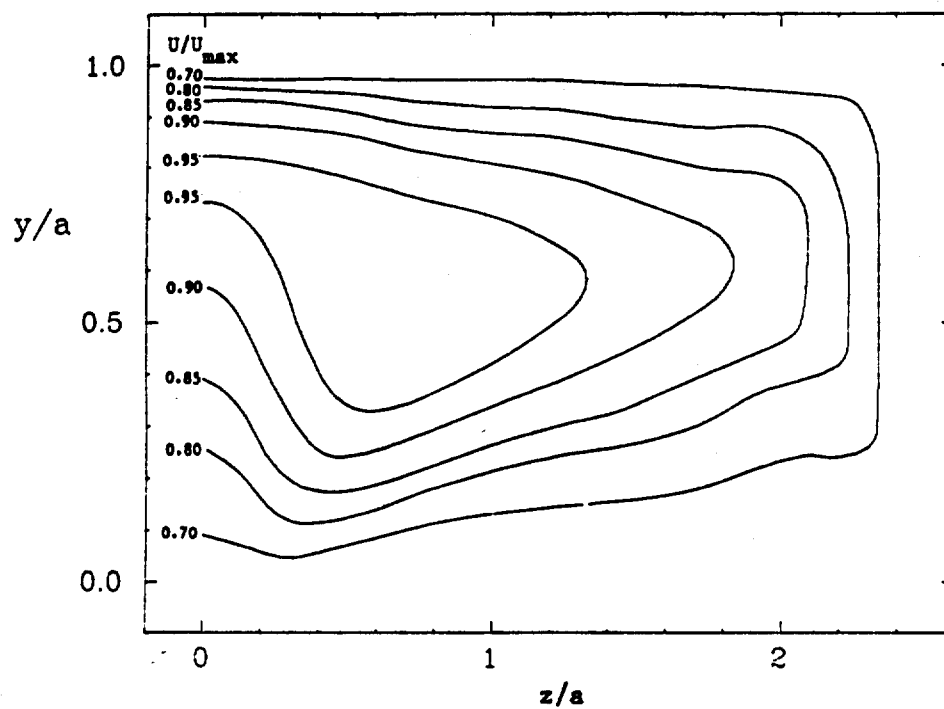
$a = 0.092 \text{ m}$
 $b = 0.225 \text{ m}$
 $c = 0.05 \text{ m}$

Operating Conditions

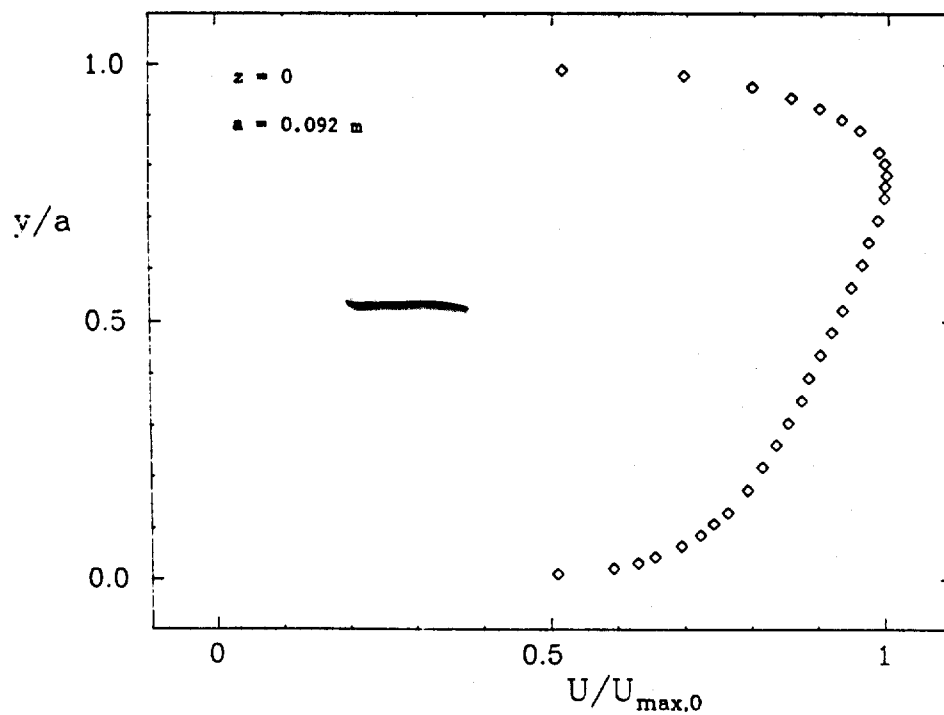
$U_{\max, o} = 14.4 \text{ mps}$ (maximum velocity in plane of symmetry)
 $U_{\max} = 15.0 \text{ mps}$ (maximum velocity in duct cross-section)
 $Re_{\max} \equiv U_{\max} D_h / \nu = 1.5 \times 10^5$
 $U_* = 0.56 \text{ m/s}$ at $y = 0$
 $U_{1*} = 0.69 \text{ m/s}$ at $y = 0$

Figure 2. Details of duct configuration and operating conditions, Case 0112.

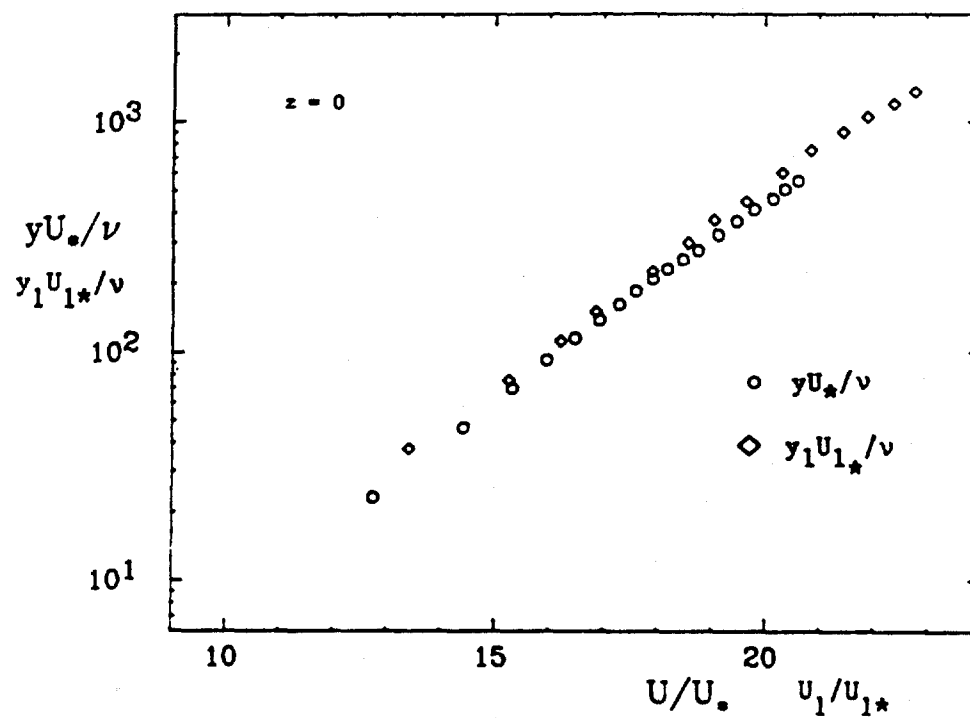
PLOT 1 CASE 0112 FILE 2



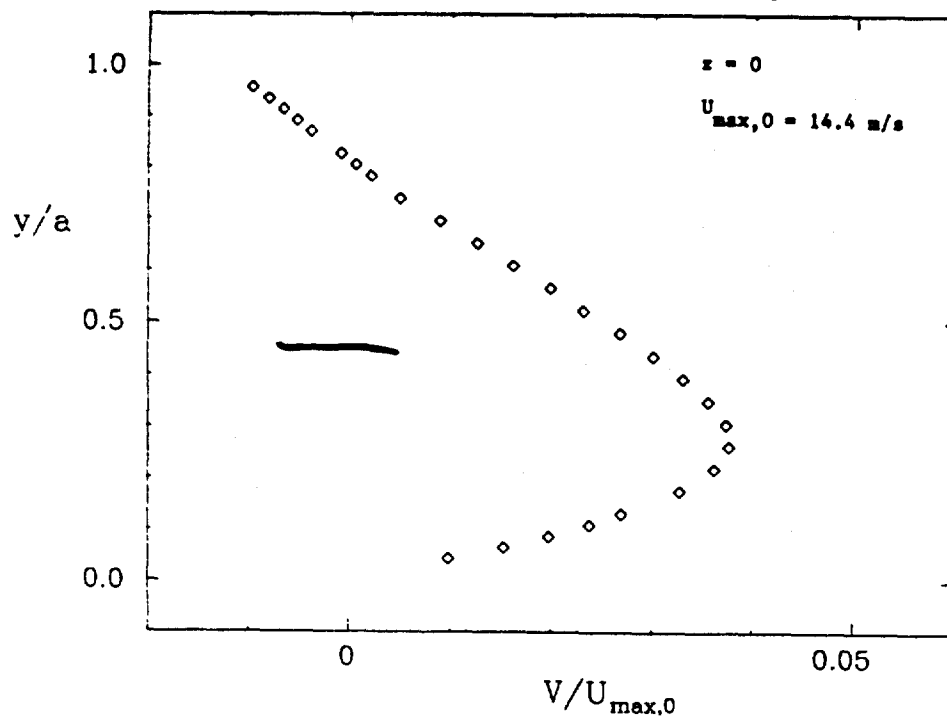
PLOT 2 CASE 0112 FILE 4



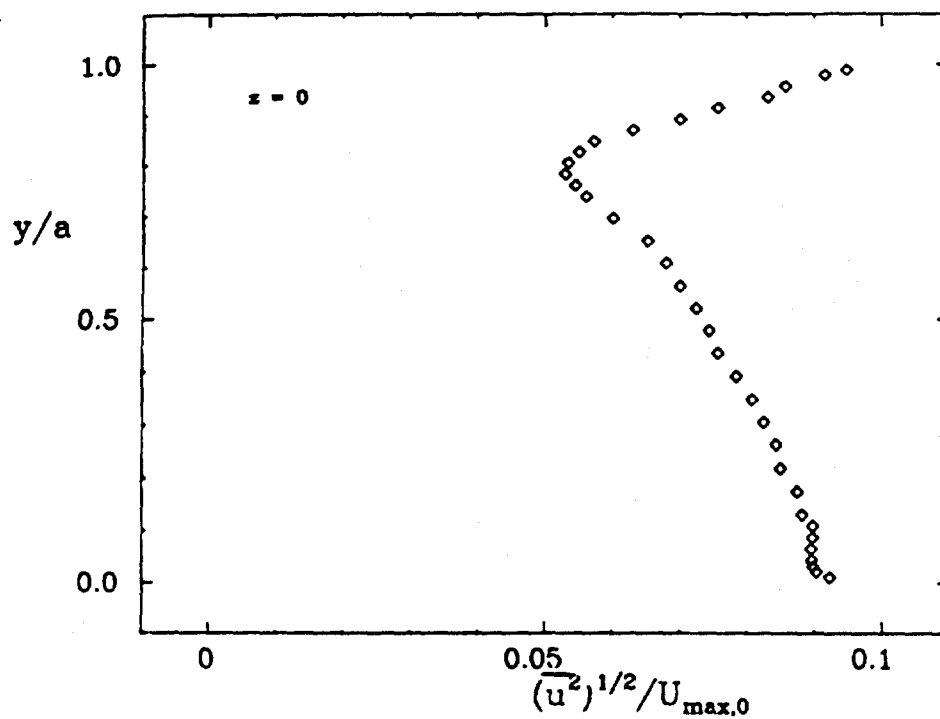
PLOT 3 CASE 0112 FILE 3



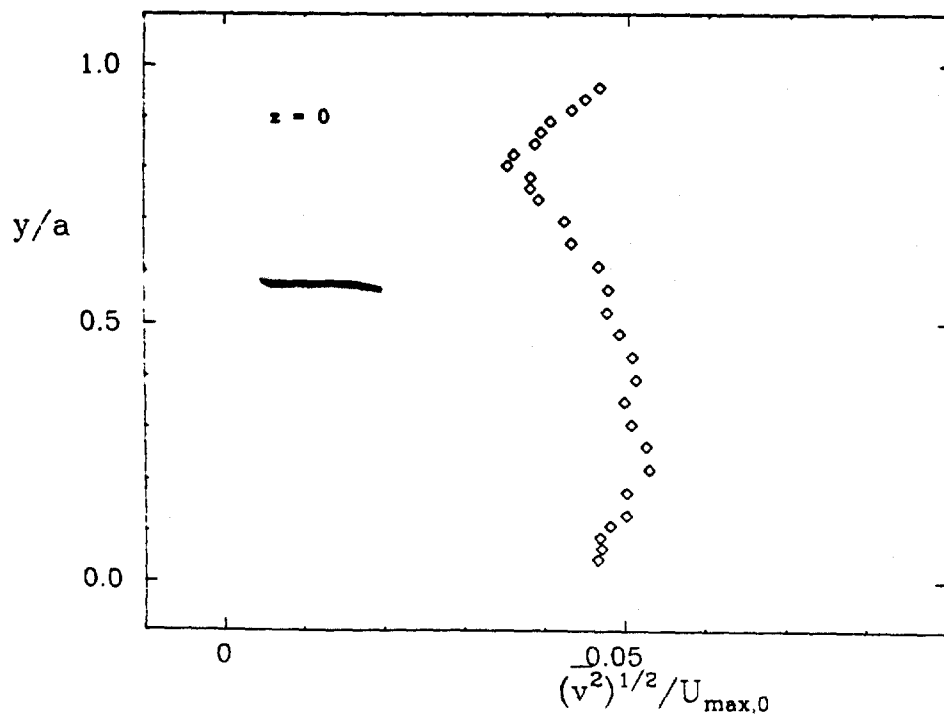
PLOT 4 CASE 0112 FILE 4



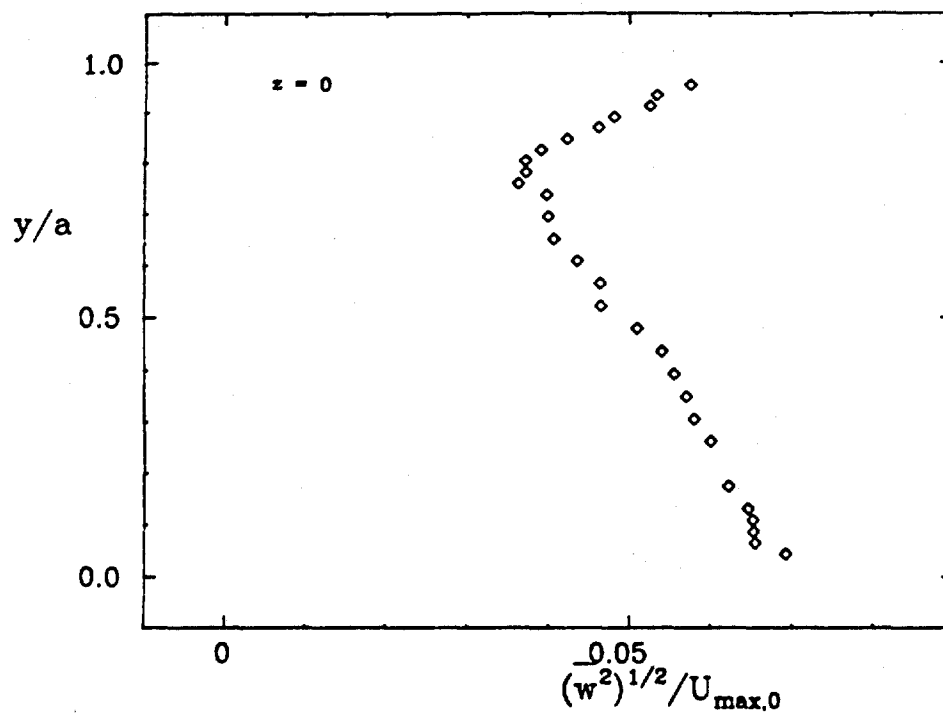
PLOT 5 CASE 0112 FILE 4



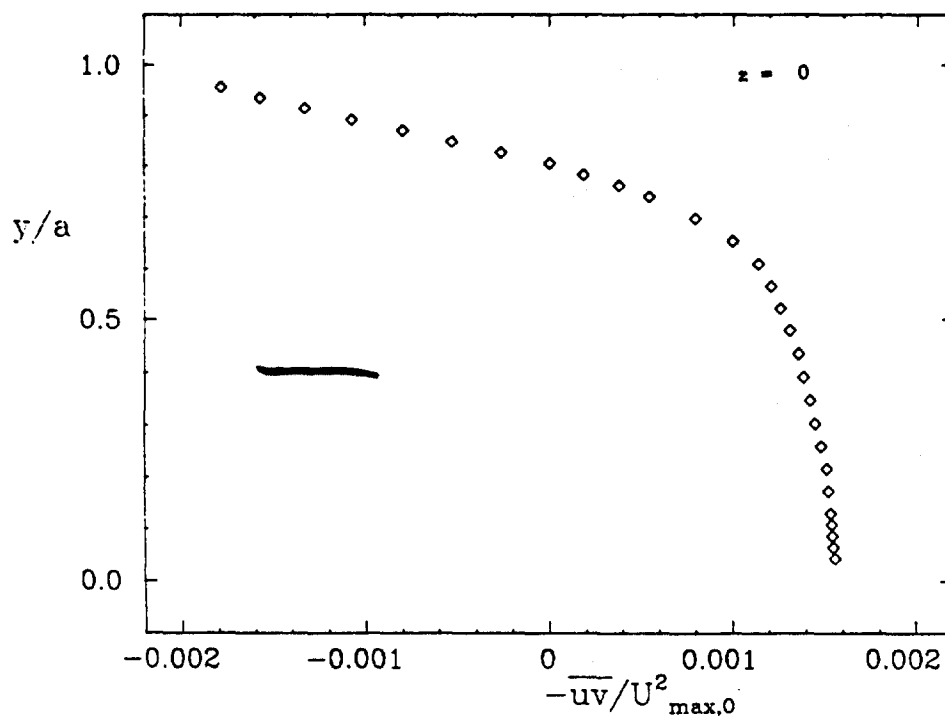
PLOT 6 CASE 0112 FILE 4



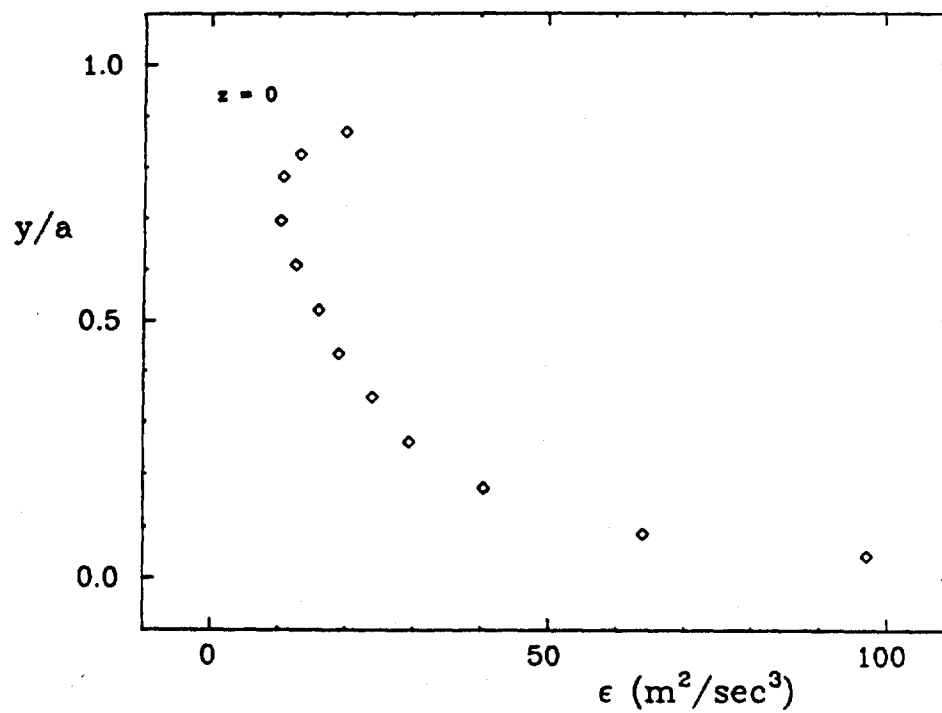
PLOT 7 CASE 0112 FILE 4



PLOT 8 CASE 0112 FILE 4



PLOT 9 CASE 0112 FILE 4



ENTRY ZONE OF ROUND TUBE

Flow 0130

Evaluator: J. B. Jones

SUMMARY



This test case is the steady axisymmetric flow of an incompressible Newtonian fluid in the inlet region of a smooth straight pipe of circular cross-section, with a uniform velocity profile and zero-thickness boundary layer at the inlet, $x/D = 0$ (see Fig. 1). Roughness elements on the tube wall near $x/D = 0$ insure that the boundary layer is turbulent. Free-stream turbulence intensity is less than 1% at $x/D = 0$.

VARIABLES AND THEIR RANGES

Variables are mean velocity (U or, in dimensionless form, U/U_b or U/U_c) as a function of radial (r/R) and axial (x/D) location for various values of Reynolds number. The region of interest extends from the pipe inlet plane to the section at which fully developed flow (i.e., zero axial gradient of all mean velocities and turbulence quantities) is attained. This occurs at an x/D value greater than 120.

For this flow, data meeting the selection criteria listed below are sparse. Although Reynolds number is an important variable, data of satisfactory quality to serve as a standard of comparison for calculations are limited to $Re = 388,000$, $Re = 550,000$, and $Re = 1,300,000$. Suitable detailed velocity-profile data are available only in the x/D range from 0 to 43.5.

A convenient parameter for correlating velocity-profile development is the blocked area fraction or blockage factor B , which is related to other velocity profile characteristics by

$$B = \frac{2\delta_{ax}^*}{R} = 1 - \frac{U_b}{U_c}$$

where $U_b = \dot{m}/\rho A$, $U_c = U$ at $r = 0$, and

$$\delta_{ax}^* = \int_0^R \left[1 - \frac{U}{U_c} \right] \frac{r}{R} dr$$

For Reynolds numbers of 100,000 and higher, the boundary layer reaches the pipe centerline at a value of x/D between 20 and 35. Of special interest is the "overshoot" phenomenon. When B (as well as several other parameters such as centerline velocity, displacement thickness, momentum thickness, and kinetic energy coefficient) is plotted against x/D , a maximum is seen to occur in the region $30 < x/D < 40$. (The

overshoot phenomenon occurs also in rectangular and parallel plane channels in turbulent flow.)

The following explicit criteria were observed in selecting data suitable for checking calculations of turbulent pipe-entrance flows:

1. The flow-passage geometry must be fully specified and verified to be a straight smooth circular pipe.
2. The flow conditions at the pipe inlet plane must be specified and must be nearly uniform across the pipe. The inlet flow must be verified as steady, swirl-free, symmetrical, and free of circumferential variations of mean quantities. Different shapes of contractions or diffusers upstream of the pipe entrance cause different velocity distributions at the inlet plane, so the radial variation of mean velocity and the free-stream turbulence intensity at the pipe inlet plane must be measured.
3. Data must be demonstrated to be reasonably free of sources of experimental error such as inlet flow distortions, pulsations, and the several possible probe errors.
4. Descriptions of measurement methods and data-reduction techniques must be adequate for evaluation and for the making of at least partial uncertainty analyses.
5. Results must be internally consistent and physically reasonable.

DATA SELECTED

The mean-velocity data selected as standards of comparison are those of Barbin and Jones (1963). The data file for this flow contains tabulated values of U/U_{\max} (range 0.529 to 1.000) vs. r/R (range 0 to 0.5) for various x/D (range 1.5 to 43.5). Static pressure data are also in the data file.

Tabulations of B vs. x/D (range 1.5 to 43.5) at $Re = 388,000$ are given by Barbin and Jones (1963) and B vs. x/D (range 12 to 84) at $Re = 550,000$ and $Re = 1,300,000$ by Miller (1971) are in the data file. Figure 2 shows the variation of B with x/D as determined in the three studies (Barbin and Jones, 1963; Miller, 1971; and Pozzorini, 1976).

FURTHER DATA NEEDS

A literature search and study have shown clearly the need for full experimental description of the mean velocity field and the turbulence velocity field in the inlet region of a pipe, extending from the inlet to a section at which fully developed flow has been established. Specific requirements are as follows:

1. The geometry must be fully specified. (In the past, contraction shapes have seldom been described to the extent that duplicates could be constructed.) Until much more is known about turbulent flow through contractions and the effects of

inlet boundary layers on pipe-inlet flow, provision for eliminating inlet boundary layers should be made.

2. Inlet flow must be fully specified and verified by measurement. (It is inadequate to say, "The inlet boundary layer was thin," or "The inlet velocity profile was uniform over at least eighty per cent of the pipe diameter.")
3. Checks of symmetry, flow steadiness, freedom from tangential mean-velocity components, and uniformity of the inlet flow must be made carefully for each flow condition studied. Pozzorini (1976) discusses the difficulties in obtaining a uniform inlet flow. The location of boundary-layer transition should be fixed, and checks should be made against circumferential variations.
4. Measurements should be made over at least a 10-to-1 range of Reynolds numbers. A minimum range of 50,000 to 500,000 is suggested.
5. Necessary corrections to velocity probe readings for effects of turbulence, wall proximity, velocity gradients, probe blockage, and shear should be made, although it is recognized that additional research is needed to establish some of these corrections.
6. Direct wall-shear-stress measurements would be advisable.
7. Careful measurements should be made to detect any periodic circumferential or axial variations of mean quantities. Evidence of an oscillatory character of flow development has been discovered, as shown by Laws et al. (1979).
8. Until a fully reliable calibration flow is available for turbulence-measuring equipment, it would be well for turbulence measurements to be checked by independent instrumentation.

REFERENCES

- Barbin, A. R., and J. B. Jones (1963). "Turbulent flow in the inlet region of a smooth pipe," Journal of Basic Engineering, Trans. ASME, Series D, 85:1, 29-34.
- Laws, E. M., E. H. Lim, and J. L. Livesey (1979). "Turbulent pipe flows in development and decay," Proceedings of the Symposium on Shear Flow, London, pp. 4.6-4.11.
- Miller, D. (1971). "Performance of straight-wall Diffusers (1971)" Part II of Internal Flow. A Guide to Losses in Pipe and Duct Systems, BHRA, Cranfield, Bedford, England, pp. 82-86, 106-109.
- Pozzorini, R. (1976). "Das turbulente Strömungsfeld in einem langen Kreiskegel-Diffusor," Ph.D. Dissertation, ETH Zürich. Eduard Truninger AG, Zürich.

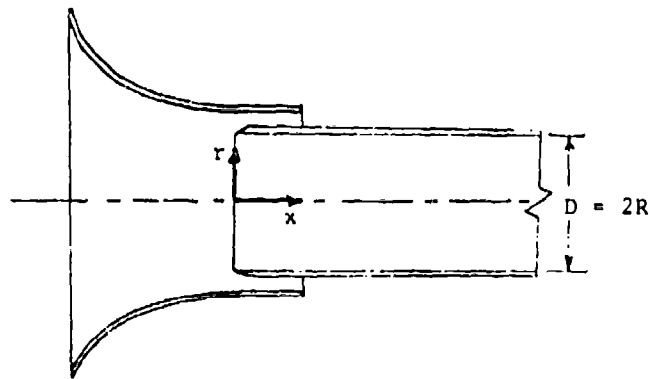


Figure 1. Nomenclature

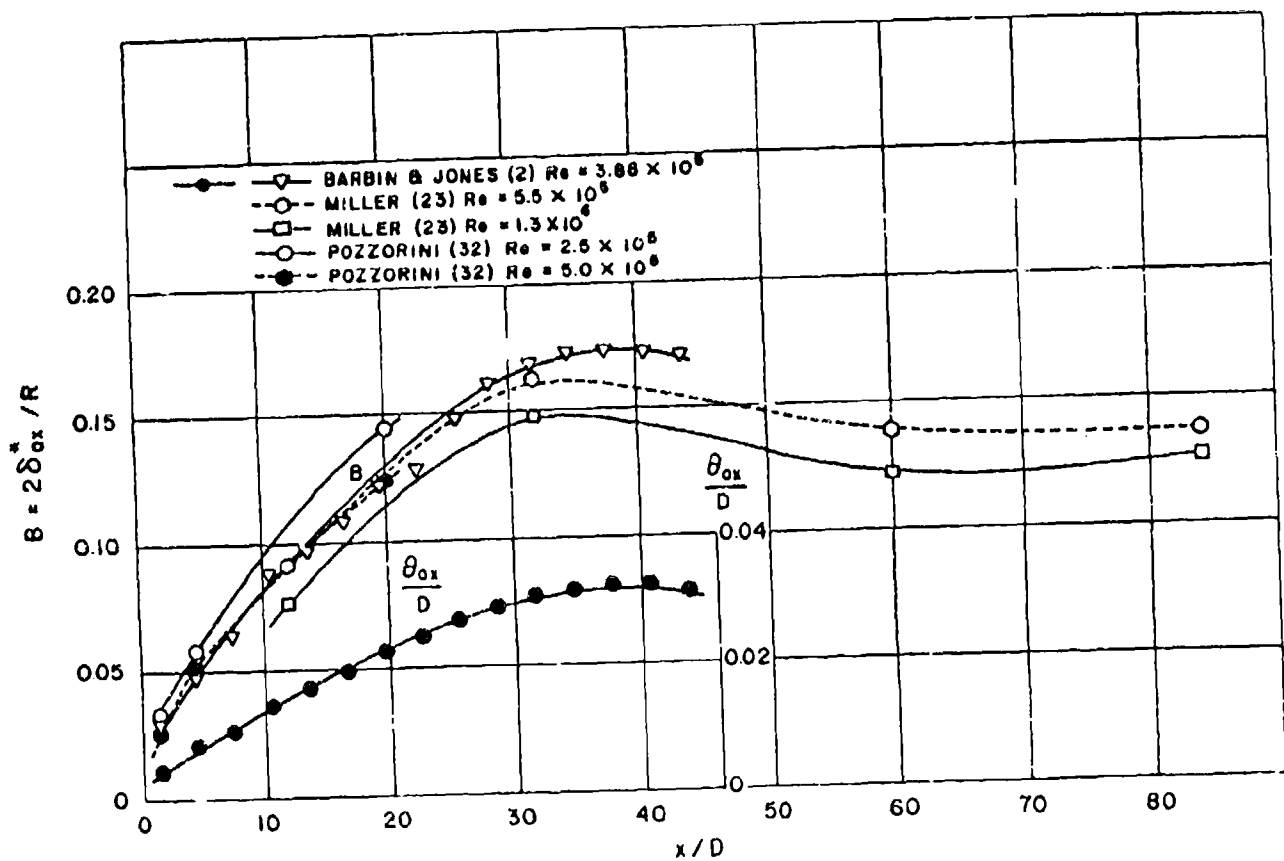


Figure 2. Results of three comparable investigations of velocity profile development

DISCUSSION

Flow 0130

There was some discussion as to whether the initial conditions were sufficiently well specified, but it was pointed out that the results may not be too sensitive to initial boundary-layer thickness as long as it is small. [Ed: This flow was not finally selected as a test case for the 1981 meeting.]

J. Jones

G. Lilley



NUMERICAL CHECKS

E. Reshotko

The Organizing Committee had proposed at an early stage that computers should first attempt to calculate certain "complex" laminar flows before proceeding to the "complex" turbulent flows. The four check cases chosen were:

1. Potential flow in 90° corner
2. Howarth flow (solution by Briley)
3. Axisymmetric jet flow (solution in Rosenhead)
4. Flow in a square cavity with a moving lid.

Each flow was presented to the meeting in turn and arguments given for its introduction as a check case.

DISCUSSION

1. The consensus was that calculation of laminar flows is not a good check for a turbulent-flow algorithm, because an algorithm that is good for turbulent flow may not be good for laminar flow. It was strongly proposed by P. Saffman and agreed by the Conference that the numerical checks proposed by Reshotko be withdrawn. [Ed: This has been done.]
2. The question of grid-size independence was considered very important and it was decided to request that computers should perform at least one independence check, namely, a doubling (approximately) of mesh size or equivalent (for example, a higher-order numerical scheme) or at least one entry flow case.*
3. Finally it was suggested someone be invited to the 1981 meeting to provide an expert review paper on the numerical issues involved in the Conference computations; for example, the review might include a discussion of the potential deterioration of accuracy if the mesh is made too small.†

*[Ed.: A halving of mesh size has been requested, or if this is not possible, a doubling.]

†B. E. Launder and W. Rodi have agreed to consider numerical problems and report to the 1981 meeting. B. E. Launder is to be the overall coordinator; details will be evolved when the computations are accumulated.

SESSION V

Chairman: A. Roshko

Technical Recorders:

E. Adams
H. L. Moses



Flow 0410

Flow 0440

Flow 0140

Flow 0430

EVALUATION OF BLUFF-BODY, NEAR-WAKE FLOWS

Flow 0410

Cases 0411, 0412, 0413 and 0414

Evaluator: B. Cantwell^{*}

SUMMARY

Any evaluation of bluff-body, near-wake flows has to deal with two problems which make a reliable evaluation very difficult.

i) The near wake is a region of high turbulence intensity and low or reverse mean velocity. It is a region which can be measured effectively only by a velocity-biased hot wire or a frequency-shifted LDA.

ii) The number of data sets for the near wake is very limited. Redundant cases do not exist, and each available case represents a "one-lab" experiment.

The remainder of this summary states selection criteria and discusses four specific possible cases.

SELECTION CRITERIA

Selection Criteria Based on Physical Considerations

1. Reynolds number: the Reynolds number should be chosen to avoid significant effects of transition.
2. Mach number: data selected for comparison with incompressible calculations should be at a Mach number less than about 0.3.
3. Surface roughness: in practice a surface-roughness height on the order of a few tens of microinches is usually satisfactory for typical cylinder dimensions. For measurements at $Re > 10^6$ the surface roughness needs to be characterized very carefully.
4. Wind-tunnel blockage: blockage should be less than about 5% to avoid the need for correction.
5. Aspect ratio, end effects, three-dimensionality: all models, regardless of aspect ratio, should include properly designed end plates (see, for example, Stansby, 1974). Venting of the separated flow zone through probe insertion should be avoided if at all possible.
6. Free-stream turbulence: free-stream turbulence levels should be less than about 0.5%.

*Department of Aero. and Astro., Stanford University, Stanford, CA 94305.

Selection Criteria Based on Measurement Considerations

1. Flying hot wire: the flying hot wire can be used effectively to make measurements in separated flows. Measurement uncertainties are somewhat higher than in ordinary hot-wire measurements, due to decreased sensitivity arising from the addition of a bias velocity. Conventional fixed hot-wire data taken in the first 5-7 diameters of the near wake are unusable.
2. Laser-Doppler with frequency shift: the LDA can provide accurate, reliable data on mean velocities and turbulence quantities in separated flows. Single particle counter processing is preferred over tracker processing. A suitable method for correcting sampling bias is essential.

Other Selection Criteria

1. The data should include measurements of C_D , C_L , and Strouhal number.
2. Velocity and stress data should be provided on a grid which is sufficiently dense to permit reasonably accurate interpolations.
3. Measurements should include both lateral and longitudinal velocity components.
4. If unsteady data are included, they should tabulate a sufficient number of points in time so that time can be treated as an independent variable.
5. Unsteady data should include sufficient information for estimating vortex circulation.
6. The data should include a specification of measurement uncertainties.
7. The data should include measurements at several Reynolds numbers and/or Mach numbers.

Case 0411. Cantwell and Coles (1980).

This data set involves measurements in the near wake of a 10.137-cm-dia: cylinder at a Reynolds number of 140,000. The experiment was carried out in the CALCIT 10-ft wind tunnel. Measurements of the streamwise and lateral velocity components were taken using two independent x-array probes mounted on the ends of a rotating arm. Data from the two probes provided independent sets of measurements which were in good agreement with each other (see Fig. 1). The two sets were averaged together to produce final velocity and turbulence data. The data are confined to a plane normal to the centerline of the cylinder covering $-3.0 \leq y/D \leq 3.0$ and $-0.5 \leq x/D \leq 8.0$. The free-stream velocity was 2120 ± 10 cm/s. The probe bias velocity was 2159.56 cm/s. The free-stream turbulence level was less than 0.6%. The cylinder model was fitted with end plates 60.96 cm in diam and 2 cm thick. The cylinder had an overall aspect ratio between the end plates of 27 to 1. The blockage ratio was 0.042. The cylinder was centerless ground and lapped to an outside surface roughness of 30 to 100 μ m. Data include measurements of the mean 360° surface pressure distribution at the centerplane position of the cylinder model. Measurements of the base-pressure distribution along one half of the span showed a very small variation suggesting good two-

dimensionality of the flow. The drag coefficient ($C_D = 1.227$), base-pressure coefficient ($C_{pb} = -1.21$), and Strouhal number ($Str = 0.179$) agreed well with other data on cylinders at the measured Reynolds number. A surface-pressure sensor was used to produce unsteady mean data at 16 phases of the vortex shedding cycle. Measurements include mean (globally averaged as well as ensemble-averaged at fixed phase) velocities \bar{U} and \bar{V} in the streamwise and lateral directions, along with all three components of Reynolds stress ($\overline{u^2}$, $\overline{v^2}$, and \overline{uv}) due to background turbulence. The data are specified on 0.1-diam centers in a grid which is 61 units in the vertical direction and 86 units in the streamwise direction. Hot-wire calibrations were updated continuously during the experiment, using the self-calibrating feature of the flying hot wire. Conventional static calibrations were used. One small region of the flow was encountered, where the velocity bias was insufficient to ensure that all velocity vectors in the ensemble were within the range of sensitivity of the wires. This occurred in a region of very high turbulence intensity (on the order of 0.6) about 1.5 diam downstream of the center of the cylinder and within ± 0.7 diam of the wake centerline. This region is covered by two sets of data arcs of the flying hot wire (see the full evaluation report for more details). The first set includes data arcs which pass through the wake at a small angle with the oncoming flow and are unaffected by probe interference. The second set includes data arcs which pass through the wake at a steep angle with the oncoming flow and experience the probe interference just described. Data in which this difficulty was encountered were deleted before final processing, and coverage of the affected area is limited to the first set of arcs with concomitant high uncertainty ($\pm 4-8\%$ in mean velocity, $\pm 10-15\%$ in Reynolds stress). A second troublesome area is in the recirculation bubble within one diameter of the cylinder center. This region is covered only by the second set of arcs which pass through the wake at a steep angle. Although the turbulence level is low in this region, the mean velocity is also very low. As a result, the small uncertainty in the measured relative velocity ($\pm 2\%$) leads to a large uncertainty ($\pm 50\%$) in the absolute velocity (compared to the local mean) when the bias velocity is subtracted. The main consequence for purposes of comparison with computation is that the flow in the mean recirculation bubble is poorly documented. The two regions just described comprise about 5% of the total area of the measurement region. Measurements outside the two regions just described are reasonably good ($\pm 2-4\%$ in mean velocity, $\pm 5-10\%$ in Reynolds stress). The data do not include information on the third (spanwise) velocity component, nor do they include averages at constant phase of the unsteady surface-pressure distribution.

Recommendation

This data set is recommended for comparison with computations. Both the steady and unsteady data are recommended without modification.

Reservations

Data within the separation bubble has high uncertainty and is quite sparse. Unsteady pressure distributions are not available.

Case 0412. Watmuff (1979) and Perry and Watmuff (1979).

This data set involves measurements in the near-wake of an oblate ellipsoid with major, middle, and minor axes equal to 220, 127, and 73 mm, respectively. Measurements were taken with the ellipsoid stationary and with the ellipsoid oscillating. Measurements of the longitudinal and lateral velocity components were made using an x-array mounted on a moving support (a linear version of the flying hot wire). The model was mounted with its middle axis aligned with the oncoming stream. Data were taken in a plane through the center of the body normal to the major axis. The dimensions of the measurement plane are 140 mm in the lateral direction and 2800 mm in the longitudinal direction; this area covers a substantial portion of the near and intermediate wake. Re based on streamwise chord was 32,500. The bias velocity of the probe was 3.8 m/s. The free-stream turbulence level was less than 0.3%. Accurate hot-wire calibrations were obtained using a dynamic calibration scheme. A modest amount of drift was noted (on the order of 2% of the inferred mean velocity over 15 hrs typically required for an experiment). The shedding frequency for the stationary ellipsoid was 12.7 Hz. In the oscillating case, the body was rocked $\pm 5^\circ$ about its cross-stream axis at a frequency close to the natural shedding frequency. A hot wire placed outside the wake was used to produce unsteady mean data at 16 phases of the shedding cycle. Measurements include mean (globally averaged as well as ensemble-averaged at fixed phase) velocities U and V in the streamwise and lateral directions, along with all three components of Reynolds stress ($\overline{u^2}$, $\overline{v^2}$, and \overline{uv}) due to background turbulence. The data do not include measurements of lift, drag, or surface pressure on the ellipsoidal model, nor do they include out-of-plane measurements in this three-dimensional flow. Model surface roughness was not specified. The blockage ratio was 0.08.

Recommendation

This data set is recommended for inclusion with the Data Library but is not recommended for comparison with computations for 1981.

Reservations

The lack of any information on lift, drag, or surface pressure is a serious flaw. The data are confined to a single plane in a three-dimensional flow. Measurements of model surface roughness would have been useful. The blockage ratio is slightly higher than is desirable. The data are limited to a single Reynolds number.

Case 0413. Castro, I. P. (1971).

This case involves pulsed-wire measurements in the near-wake of flat plates of varying porosity, including the case of zero porosity. The measurements were carried

out in a 3x2-ft test section with 41-mm-wide plates spanning the two-foot length. The velocity and turbulence data are very sparse, including measurements of only one velocity component along the centerline of the wake.

Recommendation

This data set is not recommended for comparison with computation.

Case 0414. Owen, F. K. and D. A. Johnson (1978).

This work involves frequency-shifted LDA measurements in the wake of a circular cylinder. The experiments were carried out in the Ames 2x2-ft wind tunnel on a one-inch-diam model at a Reynolds number of 167,000 and a Mach number of 0.6. Data include measurements of mean and fluctuating longitudinal and lateral velocities. Conditionally averaged data are included which provide velocity and Reynolds normal-stress data at two phases of the shedding cycle 180° apart. The data do not include information on model drag, lift, or surface pressure. The LDA data are presently in the form of velocity histograms and corrections for sampling bias have not been applied. Uncertainty estimates are not given. The data are confined to a plane normal to the cylinder axis extending 7.6 diameters downstream of the cylinder center.

Recommendation

This data set is not recommended for comparison with computations in its present form. If the following changes were made, the data could be used:

1. Correct the submitted data for sampling bias.
2. Expand the unsteady data to include at least eight phases of the shedding cycle.
3. Supplement the data with information on model drag, lift, and surface pressure, with particular attention to possible surface-shock locations.
4. Include a detailed description of wind-tunnel geometry and wall pressure, to allow blockage corrections for calculations of the transonic flow.

REFERENCES

- Cantwell, B. J. (1976). "A flying hot-wire study of the turbulent near-wake of a circular cylinder at a Reynolds number of 140,000," Ph.D. thesis, California Institute of Technology, Pasadena, California. Also B. J. Cantwell and D. E. Coles (1980), "Entrainment and transport in the near wake of a circular cylinder" (manuscript in preparation, on file at Stanford).
- Castro, I. P. (1971). "Wake characteristics of two-dimensional perforated plates normal to an airstream," J. Fluid Mech., 46, 599-609.
- Owen, F. K. and D. A. Johnson (1978). "Measurement of unsteady vortex flow fields," AIAA Paper 78-18.
- Stansby, P. K. (1974). "The effects of end plates on the base pressure coefficient of a circular cylinder," Aeronaut. Jour., (January).
- Watmuff, J. H. (1979). "Phase-averaged large-scale structures in three dimensional turbulent wakes," Ph.D. thesis, Dept. of Mech. Engrg., University of Melbourne, Australia. Also Report FM-12 by A. E. Perry and J. H. Watmuff, 1979.

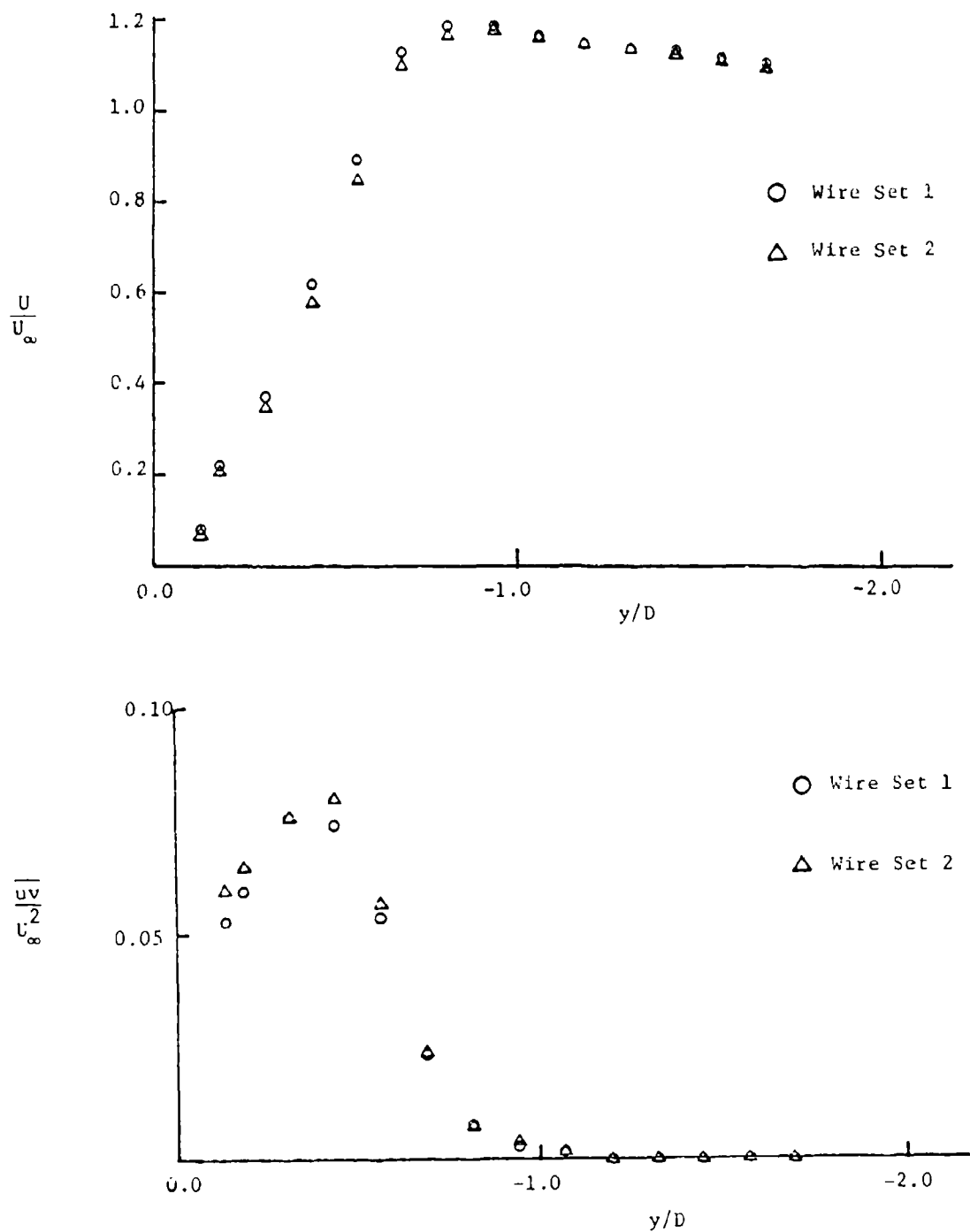


Figure 1. Mean streamwise velocity and shearing stress due to background turbulence measured by two independent x-arrays of the flying hot wire at $x/D = 1.0$. (Cantwell-Coles, 1980).

DISCUSSION

Flow 0410

A. Circular Cylinder (Cantwell/Coles)

1. The computation output should also include $C_p(\theta)$ and not only CP_{pb} .^{*}
2. A non-steady computation should also include $C_L(t)$.[†]
3. This should be on the list of entry test cases because this (non-steady) case might at this stage require a simpler approach than the methods used for the existing entry test cases, which if used, could appear too difficult.
4. A data set is needed for a two-dimensional bluff body flow with fixed separation points.

B. Wake of Ellipsoid (Perry/Watmuff)

1. It was recommended that this case should be added to the Data Library but it was not recommended as a test case for the 1980/81 Conference. This was largely on the grounds that data were not given on the body, and wake data were only given in the center plane.
2. It is necessary to obtain C_D , $C_p(\theta, x = 0)$ and the tunnel-geometry specification for the updated file.

C. Circular Cylinder at $M = 0.6$ (Owen/Johnson)

1. It was confirmed that this case should not be used in the 1981 Conference.
2. It was recommended that LDA measurements be made at $M \leq 0.25$ at a Reynolds number of approximately 140,000 to provide a suitable second data set to Case 0411.

The following comment was received from M. Morkovin after the 1980 meeting:

"I observe that from the measurements with the flying wire, the indicated mean velocity defect decreases much faster with x/D than in the results given in Abramovich and Schlichting. This is disturbing. In view of the general consensus on the desirability of redundant measurements, do Cantwell and Coles have such measurements for the mean velocity defect with x/D ? If not, would they be able to make simple additional measurements before computers tackle this challenging complex flow?"

[Ed.: This has been looked into, but so far it has not been possible to devise an experiment to do this. It remains an important action to be completed.]

^{*}[Ed.: This recommendation has been included in the specification.]

[†][Ed.: No data exist for $C_L(t)$ for this flow. Hence computation will not be required, but can be presented if desired.]

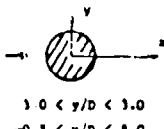
SPECIFICATIONS FOR COMPUTATION

ENTRY TEST CASE/INCOMPRESSIBLE

Case #0411; Data Evaluator: B. Cantwell
Data Takers: B. Cantwell and D. Coles

PICTORIAL SUMMARY

Flow 0410. Data Evaluator: B. Cantwell. "Evaluation of Bluff-Body, Near-Wake Flow."

Case Data Taker	Test Rig Geometry	dp/dx or C _p	Number of Stations Measured							C _f	Re	Ini- cial Condi- tion	Other Notes
			Mean Velocity		Turbulence Profiles								
			U	V or W	$\overline{u^2}$	$\overline{v^2}$	$\overline{w^2}$	\overline{uv}	Others				
Case 0411 B. Cantwell D. Coles	 -3.0 < x/D < 8.0 -0.5 < y/D < 0.5	Mean sur- face pres- sure	Yes*	Yes*	Yes*	Yes*	-	Yes*	Yes* $\overline{u^3}$, $\overline{v^3}$, $\overline{u^4}$, $\overline{v^4}$, $\overline{u^2v}$, $\overline{uv^2}$ y inter- mittency	-	1.4 × 10 ⁵ (based on cylinder dia.)	Free stream turb. level < 0.6%	Flying hot-wire data. Large body of data field. Unsteady data included.

*Location: y/D = -3.0 + 0.1 (i-1), 1 ≤ i ≤ 61; x/D = -0.5 + 0.1 (j-1), 1 ≤ j ≤ 86.

Plot	Ordinate	Abscissa	Range/Position	Comments
1	C _p	θ	0 ≤ θ ≤ 360°	Model surface pressure.
2	U _{CL} /U _{ref}	x/D	0.5 ≤ x/D ≤ 8.0	Mean centerline velocity distribution.
3	y/D	$\overline{u^2}/U_{ref}^2$	-1.5 ≤ y/D ≤ 1.5	Mean normal stress at x/D = 1.5. See note after Spec. Instructions.
4	y/D	$\overline{v^2}/U_{ref}^2$	-1.5 ≤ y/D ≤ 1.5	Mean normal stress at x/D = 1.5. See note after Spec. Instructions.
5	y/D	\overline{uv}/U_{ref}^2	-1.5 ≤ y/D ≤ 1.5	Mean shear stress at x/D = 1.5. See note after Spec. Instructions.
6 optional	y/D	$\langle uv \rangle / U_{ref}^2$	-3.0 ≤ y/D ≤ 3.0	Unsteady mean shear stress at x/D = 1.3, phase 7.
7 optional	y/D	$\langle uv \rangle / U_{ref}^2$	-3.0 ≤ y/D ≤ 3.0	Unsteady mean shear stress at x/D = 2.9, phase 7.
8 optional	y/D	$\langle uv \rangle / U_{ref}^2$	-3.0 ≤ y/D ≤ 3.0	Unsteady mean shear stress at x/D = 4.0, phase 7.
9 optional	y/D	$\langle uv \rangle / U_{ref}^2$	-3.0 ≤ y/D ≤ 3.0	Unsteady mean shear stress at x/D = 5.3, phase 7.
10 optional	V/U _{ref}	x/D	0.5 ≤ x/D ≤ 8.0	Unsteady lateral velocity component along the wake center- line at phase 7.

Special Instructions:

This data set includes both steady and unsteady data in the near wake of a circular cylinder. It is anticipated that computations for the 1980-81 Conference will concentrate on the globally averaged mean flow, Plots 1-5, although eventually large-eddy simulations of this flow may utilize the unsteady measurements. If an unsteady computation is carried out, the computer should report results for items 6-10 above marked optional. In addition, the computer should report the value of the Strouhal number for comparison with the measured Strouhal number. The computer may also report the unsteady lift $C_L(t)$, although data for comparison with $C_L(t)$ are not available.

For the computer who wishes to compute the entire flow field including tunnel walls, relevant dimensions are as follows:

Contraction ratio: 9:1.

Test section diameter: 3.048 m.

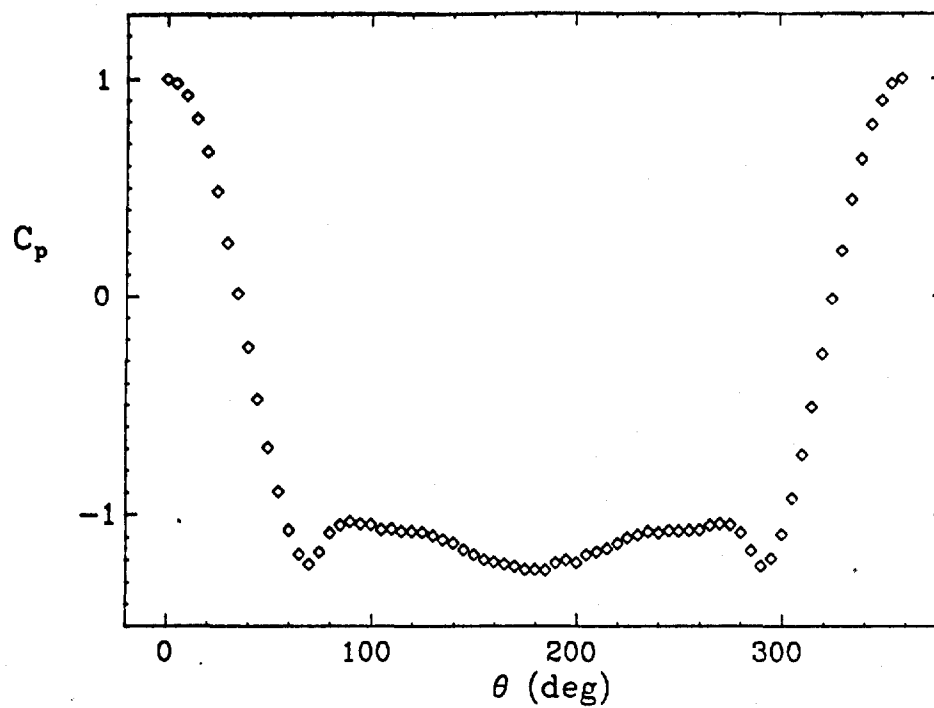
Test section length: 3.048 m.

Model diameter: 0.10137 m.

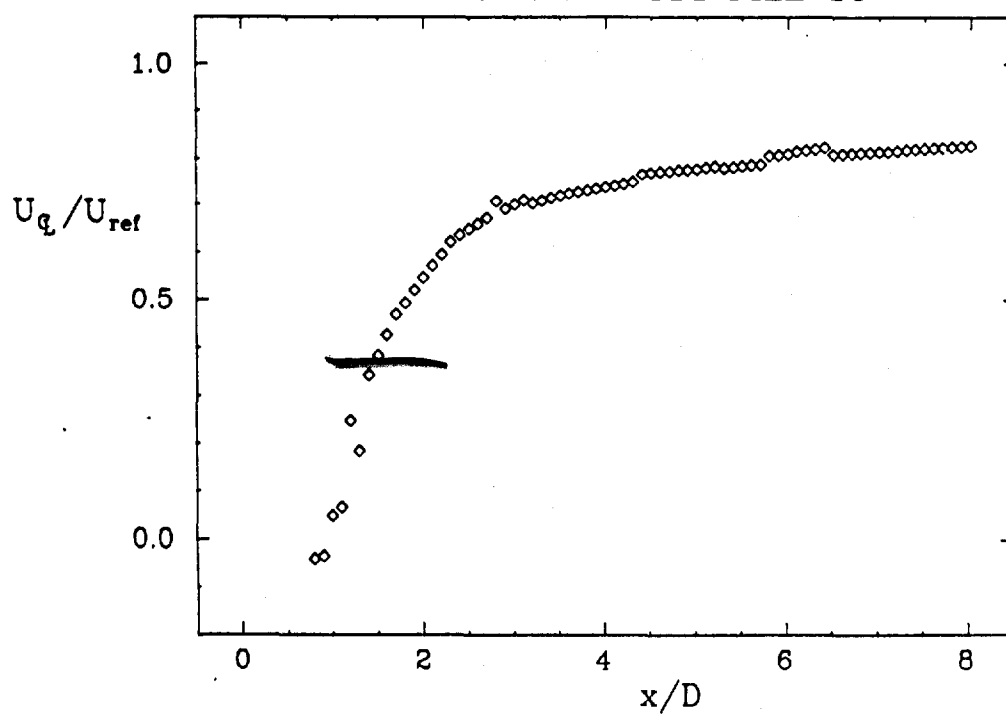
The center of the cylinder was located 0.61 m downstream of the entrance to the test section and 0.152 m above the tunnel centerline.

Note: Mean Reynolds stresses (Plots 3, 4, and 5) must be constructed by summing the mean stress due to background turbulence in file 18 with the stress due to the periodic motion constructed by squaring and averaging the unsteady mean velocity data in files 2 through 17.

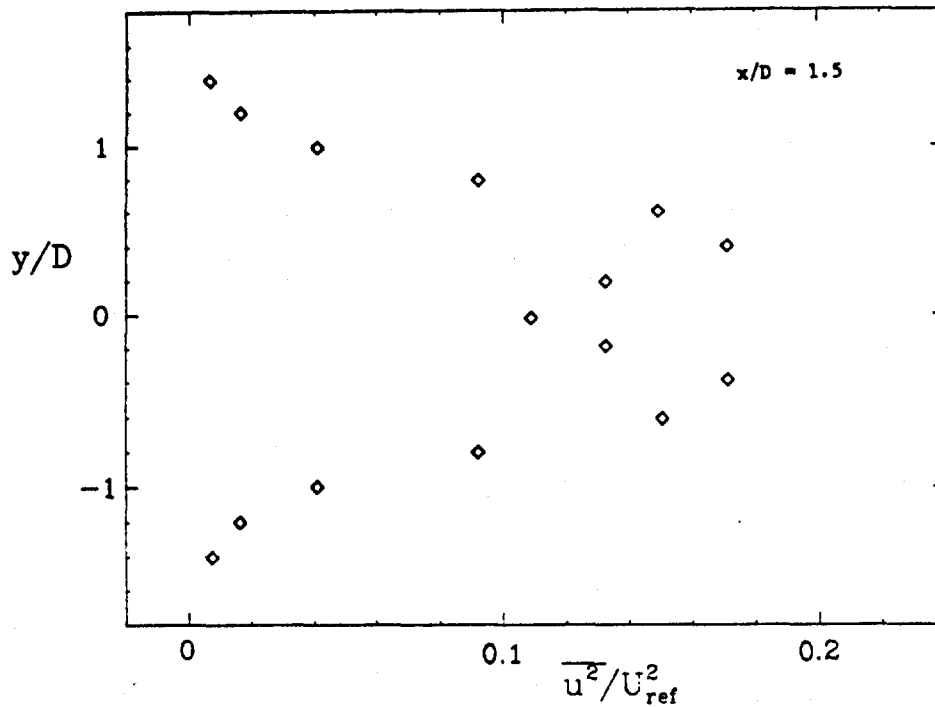
PLOT 1 CASE 0411 FILE 19



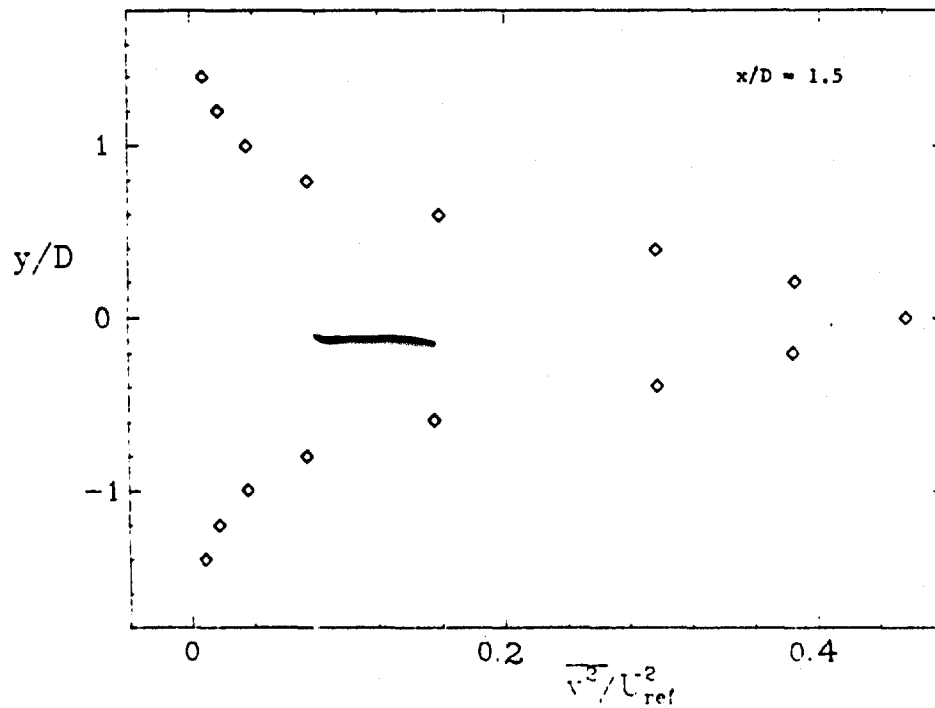
PLOT 2 CASE 0411 FILE 18



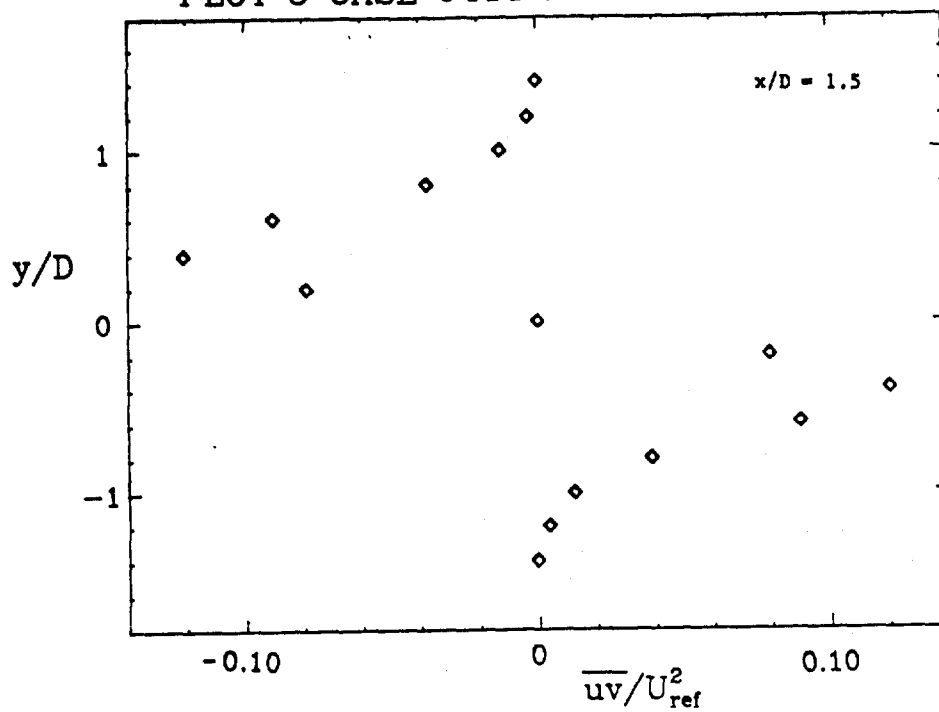
PLOT 3 CASE 0411 FILE 18



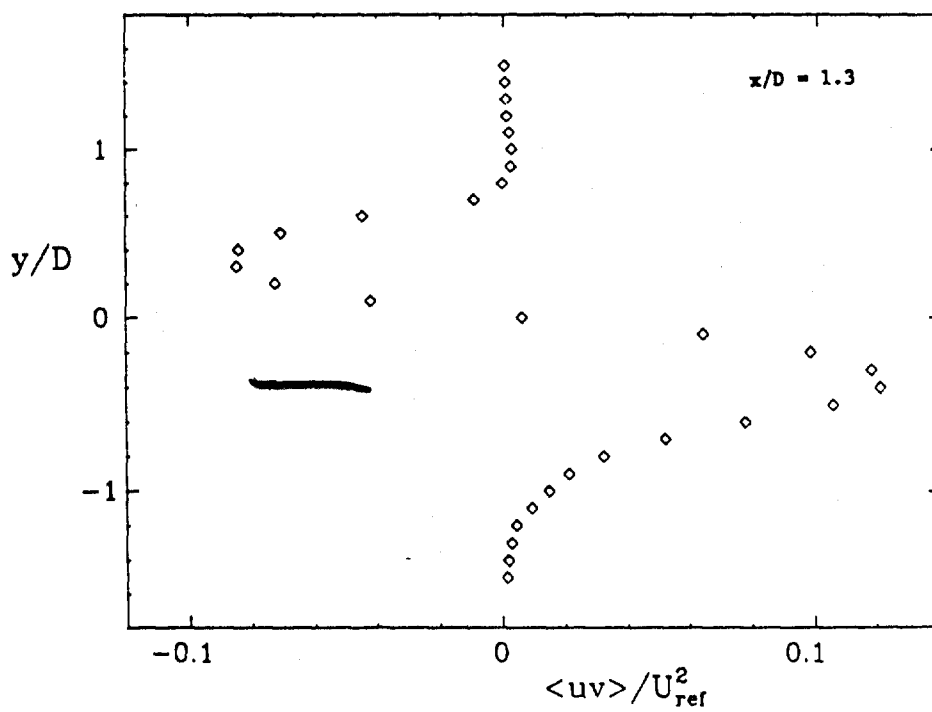
PLOT 4 CASE 0411 FILE 18



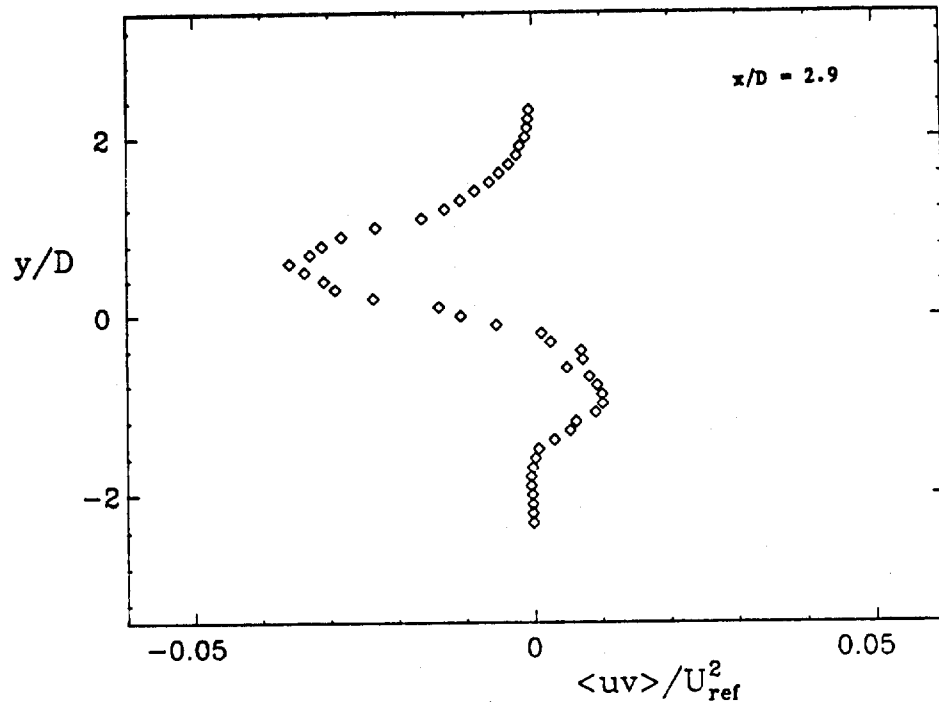
PLOT 5 CASE 0411 FILE 18



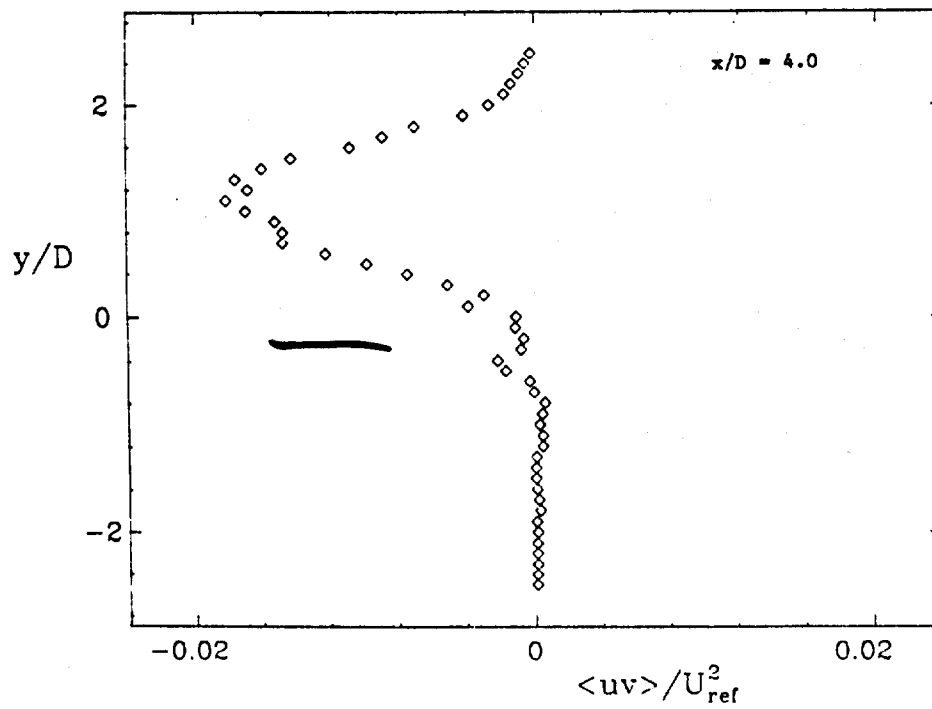
PLOT 6 CASE 0411 FILE 8



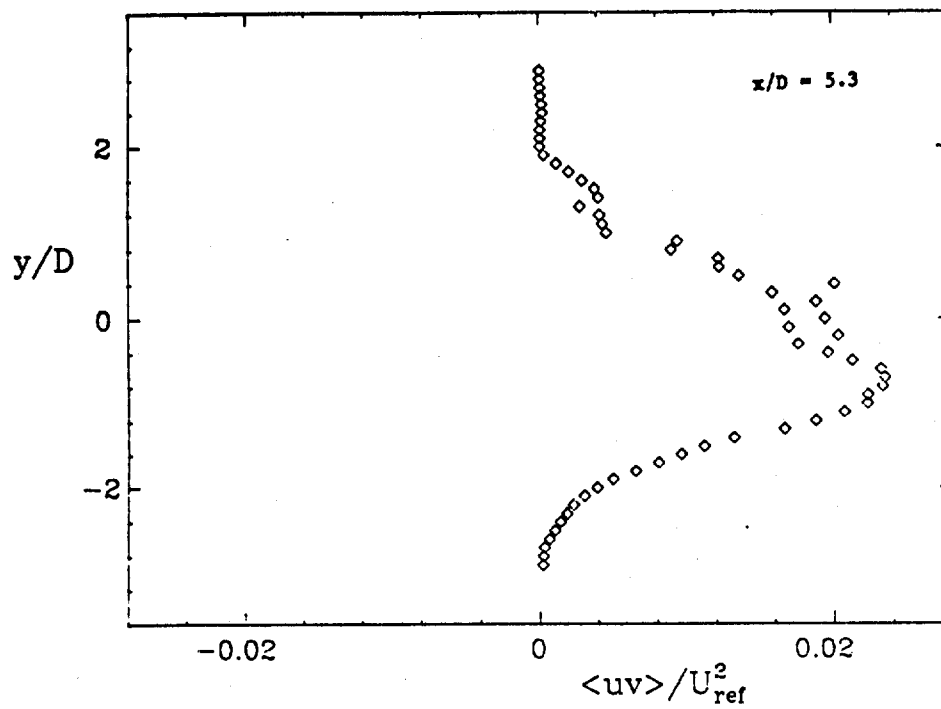
PLOT 7 CASE 0411 FILE 8



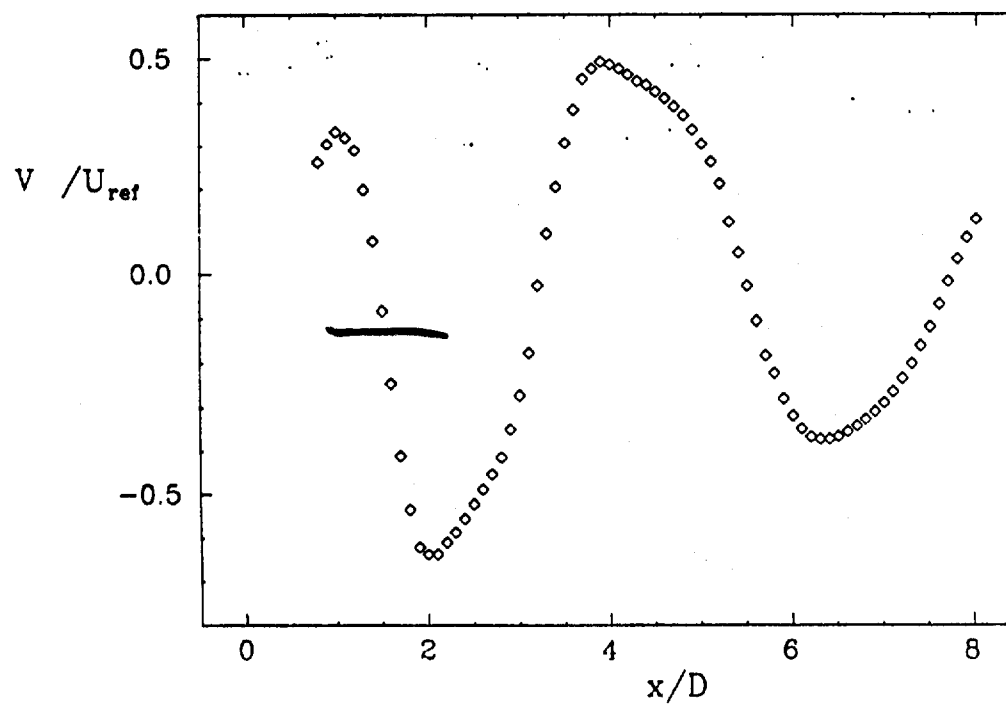
PLOT 8 CASE 0411 FILE 8



PLOT 9 CASE 0411 FILE 8



PLOT 10 CASE 0411 FILE 8



TWO-DIMENSIONAL STALLED AIRFOIL

Flow 0440

Case 0441

Evaluator: A. J. Wadcock*



SUMMARY

The only data set warranting a close scrutiny of experimental technique and an investigation of accuracy is that of Coles and Wadcock (1979). It remains to identify possible problems or limitations in this single recommended data set. The measurement technique is unconventional, and understandably some doubts have been voiced regarding both the possible disturbance to the flow being measured and the accuracy of the data obtained by the flying hot wire. The attached boundary layer is documented downstream of $x/c = 0.620$, and the near wake is covered for one chord length downstream of the airfoil trailing edge.

CALIBRATION PROCEDURES

Compound Test Section

The model was mounted between plane parallel end plates in a circular-section wind tunnel (see Figs. 3 and 5 of Wadcock, 1978). No allowance was made for boundary-layer growth on the end plates or the tunnel side walls. The usual practice of calibrating the wind tunnel by measuring the dynamic pressure q_{inf} (with the model absent) and q_{ref} (with the model present) at the same flow rate as indicated by the same pressure difference from two downstream piezometer rings is not applicable for a compound test section. At large angles of attack (i.e., high drag), a large fraction of the airflow is diverted outside the two-dimensional insert.

The main complication from the use of this compound test section arises from the need to know U_{inf} --the velocity that the flow would have at some point in the tunnel (with the model absent) for a given reference dynamic pressure defined by the piezometer rings. This complicates the presentation of both pressure and velocity data which are normally made non-dimensional by q_{inf} and U_{inf} , respectively. A pitot-static tube mounted near the wind-tunnel roof was used to measure U_{ref} . This quantity was used in all data normalizations. The position of the roof-mounted pitot-static tube is shown in Figs. 3 and 5 of Wadcock (1978). In the event that it is necessary to bound the region of calculation by including the tunnel walls, all information required for this purpose can be found in Wadcock (1978).

*NASA-Ames Research Center, Moffett Field, CA 94035.

Two-Dimensionality of the Mean Flow

To encourage uniform transition across the span, boundary-layer trips were attached to both surfaces of the airfoil. The trips were narrow strips of tape 0.15 mm thick and 4 mm wide, with a sawtooth leading edge. On the suction side, the trip was centered at $x/c = 0.025$, slightly downstream from the pressure minimum. On the pressure side the trip was centered at $x/c = 0.103$, well downstream from the stagnation point. The trips had no measurable effect on the surface-pressure distribution even near the leading edge.

A passive method of flow control which relied on simple metal sheets mounted on the side walls (see Fig. 13 of Wadcock, 1978) was found to be successful in creating two-dimensional flow. The resultant flow is shown in Figs. 11 and 14 of Wadcock (1978). Flow visualization (see Wadcock, 1978, for photograph) suggested that the separation line was reasonably straight over the central meter of the span.

Model Position

During the experiment, all measurements of probe position were referred to a coordinate system defined by the traverse mechanism whose motion was accurately aligned with the tunnel axis. The vertical traverse was repeatable to 0.0025 cm, and the horizontal travers to 0.01 cm.

With the tunnel off, the position of the airfoil with respect to the traverse system was measured as detailed in Wadcock (1978). These measurements established discrepancies between the real and ideal airfoil sections. The real surface showed a wavy pattern with a wave length of about 25 cm and an amplitude of about 0.01 cm. These discrepancies are unlikely to be important from an aerodynamic point of view.

The deflection of the model under air load was measured with the aid of a small optical proximity sensor mounted on one arm of the rotor. To obtain a strong sensor signal, a strip of gold-coated reflective tape, 0.9 cm wide and 0.007 cm thick, was attached to the wing surface in the plane of rotation of the rotor, some 11 cm to one side of the mid-span pressure orifices. With the rotor turning at standard speed, the change in sensor signal from the air-off to the air-on condition showed that the model displacement could be taken as a simple translation of 0.155 cm normal to the chord line. This displacement may have been partly model deflection and partly strut deflection, but the distinction is immaterial.

The airfoil position was finally determined by fitting the air-on location of the rear part of the suction surface to analytical formulas which describe the NACA 4412 airfoil profile. This process fixed the position of the chord line and also defined the real angle of incidence to be 13.87 ± 0.01 degrees. The streamwise position of the trailing edge was determined to an accuracy of 0.02 cm. A more detailed description of these delicate measurements can be found in Wadcock (1978).

Data Placement

The airfoil may be misplaced by 0.02 cm in x, by 0.01 cm in y, and by 0.01 degrees in angle of incidence. The position of data points along the probe arc may be uncertain by as much as 0.1 cm over and above the effect of non-simultaneous sampling, because of strut deflection and also because of systematic local irregularities in the encoder signal.

Further uncertainty in relative position occurs from vibration and buffeting of both model and strut. During the grazing traverse, observed peak-to-peak excursions in proximity sensor voltage indicated a peak-to-peak displacement of about 0.034 cm. The rms voltages and displacements were about one-fourth these values. If this excursion were all caused by displacement of the airfoil normal to the chord, the peak-to-peak motion would be 0.035 cm. If the excursion were all caused by displacement of the strut and rotor hub in the streamwise direction, the peak-to-peak motion would be 0.080 cm. Both estimates are reasonable, and the actual motion is probably a combination of the two.

The Flying Hot Wire and Related Instrumentation (see Coles et al., 1978).

The main experimental technique uses a flying hot wire mounted on the end of a whirling arm. The rectification problem is thus avoided by biasing the relative velocity. In practice, the tip speed of the whirling arm can be made large enough so that the direction of the relative flow at the probe (a standard commercial x-array) is always within the useful range of about ± 30 degrees with respect to the probe axis.

The angular position of the motor shaft was encoded by a 256-tooth precision gear and a magnetic pickup which produced a clean T-L pulse train called the encoder signal. The encoder signal controlled not only the rotor speed but also the timing (and hence the position in the flow) of the hot-wire measurements. The rotor diameter was 151.4 cm, with 256 equally spaced sampling positions. Digital data were obtained every 1.86 cm along the probe arc.

Eight of the twelve analog data channels surveyed carried miscellaneous signals (e.g., tunnel temperature, tunnel dynamic pressure, model surface pressure). Four data channels were reserved for hot-wire data from the two x-arrays, one on each arm of the rotor. The rotor tip speed during the hot-wire measurements was 375 rpm. The tip speed was 29.73 m/s. Each data file lasted for 2048 revolutions (5.46 min). There are 85 such files in the main data base.

Hot-Wire Calibration

The flying hot-wire technique encounters several problems which are not typical of the ordinary art of hot-wire anemometry. One problem is that the calibration arc occupies a considerable fraction of the tunnel test section, and nonuniformities of

the calibration flow along this arc may be important. A second problem is that absolute errors in measured velocity are conserved, and relative errors are therefore at least doubled during conversion from a reference frame fixed in the probe to a reference frame fixed in the tunnel. A third problem is that calibration of wire arrays is required over an unusually large range of velocities.

For the present experiment it was impractical to remove the airfoil model from the test section during wire calibration. Instead, the airfoil was pitched to -4 degrees (zero-lift angle), and the calibration arc was chosen to be as high and as far downstream from the airfoil as possible. The resulting calibration geometry is shown in Fig. 31 of Wadcock (1978). The magnitude of the free-stream velocity was determined at six points along the calibration arc by means of a pitot-static tube for each dynamic pressure used for wire calibration. A sample probe calibration is documented in detail in Coles et al. (1978).

Benchmark Data

The main events of the experiment were the pre-test calibration, the horizontal, vertical, grazing, and boundary-layer traverses, and the post-test calibration. The pre-test calibration was intended to anchor one end of the drifting data. However, at different times in the course of this calibration, three of the four wires showed sudden small changes in response. No way was found to pull the data together, and the pre-test calibration had to be discarded.

We were left with the post-test calibration and a series of "benchmark" files (duplicate files represented by the lowest arc in Fig. 34 of Wadcock, 1978) spaced among the data files. The key to control of drift was the determination of the mean velocity along portions of the benchmark arc which lay outside the turbulent region. The strategy used was to assume that the wire parameters changed continuously and linearly with time during the period spanning the last two benchmark runs and the post-test calibration. The details are fully documented in Wadcock (1978). Only those parts of the benchmark arc outside the boundary layer and airfoil wake were used to keep track of the hot-wire drift, as shown in Fig. 2. Agreement among all seven benchmark files is thus guaranteed over these regions of the arc. The agreement among these files documenting the passage of the probe through the wake illustrates the importance of a stable mean (as shown by the repeatability of the data) and further guarantees that the hot-wire drift was under control. This gives a measure of the internal self-consistency of the hot-wire data.

SUMMARY OF CALIBRATION PROCEDURES

The hot wires were calibrated in a nonuniform flow. An iterative inversion scheme provided information on the flow inclination along the calibration arc. Only the post-test calibration was meaningful. Control of drift was provided by use of a

set of duplicate "benchmark" files. A bootstrap procedure was necessary to establish the benchmark velocity field.

The hot-wire data were then inverted and the results stored on punched cards as "raw data."

The following uncertainty estimates have been calculated corresponding to 95% confidence levels.

Variable	Uncertainty Estimate
Intermittency	± 0.04
U, V	$\pm 0.03 U_{ref}$ ($\pm 0.02 U_{ref}$ in regions of low turbulence)
$\overline{u^2}, \overline{uv}, \overline{v^2}$	$\pm 6\%$

Note the uncertainty is expressed as an absolute value for the mean-velocity components and as a percentage for the Reynolds stresses.

DISAGREEMENT BETWEEN FLYING HOT-WIRE AND PITOT-STATIC MEASUREMENTS

At this stage of the data processing, it was observed that velocity measurements indicated by the hot wire outside both boundary layer and wake were lower than corresponding measurements made with a pitot-static tube. The disagreement is assumed to stem from the way in which (1) the flow inclination along the calibration arc was inferred, (2) the way in which the benchmark velocity field was inferred, or (3) a combination of the two. A small correction was made to the raw data to force agreement. This correction is fully discussed in Wadcock (1978); it amounted to an increase of 2% in the magnitude of the velocity relative to the probe.

The agreement in the magnitude of the velocity, after correction of the hot-wire data, is within a fraction of 1% in all cases, on both sides of the airfoil for values of U/U_{ref} from 1.0 to 1.4. Elsewhere in the flow, of course, the hot-wire data have also changed. In the free stream, the flow angles have changed by as much as one degree at the extremities of the probe arcs. In the separation bubble, the dimensionless mean velocity has changed in magnitude by about 0.02, and in angle by unknown amounts. The Reynolds stresses and higher moments, however, have merely been multiplied everywhere by constant factors close to unity.

The comparison between the corrected hot-wire data and the results of a pitot-static traverse through the wake (pitot-static tube aligned at 6 degrees to the tunnel axis) made in Fig. 23 of Wadcock (1978) shows good agreement, lending credence to the above correction.

PROBE INTERFERENCE

At an early stage of data processing, it became apparent from an inspection of intermittency data (i.e., independent of any problems with wire calibration and drift)

that there was a serious problem with probe interference. Our original expectation was that the passage of the rotor arm through the fluid would add a local increment of momentum in the direction of probe motion, but that the effect should be small because the affected fluid would move a substantial distance (two meters or more, in the case of the free stream) between successive probe passages. There is strong evidence that the effect just described was small, as expected, and that a different kind of interference was acting, arising from the extreme sensitivity of separation to slight changes in the external pressure field. Although the obstacle presented to the flow by the rotor hub was physically small, the drag was an appreciable fraction of the drag of the airfoil itself, and the blockage effect was substantial. The associated changes in velocity outside the boundary layer varied with rotor position and worked with strong leverage on the separation process.

The effect is best documented in terms of the surface pressure on the airfoil (see Fig. 37 of Wadcock, 1978). The differences among repeated measurements at any one surface pressure port were found to be strongly correlated with the streamwise position of the traverse system and almost independent of the vertical position. Wadcock (1978) provides confirmation that it was traverse position, and not probe rotation, that governed the magnitude of the effect. The largest effect occurs when the traverse system is set up for the boundary-layer traverse. The observed pressure distribution for this situation is shown in Fig. 3. The effect was not two-dimensional; the required corrections to C_p at the 1/4- and 3/4-span stations were found to be only 60 to 70% of the required corrections at midspan.

The scheme used to cope with this problem of blockage was to discard the hot-wire data for that part of each grazing or boundary-layer arc downstream of the last grazing arc--see Fig. 4. The scheme outlined here has sacrificed much of the redundancy of the original data, although two traverses at different angles remain in the important region of the separation bubble. Agreement between the two sets of arcs is illustrated in Fig. 5 for the distribution of one of the normal Reynolds stresses across the wake at a station slightly downstream from the airfoil trailing edge. The problem can be ignored for all horizontal and vertical traverse data. The main part of the separation bubble can be taken as interference-free (as can all the data in the wake), but the boundary layer up to separation cannot.

PROCESSED DATA

The data of the present experiment are awkwardly placed from the point of view of a numerical analyst. Further processing was therefore carried out to redefine the data on a rectangular grid. Mostly for convenience in describing the airfoil surface, the grid in question is aligned with the airfoil chord. Details can be found in Wadcock (1978) with information up to and including fourth moments. Wadcock (1979)

provides a partial tabulation of the processed data. Contour plots of intermittency, chordwise mean velocity, and three Reynolds stresses are shown in Figs. 6a, 6b, 6c. Shading has been used to emphasize peaks and valleys. Note that these figures are based on velocity components resolved along and normal to the chord line. Quite different values and different contours might be obtained near the airfoil if the components were resolved more nearly along and normal to the airfoil surface. The main conclusion from the Reynolds-stress data is that the separation process is relatively regular up to the trailing edge of the airfoil. The real challenge is to understand the merging process for the two shear layers just downstream of the trailing edge and the subsequent rapid relaxation toward the final state of a conventional wake far downstream.

SUNDRY COMMENTS

1. No experimental measurements of skin friction have been published, although a limited number of boundary-layer velocity profiles are tabulated in Wadcock (1978), the first point of each of which can be considered as a Preston-tube measurement. Any attempt to obtain an estimate for skin friction from a Clauser plot of the hot-wire data fails, as there is a negligible logarithmic region to the velocity profile, even at the earliest boundary-layer station for which data are available. Estimates for the skin friction will be available (from a more complete law-of-the-wall plus law-of-the-wake fit) at a later date. This will enable a momentum balance to be performed.
2. A single boundary-layer profile on the pressure surface of the airfoil at $x/c = 0.820$ is listed in the data files. This provides the only available information about the development of the boundary layer on the pressure surface:

$$R_\theta = \frac{U_{ref} \theta}{\nu} = 1090$$

$$C_f = \tau_w / q_{ref} = 0.0047$$

$$\frac{\delta}{\tau_w} \frac{dp}{dx} = -0.152$$

REFERENCES

- Coles, D., B. Cantwell, and A. J. Wadcock (1978). "The flying hot wire and related instrumentation," NASA CR-3066.
- Coles, D., and A. J. Wadcock (1979). "Flying hot-wire study of flow past a NACA 4412 airfoil at maximum lift," AIAA Jou., 17, 321
- Wadcock, A. J. (1978). "Flying hot-wire study of two-dimensional turbulent separation on a NACA 4412 airfoil at maximum lift," Thesis, California Institute of Technology, Pasadena, California.
- Wadcock, A. J. (1979). "Structure of the turbulent separated flow around a stalled airfoil," NASA CR-152263.

CASE 0441

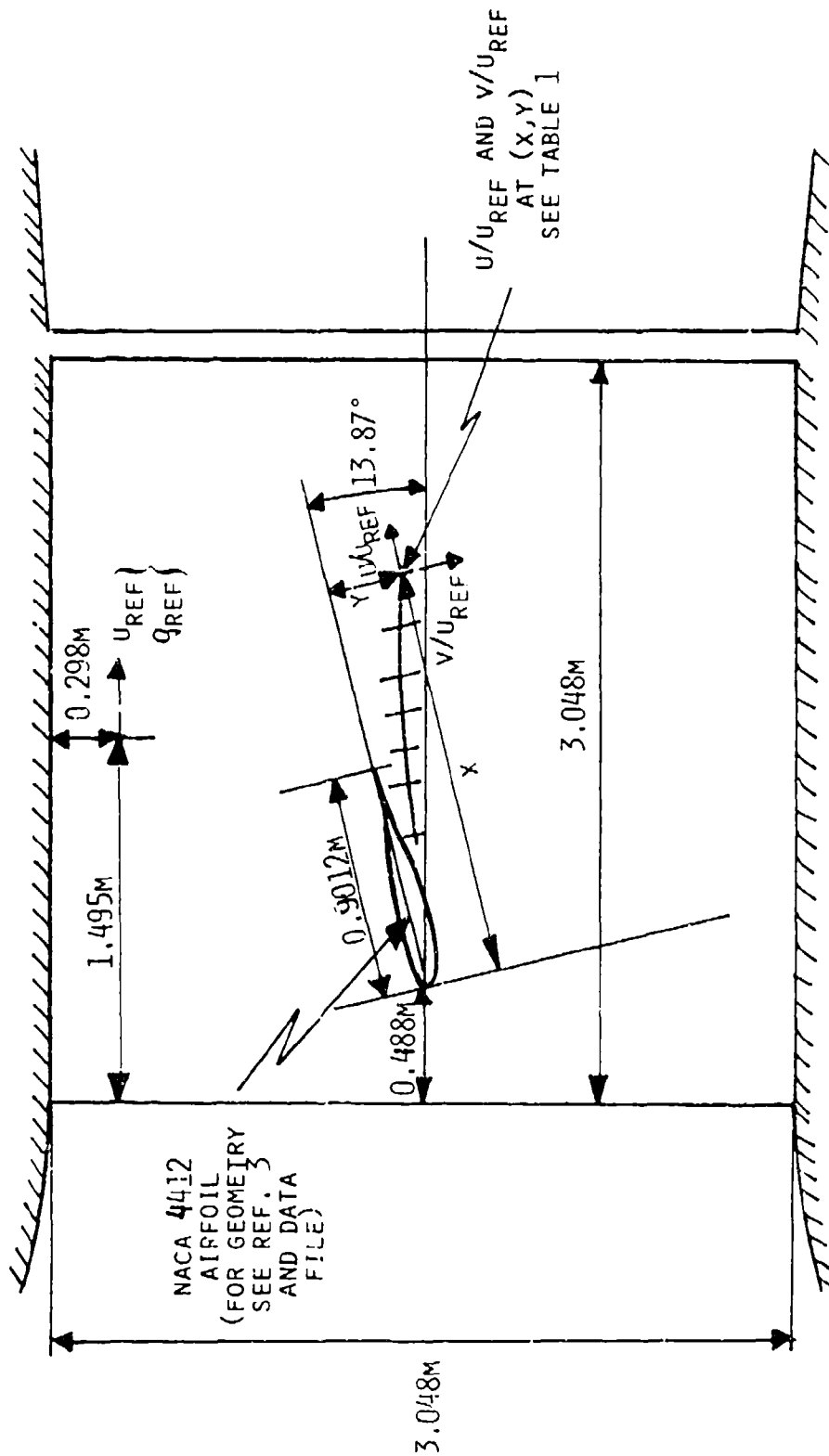


FIGURE 1 DIAGRAM SHOWING AIRFOIL IN WIND TUNNEL

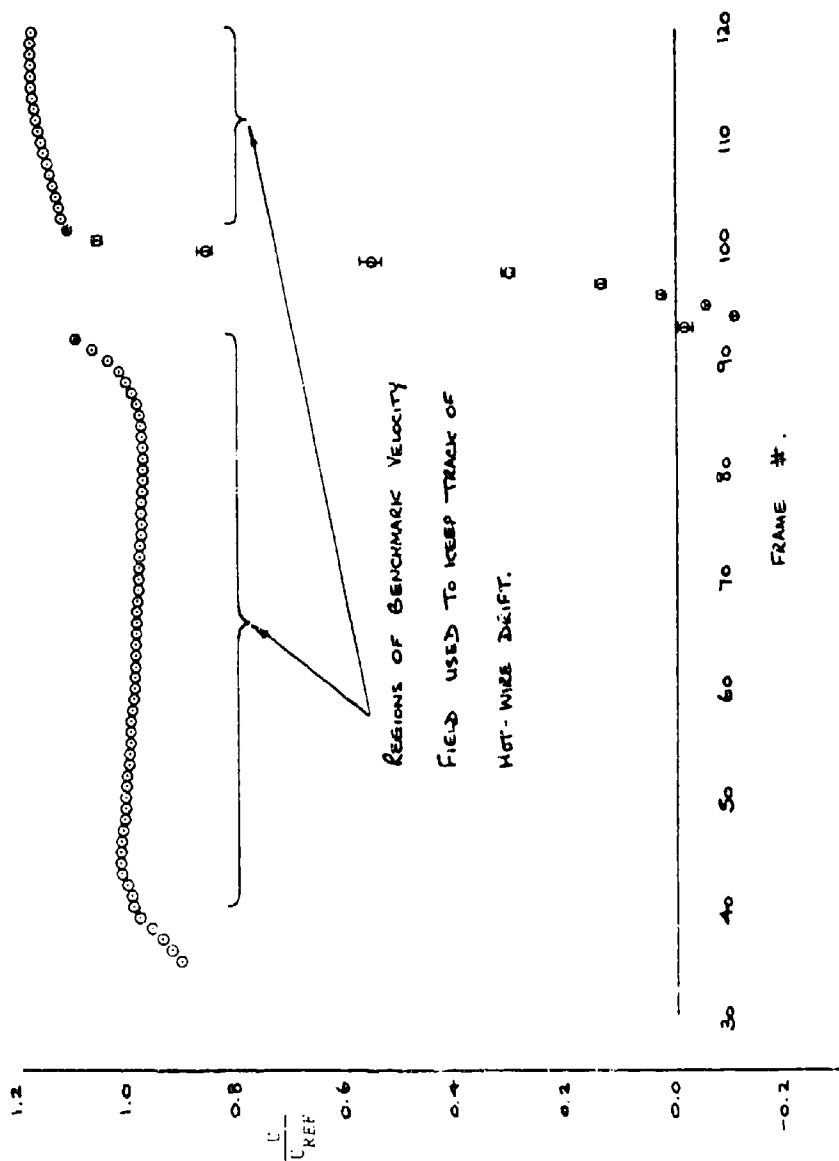


FIGURE 2. CASE 0441

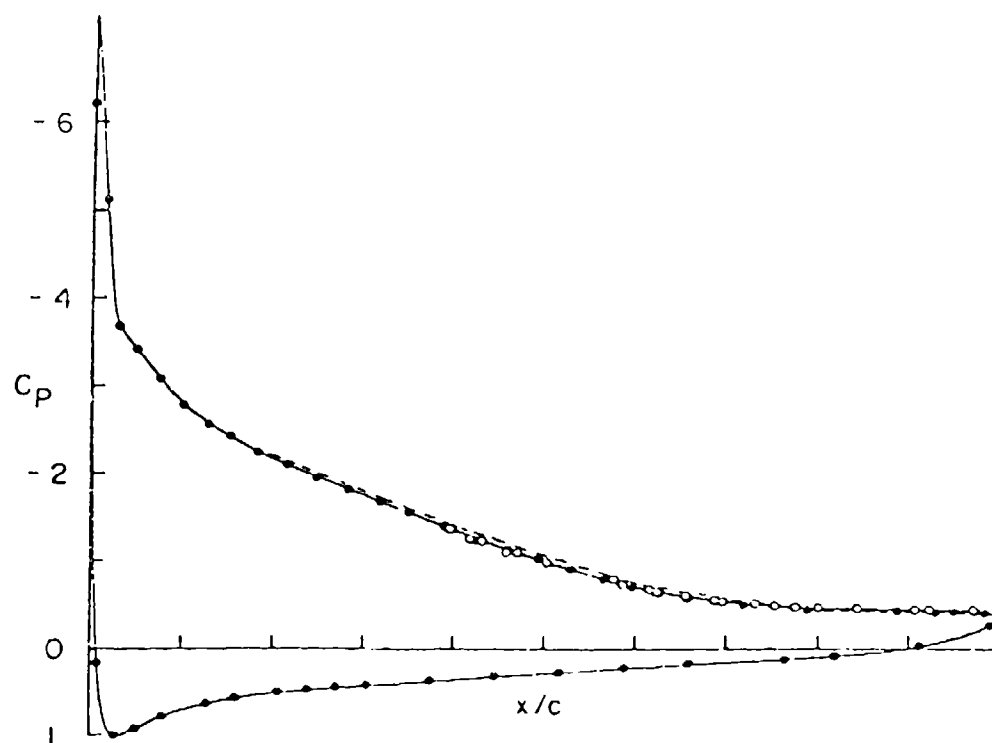


Figure 3. Case 0441, surface-pressure distribution at 14 degrees angle of incidence, with flow guides in optimum position (Run 87). Solid symbols: data at midspan. Open symbols: data at 1/4-span and 3/4-span.

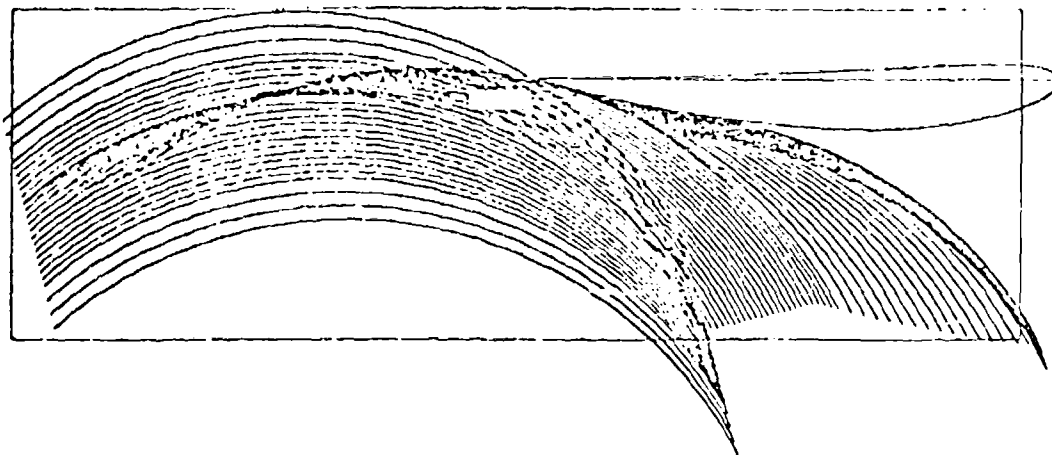


Figure 4. Case 0441, location of probe trajectories for main experiments, after downstream portion of grazing and boundary-layer traverses have been deleted. Arcs extend from Frame 40 to Frame 115. Small white rectangle shows region used for area interpolation. Large rectangle shows maximum extent of grid used for processed data.

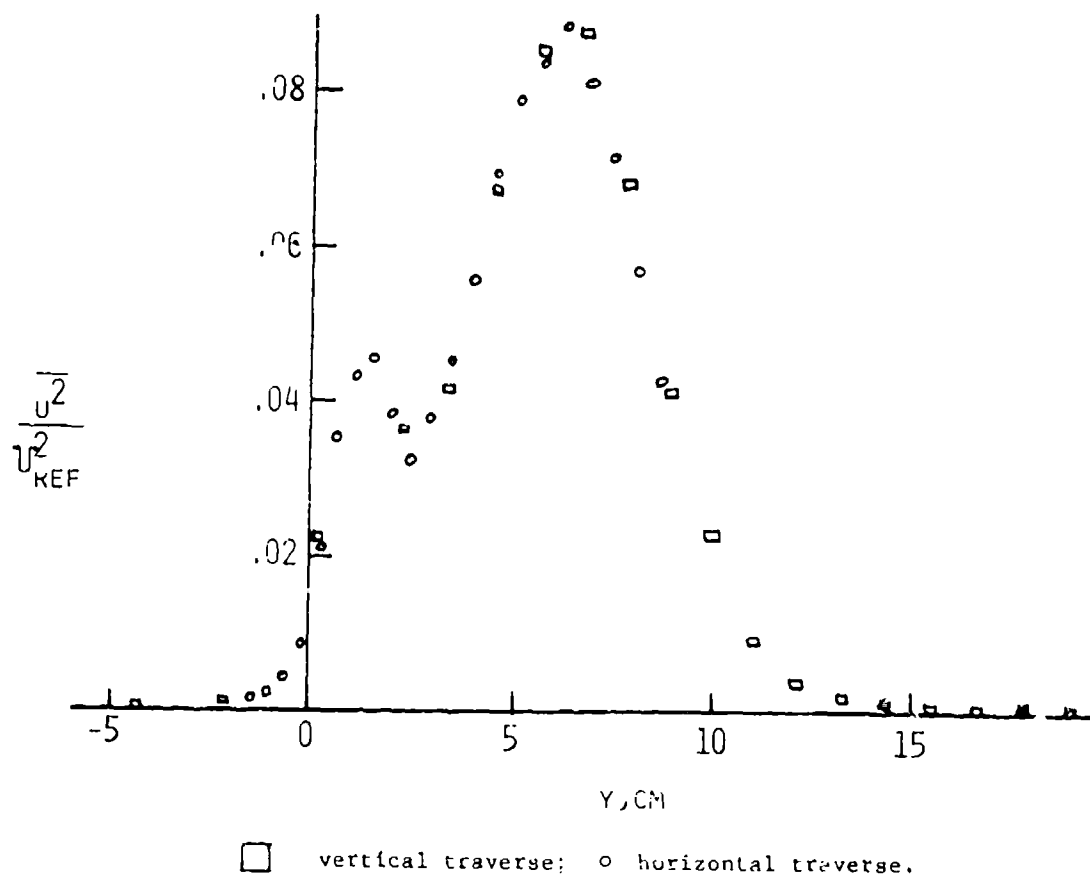


Figure 5. Case 0441, effect of rotor interference on wake thickness. Dependent variable is chordwise component of turbulent energy, evaluated by linear interpolation in corrected raw data. Station is $x = 98.86$ cm.

CASE 0441

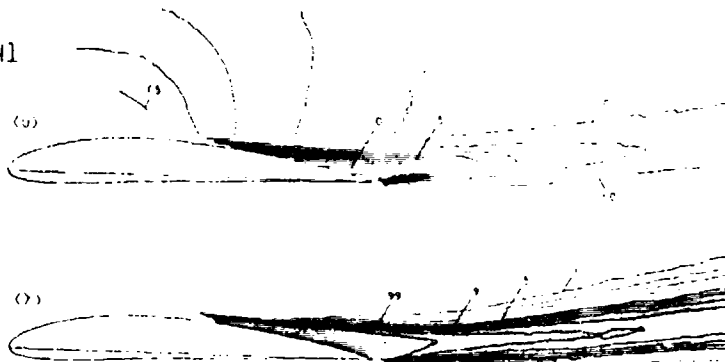


Figure 6a. Contour plots of chordwise mean velocity U/U_{ref} and intermittency factor γ . Contour interval is 0.1.

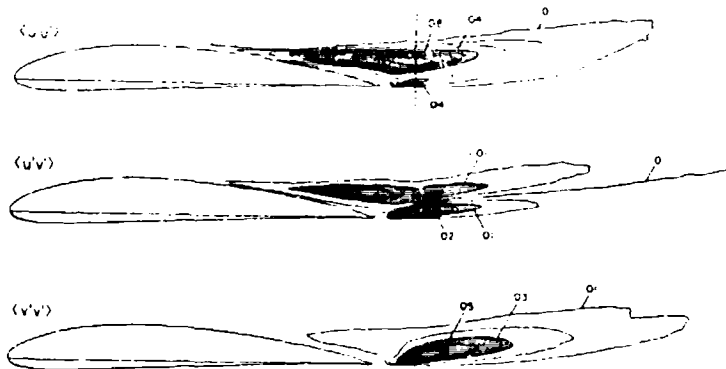


Figure 6b. Contour plots of correlations $u^2/(U_{ref})^2$, $\overline{uv}/(U_{ref})^2$, and $v^2/(U_{ref})^2$. Contour interval is 0.010 or 0.005.

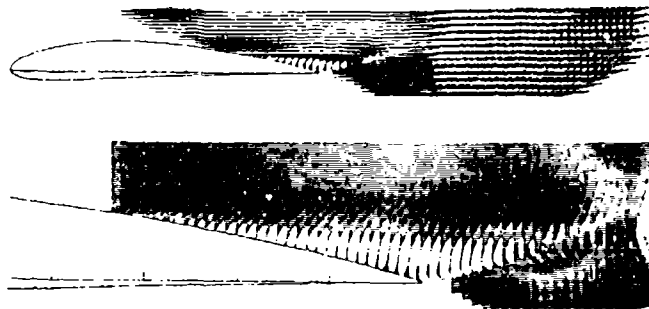


Figure 6c. Partial display of vector field of mean velocity. Top: same scale as Figs. 6a, b; bottom: close-up view of separated region. (Tick marks on chord line are at intervals of 0.1 in. x/c .)

DISCUSSION

Flow 0440

1. It was recommended that some clarification be given to the data on the wall geometry and end plates.
2. A cautionary note should be added regarding the boundary-layer data upstream of separation. These data should not be used as initial data in computations.
3. The location of the transition strips should be given in the specifications.
4. The computation output should also include profiles of mean velocity, shear stress and turbulent energy at three chordwise locations (e.g., before separation, just downstream of the trailing edge and in the reverse-flow region).
- 5 The computation output should also include x_{sep} .


SPECIFICATIONS FOR COMPUTATION
ENTRY TEST CASE/INCOMPRESSIBLE

Case #0441; Data Evaluator: A. Wadcock

Data Takers: A. Wadcock and D. Coles

PICTORIAL SUMMARY

Flow 0440. Data Evaluator: A. Wadcock. "Two-Dimensional Stalled Airfoil."

Case Data Taker	Test Rig Geometry	dp/dx of C _p	Number of Stations Measured								Re	Ini- tial Condi- tion	Other Notes
			Mean Velocity		Turbulence Profiles					C _f			
			U	V or W	$\overline{u^2}$	$\overline{v^2}$	$\overline{w^2}$	\overline{uv}	Others				
Case 0441 D. Coles A. Madcock	 $0.62 \leq x/c \leq 2.00$ $\Delta s/c = 0.0111$	Mean sur- face pres- sure	125	125	125	125	-	125	Inter- mit- tency	-	1.5×10^6 (based on air- foil chord)	Free stream turb. level < 1.5%	Aspect ratio = 2. Probe interference present for attached boundary layer data—separated zone and wake is interference- free.

Plot	Ordinate	Abscissa	Range/Position	Comments
1	C _p	100 x/c	$0 \leq 100 \ x/c \leq 100$ $-8.0 < C_p < 1.0$	Upper and lower surface pressure.
2	y/c	U/U _{ref}	$-0.13771 < y/c < 0.517$	4 curves at x/c = 0.642, 0.908, 1.1747, and 1.95146 (IX = 52, 76, 100, 170).
3	y/c	V/U _{ref}	$-0.13771 < y/c < 0.517$	4 curves at x/c = 0.642, 0.908, 1.1747, and 1.95146 (IX = 52, 76, 100, 170).
4	y/c	$\overline{u^2}/U_{ref}^2$	$-0.13771 < y/c < 0.517$	4 curves at x/c = 0.642, 0.908, 1.1747, and 1.95146 (IX = 52, 76, 100, 170).
5	y/c	$\overline{v^2}/U_{ref}^2$	$-0.13771 < y/c < 0.517$	4 curves at x/c = 0.642, 0.908, 1.1747, and 1.95146 (IX = 52, 76, 100, 170).
6	y/c	\overline{uv}/U_{ref}^2	$-0.13771 < y/c < 0.517$	4 curves at x/c = 0.642, 0.908, 1.1747, and 1.95146 (IX = 52, 76, 100, 170).

Special Instructions:

Definition of Special Symbols: c = chord; q_{inf} = dynamic pressure far upstream (model absent); q_{ref} = dynamic pressure in uniform flow (model present); U_{inf} = velocity in uniform flow (model absent), U_{ref} = velocity in uniform flow (model present); C_p = (p - p_{ref})/q_{ref}.

The data for this case are defined with respect to cartesian coordinates with the horizontal axis aligned with the airfoil chord and the origin at the airfoil leading edge. The data are contained in a two-dimensional grid with indices IX and IY with ranges

$$1 \leq IX \leq 175$$

$$1 \leq IY \leq 296$$

x/c and y/c are related to IX and IY by

$$x/c = (6.86 + IX - 1)/90.117$$

$$y/c = (-62.05 + IY - 1)/[(5)(90.117)]$$

The calculated static pressure distribution on the surface of a two-dimensional NACA 4412 airfoil at an angle of attack of 13.87° , mounted between parallel walls in the configuration shown in Fig. 1, should be compared with the measured pressure distribution at a Reynolds number (based on chord) of 1.5×10^6 . (See data on file for the airfoil geometry and C_p .)

Computors are free to set up the boundary conditions for this test case to best suit their flow-calculation method. However, they should note the finite blockage effects of the walls on the airfoil flow in the experiment. The boundary-layer growth on the wind-tunnel walls and the tunnel-wall-pressure distribution were not measured. Appropriate approximations to the starting values of δ^* , θ , and C_f at the entrance to the test section must therefore be introduced in calculation methods which set out to predict the complete flow field in the test section including the boundary-layer growth along the tunnel walls and the wall-pressure distribution.

In order to check the suitability of the chosen boundary conditions (whether from a blockage calculation or other bases) trial runs can be made of the predicted free-stream velocity distribution and compared with the measured free-stream velocity distributions on the line shown in Fig. 1 (data presented in Table 1). (The values U/U_{ref} and V/U_{ref} have been taken from the data on file). The position at which U_{ref} was measured is also shown in Fig. 1. Note that the velocity components given in the table are in the flow field above the upper surface of the airfoil, whereas U_{ref} is measured at a location below the lower surface of the airfoil. X and Y are measured along and normal to the chord line, respectively. Computors should report basis used with results.

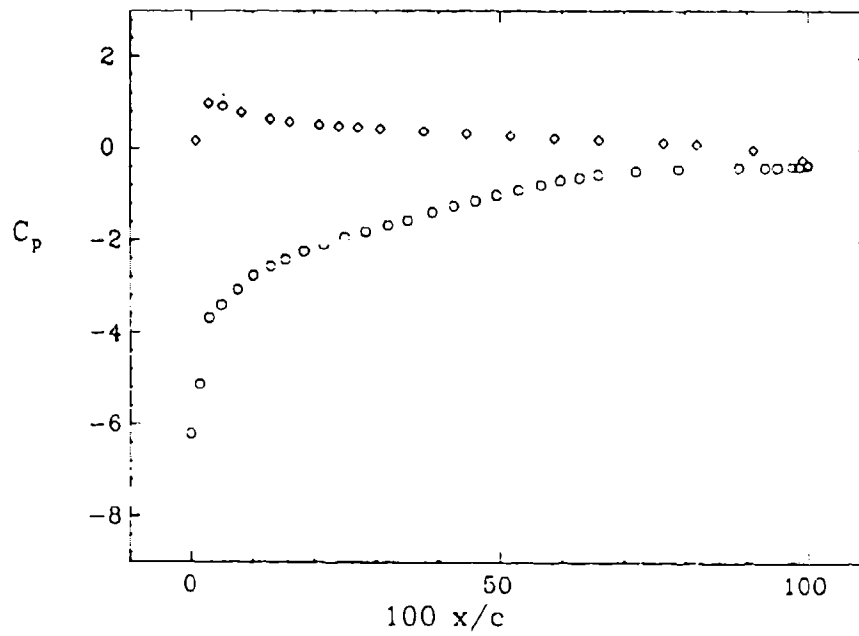
When a satisfactory prediction of the free-stream velocity distribution has been achieved in the vicinity of this line proceed with the calculation of the pressure distribution around the airfoil.

It should be noted that data on file are presented in a coordinate system aligned with the airfoil chord. Computation of quantities applicable to another coordinate system (i.e., local boundary-layer coordinates) such as δ^* , ρ , and C_f are not requested since computers who do not calculate individual normal stresses will be unable to transform Reynolds-stress data from one coordinate system to another.

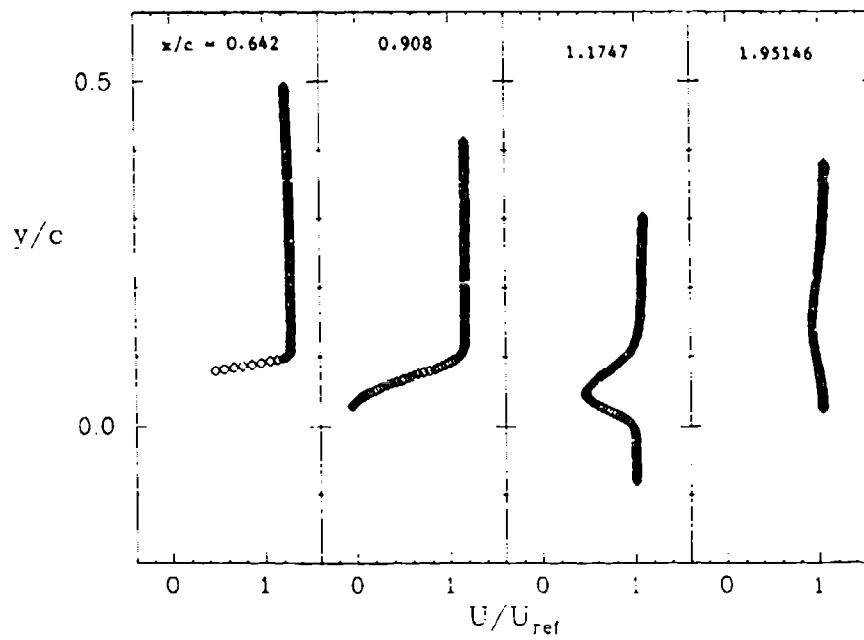
Table 1
The Values of the Measured Velocity Components in the Freestream
at Selected Positions (Wadcock, 1970)

x (m)	y (m)	U/U _{ref}	V/U _{ref}
0.6086	0.1039	1.2243	-0.0414
0.8086	0.1439	1.1688	0.0024
0.9586	0.1719	1.1102	0.0167
1.1086	0.1919	1.0532	0.0650
1.2586	0.2159	1.0485	0.1093
1.4586	0.2639	1.0523	0.1464
1.6586	0.3259	1.0532	0.1894

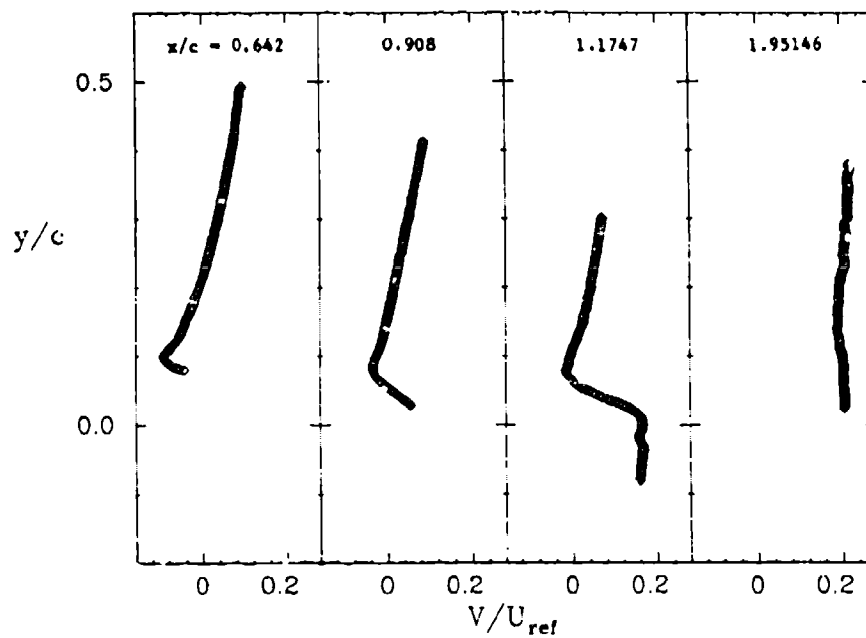
PLOT 1 CASE 0441 FILE 3



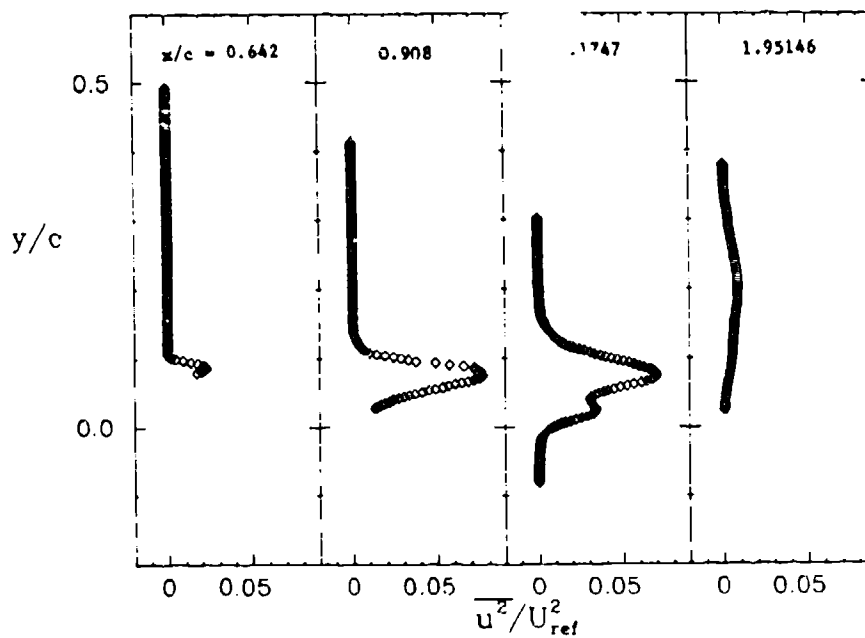
PLOT 2 CASE 0441 FILE 4



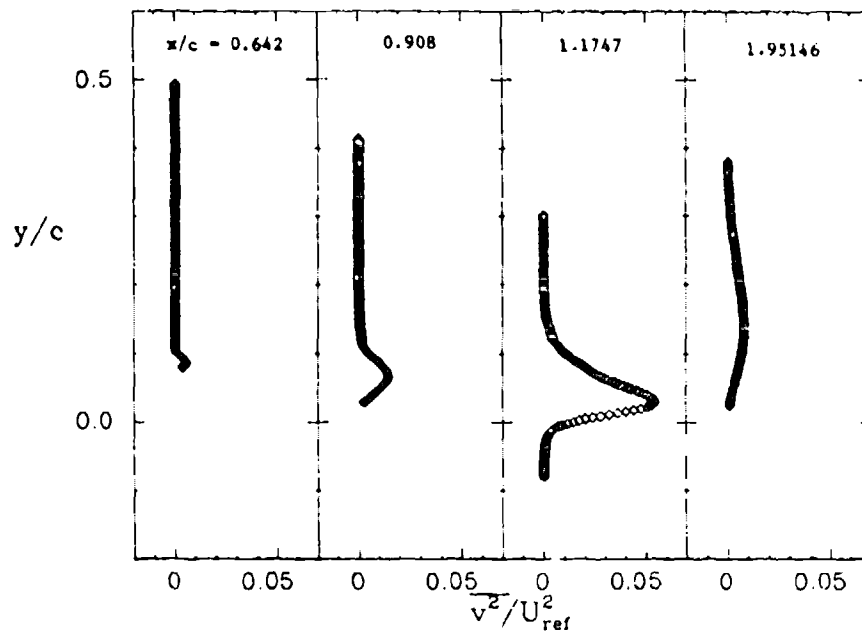
PLOT 3 CASE 0441 FILE 4



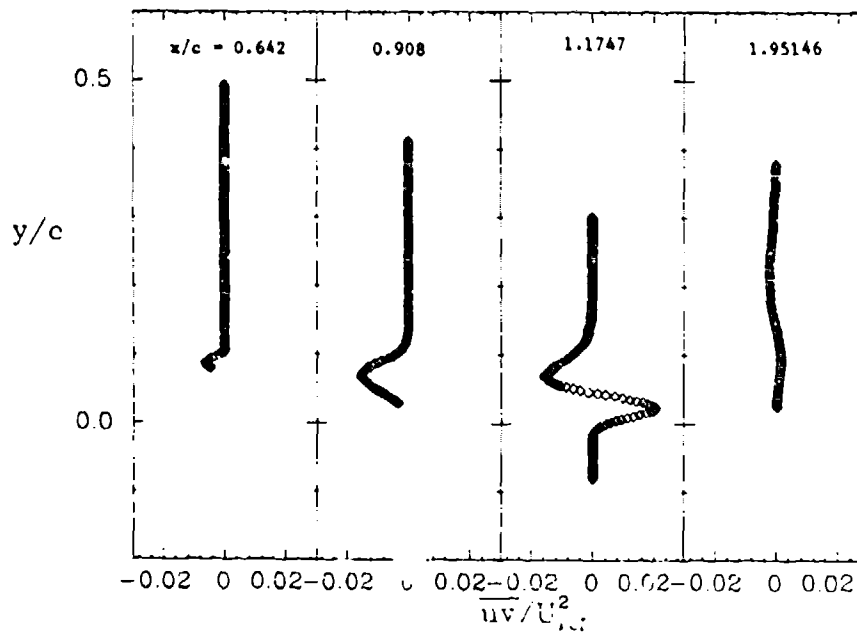
PLOT 4 CASE 0441 FILE 4



PLOT 5 CASE 0441 FILE 4



PLOT 6 CASE 0441 FILE 4



DIFFUSER FLOWS, UNSEPARATED

Flow 0140

Cases 0141, 0142, 0143

DIFFUSER FLOWS, SEPARATED

Flow 0430, Case 0431

Evaluator: P. L. Simpson*



SUMMARY

Several ground rules were used initially in this evaluation in addition to the Guidelines for Data Evaluation supplied by the Organizing Committee: (1) no new evaluation of any flow evaluated by Cole; and first has been made; (2) no flow that contained additional effects such as wall curvature, heated or cooled walls, roughness, high free-stream turbulence level, etc. has been considered; (3) no flow with only pitot-static tube measurements has been considered. Since hot-wire and laser anemometer data are available and are more informative, there is no reason to consider flows with only this type of measurement.

Only experiments where the entrance boundary layer was rather thin were considered. It is well known, however, that diffuser performance significantly depends on inlet blockage, that is on the normalized displacement thickness of the entrance flow. It is also known that calculations of diffuser flows by conventional boundary-layer procedures often agree quite well with measurements if the displacement thickness at the entrance is small, but very poorly if it is large. Because of these reasons, experimental results for thicker entry boundary layers are needed as test cases for calculation methods. This reviewer is unfortunately not aware of any such data for two-dimensional diffusers of an equally high standard as the available small entrance-blockage cases.

This survey indicates that one two-dimensional strong adverse pressure gradient flow without separation and one flow with separation are documented well enough to be used.

Initially only two-dimensional diffuser flows were considered, but later the evaluation review committee brought attention to several high-quality axisymmetric flows. Since A. Klein of MTU (Munich) had done a large amount of careful cross-checking of data for conical diffusers, his opinions on available axisymmetric diffuser data were weighed heavily.

*Southern Methodist University, Dallas, Texas 75275.

Case 0141. A. E. Samuel and P. N. Joubert (1974).

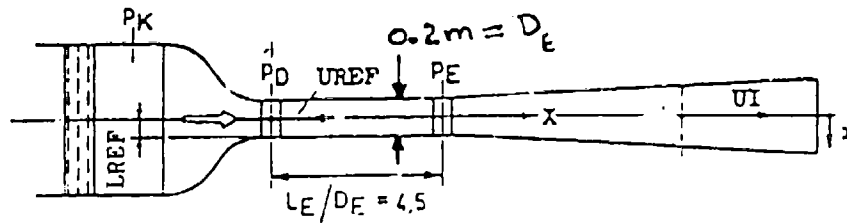
This case is very good for several reasons. $dp/dx > 0$ and $d^2p/dx^2 > 0$ which occurs in many practical cases, whereas most other data are for $dp/dx > 0$ and $d^2p/dx^2 < 0$.

This experiment was performed in a 2.5-m long region of a flexible-roof tunnel with a finely controlled streamwise pressure distribution. The flow has a strong enough pressure gradient that it appears to be approaching separation at the end of the working region, but no separation is present. The two-dimensional nature of the flow field was checked by momentum balance and velocity traverse on either side of the working section centerline. The skin-friction term and the summed momentum and pressure terms of the integrated form of the momentum integral equation differed no more than 19%, and commonly differed by less than 14%. The off-centerline velocity profiles were indistinguishable from those on the centerline. Hot-wire measurements of $\overline{u^2}$, $\overline{v^2}$, $\overline{w^2}$, $-\overline{uv}$, u spectra are presented; pitot-tube measurements are for U . The hot-wire equipment and techniques are well documented. The spectral results behave similar to the data of Klebanoff. The surface-skin-friction floating balance and Preston-tube techniques that were used are well documented with very good agreement among results. The pressure coefficient C_p was obtained from static taps on the tunnel centerline during a few hours; dC_p/dx was obtained from a special pressure-gradient probe during a period of a few days. Fluctuations in p and ρ were small; ρ was corrected for pressure and temperature changes, but not humidity; d^2C_p/dx^2 was obtained by differentiation of a smoothed dC_p/dx curve.

Cases 0142 and 0143. R. Pozzorini (1976).

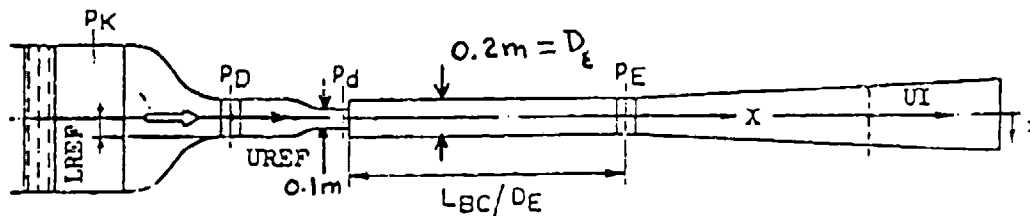
These measurements were made on a 6°-included-angle conical diffuser with an area ratio of 4. They are probably the most thorough diffuser experiments conducted to date according to A. Klein. Mean velocities were measured with pitot tubes, static-pressure probes, and a hot-wire anemometer. Shear and turbulence corrections were applied to the pitot-static data and corrections for large turbulence were applied to the hot-wire data, which included the three Reynolds normal stresses and the Reynolds shearing stress. C_f was determined by a Preston tube. Special merits of these data are: a very careful control of entrance conditions and a special search of flow asymmetry and avoidance of errors resulting from it. Experiments were conducted for three different entrance boundary-layer thicknesses: (a) thin (the potential core extends well to the diffuser exit), (b) medium (the potential core vanishes at the diffuser exit), (c) thick (the potential core is absent over most of the diffuser length).

The low-core turbulence flow with $L_E/D_E = 4.5$ and $P_K - P_D \approx 100$ mm of water should be used for Case 2 since the boundary layer at the beginning of the diffuser is developed, but still thin, and the potential core extends to the diffuser exit.



Case 0142. Pozzorini low-core turbulence flow.

The high-core turbulence flow (Pozzorini Case 3) with $LBC/DE = 7.25$ and $P_K - P_D = 25$ mm of water should be used as Case 0143, which shows marked influence of freestream turbulence.



Case 0143. Pozzorini high-core turbulence flow.

Case 0431. R. L. Simpson, Y.-T. Chew, B. G. Shivaprasad (1980).

This experiment was performed on the flat wooden bottom wall of a constant-width, variable-height, converging-diverging channel, 4.9 m long. Mean-flow and fluctuation quantities were obtained for an incompressible turbulent boundary layer undergoing separation. Complete pressure-gradient relief was not achieved in the downstream region where backflow near the wall occurred all of the time. The streamwise free-stream velocity distribution was obtained with the normal hot-wire probe mounted on a cart that was transversed in the streamwise direction. To obtain dU_e/dx at a given streamwise location, a quadratic least-squares fit to upstream and downstream data was differentiated and evaluated at that location. Active suction and tangential injection control of the side- and top-wall boundary layers was used to promote mean-flow two-dimensionality. The skin-friction terms and the summed momentum, pressure, and normal stresses terms of the integrated form of the momentum integral equation differed no more than 20%, and differed less than 16% over 80% of the length upstream of separation. The normal stresses term was important after the beginning of separation. In regions without intermittent backflow, the flow field was surveyed with hot-wire

anemometers for U , $\overline{u^2}$, $\overline{v^2}$, \overline{uv} , skewness, flatness. Fraction of time flow moves downstream, and fraction of time flow away from the wall were obtained within estimated uncertainties in regions where both techniques are valid. Measurements at the downstream end of the separated flow are available as boundary conditions on the flow. $\overline{w^2}$ measurements will be available in another Project SQUID report later in 1980.

ADVICE FOR FUTURE DATA-TAKERS

Diffuser flows with and without separation have been studied for a number of years, with most data sets being tainted with some shortcoming. Mean-flow three-dimensionality, uncertainty in the skin-friction measurements as separation is approached, insufficient documentation of and repeatability of the streamwise pressure gradient over the duration of the experiments, the use of directionally insensitive velocity measurement instrumentation are the common deficiencies. The Samuel and Joubert flow is as free of these deficiencies as humanly possible for a flow without separation. The technology is now available to overcome the previous measurement deficiencies and make acquisition of better data more routine. Computers can be used to eliminate the drudgery and exasperation that are encountered when a large amount of careful data are needed.

Directionally sensitive laser anemometers should be used for velocity measurements whenever any backflow or large spanwise turbulence is present. There is no reliable way to calibrate or correct the directionally insensitive hot-wire for these effects (Simpson, 1976). It is a waste of effort to obtain hot-wire data in the presence of backflow. The existence of such hot-wire data and the sparse amount of laser anemometer data currently available often tempt computers to compare their results with these invalid hot-wire data. Such comparisons lead to more confusion. All future data obtained with hot-wire anemometers in the presence of a widely changing instantaneous flow direction should be totally rejected.

Unfortunately laser anemometry is expensive to use and requires some time to master. By the time most graduate students become competent to use it, they finish their studies, having produced only a small amount of useful data. There is the distinct need for future diffuser research to be conducted by organizations that use laser anemometry professionally with long-term personnel.

The Rubesin et al. (1975) surface hot wire on a polystyrene substrate is a superior surface-heat-transfer skin-friction gage to anything else. It can be calibrated in laminar flow and used in turbulent flow with and without pressure gradients. It is easy to manufacture and use, so inexperienced graduate students who do nearly all such experiments can use this device successfully.

Mean-flow three-dimensionality plagues all separating turbulent boundary layers to some degree. The size of the large-scale turbulent structures becomes a sizable

fraction of the spanwise width of the flow channel at some location downstream of separation, so no two-dimensional mean flow is possible--a cellular structure strongly influenced by the side walls is probable. Several investigators believe that experiments in axisymmetric diffusers eliminate this problem, but this is not entirely true. It is clear that the peripheral variation in the flow may be nearly eliminated in an axisymmetric diffuser. However, at some streamwise location the radial and peripheral dimensions of the large-scale turbulent structures approach the radius of the diffuser. Then the flow structure is influenced by the geometrical constraints. Adjacent large-scale structures do not interact with one another as they would in a two-dimensional geometry. A cellular structure may also be produced. Data on the three-dimensional nature of separated diffuser flows are clearly needed, but will be obtained after the data-gathering task has been made less laborious.

The pressure-gradient distribution strongly influences the flow development so it is important that the pressure-gradient distribution be repeatable and thoroughly documented throughout the course of an experiment.

REFERENCES

- Pozzorini, R. (1976). "Das turbulente Strömungsfeld in einem langen Kreiskegel-Diffusor." Ph.D. Dissertation 5646, Eidgenössischen Technischen Hochschule Zürich, Ed. Truninger AG, Zürich.
- Rubesin, M. W., A. F. Okuno, G. G. Mateer, A. Brosh (1975). "A hot-wire surface gauge for skin friction and separation detection measurements," NASA TM X-62 465.
- Samuel, A. E. and P. N. Joubert (1974). "A boundary layer developing in an increasingly adverse pressure gradient," J. Fluid Mech. 66:481-505.
- Simpson, R. L. (1976). "Interpreting laser and hot-film anemometer signals in a separating boundary layer," AIAA Jou., 14:1, 124-126.
- Simpson, R. L., Y.-T. Chew, and B. G. Shivaprasad (1980). "Measurements of a separating turbulent boundary layer." Project Squid Rep. SMU.4, Purdue University.

DISCUSSION

Flows 0140, 0430

1. It was recommended that Case 0141 be designated "Boundary layer in an adverse pressure gradient."
2. It was suggested that Cases 0142 and 0143 be considered either
 - (a) as a diffuser flow of given geometry, or
 - (b) as a boundary layer flow using a given pressure distribution.*
3. It was suggested that Case 0431 will not be possible to compute as a boundary layer flow. It is therefore necessary to provide the computer with details of a streamline in the outer flow as an alternative to the pressure specification.†

The following additional comment was received after the 1980 Conference:

4. A question concerning the Samuel, Joubert flow, Case 0141, has been raised by John Moore. The data at $x = 2.9$ m and $x = 3.4$ m show disagreement between the values of U_e and velocity computed from the recorded values of C_p . We have queried Peter Joubert on this point and he confirms that the effect is real and has been encountered by other investigators in locations where the usual boundary-layer approximations do not apply. He notes that they did not use the wall pressure to find U_e but that a pitot-static tube was used to measure this quantity directly. Moreover, normal stress data are available in the data file and can be used together with the data for U_e to check the measured wall pressure.

*[Ed.: This recommendation has not been followed since a review of the complete data set for the 1981 computations indicated sufficient boundary-layer cases are available without it.]

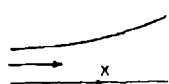
†[Ed. (SJK): We have computed this flow successfully as a boundary-layer flow. Success, in our view, depends on appropriate modeling of a detachment zone in transitory stall, but the data are entirely adequate at least for the method given by J. Bardina, A. Lyrio, S. J. Kline, J. H. Ferziger, and J. P. Johnston (to be published in J. Fluids Engrg.)

SPECIFICATIONS FOR COMPUTATION
SIMPLE CASE/INCOMPRESSIBLE

Case #0141; Data Evaluator: R. L. Simpson
Data Takers: A. Samuel and P. Joubert

PICTORIAL SUMMARY

Flow 0140. Data Evaluator: R. Simpson. "Diffuser Flowa (unseparated)."

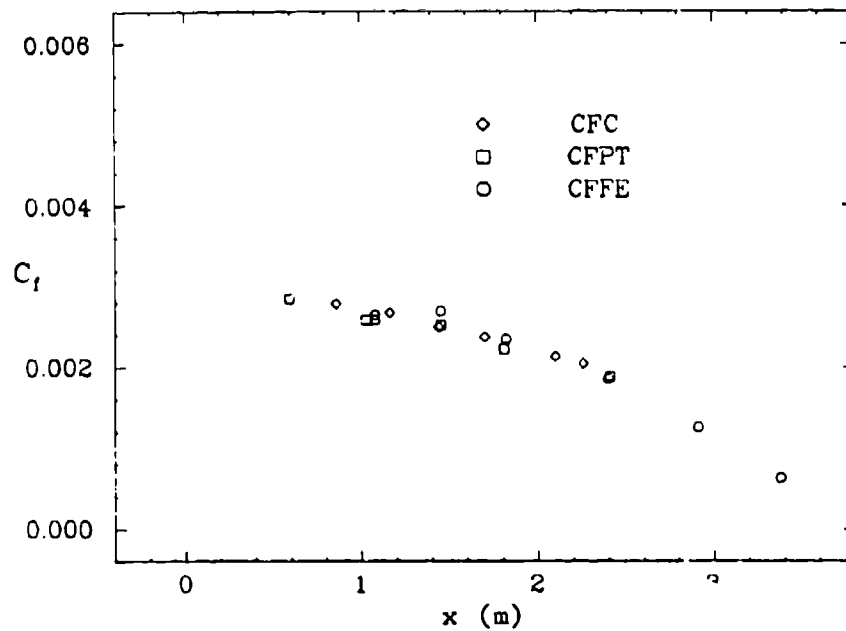
Case Data Taker	Test Rig Geometry	dp/dx or C _p	Number of Stations Measured								C _f	Re	Initial Cor.	Other Notes
			Mean Velocity		Turbulence Profiles									
			U	V or W	$\overline{u^2}$	$\overline{v^2}$	$\overline{w^2}$	\overline{uv}	Other					
Case 0141 A. Samuel P. Joubert		$\frac{dp}{dx} > 0$ $\frac{d^2p}{dx^2} > 0$	12	-	6	6	6	6		Floating balance, Preston tube, Clauser plots	1.76×10^6 per m	Turbu- lence Inten- sity 0.3%	Two-dimensionality was checked.	

Plot	Ordinate	Abscissa	Range/Position	Comments
1	C _f	x	$1.04 \leq x \leq 3.39$ m	
2	y	(\overline{uv}/U_e^2)	$0 \leq y \leq 0.040$ m	3 curves at x = 1.04, 1.44, 1.79 m.
3	y	\overline{uv}/U_e^2	$0 \leq y \leq 0.040$ m	3 curves at x = 2.38, 2.89, 3.39 m.
4	y	U/U _e	$0 \leq y \leq 0.10$ m	2 curves at x = 2.87, 3.40 m.

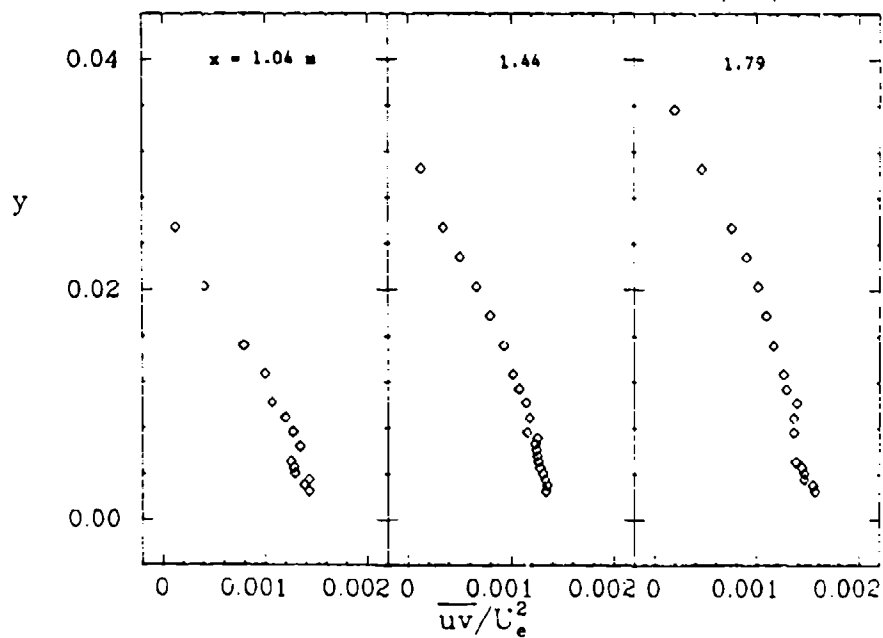
Special Instruction:

Note C_f is normalized on the reference velocity U_{ref} at x = 0, the first pressure tap, and not the local U_e.

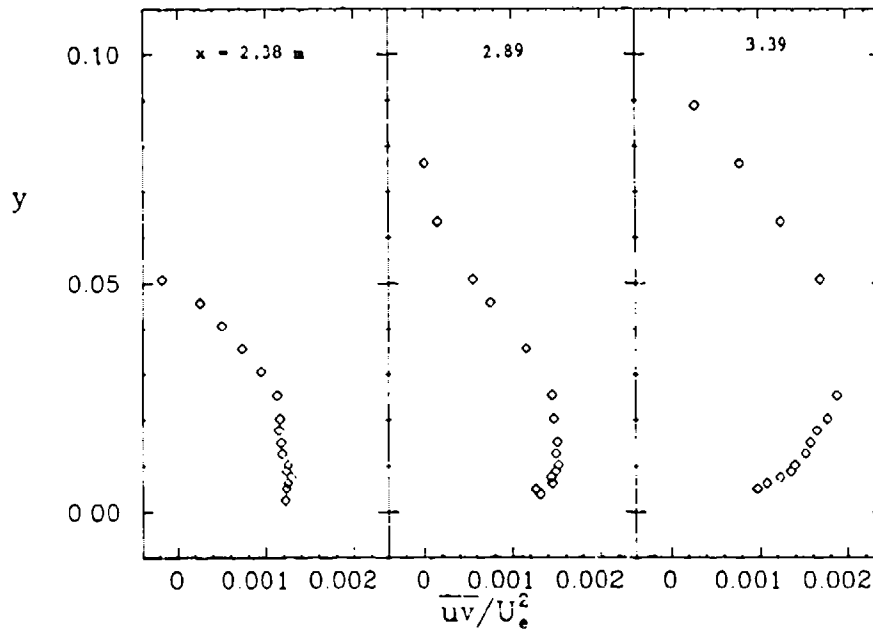
PLOT 1 CASE 0141 FILE 4



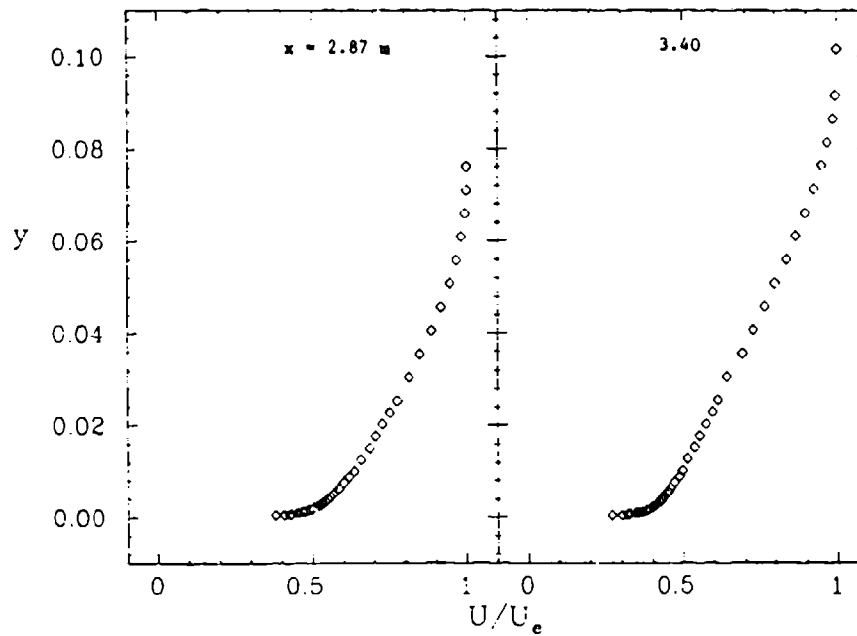
PLOT 2 CASE 0141 FILE 25,26,27



PLOT 3 CASE 0141 FILE 28,29,30



PLOT 4 CASE 0141 FILES 14,16



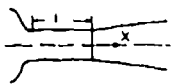
SPECIFICATIONS FOR COMPUTATION

ENTRY CASE/INCOMPRESSIBLE

Case #0142; Data Evaluator: R. L. Simpson
Data Taker: R. Pozzorini (Low-Core Turbulence)

PICTORIAL SUMMARY

Flow 0140. Data Evaluator: R. Simpson. "Diffuser Flows (unseparated)."

Case Data Taker	Test Rig Geometry	dp/dx or C _p	Number of Stations Measured								C _f	Re	Ini- tial Condi- tion	Other Notes
			Mean Velocity		Turbulence Profiles									
			U	V or W	$\overline{u^2}$	$\overline{v^2}$	$\overline{w^2}$	\overline{uv}	Others					
Case 0142 R. Pozzorini	 1/d = 4.5; Area Ratio 4; Cone Angle 6°	> 0	12	12	12	12	12	12	-	Flassee pipe, Pres- ton tube	2.34 x 10 ⁵ (based on inlet pipe radius)	Turbu- lence inten- sity 0.31%	Conical diffuser -core (low turbulence).	

Plot	Ordinate	Abscissa	Range/Position	Comments
1	C _f	x	-0.055 ≤ x ≤ 1.90 m	
2	C _{pw}	x	-0.055 ≤ x ≤ 1.90 m	C _{pw} = (P - P _D) / 1/2 ρ _{ref} U _{ref} ² Ref values and P _D at locations shown on sketch in Summary, Case 0142 above.
3	r	U/U _I	0 ≤ r ≤ D/2	2 curves at x = 0.5723 m and x = 1.813 m (Files 22, 27).
4	r	\overline{uv}/U_I^2	0 ≤ r ≤ D/2	5 curves at x = -0.055, 0.1908, 0.5723, 1.049, 1.813 m. (Files 16, 19, 22, 24, 27).

Special Instruction:

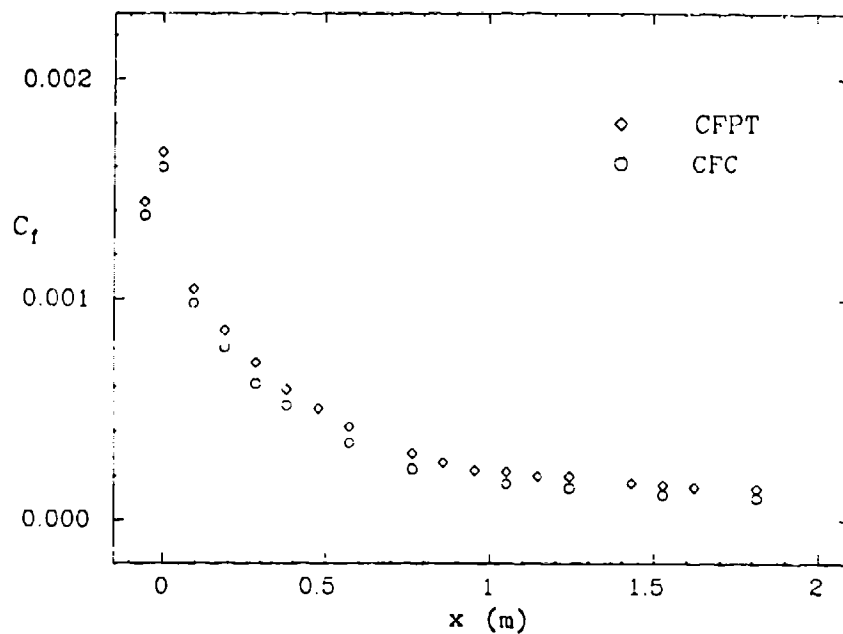
P = wall pressure at given x.

U_I = velocity at tunnel centerline.

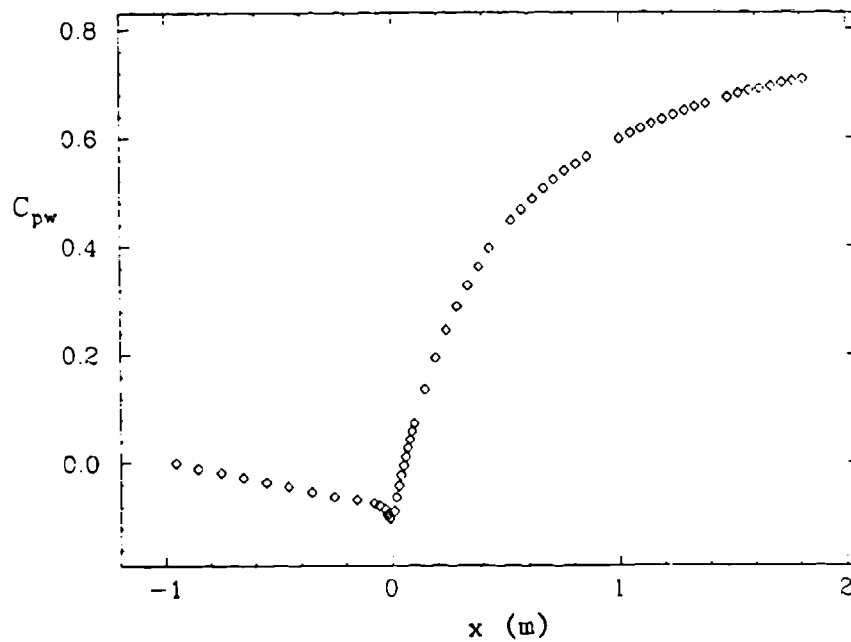
P_D, P_{ref}, U_{ref} are defined in summary.

This case refers to Pozzorini's Case 2 with L_E/D_E = 4.5 and P_K - P_D = 100 mm;
see Summary.

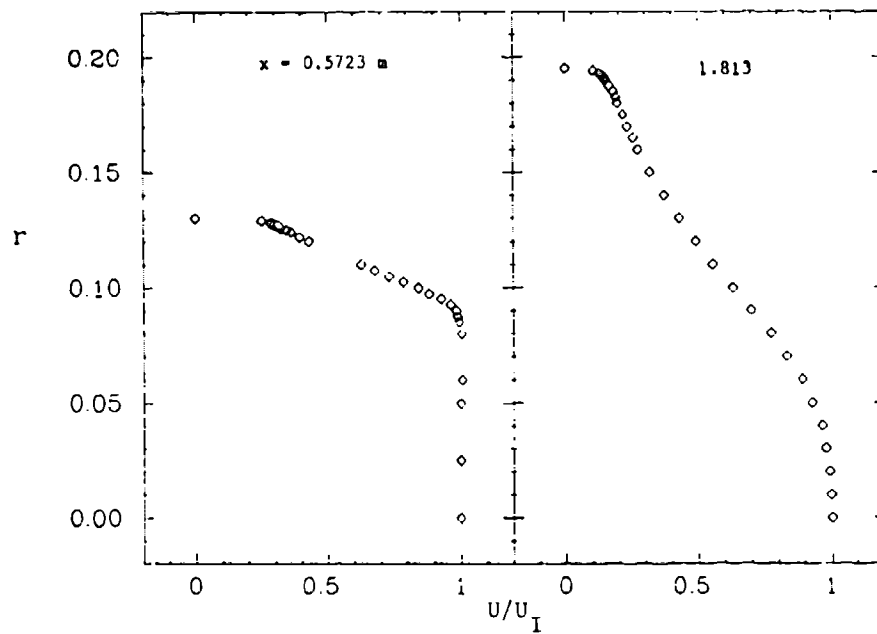
PLOT 1 CASE 0142 FILE 2



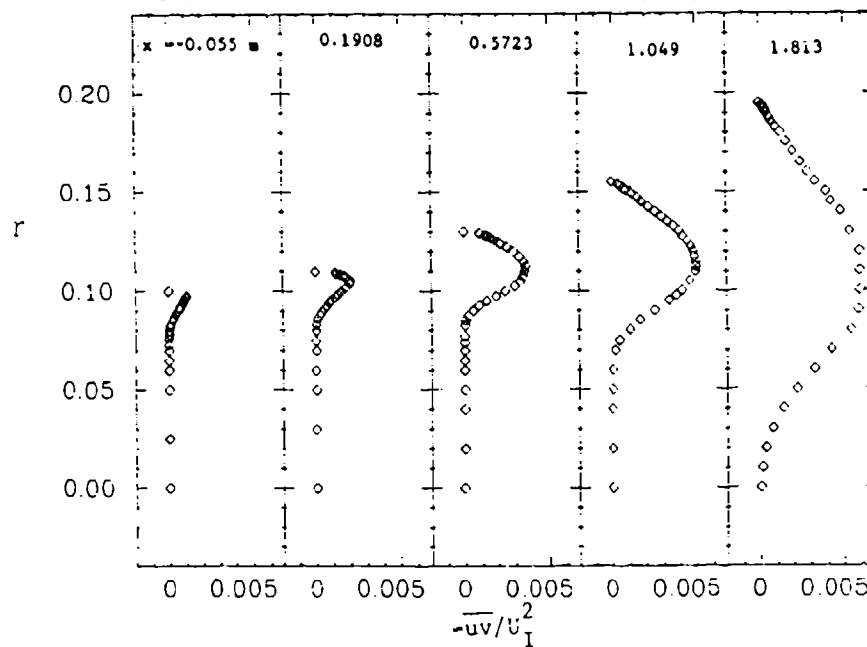
PLOT 2 CASE 0142 FILE 2



PLOT 3 CASE 0142 FILES 22,27



PLOT 4 CASE 0142 FILES 16,19,22,24,27



SPECIFICATIONS FOR COMPUTATION

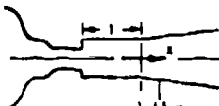
ENTRY CASE/INCOMPRESSIBLE

Case #0143; Data Evaluator: R. L. Simpson

Data Taker: R. Pozzorini (High-Core Turbulence)

PICTORIAL SUMMARY

Flow 0140. Data Evaluator: R. Simpson. "Diffuser Flows (unseparated)."

Case Data Taker	Test Rig Geometry	dp/dx or C _p	Number of Stations Measured								E _h	Initial Condi- tion	Other Notes
			Mean Velocity		Turb. Profiles								
			U	V or W	$\overline{u^2}$	$\overline{v^2}$	$\overline{w^2}$	\overline{uv}	Others	C _f			
Case 0143 S. Pozzorini	 1.45 m 1.81 m 1/d = 7.25; Area Ratio 4; Cone Angle 6°	> 0	5	6	6	6	6	6	-	Elasmer plots, Pres- ton tube	1.27 + 105 (based on inlet pipe radius)	Turbu- lence inten- sity 18%	Conical diffuser —core (high turbulence).

Plot	Ordinate	Abscissa	Range/Position	Comments
1	C _f	x	-0.055 ≤ x ≤ 1.90 m	
2	C _{pw}	x	-0.055 ≤ x ≤ 1.90 m	C _{pw} = (P - P _D) / 1/2 ρ _{ref} U _{ref} ² Ref values, P _D at locations shown on sketch in Summary, Case 0143 above.
3	r	U/U _I	0 ≤ r ≤ D/2	2 curves at x = 0.5723, x = 1.813 m. (Files 37, 39).
4	r	\overline{uv}/U_I^2	0 ≤ r ≤ D/2	5 curves at x = -0.055, 0.0953, 0.5723, 1.049, 1.813 m. (Files 35, 36, 37, 38, 39).

Special Instruction:

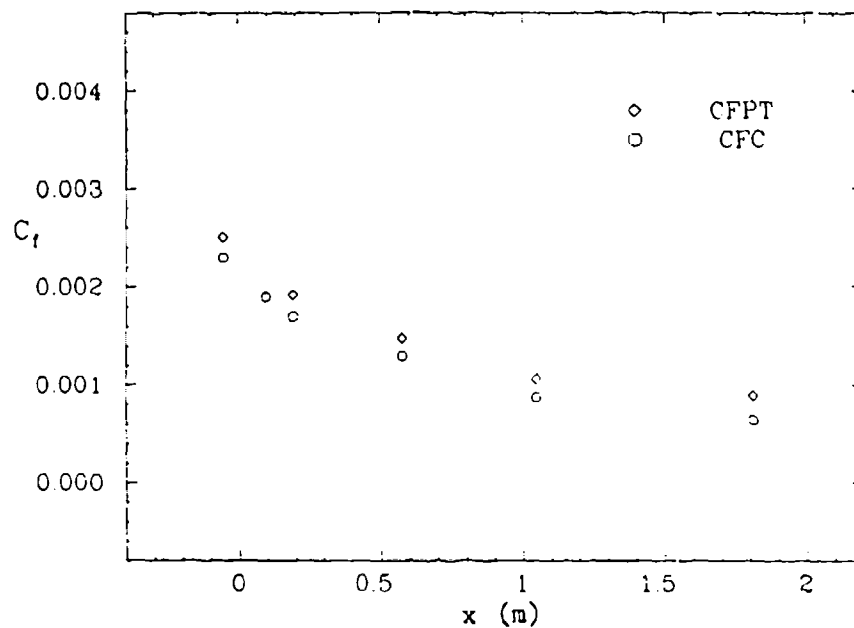
P = wall pressure at given x.

U_I = velocity at tunnel centerline.

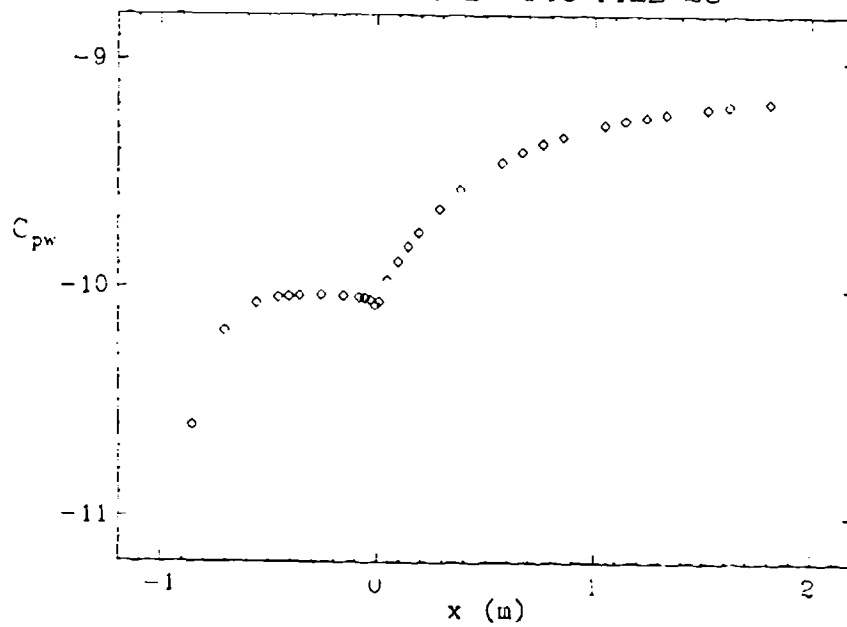
P_D, P_{ref}, U_{ref} are defined in summary.

This case refers to Pozzorini's Case 3 with L_{BC}/D_E = 7.25, P_K - P_D = 25 mm of water; see Summary.

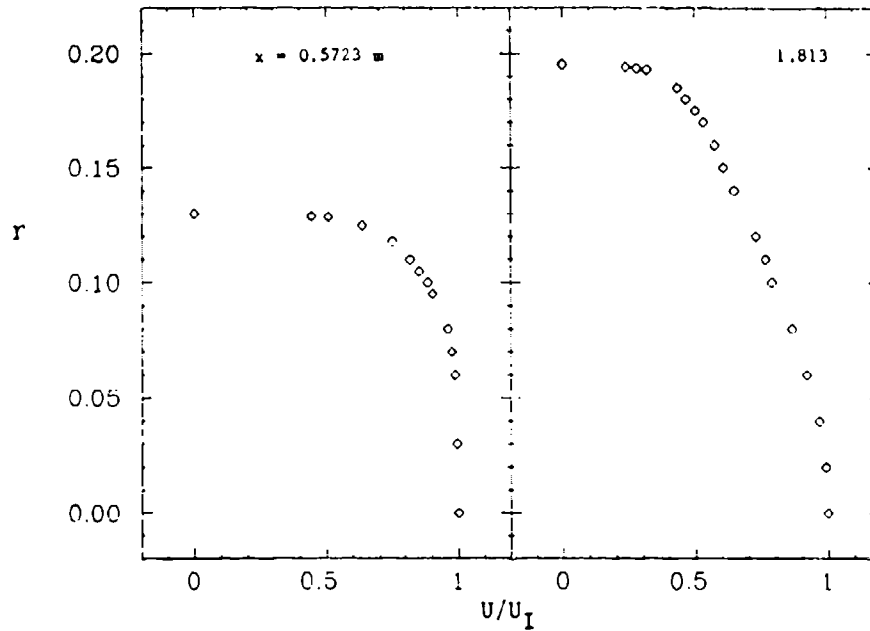
PLOT 1 CASE 0143 FILE 28



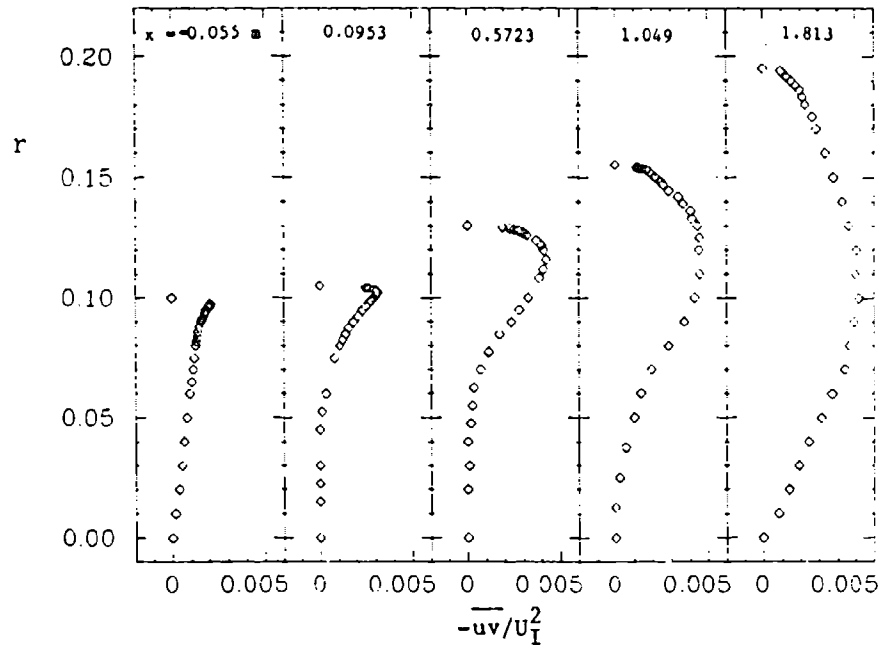
PLOT 2 CASE 0143 FILE 28



PLOT 3 CASE 0143 FILES 37,39



PLOT 4 CASE 0143 FILES 35,36,37,38,39




SPECIFICATIONS FOR COMPUTATION
ENTRY CASE/INCOMPRESSIBLE

Case #0431; Data Evaluator: R. L. Simpson
Data Taker: R. Simpson, Y.-T. Chew, B. G. Shivaprasad

PICTORIAL SUMMARY

Flow 0430. Data Evaluator: R. Simpson. "Diffuser Flow (Separated)."

Case Data Taker	Test Rig Geometry	dp/dx or C _p	Number of Stations Measured								C _f	Re	Ini- tial Condi- tion	Other Notes
			Mean Velocity		Turbulence Profiles									
			U	V or W	$\overline{u^2}$	$\overline{v^2}$	$\overline{w^2}$	\overline{uv}	Others					
Case 0431 R. Simpson Y. Chew B. Shivaprasad		< 0 up stream of throat > 0 down- stream	21*	-	21*	11*	6*	11*		Pres- ton tube	1.07 x 10 ⁶ per m	Turbu- lence inten- sity 0.11	Platens, skewness, and fraction of time flow moves downstream is available. Two-dimensionality was checked. Position of an inviscid streamline near the upper wall is given.	

*Hot-wire measurement.

†Laser Doppler measurement.

Plot	Ordinate	Abscissa	Range/Position	Comments
1	$C_{f,LT}$	x	$0.905 \leq x \leq 4.34$ m	
2	y	\overline{uv}/U_0^2	$0 \leq y \leq \delta$	3 curves at x = 2.673, 3.327, 3.972 m.
3	y	U/U_0	full channel	5 curves at x = 1.632, 2.197, 2.673, 3.01, 3.286 m.
4	y	U/U_0	full channel	5 curves at x = 3.416, 3.524, 3.680, 3.972, 4.430 m.
5	y	$\overline{u^2}$	full channel	5 curves at x = 1.632, 2.700, 2.673, 3.01, 3.286 m.
6	y	$-\overline{uv}$	full channel	5 curves at x = 3.416, 3.524, 3.680, 3.972, 4.430 m.
7	y	γU	full channel	5 curves at x = 3.416, 3.524, 3.680, 3.972, 4.430 m. $\gamma U \triangleq$ fraction of time flow moves in downstream direction.

Special Instructions:

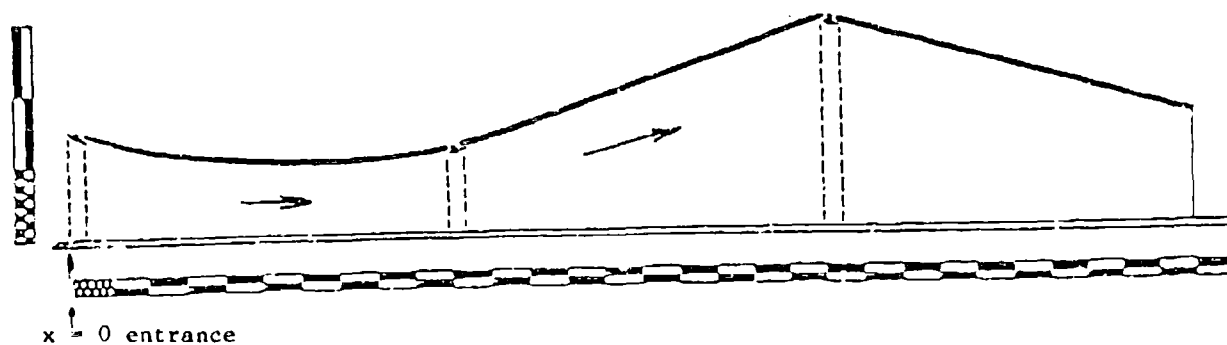
1. In Plot 1, indicate location of computed $C_f = 0$ by an arrow.
2. Start computations at x = 0.805 m; plot from x = 0.905 m. x = 0 is step which trips boundary layer; see sketch 1 below.
3. This flow can be computed parabolically (by inviscid core and boundary layers plus matching) or elliptically as desired by computer groups. If the flow is

done elliptically, the laser data at 4.34 m and the hot-wire data at 4.31 m can be used for downstream data; if these data are so used, they should be specially marked on any output. Computers using parabolic methods can:

- (i) Take the effective streamline near the upper wall as a boundary for the channel. See data attached to this specification as Table 1. Or,
- (ii) Compute boundary layer on upper wall.

The basis employed should be clearly stated in any event.

4. $C_{fLT} = C_f$ based on Ludwig-Tillman correlation.



Sketch 1. Sideview schematic of the test section. Major divisions on scales: 10 inches. Note baffle plate upstream of blunt leading edge on bottom test wall and upper wall jet boundary-layer controls.

Table 1. (Case 0431)
Position of an Inviscid Flow Streamline Near the Upper Wall

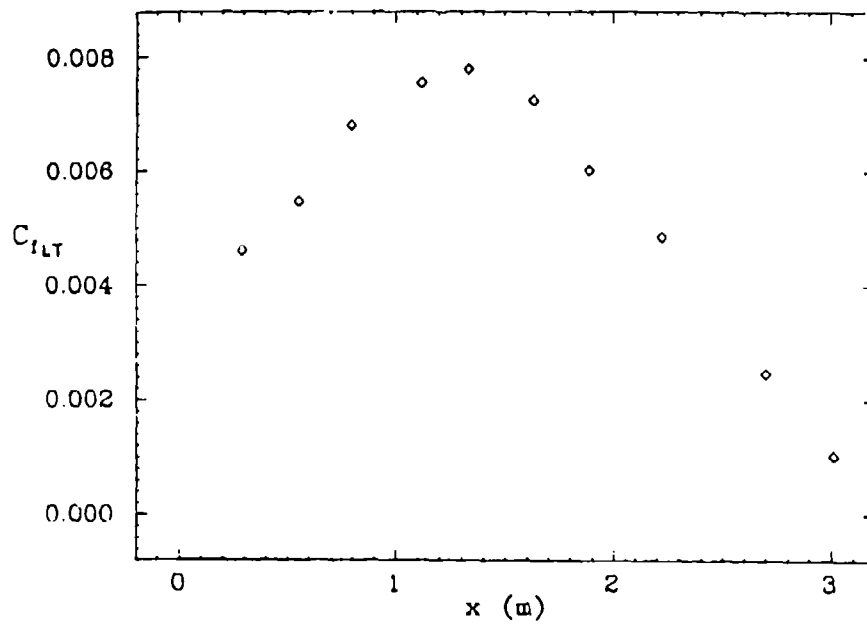
x, meters	y, meters
0.289	0.2541
0.553	0.2314
0.794	0.2118
1.118	0.1954
1.334	1.1879
1.632	0.1881
1.886	0.1933
2.223	0.2042
2.701	0.2355
2.855	0.2535
3.011	0.2731
3.115	0.2894
3.230	0.3099
3.417	0.3473
3.681	0.3935
3.973	0.4565
4.341	0.5149

$Y(x)$ calculated by:

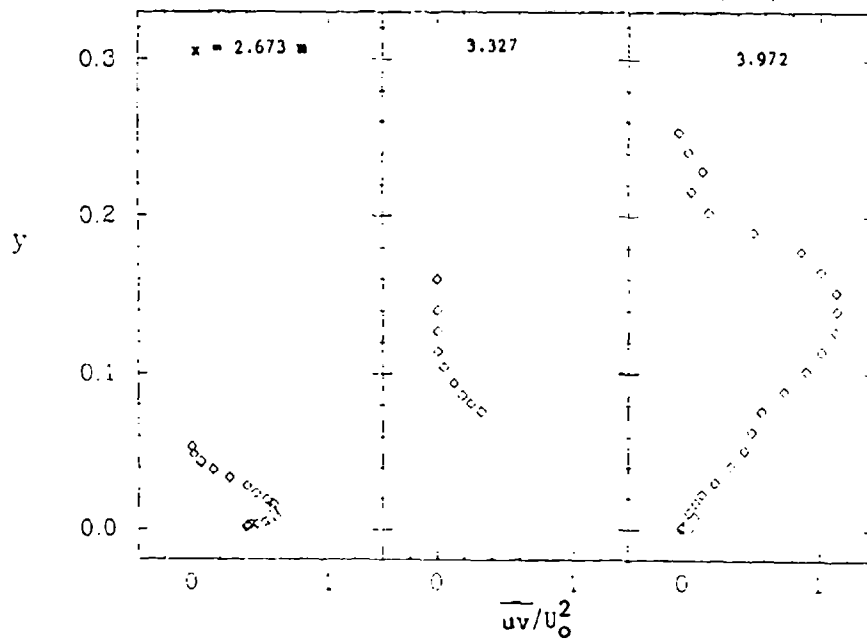
$$U_{\infty}(x) [Y(x) - \delta^*] = \psi = \text{constant}$$

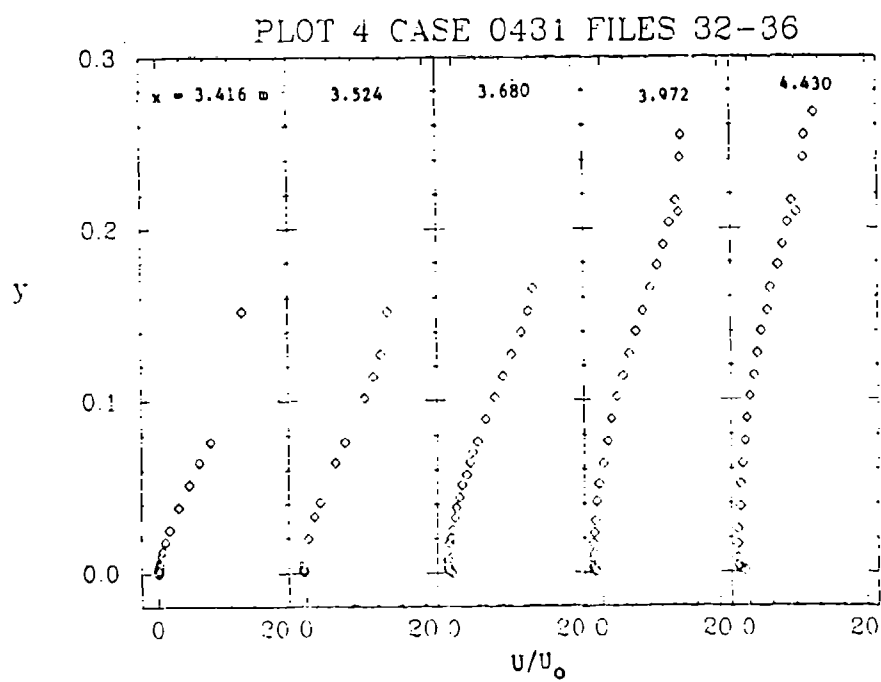
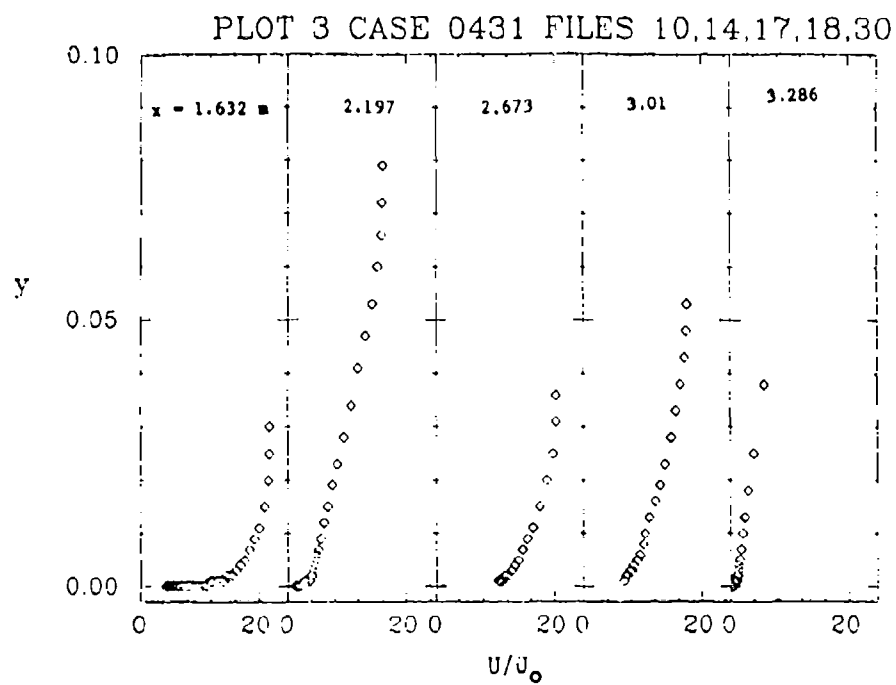
where δ^* is the test wall displacement thickness.

PLOT 1 CASE 0431 FILE 2

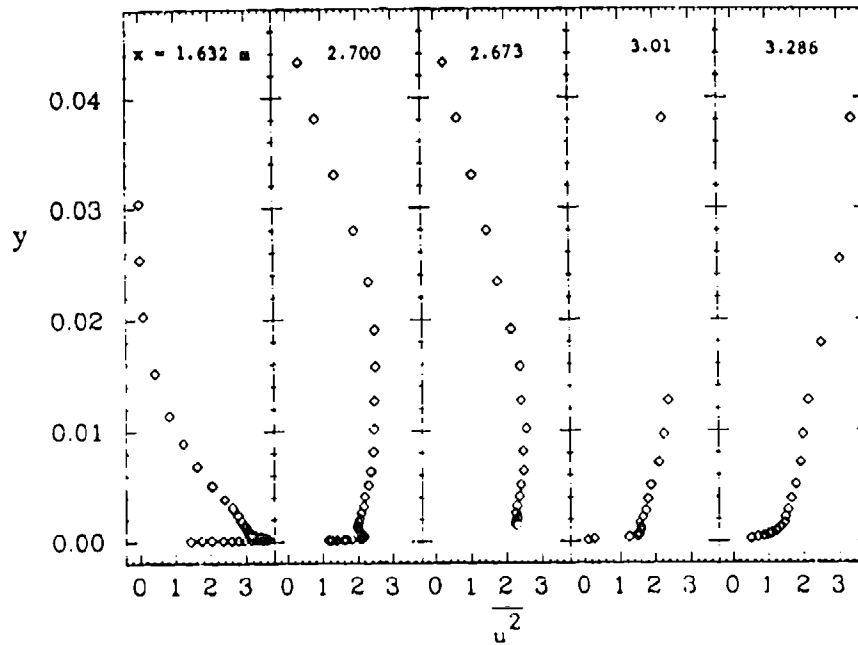


PLOT 2 CASE 0431 FILES 18,21,35

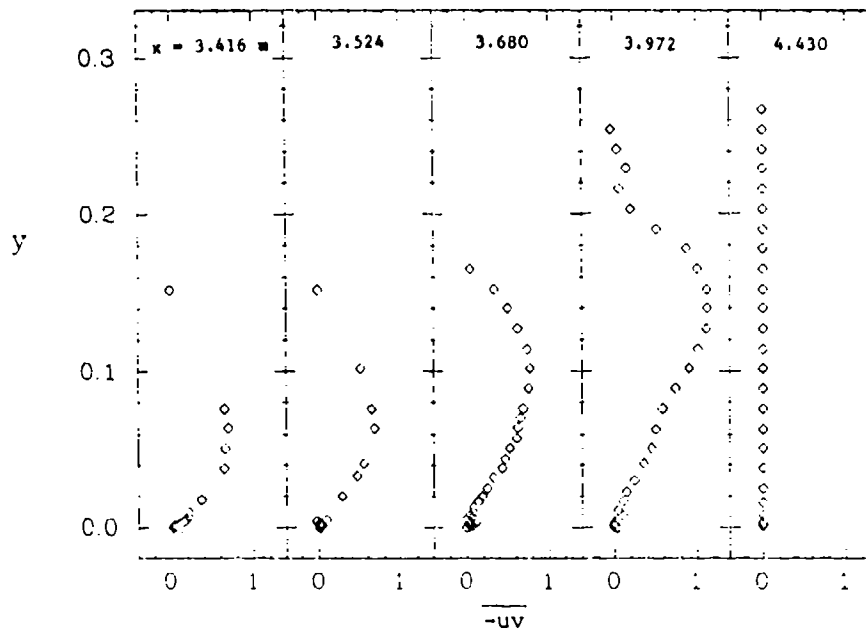


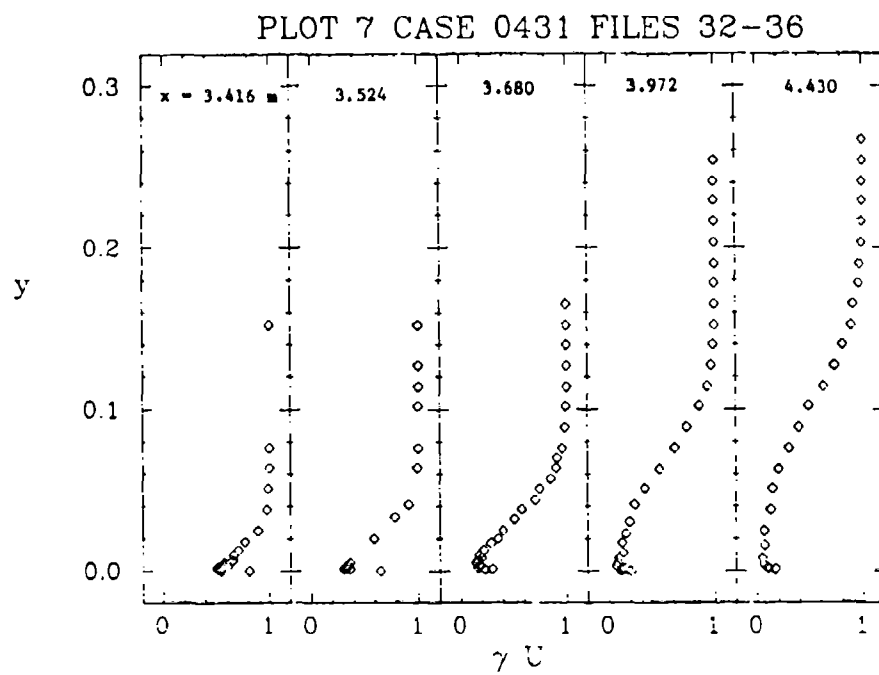


PLOT 5 CASE 0431 FILES 10,13,18,27,30



PLOT 6 CASE 0431 FILES 32-36





SESSION VI

Chairman: E. Reshotko

Technical Recorders:

R. Westphal
D. J. Cockrell



Flow 0420

Predictive Cases:

Flow 0110 and Flow 0420

Flow 9000

Flow 0430

BACKWARD-FACING STEP FLOW

Flow 0420

Case 0421

Evaluators: J. K. Eaton and J. P. Johnston^{*}

SUMMARY

Data sets for subsonic, turbulent flows over two-dimensional backward-facing steps have been evaluated for their suitability as test cases for computational procedures. This report summarizes the procedures and results of the data evaluation. More detailed discussions of the results of the data review may be found in Eaton and Johnston (1980a and b).

SELECTION CRITERIA

The selection criteria are grouped into four general categories: (1) adequacy of instrumentation, (2) adequacy of the experimental facility, (3) completeness of the data, and (4) agreement of the turbulence data with common trends.

(1) A laser anemometer or a pulsed-wire anemometer should be used for mean velocity and turbulence measurements in the separated flow zone. Hot-wire anemometers and pitot tubes may be used downstream of reattachment. Averaging times of 2000-5000 throughflow times should be used for all quantities to minimize scatter.

(2) The flow must be two-dimensional in order to allow accurate comparison with computations. Two-dimensionality should be checked by direct momentum balance. If this is not possible, the step aspect ratio (step span/step height) should be greater than 10 and the spanwise uniformity of the flow should be carefully checked. The boundary layer at separation should be fully turbulent with a momentum thickness Reynolds number of at least 1000. The free-stream turbulence level should be low, 0(0.1%).

(3) The initial condition must be specified, including detailed mean-velocity and turbulence profiles in the boundary layer upstream of separation. Within the zone of separated flow, the data should include profiles of mean velocity \bar{U} , as well as u^2 and uv . Downstream of reattachment, the mean-velocity profiles should be sufficiently detailed to obtain the skin friction from a Clauser plot. Wall static-pressure data should be available, as well as mean-velocity profiles for the boundary layer on the wall opposite the step (if any).

(4) The turbulence intensity and Reynolds shear stress should follow the common trend exhibited by the bulk of the existing data sets. They should both increase

^{*}Dept. of Mech. Eng., Stanford University, Stanford, CA 94305.

downstream of the separation point and then rapidly decay, beginning somewhere near reattachment. The peak value of the Reynolds shear stress, $-\overline{uv}/U_0^2$, should be approximately 0.011 ± 0.002 . The peak values of $\overline{u^2}/U_0^2$ should be approximately 0.04 ± 0.005 . These values have been established using the available laser-anemometer data.

SELECTED DATA SETS

Unfortunately, none of the available data sets met all of the selection criteria listed above. The data set of Kim et al. (1978) was selected as the backward-facing-step test case because it meets more of the selection criteria than any other currently available data set. Several new data sets by Eaton and Johnston (1980c), Tropea and Durst (1980), and Kuehn and Seegmiller (1980) will be available in the near future. These data sets appear to promise more accurate turbulence data than are currently available. However, they must be subject to external review before they can qualify as legitimate test cases.

The experiment of Kim et al. (1978) was conducted in a single-sided, two-dimensional sudden expansion (see Fig. 1). The experiment was very well documented and has several advantageous features: (1) a turbulent boundary layer at separation, (2) excellent spanwise uniformity, and (3) complete initial and boundary-condition specifications.

The data set does not meet the selection criterion specified under "Instrumentation." The mean-velocity profiles were measured with pitot tubes rather than the preferred instruments. However, the measurements are reasonably accurate, except within the reattachment region ($6 < x/H < 8$). The mean-velocity data can be confidently used for comparison with computer calculations in all other regions of the flow.

The only really serious drawback to this experiment is that the turbulence quantities were measured with an x-array hot wire. The maximum values of the shear stress ($-\overline{uv}$) and the normal stresses are substantially lower than those measured with laser-anemometer or pulsed-wire techniques in other backward-facing-step experiments (see Fig. 2). The reviewers feel that the turbulence data within the separated shear layer should therefore not be used for comparison with calculations. These data have not been included in the compilation. Computers who would like to compare their calculated turbulent shear-stress levels to experimental data should use the "best guess" line from Fig. 2.

The data set of Chandrasuda (1975) has also been selected for eventual compilation in the data library. It contains the only known measurements of triple products in a backward-facing-step flow. The boundary layer at separation is laminar, making it unsuitable for use at the 1981 meeting.

RECOMMENDATIONS FOR FUTURE WORK

The reattachment process is still relatively poorly understood, despite the large number of experiments on the backward-facing-step flow. The biggest problem has been the lack of suitable instruments for use in reattaching flows. Now that suitable instruments are available, one or two careful experiments should be undertaken to supply accurate data for checking flow calculations. These experiments should meet all of the criteria laid out in Eaton and Johnston (1980a).

The effect of system geometry and streamwise pressure gradient on reattachment should be investigated. A number of studies of this effect have already commenced. Kuehn and Seegmiller at NASA-Ames Research Center are continuing their work on this subject. Their preliminary work pointed out the substantial effect of pressure gradient. Additional studies are being undertaken by Tropea and Durst at the University of Karlsruhe and, in our laboratory, by Westphal, Eaton, and Johnston, and by Pronchick and Kline.

Systematic studies of the effect of the thickness of the separating boundary layer and the effect of the free-stream turbulence level may also be useful. Neither of these effects appears to be as important as the pressure gradient.

Further experiments are needed on the evolution of flow structure within the reattachment zone. The rapid decay of turbulence energy within the reattachment zone has not been adequately explained. In particular, the two-stage decay noted in many experiments is not well understood.

Measurements of the near-wall velocity and the skin friction should be made in the separated flow region. Many computational procedures assume that the skin friction is negligible in the reversed-flow region. However, our own recent measurements suggest that the skin friction is actually quite large. These are the only known skin-friction measurements in the reversed-flow region, other than a single point reported by Chandrsuda (1975). Further measurements of skin friction are needed to check the available data and to understand the variation of skin friction with various flow parameters.

The cause of low-frequency motions of the reattaching shear layer should be further investigated. Such motions have been observed in some experiments (e.g., Eaton and Johnston (1980b) and Tropea and Durst (1980), but not in others (Chandrsuda, 1975). Large-scale, low-frequency motions may be of considerable technological importance.

REFERENCES

- Chandrsuda, C. (1975). "A reattaching turbulent shear layer in incompressible flow," Ph.D. thesis, Dept. of Aeronautics, Imperial College of Science and Technology, London, SW7 2BY.
- Eaton, J. K., and J. P. Johnston (1980a). "An evaluation of data for the backward-facing-step flow," prepared for the 1980-81 Stanford Conference on Complex Turbulent Flows.
- Eaton, J. K., and J. P. Johnston (1980b). "A review of research on subsonic turbulent-flow reattachment," Paper No. 80-1438, AIAA 13th Fluid and Plasma-dynamics Conference, Snowmass, Colorado.
- Eaton, J. K., and J. P. Johnston (1980c). "Turbulent flow reattachment: an experimental study of the flow and structure behind a backward-facing step," Report MD-39, Dept. of Mech. Eng., Stanford University, Stanford, California.
- Kim, J., S. J. Kline, and J. P. Johnston (1978). "Investigation of separation and reattachment of a turbulent shear layer: flow over a backward-facing step," Report MD-37, Dept. of Mech. Eng., Stanford University, Stanford, California.
- Kuehn, D., and H. Seegmiller (1980). Private communication.
- Tropea, C., and F. Durst (1980). Private communication.

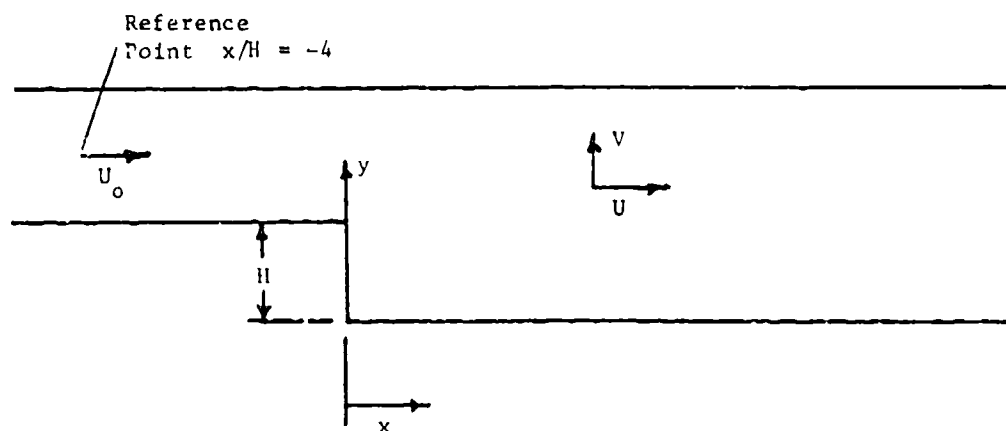


Figure 1. Test section configuration of Kim et al. (1978).
 $H = 3.81$ cm; area ratio = 1.5.

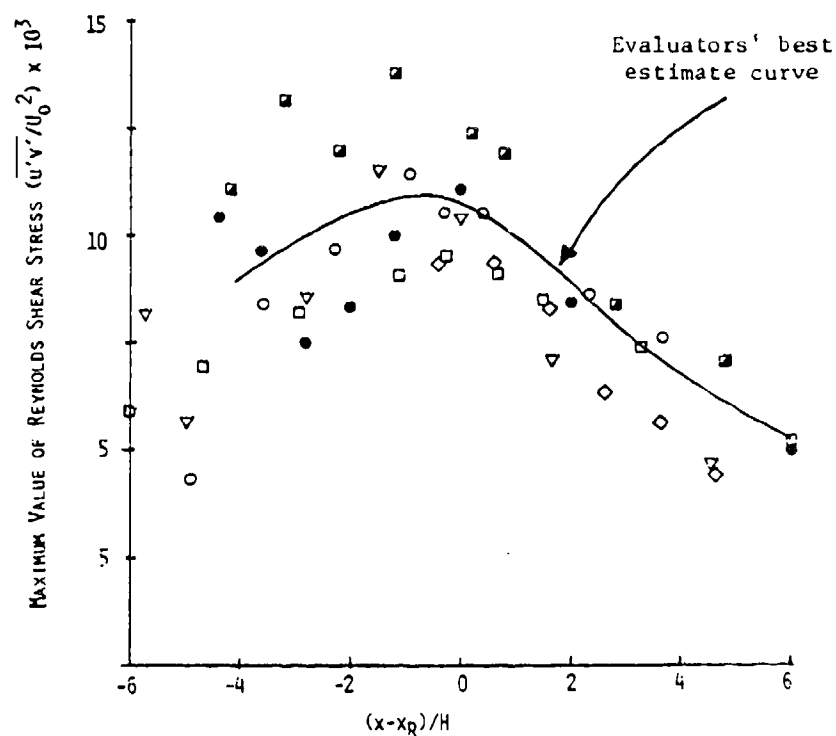


Figure 2. Reynolds shear-stress data and "best guess" line for experiment of Kim et al. (1978).
 ○ Baker; ◇ Chandrsuda; □ Kim et al.; ▽ Kuehn and Seegmiller;
 ● Smyth; ■ Tropea and Durst.

DISCUSSION

Flow 0420

1. F. Durst and C. Tropea (Karlsruhe) noted that laser-doppler anemometer data are now available for the backward-facing step and request a wording change in the evaluation report.
2. C. Tropea questioned the selection of the $x/h = 4$ station as the only station in the separated region where comparisons are requested. He also suggested the mean normal velocity as a sensitive and desirable comparison within the separated region.
3. E. P. Sutton showed the susceptibility of sudden expansions to upstream disturbance using some of his own data as example. These data were for a laminar separating layer; it was accepted that higher Reynolds number separating boundary layers would not be as susceptible to disturbance effects in the initial region.
4. No changes were recommended to the specification for Case 0421.

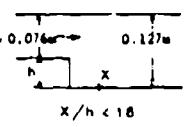
SPECIFICATIONS FOR COMPUTATION
CENTRAL, ENTRY CASE/INCOMPRESSIBLE

Case #0421; Data Evaluators: J. K. Eaton and J. P. Johnston

Data Takers: J. Kim, S. Kline, and J. Johnston

PICTORIAL SUMMARY

Flow 0410. Data Evaluators: J. Eaton and J. Johnston. "Reattached-Facing Step Flow."

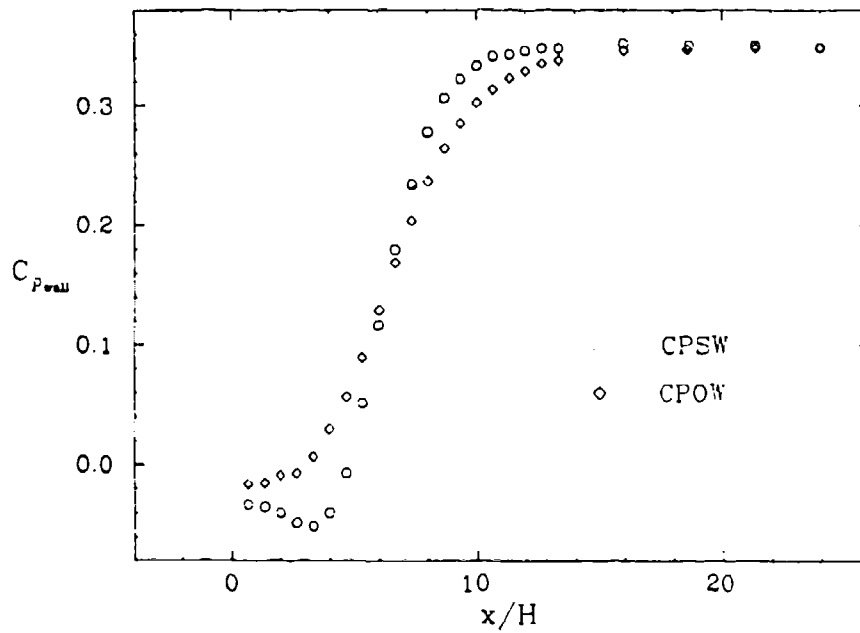
Case Data Taker	Test Rig Geometry	$\frac{dp}{dx}$ or C_p	Number of Stations Measured								C_f	Re	Initial Condi- tion	Other Notes
			Mean Velocity		Turbulence Profiles									
			U	V or W	$\overline{u^2}$	$\overline{v^2}$	$\overline{w^2}$	\overline{uv}	Others					
Case 0421 J. Kim S. Kline J. Johnston		Wall pres- sure	12	-	6	6	-	6	Inter- mit- tency	Reattach- ment length about 7h (based on h)	4.5 $\times 10^4$ (based on h)	6/h = 0.3	Aspect ratio 16. Data inadequate in zones of high turbulence and oscillating flow. Laser data needed. Reattached layer well documented. Pressure on upper and lower walls available.	

Plot	Ordinate	Abscissa	Range/Position	Comments
1	$C_{p_{wall}}$	x/H	$-4 < x/H < 16$	Plot on step-wall side. (Opposite side optional.)
2	$-\overline{uv}_{max}/U_0^2$	$(x-x_R)/H$	$-10 < (x-x_R)/H < 10$	$-\overline{uv}_{max}$ = maximum $-\overline{uv}$ from profile at given x.
3	y/H	U/U_0	full channel	At $x/H = 5.33, 8.00, 13.33$.
4	$-\overline{uv}/U_0^2$	y/H	full channel	At $x/H = 7.66, 10.3, 15.67$.

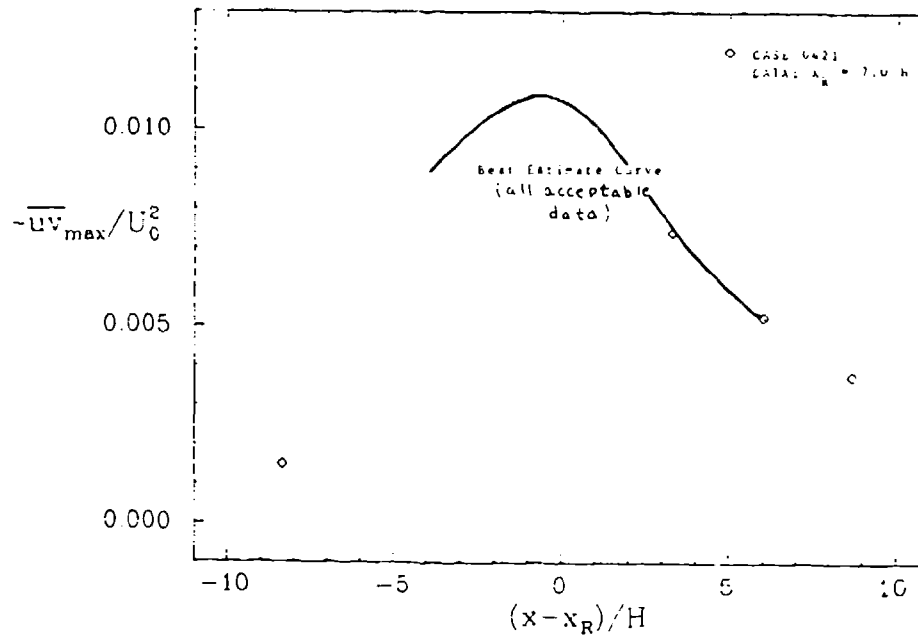
Special Instructions:

- $$C_{p_{wall}} = \frac{\Delta P_{wall} - P_0}{\frac{1}{2} \rho U_0^2}$$
 P_0 = pressure at $x/H = -4$
 U_0 = freestream velocity at $x/H = -4$
- Take x_R = location of reattachment as computed by your program, report value of x_R .
- Plot 2 shows data from the file on Case 0421 for $(\overline{uv})_{max}/U_0^2$. The full line shows the best estimate drawn through all acceptable data for $-\overline{uv}_{max}/U_0^2$; it is taken from Fig. 2 above.

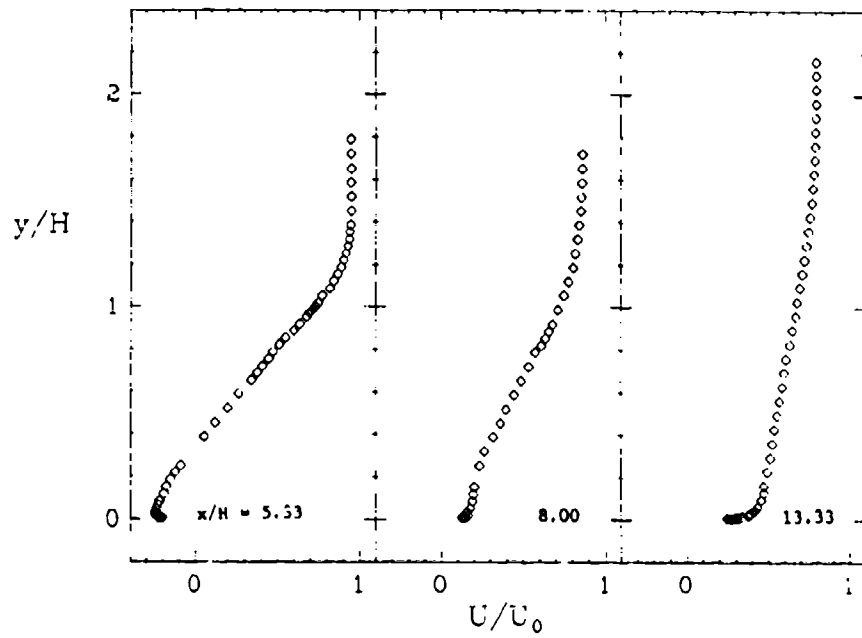
PLOT 1 CASE 0421 FILES 2-3



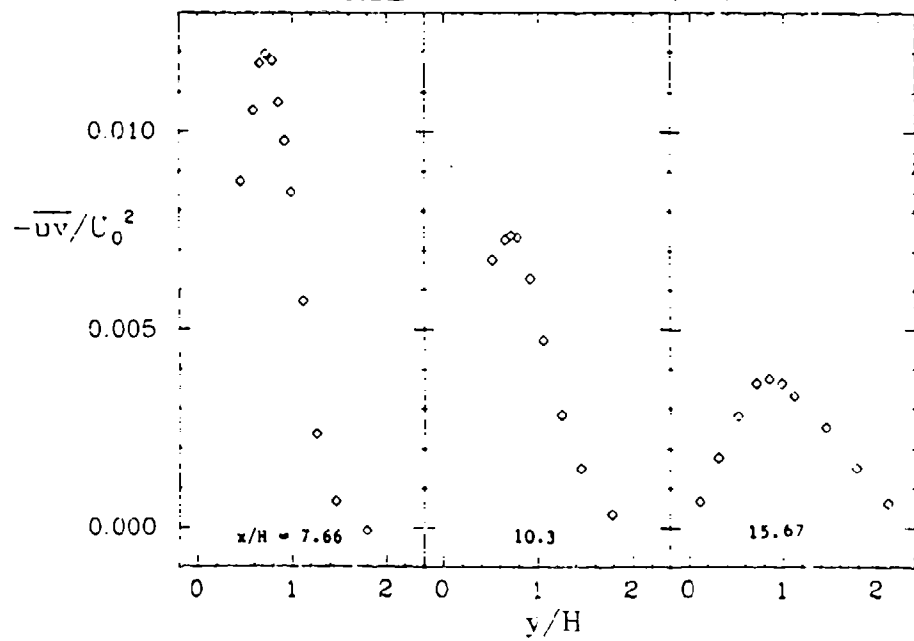
PLOT 28 CASE 0421 FILES 27-32



PLOT 3 CASE 0421 FILES 19,22,25



PLOT 4 CASE 0421 FILES 28,30,32



AN OVERVIEW OF THE PREDICTIVE TEST CASES

by John K. Eaton*

One of the unique features of the 1980-81 Conference is the inclusion of "predictive test cases" for several classes of flows. Initial conditions and boundary geometries (or boundary data) will be supplied for these cases as they would be for an ordinary test case. However, the experimental data will not be supplied since the experiments have not been completed. The experimental data will be presented with the predictions at the 1981 meeting. Therefore, any successful calculation of the flow field will require a truly predictive computational procedure.

There are two major reasons for the addition of the predictive test cases. First, computational fluid mechanics is now being applied to practical engineering problems. Users of computational procedures (primarily industrial concerns) must have some way of assessing their applicability to complex-flow configurations that are beyond the range of the available data base. The predictive test cases will test the ability of computational procedures to extrapolate from the current data base. Secondly, the predictive test cases will help the research community to assess the usable scope of various turbulence models. Some models may require considerably more "fine tuning" than others; predictive cases will be a significant test of scope.

The experimental work for the predictive test cases is being coordinated by Prof. J. K. Eaton and S. J. Kline at Stanford University. However, the actual experiments are being conducted at various laboratories throughout the world. Some of the experiments were suggested to the researchers by the Organizing Committee. The experimenters already have considerable experience in making the type of measurements suggested by the Organizing Committee. The remainder of the predictive test cases are ongoing experiments whose timetables happen to mesh well with the conference schedule.

Most of the experiments are currently in the preliminary stages. The bulk of the experimental data will be obtained during the period between the two conferences. The timetable for most of the experiments is such that the experimenters would probably first publish their results in the summer of 1981. However, they have agreed to withhold publication or private communication of any results until the 1981 conference.

The predictive cases include: i) developing flow in a square duct with an asymmetric inlet flow; ii) four kinds of geometric modification of the backward-facing step flow; iii) a diffuser flow; iv) a shock-boundary layer interaction experiment; and v) a transonic airfoil experiment. Details of the cases are given in the attached specifications. They are mostly perturbations of the existing test cases. Therefore,

*Asst. Professor, Dept. of Mech. Engr. Stanford University, Stanford, Ca 94305.

the numerical procedures and turbulence models should not require large changes. We cannot guarantee that useful data sets will be obtained for these flows in time for the 1981 meeting. It appears that most of the experiments have set reasonably conservative timetables. We can reasonably expect to obtain useful data for at least one-half of the cases in time for the 1981 meeting.

One major problem is that the experimental data will not be available for public scrutiny prior to its use at the 1981 conference. There is a danger that undue importance will be attached to a data set which may be highly inaccurate. Researchers in complex turbulent flows frequently encounter unexpected measurement difficulties or uncontrolled flow disturbances. We are taking several precautions to try to avoid using data which are affected by such problems. First of all, the experiments are being conducted by researchers with considerable experience. The experimenters have all previously made measurements in flows similar to their predictive test case. Secondly, by showing the experimental plans prior to the acquisition of data, we hope to obtain suggestions, and guidance from other conference participants. As an added precaution, data will be repeated in two labs for Case 0422.

The predictive test case data will all be reviewed prior to the 1981 meeting. The review will be similar to the evaluation of the regular test cases which was done for the 1980 conference. Any problems with a given data set will be reported at the 1981 meeting. Any data set the Evaluation Committee deems inadequate will be rejected. In addition, one knowledgeable researcher will oversee the experiment as it progresses. This will allow the experimenter to rectify problems before he has completed the experiment.

We hope that with these precautions we will be able to supply new data sets which are useful for checking computational methods.

PROCEDURES

The computers were supplied with the boundary geometry and detailed initial conditions for four predictive cases (P1 to P4) in January 1981. The instructions to computers are listed in the Appendix to this summary.

LIST OF PREDICTIVE TEST CASES

<u>Case 0113 (P1).</u>	Asymmetric Flow in a Square Duct
<u>Case 0422 (P2).</u>	Backward-Facing Step: Variable Opposite-Wall Angle
<u>Case 0423 (P3).</u>	Backward-Facing Step: Turned Flow Passage
<u>Case 0424 (P4).</u>	Backward-Facing Step: Variable Area Ratio
<u>Case Y.</u>	Flow in a Planar Diffuser with Downstream Tailpipe
<u>Case 6.</u>	Shock-Boundary Layer Interaction

APPENDIX

Instructions to Computers Regarding Predictive Cases

FORMAT, TAPE ORGANIZATION

Since we will be printing results from the tapes, it is important that you use standard format and tape organization. Please:

1. Follow the precise order of file labeling indicated.
2. Report N wherever requested.
3. Format using nE13.6 ($n \leq 6$).
4. Use 9-track, odd-parity, phase-encoded, unlabeled tape written at a density of 1600 bits per inch according to EBCDIC code. Record format: fixed and blocked. Record length: 80 bytes; 100 records per block; blocksize = 8000 bytes. Report to us separately in writing, and at head of tape, the full details of formatting and tape organization.

Since these are predictive cases, no detailed experimental data are being supplied apart from initial conditions. In each predictive case the specification calls for the creation of an appropriate number of computer output data files as binary or trinary arrays in accordance with the following format:

FORM OF OUTPUT DATA

Please note that all output data requested in the predictive cases are non-dimensional. Please report on tape in non-dimensional form using the normalizations specified so that shifts in units or normalization will not be necessary.

Since we will need to produce output plots at Stanford on short turn-around times with limited personnel, these details are important to the evaluation of your results.

We will need to have the tapes at Stanford by 15 July 1981 in order to compile and disseminate results before the September meeting.

ASYMMETRIC FLOW IN A SQUARE DUCT

Flow 0110

Case 0113 (P1)

Description by John K. Eaton

SUMMARY

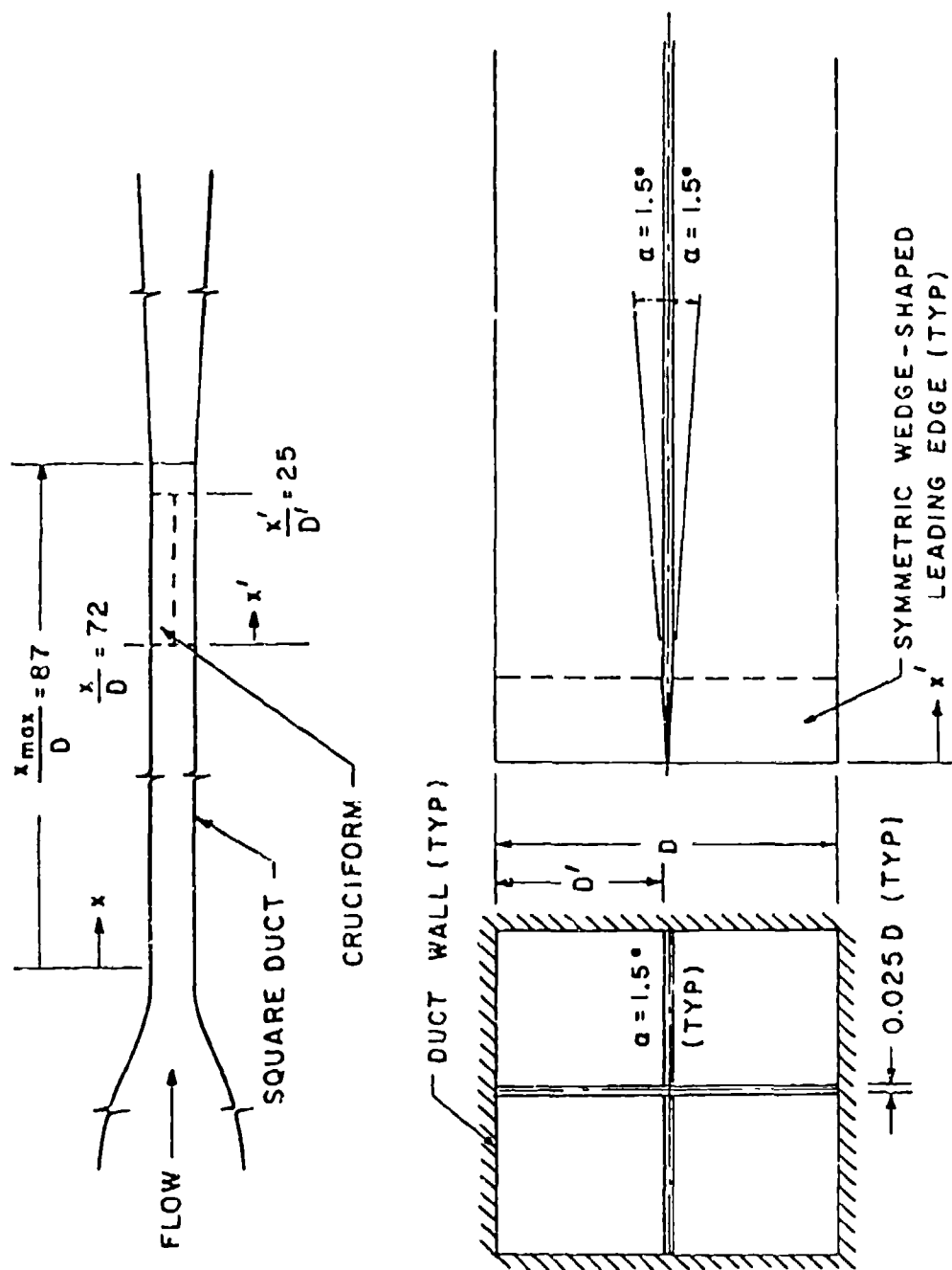


GENERAL FEATURES

In this test case, a cross-shaped insert (cruciform) will be inserted into a smooth-walled square duct and positioned as shown in Fig. 1. The cruciform consists of two intersecting, smooth-walled flat plates, each of which spans the duct and has a symmetric wedge-shaped leading edge. The thickness of each plate is $0.025D$, and the wedge half-angle of each leading edge, α , is 1.5 degrees. The cruciform and duct form four square flow passages. Flow within each passage consists of well-developed boundary layers initiated at the square duct inlet ($x/D = 0$) which continue along the duct walls, and new boundary layers initiated at the leading edge of the cruciform ($x'/D' = 0$) which develop along the cruciform walls. The interactions which occur downstream of the leading edge are locally symmetric about corner bisectors (diagonals) which intersect the axial centerline of the cruciform, but are asymmetric about the other corner bisectors. Data will be taken with the leading edge of the cruciform positioned at $x/D = 72$, as shown in Fig. 1, for a high Reynolds number operating condition ($Re_D \equiv U_D D/\nu = 2.5 \times 10^5$).

SPECIFICATION OF INITIAL CONDITIONS AND COMPUTATIONAL RANGE

Computations should be started at the inlet of the square duct ($x/D = 0$) where a potential-type, uniform mean flow can be assumed. This condition corresponds to specifying $U = U_D$, $V = 0$, $W = 0$ at $x/D = 0$ and letting all turbulence-related correlations be zero. Local flow development in the square duct should be computed over the interval $0 \leq x/D \leq 72$, with an appropriate change in the boundary conditions when $x/D \geq 72$ ($x'/D' \geq 0$) in order to predict flow in the passages formed by the cruciform and duct. The computations can be terminated at $x'/D' = 24.6$ if a parabolic-type code is used, which corresponds to the last streamwise location where data will be taken.



CRUCIFORM LEADING EDGE DETAIL

Figure 1. Square duct flow facility with cruciform in position.

DISCUSSION

Case 0113 (P1)

E. P. Sutton raised the question of need for rounding plate leading edge. Discussion led to general agreement (J. P. Johnston, F. Gessner) that rounding may be undesirable in view of laminar flow results and that, at worst, the sharp leading edge would only cause very short, occasional separation regions which would be practically unimportant.

J. Hunt suggested that changes to the turbulence structure may be an important effect of the cruciform.

I Greber suggested the need to specify some type of vector output, possibly contour plots.

E. Reshotko noted the necessity to ensure that the four flow channels within the cruciform are independent by adjusting the downstream pressure.

After discussion, there was general agreement that the current cruciform blockage is acceptable and the 3° leading edge is adequate.

J. Hunt and D. J. Cockrell recommended flow visualization, if possible, to ensure complete flow documentation.

PREDICTIVE CASE

SPECIFICATIONS FOR COMPUTATION

Case #0113 (P1); Coordinator: J. K. Eaton

File #	Independent Variable(s) (Label)	Dependent Variable(s) (Output)	Range of Independent Variable(s); Locations	Comments
P1-1	1-55	U/U_b	at $x/D = 70$	For location of points 1-55, see Fig. 2. For each of files P1-1 through P1-9, create a binary array with labels 1 through 55 and associated output values for variables indicated. Use file numbers indicated.
P1-2	1-55	V/U_b	at $x/D = 70$	
P1-3	1-55	W/U_b	at $x/D = 70$	
P1-4	1-55	$\overline{u^2}/U_b^2$	at $x/D = 70$	
P1-5	1-55	$\overline{v^2}/U_b^2$	at $x/D = 70$	
P1-6	1-55	$\overline{w^2}/U_b^2$	at $x/D = 70$	
P1-7	1-55	\overline{uv}/U_b^2	at $x/D = 70$	
P1-8	1-55	\overline{uw}/U_b^2	at $x/D = 70$	
P1-9	1-55	\overline{vw}/U_b^2	at $x/D = 70$	
P1-10	1-N	$y/D, z/D$	locating points for isotach $U/U_c = 0.70$ $x/D = 70$	For each of files P1-10 through P1-14, create a 3-element array with labels 1-N for N points specifying the given isotach location. Report the value of N for each file in writing and at head of file on tape. See instruction 3.
P1-11	1-N	$y/D, z/D$	locating points for isotach $U/U_c = 0.80$ $x/D = 70$	
P1-12	1-N	$y/D, z/D$	locating points for isotach $U/U_c = 0.85$ $x/D = 70$	

File #	Independent Variable(s) (Label)	Dependent Variable(s) (Output)	Range of Independent Variable(s); Locations	Comments
P1-13	1-N	y/D, z/D	locating points for isotach $U/U_c = 0.90$ $x/D = 70$	
P1-14	1-N	y/D, z/D	locating points for isotach $U/U_c = 0.95$ $x/D = 70$	
P1-15	z/a	$\tau_{w,y}/\tau_{w,y}$	$0 \leq z/a \leq 1$ $x/D = 70$	For file P1-15, create a binary array of N elements. Report value of N in writing and at head of file.
P1-16	1-N	y'/a, z'/a	$U/U_{max} = 0.80$ $x'/D' = 8.2$	For each of files P1-16 through P1-27, create a 3-element array with labels 1-N specifying the given isotach location. Report the value of N for each file in writing and at head of file on tape.
P1-17	1-N	y'/a, z'/a	$U/U_{max} = 0.85$ $x'/D' = 8.2$	
P1-18	1-N	y'/a, z'/a	$U/U_{max} = 0.90$ $x'/D' = 8.2$	
P1-19	1-N	y'/a, z'/a	$U/U_{max} = 0.95$ $x'/D' = 8.2$	
P1-20	1-N	y'/a, z'/a	$U/U_{max} = 0.80$ $x'/D' = 16.4$	
P1-21	1-N	y'/a, z'/a	$U/U_{max} = 0.85$ $x'/D' = 16.4$	
P1-22	1-N	y'/a, z'/a	$U/U_{max} = 0.90$ $x'/D' = 16.4$	
P1-23	1-N	y'/a, z'/a	$U/U_{max} = 0.95$ $x'/D' = 16.4$	
P1-24	1-N	y'/a, z'/a	$U/U_{max} = 0.80$ $x'/D' = 24.6$	
P1-25	1-N	y'/a, z'/a	$U/U_{max} = 0.85$ $x'/D' = 24.6$	

File #	Independent Variable(s) (Label)	Dependent Variable(s) (Output)	Range of Independent Variable(s); Locations	Comments
P1-26	1-N	$y'/a, z'/a$	$U/U_{max} = 0.90$ $x'/D' = 24.6$	
P1-27	1-N	$y'/a, z'/a$	$U/U_{max} = 0.95$ $x'/D' = 24.6$	
P1-28	x'/D'	C_p	$0 \leq x'/D' \leq 25$	For file P1-28, create an array of N binary elements with labels of x'/D' showing values of C_p . Report the value of N for each file in writing and at head of file.
P1-29	y'/a'	$U/U_{b,m}$	$0 \leq y'/a' \leq 1$ $x'/D' = 8.2$	For each of files P1-29 through P1-49, create a binary array of N elements with labels of y'/a' . Report the value of N for each file in writing and at head of file on tape.
P1-30	y'/a'	$U/U_{b,m}$	$0 \leq y'/a' \leq 1$ $x'/D' = 16.4$	
P1-31	y'/a'	$U/U_{b,m}$	$0 \leq y'/a' \leq 1$ $x'/D' = 24.6$	
P1-32	y'/a'	$V'/U_{b,m}$	$0 \leq y'/a' \leq 1$ $x'/D' = 8.2$	
P1-33	y'/a'	$V'/U_{b,m}$	$0 \leq y'/a' \leq 1$ $x'/D' = 16.4$	
P1-34	y'/a'	$V'/U_{b,m}$	$0 \leq y'/a' \leq 1$ $x'/D' = 24.6$	
P1-35	y'/a'	$\overline{u^2}/U_{b,m}^2$	$0 \leq y'/a' \leq 1$ $x'/D' = 8.2$	
P1-36	y'/a'	$\overline{u^2}/U_{b,m}^2$	$0 \leq y'/a' \leq 1$ $x'/D' = 16.4$	
P1-37	y'/a'	$\overline{u^2}/U_{b,m}^2$	$0 \leq y'/a' \leq 1$ $x'/D' = 24.6$	
P1-38	y'/a'	$\overline{v^2}/U_{b,m}^2$	$0 \leq y'/a' \leq 1$ $x'/D' = 8.2$	

File #	Independent Variable(s) (Label)	Dependent Variable(s) (Output)	Range of Independent Variable(s); Locations	Comments
P1-39	y'/a'	$\overline{v^2}/U_{b,m}^2$	$0 \leq y'/a' \leq 1$ $x'/D' = 16.4$	
P1-40	y'/a'	$\overline{v^2}/U_{b,m}^2$	$0 \leq y'/a' \leq 1$ $x'/D' = 24.6$	
P1-41	y'/a'	$-\overline{uv}/U_{b,m}^2$	$0 \leq y'/a' \leq 1$ $x'/D' = 8.2$	
P1-42	y'/a'	$-\overline{uv}/U_{b,m}^2$	$0 \leq y'/a' \leq 1$ $x'/D' = 16.4$	
P1-43	y'/a'	$-\overline{uv}/U_{b,m}^2$	$0 \leq y'/a' \leq 1$ $x'/D' = 24.6$	
P1-44	y'/a'	$-\overline{vw}/U_{b,m}^2$	$0 \leq y'/a' \leq 1$ $x'/D' = 8.2$	
P1-45	y'/a'	$-\overline{vw}/U_{b,m}^2$	$0 \leq y'/a' \leq 1$ $x'/D' = 16.4$	
P1-46	y'/a'	$-\overline{vw}/U_{b,m}^2$	$0 \leq y'/a' \leq 1$ $x'/D' = 24.6$	
P1-47	y'/a'	$K/U_{b,m}^2$	$0 \leq y'/a' \leq 1$ $x'/D' = 8.2$	
P1-48	y'/a'	$K/U_{b,m}^2$	$0 \leq y'/a' \leq 1$ $x'/D' = 16.4$	
P1-49	y'/a'	$K/U_{b,m}^2$	$0 \leq y'/a' \leq 1$ $x'/D' = 24.6$	
P1-50	z/D'	$\tau_{w,y}/\tau_{w,y}$	$0 \leq z/D' \leq 1$ $x'/D' = 8.2$	For each of files P1-50 through P1-52, create a binary array of N elements with labels z/D' , reporting values of $\tau_{w,y}/\tau_{w,y}$. Report the value of N for each file in writing and at head of file.
P1-51	z/D'	$\tau_{w,y}/\tau_{w,y}$	$0 \leq z/D' \leq 1$ $x'/D' = 16.4$	
P1-52	z/D'	$\tau_{w,y}/\tau_{w,y}$	$0 \leq z/D' \leq 1$ $x'/D' = 24.6$	

File #	Independent Variable(s) (Label)	Dependent Variable(s) (Output)	Range of Independent Variable(s); Locations	Comments
P1-53	y/D'	$\tau_{w,z}/\tau_{w,z}$	$0 \leq y/D' \leq 1$ $x'/D' = 8.2$	For each of files P1-53 through P1-55, create a binary array of N elements with labels y/D', reporting values of $\tau_{w,z}/\tau_{w,z}$. Report the value of N for each file in writing and at head of file.
P1-54	y/D'	$\tau_{w,z}/\tau_{w,z}$	$0 \leq y/D' \leq 1$ $x'/D' = 16.4$	
P1-55	y/D'	$\tau_{w,z}/\tau_{w,z}$	$0 \leq y/D' \leq 1$ $x'/D' = 24.6$	

Special instructions:

1. Instructions for predictive case files format are given in the Appendix to the Overview of Predictive Test Cases.
2. Files P1-1 through P1-15 constitute input data at $x/D = 70$, two diameters upstream of the cruciform. You should compute these data by computing square channel flow of Case 0111. The data in these files (P1-1 through P1-15) will be used to evaluate if the particular method employed works well in the symmetric flow in the larger channel before the more complex asymmetric case is carried out.
3. Isotachs in files P1-10 through P1-14 are to cover domain $0 \leq y/a \leq 1$; $0 \leq z/a \leq 1$.
4. Note two coordinates used (see Fig. 1). x', y' etc. refer to section with inset cruciform.

Nomenclature

a	half-width of square duct (Fig. 2)
a'	diagonal width of modified flow passage (Fig. 3)
C_p	static pressure coefficient: $C_p \equiv (p_o - p)/(1/2 \rho U_{b,m}^2)$
D	width of square duct (Fig. 1)
D'	width of modified flow passage (Fig. 1)
K	turbulence kinetic energy
p_o	static pressure at $x'/D' = 0$
p	static pressure
Re_b	bulk Reynolds number: $Re_b \equiv U_b D/\nu$
u, v, w	fluctuating velocity components in the x-, y-, and z-direction, respectively
$\overline{u^2}, \overline{v^2}, \overline{w^2}$	Reynolds-normal-stress components
$-\overline{uv}, -\overline{vw}, -\overline{uw}$	Reynolds-shear-stress components
U, V, W	mean-velocity components in the x-, y-, and z-directions, respectively
U_b	bulk velocity in square duct ($0 \leq x/D \leq 72$)

$U_{b,m}$	bulk velocity in modified flow passage ($0 < x'/D' \leq 25$)
U_c	axial centerline velocity in square duct
U_{max}	maximum axial velocity in modified flow passage
V'	transverse velocity component in the y' -direction
x, y, z	Cartesian coordinates (Fig. 2)
x'	axial distance measured from leading edge of cruciform (Fig. 1)
y'	diagonal coordinate measured from corner (Fig. 3)
$\Delta y, \Delta z$	distance increments (Fig. 2)
α	wedge half-angle (Fig. 1)
μ	absolute viscosity
ν	kinematic viscosity
ρ	fluid density
$\tau_{w,y}$	local wall shear stress on the wall $y = 0$ (Fig. 3): $\tau_{w,y} \equiv \mu(\partial U / \partial y)_{y=0}$
$\overline{\tau_{w,y}}$	integrated average value of $\tau_{w,y}$ along the wall $y = 0$
τ_{w,z_1}	local wall shear stress on the wall $z = z_1$ (Fig. 3): $\tau_{w,z_1} \equiv \mu(\partial U / \partial z)_{z=z_1}$
$\overline{\tau_{w,z_1}}$	integrated average value of τ_{w,z_1} along the wall $z = z_1$

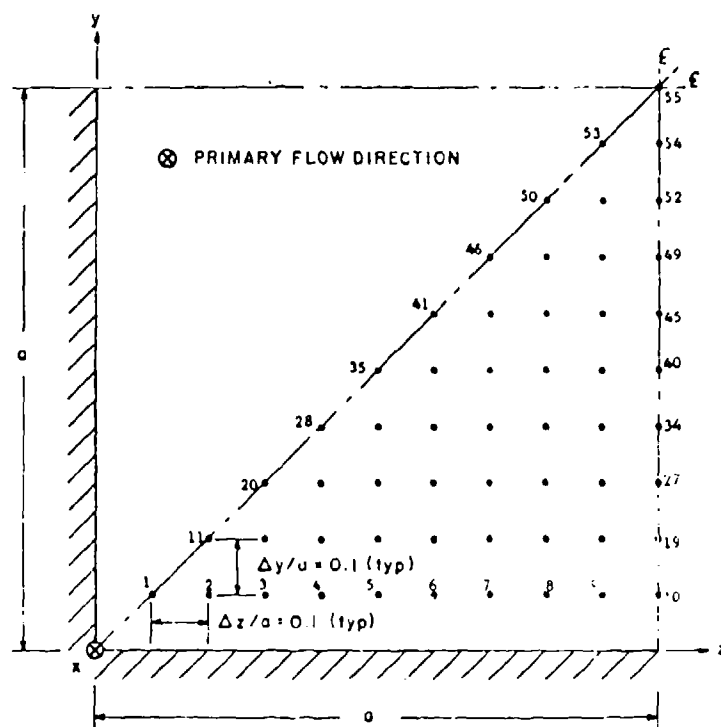


Figure 2. Data point locations (●) in an octant of the square duct. Numbers refer to locations in files P1-1 through P1-15. Numbers sequential left to right on each row.

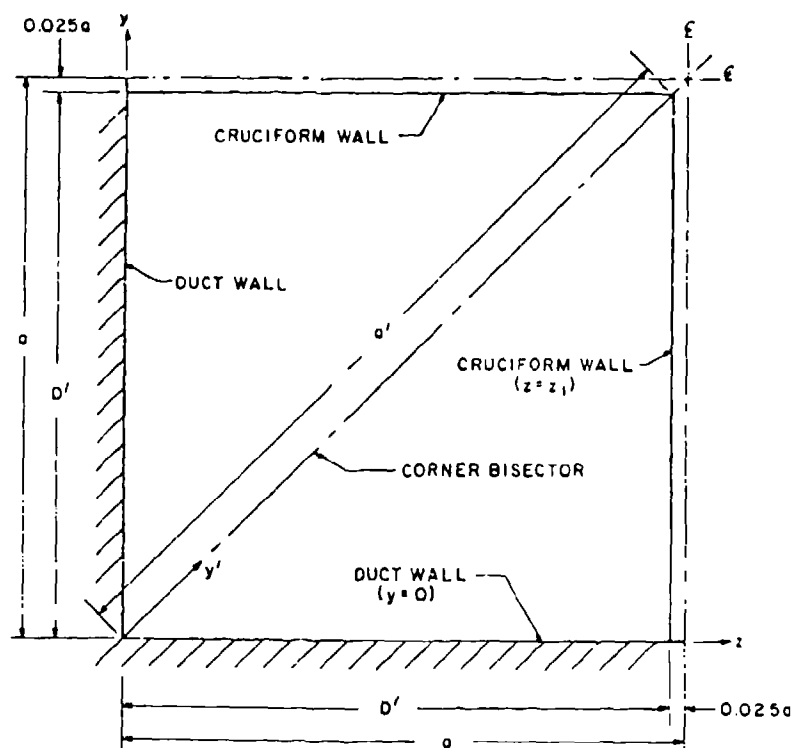


Figure 3. Reference dimensions and coordinates for modified flow passage formed by cruciform and square duct.

BACKWARD-FACING STEP: VARIABLE OPPOSITE-WALL ANGLE

PREDICTIVE TEST P2

Flow 0420

Case 0422

Description by John K. Eaton

SUMMARY

GENERAL DESCRIPTION

Measurements are being made in a single-sided sudden expansion. The wall opposite the step is set at various angles as shown in Fig. 1. The step aspect ratio (channel span/step height) is twelve; this should be adequate to provide good two-dimensionality. The spanwise uniformity has been checked in this apparatus.

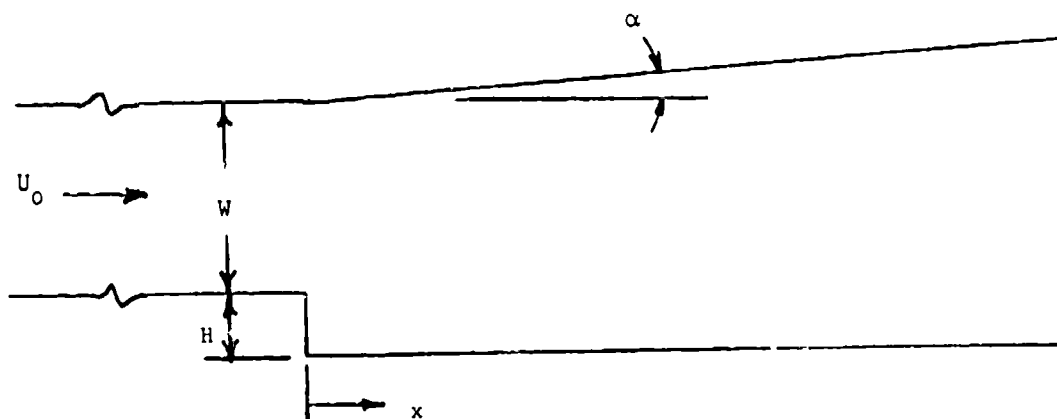
Measurements will be provided for angles in the range $-2 \leq \alpha \leq 10$ degrees. The reattachment length will be measured as a function of α . Wall-static-pressure data will be provided for angles of -2 , 0 , 6 , and 10 degrees. A detailed data set, including mean velocity and Reynolds shear-stress profiles, will be supplied for $\alpha = 6^\circ$. Profiles of \bar{U} and \overline{uv} will be provided along the centerline in the separated region and downstream of reattachment to $x/h = 20$.

DETAILED FLOW GEOMETRY

The test section geometry is shown in Fig. 1. The initial conditions are specified at a station four step heights upstream of the step. The free-stream velocity is 44 m/s at this point. The boundary layers on both the step-side and opposite walls are fully turbulent. Various parameters describing the boundary layers are compiled in Table 1. The step-wall boundary layer is thicker because it is tripped with the sandpaper roughness. The entire wind tunnel is sketched in Fig. 2 which illustrates the exit conditions.

TABLE 1
Boundary-Layer Parameters Measured at $x/H = -4$

	Step-Side Wall	Opposite Wall
δ_{99}	1.69 cm	1.41 cm
δ^{**}	0.257 cm	0.240 cm
θ	0.190 cm	0.172 cm
H	1.351	1.398
C_f	0.0030	0.0028
Re_θ	5500	5000



$H = 1.27 \text{ cm}$
 $W = 10.16 \text{ cm}$
 $\alpha = -2 \text{ to } 10 \text{ degrees}$
 $U_0 = 44 \text{ m/s}$

Figure 1. Sketch of wind-tunnel test section (not to scale).

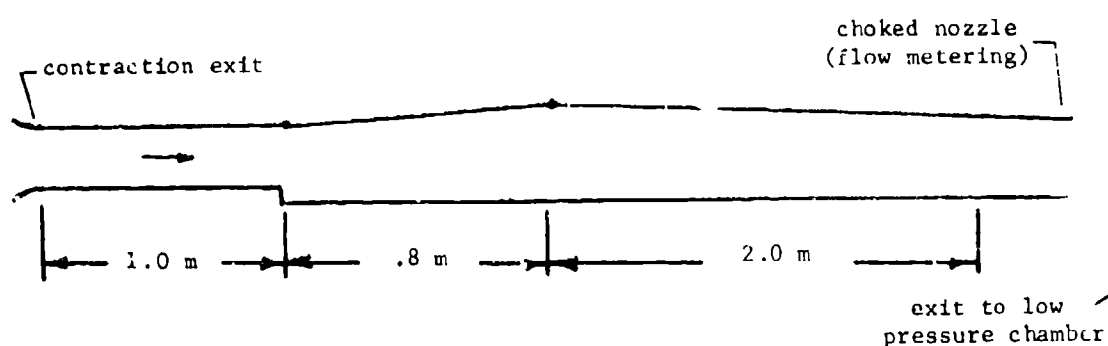


Figure 2. Sketch of wind tunnel (not to scale).

DISCUSSION

Flow 0420 (P2)

For this flow there was general agreement that α should be slightly negative for at least one test of this case.*

It was expected that experimenters will generally measure all quantities they can in the time available. F. Gessner, J. Eaton, D. J. Cockrell, and C. Tropea agreed that the mean normal velocity data would be desirable, at least for stations ahead of reattachment. E. Reshotko suggested that as much data should be obtained for this case as for Case 0421.

*[Ed.: This is planned.]

ENTRY CASE/PREDICTIVE TEST

SPECIFICATIONS FOR COMPUTATION

Case #0422; Coordinator: J. K. Eaton

File #	Independent Variable(s) (Label)	Dependent Variable(s) (Output)	Range of Independent Variable(s); Locations	Comments
P2-1	x/H	$C_{P_{wall}}$	$-4 \leq x/H \leq 16$	$C_{P_{wall}}$ is for step-side wall. See instruction 2. $\alpha = -2^\circ$
P2-2	x/H	$C_{P_{wall}}$	$-4 \leq x/H \leq 16$	$\alpha = 0^\circ$
P2-3	x/H	$C_{P_{wall}}$	$-4 \leq x/H \leq 16$	$\alpha = 6^\circ$
P2-4	x/H	$C_{P_{wall}}$	$-4 \leq x/H \leq 16$	$\alpha = 10^\circ$
P2-5	α	x_R	$-2 \leq \alpha \leq 10^\circ$	$x_R \triangleq$ point where $\tau_w = 0$ in computations.
P2-6	y/H	U/U_0	full channel	$x/H = 4$.
P2-7	y/H	U/U_0	full channel	$x/H = 16$.
P2-8	y/H	U/U_0	full channel	At computed x_R .
P2-9	y/H	\overline{uv}/U_0^2	full channel	$x/H = 4$.
P2-10	y/H	\overline{uv}/U_0^2	full channel	$x/H = 16$.
P2-11	y/H	\overline{uv}/U_0^2	full channel	At computed x_R .

Special Instructions:

1. Instructions for predictive case files format are given in the Appendix to the Overview of Predictive Test Cases.
2. For each file indicated in this case, create a binary array of N elements. Report value of N for each file in writing and at head of file.
3. Compute results along centerline; two-dimensionality can be assumed.
4. ()₀ station: $x/H = -4$.

BACKWARD-FACING STEP: TURNED FLOW PASSAGE

PREDICTIVE TEST P3

Flow 0420

Case 0423

Description by John K. Eaton

SUMMARY

GENERAL DESCRIPTION

Measurements are being made in a single-sided sudden expansion. The duct downstream of the expansion has parallel walls, but can be set at an angle, α , to the upstream duct as shown in Fig. 1. The corner on the wall opposite the step has been smoothed to prevent separation; see Fig. 1. The step aspect ratio (channel span/step height) is twelve; this should be adequate to provide good two-dimensionality. The two-dimensionality will be checked by momentum and mass balance calculations and by spanwise uniformity checks.

Measurements will be provided for angles in the range $0 \leq \alpha \leq 15$ degrees. The reattachment length will be measured as a function of α and wall-static-pressure data will be provided for angles of 0, 5, 10, and 15°. A detailed data set including mean-velocity and turbulence-intensity profiles will be supplied for the 10-degree configuration. Profiles will be provided in the separated region and downstream of reattachment to $x/L \approx 20$.

DETAILED FLOW GEOMETRY

The test section geometry is shown in Fig. 1. The initial conditions are specified at station ()₀ where $x/H = -3$. At station ()₀, the free-stream velocity is 12 m/s. The boundary layers on both walls of the channel are turbulent (parameters tabulated in Table 1). The step-wall boundary layer is thicker because a thicker trip was used. The test section extends a distance of 1.6 m downstream of the expansion. At 1.6 m the flow exits into a large room.

TABLE 1
Boundary-Layer Parameters Measured at $x/H = -3$

	Step-Side Wall	Opposite Wall
δ_{99}	1.78 cm	1.26 cm
δ^*	0.246 cm	0.183 cm
θ	0.180 cm	0.135 cm
H	1.363	1.358
C_f	0.0042	0.0045
Re_θ	1460	1070

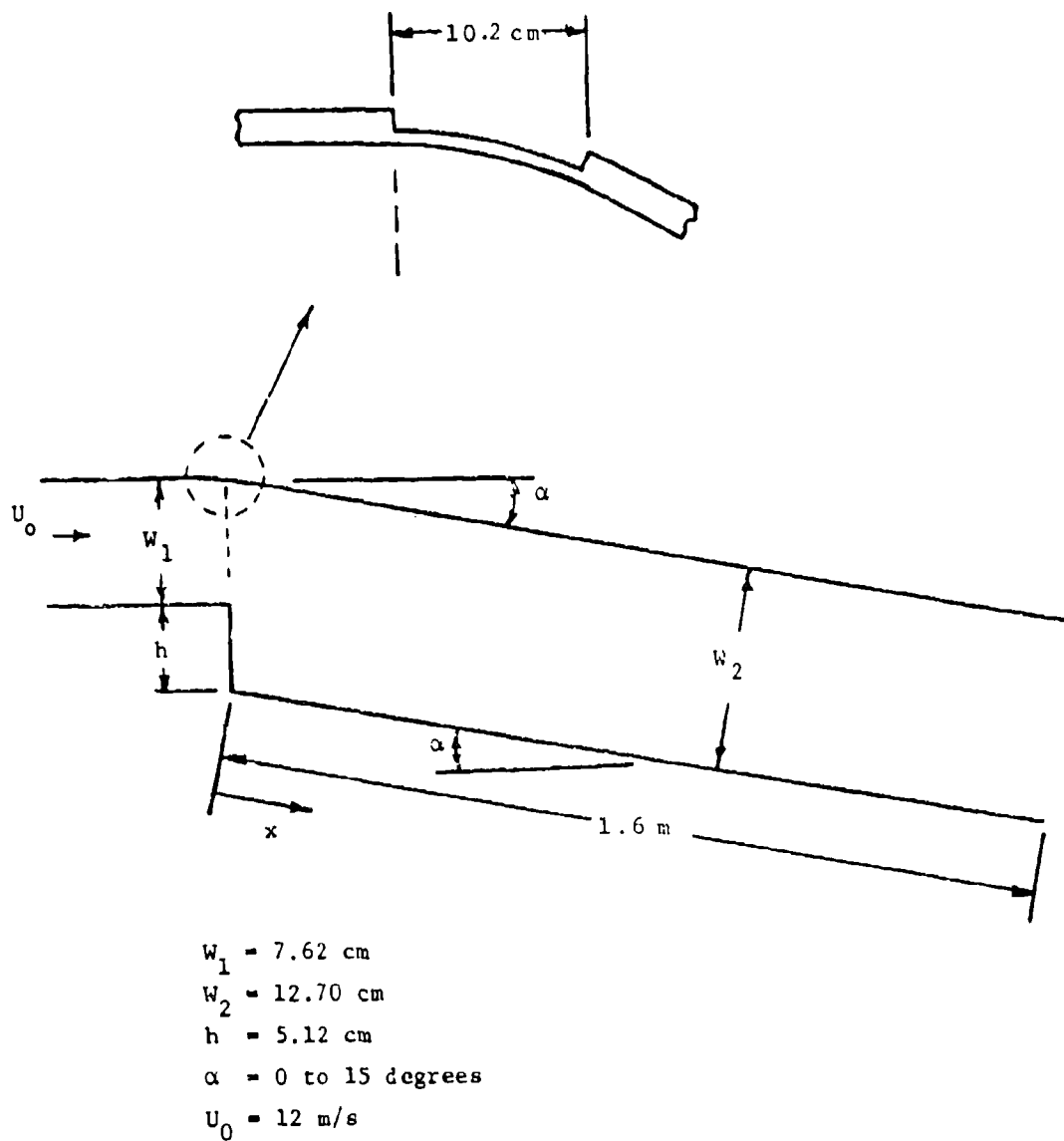


Figure 1. Wind-tunnel configuration.

ENTRY CASE/PREDICTIVE TEST
SPECIFICATIONS FOR COMPUTATION
Case #0423; Coordinator: J. K. Eaton

File #	Independent Variable(s) (Label)	Dependent Variable(s) (Output)	Range of Independent Variable(s); Locations	Comments
P3-1	x/H	$C_{p_{w,s}}$	$-3 \leq x/H \leq 20$	See instructions 1, 2, 3, 4, 5. $\alpha = 0^\circ$.
P3-2	x/H	$C_{p_{w,s}}$	$-3 \leq x/H \leq 20$	$\alpha = 5^\circ$. for step-side wall
P3-3	x/H	$C_{p_{w,s}}$	$-3 \leq x/H \leq 20$	$\alpha = 10^\circ$.
P3-4	x/H	$C_{p_{w,s}}$	$-3 \leq x/H \leq 20$	$\alpha = 15^\circ$.
P3-5	x/H	$C_{p_{w,o}}$	$-3 \leq x/H \leq 20$	See instructions 1, 2, 3, 4, 5. $\alpha = 0^\circ$.
P3-6	x/H	$C_{p_{w,o}}$	$-3 \leq x/H \leq 20$	$\alpha = 5^\circ$. for wall opposite step
P3-7	x/H	$C_{p_{w,o}}$	$-3 \leq x/H \leq 20$	$\alpha = 10^\circ$.
P3-8	x/H	$C_{p_{w,o}}$	$-3 \leq x/H \leq 20$	$\alpha = 15^\circ$.
P3-9	α	x_R	$0 \leq \alpha \leq 15^\circ$	$x_R \triangleq$ point where $\tau_w = 0$ in computations.
P3-10	y/R	U/U_o	full channel	$x/H = 4.5$; $\alpha = 10^\circ$.
P3-11	y/H	U/U_o	full channel	$x/H = 15.8$; $\alpha = 10^\circ$.
P3-12	y/H	U/U_o	full channel	$x/H = x_R$; $\alpha = 10^\circ$.

Special Instructions:

1. Instructions for predictive case files format are given in the Appendix to the Overview of Predictive Test Cases.
2. For each file in this case, create a binary array of N elements; report the number of elements in each file in writing and at head of file.
3. Take x_R = location of reattachment ($\tau_w = 0$) computed by your program.
4. $U_o = 12$ m/s; ()_o = station $x/H = -4$.

5. $C_{p_{w,s}} = \frac{P_{wall} - P_o}{\frac{1}{2} \rho U_o^2}$ on step-side wall.

$C_{p_{w,o}} = \frac{P_{wall} - P_o}{\frac{1}{2} \rho U_o^2}$ on wall opposite step.

BACKWARD-FACING STEP: VARIABLE AREA RATIO

PREDICTIVE TEST P4

Flow 0420

Case 0424

Description by S. J. Kline

SUMMARY

GENERAL DESCRIPTION

This case has the same geometry and nomenclature as Cases 0421, 0422, and 0423 ($\alpha = 0^\circ$). This case consists of running with various area ratios using a sufficient number of values so that results can be extrapolated to the limiting values (0, 1) for the inverse area ratio (A_1/A_2).

The initial data are those for Case 0422. If you desire to investigate the effects of variation in initial R_θ , we will be happy to receive output on that effect also.

We suggest computers do not do this case unless they have set up Case 0421, 0422, or 0423, so that only a few additional production runs are required to obtain the output requested.

ENTRY CASE/PREDICTIVE TEST

SPECIFICATIONS FOR COMPUTATION

Case #0424 (P4); Coordinator: J. K. Eaton

File #	Independent Variable(s) (Label)	Dependent Variable(s) (Output)	Range of Independent Variable(s); Locations	Comments
P4-1	A_1/A_2	x_R/H	$0 < A_1/A_2 < 1$	<ol style="list-style-type: none"> 1. H = step height A_1 = upstream area A_2 = downstream area See Fig. 1, Case 0421, p. 103. 2. Compute for enough values of A_1/A_2 to establish limiting values of x_R/H at $A_1/A_2 = 0$ and $A_1/A_2 = 1$ by extrapolation of x_R/H. 3. x_R/H = value of x/H where computed value of $\tau_w = 0$.

Special Instructions:

1. Instructions for predictive case files format are given in the Appendix to the Overview of Predictive Test Cases.
2. Create a binary array for file P4-1 of N elements. Report the value of N in writing and at head of file.
3. Special comment: Since the geometry and flow are the same as Cases 0421, 0422, 0423 ($\alpha = 0^\circ$) with some possible variations in inlet conditions, it should be relatively easy to run the computations for file P4-1, if you do any of Cases 0421, 0422, or 0423. Please use the initial conditions of Case 0422 (see specifications for Case 0422, instruction 5).

FLOW IN A PLANAR DIFFUSER WITH TAILPIPE

PREDICTIVE CASE γ^*

Presentation Prepared by John K. Eaton

GENERAL DESCRIPTION

The flow through a wide-angle, planar diffuser with a downstream duct (tailpipe) will be investigated. The diffuser will stall on one of the diverging walls, and the flow will reattach in the tailpipe. The flow geometry is shown in Fig. 1. The total included angle (2θ) for the diffuser will be 50° . The boundary layers on all four walls of the inlet duct are turbulent.

Measurements of the wall static pressure will be supplied for the range $-5 \leq x/W_1 \leq 75$. In addition, mean velocity, turbulence intensity, and Reynolds stress ($-\overline{u'v'}$) profiles will be measured upstream of separation and downstream of reattachment. The mean velocity and turbulence data will be obtained using hot-wire anemometry and pitot probes.

DETAILED FLOW SPECIFICATIONS

The dimensions of the experimental facility are shown in Fig. 1. Inlet profiles of mean velocity and turbulence intensity have been measured at $x/W_1 = -5$. We have requested that the experimenter also provide a Reynolds shear stress ($-\overline{u'v'}$) profile for this location. The mean velocity and turbulence intensity profiles measured on the channel centerline ($z = 0$) are shown in Figs. 2 and 3.

Spanwise profiles were measured to check the two-dimensionality of the inlet flow but are not shown here. The profiles show that the end-wall boundary layers are approximately 1.6 cm thick at $x/W_1 = -5$. The core velocity is somewhat non-uniform in the spanwise direction; the edge velocity for the upper end-wall boundary layer is about 2% higher than the edge velocity of the lower end-wall boundary layer. The effect of this on the uniformity of the downstream flow will be investigated at a later date.

SPECIFICATION FOR COMPUTATIONS

Computations should begin at or upstream of the first station $x/W_1 = -5$. The computation should continue to $x/W_1 = 75$. Three types of output are required:

*This case was not finally accepted as a predictive case for the 1981 Conference. This arose because of certain irregularities in the data, including three-dimensional effects which could not be corrected before January 1981, the deadline for submitting predictive case specifications to computers.

(1) plots of global variables, (2) plots of mean-flow velocity profiles, and (3) plots of turbulence intensity and turbulent shear stress.

The global variables should be plotted against x/W_1 (abscissa) for $-5 \leq x/W_1 \leq 75$ at a scale of 1 cm = 5. The global variables are specified below.

- (a) Skin friction plotted as $c_f = \tau_w / \frac{1}{2} \rho U_{c1}^2$, where U_{c1} is free-stream velocity at $x/W_1 = -5$.

Abscissa: x/W_1 ; range, $-5 \leq x/W_1 \leq 75$; scale, 1 cm = 5.

Ordinate: c_f ; range, 0 to 2×10^{-3} ; scale, 1 cm = 2×10^{-4} .

- (b) The static pressure on the diverging and parallel walls plotted as $c_p = (p - p_1) / \frac{1}{2} \rho U_{c1}^2$ (p_1 is the static pressure at $x/W_1 = -5$).

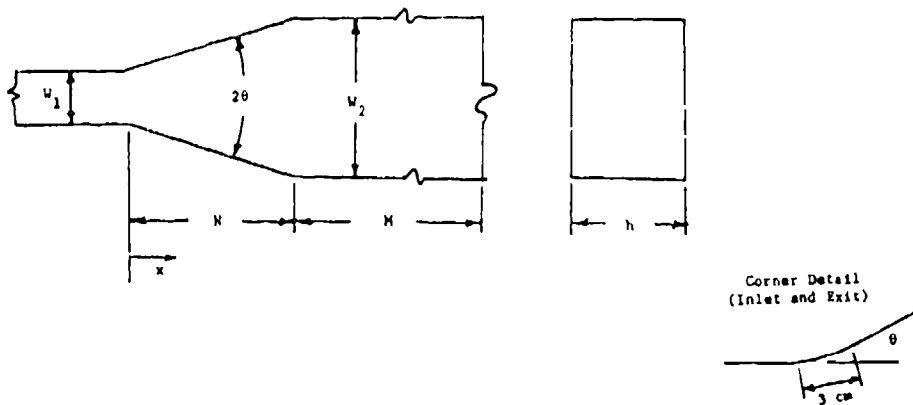
Abscissa: x/W_1 (same range and scales as described above).

Ordinate: c_p ; range, -0.1 to 1.0; scale, 1 cm = 0.1.

- (c) The momentum and displacement thicknesses should be plotted on the same figure.

Abscissa: x/W_1 (same range and scales as described above).

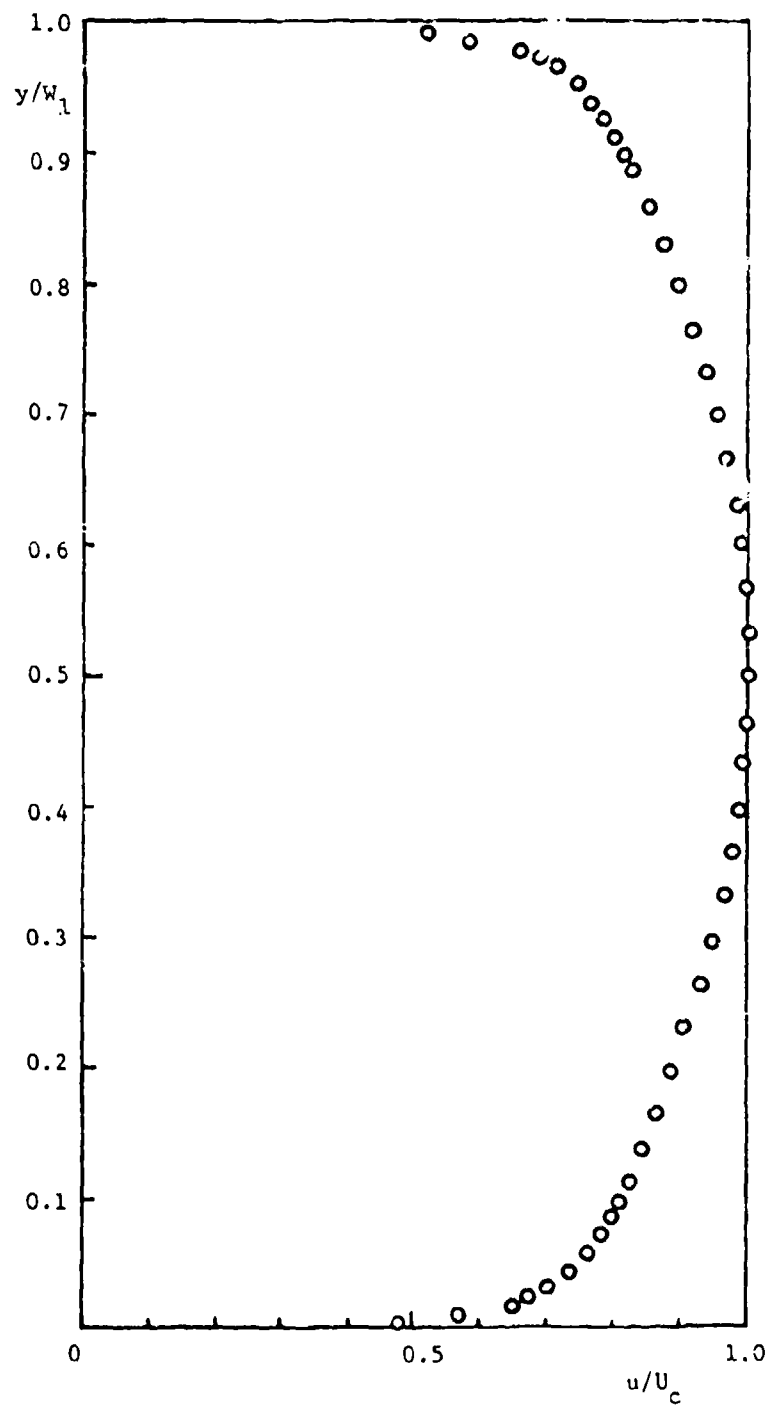
Ordinate: θ, δ^* ; scale, 1 cm = 1 cm.



$2\theta = 50^\circ$
 $W_1 = 3 \text{ cm}$
 $W_2 = 31 \text{ cm}$
 $N = 30 \text{ cm}$
 $M = 180 \text{ cm}$
 $h = 16 \text{ cm}$

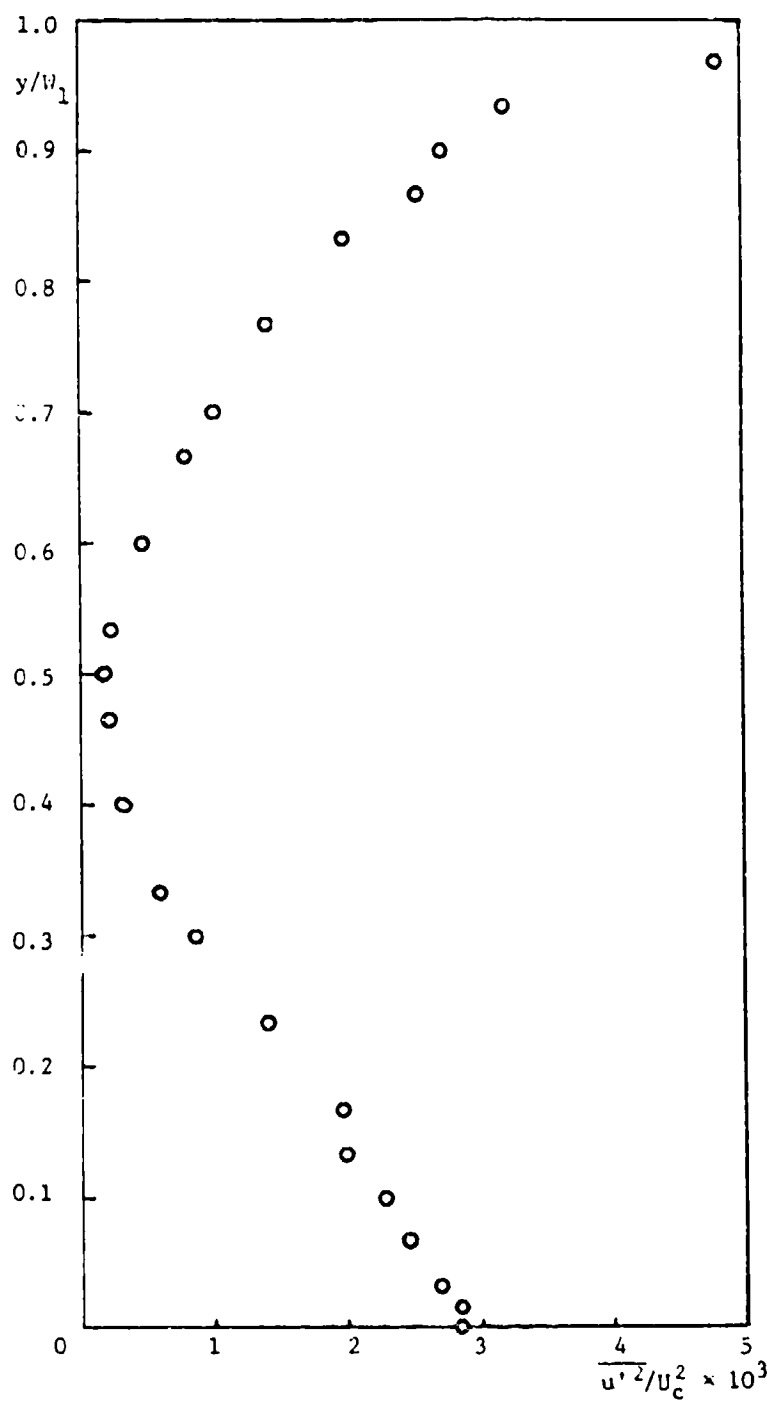
inlet station at $x/W_1 = -5$
 $U_c(x/W_1 = -5) = 44.5 \text{ m/s}$
 $\nu = 1.63 \times 10^{-5} \text{ m}^2/\text{s}$

Figure 1. Test facility configuration.



$2\theta = 50^\circ$, $N/W_1 = 10$, $AR = 10.3$, $U_c = 44.5 \text{ m/s}$

Figure 2. Inlet cross-stream direction velocity profile.



$2\theta = 50$, $N/w_1 = 10$, $AR = 10.3$ (at $x/w_1 = -5$)

Figure 3. Inlet cross-stream direction turbulence profile.

SHOCK-BOUNDARY LAYER INTERACTION

Preliminary Specification -- Predictive Case δ^*

Presentation Prepared by John K. Eaton

GENERAL DESCRIPTION

In this experiment, a shock-boundary layer interaction will be studied at various free-stream Mach numbers. A turbulent boundary layer will be grown on a flat plate and the impinging shock will originate at a separate shock generator (see Fig. 1). Both the flat plate and the shock generator will span a 1x1-ft supersonic wind tunnel.

Measurements will include wall static pressure, mean velocity profiles, and skin-friction measurements. Data will be obtained for the conditions shown in Table 1. There is a possibility of obtaining data at higher Reynolds numbers by modifying the test plate. This will depend on the extent of the region of two-dimensional flow.

DETAILED FLOW SPECIFICATIONS

A detailed flow specification cannot be given at this time. Preliminary work will be done with a laminar boundary layer to check the flow two-dimensionality. If the preliminary work indicates that the flow conditions are well controlled, the initial condition data for the turbulent boundary layer case will be sent to computers.

TABLE 1
Test Conditions

M	Max Re (based on plate length)
1.6	2.1×10^6
2.0	2.2
2.5	2.3
3.0	1.8
3.5	1.5
4.0	1.2

*This case was not finally accepted as a predictive case for the 1981 Conference. The elimination of adverse three-dimensional effects proved too difficult to solve in the time available before January 1981.

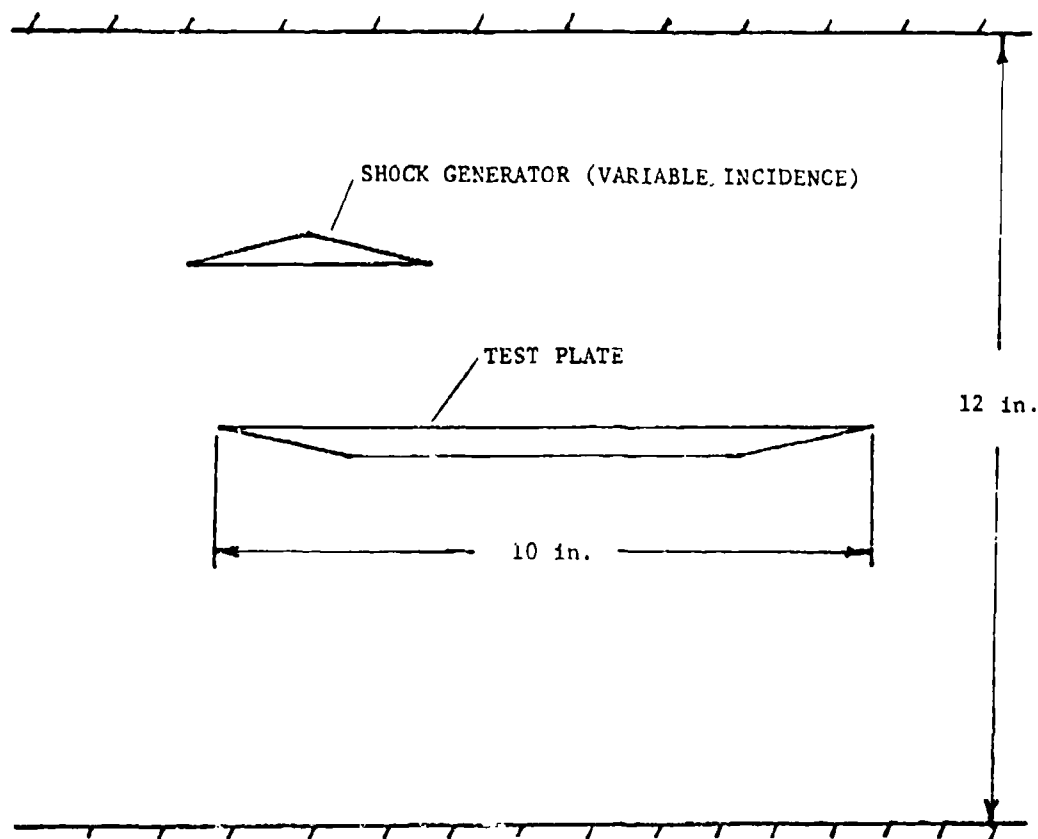


Figure 1. Wind Tunnel Configuration

DISCUSSION

Predictive Case δ

E. P. Sutton suggested technical oversight is necessary to ensure the best chance of obtaining two-dimensional flow. J. Eaton remarked that S. Bogdonoff had already agreed to provide technical oversight for this case.

TRANSONIC AIRFOIL

Preliminary Specification - Predictive Case ϵ *

Presentation Prepared by John K. Eaton

GENERAL DESCRIPTION

Data are being obtained for a NACA 64A010 airfoil with a 15.24-cm chord. Complete data sets will be obtained for three angles of attack (0, 2, and 4 degrees) at a Mach number of 0.8. Two additional cases will be investigated: i) a low Mach number case, and ii) a higher Mach number, low-angle-of-attack case, which gives severe separation. The experiments are being conducted in a 6" x 22" transonic wind tunnel. The top and bottom walls of the wind tunnel are perforated. Boundary-condition data including \bar{U} and \bar{V} on the upper and lower wind tunnel walls will be supplied.

Measurements will include mean and rms pressure on the airfoil surface. A two-component, frequency-shifted, laser-doppler velocimeter system will be used to obtain measurements of \bar{U} , \bar{V} , $\overline{u'^2}$, $\overline{v'^2}$, and $\overline{u'v'}$. Measurements will be made upstream of the model, along the model surface, and in the near and far wakes.

DETAILED FLOW SPECIFICATIONS

Detailed flow specifications will be issued after the experimenter has measured the boundary-condition data. These data should be sent to computers by January 31, 1981.

DISCUSSION

Predictive Case ϵ

There was general agreement with E. P. Sutton's observation that, since only the top and bottom tunnel walls are perforated, the side-wall boundary layers could be troublesome in this experiment. M. Childs and J. Spreiter were suggested as possible technical reviewers for this experiment.

*This case was not finally accepted as a predictive case for the 1981 Conference. There were reservations regarding the small aspect ratio of the airfoil and the inherent difficulties in avoiding three-dimensional effects. There was also insufficient time to properly document the data in time for the specifications to be submitted to computers by January 1981. This experiment is currently being completed.

DISCUSSION

General Predictive Cases

1. It was recommended that all the predictive test cases proposed should be retained.
2. The need for specifying initial, boundary and downstream conditions were extensively discussed for all predictive cases.
3. E. Reshotko, J. Eaton, G. Sovran, and J.P. Johnston favored giving complete geometric information, together with mean and turbulence quantities at an initial plane, to computers.
4. R. Durst favored providing downstream conditions for those with elliptic codes.
5. J. Hunt suggested that some spectral data and/or information concerning scales would be needed by some methods.

There was broad agreement that better specification of test geometries, including exhaust conditions, would be needed. The issue of whether flow specifications favor particular calculation schemes was raised and discussed, but not resolved.*

*[Ed.: In the step case, specifications will give geometry and initial conditions. Computers requiring downstream boundary data can generate them by employing a fictitious tailpipe of sufficient length for their purpose.]

FLOWS WITH BUOYANCY FORCES

Flow 9000

Evaluator: J. C. Wyngaard*

SUMMARY

(From Letter from J. C. Wyngaard to S. J. Kline, 7/15/1980)

In January 1980 you asked me to evaluate in more detail buoyancy-influenced flows for the 1980-81 AFOSR-HTTM Stanford Conference on Complex Turbulent Flows. I agree to undertake the task, and in April I expected to have an evaluation done by sometime in June.

I agree that an important part of turbulence modeling is the ability to calculate flows with strong buoyancy forces. I also agree that such an evaluation should include both unstably and stably stratified flows from laboratory and geophysical environments. However, my reflection and research over the past few months has convinced me that an evaluation of these flows, to the standards you have established, is not possible at this time.

The boundary layers in the lower atmosphere and the upper ocean are perhaps the most accessible sources of buoyancy-influenced geophysical turbulence. They are found in states ranging from essentially free convection through neutral shear flow to stable stratification. They have extremely large Reynolds-number turbulence, are often quasi-steady and locally homogeneous, and thus are often well-suited to one-dimensional idealizations. By contrast, stratified flows in the laboratory often have Reynolds numbers so low that their structure is Reynolds-number-dependent; in addition, it can be difficult to find laboratory flows as nearly one-dimensional as geophysical ones and having arbitrary states of stratification (flux Richardson number) and negligible containment effects. Thus a successful evaluation would have to be based largely on geophysical data.

Over the past 5-10 years, a large number--certainly several dozens--of papers have appeared which deal with the modeling of these geophysical boundary layers. Most of these models are variants of the second-order type developed for use in shear flows, and often they are able, with some tuning for convective or stable stratification effects, to reproduce what is known of the broad features of these boundary layers. Many of these papers do include some attempts at comparisons with measurements.

*National Center for Atmospheric Research, P.O. Box 3000, Boulder, CO 80307.

There are several points I would like to make about this activity. The first is that, broadly speaking, our knowledge of the structure of these geophysical boundary layers does not approach that of laboratory shear flows. While I believe that the first measurements of the Reynolds shear stress and heat flux budget were done in the atmosphere, not in the laboratory, this is not typical. Rather, we simply do not yet have the exhaustive sets of carefully taken, statistically reliable, complete measurements of the mean and turbulent structure of geophysical boundary layers that are needed for flow documentation.

A second point is that because our documentation of the structure of these geophysical flows lags so far behind that of laboratory shear flows, I fear that model verification and refinement is being fairly widely neglected. I pointed out some aspects of this in a manuscript which will appear in Turbulent Shear Flows II, the proceedings of the 1979 London conference. In particular, I argued that in convectively driven turbulence the pressure covariances, transport terms, and the dissipation rates in the second-moment equations behave quite differently than in shear flow, and that the widely used shear-flow closures for these terms are incorrect. In order to show this, however, I had to average over many sets of measurements and experiments, and the conclusions are more qualitative than quantitative. Given this situation, perhaps it is natural that buoyant-flow modelers do not seem to work as hard on model verification as shear-flow modelers do.

Thus I feel that the buoyant-flow evaluation could not now be done to shear-flow standards. While many of us in the field believe that contemporary models do make significant errors in their predictions of convective turbulence structure, it is all but impossible to document this adequately at this time. I think that an attempt to do such an evaluation, in the context of your conference, might ultimately turn out to be a disservice to the community.

Perhaps what we need instead for buoyancy-influenced flows is a monograph such as Townsend has done for shear flows. Important topics might include, for convective flows, such active research areas as

1. structure of the overlying entrainment region
2. deviations from Monin-Obukhov similarity in the surface layer
3. the nature of the pressure transport of turbulent kinetic energy, known to be important at the bottom and top
4. the behavior of the turbulent transport (third-moment divergence) terms
5. the effects of baroclinity (i.e., vertical variation in the horizontal mean pressure gradient) on boundary-layer structure
6. effects of entrainment on boundary-layer structure
7. the vertical profiles of dissipation rates of turbulent kinetic energy and scalar variance

8. validity of local closures in convection
9. influence of the shape of the buoyancy-flu. profile on boundary-layer structure.

These point could be discussed in the context of the underlying physics, and what data do exist could be included, with the appropriate caveats. While each of these points concerns a key structural aspect, I emphasize that none is now well-enough measured to be included in a data archive. One could make a comparable list, and statement, for stably stratified flows.

I hope that my position does not cause you serious problems with your conference. After these months of reflection, however, it is the only one I feel comfortable with. I would be happy to discuss any of the points with you in more detail.

DISCUSSION

Flow 9006

B. Launder: I am in general agreement with John Wyngaard's statement but I feel his viewpoint seems to be unduly pessimistic. The data may not achieve the degree of precision of the laboratory non-buoyant data, but they are certainly good enough to do at least some coarse sorting out among turbulence models now in use. One might also remark that "answers" for buoyant flows are generally not needed with quite the precision required in aerodynamics (a factor of 2 on effective diffusivity is often close enough). I would also underline my earlier observation (when the question of commissioning a buoyant-flow survey was raised) that because buoyant flows involve coupling between turbulent heat and momentum fluxes, it would seem more informative to precede such a survey with one relating to heat-transport mechanics with negligible buoyancy effects.

Recommendation: Buoyancy effects would require a more detailed study, including also the matter of scalar transport. It is unlikely that this can be done in time to be meaningful for the 1981 Conference. It was confirmed that this flow should not be used for the 1981 Conference.

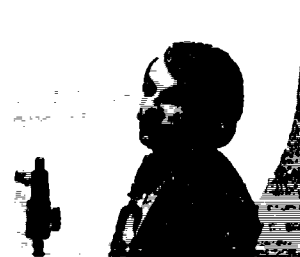
FLOWS WITH SWIRL

Flow No. 0340

Evaluator: A. P. Morse*

SUMMARY

(presented at the 1980 Conference by A. P. Morse)[†]



INTRODUCTION

This summary deals only with free swirling flows (flows in which the main region of interest is remote from solid walls). A full report has been submitted to the Stanford 1980-81 Organizing Committee, Morse (1980b). The addition of swirl has large-scale effects on free jet development. In particular, the rate of mixing increases with swirl intensity. Thus swirling jets spread more quickly, and the mean velocities decay more rapidly than in a non-swirling jet. In a strongly swirling jet the gradients of static pressure set up across the flow field introduce adverse axial pressure gradients in the region of swirl decay, and these may be strong enough to cause reversal of the forward velocities near the jet axis. Thus a recirculation zone is set up downstream of the jet orifice. Weaker swirl leads to less strong curvature of the stream lines, and the flow is then amenable to analysis as a thin shear layer. Even so, the spreading rate may reach as much as twice that of a non-swirling jet. The enhanced mixing resulting from the adverse pressure gradient leads to increases in the turbulence intensities. Further downstream, where the swirl field is weakened, the turbulence levels and the spreading rate reduce approximately to those of the non-swirling jet.

EXPERIMENTAL INVESTIGATIONS

A summary of previous investigations of free swirling flows is given in Table 1 of which five are considered to display satisfactory internal consistency. These are presented in Table 2, alongside the earlier measurements of Rose (1962) and Pratte and Keffer (1972). All five cases are suitable test cases for comparison with computations.

*Dept. of Mech. Engr., Imperial College, London SW7 2BY, England.

[†]The report on this flow was received too late to evaluate it and review it in accordance with the standard procedure. It is accordingly not a test case for the 1981 Conference.

The swirl number, S , in Tables 1 and 2 is defined as

$$S = \frac{G_\theta}{RG_x}$$

where R is a characteristic dimension of the flow (usually the nozzle radius), G_x is the axial momentum flux, and G_θ is the angular momentum flux.

The data of Hösel (1978) and Fornoff (1978) refer to a single jet exhausting into the stagnant atmosphere. The exit diameter of the jet nozzle was 20 mm. Morse (1980a) also studied the single jet (exit diameter 25.4 mm) and extended the investigation to the case of a jet exhausting into a uniform stream of low turbulence intensity. The initial velocity ratio of the two streams (inner-to-outer) was 2.70. The velocity of the outer jet remained constant (to within $\pm 2\%$) over the axial range of measurement.

Co-axial jet flows were also studied by Hellat (1979) and Ribeiro and Whitelaw (1980). In the latter case, the flow originated from concentric pipes of an internal diameter ratio of 2.79, the two jet streams being separated initially by a wall thickness of 0.34 times the (internal) radius of the inner pipe. The ratio of the maximum jet velocities (inner-to-outer) at the exit plane was 0.71. Recirculation did not occur. Hellat's flows were generated in concentric pipes of an internal diameter ratio of 2.07. The investigation covered three swirling flows, one without recirculation and two with; unfortunately, for the highest swirl number, the axial distance covered by the measurements was insufficient to cover the whole of the area in which flow reversal occurred.

All of the cases recommended as suitable for prediction entailed measurements of the three components of the mean velocity vector and all six non-zero Reynolds stresses. Hösel and Fornoff used laser-Doppler anemometry, the remaining authors hot-wire anemometry.

The experimental flow conditions at the nozzle exit are given in the references below. The accuracy of the measured data is typical of that in jet or mixing-region flows (see Flow 0310).

TEST CASES

Case 0341. Ribeiro, M. M. and J. H. Whitelaw, J. H. (1980). "Co-Axial Jets With and Without Swirl"

In this experiment values of U , V , W and all $\overline{u_i u_j}$ were measured for swirl numbers $S = 0$ and $S = 0.31$ for downstream distances up to $x/D = 6$. The external field was stationary. This test case involves the theoretical and experimental comparison between the variation of the centerline values of U , u^2 and v^2 with x/D , as well as the decay of the maximum swirl velocity.

Case 0342. Morse, A. P. (1980a). "Axisymmetric Free-Shear Flows With and Without Swirl"

This case is similar to Case 0341 with the addition that for $S = 0.32$ results are given for the jet issuing into a uniform flow in which the inner to the outer velocity ratio is 2.70.

Case 0343. Hösel, W. (1978). "Drallstrahlenuntersuchungen mit einem Weiterentwickelten Laser-Doppler-Messverfahren"

This case is similar to Case 0341 in which the external field is stationary, but the swirl numbers tested are $S = 1.33$ and 1.70 .

Case 0344. Hellat, J. (1979). "Turbulente Strömung und Mischung in Erdgas--Diffusion Flammen mit Luftdrall"

This case is similar to Case 0341 but has an extended range of S covering $S = 0.40, 1.15$, and 2.28 .

Case 0345. Fornoff, M. (1978). "Experimentelle und Theoretische Untersuchung von Drallstrahlen"

This case is similar to Case 0341 but has an extended range of x/D up to 40, for $S = 0.53$. This range of x/D was covered in Case 0343 for larger values of S .

CONCLUSIONS

Reliable data are scarce for free-swirling jet flows, particularly those for flows with recirculation (i.e., at high values of the swirl number). In this context, the measurements of Hösel (1978) and Hellat (1979) probably represent the best available at present. Neither set of data is however recommended as a suitable test case for prediction. Hösel's data display too large a variation in the axial and angular momentum fluxes (see Table 2) and, although symmetry is excellent, the profiles do not contain sufficient measurement points for good definition, particularly in the near-field of the flow. Moreover, the first full description of the mean-velocity and Reynolds-stress components is only available at $x/D = 2.0$, so that the prime region of interest (the recirculation zone) cannot be covered in the computations. Hellat's data are of greater internal consistency, but only extend over the axial range $0.6 \leq x/D \leq 2.8$. In Hellat's flow with the highest swirl number $S = 2.28$; this x/D range does not cover the region of recirculation.

The data of Ribeiro and Whitelaw (1980) and Morse (1980a) have been selected as suitable cases for comparison with computation. These are summarized in Table 2. The former data cover one flow (in a coaxial jet arrangement), the latter three. However, of the latter flows, that for the lowest swirl number ($S = 0.26$) displays too large a variation in the angular momentum flux and is recommended only as a back-up case for the flows of higher swirl number.

The three flows selected satisfy the requirements of good conservation of the momentum fluxes, symmetry and internal consistency of the magnitudes of the shear stresses \overline{uv} and \overline{vw} with the mean velocity profiles. The flows do not entail recirculation and may be computed by a parabolic "marching-type" procedure as in Morse (1980a).

ADVICE TO COMPUTERS

The magnitude of the shear stress \overline{uw} governing the axial diffusion of angular momentum is at least an order of magnitude higher than would be expected from the use of isotropic "turbulent viscosity" hypothesis. In the near field of the flow, \overline{uv} is comparable to \overline{uw} and \overline{vw} (see Fig. 1). Despite its large magnitude, the influence of \overline{uw} on the development of the flow is small. Axial diffusion of angular momentum is only of significance in the outer part of the flow (see Figs. 2a and 2b), while the production of \overline{uv} by the action of \overline{uw} is small compared to the production against the radial velocity gradient $\partial U/\partial r$ (see Fig. 3). Consequently, the inclusion of \overline{uw} in the calculation procedure is not necessary. This situation is not, however, appropriate, for flows with recirculation; there axial diffusion is important, and the production of \overline{uv} by \overline{uw} is comparable to, or even larger than that by $-\overline{v^2}(\partial U/\partial r)$.

REFERENCES

- Chigier, N. A., and J. M. Beer (1964). "Velocity and static-pressure distributions in swirling air jets issuing from annular and divergent nozzles," ASME, J. of Basic Eng., 788.
- Chigier, N. A., and A. Chervinsky (1967). "Experimental investigation of swirling vortex motions in jets," ASME, J. of Appl. Mech., 89, Series E, 443.
- Craya, A., and M. Darrigol (1967). "Turbulent swirling jet," Phys. Fluids Suppl., Boundary Layers and Turbulence, 197.
- Fornoff, M. (1978). "Experimentelle und Theoretische Untersuchung von Drallstrahlen," Diplomarbeit, University of Karlsruhe, West Germany.
- Hellat, J. (1979). "Turbulente Strömung und Mischung in Erdgas--Diffusion Flammen mit Luftdrall," Dissertation Thesis, University of Karlsruhe, West Germany.
- Hösel, W. (1978). "Drallstrahlenuntersuchungen mit einem Weiterentwickelten Laser-Doppler-Messverfahren," Rept. SFB 80/E/120, University of Karlsruhe, West Germany.
- Kawaguchi, O., and T. G. Sato (1971). "Experimental investigations of premixed swirling jet flames," Bulletin JSME, 14:69, 248.
- Keer, N. M., and D. Fraser (1965). "Swirl, Part I: Effect on axisymmetrical turbulent jets," J. Inst. Fuel, 519.
- Maier, P. (1967). "Untersuchung Isothermer Turbulenter Drallfreistrahlen und Turbulenter Drallflammen," Dissertation Thesis, University of Karlsruhe, West Germany.

- Mathur, M. L., and N. R. L. MacCallum (1967). "Swirling air jets issuing from vane swirlers. Part I: Free jets," J. Inst. Fuel, 214.
- Morse, A. P. (1980a). "Axisymmetric free shear flows with and without swirl," Ph.D. Thesis, University of London.
- Morse, A. P. (1980b). "An evaluation of data for flows with swirl--Flow 0340," prepared for the 1980-81 Stanford Conference on Complex Turbulent Flows.
- Pratte, B. D., and J. F. KEFFER (1972). "The swirling turbulent jet," ASME, J. Basic Eng., 94, Series D, 739.
- Ribeiro, M. M., and J. H. Whitelaw (1980). "Co-axial jets with and without swirl," J. Fluid Mech., 96, 769.
- Rose, W. G. (1962). "A swirling round turbulent jet. Part I: Mean-flow measurements," ASME, J. Appl. Mech., 29, Series E, 615.
- Syred, N., N. A. Chigier, and J. M. Beer (1971). "Turbulence measurements in swirling recirculating flows," Symposium on Internal Flows, University of Salford, Paper 13, B27.

TABLE 1
Summary of Experimental Investigations of Free-Swirling Flows

Author(s)	Method of Swirl Generation	Measurement Technique	Range of Axial Distance	Range of Swirl Number	Recirculation?	Measured Quantities
Rose (1962)	rotating pipe	hot-wire	0.235-15.0	0-0.23	No	U, V, W, u_1^2
Chigier and Beer (1964)	tangential ports	impact probe	0-6.0	0.39-1.43	Yes	U, W
Keer and Fraser (1965)	vanes	impact probe	11.7-19.0	0-0.72	No	U, V, W
Chigier and Chervinsky (1967)	tangential ports	impact probe	1.0-15.0	0.13-0.66	Yes	U, W, P
Mathur and MacCallum (1967)	vanes	impact probe	0.6-20.0	0-2.7	Yes	U, W, P
Maier (1967)	vanes	impact probe	0.27-30.0	1.75-2.9	Yes	U, W
Craya and Darrigol (1967)	tangential ports	hot-wire	1.0-15.0	0-1.58	Yes	$U, V, W, \text{all } u_i u_j$
Syred, Chigier and Beer (1971)	tangential ports	hot-wire	0-2.0	2.2	Yes	U, W, u^2, v^2, w^2, uv
Kawaguchi and Sato (1971)	tangential ports	hot-wire	0.1-4.0	0.6-0.9	Yes	U, W, u_1^2, P
Pratte and Keffer (1972)	rotating pipe	hot-wire	1.0-30.0	0.3	No	$U, W, \text{all } u_i u_j$
Hösel (1978)	tangential ports	LDA	0.25-40.0	0-1.7	Yes	$U, V, W, \text{all } u_i u_j$
Fornoff (1978)	tangential ports	LDA	0.25-40.0	0.53	No	$U, V, W, \text{all } u_i u_j$
Hellat (1979)	tangential ports	hot-wire impact probe	0.56-2.79	0-2.28	Yes	$U, V, W, \text{all } u_i u_j$
Ribeiro and Whitelaw (1980)	tangential ports	hot-wire	0-6.0	0.32	No	$U, V, W, \text{all } u_i u_j$
Morse (1980a)	tangential ports	hot-wire	0.5-20.0	0-0.40	No	$U, V, W, \text{all } u_i u_j$

TABLE 2

Summary of Principal Test Cases Examined, Showing Standard Deviations in Momentum Fluxes and Swirl Number

Author(s)	Swirl Number		Variation in G_x	Variation in G_θ	Variation in S	Range of Profiles Measured (x/D)
	Quoted Value	Mean Computed Value	σ (%)	σ (%)	σ (%)	
Rose (1962)	-	0.23	8.3	18.5	11.6	0.235-15.0
Pratte and Keffer (1972)	0.30	0.26*	16.0*	34.4*	41.6*	1.0-50.0
		0.35	19.9	29.1	38.7	
Hösel (1978)	1.00	1.33	8.9	20.8	12.8	0.25-40.0
	1.30	1.70	15.5	22.5	16.3	
Fornoff (1978)	0.50	0.53	16.9	28.1	21.4	0.25-40.0
Hellat (1979)	0.40	0.40	6.8	6.0	7.4	0.56-2.79
	1.10	1.15	4.2	4.2	4.2	
	2.20	2.28	5.0	3.9	8.4	
Ribeiro and Whitelaw (1980)	0.26	0.31	8.2	6.0	3.3	0-6.0
Morse (1980a)	0.25	0.26	11.9	19.6	11.8	0.5-15.0
	0.32	0.32	2.1	2.8	3.9	1.0-20.0
	(finite U_∞)					
	0.36	0.40	6.9	10.2	9.1	0.5-15.0

* denotes without turbulence terms.

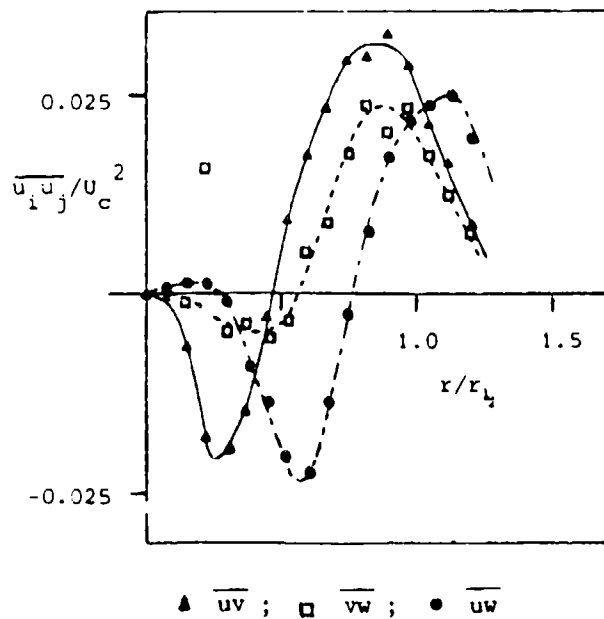
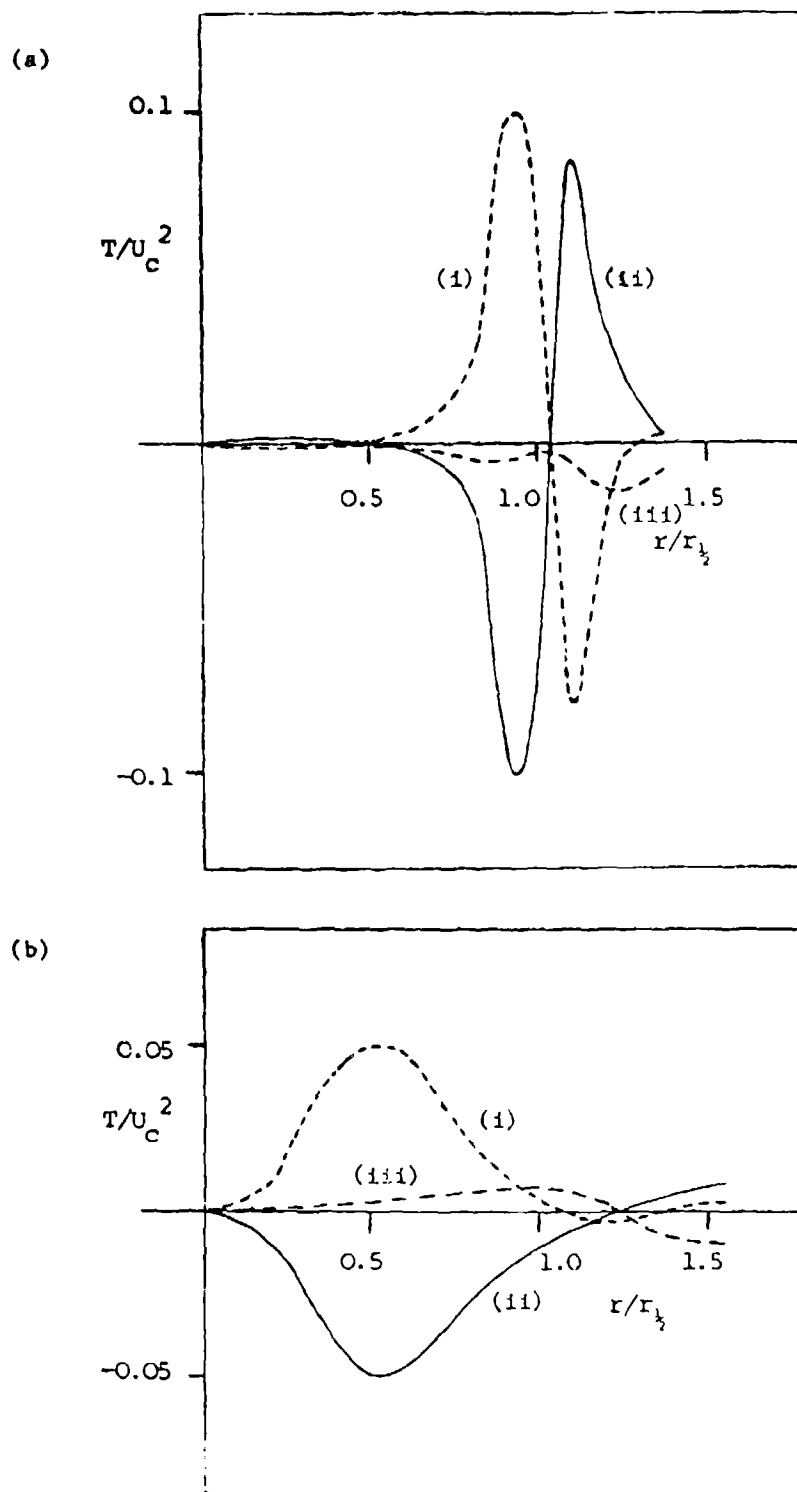
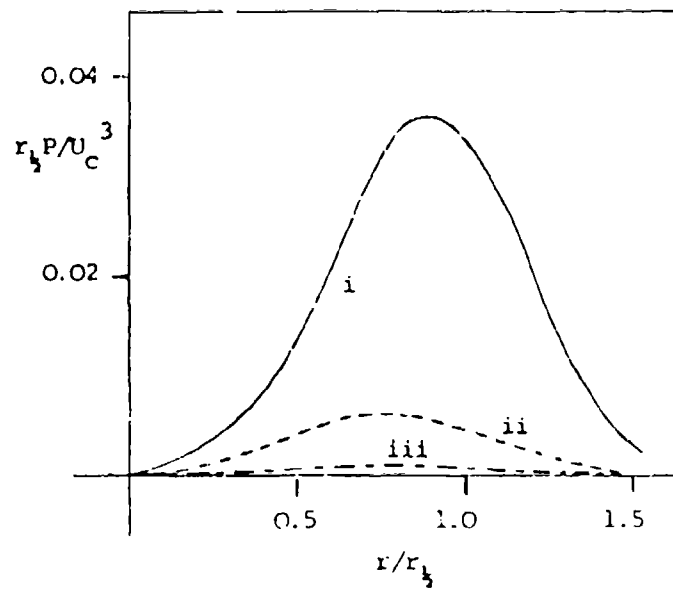


Figure 1. Shear-stress levels at $x/D = 1.0, 6.0$. Data of Ribeiro and Whitelaw (1980), $S = 0.31$.



$$T = (1) - \left[U \frac{\partial}{\partial x}(rW) + V \frac{\partial}{\partial r}(rW) \right]; \quad (11) = \frac{1}{r} \frac{\partial}{\partial r}(r^2 \overline{vw}); \quad (111) = -r \frac{\partial \overline{uw}}{\partial x}$$

Figure 2. (a) Angular momentum balance at $x/D = 0.5$ and (b) at $x/D = 4.0$. Data of Morse (1980a); $S = 0.40$.



$$P = (i) \overline{-v^2 \frac{\partial U}{\partial r}}; \quad (ii) \overline{2uw \frac{W}{r}}; \quad (iii) \overline{uv \frac{V}{r}}$$

Figure 3. Components of production of \overline{uv} at $x/D = 2.0$. Data of Morse (1980a), $S = 0.4$.

SESSION VII

Chairman: L. W. Carr

Technical Recorders:

B. Afshari
F. A. Dvorak



Flow 0360/0390

Flow 0380

Flow 8500

Flow 8100/8200

Flow 8400

Flow 8410

WAKES OF ROUND BODIES

Flow 0360

Case 0361

AXISYMMETRIC BOUNDARY LAYER WITH STRONG STREAMWISE AND TRANSVERSE CURVATURE

Flow 0390

Evaluator: V. C. Patel*



SUMMARY

In the evaluation of axisymmetric wake data, emphasis has been placed on the near-wakes of elongated, streamlined bodies for several reasons. First, far wakes can be classified as simple shear layers, and can be dealt with separately. Second, reliable data in the near-wakes of bluff bodies, with large regions of recirculation, are not available. Third, other test cases for separated flows are being considered for the Conference. The boundary layer over a long slender body thickens rapidly over the rear 5-10% of the body length, and the region over which available first-order boundary-layer theory fails as a result of the transverse and longitudinal curvature effects and normal pressure gradients is quite large. The upstream effects continue to influence the flow in the near-wake. Consequently, a complex turbulent shear flow exists over the tail of the body and in the near-wake; the entire region is characterized by strong viscous-inviscid interaction.

CRITERIA

Before embarking on a detailed review of any particular set of wake data to determine its suitability as a test case for calculation methods developed for complex turbulent shear flows, the criteria that were utilized in making a preliminary selection for further in-depth review are listed. Only those data sets which appeared to meet the following criteria were considered further.

- (a) The initial and boundary conditions must be well documented. In the case of the wake of a round body, the initial conditions may be provided by measurements either in the boundary layer over the body or in the wake just downstream of the body. The boundary conditions should include, at least, the variation of velocity or pressure at the edge of the wake and the pressure distribution over the tail of the body.
- (b) The data must contain information on the near-wake. This requirement stems from the generally held belief that a round wake becomes fully

*Iowa Inst. of Hydraulics Research, University of Iowa, Iowa City, IA 52240.

developed and attains near self-preservation within a distance of the order of one or two body diameters and that the subsequent wake flow can be treated adequately by thin shear-layer approximations. Data which are restricted to the far wake are therefore not suitable as test cases.

- (c) The measurements must include profiles of both pressure and mean velocity as well as turbulence quantities (Reynolds stresses, at a minimum). The flow in the near-wake qualifies as a complex shear flow due to the influence of the extra rates of strain (generated by the body curvatures), higher-order boundary-layer effects (i.e., normal pressure gradients), localized separation, and viscous-inviscid interaction. Fairly detailed data are therefore required in order to test the performance of calculation methods in this environment.

AVAILABLE DATA

Rodi (1975) reviewed data from several previous experiments in axisymmetric wakes. Although his review was confined largely to the asymptotic and self-preservation aspects, it indicated that most of the data available up to that time were acquired in the wakes of bluff bodies with large regions of recirculation and were confined to large distances downstream of the body. Furthermore, several did not include turbulence measurements. The only exception to this was the data of Chevray (1968) in the near-wake of a prolate spheroid. Chevray's measurements included mean velocity and Reynolds stresses at a station upstream and at several stations downstream of the small region of separated flow at the tail. This data set could form an ideal test case for boundary-layer calculation methods designed to handle small pockets of separated flow (so-called inverse calculations) and extend into the near-wake, and was therefore examined in detail.

Interest in axisymmetric wakes has increased in recent years due to possible naval applications, and several new experiments have been reported since Rodi's review. Schetz et al. have made mean-velocity and Reynolds-stress measurements in the wakes of three bodies of revolution. In all cases, data were obtained over the range $2 < x/D < 40$, where x is the distance from the tail and D is the maximum diameter of the body. The mean-velocity profiles indicated near self-similarity over this region. Consequently, it was concluded that the data do not include the important near-wake regions. Furthermore, no information is available either on the boundary layer over the body or the condition of the flow at the tail. These data therefore did not satisfy the established criteria.

The boundary layer over the tail of a streamlined, sharp-tailed, axisymmetric body has been investigated by Patel et al. (1974). In fact, they modified the 6:1

spheroid model of Chevray (1968) by attaching a conical tailpiece to eliminate the separation. Although their detailed measurements were confined to the thick boundary layer, they may be of interest in wake studies since the flow over the tail possesses many of the features of importance in the modeling of near-wakes. Their data may therefore be useful in testing boundary-layer as well as near-wake calculation procedures and have been evaluated.

The more recent experiments of Patel and Lee (1977) and Huang et al. (1978) have included not only the thick boundary layer over the tail but also the near-wake. Together, they provide static-pressure, mean-velocity, and Reynolds-stress data on three different bodies with different surface-curvature and boundary-layer histories. These were examined with a view to determine their suitability as test cases.

In summary, the following sets of axisymmetric flow data were evaluated:

- Chevray (1968), Spheroid;
- Patel et al. (1974), Modified spheroid;
- Patel and Lee (1977), Low-drag body;
- Huang et al. (1978), Afterbody 1 and 2.

After the completion of these reviews, a preliminary report by Huang et al. (1980), describing yet another data set on a third body of revolution, was received. Although this appears to address some of the criticisms of the previous measurements, a detailed evaluation could not be carried out within the required time frame.

RECOMMENDATIONS

Detailed evaluations of the five data sets are contained in the Review Report. The resulting recommendations are summarized below.

- (a) The data of Patel and Lee (1977) and Huang et al. (1978) contain some uncertainties which make them unsuitable as test cases.
- (b) The thick-boundary-layer data of Patel et al. (1974) are recommended as a test case for complex wall shear layers rather than for axisymmetric near-wakes since the measurements were not continued into the wake.
- (c) The recently completed measurements of Huang et al. (1980) should be considered in future evaluations.
- (d) The measurements of Chevray (1968) represent by far the most complete data set in the wake of a streamlined axisymmetric body and is recommended as a test case. The static pressure, mean velocities, and Reynolds stresses have been measured with acceptable accuracy and the flow is judged to be axisymmetric. As a test case, it is of special interest since it contains a small embedded region of flow reversal near the tail. It is suggested that the calculations start from the

boundary layer over the body, continue through the separated flow and near-wake, to the far wake.

Starting the solutions at the first measurement station, $x/D = -0.25$, is not recommended since the effects of normal pressure gradients and transverse curvature are already significant at this station. Note that, at the NASA-Langley Conference of 1972, where this data set was used as a test case, the calculations were started downstream of the separation bubble. This is not recommended for the present Conference.

COMMENTS FOR FUTURE EXPERIMENTERS

The crucial uncertainty in data of this type concerns adequate documentation of axial symmetry, particularly since several investigators have reported that the flow over the tail of the model and in the near-wake is quite sensitive to small changes in model alignment and mounting arrangement. Another uncertainty stems from the difficulties of making accurate measurements of static pressure across the thick tail boundary layer and the near-wake. These are especially important in the quantification of the overall effects of viscous-inviscid interaction. A comprehensive documentation of the flow at a well-defined initial station is also important if the subsequent data are to provide a measure of the influence of such factors as extra rates of strain and normal pressure variation. Finally, the question of what constitutes a "near-wake" (or the approach to asymptotic conditions) and how it is influenced by the initial conditions (i.e., whether the wake starts from attached flow at the tail or separation over the body) cannot be answered with the present data. Additional experiments are needed, including measurements in separated flows. These are some of the points which should be addressed in the design of future experiments.

REFERENCES

- Chevray, R. (1967). "The turbulent wake of a round body," ASME, J. Basic Eng., 90, 275-284 (see also Ph.D. Thesis, The University of Iowa, 1967).
- Huang, T. T., N. Santelli, and G. Belt (1978). "Stern boundary-layer flow on axisymmetric bodies," Proc. Twelfth Symp. on Naval Hydromechanics, National Academy of Sciences, pp. 127-157.
- Huang, T. T., N. C. Groves, and G. Belt (1980). "Boundary-layer flow on an axisymmetric body with an inflected stern," Preliminary Report, DWT-NSRDC.
- Patel, V. C., A. Nakayama, and R. Damian (1974). "Measurements in the thick axisymmetric turbulent boundary layer near the tail of a body of revolution," J. Fluid Mech., 63, 345-362 (see IIHR Report No. 142, 1973, for tabulated data).
- Patel, V. C., and Y. T. Lee (1977). "Thick axisymmetric turbulent boundary layer and near wake of a low-drag body of revolution," Iowa Institute of Hydraulic Research, The University of Iowa, IIHR Report No. 210 (see also Turbulent Shear Flows, Vol. I, pp. 127-153, Springer-Verlag, 1979).

Rodi, W. (1975). "A review of experimental data of uniform density free turbulent boundary layers," Studies in Convection, B. E. Launder, ed., Academic Press, pp. 79-165.

DISCUSSION

Flows 0360/0390

1. The Conference agreed that the data of Chevray should form the test case (Case 0361) for the wake from a streamlined axisymmetric body.
2. At the suggestion of T. T. Huang it was agreed that the data for Flow 0390 should be left for future evaluation.

SPECIFICATIONS FOR COMPUTATION

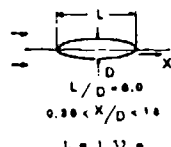
ENTRY CASE/INCOMPRESSIBLE

Case #0361; Data Evaluator: V. C. Patel

Data Taker: R. Chevray

PICTORIAL SUMMARY

Flow 0360. Data Evaluator: V. Patel. "Wakes of Round Bodies (Asymmetric Wakes)."

Case Data Taker	Test Rig Geometry	dp/dx or C _p	Number of Stations Measured							C _f	Re	Initial Condition	Other Notes
			Mean Velocity		Turbulence Profiles								
			U	V or W	$\overline{u^2}$	$\overline{v^2}$	$\overline{w^2}$	\overline{uv}	Others				
Case 0361 R. Chevray	 L/D = 8.0 0.30 < X/D < 1.0 L = 1.32 m	Negligible tunnel blockage effect	12	2	12	12	12	12	-		2.75 × 10 ⁶ (based on L)	Free stream turbulence 0.2%	Model 1.42 m long, 0.254 m maximum diam. spheroid. Static pressure distribution across wake is provided. Model surface pressure not measured.

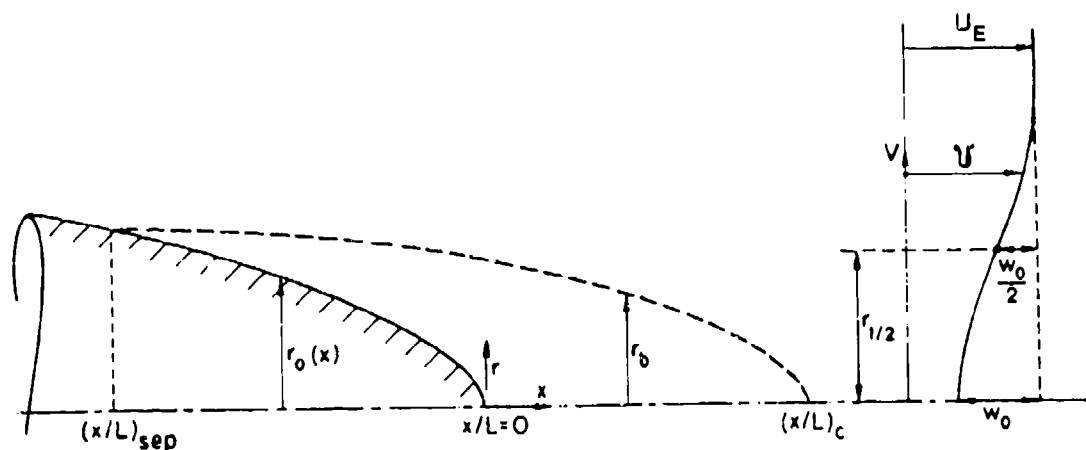
Plot	Ordinate	Abcissa	Range/Position	Comments
1	$C_p = P_A/q_{ref}$	r/R_{ref}	$0 \leq r/R_{ref} \leq 2$	5 curves at $X/R_{ref} = -0.5, 0, 0.5, 1.0, 2.0$.
2	r/R_{ref}	U/U_∞	$0 \leq r/R_{ref} \leq 1$	5 curves at $X/R_{ref} = -0.5, 0.5, 2.0, 6.0, 36.0$.
3	r/R_{ref}	$(\overline{uv})/U_\infty^2$	$0 \leq r/R_{ref} \leq 1$	5 curves at $X/R_{ref} = -0.5, 0.5, 2.0, 6.0, 36.0$.
4	r/R_{ref}	$(\overline{u^2})^{1/2}/U_\infty$	$0 \leq r/R_{ref} \leq 1$	5 curves at $X/R_{ref} = -0.5, 0.5, 2.0, 6.0, 36.0$.
5	r/R_{ref}	$(\overline{v^2})^{1/2}/U_\infty$	$0 \leq r/R_{ref} \leq 1$	5 curves at $X/R_{ref} = -0.5, 0.5, 2.0, 6.0, 36.0$.
6	r/R_{ref}	$(\overline{w^2})^{1/2}/U_\infty$	$0 \leq r/R_{ref} \leq 1$	5 curves at $X/R_{ref} = -0.5, 0.5, 2.0, 6.0, 36.0$.

Special Instructions: (compiled by S. J. Kline)

Due to the separation bubble at the tail, it is expected that most calculators attempting this case will use interactive or inverse solution procedures. Experimental information required for such calculations should be minimal. Some caution is advised in matching the calculations with experiment since the first measuring station ($X/L = -0.0417$, $X/R = -0.5$) is just ahead of separation.

It is suggested that the influence of the transition device be taken into account by matching the calculations at $X/L = -0.314$ with the boundary-layer measurements of Patel et al. after scaling the latter data for the difference in the Reynolds numbers of the two experiments. This is recommended since the same model was used in both, and the boundary layer at the match station is expected to remain unaffected by the small change in tail geometry shown on Fig. 2 below. This expectation is confirmed by rescaling and plotting the displacement thickness lines for the two cases, as shown on Fig. 3 below (computations by V. C. Patel). Regarding these computations, Patel remarks that he has accomplished this [scaling] as follows:

- (a) the integral parameters R_θ , H , C_f , and δ/r_0 have been scaled using proper relations to obtain corresponding values of the higher Re of Chevray;
- (b) since the velocity profile of Patel et al. is in excellent agreement with the Coles profile family, this has been used in conjunction with the new (scaled) integral parameters to obtain the velocity profile. Both profiles are listed in detail in the accompanying computer output (Tables 1 and 2 contain profile data as supplied by V. C. Patel);
- (c) since the Reynolds-stress measurements of Patel et al. agreed with those of Klebanoff (see J. Fluid Mech. paper, Fig. 12), this information can be used together with the proper U_e , C_f , and δ to obtain the stresses, IF REQUIRED BY THE COMPUTER. \overline{uv} distribution is also given in the computer output.



L = body length = 60"; R = max. body rad = 10"; $D = 2R$

Figure 1. Notation for Case 0361.

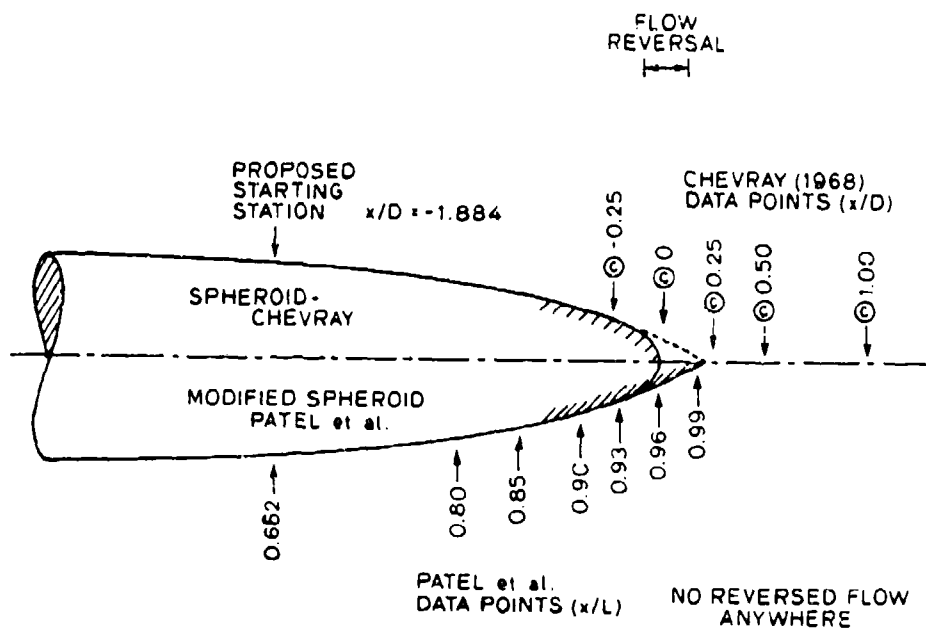
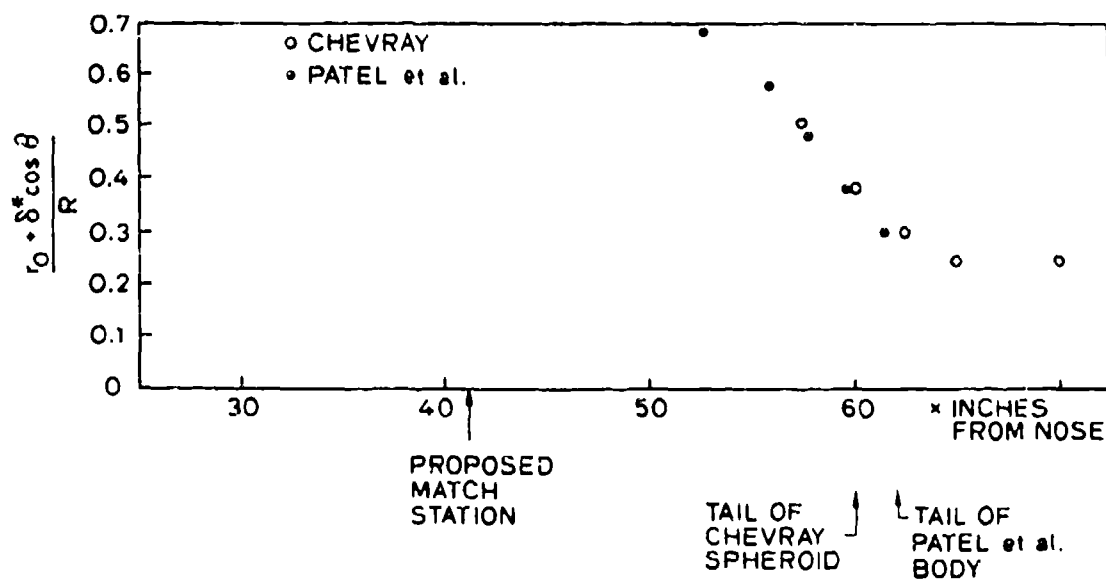


Figure 2. Changes in tail geometry.



Note: Displacement surface is same, within experimental uncertainty, in both experiments.

Figure 3. Distance to the displacement surface from the axis.

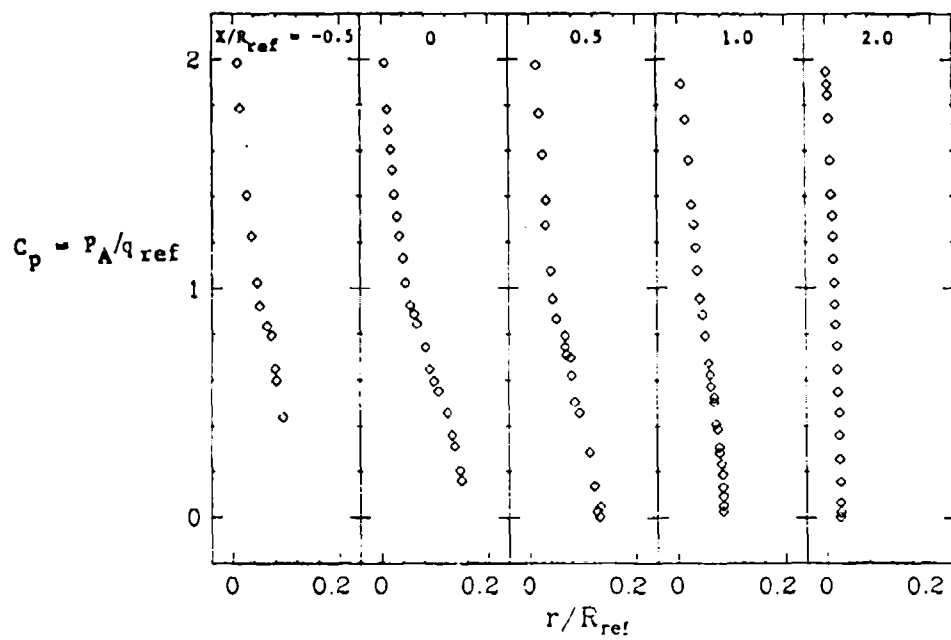
TABLE 1. Profile Data (Patel et al., 1974)
X/L = 0.662 (Nomenclature follows standard computer symbols, pp. iii-v)

UE, m/s RDELS	12.00 1767	DELS, m CF	0.00221 0.0034	HS DEL, m	1.455 0.01790
	Y, mm	U/UE	KAY/UE	-U1V1/UE**2	
	0.000	0.000	0.000000	0.000000	
	0.321	0.357	0.005667	0.001700	
	0.342	0.370	0.005667	0.001700	
	0.364	0.383	0.005667	0.001700	
	0.389	0.397	0.005667	0.001700	
	0.416	0.410	0.005667	0.001700	
	0.444	0.423	0.005667	0.001700	
	0.476	0.437	0.005667	0.001700	
	0.509	0.451	0.005667	0.001700	
	0.546	0.465	0.005667	0.001700	
	0.586	0.479	0.005667	0.001700	
	0.629	0.494	0.005667	0.001700	
	0.676	0.508	0.005667	0.001700	
	0.726	0.523	0.005667	0.001700	
	0.782	0.537	0.005667	0.001700	
	0.842	0.552	0.005667	0.001700	
	0.907	0.563	0.005667	0.001700	
	0.980	0.571	0.005666	0.001700	
	1.059	0.578	0.005665	0.001700	
	1.147	0.586	0.005664	0.001699	
	1.244	0.595	0.005661	0.001698	
	1.350	0.603	0.005656	0.001697	
	1.468	0.612	0.005650	0.001695	
	1.598	0.620	0.005641	0.001692	
	1.741	0.629	0.005630	0.001689	
	1.898	0.638	0.005615	0.001685	
	2.072	0.648	0.005596	0.001679	
	2.263	0.657	0.005572	0.001672	
	2.474	0.667	0.005541	0.001662	
	2.706	0.677	0.005503	0.001651	
	2.962	0.687	0.005455	0.001636	
	3.243	0.698	0.005396	0.001619	
	3.553	0.709	0.005324	0.001597	
	3.895	0.720	0.005236	0.001571	
	4.270	0.732	0.005130	0.001539	
	4.682	0.745	0.005002	0.001501	
	5.136	0.758	0.004850	0.001455	
	5.634	0.772	0.004669	0.001401	
	6.180	0.786	0.004456	0.001337	
	6.780	0.802	0.004207	0.001262	
	7.437	0.818	0.003920	0.001176	
	8.157	0.835	0.003591	0.001077	
	8.945	0.854	0.003220	0.000966	
	9.806	0.873	0.002807	0.000842	
	10.748	0.893	0.002356	0.000707	
	11.777	0.913	0.001877	0.000563	
	12.902	0.934	0.001384	0.000415	
	14.133	0.954	0.000900	0.000270	
	15.481	0.972	0.000465	0.000139	
	15.962	0.988	0.000136	0.000041	
	18.595	1.000	0.000000	0.000000	

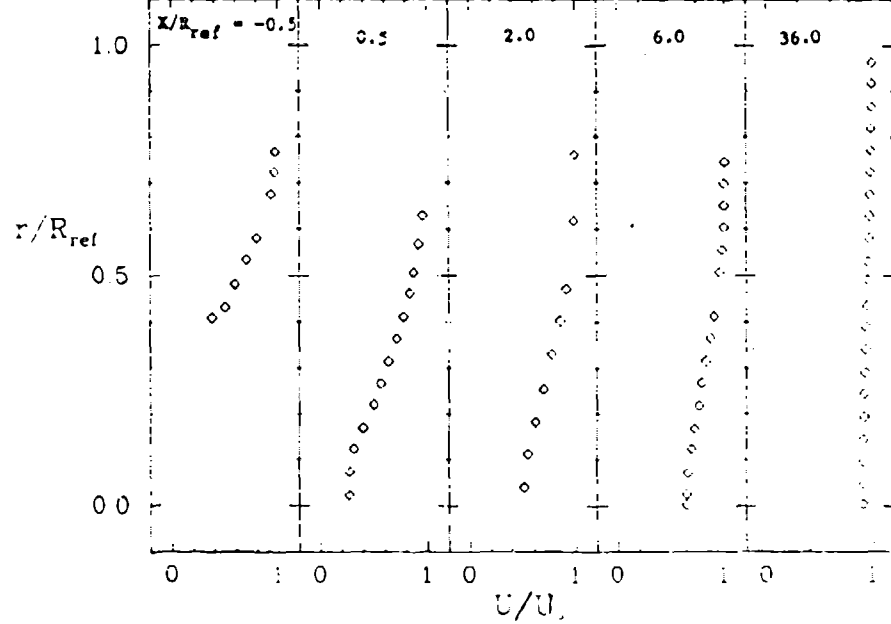
TABLE 2. Profile Data (Chevray, 1968, after re-scaling)
 $X/D = -1.884$ (Nomenclature follows standard computer symbols, pp. iii-v)

UE, m/s	27.43	DELS, m	0.00184	HS	1.405
RDELS	3369	CF	0.0030	DEL, m	0.01528
Y, mm	U/UE	KAY/UE**2	-U1V1/UE**2		
0.000	0.000	0.000000	0.000000		
0.148	0.334	0.005000	0.001500		
0.159	0.348	0.005000	0.001500		
0.171	0.362	0.005000	0.001500		
0.184	0.376	0.005000	0.001500		
0.199	0.390	0.005000	0.001500		
0.214	0.404	0.005000	0.001500		
0.231	0.419	0.005000	0.001500		
0.250	0.434	0.005000	0.001500		
0.271	0.449	0.005000	0.001500		
0.293	0.464	0.005000	0.001500		
0.318	0.479	0.005000	0.001500		
0.345	0.495	0.005000	0.001500		
0.375	0.510	0.005000	0.001500		
0.408	0.525	0.005000	0.001500		
0.444	0.533	0.005000	0.001500		
0.485	0.541	0.005000	0.001500		
0.530	0.549	0.004999	0.001500		
0.581	0.558	0.004998	0.001499		
0.638	0.567	0.004997	0.001499		
0.701	0.575	0.004995	0.001498		
0.772	0.584	0.004992	0.001498		
0.850	0.594	0.004988	0.001496		
0.938	0.603	0.004983	0.001495		
1.037	0.613	0.004976	0.001493		
1.146	0.622	0.004967	0.001490		
1.269	0.632	0.004955	0.001487		
1.406	0.642	0.004940	0.001482		
1.558	0.652	0.004921	0.001476		
1.729	0.662	0.004897	0.001469		
1.919	0.673	0.004866	0.001460		
2.132	0.684	0.004828	0.001448		
2.369	0.695	0.004780	0.001434		
2.633	0.706	0.004720	0.001416		
2.928	0.718	0.004645	0.001394		
3.257	0.731	0.004554	0.001366		
3.623	0.744	0.004442	0.001333		
4.031	0.757	0.004306	0.001292		
4.486	0.772	0.004141	0.001242		
4.991	0.787	0.003944	0.001183		
5.553	0.804	0.003710	0.001113		
6.176	0.821	0.003434	0.001030		
6.868	0.840	0.003114	0.000934		
7.634	0.860	0.002747	0.000824		
8.483	0.881	0.002336	0.000701		
9.422	0.903	0.001887	0.000566		
10.461	0.926	0.001412	0.000424		
11.611	0.948	0.000933	0.000280		
12.886	0.969	0.000490	0.000147		
14.302	0.987	0.000146	0.000044		
15.884	1.000	0.000000	0.000000		

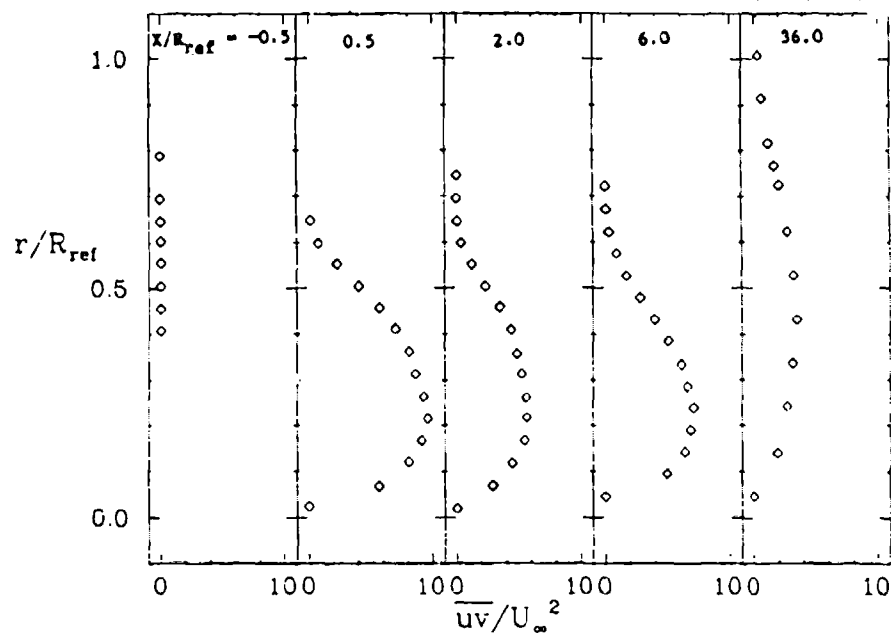
PLOT 1 CASE 0361 FILES 2-6



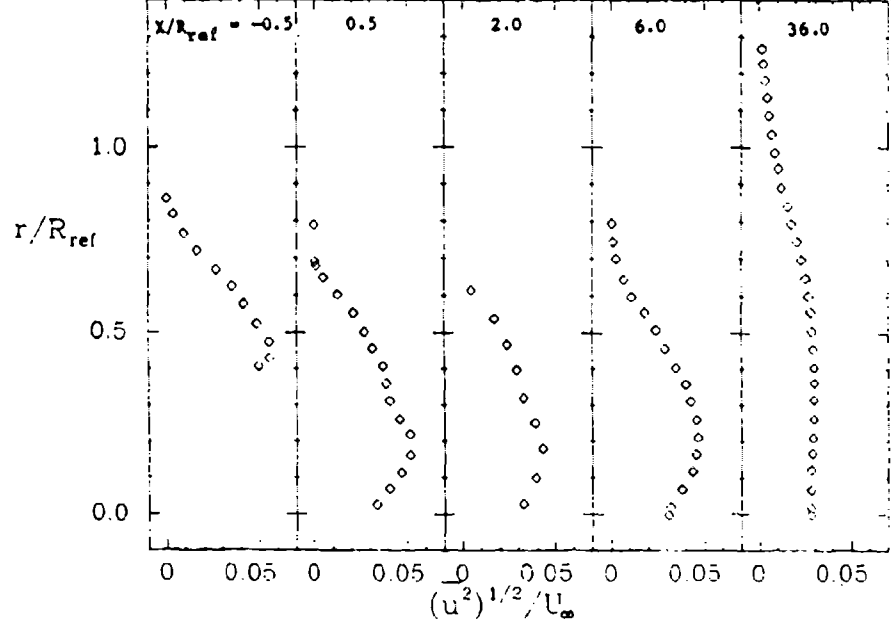
PLOT 2 CASE 0361 FILES 8,10,12,14,19

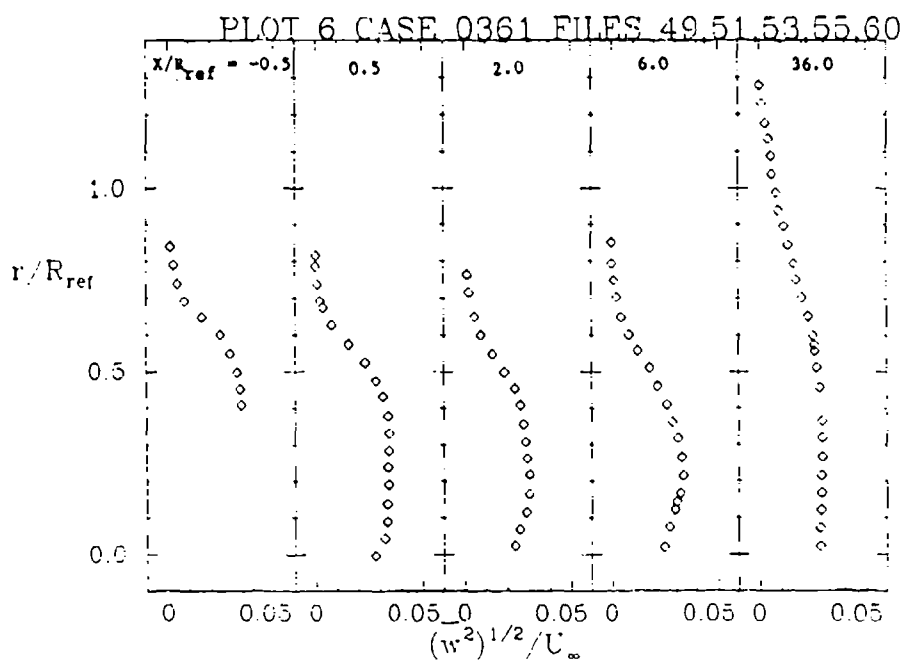
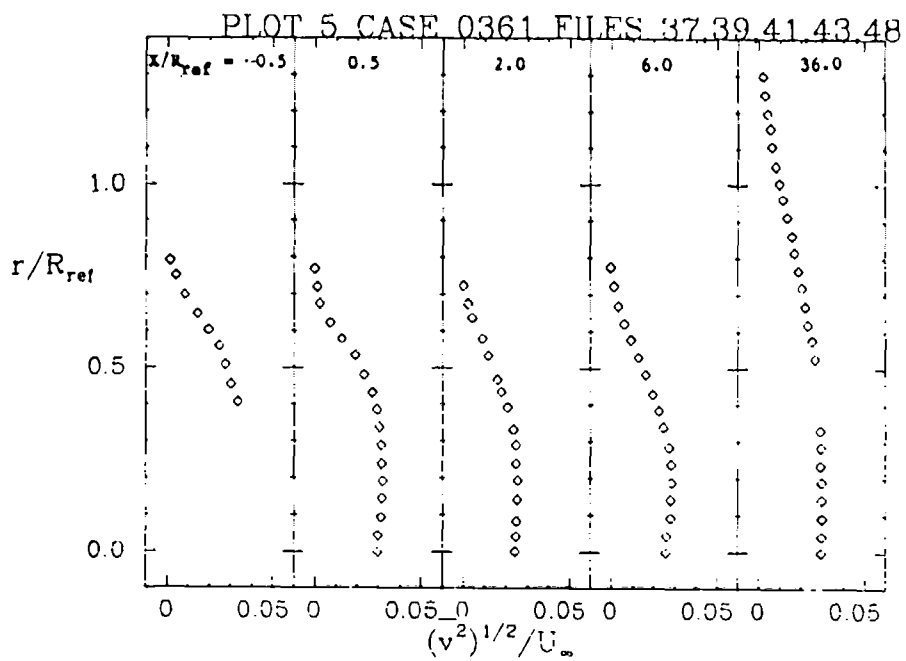


PLOT 3 CASE 0361 FILES 61,63,65,67,72



PLOT 4 CASE 0361 FILES 25,27,29,31,36





WAKES OF TWO-DIMENSIONAL BODIES

Flow 0380

Evaluator: V. C. Patel

SUMMARY

Extensive measurements have been made, over several decades, in the wakes of two-dimensional bodies. The available data fall into three broad categories, depending upon the distance from the body: (a) far wakes (or asymptotic or fully developed) wakes, characterized by "small" velocity defects, (b) far wakes subjected to perturbations, such as pressure gradients or stratifications, and (c) near wakes. Far wakes have been discussed extensively in the literature and are not considered here. Data on the influence of externally imposed pressure gradients on far (small-defect) wakes are available (see, for example, Narasimha and Prabhu, 1972; Prabhu and Narasimha, 1972; and Prabhu, 1971). These are of interest in connection with the response of fully developed turbulence to perturbations and may also provide good test cases for turbulence models. The present survey, however, is confined to near wakes.

REVIEW OF NEAR-WAKE DATA

The available near-wake data can be subdivided into five categories on the basis of the body geometry and the flow conditions at the trailing edge. These are briefly reviewed in turn.

Symmetric Wake of a Smooth Flat Plate

This is the simplest of near-wake flows. There are at present a number of data sets of incompressible flow data in this category (Andreopoulos, 1978; Chevray and Kovasznay, 1969; Fayet et al., 1971a; 1971b; Pot, 1979; Ramaprian et al., 1980; Solignac, 1973; and Tsen and Fayet, 1971). Quite detailed information is available on five of these. The major features of the models, and trailing-edge and boundary-layer characteristics are summarized in the Review Report. Together these experiments appear to cover a wide range of Reynolds number and initial conditions at the trailing edge. We shall return to these data later on.

Symmetric Wakes with Pressure Gradients

In this category we may consider the near wake of a flat plate with an externally imposed pressure gradient or wakes of airfoil-like bodies with self-induced longitudinal pressure gradients.

Among the data of the first kind are those of Chevray and Kovasznay (1969) et al. (1971c; 1972a), who repeated their measurements on a flat plate with an adverse streamwise pressure gradient imposed by contoured sidewalls.

Visnawath et al. (1979) have made measurements in the boundary layer and the wake of a model consisting of a flat-plate middle body, a rounded nose section, and sharp-edged symmetric aft flap. With no flap deflection, the wake is symmetric and resembles that of a thin airfoil. In fact, this experiment is somewhat similar to that of Chevray and Kovasznay (1969), Fayet et al. (1971a), and Tsien and Fayet (1971), but it has been included here since the pressure gradients over the trailing edge are significant. There are two data sets, corresponding to $M = 0.4$ and 0.7 , and the measurements include static-pressure distributions on the model and tunnel walls, mean-velocity profiles in the boundary layer on the aft portion of the model and at several stations in the wake, and Reynolds stresses $\overline{u^2}$, $\overline{v^2}$, and \overline{uv} at most of the above stations. This data set is being reviewed by P. Drescher.

The early measurements of Preston and Sweeting on a Joukowski airfoil at zero incidence also fall in this category, but these were restricted to static-pressure and mean-velocity traverses.

Asymmetric Near Wakes

There are many data sets in this category. M. Firmin of RAE reports that several recent data sets from two different airfoils (RAE 2822 and RAE 101) are available over a range of incidence, Reynolds number, and Mach numbers, but are all restricted to mean flow measurements using pitot and static tubes. The relevant information is contained in RAE TM Aero 1725, RAE TR 71127, and AGARD Advisory Report No. 138. In the latter, Cook et al. (1978) provide a detailed account of the data and their accuracy for the measurements on the RAE 2822 airfoil at several values of Re , M , and α . It is believed that similar data on other airfoils have been gathered over the years in the aircraft industry and related research establishments, but the evaluator is not aware of corresponding turbulence measurements.

The study of Visnawath et al. (1979) referred to earlier also provides asymmetric-wake data, since one experiment was performed with the aft flap deflection of 6.5° . The measurements include static pressure, mean velocities, and Reynolds stress ($\overline{u^2}$, $\overline{v^2}$, \overline{uv}).

Two sets of asymmetric-wake data gathered by Fayet et al. (1971c; 1972b) describe measurements in the wake of their flat-plate model fitted with sandpaper roughness on one side. The wake was also subjected to a symmetric adverse longitudinal pressure gradient by means of contoured sidewalls. The last in this series of reports (Fayet et al., 1972c) describes experiments in the asymmetric wake of the smooth flat plate at an incidence of 10° . In all cases, the data include static pressure, mean velocities, and Reynolds stresses.

The most recent, and perhaps the most detailed, measurements in asymmetric wakes have been carried out by Andreopoulos (1978) and Ramaprian et al. (1980). Both

utilize roughness on one side of a flat-plate model to realize the asymmetry. The data from the former experiment have been reviewed, while those from the latter are still undergoing analysis.

Finally, Ramaprian et al. are continuing their wake studies by making measurements in the wake of a super-critical airfoil at moderate incidence. This experiment will be completed during the fall of 1980.

Infinite Swept-Wing Wakes

The evaluator is aware of three experiments in this category. Cousteix et al. (1979) have made measurements in the wake of a wing, swept at $22\frac{1}{2}^\circ$, at an incidence of $18\frac{1}{2}^\circ$. The boundary layer on the top surface is close to separation and the cross flows are of the order of 40° . The top and bottom asymmetry is high and the three-dimensionality is also large. The measurements include pressures, mean velocities, and the six Reynolds stresses. A preliminary report describing the experiment and data is now available.

The experiment of Bradshaw et al. (1980) is similar to the above and is in progress. Preliminary information received thus far indicates that the wing consists of a contoured upper surface and a flat lower surface. The angle of sweep is 35° . Quite detailed measurements are planned for the region downstream of the trailing edge. It is expected that a complete data set will be available soon.

The third set of data is due to Cook et al. (1979), who have made measurements of the distributions of Mach number, flow direction, and static pressure through the wake and boundary layer of a wing of constant chord and RAE 101 section at sweep angles of 20 and 28° , and incidences of $\pm 1.88^\circ$. However, turbulence data were not collected.

Wakes Starting with Flow Separation

Near-wakes involving flow separation have not been reviewed here in detail. Nevertheless, it appears that more and more data are being obtained with geometries involving separation.

A recent report by Solignac (1979) describes measurements in an axisymmetric apparatus to simulate the flow over the trailing edge of a two-dimensional airfoil, with separation on the upper surface. Hot-wire and laser anemometry has been used to measure the mean and turbulence velocities, but it appears that the resolution of the measurements in the separation zone is not complete.

Young and Hoad (1979) have reported two sets of NASA measurements on stalled airfoils using laser anemometry.

SELECTION OF TEST CASES

Ideally, it is desirable to have available one reliable and complete data set in each of the five classes of two-dimensional wakes listed above. As the summary

indicated, however, there are many data sets in each category and therefore the task of evaluation and selection is quite considerable. Furthermore, many of the experiments are either in progress or were completed well after the present review process was started. A decision was therefore made to examine only the data from the most simple experiments first in the hope that the others will be evaluated later on. The cases selected for evaluation were: (a) the wake of a smooth flat plate and (b) the asymmetric wake of a flat plate roughened on one side.

The criteria used in the selection of test cases are as follows:

- (a) Fully developed ($Re > 3000$, say) turbulent boundary layer on the plate, so that low Reynolds number effects are absent.
- (b) Well-documented initial conditions, either in the boundary layer on the plate or at the trailing edge.
- (c) Sufficiently detailed data in the near wake, including at least the mean velocity and Reynolds stress profiles.
- (d) Acceptable level of accuracy and two-dimensionality.

AVAILABLE DATA

Considering first the wake of a smooth flat plate, the data of Andreopoulos (1978), Chevray and Kovasznay (1969), Fayet et al. (1971a; 1971b), Ramaprian et al. (1980), Solignac (1973), and Tsen and Fayet (1971) were examined and it was concluded that the earlier data had been superseded by the more recent and detailed measurements of Andreopoulos (1978) and Ramaprian et al. (1980). Since the experiments of Ramaprian et al. (1980) were in progress, and the data could not be analyzed within the required time frame, only the data of Andreopoulos were reviewed in detail. The evaluation is described in the Review Report. Finally, Pot (1979) describes another experiment in the wake of a flat plate but the report was received in the later stages of the review process and his data could not be evaluated in time for this summary. It is hoped to continue the evaluation and make an oral report at the Conference.

In the case of the asymmetric wake of a flat plate with roughness on one side, there are several sets of data: Andreopoulos (1978), Fayet et al. (1971c; 1972b), and Ramaprian et al. (1980). Again, only the data of Andreopoulos have been evaluated in detail.

RECOMMENDATIONS

The detailed evaluation of the symmetric-wake data of Andreopoulos (1978) indicated that they are suitable as a test case. Perhaps the only limitation of the data is that the measurements do not extend into the far wake, where we hope to recover the classical asymptotic solution. This drawback did not come into focus until the recent data of Pot (1979) were examined. The latter show that the growth and decay rates, and the Reynolds-stress profiles, do not reach asymptotic conditions until $x/\theta \sim 400$,

whereas the measurements of Andreopoulos extend only up to $x/\theta \sim 40$. In view of this, it is suggested that calculations for this case be continued up to $x/\theta = 1000$, and that the predictions in the range $400 < x/\theta < 1000$ be compared with the results of asymptotic theory. An alternative is to replace the data of Andreopoulos with those of Pot as a test case, provided an evaluation of the latter data confirms their acceptability relative to the other criteria. It is also suggested that calculations for this test case start in the boundary layer just upstream of the trailing edge so that the problem of continuing the calculation through the discontinuity in the boundary conditions is faced squarely.

With regard to the asymmetric case, the data of Andreopoulos are again recommended as a test case. Here also the calculations should be compared with asymptotic theory in the far wake. An additional uncertainty in this case stems from the finite thickness of the trailing edge (resulting from the sandpaper on one side of the plate), the influence of which is evident from the peaks in the turbulence measurements in the near wake. Similar results are also seen in the symmetric-wake experiments of Ramaprian et al. (1980) and Pot (1979), in which the trailing edges were not as sharp as those of Andreopoulos' model. Calculators would need to be cognizant of this influence of initial conditions and it would be interesting to see whether calculation methods are responsive to the trailing-edge geometry.

REFERENCES

- Andreopoulos, J. (1978). "Symmetric and asymmetric near wake of a flat plate," Ph.D. Thesis, Imperial College, London.
- Bradshaw, P., et al. (1980). Private communication, Imperial College, London.
- Chevray, R., and L. S. G. Kovasznay (1969). "Turbulence measurements in the wake of a thin flat plate," AIAA Jou., 7, 1641-1643.
- Cook, P. H., M. A. McDonald, and M. C. P. Firmin (1978). "Aerofoil RAE 2822--pressure distributions, and boundary layer and wake measurements," in Experimental Data Base for Computer Program Assessment, AGARD Advisory Report 138, pp. A6.1-A6.77.
- Cook, P. H., M. A. McDonald, and M. C. P. Firmin (1979). "Wind tunnel measurements of the mean flow in the turbulent boundary layer and wake in the region of the trailing edge of a swept wing at subsonic speeds," RAE Tech. Rept. 79062.
- Cousteix, J., et al. (1979). Private communication, CERT, Toulouse, France.
- Fayet, J., H. Garem, and L. F. Tsen (1971a). "Montage et expérience sur le sillage symétrique d'une plaque plane, dans un écoulement uniforme," Rept. 70/145, CEAT, Poitiers, France.
- Fayet, J., H. Garem, and L. F. Chen (1971b). "Mesure de l'énergie cinétique turbulente dans un sillage symétrique d'une plaque plane dans un écoulement uniforme," Rept. December 1971, CEAT, Poitiers, France.

- Fayet, J., J. H. Garem, and L. F. Tsen (1971c). "Montage et expériences sur les sillages symétrique et dissymétrique d'une plaque plane dans un écoulement avec gradient de pression," Rept. 70/145, CEAT, Poitiers, France.
- Fayet, J., J. H. Garem, and L. F. Tsen (1972a). "Energie turbulente dans un sillage symétrique d'une plaque plane en écoulement décéléré," Rept. March 1972, CEAT, Poitiers, France.
- Fayet, J., J. H. Garem, and L. F. Tsen (1972b). "Tensions du Reynolds dans un sillage dissymétrique d'un profil en écoulement décéléré," Report June 1972, CEAT, Poitiers, France.
- Fayet, J., J. H. Garem, and L. F. Tsen (1972c). "Sillage crée par une plaque plane inclinée à 10° placée dans un gradient de pression positif," Report December 1972, CEAT, Poitiers, France.
- Narasimha, R., and A. Prabhu (1972). "Equilibrium and relaxation in turbulent wakes," J. Fluid Mech., 54, 1.
- Pot, P. J. (1979). "Measurements in a 2-D wake and in a 2-D wake merging into a boundary layer, data report," NLR TR-79063 L (Provisional Issue).
- Prabhu, A. (1971). Ph.D. Thesis, Indian Institute of Science, Bangalore, India.
- Prabhu, A., and R. Narasimha (1972). "Turbulent non-equilibrium wakes," J. Fluid Mech., 54, 20.
- Ramaprian, B. R., V. C. Patel, and M. S. Sastry (1980). Unpublished data, Institute of Hydraulic Research, University of Iowa.
- Solignac, J.-L. (1973). "Calcul du sillage turbulent bidimensionnel en aval d'un obstacle mincé," Fourth Canadian Cong., Applied Mechanics, Montreal, Canada.
- Solignac, J.-L. (1979). "Etude expérimentale de la confluence avec décollement sur un arrière-corps de révolution," Tech. Rept. 1971-151, ONERA, France.
- Tsen, L. F., and J. Fayet (1971). "Etude du développement d'un sillage turbulent dans un écoulement avec gradient de pression," Rept. 70/145 Final, CEAT, Poitiers, France.
- Viswanath, P. R., J. W. Cleary, H. L. Seegmiller, and C. C. Horstman (1979). "Trailing edge flows at high Reynolds number," AIAA Paper 79-1503.
- Young, W. H., and D. R. Hoad (1979). "Comparison of two flow surveys above stalled wings," AIAA Paper 79-0147 (see also NASA TN D-8408, 1977; NASA TP-1266, 1978; NASA TM-74040, 1978).

FLOW IN THE WAKE OF FLAT PLATE WITH SYMMETRIC WAKE
AND ASYMMETRIC INITIAL BOUNDARY LAYERS

Flow 0380

Cases 0381, 0382

Evaluator: V. C. Patel

Data Taker: J. Andreopoulos

SUPPLEMENT TO SUMMARY*

CASE 0381. WAKE OF SMOOTH FLAT PLATE

This experiment was performed in the wake of a smooth flat plate at $M \sim 0.1$. The measurements included the following:

- (a) Mean velocity profiles at 10 streamwise stations, $x/\delta_0 = 0.0935, 0.187, 0.374, 0.561, 0.935, 1.869, 3.738, 5.607, \text{ and } 9.35$.
- (b) Reynolds stresses $\overline{u^2}, \overline{v^2}, \overline{uv}$ at 6 stations, $x/\delta_0 = 0, 0.467, 0.935, 1.869, 3.738, \text{ and } 7.477$.
- (c) Triple correlations $\overline{u^3}, \overline{uv^2}, \overline{u^2v}, \overline{v^3}$, at the 6 stations in (b).
- (d) Conditional averages to study the mixing in the central part of the wake.

The following comments concern the first three items (a-c) and are based on the information contained in Andreopoulos (1978) and further input from the experimenter.

Test Facility

The experiment was conducted in a 91×91 cm closed-circuit wind tunnel (maximum speed 45 m/s, ambient turbulence level 0.05%). The model was 3080 mm long and 28 mm thick. The leading edge, 80 mm long, was based on the NACA 0009 section. The rear 450 mm length was tapered to yield a sharp trailing edge, included TE angle of 3.5° and a reported TE thickness of 0.07 mm. The boundary layer was tripped by means of 50-mm-wide sandpaper strips just downstream of the 80 mm leading edge.

The model spanned the working section and was mounted horizontally at the mid-span of the tunnel. The leading edge of the plate was located "just downstream" of the tunnel contraction.

All tests were conducted with a velocity of $U_e = 33.5$ m/s monitored at the end of the tunnel contraction. U_e is used as the reference velocity throughout the presentation of the data. It is assumed that U_e remains constant along the shear layer

* Edited by S. J. Kline. This flow was added by the Organizing Committee after the 1980 meeting in order to provide cases comparing symmetric and asymmetric initial conditions and because it contains measurements of third-order correlations as a check for turbulence models.

(i.e., it is taken as the velocity outside the boundary layer and the wake). Thus, blockages, due to tunnel walls, model, boundary layer, and wake, and taper of the plate are neglected.

Two-Dimensionality

Checks for two-dimensionality were made at the trailing edge ($x/\delta_0 = 0$) and the most downstream station ($x/\delta_0 = 9.35$). Pitot traverses indicated two-dimensional flow within 1 to 2% of the mean velocity profiles over 70% of the plate span (i.e., over $12\delta_0$) at the trailing edge and over 50% of the tunnel width (i.e., over $8.5\delta_0$) at $x/\delta_0 = 9.35$. The profiles of $\overline{u^2}$ at two spanwise locations at $x/\delta_0 = 9.35$ agreed within 4%. Also, Clauser charts for the wall shear stress at ± 200 mm (i.e., $\pm 3.74\delta_0$) from the centerline gave C_f values with 5% of the centerline value at the trailing edge. These checks for two-dimensionality are considered marginally adequate. Note that the effective aspect ratio of the two-dimensional part of the wake (i.e., span/ $2\delta_0$) is of the order of 5 and the geometric aspect ratio (tunnel width/ $2\delta_0$) is 8.5. Drawing from the experience of experiments in nominally two-dimensional boundary layers, this is considered marginal since it invites flow convergence or divergence at the centerline due to the growth of the untreated corner boundary layers. Also, the spanwise contamination (or some other factor) reduces the region of two-dimensionality from 70% of tunnel width (at TE) to 50% (at $x = 9.5\delta_0$) in a distance of only 4.25 wake widths. This would suggest that it would have been difficult to justify two-dimensionality of the flow beyond the last measuring station.

Free-Stream Conditions

This experiment corresponds to an idealized flow in which the static pressure should remain constant along the stream. However, no pressure measurements are reported. Andreopoulos (1978) acknowledges the existence of "the small pressure gradient which was due to the gradually reduced thickness of the flat plate at the trailing edge" on p. 159, while discussing the values of C_f in the asymmetric wake, but no information was reported on the magnitude of the pressure gradients involved.

If two-dimensionality is accepted, and it is assumed that the pressure is constant along the shear layer, the momentum thickness should remain constant in the wake. It has been found that the values of θ/δ_0 tabulated on p. 44 and plotted in Figure 4.4 on p. 64 of Andreopoulos (1978) are in error. The integral parameters have been re-evaluated by Andreopoulos at the reviewer's request.* These show that θ remains constant in the wake within $\pm 2\%$ and therefore the flow may be regarded as two-dimensional, and the influence of streamwise pressure gradient may be neglected in the wake.

*[Ed.: The corrected values have been put on the tape file; see File 1 of this case.]

With regard to the boundary layer on the plate, the experimenter acknowledges the presence of a small pressure gradient. The mean velocity profile at $x = 0$ (the trailing edge) shown in the logarithmic plot of Figure 4.3 of Andreopoulos (1978) indicates a wake component ($\Delta U/U_*$) of 3.8 (the evaluator's estimate is 3.0). This is considerably higher than the value of 2.6 usually attributed to a flat-plate boundary layer, and suggests that the upstream boundary layer has developed in an adverse pressure gradient. An equivalent equilibrium pressure-gradient parameter $\beta \equiv (\delta^*/U_*)(dp/dx)$ can be estimated using the correlation*

$$\frac{\Delta U}{U_*} = \frac{2\pi}{\kappa}, \quad \pi = 0.8(\beta + 0.5)^{0.75}$$

With $\kappa = 0.418$, we have $\beta = 0.49$. The existence of an adverse pressure gradient is further confirmed by the lower value of C_f and the higher value of H at $x = 0$ than those observed in other flat-plate boundary-layer experiments (e.g., for $R_\theta = 13,040$, Wieghardt-Stanford (1968) IDENT 1420 - gives $C_f = 0.00247$, $H = 1.334$, while the present experiment at $R_\theta = 13,600$ yields $C_f = 0.0023$ and $H = 1.389$).

Mean Velocity Profiles

1-mm-dia pitot probes and 2-mm-dia static probes were used, together with Betz manometers, to make these measurements. The profiles are shown in Figures 4.1-4.3. The mean velocities recorded with hot wires agreed with the pitot-static results within 5%. The pitot and static probes were small enough, relative to the wake width, for probe-displacement effects to be considered negligible.

The velocity profiles contain a sufficient number of data points to enable an accurate evaluation of the integral parameters. As noted earlier, values in Andreopoulos (1978) are incorrect and should be replaced by those given by the evaluator; see data tape.

The velocity profiles appear to be symmetric about the wake centerline. The graphs show U/U_e going to 1.0 at both edges of the wake at all 10 stations. Since U_e is the constant reference velocity, this suggests that the free-stream velocity, and therefore the pressure, remained constant along the wake.

Reynolds Stresses ($\overline{u^2}$, $\overline{v^2}$, \overline{uv})

These were measured with linearized DISA hot wires at 6 stations. Note that w^2 WAS NOT MEASURED. The turbulence measuring stations do not all coincide with the stations where the mean velocity profiles were measured. The common stations are $x/\delta_0 = 0, 0.935, 1.869, \text{ and } 3.738$.

The data shown in Figures 4.5-4.23 of Andreopoulos (1978) were obtained digitally (i.e., by processing recorded signals after A + D conversion) from x-wire traverses.

*D. E. Coles' wall-wake correlation in the form given by White (1974).

$\overline{u^2}$ obtained from analog equipment agreed with the digital values with a maximum experimental scatter of 5% (see p. 49). This appears reasonable with regard to hot-wire measurements of Reynolds stresses and may be used as the confidence level.

There is no way to assess the accuracy of the hot-wire measurements directly. However, the profiles of $\overline{u^2}$ and $\overline{v^2}$ are reasonably (within 5%) symmetric about the wake centerline while those of \overline{uv} are, as expected, antisymmetric. Since the streamwise region of flow development is roughly 8 times the shear-layer thickness, it is expected that the symmetry, once established at the trailing edge, would persist.

Andreopoulos does not present any comparison between his turbulence data and those of others to establish credibility, although some could have been made. The evaluator has undertaken this task. Figure 1 shows conventional plots of the Reynolds normal and shear stresses measured at the trailing edge. The flat-plate data of Klebanoff and similar measurements in two other experiments are included for comparison. U_∞ and δ values quoted by the experimenters are used.

It is seen that Andreopoulos' shear-stress measurements are somewhat higher than those of Klebanoff and imply a small local adverse pressure gradient. A similar conclusion could also be drawn from the measured u' although v' is in reasonable agreement with Klebanoff's data.

The Reynolds stresses $\overline{u^2}$, $\overline{v^2}$, and \overline{uv} measured at the most downstream station ($x = 400$ mm) have also been compared with similar measurements made by Chevray and Kovasznay (1960) and by Ramaprian, Patel and Sastry (1979) (see Fig. 2). Since the proper scaling laws for near-wakes are not known, such comparisons should be interpreted with caution. Nevertheless, examination of the data at similar non-dimensional distances ($x/\delta_0 = 8$) from the trailing edge shows that all three sets of data are in reasonable agreement except that the values of Andreopoulos are somewhat larger in the outer parts of the wake. This is perhaps due to the differences in the initial conditions at the trailing edge.

Triple Products ($\overline{u^3}$, $\overline{uv^2}$, $\overline{u^2v}$, and $\overline{v^3}$)

These are shown in Figures 4.24-4.47 of Andreopoulos (1978). Products involving w were not measured. It is again difficult to establish the reliability of the data since a standard for comparison is not available. Nevertheless since the Imperial College group has had extensive experience with hot-wire anemometry, these results appear to represent the state of the art in data acquisition. The profiles of triple products do not exhibit the same level of symmetry or asymmetry as the Reynolds stresses. One measure of the accuracy of the data is therefore the departure of the data from the expected symmetry or asymmetry. Examination of the data on this basis

suggests a scatter of the order of 20% of the respective maximum values. This, I believe, could be used as a rough guide for most triple-velocity-product measurements.

The measurements at the trailing edge ($x = 0$) have also been compared by the reviewer with some previous measurements in the boundary layers made by Bradshaw and his students. These again agreed within the 20% bracket mentioned above.

CASE 0382. ASYMMETRIC WAKE BEHIND PLATE WITH ONE SIDE ROUGH

This experiment was conducted in the same facility as the symmetric wake experiment. The smooth plate used for the symmetric wake was roughened on one side to generate an asymmetric wake. The measurements consist of the following:

- (a) Mean velocity profiles at 6 streamwise stations: $x = 0, 25, 50, 100, 200,$ and 400 mm.
- (b) Reynolds stresses $\overline{u^2}, \overline{v^2}, \overline{uv}$ at 4 stations: $x = 0, 25, 100,$ and 400 mm.
- (c) Triple correlations $\overline{u^3}, \overline{u^2v}, \overline{uv^2},$ and $\overline{v^3}$ at the 4 stations in (b).
- (d) Intermittency.
- (e) Conditional averages to study the mixing in the central part of the wake.

This evaluation is restricted to the first four items (a-d) and is based on the information in Andreopoulos (1978).

Since the test facility and experimental procedures were reviewed in detail in connection with the symmetric case, only the differences between the two data sets will be discussed. The comments on the accuracy of the measurements in Case 0381 apply to this case also.

Test Facility

One side of the flat-plate model was roughened by sand paper with a roughness height of 1 mm, giving a trailing-edge thickness of 1 mm (in place of the 0.07 mm in the symmetric smooth-plate case).

Two-Dimensionality

Tests made for two-dimensionality in the symmetric case are not reported (in Andreopoulos, 1978) for the asymmetric case. However, a private communication from Andreopoulos indicates that such tests gave results similar to those in the symmetric case. The writer believes that the two-dimensionality or lack of it would not be affected by the small change in geometry.

*[Ed.: See also report of Ad-Hoc (Newman) Committee in the Proceedings of the 1980 meeting on expected uncertainty in hot-wire data.]

Free-Stream Conditions

As in Case 0381, pressure measurements were not made. Although the experimenter mentions "small pressure gradient which was due to the gradually reduced thickness of the flat plate at the trailing edge" in connection with the determination of C_f on the rough side, the pressure gradient can only be estimated from the velocity defect ($\Delta U/U_*$) on the logarithmic plot of Figure 5.11 of Andreopoulos (1978). The defect on the smooth side (≈ 3.2) is smaller than that observed (3.8) in the symmetric experiment, implying a smaller effective pressure gradient. The reason for this is not entirely clear, but it correlates with the larger value of C_f (0.0024 instead of 0.0023).

As in the symmetric case, the re-evaluated momentum thickness remains constant within 2%.

Mean Velocity Profiles

The profiles measured by pitot-static probes are presented in Figures 5.1-5.6 of Andreopoulos (1978). The comments on accuracy made in connection with the symmetric case continue to apply, except of course symmetry can no longer be used as a check for flow quality.

Reynolds Stresses ($\overline{u^2}$, $\overline{v^2}$, \overline{uv})

These data are shown in Figures 5.14 through 5.25 of Andreopoulos (1978). Since the measurement techniques were the same as those in the symmetric case, the previous estimate of 5% accuracy is assumed to be reasonable.

A comparison between the Reynolds stresses at the trailing edge measured on the smooth surface side in the asymmetric wake (Case 0381) and those measured in the symmetric wake (Case 0382) shows excellent agreement, and is an indication of the reliability and repeatability of the measurements.

It should be noted that the value of C_f at the trailing edge on the rough side was assigned by extrapolation of the measured \overline{uv} .

Triple Products ($\overline{u^3}$, $\overline{u^2}$, $\overline{uv^2}$, $\overline{v^3}$)

These are plotted in Figures 5.30 through 5.45 of Andreopoulos (1978). The accuracy of these measurements appear to be the same as those in the symmetric data. The fact that two sets of data were collected at each station, with the lower and upper (smooth and rough) surface boundary layers heated at different times (for conditional sampling), and they are in good overall agreement, suggests that the flow was not influenced by the small amount of heat addition (i.e., buoyancy effects can be considered negligible).

NOTE ON DATA PRESENTATION

As indicated in the preliminary data-evaluation report, the results presented in Andreopoulos (1978) contain several errors and inconsistencies. J. Andreopoulos has now provided the tabulated integral parameters, mean-velocity profiles, and turbulence data. It is recommended that the tabulated data be used in further analysis; see data tape for this case.

ADVISES FOR FUTURE DATA TAKERS

If simple two-dimensional wake flows such as those reported by Andreopoulos are to be used as test cases for modern calculation methods, calculations should start from the boundary layer somewhere on the body and continue into the wake so that the important problem of the discontinuity in the boundary conditions at the trailing edge is addressed realistically. Starting the solutions in the wake, with measured profiles as inputs, circumvents this important flow problem.

The ideal test case should possess the following features:

- (i) well-documented data in the upstream boundary layer;
- (ii) sufficiently detailed data over a reasonable downstream distance in the wake, including at least the mean velocity and Reynolds-stress profiles;
- (iii) two-dimensionality, or documented measure of three-dimensionality.

From the discussion of Andreopoulos' data it is clear that they fail only on one count, namely insufficient information on the upstream boundary layer. Since the geometry is simple, it should be possible to "invent" reasonable upstream starting conditions. In both cases, this would require the prescription of an "effective" pressure gradient due to the taper on the plate, and in the asymmetric case it may be necessary to determine an equivalent roughness height.

REFERENCES

- AFOSR-IFP-Stanford 1968 Conference on Computation of Turbulent Boundary Layers, Vol. II, D. E. Coles and E. Hirst, eds.
- Andreopoulos, J. (1978). "Symmetric and asymmetric near wake of a flat plate," Ph.D. Thesis, Dept. of Aero Engr., Imperial College, London.
- White, F. M. (1974). Viscous Fluid Flow, McGraw-Hill Book Co., New York 70481.

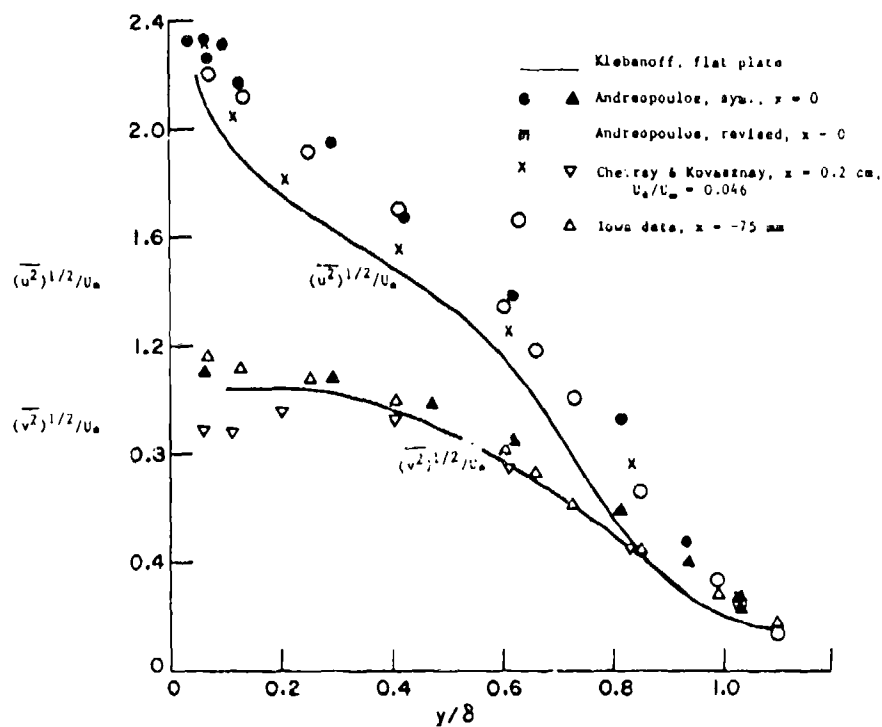


Figure 1a. Reynolds normal stresses of various observers.

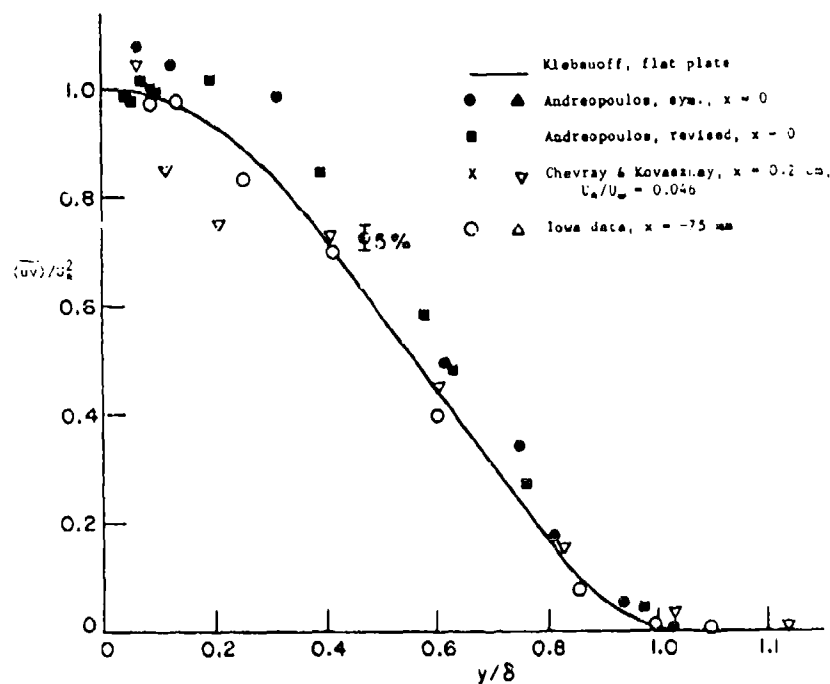


Figure 1b. Reynolds shear stresses of various observers.

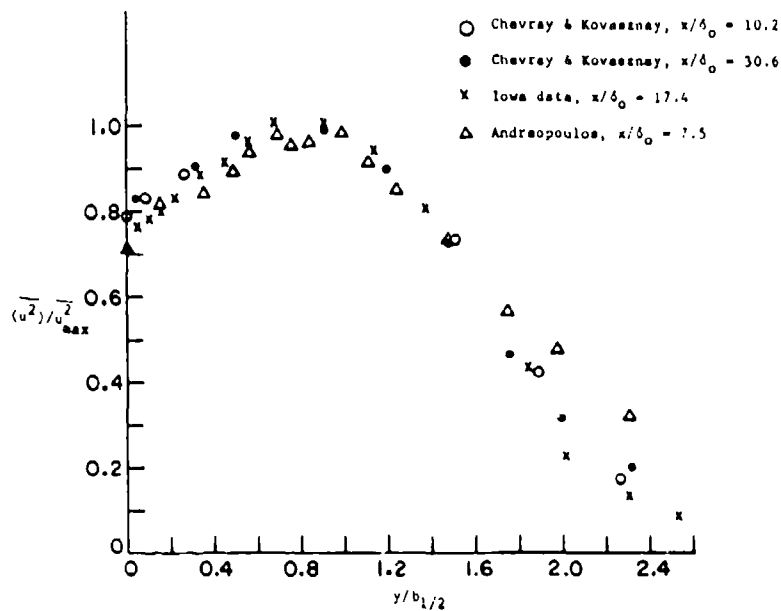


Figure 2a. Reynolds normal stress at most downstream stations of various observers.

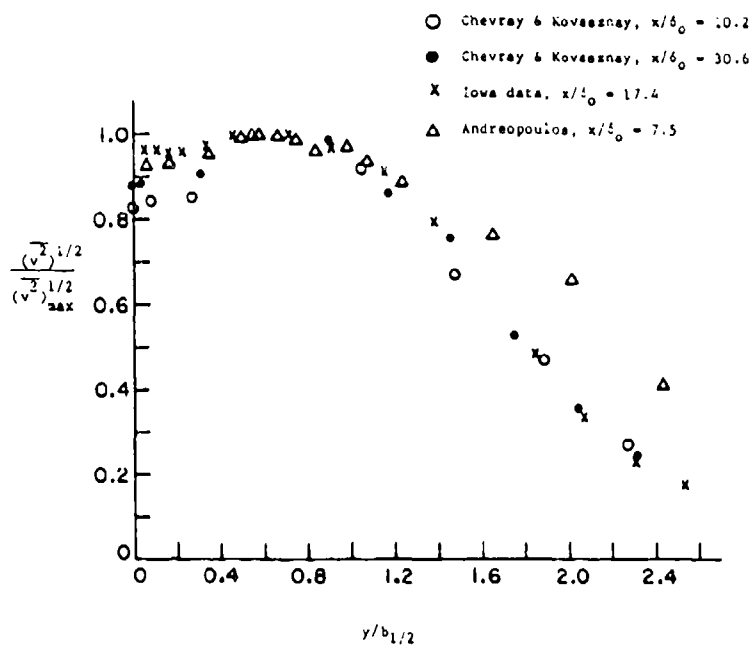


Figure 2b. Reynolds normal stress at most downstream stations of various observers.

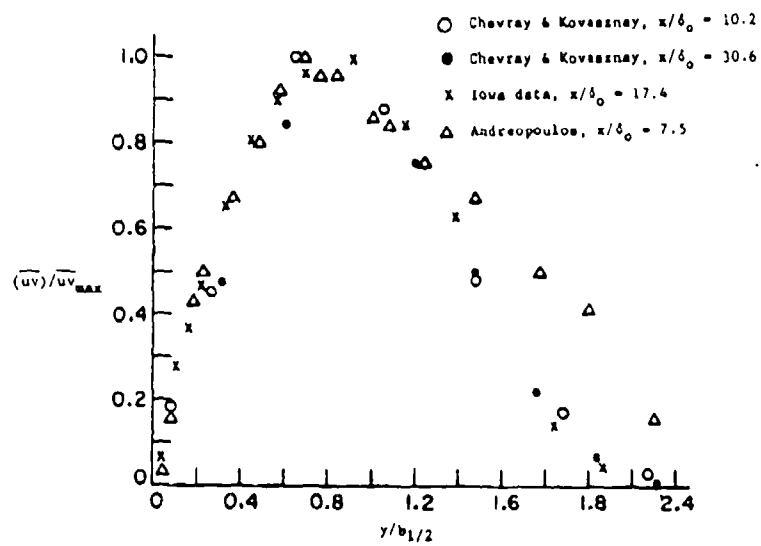


Figure 2c. Reynolds shear stress at most downstream stations of various observers.

SPECIFICATIONS FOR COMPUTATION

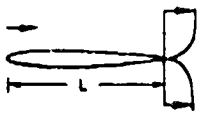
ENTRY CASE/INCOMPRESSIBLE

Case #0381; Data Evaluator: V. C. Patel

Data Taker: J. Andreopoulos

PICTORIAL SUMMARY

Flow 0380. Data Evaluator: V. C. Patel. "Wakes of Two-Dimensional Bodies."

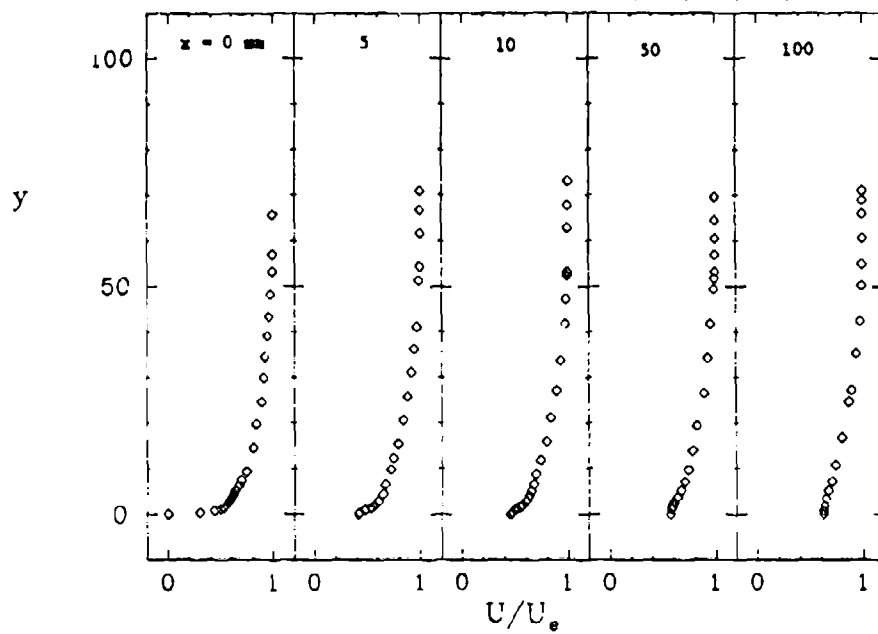
Case Data Taker	Test Rig Geometry	dp/dx or C _p	Number of Stations Measured								C _f	Re	Ini- tial Condi- tion	Other Notes
			Mean Velocity		Turbulence Profiles									
			U	V or W	$\overline{u^2}$	$\overline{v^2}$	$\overline{w^2}$	\overline{uv}	Others					
Case 0381 J. Andreopoulos			10		4	4	-	4	Triple cor- rela- tions	-	6.8 × 10 ⁶ (based on L)	Free- stream turb. < 0.05%	Symmetrical Case. Conditional averages to study the mixing in the central part of wake.	

Plot	Ordinate	Abcissa	Range/Position	Comments
1	y	U/U _e	0 ≤ y ≤ 100 mm	5 profiles at x = 0, 5, 10, 50, 100 mm.
2	y	\overline{uv}/U_e^2	-50 ≤ y ≤ 50 mm	3 profiles at x = 50, 100, 400 mm.
3	y	$\overline{u^2}/U_e^2$	-50 ≤ y ≤ 50 mm	3 profiles at x = 25, 100, 400 mm.
4	y	$\overline{v^2}/U_e^2$	-50 ≤ y ≤ 50 mm	3 profiles at x = 25, 100, 400 mm.
5	y	$\overline{uv^2}/U_e^3$	-50 ≤ y ≤ 50 mm	3 profiles at x = 25, 100, 400 mm.
6	y	$\overline{u^2v}/U_e^3$	-50 ≤ y ≤ 50 mm	3 profiles at x = 25, 100, 400 mm.

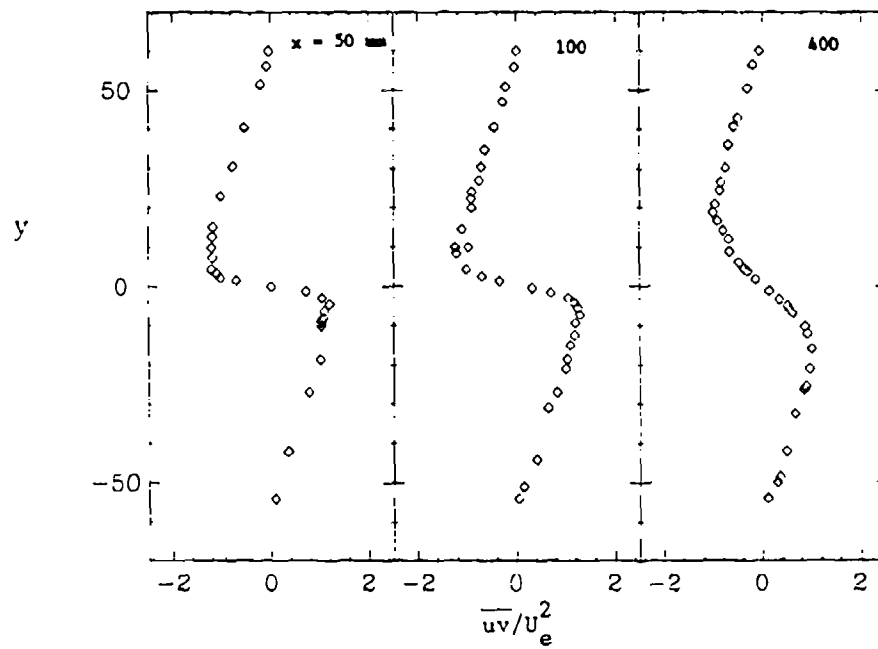
Special Instructions:

1. $\theta_0 = \theta_{\text{initial}} = 11.69^\circ$.
2. Calculations should begin just upstream of the trailing edge ($x/\theta_0 = 0$) and preferably continued to $x/\theta_0 = 1200$ to check limiting asymptotic form.

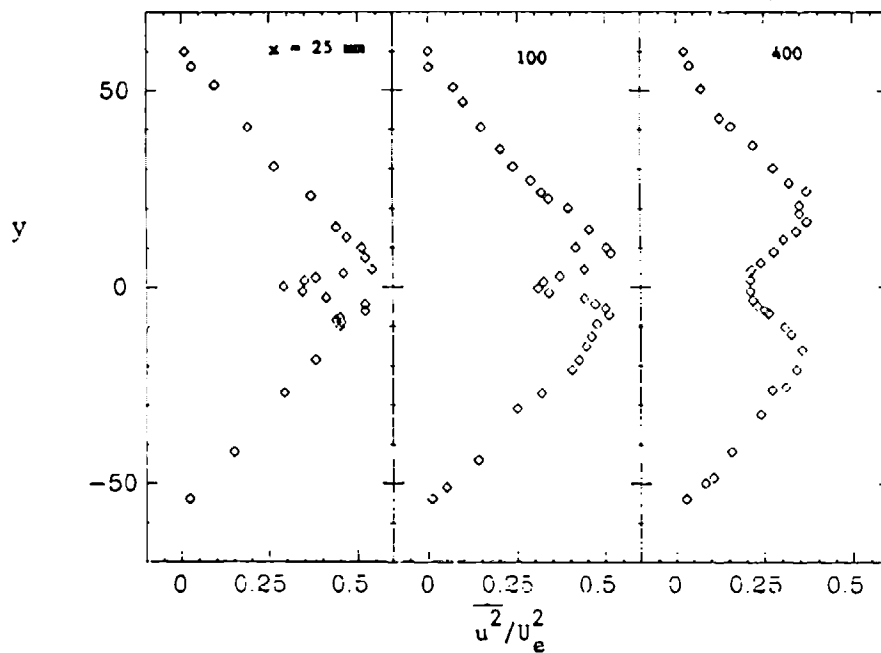
PLOT 1 CASE 0381 FILES 12,14,15,22,27



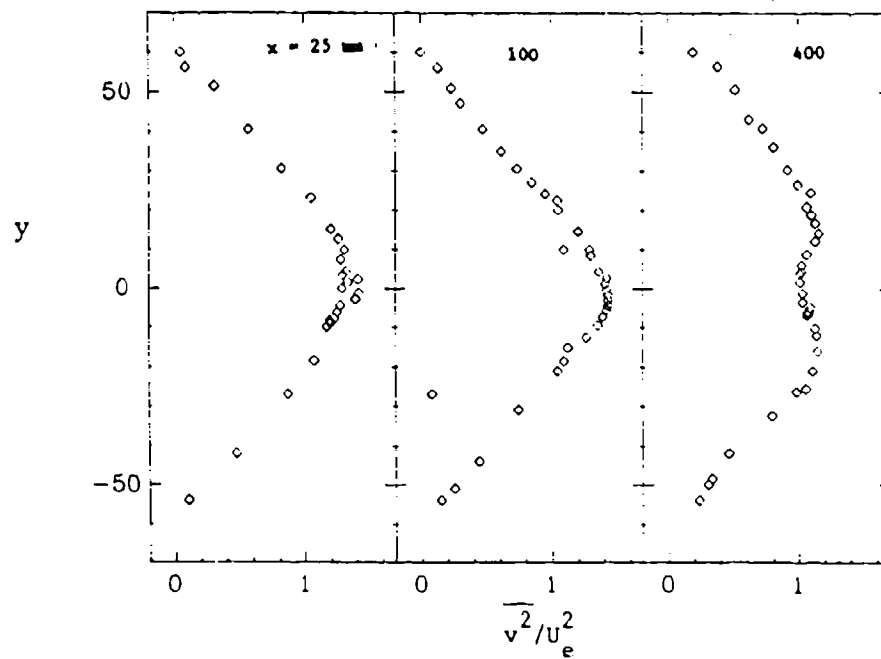
PLOT 2 CASE 0381 FILES 6,7,8



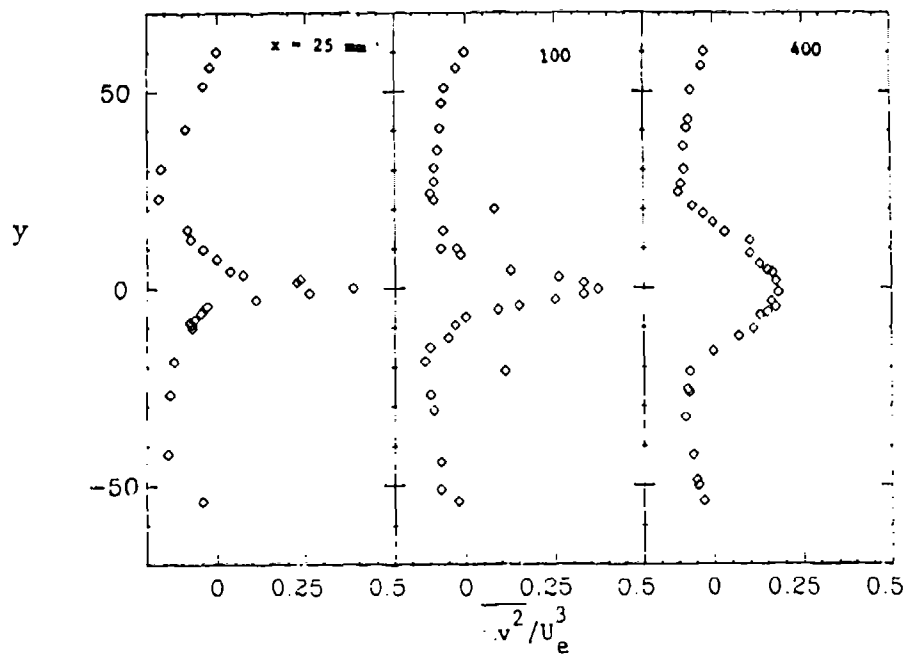
PLOT 3 CASE 0381 FILES 6,7,8



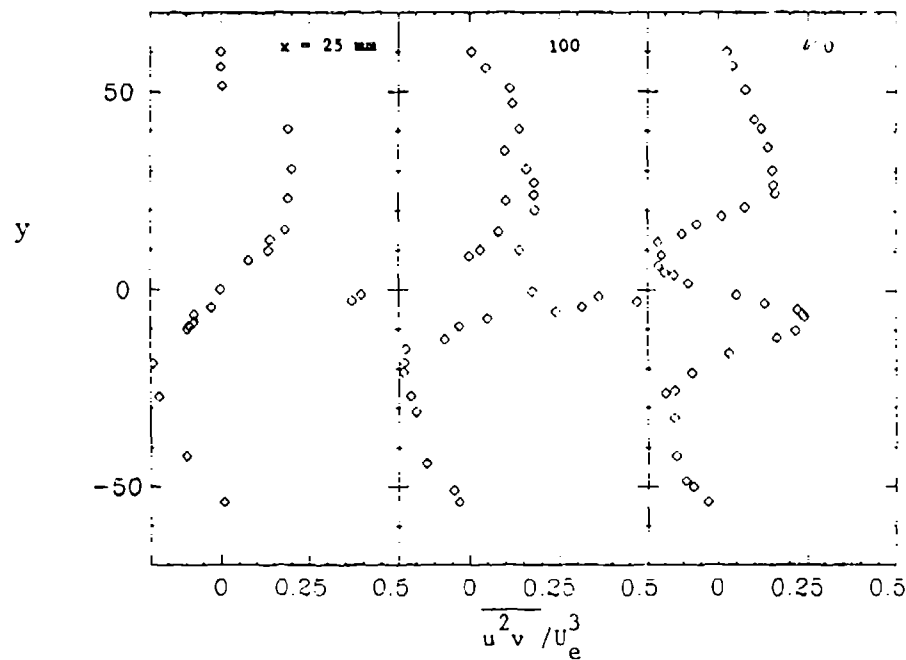
PLOT 4 CASE 0381 FILES 6,7,8



PLOT 5 CASE 0381 FILES 6,7,8



PLOT 6 CASE 0381 FILES 6,7,8



SPECIFICATIONS FOR COMPUTATION

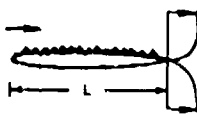
ENTRY CASE/INCOMPRESSIBLE

Case #0382; Data Evaluator: V. C. Patel

Data Taker: J. Andreopoulos

PICTORIAL SUMMARY

Flow 0380. Data Evaluator: V. C. Patel. "Wakes of Two-Dimensional Bodies."

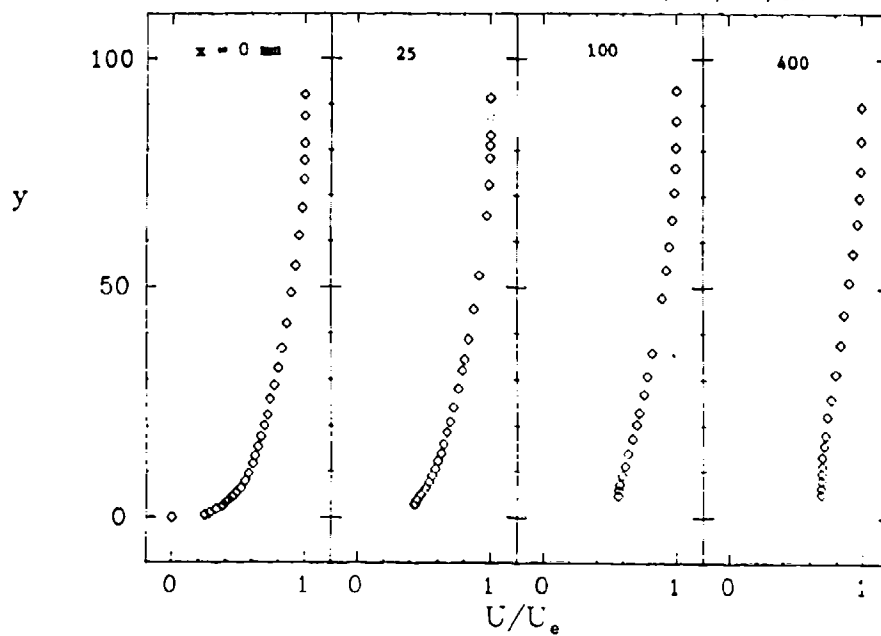
Case Data Taker	Test Rig Geometry	$\Delta p/\Delta x$ or C_p	Number of Stations Measured							C_f	Re	Ini- tial Con- di- tion	Other Notes
			Mean Velocity		Turbulence Profiles								
			U	V or W	$\overline{u^2}$	$\overline{v^2}$	$\overline{w^2}$	\overline{uv}	Others				
Case 0382 J. Andreopoulos			6		4	4	-	4	Triple cor- rela- tions		6.8×10^6 (based on L)	Free- stream turb. < 0.01%	Asymmetrical Case. Conditional averages to study the mixing in the central part of wake.

Plot	Ordinate	Abcissa	Range/Position	Comments
1	y	U/U_e	$0 \leq y \leq 100 \text{ mm}$	4 profiles at $x = 0, 25, 100, 400 \text{ mm}$.
2	y	\overline{uv}/U_e^2	$-50 \leq y \leq 50 \text{ mm}$	3 profiles at $x = 25, 100, 400 \text{ mm}$.
3	y	$\overline{u^2}/U_e^2$	$-50 \leq y \leq 50 \text{ mm}$	3 profiles at $x = 25, 100, 400 \text{ mm}$.
4	y	$\overline{v^2}/U_e^2$	$-50 \leq y \leq 50 \text{ mm}$	3 profiles at $x = 25, 100, 400 \text{ mm}$.
5	y	$\overline{uv^2}/U_e^3$	$-50 \leq y \leq 50 \text{ mm}$	3 profiles at $x = 25, 100, 400 \text{ mm}$.
6	y	$\overline{u^2v}/U_e^3$	$-50 \leq y \leq 50 \text{ mm}$	3 profiles at $x = 25, 100, 400 \text{ mm}$.

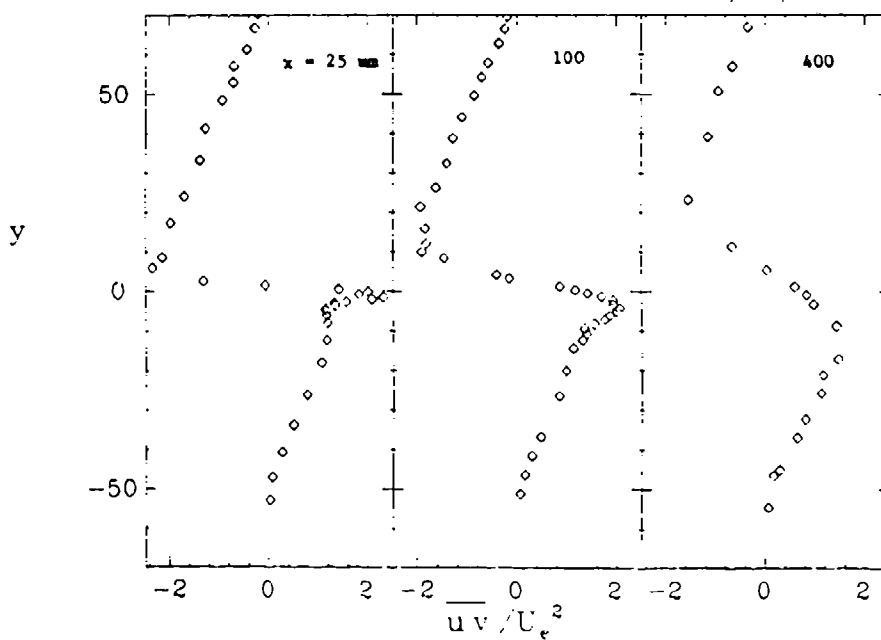
Special Instructions:

- $\theta_0 = \theta_{\text{initial}} = 15.4 \text{ mm}$.

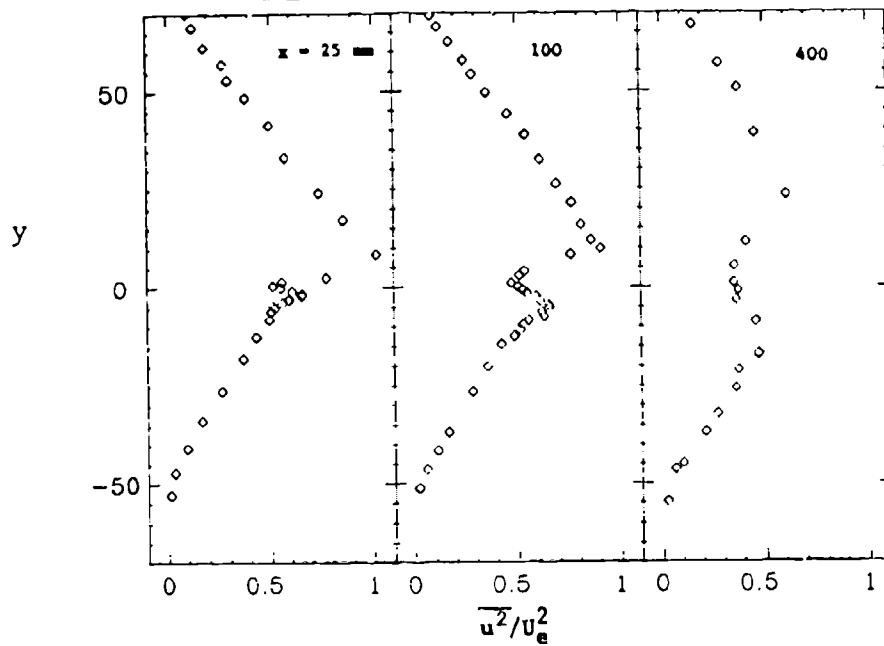
PLOT 1 CASE 0382 FILES 40,42,45,49



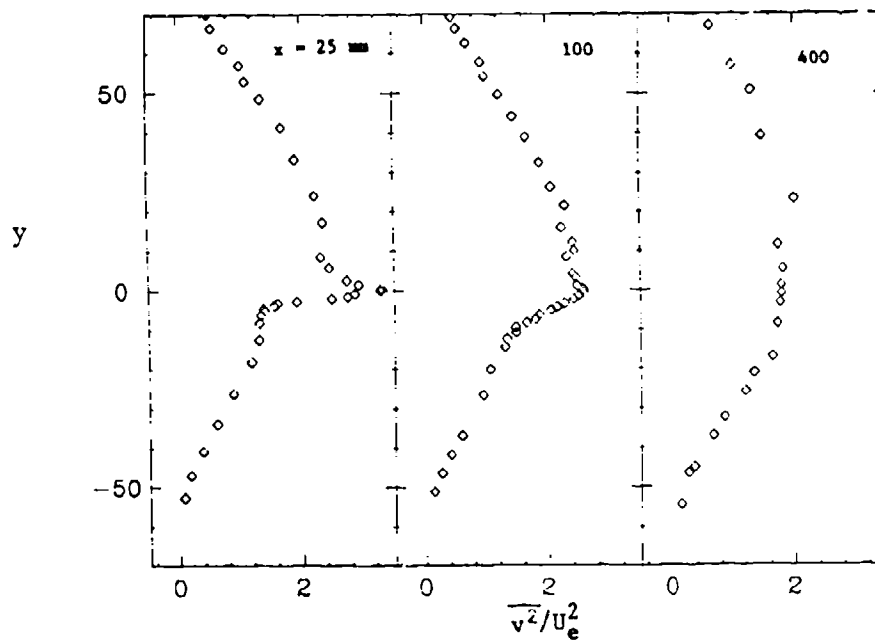
PLOT 2 CASE 0382 FILES 9,10,11



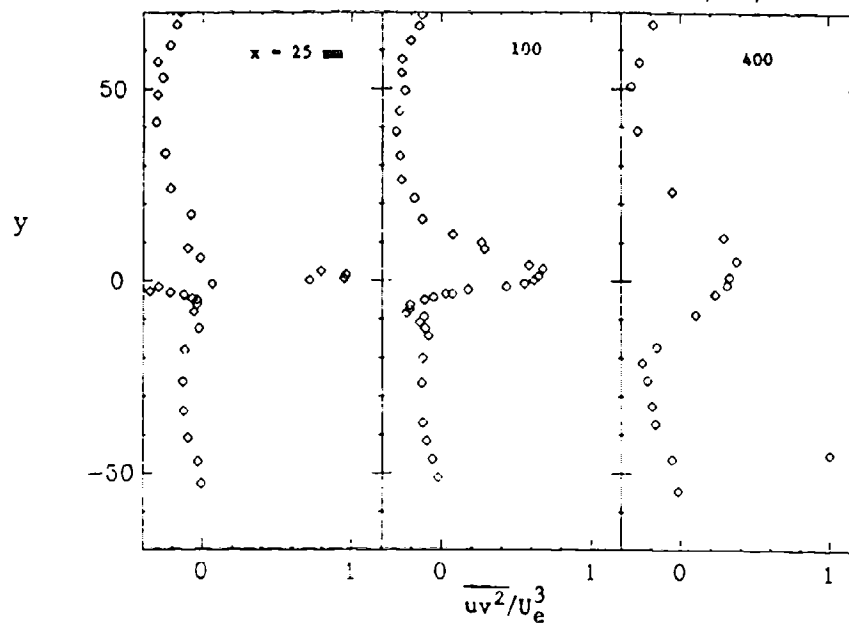
PLOT 3 CASE 0382 FILES 9,10,11



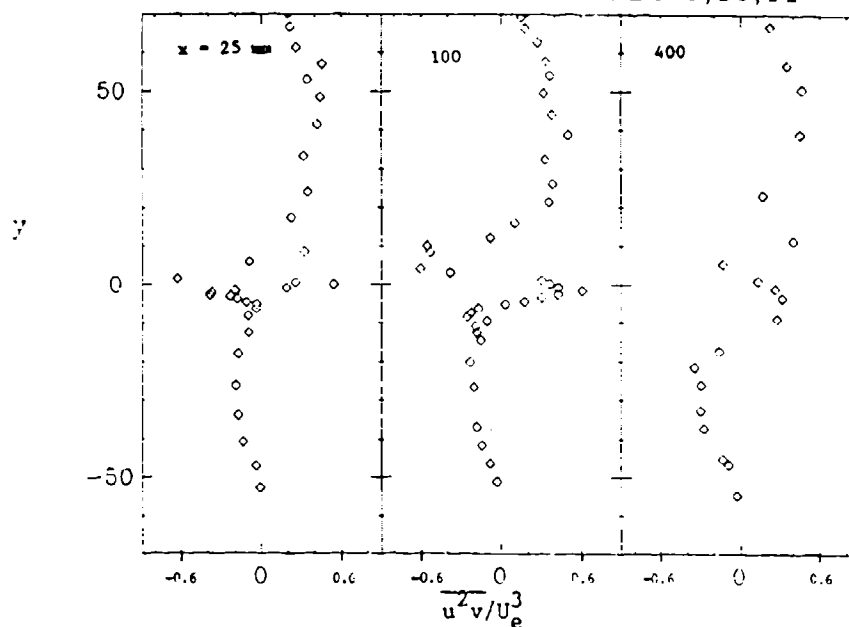
PLOT 4 CASE 0382 FILES 9,10,11



PLOT 5 CASE 0382 FILES 9,10,11



PLOT 6 CASE 0382 FILES 9,10,11



COMPRESSIBILITY EFFECTS ON FREE-SHEAR LAYERS

Flow 8500

Case 8501

Evaluator: P. Bradshaw*

SUMMARY

SELECTION CRITERIA AND FLOWS SELECTED

It appears that the plot of spreading rate against Mach number for plane or effectively plane free-shear layers ("mixing layers" or "half-jets") given by Birch and Eggers (1972, p. 36) in the Langley free-shear-layer meeting proceedings can still be regarded as definitive. Indeed, the only subsequent work appears to be that listed in Armstrong et al. (1976), Ikawa and Kubota (1975), Harvey and Hunter (1975), and Wagner (1973). Of these, the Mach 5 results are stated to be "nearly fully developed." Ikawa's measurements at $M = 2.46$ extended only to about sixty boundary-layer thicknesses downstream of the exit, while the Mach 19 data were taken only a few boundary-layer thicknesses from the exit. Therefore, the Mach 19 data provide a rather wide choice of extrapolation for the "Langley" curve, while the measurements at lower Mach number are in reasonable agreement with that curve. Armstrong's flow (1976) is subsonic, and Lau's (1980) for $M < 1.7$ only; the behavior of the spreading rate for $M < 1.5$ in Plot 4 is largely conjectural.

The full horrors of the sensitivity of free-shear layers to initial and boundary conditions have only been realized since the work reported at the Langley meeting, but even then it was fairly clear that some of the supersonic-mixing-layer data were anomalous. It is probably too facile to denounce any measurement with a higher-than-usual spreading rate as being the result of disturbed or anomalous flow, but the "Langley" consensus curve does indeed seem to reject the data with higher spreading rates (i.e., lower σ). The present test case is intended to represent the asymptotic spreading rate for $x \rightarrow \infty$, as in the low-speed test case (Flow 0310).

As is well known, the effect of density differences on the spreading rate of a low-speed free-shear layer is very much smaller than if the density difference were produced by high Mach number in a homogeneous fluid. Again, there seem to have been no significant extra data since those reviewed by Birch and Eggers (1972). The conclusions of that review were that the trend of spreading rate with density ratio is obscure, while the effect of density ratio on the percentage change of spreading rate with the velocity ratio was small. For the present purposes it is proposed to accept

*Imperial College, Prince Consort Road, London, SW7 2BY, England

the latter conclusion, relying on the measurements of Brown and Roshko for the variation of σ with the ratio of secondary-stream to primary-stream density ρ_2/ρ_1 . Brown and Roshko state that the inverse of the relative spreading rate σ_0/σ is equal to 1.33 at $\rho_2/\rho_1 = 7$ and to 0.74 at $\rho_2/\rho_1 = 1/7$. Compared with the variation of σ with Mach number, the effect of density is small. For purposes of distinguishing the variable-density and compressible cases, it should therefore not be necessary to enter into detailed arguments about accuracy of the Brown and Roshko measurements.

The mixing-layer data are probably the most suitable for testing models of compressibility effects on turbulent flow, because those effects are likely to depend more on the fluctuating Mach number than on the mean Mach number. Taking a typical velocity fluctuation as $\sqrt{(\text{max kinematic shear stress})}$, $\sqrt{(\tau_m/\rho)}$, for simplicity we find that the Mach number fluctuation is $M_e \sqrt{|\tau_m/\rho_e U_e^2|}$. In the mixing layer, the quantity under the square root sign is of order 0.01 at low Mach number, while in a boundary layer it is of order $(C_f/2)$, say 0.001 to 0.002 at low Mach number. Thus compressibility effects appear at much lower M_e in mixing layers than in boundary layers and are significant at speeds well below those at which serious measurement uncertainties, real gas effects, etc., begin to affect boundary-layer data.

ADVICE FOR FUTURE DATA TAKERS

It is easy to demand that experimenters should choose a large enough spatial scale and total pressure to ensure full self-preserving development of the mixing layer well before the end of the test section; but it is less easy to achieve it, particularly since the length required to achieve self-preservation probably increases with Mach number as the spreading rate decreases. The recommendations in S. F. Birch's evaluation report on low-speed mixing layers apply with even greater force. This writer recommends that if the object is to investigate the self-preserving flows only, that the nozzle boundary layer should be kept laminar, if possible, partly to keep it thin and partly because full development seems to be achieved more rapidly, at least for single-stream mixing layers. However, a test case for calculations beginning at the exit is better conditioned if the initial boundary layer is turbulent (see report of Ad-Hoc Committee No. 5, Session XIII). The problem of mixing-layer development for various initial conditions deserves study at any Mach number. Mean velocity measurements should always be accompanied by short-exposure Schlieren or shadowgraph pictures to show up the eddy structure.

REFERENCES

- Armstrong, R. R., H. V. Fuchs, A. Michalke, and U. Michel (1976). "Influence of Mach number on pressure fluctuations relevant to jet noise," presented at the 1976 Noise Control Conference, Warsaw.
- Birch and Eggers (1972). "Free turbulent shear flows," NASA SP-321, Vol. 1.
- Harvey, W. D., and W. W. Hunter, Jr. (1975). "Experimental study of a free turbulent shear flow at Mach 19 with electron-beam and conventional probes," NASA TN D-7981.
- Ikawa, H., and T. Kubota (1975). "Investigation of supersonic turbulent mixing layer with zero pressure gradient," AIAA Jou., 13, 566.
- Lau, J. C. (1980). "Mach number and temperature effects on jets," AIAA Jou., 18, 609. See also J. Fluid Mech., 93, 1 (1979).
- Wagner, R. D. (1973). "Mean flow and turbulence measurements in a Mach 5 free shear layer," NASA TN D-7366. See also E. L. Morrisette, S. F. Birch, and R. D. Wagner (1973). "Mean flow and turbulence measurements in a Mach 5 shear layer," Fluid Mechanics of Mixing, E. M. Uram and V. W. Goldschmidt, eds. (1973), p. 79, ASME, New York.

DISCUSSION

Flow 8500

The committee agreed with P. Bradshaw's suggestions that: (1) since in some computations it is not possible to solve for a flow with $U_2 = 0$, it is acceptable to extrapolate V_2 to zero from two or more cases with low U_2 values; (2) the calculations must be performed from $M = 0$ through the range of Mach numbers.

G. Settles' remark about a new set of data at $M = 3$, which falls on Bradshaw's curve, was brought up by the committee. The committee observed the fact that, as mentioned by G. Settles, Horstman has successfully computed the spreading rate in a compressible flow. Also, Saffman and Oh (as mentioned by D. Bushnell) have carried out similar calculations.

The committee questioned the validity of the postulate for high ratio of density for the low Mach number case of the problem. They stated that the specifications of the problem for this case are not clear.

During the discussions after the presentation, Dr. Saffman suggested that calculations be carried out for unequal stagnation temperatures. Also, A. Koshko questioned the validity of calculations of spreading rate at low-speed flows (low M).

SPECIFICATIONS FOR COMPUTATION

SIMPLE CASE/COMPRESSIBLE

Case 8501; Data Evaluator: P. Bradshaw

Data Takes: Various

PICTORIAL SUMMARY

Flow 8500. Data Evaluator: P. Bradshaw. "Compressible Effects on Free Shear Layers."

Case Data Taker	Test Rig Geometry	dp/dx or C _p	Number of Stations Measured							C _f	Re	Initial Condi- tion	Other Notes
			Mean Velocity		Turbulence Profiles								
			U	V or W	$\overline{u^2}$	$\overline{v^2}$	$\overline{w^2}$	\overline{uv}	Others				
Case 8501 Various data takers			Smoothed curve of dp/dx vs. M gives.										Shear layer spreading rate vs Mach number.

Plot	Ordinate	Abscissa	Range/Position	Comments
1	δ/x or $(\frac{d\delta}{dx})$	M	$0 \leq M \leq 19$ $0.02 \leq d\delta/dx \leq 0.15$	Classical spreading rate vs Mach number distribution.

Special Instructions:

Definition of Special Symbols:

δ/x is tabulated in the file. The equivalence of δ/x and $d\delta/dx$ implies the use of the linear, asymptotic relation between δ and x using an appropriate value of starting length x_0 .

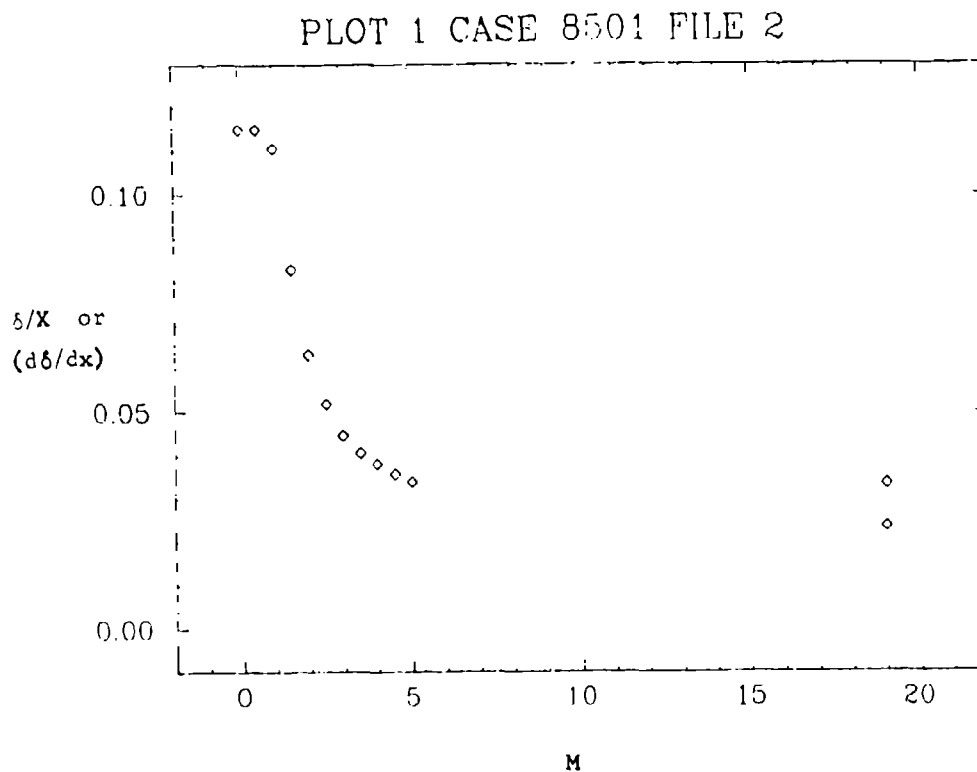
δ = mixing-layer thickness between $U/U_e = \sqrt{0.1}$ and $\sqrt{0.9}$.

The test case is to reproduce the curve of spreading rate presented in the proceedings of the "Langley" meeting (see NASA SP-321). All flows were nominally plane, simple mixing layers in nominally still air. The total temperature of the stream and the ambient air were nominally the same. For uniformity with the test cases for low-speed mixing layers (Flow 0310), the data correlation presented in SP-321 has been converted into a graph of $d\delta/dx$ vs M , where δ is the distance between points on the velocity profile at which the velocity is $\sqrt{0.1} \approx 0.316$ and $\sqrt{0.9} \approx 0.949$ times the maximum. We have taken $d\delta/dx = 1.3/\sigma$ for an error-function profile. The "Langley" values have been modified to agree with the consensus value of $d\delta/dx$ at $M = 0$ (0.115), see Flow 0310. The range of values of $d\delta/dx$ at $M = 19$ data from NASA TN D-7981 (1975) has been bracketed by two points at that Mach number on the curve; no interpolation between $M = 5$ and $M = 19$ is offered. With the exception of $M = 19$, the points on Plot 1 are derived from the curve in SP-321 and are not data points.

Since computers are required to produce asymptotic values of $d\delta/dx$ after the effect of initial conditions has died away, the choice of starting profiles can be left to the computer. The error-function velocity profile is adequate for starting, but the origin of the error function (the half-velocity point) depends on the density profile which is uncertain. At low M , constancy of $\int U^2 dy$ requires the origin of the error function to be at $\eta = 0.043$ (i.e., $U/U_e = 0.5$ at $\eta = 0.043$ leading to $U/U_e = 0.71$ at $\eta = 0$); for practical profiles this is an overestimate.

The data refer to a secondary stream speed which is nominally zero. Computers whose programs will not run satisfactorily for mixing layers in still air should perform at least two runs with small values of secondary stream speeds, and extrapolate to zero speed.

In order to distinguish between the effects of compressibility and of density gradient as such, computers are requested--if their programs permit--to perform runs at low Mach number on mixing layers with different densities in the primary and secondary streams; again, results for zero secondary speed may be obtained by extrapolation. Runs should be carried out at density ratios of 7 and 1/7. Higher Mach number runs with different total temperature in the exit flow or ambient air would be of interest but no reliable data exist for comparison.



SUPERSONIC FLOW OVER A FLAT PLATE

Flows 8100 (Insulated Wall) and 8200 (Cooled Wall)

Cases 8101, 8201

Evaluators: M. W. Rubesin and C. C. Horstman*

SUMMARY

SELECTION CRITERIA AND FLOWS SELECTED

Many experiments have been conducted to provide measurements of the mean properties of a compressible turbulent boundary layer on a flat plate in supersonic flow. These properties include profiles of the mean velocity and temperature and the surface quantities of skin friction, recovery factor, and Stanton number. Although each experiment is of limited range or scope, in their aggregate these experiments cover a large range of Mach number and surface-temperature conditions. It has been shown (Hopkins and Inouye, 1971; Bradshaw, 1977; Hopkins et al., 1972) that the van Driest II mixing-length theory can be used to correlate both the skin friction and the inner-region profile data. Skin friction is represented by the van Driest II theory to about $\pm 10\%$ over the range $2.8 < M < 7.4$ and $0.2 < T_w/T_{aw} < 1.0$. At lower surface temperatures, the theory overpredicts the skin-friction data by about 20% when $T_w/T_{aw} \approx 0.1$. In addition, the incompressible "law of the wall" has been shown to fit the mean velocity data up to a Mach number of 7.0, for both insulated and cooled walls ($T_w/T_{aw} \approx 0.3$), by the theoretically suggested expedient of redefining an "equivalent incompressible velocity" as

$$U^* = \int_0^U \sqrt{\rho/\rho_w} dU$$

and utilizing wall properties in defining y^+ . Finally, recovery factors $r = (T_{aw} - T_e)/(T_T - T_e)$ have been shown to remain close to a value of 0.88 over large ranges of Mach number (van Driest, 1956).

These mean data were obtained, for the most part, without accompanying turbulence measurements. Hot-wire measurements in the period when most of the mean measurements were obtained were confused by density fluctuations, and the laser-Doppler anemometer had not yet been developed. As hot-wire data-reduction techniques improved and as the LDV was developed, profiles of the turbulence moments were measured on wind-tunnel walls, where pressure gradients were zero, rather than on flat-plate models (Johnson and Rose, 1975; Acharya et al., 1979; Dimotakis et al., 1979). One reason for this

*NASA-Ames Research Center, Moffett Field, CA 94035.

was that thicker boundary layers are known to reflect their upstream history of continuous acceleration. The total enthalpy in such boundary layers is known to relate to local velocity in a parabolic fashion, rather than the linear Crocco relationship that occurs on flat plates. Thus these turbulence measurements may not be identical to those on flat plates. Accordingly, the primary test of the computational techniques as applied to flat plates will be comparisons of the computed mean properties with those expected from the van Driest II method. As examples, when the van Driest II method is applied to the Kármán-Schön herr skin-friction law, the results shown in Figs. 1 and 2 are obtained.

RECOMMENDATIONS FOR FUTURE DATA TAKERS

Improvements in the operation and interpretation of the data from laser-Doppler and hot-wire anemometers in recent years makes it possible to consider these instruments for gathering data of turbulence parameters upon which turbulence-model improvements can be made. The relatively small models associated with supersonic wind tunnels utilized for studies of fluid mechanics suggest that measurements within attached boundary layers can be performed with greater spatial resolution when these boundary layers occur on the wind-tunnel walls. Such boundary layers in the portion of the nozzle where the pressure gradient has become zero are not identical to those on flat plates. These boundary layers retain a memory of their upstream history. Thus, measurements at a single station are not adequate. The turbulence-model equations are rate equations in which the mechanisms of production, dissipation, and diffusion compete. To study these processes in a region of zero pressure gradient, it is necessary to have data at successive stations so that the rate of change of the dependent variables between these stations can be measured. Thus, measurements have to be made over a sequence of axial stations covering about 100 boundary-layer thicknesses in the zero-pressure-gradient region on the nozzle walls to effectively represent a flat plate.

The instruments should be applied to measure all the quantities they can. Measurements of all the components of the Reynolds stress tensor will be most useful in guiding modeling through two-equation modeling to models that account for the lack of equilibrium between mean strain and turbulence stress. The Reynolds stresses $\overline{\rho v w}$ and $\overline{\rho u w}$ are good tests of the two-dimensionality of these "pseudo" flat-plate boundary layers. Efforts should be expended to assess both the Morkovin hypotheses and Favre mass-weighting in a quantitative manner through the careful comparison of LDV and hot-wire measurements.

Of the equations utilized in second-order modeling, the scale equation, be it expressed as a length scale, frequency scale, or dissipation rate, has the weakest theoretical foundation. Although the boundary layers on the wall of a wind tunnel

have only a gradually varying scale, the relative thickness of the boundary layer suggests measurements on walls as the place to try two-point correlation-length measurements, multipoint measurements, or other measurements directed toward defining better scale equations in compressible flow.

Finally, some thought should be given to experiments designed to guide the next generation of modeling, when some of the dynamics of the largest scales are calculated and when the models account for the contribution of the remaining scales. These measurements will have to consider the phase relationship for at least the largest scales. This will modify data-recording techniques, as it will require continuous recording of the raw data in time, with subsequent computer analysis. The use of rms meters or correlators will no longer be appropriate. Studies will have to be made to increase LDV seeding so that "continuous" data of the largest eddies can be achieved. Histograms will lose much of their meaning. The continuous, high-frequency response characteristics of hot wires should lead to multi-sensor experiments here. Again, multipoint measurements will be critical.

REFERENCES

- Acharya, M., C. C. Horstman, and M. I. Kussoy (1979). "Reynolds number effects on the turbulence field in compressible boundary layers," AIAA Jou., 17:4, 380-386.
- Bradshaw, P. (1977). "Compressible turbulent shear layers," Ann. Rev. Fluid Mech., 9, 33-54.
- Dimotakis, P. E., D. J. Collins, and D. B. Lang (1979). "Measurements in the turbulent boundary layer at constant pressure in subsonic and supersonic flow," Arnold Engineering Development Center, AEDC-TR-79-49.
- Hopkins, E. J., and M. Inouye (1971). "An evaluation of theories for predicting turbulent skin friction and heat transfer on flat plates at supersonic and hypersonic Mach numbers, AIAA Jou., 9:6, 993-1003.
- Hopkins, E. J., E. R. Keener, T. E. Polek, H. A. Dwyer (1972). "Hypersonic turbulent skin-friction and boundary-layer profiles on nonadiabatic flat plates," AIAA Jou., 10:1, 40-48.
- Johnson, D. A., and W. C. Rose (1975). "Laser velocimeter and hot-wire anemometer comparison in a supersonic boundary layer," AIAA Jou., 13, 512-514.
- Van Driest, E. R. (1956). "The problem of aerodynamic heating," Aero. Engrg. Review (October, 1956).

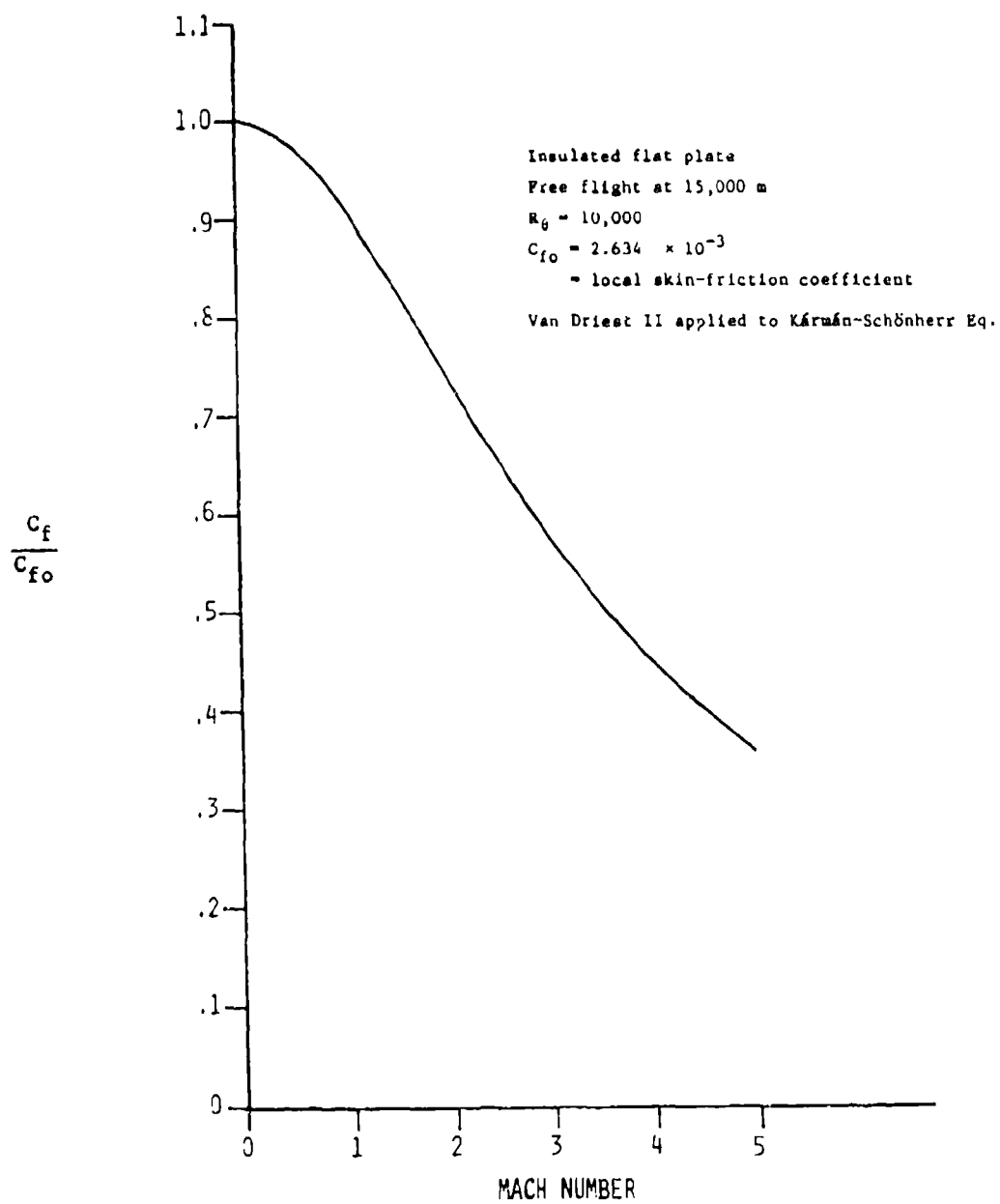


Figure 1. Case 8101, Mach number effect on skin friction.

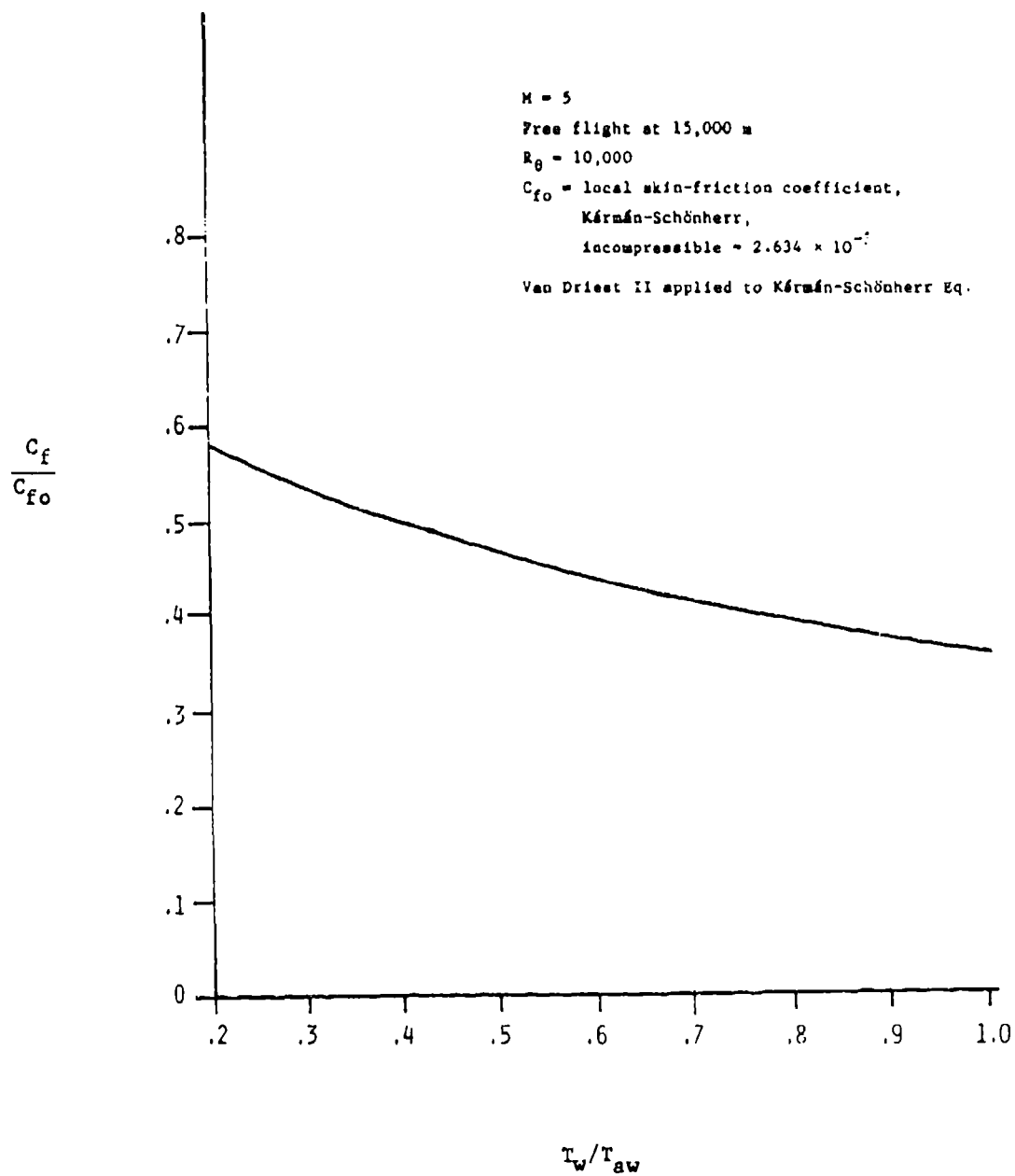


Figure 2. Case 8201, Effect of surface cooling on skin friction.

DISCUSSION

Flows 8100/8200

1. The Conference accepted Cases 8101 and 8201 as valid test cases.
2. In response to P. Bradshaw's question about the maximum frequency of data recording, M. Rubesin responded that with state-of-the-art equipment a frequency of 105 Hz can be recorded on FM tape recorders.

SPECIFICATIONS FOR COMPUTATION

SIMPLE CASE/COMPRESSIBLE

Case #8101; Data Evaluators: M. Rubesin, C. Horstman

Data Takers: Various, composite curves

PICTORIAL SUMMARY

View 8100. Data Evaluators: M. Rubesin and C. Horstman. "Supersonic Flow Over a Flat Plate (Insulated Wall)."

Case Data Taker	Test Rig Geometry	dp/ds or C _p	Number of Stations Measured								C _f	Re	Ini- tial Condi- tion	Other Notes
			Mean Velocity		Turbulence Profiles									
			U	V or W	$\overline{u^2}$	$\overline{v^2}$	$\overline{w^2}$	\overline{uv}	Others					
Case 8101 Various data takers			C _f /C _{f0} vs. M											Effect of compressibility on skin friction.

Plot	Ordinate	Abscissa	Range/Position	Comments
1	C _f /C _{f0}	M	0 ≤ C _f /C _{f0} ≤ 1.1 0 ≤ M ≤ 5.0	Skin friction vs Mach Number. C _{f0} = 0.002634.

Special Instructions:

1. This test case considers the development of the turbulent boundary layer on an adiabatic flat plate moving through the atmosphere at high speeds. For this example, the computer is to consider flight at an altitude of 15,000 m in the Mach number range 0 < M < 5. Computers should compute the ratio of the local skin-friction coefficient to the Kármán-Schönher incompressible value, both evaluated at a momentum-thickness Reynolds number of 10,000, for M = 1, 2, 3, 4, 5.

The recovery factor, $r = (T_{aw} - T_{\infty}) / (T_T - T_{\infty})$, should also be plotted as a function of Mach number. T_{aw} is the adiabatic wall temperature, T_T is stagnation temperature, and T_{∞} is the free-stream temperature at the prescribed altitude.

At the M = 5 condition, the computers are to plot their velocity profiles as $u^* / \sqrt{\tau_w / \rho_w}$ vs $\log_{10}(y \sqrt{\tau_w / \rho_w} / \nu_w)$. Note that the recovery factor and velocity profiles are output only. Data are not provided for comparison.

2. Computers are requested to produce the following additional results not backed by data for the purpose of checking consistency of models.

Plot	Ordinate	Abcissa	Range/Position	Comments
A	r	M	$0.5 \leq r \leq 1.5$ $0 \leq M \leq 5.0$	Recovery factor vs Mach number. <u>Output only.</u>
B	U^{*+}	$\log_{10} y^+$	$0 \leq U^{*+} \leq 30$ $0 \leq \log_{10} y^+ \leq 4$	Velocity profile at $M = 5$. $U^* = \int_0^U \sqrt{\rho/\rho_w} dU, \quad w = \text{wall.}$ $U^{*+} = U^* / \sqrt{\tau_w/\rho_w}.$ $y^+ = y \frac{\sqrt{\tau_w/\rho_w}}{\nu_w}.$

SPECIFICATIONS FOR COMPUTATION

SIMPLE CASE/COMPRESSIBLE

Case #8201; Data Evaluators: M. Rubesin, C. Horstman

Data Takers: Various, Composite Curve

PICTORIAL SUMMARY

Flow #200. Data Evaluators: M. Rubesin and C. Horstman. "8 versonic Flow Over a Flat Plate (Cooled Wall)."

Case Data Taker	Test Rig Geometry	dp/dx or C _p	Number of Stations Measured							C _f	Re	Ini- tial Condi- tion	Other Notes
			Mean Velocity		Turbulence Profiles								
			U	V or W	$\overline{u^2}$	$\overline{v^2}$	$\overline{w^2}$	\overline{uv}	Others				
Case 8201			C _f /C _{f0} vs. T _w /T ₀										Effect of surface cooling on skin friction.
Various data takers													

Plot	Ordinate	Abscissa	Range/Position	Comments
1	C _f /C _{f0}	T _w /T _{aw}	0 ≤ C _f /C _{f0} ≤ 0.8 0.2 ≤ T _w /T _{aw} ≤ 1.0	Plot at M = 5, C _{f0} = 0.002634. At R _θ = 10,000.

Special Instructions:

1. This test case considers the effect of changing the surface temperature of the flat plate in Case 8101. For the case of the flat plate moving at a Mach number of 5 at an altitude of 15,000 m, the computers should compute the effects of altering the plate temperature on the local skin-friction coefficient at a momentum thickness Reynolds number of 10,000.
2. Computers are requested to include the following additional results not backed by data for the purpose of checking consistency of models.

Plot	Ordinate	Abscissa	Range/Position	Comments
A	U ⁺	log ₁₀ y ⁺	0 ≤ U ⁺ ≤ 20 0 ≤ log ₁₀ y ⁺ ≤ 4	Velocity profile at M = 5 and T _w /T _{aw} = 0.3. T _{aw} is adiabatic wall temp. $U^+ = \int_0^U \sqrt{\rho/\rho_w} dU, \quad w = \text{wall}.$ $U^{*+} = U^*/\sqrt{\tau_w/\rho_w}.$ $y^+ = y \frac{\sqrt{\tau_w/\rho_w}}{\nu_w}.$

BOUNDARY LAYERS IN AN ADVERSE PRESSURE GRADIENT
IN AN AXISYMMETRIC INTERNAL FLOW

Flow 8400
Cases 8401, 8402, 8403

BOUNDARY LAYERS IN AN ADVERSE PRESSURE GRADIENT
IN TWO-DIMENSIONAL FLOW

Flow 8410
Case 8411

Data Evaluators: M. W. Rubesin and C. C. Horstman



SUMMARY*

(presented by H. H. Fernholz[†])

INTRODUCTION

These nominally two-dimensional or axisymmetric compressible turbulent boundary-layer flows along straight walls were selected by M. Rubesin and C. C. Horstman from among the variable-pressure-gradient, reflected-wave cases presented and discussed in AGARDographs 223 and 253 by Fernholz and Finley (1977, 1980). The boundary layers along aerodynamically smooth and nominally adiabatic walls were unseparated. No information is available about the state of the tunnel boundary layers or the turbulence and noise level in the test section (environment). None of the experiments listed below as Cases 8401, 8402, 8403, and 8411 provides an ideal set of measurements as defined in AG 253 but three of the four flows contain the minimum information to serve as a test case. Cases 8401, 8411, and 8402 are described below as presented in AG 223, while the description of Case 8403 was given by Kussoy et al. (1978).

Case 8401.[#] Peake et al. (1971), (CAT 7102)[‡]

Peake et al. (1971) made their measurements in the boundary layer generated on the inner surface of a cylinder mounted on the centerline of the wind tunnel. The pressure field in the axial and normal direction is shown in Fig. 1. The initial profile 01 departs considerably from the logarithmic law of the wall (see Fig. 2), and

*Herman-Fottinger Institut für Thermo- und Fluidodynamik, Technische Universität, D-1000 Berlin 12, W. Germany.

[†]This summary is based on information published by Fernholz and Finley (1980).

[#]This case was not finally selected as a test case for the 1981 Conference. The data set is, however, in the Data Library.

[‡]This number denotes the experiment in AGARDograph 223.

this departure from the log-law and the difference between profile 01 and the initial profile of the zero-pressure-gradient case may therefore be caused by adverse streamwise pressure gradients, by the pressure increase in the normal direction, or by both. Discrepancies may also, in part, spring from the resulting errors in data reduction, since the normal pressure gradient will result in the Mach number in the outer region being less than that calculated assuming constant pressure.

Profile 02 is in a region where normal pressure gradients should be negligible. For this, and the succeeding profiles, the slope of the inner region suggests that there may be errors in the skin-friction values. Profile 03 is again subject to both longitudinal and normal pressure gradients, this time of a sense to cause the Mach numbers in the outer region to be greater than assumed. The appearance on the log-law plot is again much as would be expected of a subsonic adverse-pressure-gradient layer. The succeeding profiles 04 and 05, in a zero-pressure-gradient region, appear--if anything--more as expected of a favorable pressure-gradient flow on the log-law plot.

Case 8402.* Lewis et al. (1972), (CAT 7201)

The tests were performed on the inner surface of a cylinder mounted on the centerline of the wind tunnel. A pressure gradient could be imposed by a center body, causing an adverse pressure gradient followed by a favorable one (Fig. 3). Lewis et al. (1972) did not measure the wall shear stress directly but used the curve-fitting procedure of Coles and Hirst (1969) applied to equivalent incompressible velocity profiles transformed as suggested by van Driest (1951). However, the calibration function for the Stanton tubes was presented as evidence of consistency. All velocity profiles therefore agree very well with the log-law (Figs. 4 and 5) and their wake components ΔU^+ behave as in an incompressible variable pressure-gradient boundary layer. The profiles show both the behavior characteristic of the specific pressure gradient and--after a change in pressure gradient--the effects of upstream history (cf. the log-law plot in Fig. 5 and the outer law plots shown in AG 253). The development of the boundary layer near stations 13 and 14 shows "simple wave effects." Profiles 08 to 12 show the classic low-speed adverse pressure-gradient behavior. Then the adverse pressure gradient stops at or just downstream of station 14 to be followed by a favorable pressure gradient. Consequently the whole of profile 14 and probably most of the outer part of 13 are in fact in a simple-wave, favorable pressure-gradient region with the pressure-gradient parameter Π_0 unchanged between 12 and 14!

*This case was not finally used for the 1980/81 Conference. The data set is, however, in the Data Library.

Case 8403. Kussov et al. (1978), (CAT 7802 S)*

A particularly fully instrumented study is that made by Kussov et al. (1978). The test boundary layer was formed on the inner surface of a cylindrical test section attached to the exit of the axisymmetric nozzle. One of six center bodies could be sting-mounted on the axis of the test section. The center bodies were designed to impose a shock-free compression on the boundary layer followed, where geometry allowed, by firstly a constant-pressure region and finally an expansion. The center bodies could be traversed along the centerline so that their associated pressure fields moved past a single, fixed instrumentation port in the tunnel wall about 2.90 m downstream of the tunnel throat. The position of measuring "stations" is given by their x-position relative to the nose of the center body. The center bodies traversed by about 0.22 m, and over this distance the thickness of the boundary layer entering the interaction varied by about 6%.

Two of these cases (center bodies II and IV at $Re_x = 35.3 \times 10^6$) include full profile measurements, at close streamwise intervals. The wave structures produced in both cases consist of a compression followed by an expansion. The wave structures are relatively concentrated, in that the streamwise extent--at any given value of y --is of the same order as the boundary-layer thickness so that the "reflected wave" region is entirely submerged in the boundary layer.

The static-pressure fields are shown in the form of profile measurements. In each case the static-pressure distribution in the flow direction at the wall ($y = 0$) is shown, as also are values for $y = 60$ mm corresponding to a traverse well outside the boundary layer. There are two values for p_0 , depending on whether data are taken from wall-pressure runs or from profile runs. The differences are not great. An incoming wave at $y = 60$ mm leads the wall-pressure change that it causes by about 120 mm (Fig. 6). For series 01--the more moderate pressure gradient--the wall pressure is initially constant, then rises as the compression reaches the wall and is reflected before continuing at a constant level to the end of the test zone. The expansion wave does not reach the wall, although the outer part of the downstream profiles (10-13) is affected. The outgoing reflected wave initially appears more concentrated and stronger than might be expected (see the "bulge" in the inner part of profiles 03 and 09).

Two values for the displacement surface are shown, one for D STAR calculated allowing for varying static pressure as suggested in §7 of AG 253, the other representing the authors' δ_1 values[†] calculated as for a zero normal-pressure-gradient

*This case will be presented in a supplementary volume of the data catalogue in AG-223.

†For the definition of the displacement thicknesses δ_1 and D STAR, see AG 223, pp. 14-15.

case. It is interesting that for both series 01 and 02, the conventional expression suggests a marked dip in the displacement surface in the zone where the incoming pressure wave approaches the wall. If this were in fact present, an expansion-compression-expansion wave would propagate outwards from the affected area. There is little sign of any such structure either in the static-pressure profiles, or in the wall-pressure variation.

It is evident from the foregoing that any attempt at accounting for pressure history effects in the velocity profiles must take into consideration the history of the particular part of the layer under discussion. In a wave structure whose dimensions are comparable with the boundary-layer thickness, the past history of the inner and outer layers may be very different.

For the more abrupt pressure gradient of series 02 (Fig. 7) the wall pressure, after an initial constant pressure region (02), rises to a plateau (10 to 12) but the expansion wave then reaches the wall and the pressure falls markedly in the region described by the last two profiles (13 and 14). There is evidence of a strong compression wave entering the test section in the outer part of the last profile.

There is again a localized dip in the authors' δ_1 value where the compression wave reaches the wall. The D STAR value, if anything, shows the reverse tendency. Both here and to a lesser extent for series 01, the wall pressure seems a little low in relation to the general pressure level in the inner part of the boundary layer in a way which is not explained easily in terms of the wave structure.

The observed pressure variation suggests that there is a weak outgoing expansion wave in this region, or alternatively that the probes are affected by the wall and the wave structure so as to give a slightly high reading when close to the wall.

Wall-law profiles are shown for series 01 and 02 (Figs. 8 and 9, respectively). Profiles 02, 04, and 03 are only slightly, if at all, affected by the incoming wave structure and appear as typical zero-pressure-gradient profiles in both shape and position in the log-law plot. 07 is at the start of the adverse-pressure gradient as observed at the wall and 09 at the end.

Series 02 shows the same general behavior. The initial zero-pressure-gradient profile of 03 develops an increased wake component by 07, at the start of the adverse-pressure gradient at the wall, which becomes increasingly exaggerated in profiles 09 and 10 before decreasing in 12 and 14, where the wall-pressure gradient is favorable.

Case 8411. Zwarts (1970), (CAT 7007)

Zwarts (1970) conducted his experiment on the floor of a 0.13-m square wind tunnel. A contoured splitter plate was designed by the method of characteristics to give a Mach number distribution on the tunnel floor such that the initial flow at $M_\delta = 4$ passed through a constant Mach number gradient falling to $M_\delta = 3$ over a distance of

0.13 m, followed by a second region of constant Mach number flow. Surface-flow-visualization tests showed that there was considerable flow convergence in the adverse-pressure-gradient region as well as divergence in the zero-pressure-gradient region. This was attributed to inflow/outflow from the tunnel side wall driven by the significant pressure differences normal to the test surface (length-to-width ratio of the tunnel floor is about 8).

The pressure gradient is imposed as a reflected wave, so that normal-pressure gradients should be negligible except at the start and end of the adverse-pressure gradients (profiles 03, 15, and 16). Unfortunately no static-pressure traverses were carried out.

The author offers skin-friction values deduced from several calibration functions. We have selected data evaluated from the TR-method of Hopkins and Kenner (1966) which gives the smallest values of c_f . Agreement of the velocity profiles with the logarithmic law is fair (Fig. 10) though almost all profiles lie low, which means that the skin-friction velocity is still too high. The outer-law representation is shown in Fig. 11, indicating clearly upstream-history effects.

ADVICE FOR FUTURE DATA TAKERS

Experimentalists who intend to perform further experiments in two-dimensional compressible turbulent boundary layers will find hints about gaps in our knowledge in AG 223, 253, and, when available, in Vol. III of this series (to be published 1981). As for the cases presented here a few suggestions for the two boundary-layer flows, 8402 and 8403, are appropriate. Both experiments should be repeated with cooled walls with isothermal and variable wall temperature. Before doing this the problems connected with skin-friction measurements in adverse- and favorable-pressure-gradient turbulent boundary layers must be solved (measuring techniques and calibration curves for Preston tubes).

We have to know more about the environment, i.e., the noise level and the turbulence level in the test section. In order to allow for a complete computation of the boundary layer, location and length of the transition region must be known. Existing turbulence models can only be improved if more and reliable turbulence data are performed. Here we have a large deficit with Case 8402. For this flow we would also like to see measurements of static pressure profiles at least at critical stations.

Finally it would be advantageous to have flows with steeper pressure gradients in order to be able to study compressible boundary layers near separation or relaminarization for a favorable pressure gradient. This latter type of flow is certainly most rewarding though it does not appear in the list of flow cases under consideration.

ACKNOWLEDGMENT

This summary presented at the 1980 Conference was based on information recorded in AGARDographs 223 and 253. The author thanks his co-author, J. P. Finley, for permission to reproduce the information from these two reports.

REFERENCES

- Coles, D. E., and E. A. First (1969). Proceedings, 1968 AFOSR-IFP-Stanford Conference on Computation of Turbulent Boundary Layers, Vol. II, Compiled Data, Stanford University, Stanford, CA, 94305.
- Fernholz, H. H., and P. J. Finley (1977). "A critical compilation of compressible turbulent boundary layer data," AGARD-AG-223.
- Fernholz, H. H., and P. J. Finley (1980). "A critical commentary on mean flow data for two-dimensional compressible turbulent boundary layers," AGARD-AG-253.
- Hopkins, E. J., and E. R. Kenner (1966). "Study of surface Pitots for measuring turbulent skin friction at supersonic Mach numbers--adiabatic wall," NASA TN D 3478 (CAT 6601).
- Kussoy, M. I., C. C. Horstman, and M. Aclarya (1978). "An experimental documentation of pressure gradient and Reynolds number effects on compressible turbulent boundary layers," NASA TM 78488 (CAT 7802 S).
- Lewis, J. E., R. L. Gran, and T. Kubota (1972). "An experiment on the adiabatic compressible turbulent boundary layer in adverse and favourable pressure gradients," J. Fluid Mech., 51, 657-672 (CAT 7201).
- Peake, D. J., G. Brakmann, and J. M. Romeskie (1971). "Comparison between some high Reynolds number turbulent boundary layer experiments at Mach 4 and various recent calculation procedures," Nat. Res. Council of Canada and AGARD CP-93-71 Paper II (CAT 7102).
- Van Driest, E. R. (1951). "Turbulent boundary layer in compressible fluids," J. Aero. Sci., 18, 145-160.
- Zwarts, F. (1970). "Compressible turbulent boundary layers," Ph.D. Thesis, McGill Univ., Mech. Engr. Dept. (CAT 7007).

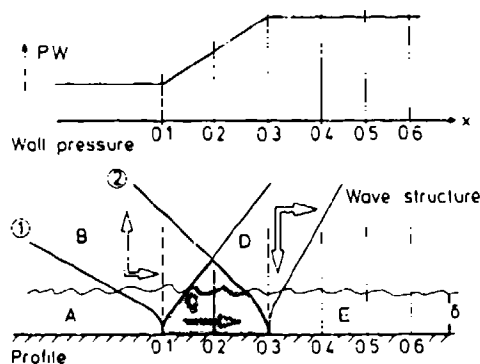


Figure 1. Sketch showing measuring stations (from AG 253).

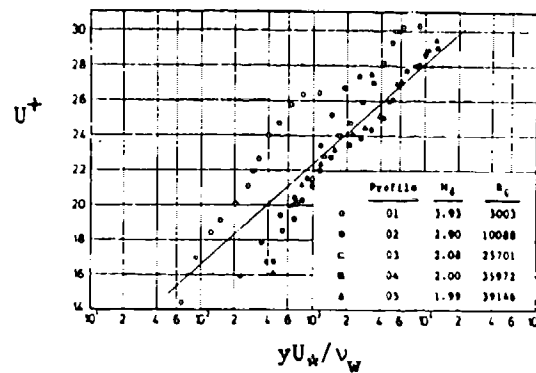


Figure 2. Law-of-the-wall for a compressible boundary layer (adiabatic wall, adverse pressure gradient, defined origin); Peake et al. (1971). c_1 from Preston tube (from AG-253).

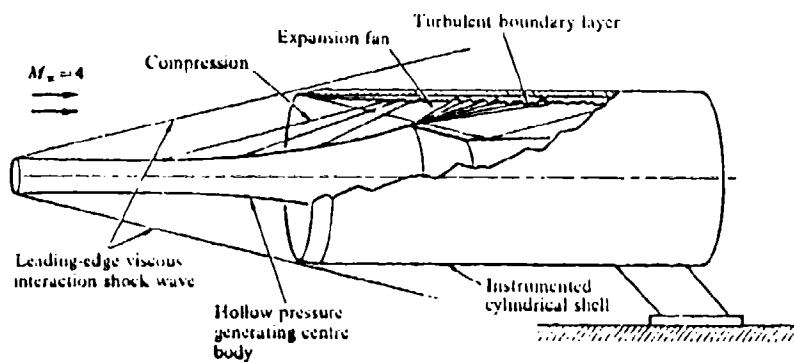


Figure 3. Wind-tunnel model.

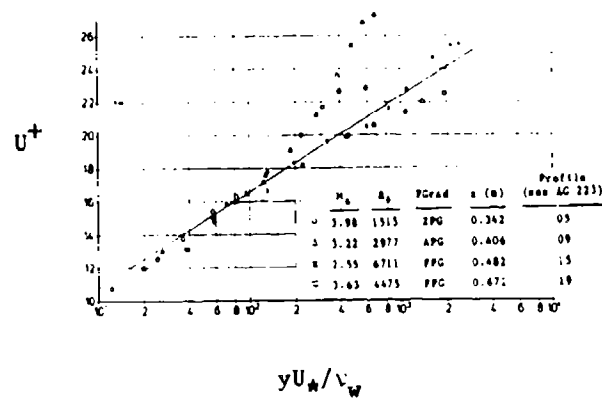


Figure 4. Comparison of log-law with measurements (Lewis et al., 1972). Adiabatic wall, variable pressure gradient (axisymmetric configuration); (from AG-253).

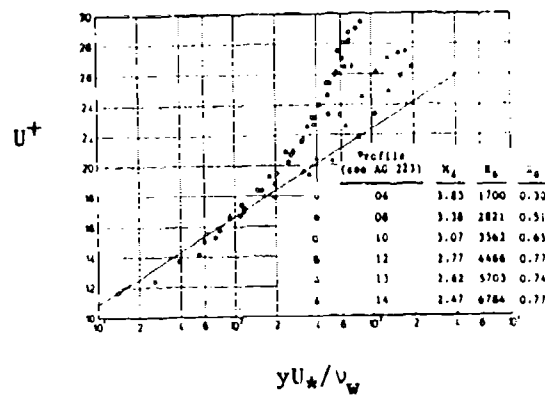


Figure 5. Law-of-the-wall for a compressible boundary layer (adiabatic wall, adverse pressure gradient, defined origin); Lewis et al. (1972). c_1 from transformed log-law (from AG-253).

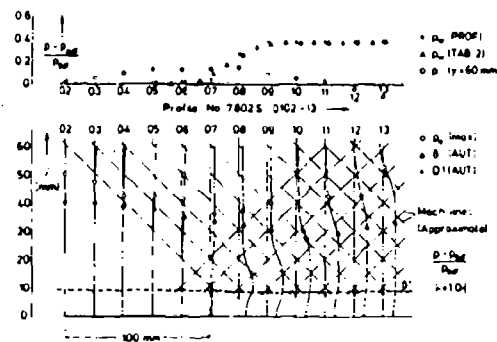


Figure 6. Pressure distribution in wave-interaction region--Series 01 (from AG-253).

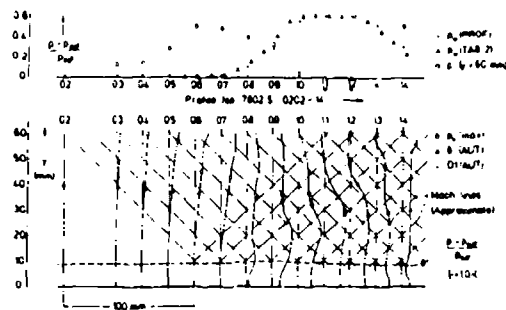


Figure 7. Pressure distribution in wave-interaction region--Series 02 (from AG-253).

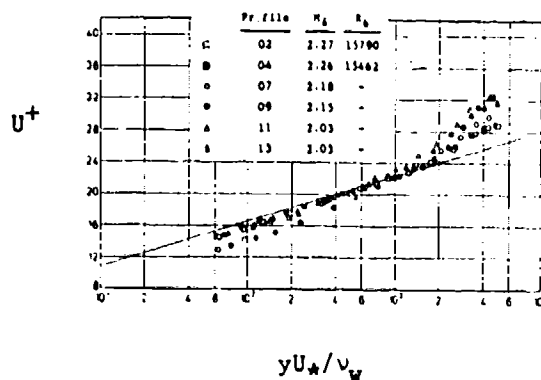


Figure 8. Law-of-the-wall for an axisymmetric compressible boundary layer (adiabatic wall, variable pressure gradient, origin not defined); Kussoy et al. (1978). c_1 from heated-wire gauge (from AG-253).

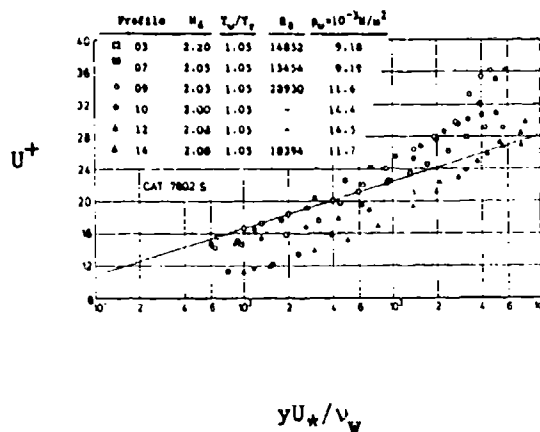


Figure 9. Law-of-the-wall for an axisymmetric compressible boundary layer (adiabatic wall, variable pressure gradient, origin not defined); Kussoy et al. (1978). c_1 from heated-wire gauge (from AG-253).

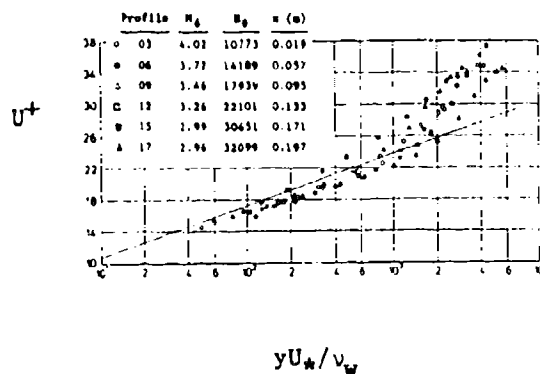


Figure 10. Law-of-the-wall for a compressible boundary layer (adiabatic wall, adverse pressure gradient, origin not defined); Zwarts (1970). c_1 from Preston tube (from AG-253).

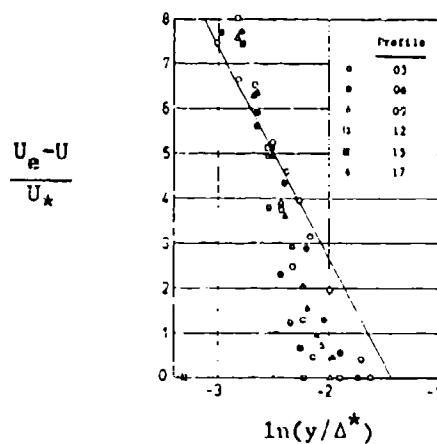


Figure 11. Outer law for a compressible turbulent boundary layer in an adverse pressure gradient (adiabatic wall, origin not defined); Zwarts (1970), (from AG-253).

BOUNDARY LAYER IN ADVERSE PRESSURE GRADIENT IN AN AXISYMMETRIC FLOW

Flow 8400

Case 8403

BOUNDARY LAYER IN ADVERSE PRESSURE GRADIENT IN TWO-DIMENSIONAL FLOW

Flow 8410

Case 8411

Data Evaluators: M. R. Rubesin and C. C. Horstman

SUPPLEMENT (Prepared by G. M. Lilley) to the
Summary Presented by H. K. Fernholz Concerning
Test Cases 8403 and 8411

CASE 8403

The test boundary layer in this flow (see Fig. 1) is formed on the inside of a constant-diameter tube over an extensive range of Reynolds number at a nominal free-stream Mach number of 2.3. The region of adverse pressure gradient was generated by a shaped center body, and its magnitude was greater than in the other test cases. The measured wall-pressure distributions are listed in the data files. The tests were conducted in the NASA-Ames Research Center's high-Reynolds-number blowdown facility and are reported in Acharya et al. (1978a,b); Acharya et al. (1979); and Kussoy et al. (1978). The tube diameter was 0.2417 m, and the length was 0.27 m. The useful test-run time in the facility varied from 5 to 60 min. The range of stagnation pressures was 0.33 to 9.0 atm, giving a free-stream unit-Reynolds-number range of 4×10^6 to 108×10^6 per meter. The total temperature was 278°K.

The measured upstream boundary-layer profiles verified that the flow in the test region of the tube was fully turbulent. The free-stream test conditions, including the initial boundary-layer characteristics at $x = 0.1$ m, are listed in Table 1 for four test runs, each at different values of stagnation pressure. In each test case, a slight Mach-number gradient ($-0.05/m$) existed ahead of the interaction due to boundary-layer growth in the tube.

The surface roughness on the inside of the duct was approximately $0.4 \mu m$ and was an order of magnitude less than the minimum (linear) sublayer thickness encountered in these tests.

Instrumentation and Measurements

The wall static pressure holes were 0.050 cm in diameter and were spaced at intervals of 5.08 cm along the tube. The wall shear was measured by (1) Preston tube, (2) heated-wire technique, and (3) law-of-the-wall plots. The outside diameter of the Preston tube was 0.152 cm. The platinum-10% rhodium heated wire was 0.000254 cm in

diameter and 0.635 cm long. The flow field was measured from Pitot pressure and total temperature traverses. The miniature Pitot tube had a total thickness of 0.0127 cm and a width, parallel to the surface, of 0.10 cm. The total-temperature thermocouple probe was based on the design proposed by Vas (1971).

The fluctuating quantities were measured by hot wires. Both single-hot-wire and dual-wedge hot-film probes were used to obtain the three fluctuating velocity components and the turbulent shear stress. Another hot wire with epoxy support measured mass flow and total temperature fluctuations.

Benchmark Data

The tests were conducted at four values of stagnation pressure. The free-stream conditions and the initial boundary-layer thicknesses at $x = 0.10$ m are given in Table 1. The Reynolds number $Re(x'_0)$ was based on the distance from the nozzle throat.

The following measured quantities are included in the data files:

a. Surface (mean):

$p_w/p_{w\infty}$, $\tau_w/\tau_{w\infty}$, $C_f \times 10^3$ as functions of x , where $C_f = \tau_w / \frac{1}{2} \rho_\infty U_\infty^2$.

b. Integral boundary-layer properties:

δ , δ^* , θ , (in cm) as functions of x .

c. Flow field (mean):

M , p/p_∞ , ρ/ρ_∞ , T/T_∞ , U/U_∞ , $\rho U/\rho_\infty U_\infty$, $T_T/T_{T\infty}$ as functions of y at various x -stations.

d. Flow field (fluctuating)

$\overline{(u^2)}^{1/2} / \rho_\infty U_\infty$, $\langle \rho' \rangle / \rho_\infty$, $\overline{(u^2)}^{1/2} / U_\infty$, $\overline{(v^2)}^{1/2} / U_\infty$, $\overline{(w^2)}^{1/2} / U_\infty$, $\sqrt{\overline{\rho'^2}} / U_\infty$, $(\tau / \rho_\infty U_\infty^2) \times 10^3$.

The axial distance x is measured from the nose of the center body. The coordinate y is normal to the wall.

Uncertainty Estimates

The following uncertainties are estimated from the basic measurement uncertainty:

$$\begin{aligned} p_w &= \pm 5\% \\ \tau_w &= \pm 15\% \\ y &= \pm 0.01 \text{ cm} \\ T_T &= \pm 0.5\% \\ p &= \pm 10\% \\ T &= \pm 6\% \\ \rho &= \pm 12\% \\ U &= \pm 3\% \\ \overline{(u^2)}^{1/2}, \overline{(v^2)}^{1/2}, \overline{(w^2)}^{1/2} &\pm 15\% \\ \tau &\pm 20\% \end{aligned}$$

CASE 8411[†]

This flow is Case 7007 of the Fernholz-Finley (1977) collection. The original data were obtained by Zwarts (1970). The test boundary layer was formed on the floor of the NAE 12.7 cm x 12.7 cm (5"x5") blowdown wind tunnel at a free-stream Mach number of 4. The test section commenced about 0.75 m downstream of the nozzle throat so that the starting boundary-layer thickness was about 10 mm. A compression wedge in the form of a contoured splitter plate was designed to give a Mach-number distribution on the tunnel floor such that the initial flow at $M = 4$ passed through a constant Mach-number-gradient falling to $M = 3$ over a distance of 0.15 m, followed by a second region of constant-Mach-number flow. A sketch of the apparatus is given below (see Fig. 2 taken from Zwarts, 1970). The measured test wall-pressure distribution is listed in the data files.^{*} The undisturbed boundary-layer Reynolds number is $R_0 = 3.5 \times 10^4$.

The test surface roughness was less than 0.9 μm , and it was not actively cooled. The wall temperature was not measured, but was assumed to be between room temperature (same as total temperature) and the adiabatic wall temperature.

The length-to-width ratio of the tunnel floor (test surface) was about 8. Surface flow-visualization tests showed there was considerable flow convergence in the region of the adverse pressure gradient, as well as flow divergence in the region of zero pressure gradient. The data on file, however, are presented for the centerline region only where the transverse Mach number gradient was small. At 38 mm from the tunnel centerline, measurements obtained from pitot traverses and Preston tubes showed differences in C_f and δ^* , from their centerline values, of up to 10% and 5%, respectively.

No boundary-layer trip was used, as it was presumed that the prevailing high Reynolds number would ensure fully turbulent boundary-layer flow a short distance downstream of the throat.

Instrumentation and Measurements

The test wall was provided with 48 static holes of 1.04 mm diam. They covered the test surface in the range $x = 0$ to $x = 0.4318$ m. Pitot probes of 0.419 mm outside diameter were used for the profile traverses. The probes emerged from the wall normally, and were curved to finish parallel with the surface; their end faces were ground square. These probes were also used as Preston tubes. Additional Preston-tube data were obtained using a pitot tube of 0.813 mm diam.

[†]A fuller description of this flow is given in AGARDograph 223.

^{*}Data on file prepared by M. W. Rubesin and C. C. Horstman, NASA-Ames Research Center, Moffett Field, CA 94035.

Pitot-tube displacement and shear corrections were applied.
 For details of temperature measurements, see Zwarts (1970).
 No turbulence measurements were made.

Benchmark Data

1. The free-stream flow conditions in this test case were as follows:

Free-stream Mach number	$M_\infty = 4.02$
Free-stream total temperature	$T_T = 295^\circ\text{K}$
Free-stream static temperature	$T_\infty = 69.57^\circ\text{K}$
Free-stream velocity	$V_\infty = 672.2 \text{ m/s}$
Free-stream static pressure	$p_\infty = 9.455 \times 10^3 \text{ N/m}^2$
Wall temperature	$T_w = 275^\circ\text{K}$

Starting values of boundary layer at $x = -0.635 \text{ cm}$:

Total thickness	$\delta_\infty = 1.088 \text{ cm}$
Displacement thickness	$\delta_\infty^* = 0.447 \text{ cm}$
Momentum thickness	$\theta_\infty = 0.056 \text{ cm}$

2. The data file contains values of:

- a) p_w , θ , C_f , H , U_e , and M_e as functions of x and y .
- b) profiles of U/U_e as functions of y at selected x -stations.

The x -coordinate is measured in the streamwise direction from an arbitrary location in the wind tunnel. The y -coordinate is normal to the test surface. The skin-friction coefficient C_f is defined with respect to properties external to the boundary layer

$$C_f = \tau_w / \frac{1}{2} \rho_\infty U_e^2$$

Uncertainty Limits

The uncertainties, estimated from the basic measurement uncertainty, are as follows:

$$p_w = \pm 2\%$$

$$C_f = \pm 10\%$$

$$U = \pm 3\%$$

$$H = \pm 5\%$$

Table 1
Free-Stream Test Conditions

Test Conditions	p_T (N/m ²)			
	31600	97070	302900	901500
T_T (°K)	278	278	278	278
M_∞	2.21	2.24	2.33	2.36
p_∞ (N/m ²)	2909	8528	23111	65638
T_∞ (K)	140.5	138.6	133.2	131.4
T_w (K)	278	278	278	278
ρ_∞ (kg/m ³)	0.0723	0.2149	0.6045	1.7399
U_∞ (m/s)	525.3	529.2	538.8	542.1
δ_c (cm)	4.0	4.0	4.0	4.0
δ_o^* (cm)	0.97	0.85	0.85	0.80
θ_o (cm)	0.26	0.23	0.23	0.21
$Re(x_o')$	11.7×10^6	35.3×10^6	105×10^6	314×10^6
$Re(\delta_o)$	0.16×10^6	0.49×10^6	1.44×10^6	4.32×10^6
$Re(\theta_o)$	1.04×10^4	2.82×10^4	8.28×10^4	22.7×10^4

REFERENCES

- Acharya, M., M. I. Kussoy, and C. C. Horstman (1978a). "Reynolds number and pressure gradient effects on compressible turbulent boundary layers," AIAA Paper #78-199.
- Acharya, M., M. I. Kussoy, and C. C. Horstman (1978b). "Reynolds number and pressure gradient effects on compressible turbulent boundary layers," AIAA Jou., 16, 1217.
- Acharya, M., C. C. Horstman, and M. I. Kussoy (1979). "Reynolds number effects on the turbulence field in compressible turbulent boundary layers," AIAA Paper 79-4044 (1978) and AIAA Jou., 17, 380.
- Fernholz, H. H., and P. J. Finley (1977). "A critical compilation of compressible turbulent boundary layer data," AGARDograph No. 223.
- Kussoy, M. I., C. C. Horstman, and M. Acharya (1978). "An experimental documentation of pressure gradient and Reynolds number effects on compressible turbulent boundary layers," NASA TM 78,488.
- Vas, I. E. (1971). "Flow field measurements using a total temperature probe at hypersonic speeds," AIAA Paper 71-273.
- Zwarts, F. J. (1970). "The compressible turbulent boundary layer in a pressure gradient," Thesis, McGill University, Montreal.

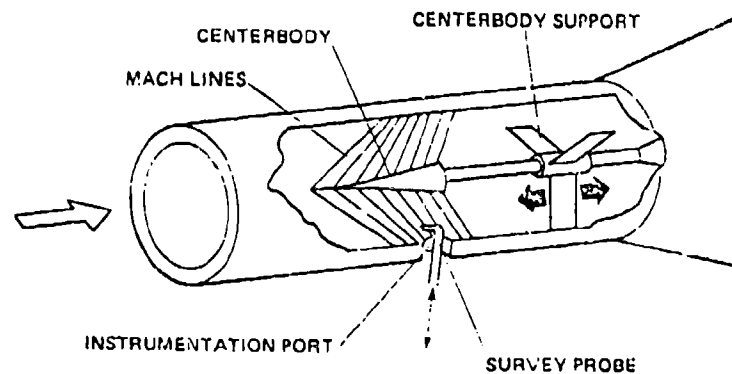


Figure 1. Test configuration for Case 8403.

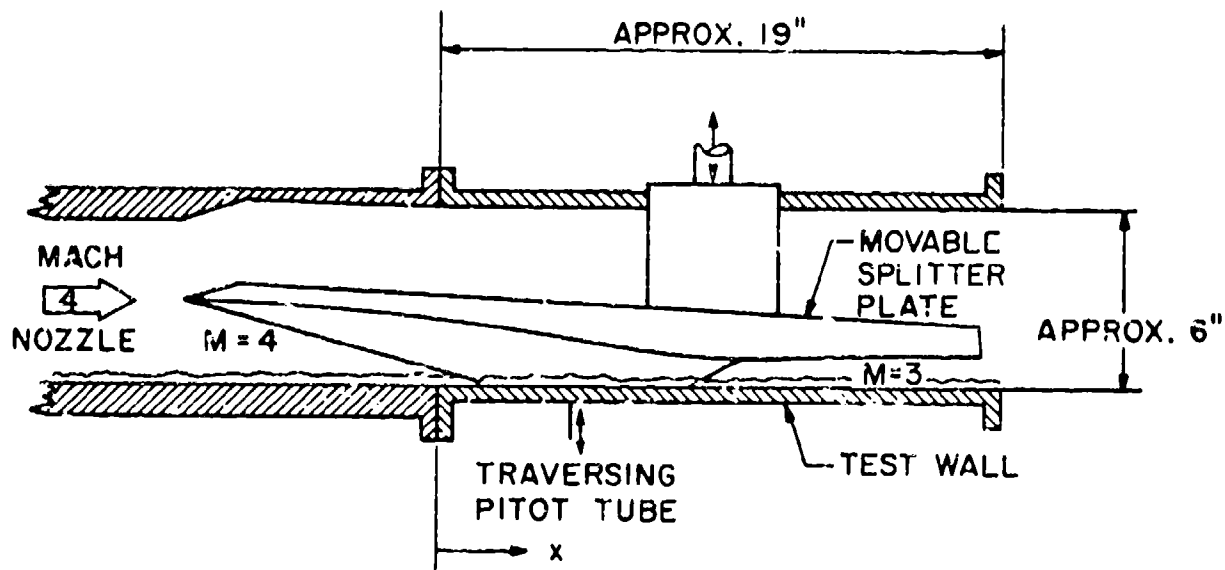


Figure 2. Schematic of apparatus for Case 8411.

DISCUSSION

Flows 8400 and 8410

1. The Conference stated that high values of the adverse-pressure-gradient parameter H_0 and the large number of measurement stations were the principal, appropriate criteria in selection of test cases in this class of compressible flows.
2. The Conference agreed that Case 8401 should be excluded from the test cases because of its questionable starting profile.
3. Concerning Case 8403, the Conference observed that, at downstream profiles, the law of the wall, based on measured skin friction, falls lower than that of Coles, for the higher pressure gradient cases.

SPECIFICATIONS FOR COMPUTATION

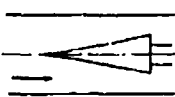
SIMPLE CASE/COMPRESSIBLE

Case #8403; Data Evaluators: M. Rubesin, C. Horstman

Data Takers: M. Kussoy, C. Horstman, M. Acharya

PICTORIAL SUMMARY

Flow 8/00. Data Evaluators: M. Rubesin and C. Horstman. "Boundary Layers in an Adverse Pressure Gradient in an Axisymmetric Internal Flow."

Case Data Taker	Test Rig Geometry	dp/dx or C _p	Number of Stations Measured										C _f	Re	M _∞	Other Notes
			Mean Velocity		Turbulence Profiles											
			U	V or W	$\overline{u^2}$	$\overline{v^2}$	$\overline{w^2}$	\overline{uv}	Others							
Case 8403 M. Kussoy C. Horstman M. Acharya		> 0	8	-	8	8	8	8	8	8	8	1.6 x 10 ⁶ to 4.22 x 10 ⁶ (based on d _g)	2.3	Axisymmetric. Profile data for 4 pres- sure gradients. Skin friction data for 6 pres- sure gradients, each at 4 Reynolds numbers.		

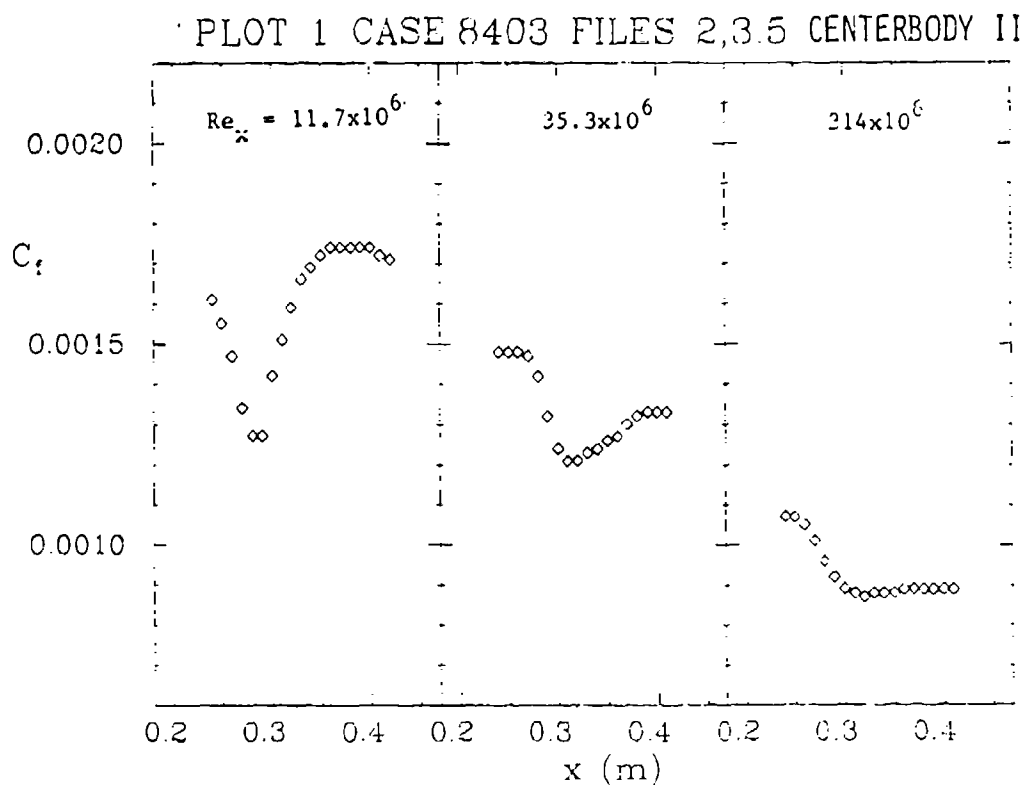
Plot	Ordinate	Abcissa	Range/Position	Comments
1	C _f	x	0.20 ≤ x ≤ 0.40 m 0.0005 ≤ C _f ≤ 0.002	Three curves for centerbody II at Re _x = 11.7, 35.3, and 314 × 10 ⁶ .
2	C _f	x	0.20 ≤ x ≤ 0.40 m 0.0005 ≤ C _f ≤ 0.002	Three curves for centerbody IV at Re _x = 11.7, 35.3, and 314 × 10 ⁶ .
3	C _f	x	0.20 ≤ x ≤ 0.40 m 0.0005 ≤ C _f ≤ 0.002	Three curves for centerbody VI at Re _x = 11.7, 35.3, and 314 × 10 ⁶ .
4	H	x	0.20 ≤ x ≤ 0.40 m 1 ≤ H ≤ 5	One curve for centerbody II at Re _x = 35.3 × 10 ⁶ .
5	H	x	0.20 ≤ x ≤ 0.40 m 1 ≤ H ≤ 5	One curve for centerbody IV at Re _x = 35.3 × 10 ⁶ .
6	y	U/U _∞	0 ≤ y ≤ 0.04 m 0 ≤ U/U _∞ ≤ 1	Three curves for centerbody II at x = 0.1775, 0.3175 and 0.3975 m.
7	y	√K/U _∞	0 ≤ y ≤ 0.04 m 0 ≤ √K/U _∞ ≤ 0.1	Three curves for centerbody II at x = 0.1775, 0.3175 and 0.3975 m.
8	y	τ/ρ _∞ U _∞ ²	0 ≤ y ≤ 0.04 m 0 ≤ τ/ρ _∞ U _∞ ² ≤ 0.0015	Three curves for centerbody II at x = 0.1775, 0.3175 and 0.3975 m.
9	y	U/U _∞	0 ≤ y ≤ 0.04 m 0 ≤ U/U _∞ ≤ 0.1	Three curves for centerbody IV at x = 0.144, 0.324 and 0.384 m.

Plot	Ordinate	Abscissa	Range/Position	Comments
10	y	\sqrt{K}/U_∞	$0 \leq y \leq 0.04 \text{ m}$ $0 \leq \sqrt{K}/U_\infty \leq 0.1$	Three curves for centerbody IV at $x = 0.144, 0.324$ and 0.384 m .
11	y	$\tau/\rho_\infty U_\infty^2$	$0 \leq y \leq 0.04 \text{ m}$ $0 \leq \tau/\rho_\infty U_\infty^2 \leq 0.015$	Three curves for centerbody IV at $x = 0.144, 0.324$ and 0.384 m .

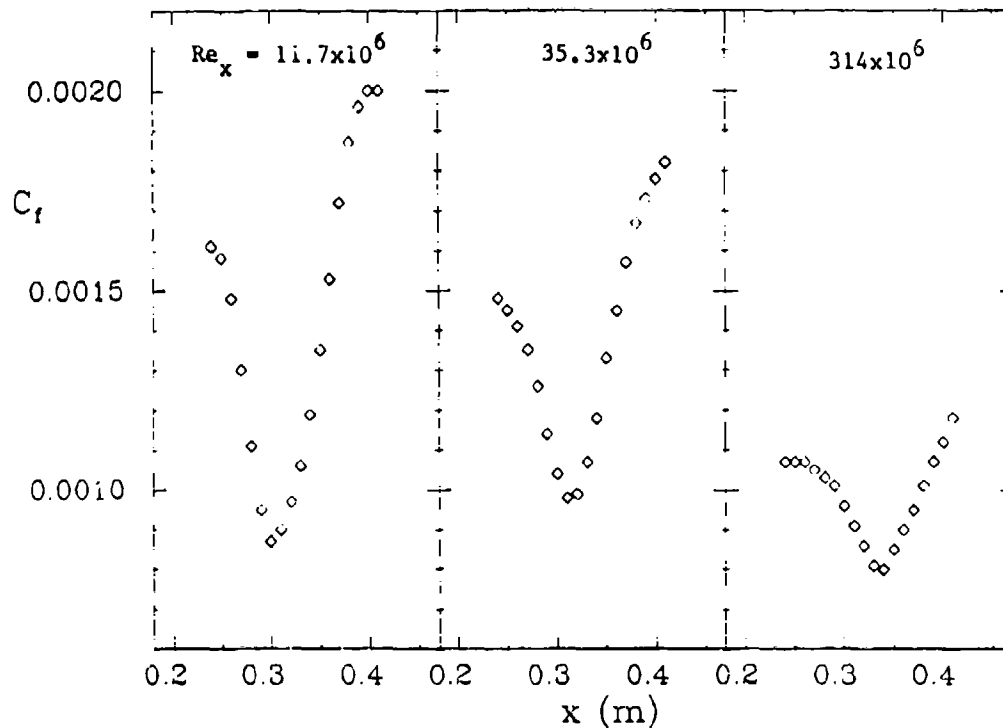
Special Instructions:

$$C_f = \tau_w / \left(\frac{1}{2} \rho_\infty U_\infty^2 \right).$$

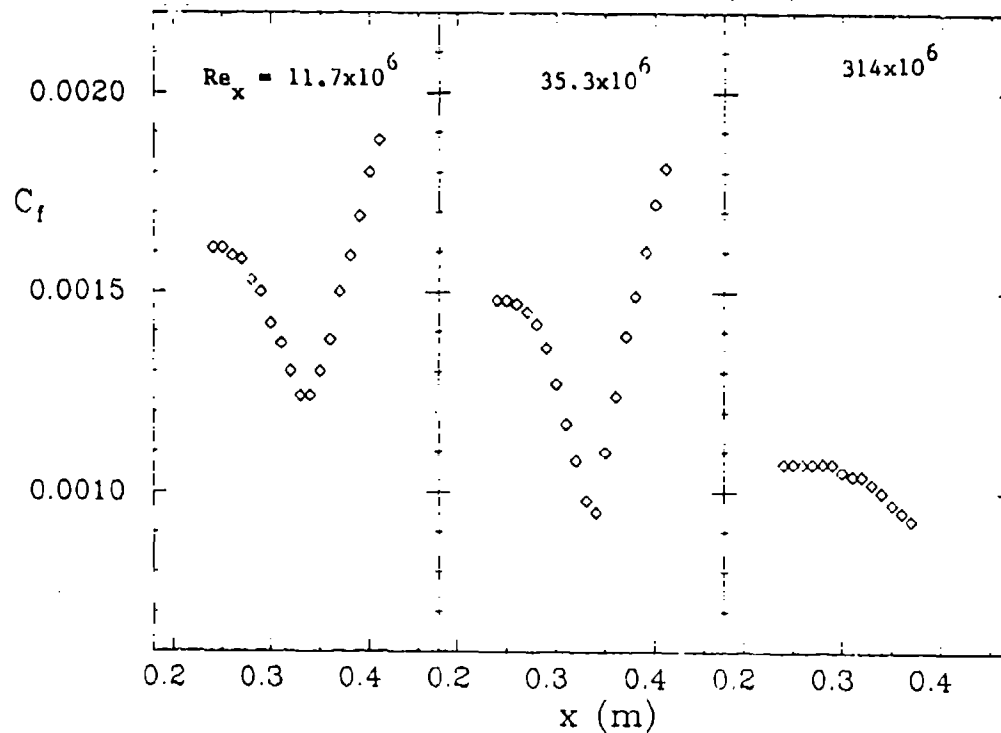
This test case considers a series of axisymmetric adverse pressure gradients at several different Reynolds numbers. The upstream conditions are prescribed at $x = 0 \text{ cm}$. Boundary-layer edge conditions are calculated using isentropic relations from the prescribed wall-pressure distribution. $()_\infty$ is defined in Table 1 above.



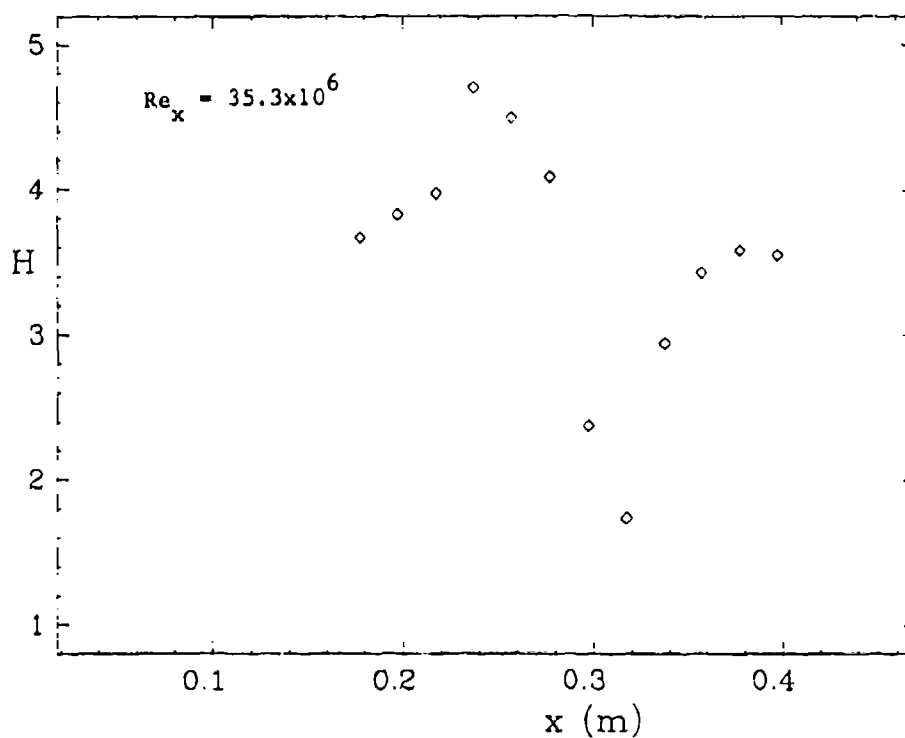
PLOT 2 CASE 8403 FILES 6,7,9 CENTERBODY IV



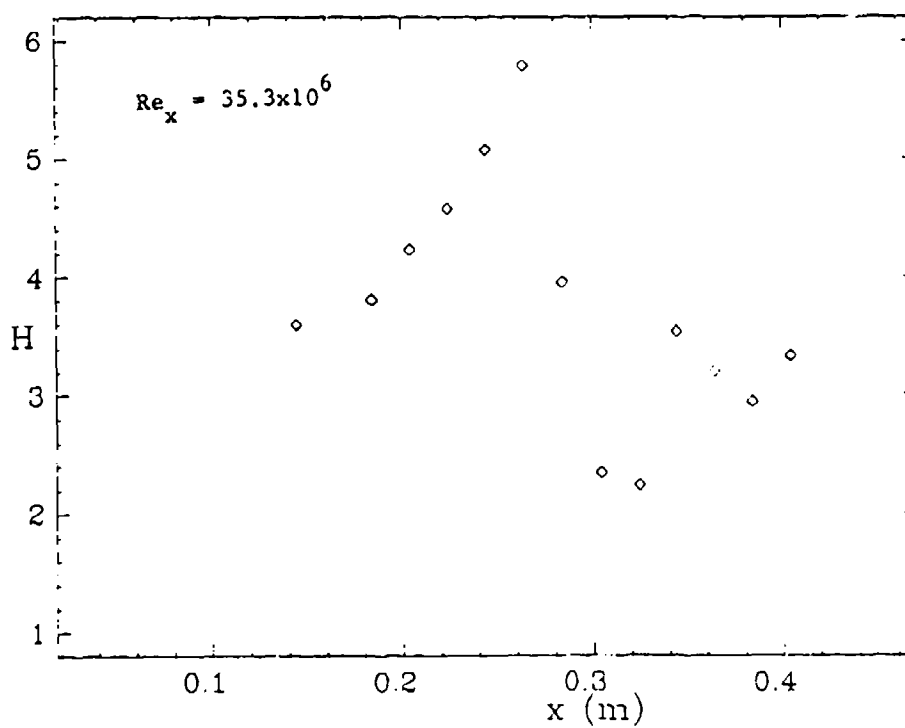
PLOT 3 CASE 8403 FILES 10,11,13 CENTERBODY IV



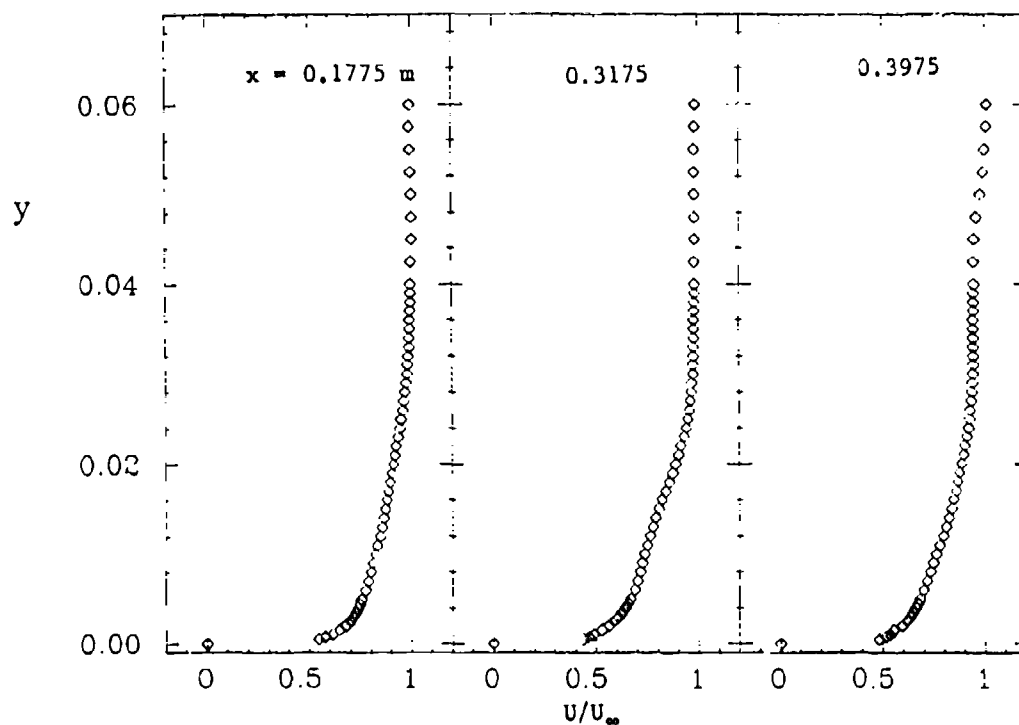
PLOT 4 CASE 8403 FILE 14 CENTERBODY II



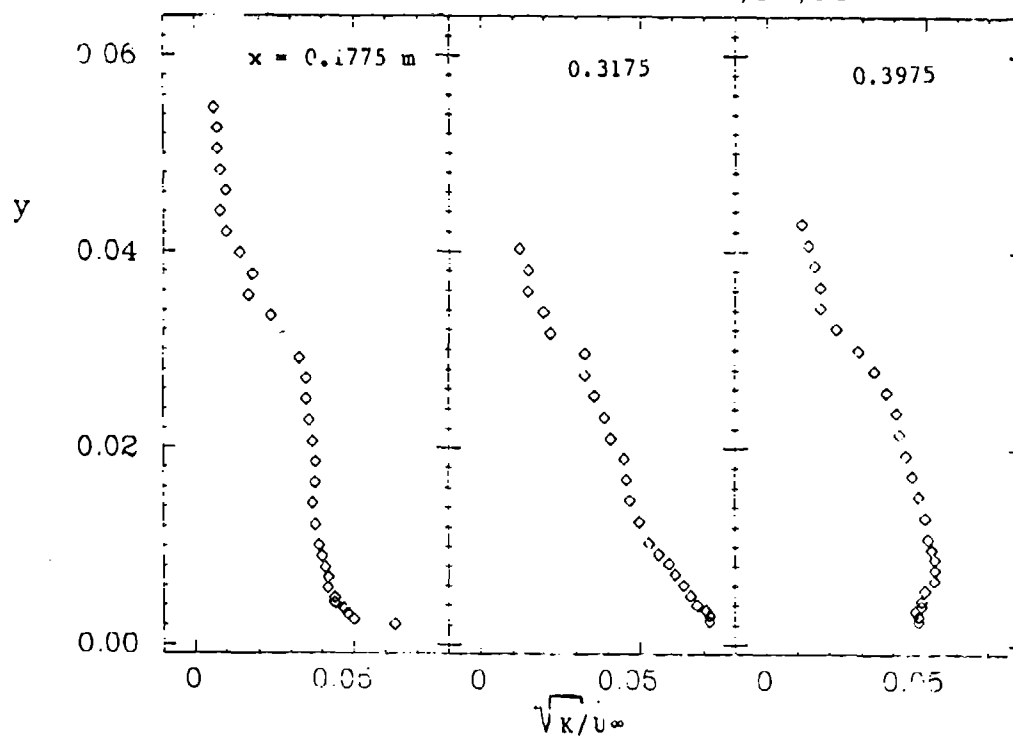
PLOT 5 CASE 8403 FILE 15 CENTERBODY VI



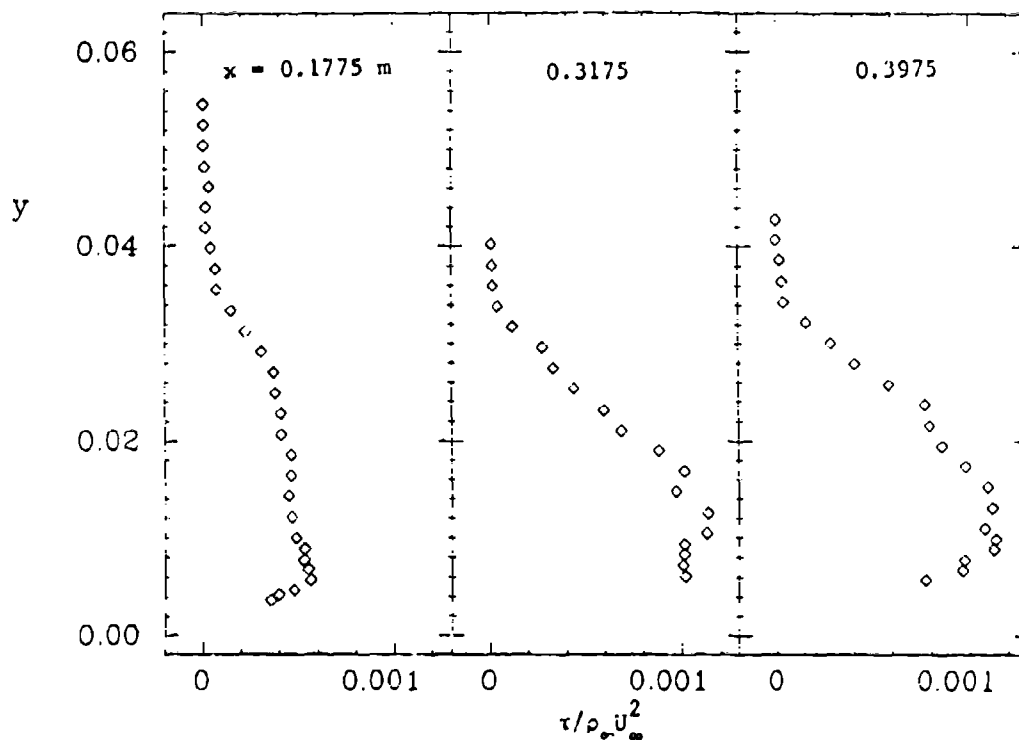
PLOT 6 CASE 8403 FILES 17,21,23 CENTERBODY II



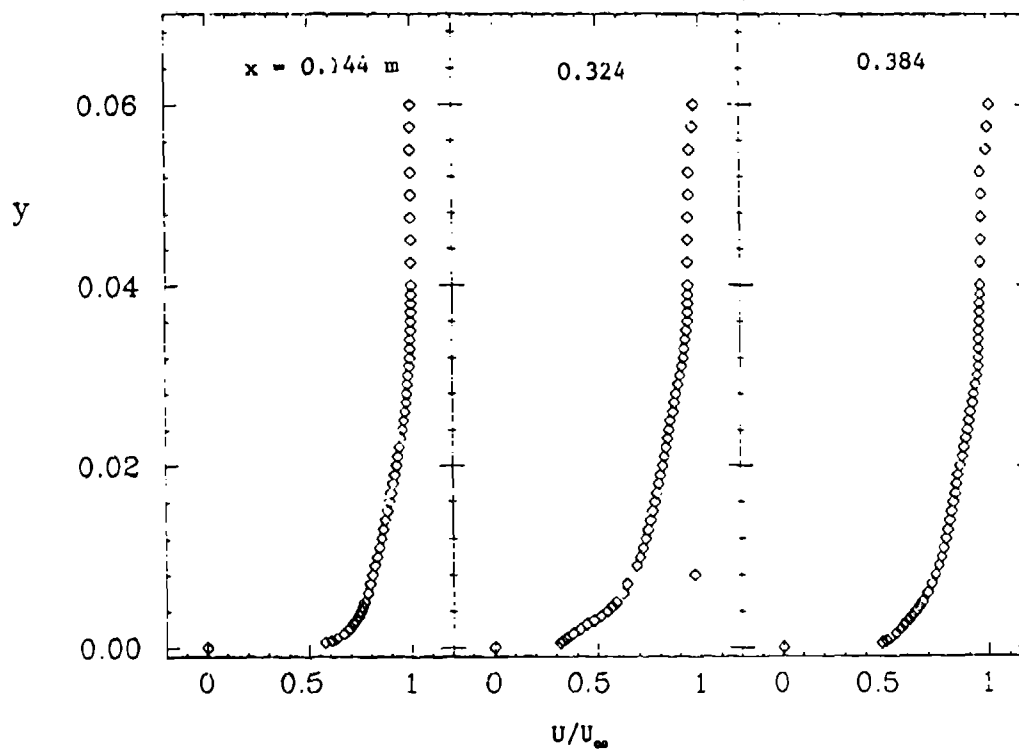
PLOT 7 CASE 8403 FILES 33,37,39 CENTERBODY II



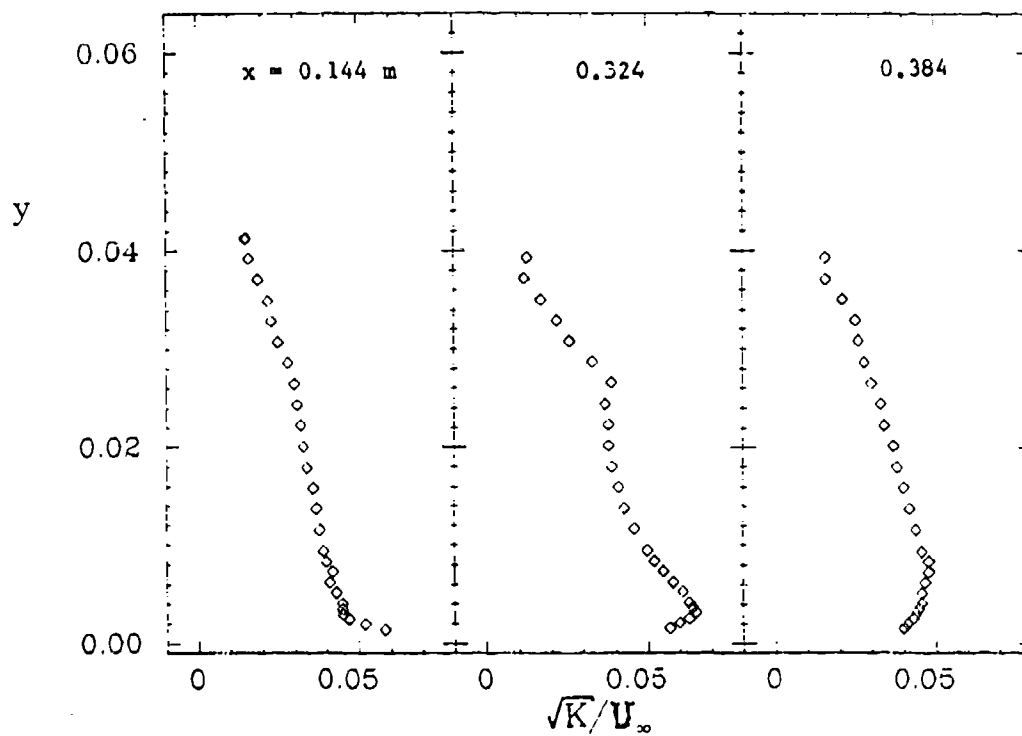
PLOT 8 CASE 8403 FILES 33,37,39 CENTERBODY II



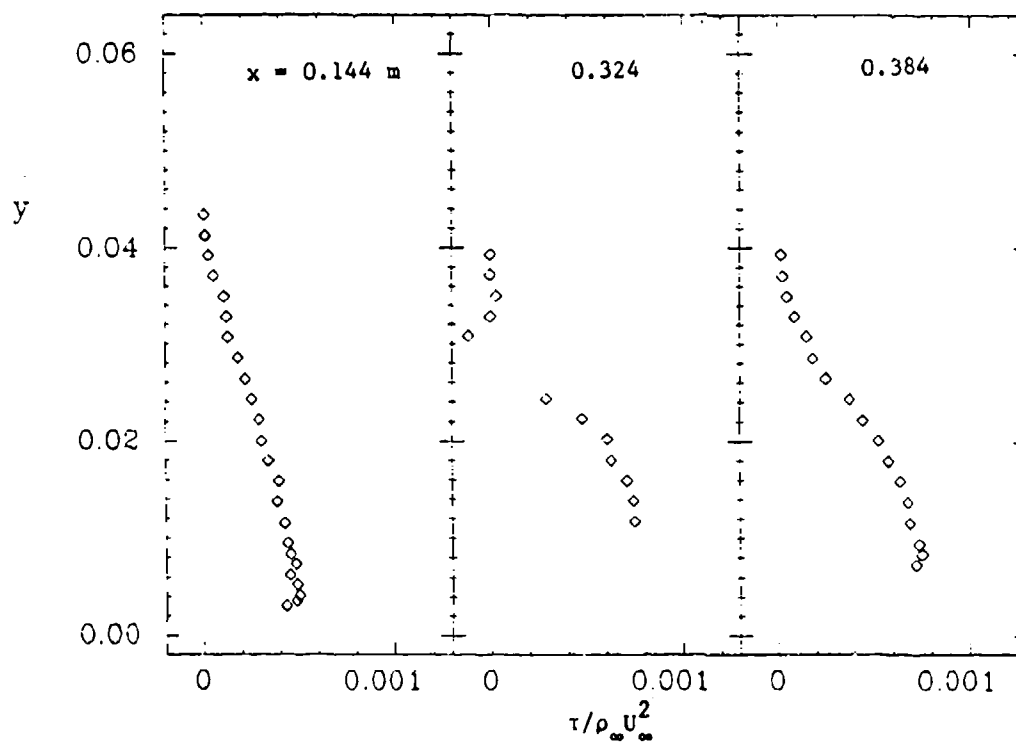
PLOT 9 CASE 8403 FILES 24,28,30 CENTERBODY IV



PLOT 10 CASE 8403 FILES 40,44,46 CENTERBODY IV



PLOT 11 CASE 8403 FILES 40,44,46 CENTERBODY IV



SPECIFICATIONS FOR COMPUTATION


SIMPLE CASE/COMPRESSIBLE

Case #8411; Data Evaluators: M. Rubesin and C. Horstman

Data Taker: F. J. Zwarts

PICTORIAL SUMMARY

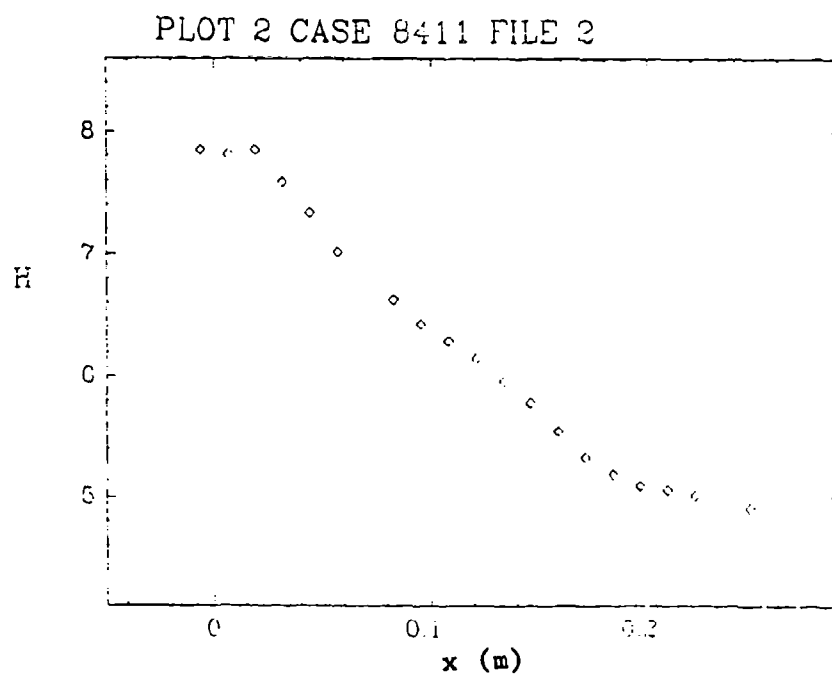
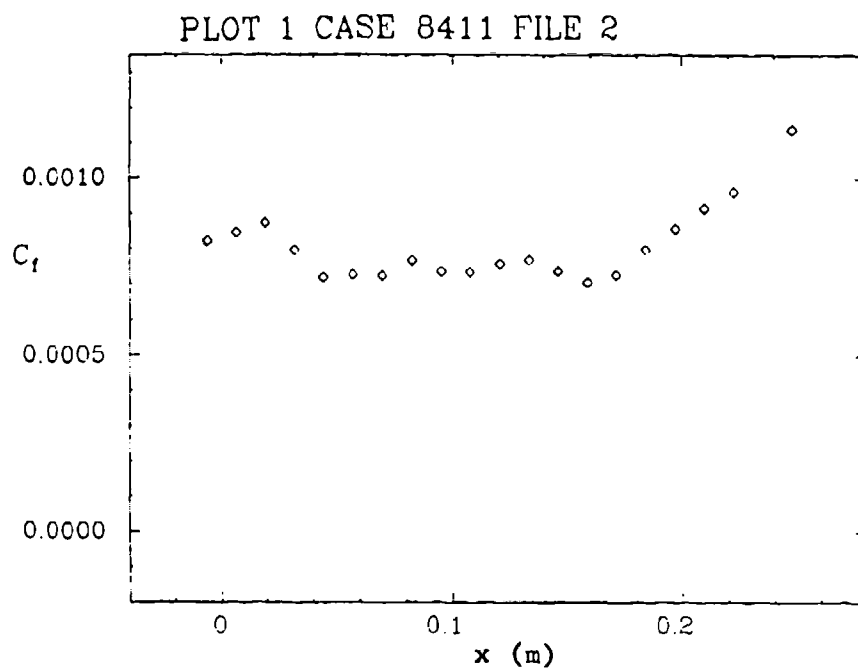
Flow 8410. Data Evaluators: M. Rubesin and C. Horstman. "Boundary Layer in an Adverse Pressure Gradient in 2-Dimensional Flow."

Case Data Taker	Test Rig Geometry	dp/dx or C _p	Number of Stations Measured							C _f	Re	M _∞	Other Notes
			Mean Velocity		Turbulence Profiles								
			U	V or W	$\overline{u^2}$	$\overline{v^2}$	$\overline{w^2}$	\overline{uv}	Others				
Case 8411 F. Zwarts		> 0	6	-	-	-	-	-	-	Pres- ton probe	3.5 x 10 ⁴ (based on S ₀)	4	

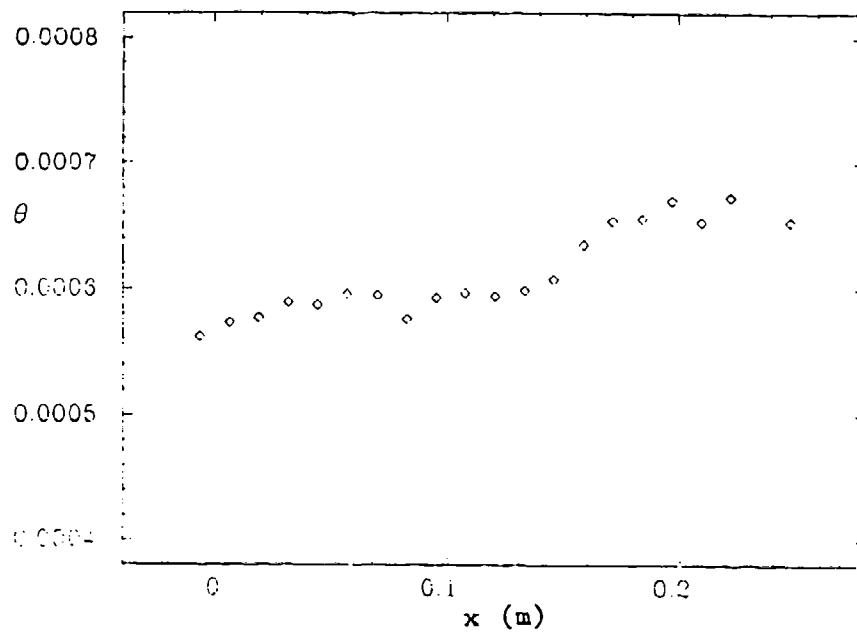
Plot	Ordinate	Abscissa	Range/Position	Comments
1	C _f	x	-0.02 ≤ x ≤ 0.20 m	
2	H	x	-0.02 ≤ x ≤ 0.20 m	
3	θ	x	-0.02 ≤ x ≤ 0.20 m	
4	y	U/U _e	0 ≤ U/U _e ≤ 1.0	At x = 0.01905, 0.09525 and 0.19683 m.

Special Instructions:

This test case considers a two-dimensional adverse pressure gradient. The upstream conditions are prescribed at $x = -0.635$ cm. Boundary-layer edge conditions are calculated using isentropic relations from the prescribed wall-pressure distribution.



PLOT 3 CASE 8411 FILE 2

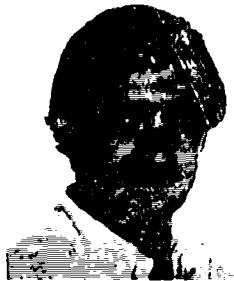


SESSION VIII

Chairman: J. L. Lunley

Technical Recorders:

S. Pronchick
H. Nagib



Flow 0370

Flow 0260

HOMOGENEOUS TURBULENT FLOWS

Flow 0370

Cases 0371, 0372, 0373, 0374, 0375, 0376

Evaluator: J. H. Ferziger*



SUMMARY

In the companion paper (Ferziger, 1980) homogeneous turbulent flows were divided into three classes containing a total of six cases. These are as follows:

1. Flows with dissipation only
Case 0371: Homogeneous isotropic turbulence
2. Flows with redistribution and dissipation
Case 0372: Homogeneous turbulence with rotation
Case 0373: Return to isotropy after straining
3. Flows with production, redistribution, and dissipation
 - a. Strained turbulence
Case 0374: Plane strain
Case 0375: Axisymmetric strain
 - b. Case 0376: Sheared turbulence

CRITERIA FOR SELECTION

This summary contains recommendations concerning which data are considered sufficiently reliable and accurate to be used as the targets for computational modeling. The criteria for acceptability are: (1) the data from different experiments agree; (2) the data be in at least rough agreement with generally accepted theory (as differentiated from modeling); (3) the effects reported extend beyond the uncertainty of the data. Except for Case 0371, the data do not meet all of these criteria, and the recommendations are therefore made with reservations.

These flows are amenable to accurate simulation without modeling at low Reynolds number. The results of such computations were not reviewed in Ferziger (1980) and will not be presented here. In the opinion of the author, computations of this type (precise modeling) should be considered as complementing the experimental results, and should be used in the future as a check on modeling.

All of the flows are to be regarded as homogeneous flows for purposes of computation. They are to be simulated from time $t = 0$ to the final time given with the data. In all cases, the initial values of the components of the Reynolds stress have been provided along with any other data about the flow needed to carry out the

*Mech. Eng. Dept., Stanford University, Stanford, CA 94305.

simulation. In order that all computers start with the same initial conditions, we have further provided an estimate of the dissipation at the initial time. These were found by the present author by curve-fitting the data and differentiating the result. The values for dissipation must be regarded as having an uncertainty on the order of $\pm 20\%$. It is recommended that the computers use the values provided; if any adjustments are made, they should be clearly stated in the entry papers.

CASE 0371. HOMOGENEOUS ISOTROPIC TURBULENCE

This is one of the best-documented flows in the turbulence literature. It is well established that, at least at Reynolds numbers based on Taylor microscale greater than 20, the turbulent kinetic energy decays according to the power law:

$$q^2 \sim (t - t_0)^{-n}$$

The exponent is well established as 1.25 ± 0.06 ; the effective origin varies somewhat. The Comte-Bellot/Corrsin (1966) case is representative of the better data on this flow and is recommended as Case 0371. The specifications are given in Table 1 below.

— In this flow (and some of the following ones) we have assumed $v^2 = w^2$ although w^2 was not measured. Note that Cases 0372A, 0375A, and 0375C are also essentially decaying homogeneous isotropic turbulence.

CASE 0372. ROTATING HOMOGENEOUS TURBULENCE

The data for this flow (and those below) are not as well established as those for the case of decaying turbulence presented above, and more caution is needed. For this flow, the best data are those of Wigeland and Nagib (1978). As we have pointed out in the companion paper, these data contain anisotropy in both intensities and length scales. The Wigeland-Nagib case which appears to be most free of difficulties has been selected as a test case. The calculations should be done at the three different rotation rates given in Table 1.

CASE 0373. RETURN TO ISOTROPY

There are only two examples of this flow available--those of Uberoi (1956) and Tucker and Reynolds (1968). Both sets of data appear reasonable, but they are sufficiently different that they are hard to compare. The specifications for these flows (which are the conditions at the end of the contraction) are given in the table.

CASE 0374. TURBULENCE UNDERGOING PLANE STRAIN

There are two types of strain data in the literature: plane strain and axisymmetric strain. They are treated separately. The results of two experiments on the effect of plane strain on turbulence are recommended--those of Townsend (1956) and

Tucker and Reynolds (1968). It is suggested that both flows be computed. The initial data and strain rates are given in Table 1.

CASE 0375. TURBULENCE UNDERGOING AXISYMMETRIC STRAIN

The best data on axisymmetric strain are those of Tan-atichat (1980). This work contains a number of cases of which two have been selected as displaying the desired effects without inconsistency. The strain rate is not constant in these flows, and additional data needed are given in Table 2.

CASE 0376. SHEARED TURBULENCE

Of the experiments on sheared homogeneous turbulence, the one by Champagne et al. (1970) seems to provide the best data for low shear rate and that of Harris et al. (1977) provides the only data for large shear rate.

REFERENCES

- Champagne, F. H., V. G. Harris, and S. Corrsin (1970). "Experiments on nearly homogeneous turbulent shear flow," J. Fluid Mech., 41, 81.
- Comte-Bellot, G., and S. Corrsin (1966). "The use of a contraction to improve the isotropy of grid-generated turbulence," J. Fluid Mech., 25, 657.
- Ferziger, J. H. (1980). "Homogeneous turbulent flows: a review and evaluation," Report for the 1980-81 AFOSR-HTTM-Stanford Conference on Complex Turbulent Flows.
- Harris, V. G., J. A. H. Graham, and S. Corrsin (1977). "Further experiments in nearly homogeneous turbulent shear flow," J. Fluid Mech., 81, 657.
- Tan-atichat, J. (1980). "Effects of axisymmetric contractions on turbulence of various scales," Ph.D. Thesis, Illinois Institute of Technology. See also: Tan-atichat, J., H. M. Nagib, and R. E. Drabka, "Effects of axisymmetric contractions on turbulence of various scales," NASA CR 165136, 1980.
- Townsend, A. A. (1956). "The uniform distortion of homogeneous turbulence," Q. J. Mech. Appl. Math., 7, 104.
- Tucker, H. J., and A. J. Reynolds (1968). "The distortion of turbulence by irrotational plane strain," J. Fluid Mech., 32, 657.
- Uberoi, M. S. (1956). "Effect of wind tunnel contraction on free stream turbulence," J. Aero. Sci., 734.
- Wigeland, R. A., and H. M. Nagib (1978). "Grid-generated turbulence with and without rotation about the streamwise direction," Fluids and Heat Transfer Report R78-1, Illinois Inst. of Tech., Chicago, IL.

Table 1

Specifications - Homogeneous Turbulent Flow 0370, Cases 0371, 0372, 0373, 0374, 0375, 0376

Note: Take all flows to be homogeneous. Compute $\overline{u^2}$, $\overline{v^2}$, and $\overline{w^2}$ from the initial time (assumed $t = 0$) until the final time specified. All intensities are in units of m^2/sec^2 ; the dissipation is in units of m^2/sec^3 , and the final time in seconds. Plot requested quantities vs time for $0 < t < t_f$. See the notes below and the text for other details.

Case Title	Case No.	File	Variables Plotted	Initial Conditions ($t = 0$)				Final Time, t_f secs.	Other data ^{2*}
				$\overline{u^2}$	$\overline{v^2}$	$\overline{w^2}$	ϵ^1		
Isotropic turbulence ³ Comte-Bellot & Corraïn 0371	2		q^2	0.306	0.254	0.254	15.52	0.35	---
Rotating turbulence ³ Wigeland & Nagib	3	0372A	q^2	7.34×10^{-2}	5.12×10^{-2}	5.12×10^{-2}	23.55	0.048	(Screen 5, 9 m/s) $\Omega = 0 \text{ sec}^{-1}$
	4	0372B	$q^2, u/v$	7.25×10^{-2}	5.25×10^{-2}	5.25×10^{-2}	21.19	0.047	$\Omega = 20 \text{ sec}^{-1}$
	5	0372C	$q^2, u/v$	7.99×10^{-2}	6.02×10^{-2}	6.02×10^{-2}	23.45	0.046	$\Omega = 80 \text{ sec}^{-1}$
Return to isotropy Uberoi	6	0373A	u^2, v^2	1.99×10^{-4}	1.54×10^{-3}	1.54×10^{-3}	33.62×10^{-4}	0.21	(CR=4, Re=3710)
	7	0373B	u^2, v^2	3.69×10^{-4}	3.31×10^{-3}	3.31×10^{-3}	15.04×10^{-3}	0.048	(CR=9, Re=3710)
	8	0373C	u^2, v^2	1.35×10^{-3}	9.26×10^{-2}	9.26×10^{-2}	9.06×10^{-2}	0.024	(CR=4, Re=6,500)
	9	0373D	u^2, v^2	3.12×10^{-3}	2.43×10^{-2}	2.43×10^{-2}	17.11×10^{-2}	0.074	(CR=4, Re=12,300)
Tucker & Reynolds	10	0373E	u^2, v^2, w^2	1.29×10^{-2}	1.79×10^{-2}	4.2×10^{-3}	1.89×10^{-2}	0.16	
Plane strain Townsend	11	0374A	u^2, v^2, w^2	2.44×10^{-2}	2.66×10^{-2}	2.20×10^{-2}	0.59	0.16	Strain rate $-\partial v/\partial y = \partial w/\partial z$ $= 9.4 \text{ sec}^{-1}$
Tucker & Reynolds ⁴	12	0374B	u^2, v^2, w^2	4.02×10^{-2}	3.07×10^{-2}	2.68×10^{-2}	0.63	0.396	$-\partial v/\partial y = \partial w/\partial z$ $= 4.45 \text{ sec}^{-1}$

Table 1 cont.

Table 1 (cont.)

Case Title	Case No.	File	Variables Plotted	Initial Conditions ($t = 0$)			Final Time, t_f secs.	Other data ^{2*}
				$\overline{u^2}$	$\overline{v^2}$	$\overline{w^2}$		
Axisymmetric strain Tan-atichat ⁵	0375A	13	u^2, v^2	3.75×10^{-3}	2.51×10^{-3}	2.51×10^{-3}	0.037	(CR = 1)
	0375B	14	u^2, v^2	3.53×10^{-3}	2.46×10^{-3}	2.46×10^{-3}	0.039	(CR = 9)
	0375C	15	u^2, v^2	2.95×10^{-3}	2.12×10^{-3}	2.12×10^{-3}	0.022	(CR = 1)
	0375D	16	u^2, v^2	2.58×10^{-3}	2.16×10^{-3}	2.16×10^{-3}	0.024	(CR = 9)
	0375E	17	u^2, v^2	1.90×10^{-3}	1.72×10^{-3}	1.72×10^{-3}	0.016	(CR = 16)
Shear								
Champagne et al.	0376A	18	u^2, v^2, w^2, uv	6.29×10^{-2}	5.51×10^{-2}	4.98×10^{-2}	1.08	$\overline{uv}(0) = -1.54 \times 10^{-4}$ $\partial U / \partial y = 12.9 \text{ sec}^{-1}$
	0376B	19	u^2, v^2, w^2, uv	1.87×10^{-1}	7.50×10^{-2}	9.32×10^{-2}	1.61	$\overline{uv}(0) = -5.74 \times 10^{-2}$ $\partial U / \partial y = 4.8 \text{ sec}^{-1}$

*CR = contraction ratio; Ω = angular velocity, rads/sec.

** See Note 5 below.

¹For a discussion of the values of the dissipation, see the text.²Data in parentheses are for identification purposes and are not needed in the calculation.³Some computers may wish to treat these flows as isotropic.⁴The axis nomenclature has been changed from that of the original author to reduce possible confusion.⁵For additional data including the velocity history of these flows, see Table 2.

Table 2
Some Additional Data for Flow 0375

<u>Case 0375B</u>			
<u>x (cm)</u>	<u>U (m/s)</u>	<u>t (sec)</u>	<u>dU/dx (sec⁻¹)</u>
0	2.59	0.0000	9.6
3	3.07	0.0107	24.8
6	4.26	0.0192	58.4
9	6.99	0.0248	135
12	12.81	0.0281	238
14	17.25	0.0294	183
16	19.61	0.0305	56.5
18	20.60	0.0315	0.0

<u>Case 0375D</u>			
<u>x (cm)</u>	<u>U (m/s)</u>	<u>t (sec)</u>	<u>dU/dx (sec⁻¹)</u>
0	2.04	0.0000	7.6
3	2.43	0.0136	19.5
6	3.36	0.0243	46.2
9	5.51	0.0314	104
12	9.88	0.0356	181
14	13.37	0.0373	146
16	15.22	0.0387	44.5
18	15.57	0.0400	0.0

<u>Case 0375E</u>			
<u>x (cm)</u>	<u>U (m/s)</u>	<u>t (sec)</u>	<u>dU/dx (sec⁻¹)</u>
0	1.73	0.0000	6.3
3	2.06	0.0161	19.1
6	2.96	0.0284	36.4
9	4.57	0.0368	102
12	12.04	0.0412	397
14	19.40	0.0425	308
16	23.73	0.0434	107
18	24.29	0.0443	0.0

DISCUSSION

Flow 0370


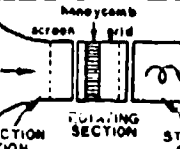
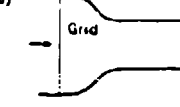

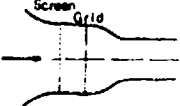

The Conference suggested that:

1. Estimates of the dissipation rate and/or the characteristic turbulence scales, based on the experimental results, should be included in the specifications of these various flow cases to eliminate variability in estimating these important parameters by computers.*
2. One case of the rotating homogeneous turbulence experiments of Wigeland and Nagib (Screen #5, $U_\infty = 6$ m/s) should be included as a test case.*
3. The experiment of Tucker and Reynolds should also be used as a test case for the return to isotropy.*
4. The experiment of Gence and Mathieu (J. Fluid Mech., 1979) should also be included as a test case for plane strain.
5. It is well accepted, based on experiments and theory, that the turbulence energy increases monotonically for the cases of strained and sheared homogeneous turbulence.
6. The value of the exponent n for the decay of turbulence energy in homogeneous turbulence, given by J. Ferziger, is intended to represent isotropic high Reynolds number grid-generated turbulence, which is void of the influence of turbulence upstream of the grid. As documented by Comte-Bellot and Corrsin, this exponent increases slightly with decreasing Reynolds number. In axisymmetric (i.e., non-isotropic) turbulence or in the presence of substantial upstream turbulence, this exponent is often smaller than the value given by Ferziger, e.g., see Wigeland and Nagib, or Tsuji (J. Phys. Soc. Japan, 10, 7 (1955), and 11, 10 (1956)).
7. The proposed numerical experiments at $R_\lambda < 80$ using exact calculations of homogeneous flows are highly recommended.

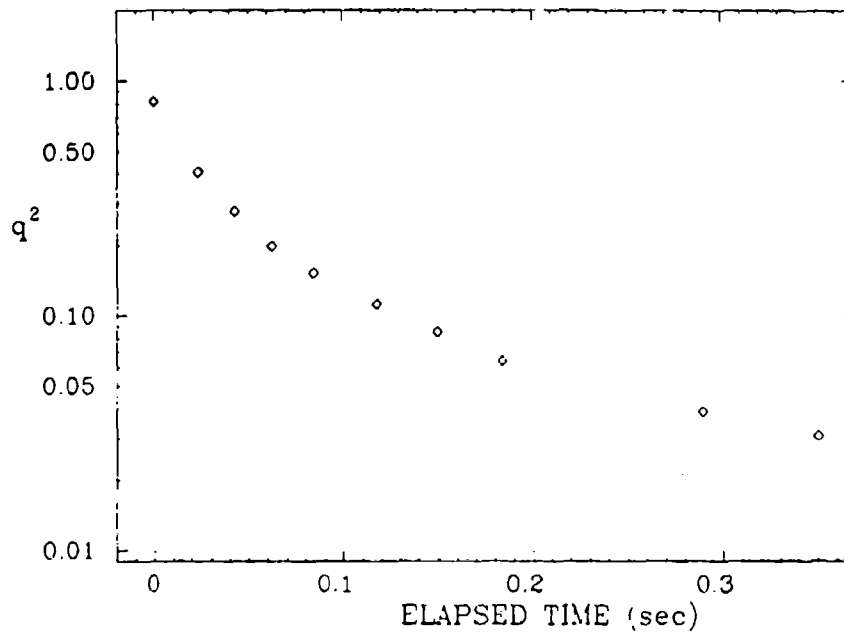
*[Ed.: This task has been done by J. H. Ferziger after the 1980 meeting and the results incorporated above.]

PICTORIAL SUMMARY

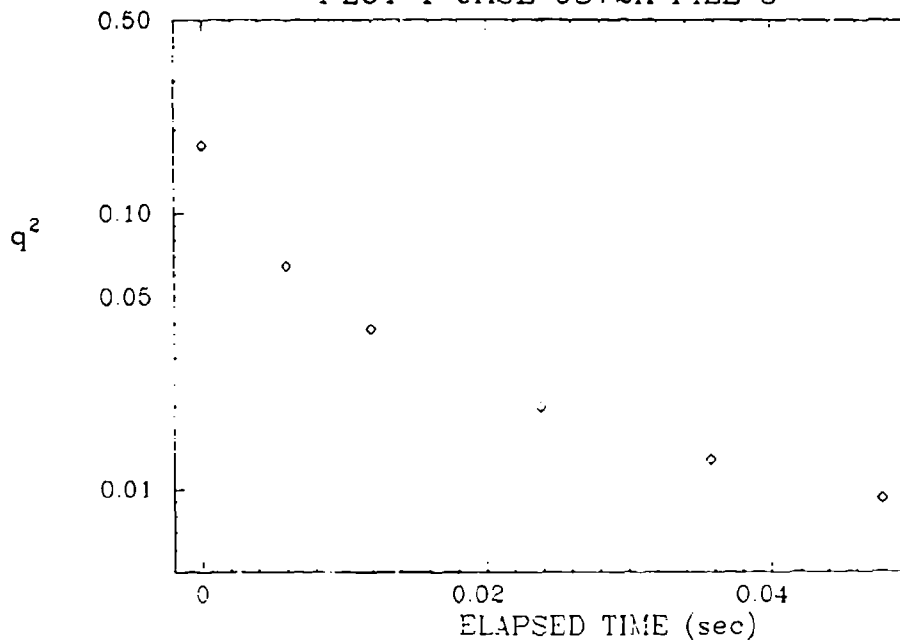
Flow 0370. Data Evaluator: J. Ferniger. "Homogeneous Turbulent Flows."

Case Data Taker	Test Rig Geometry	dp/dx or C_f	Number of Stations Measured								C_f	Re	Initial Condi- tion	Other Notes
			Mean Velocity		Turbulence Profiles									
			U	V or W	$\overline{u^2}$	$\overline{v^2}$	$\overline{w^2}$	\overline{uv}	Others					
Case 0371 G. Comte-Bellot S. Corrsin		zero	Yes	-	Yes	Yes	-	-	Auto- correla- tion Energy spectra	-	1600 3200 (based on M)	-	Homogeneous isotropic turbulence. Grid 3 cases	
Case 0372 H. Wigeland H. Magib (0372A,B,C)		-	Yes	-	Yes	Yes	-	-	-	-	-	-	Rotating homogeneous turbulence.	
Case 0373 M. Uberoi (0373a,b,c,d) H. Tucker A. Reynolds (0373e)		zero	Yes	-	Yes	Yes	-	-	Spectra of $\overline{u^2}$, $\overline{v^2}$	-	3710 (based on M)	-	Returns to isotropy. Contraction 3 cases.	
Case 0374 A. Townsend (0374a) H. Tucker A. Reynolds (0374b)		-	Yes	-	Yes	Yes	Yes	-	Longi- tudinal spec- tra	-	-	-	Plane strained homo- geneous turbulence.	
Case 0375 J. Yan-sichat (0375a,b,c,d,e)		-	Yes	-	Yes	Yes	-	Yes	Spectra cross- covari- ance	-	270 to 8100 (based on M)	-	Axisymmetric strained homogeneous turbulence. Grid 6 cases. Contraction 7 cases.	
Case 0376 F. Champagne V. Harris S. Corrsin (0376a) V. Harris J. Graham S. Corrsin (0376b)		zero	Yes	-	Yes	Yes	Yes	Yes	Auto- correla- tion	-	-	-	Sheared homogeneous turbulence.	

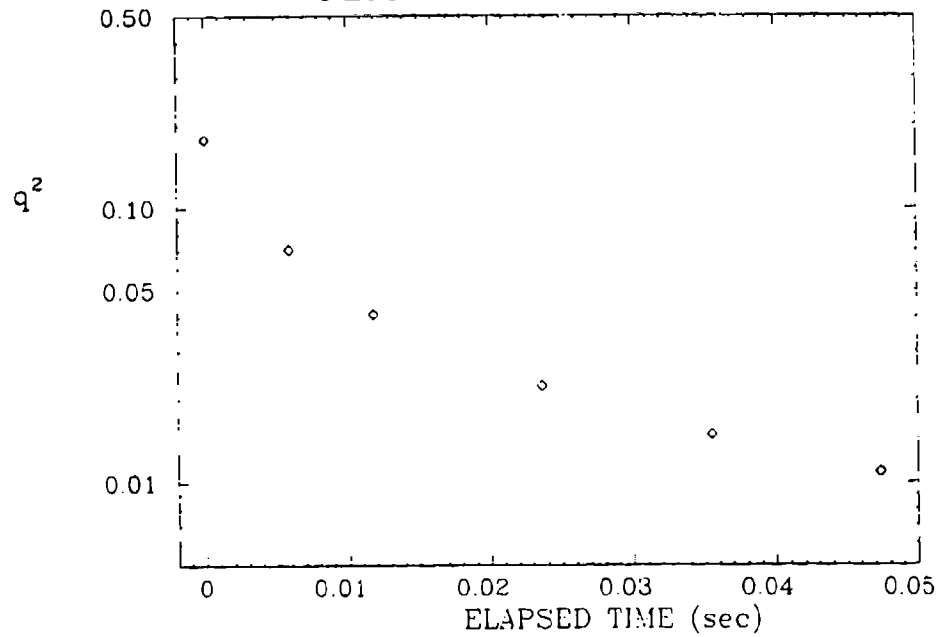
PLOT 1 CASE 0371 FILE 2



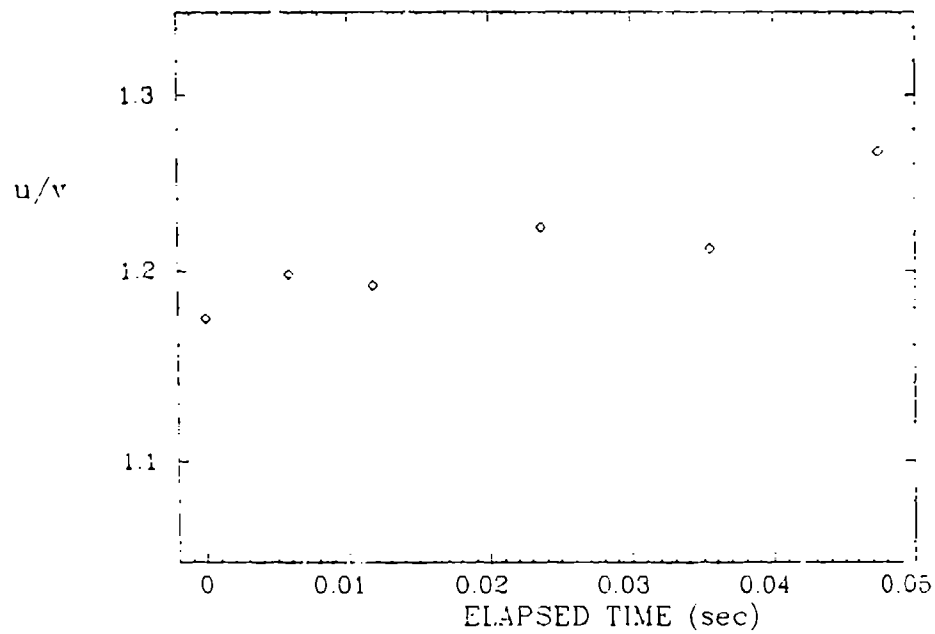
PLOT 1 CASE 0372A FILE 3

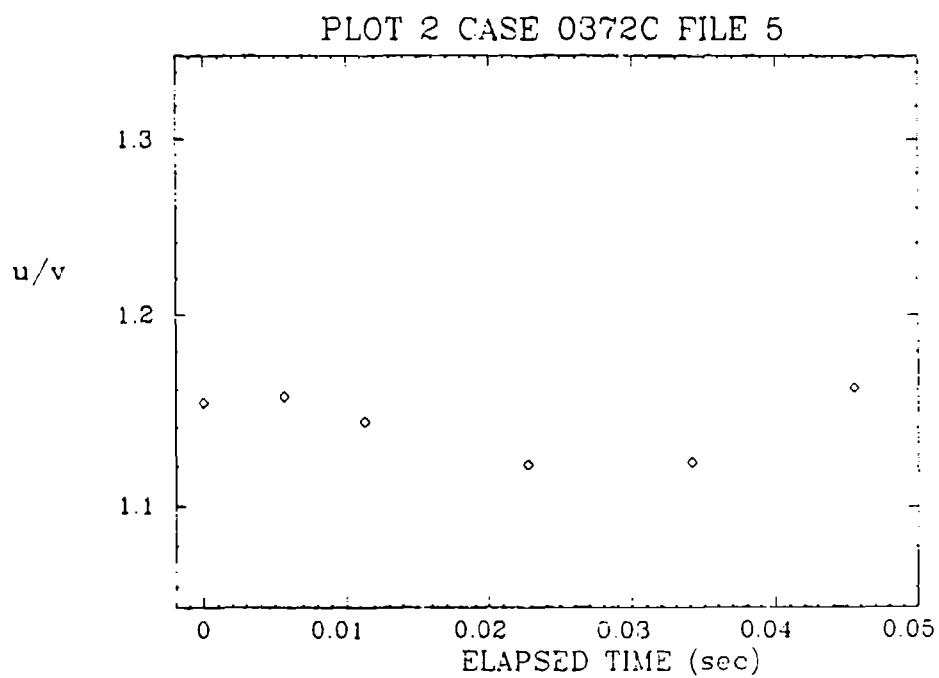
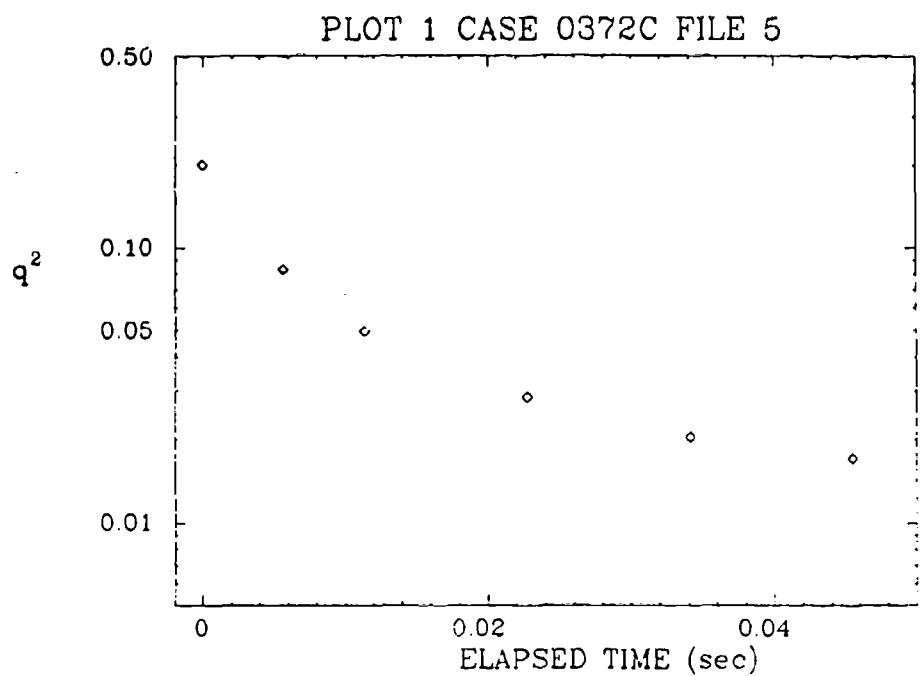


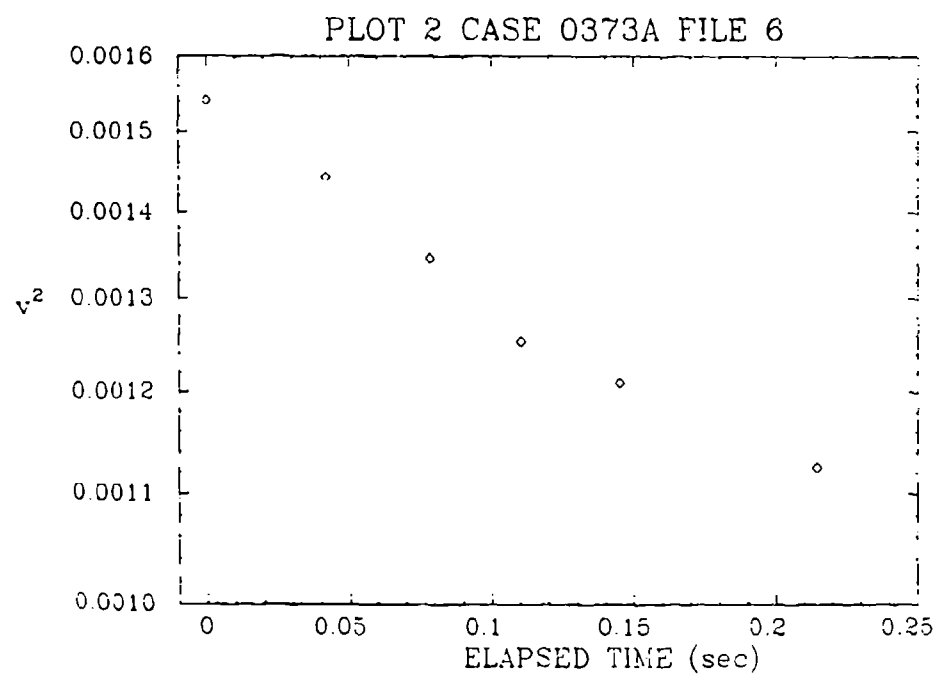
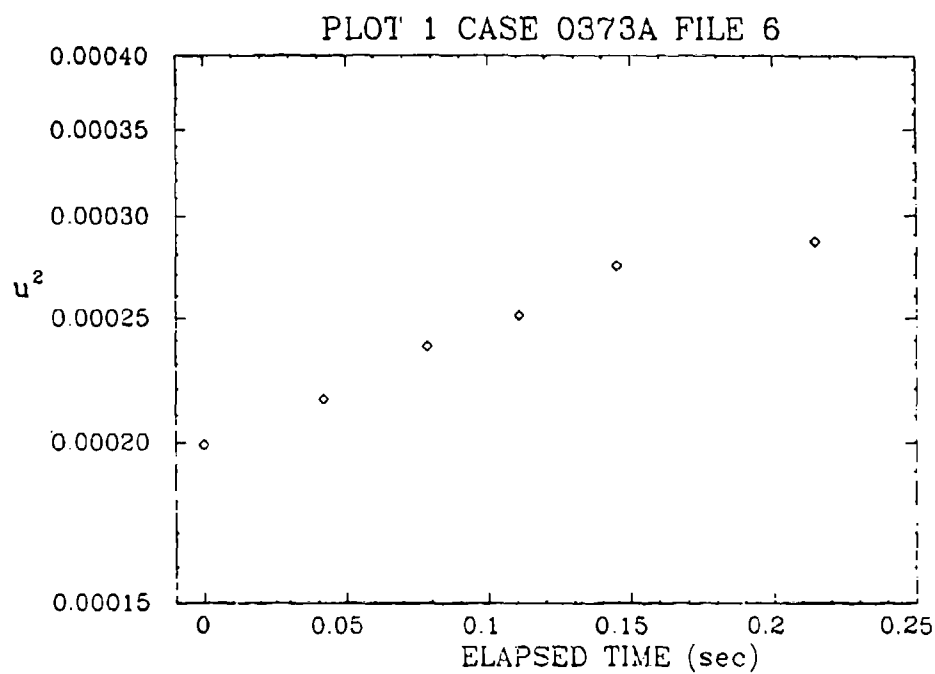
PLOT 1 CASE 0372B FILE 4

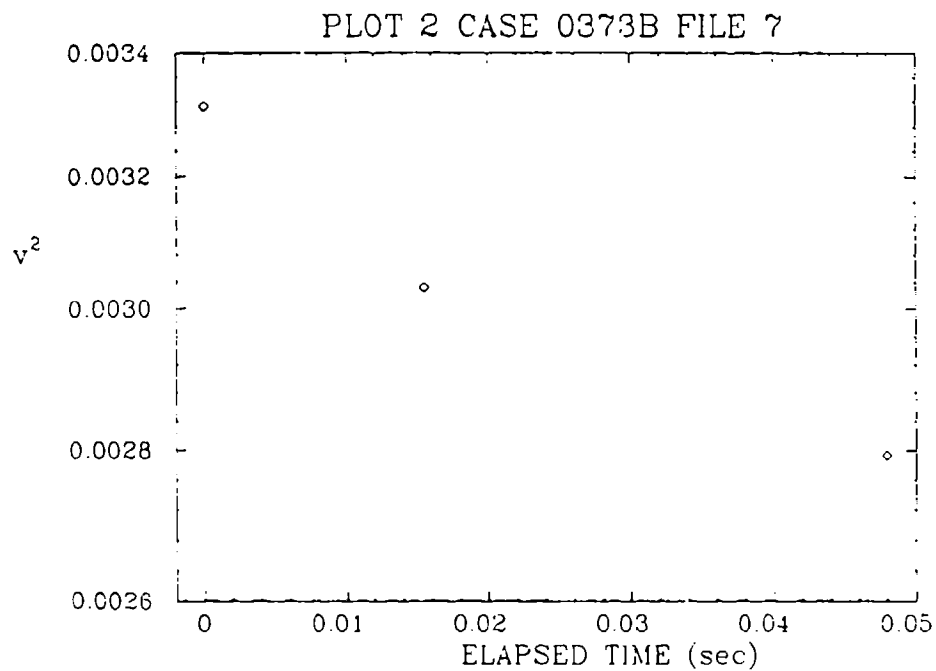
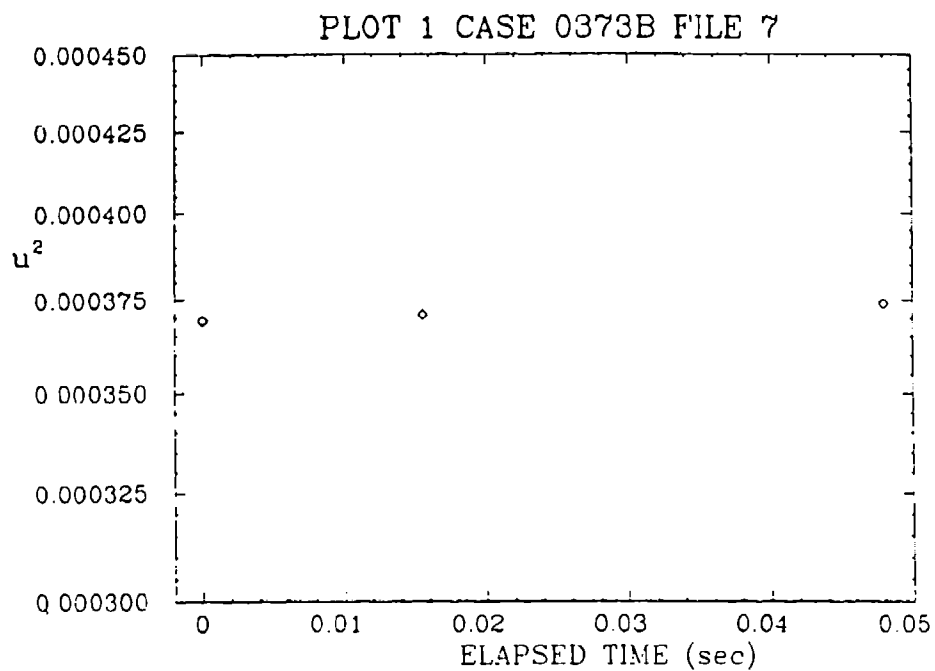


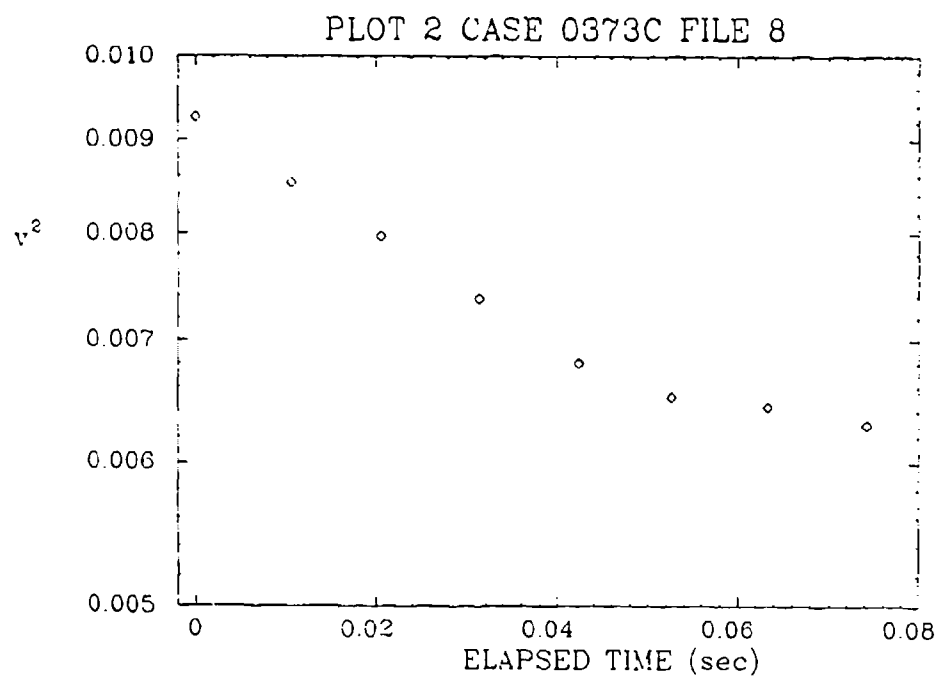
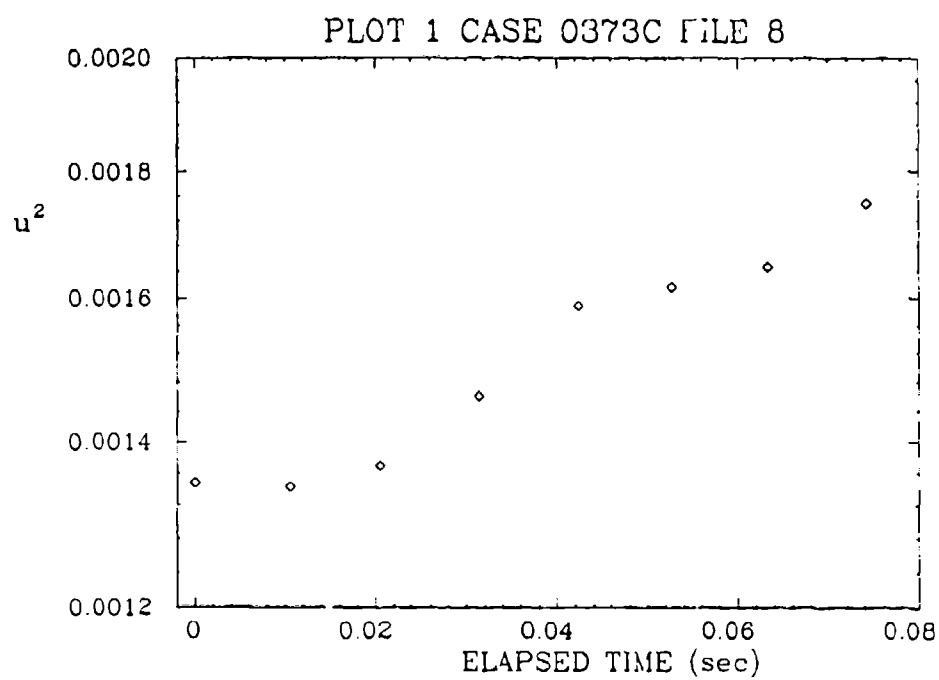
PLOT 2 CASE 0372B FILE 4



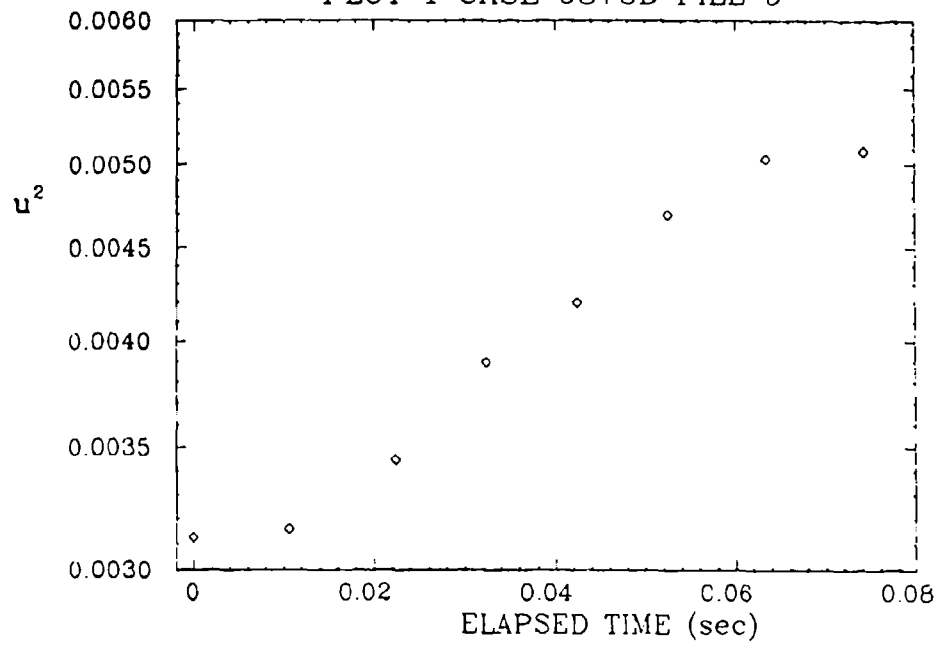




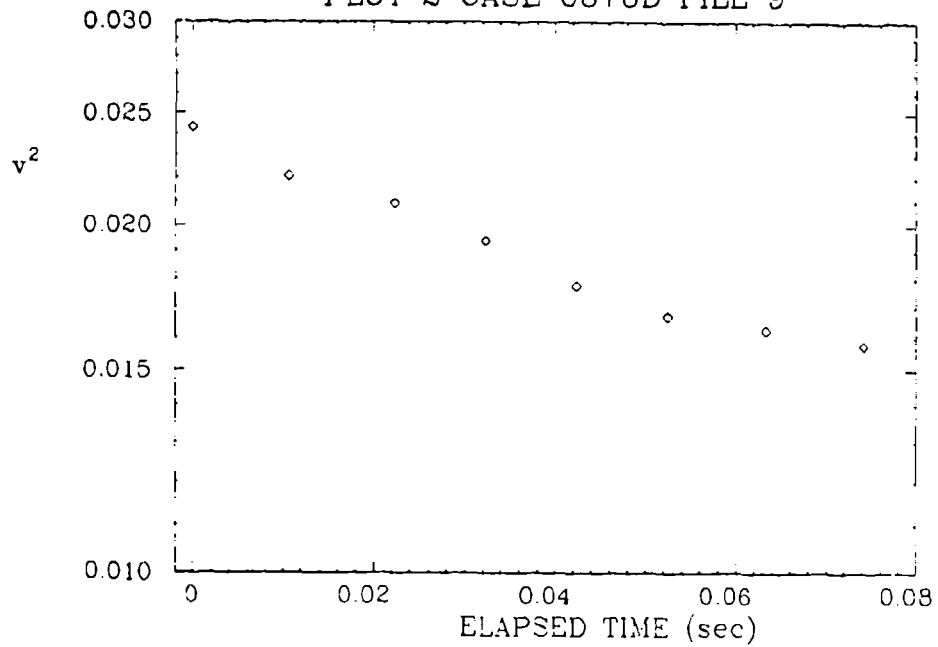


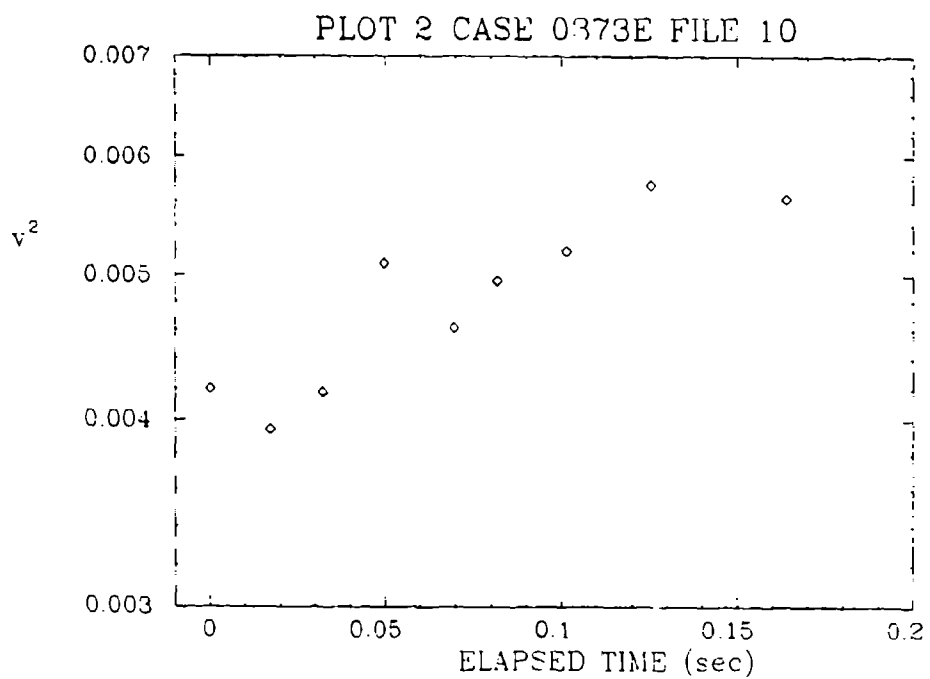
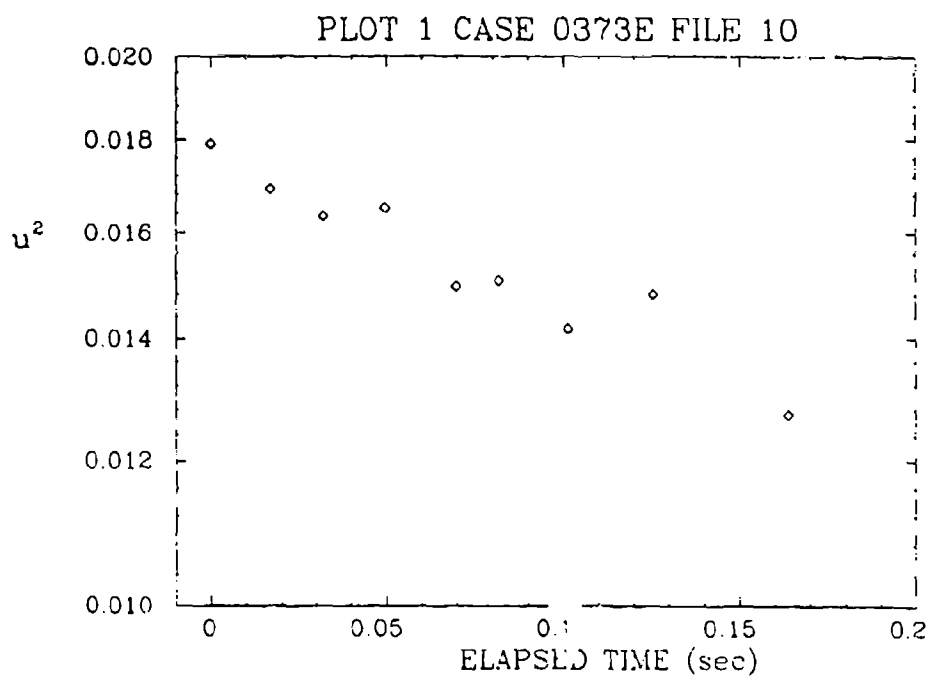


PLOT 1 CASE 0373D FILE 9

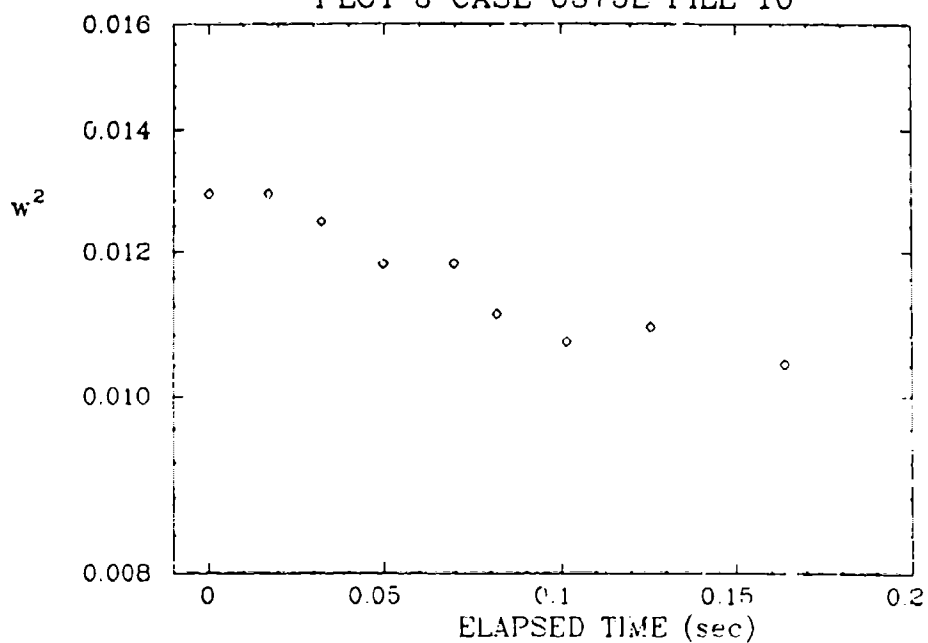


PLOT 2 CASE 0373D FILE 9

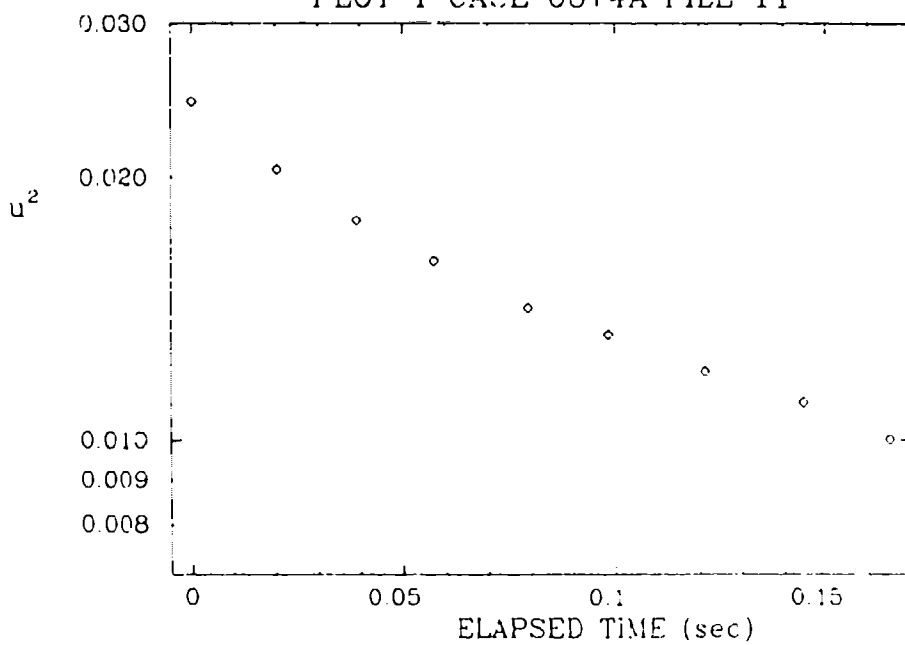




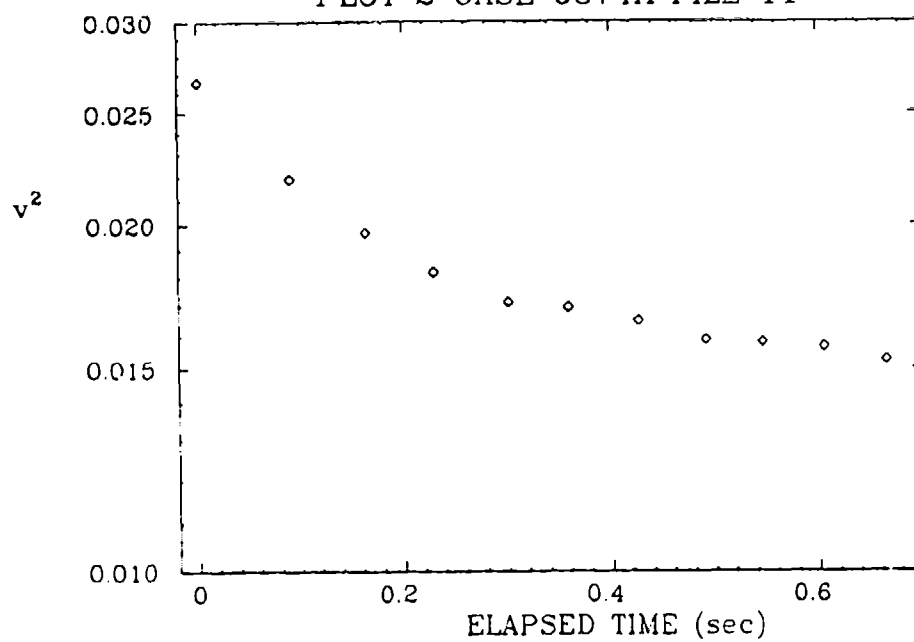
PLOT 3 CASE 0373E FILE 10



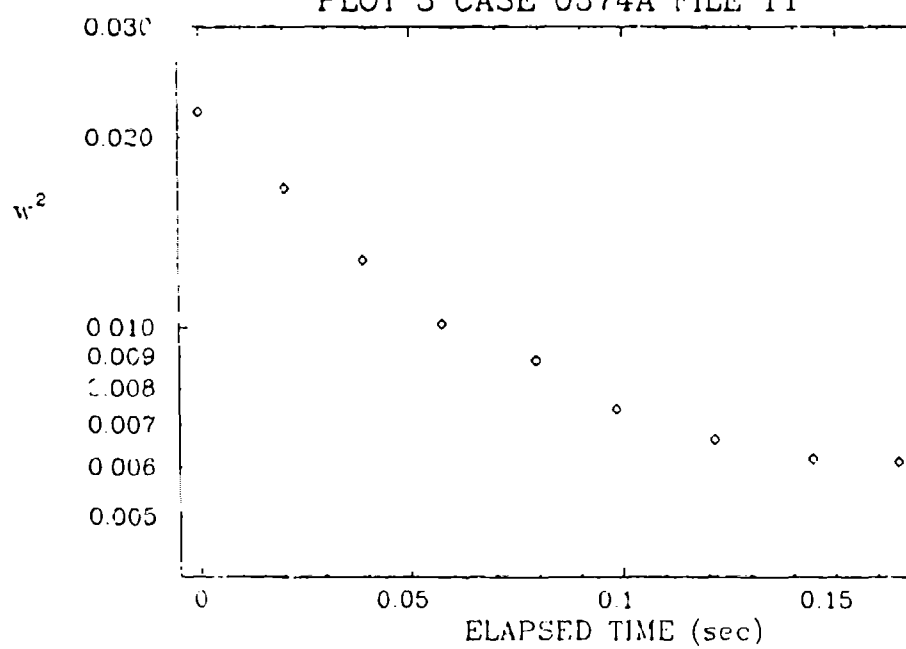
PLOT 1 CASE 0374A FILE 11

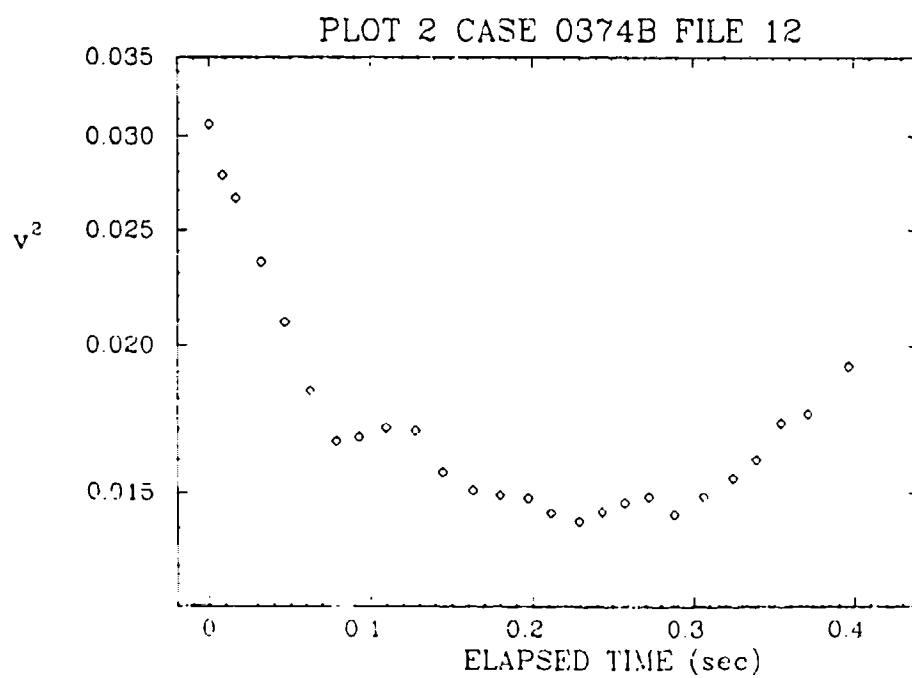
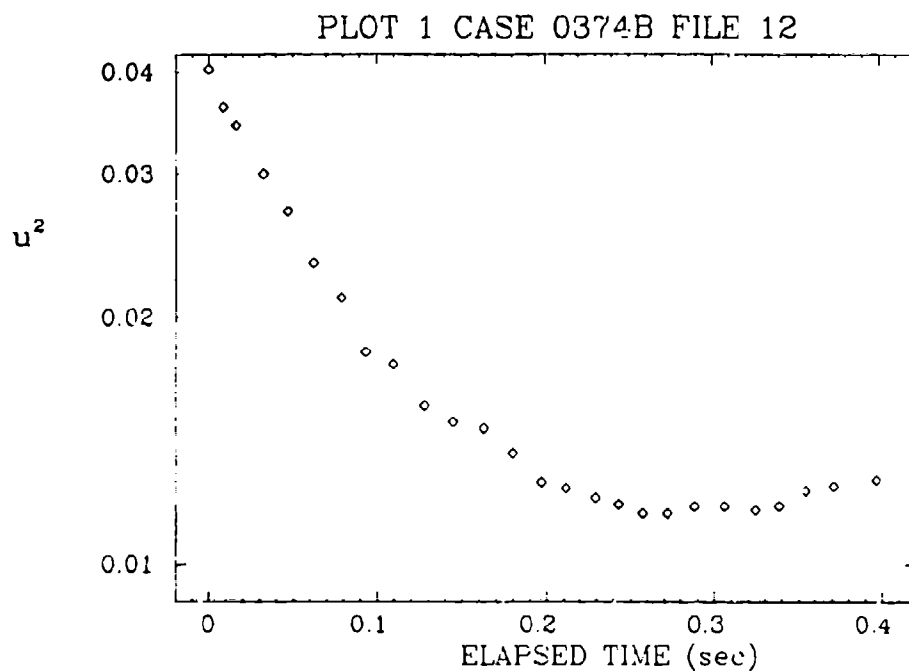


PLOT 2 CASE 0374A FILE 11

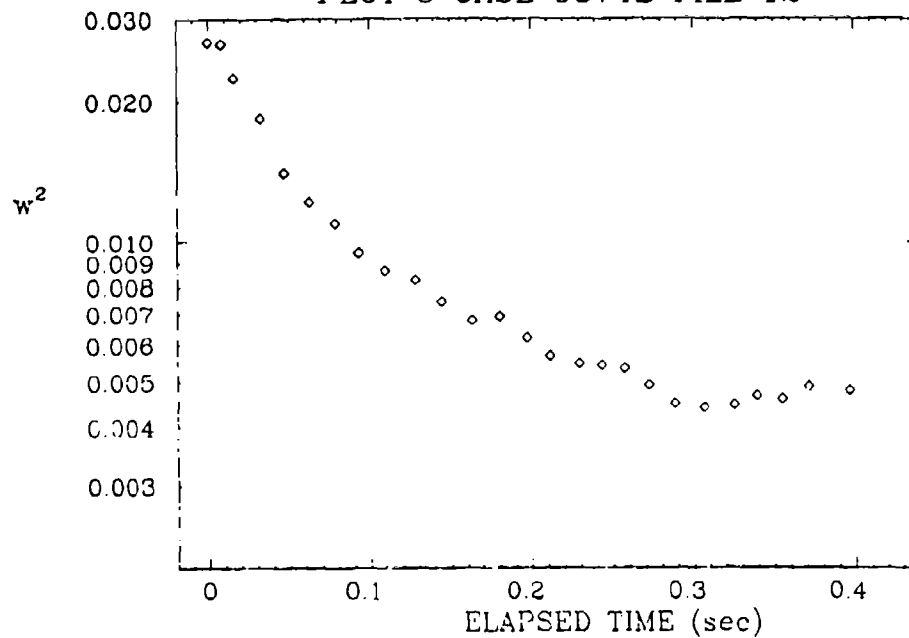


PLOT 3 CASE 0374A FILE 11

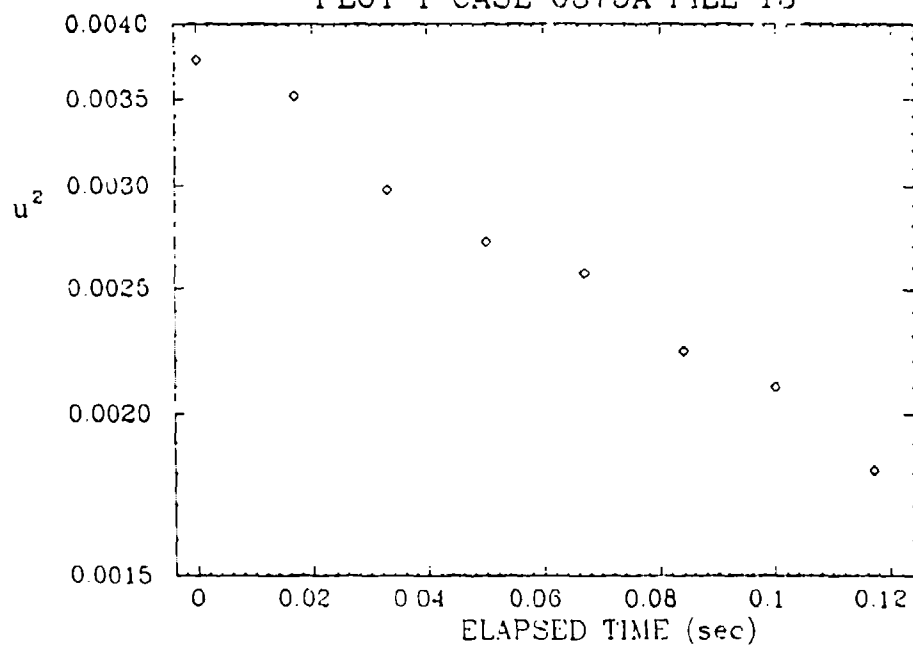




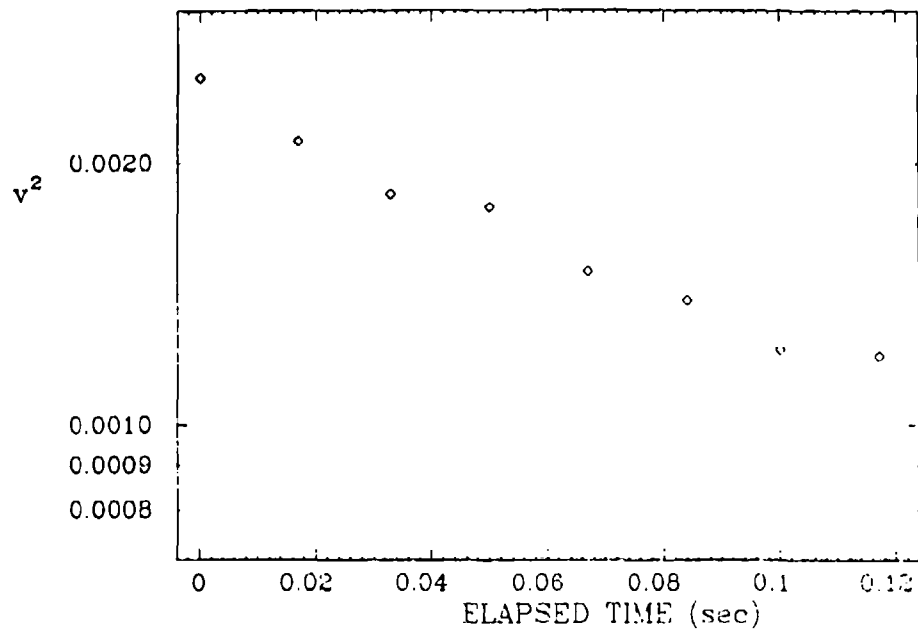
PLOT 3 CASE 0374B FILE 12



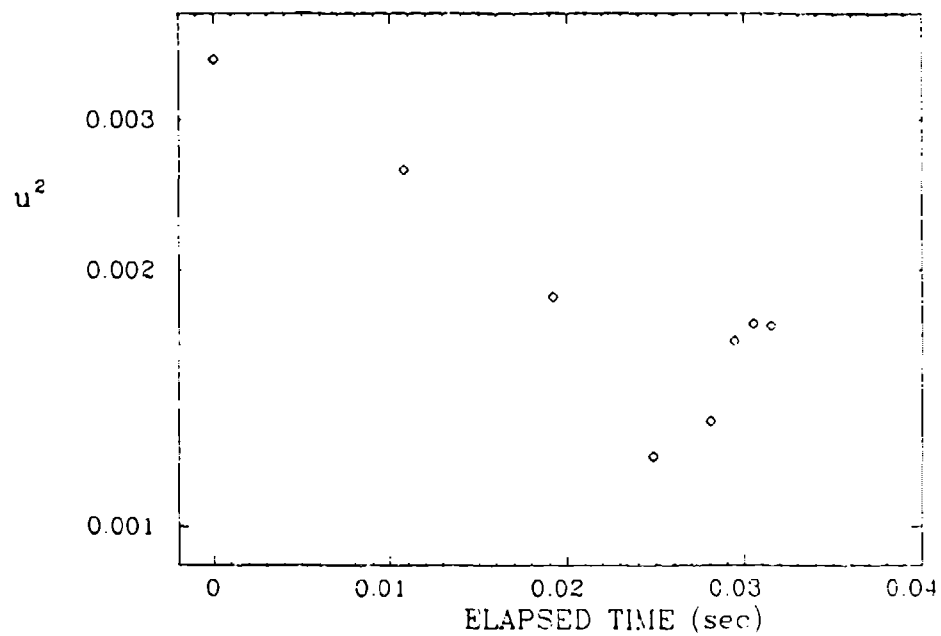
PLOT 1 CASE 0375A FILE 13



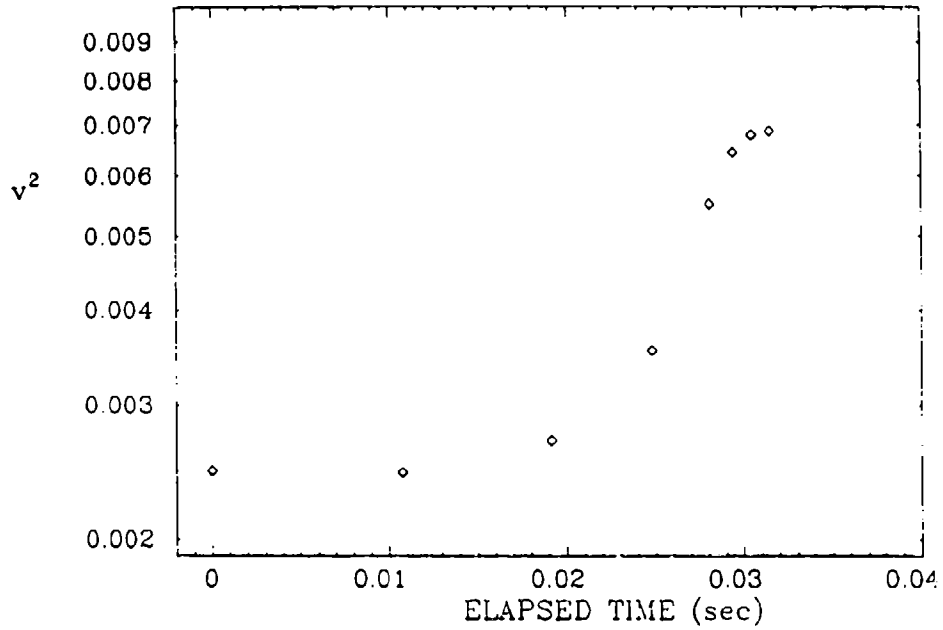
PLOT 2 CASE 0375A FILE 13



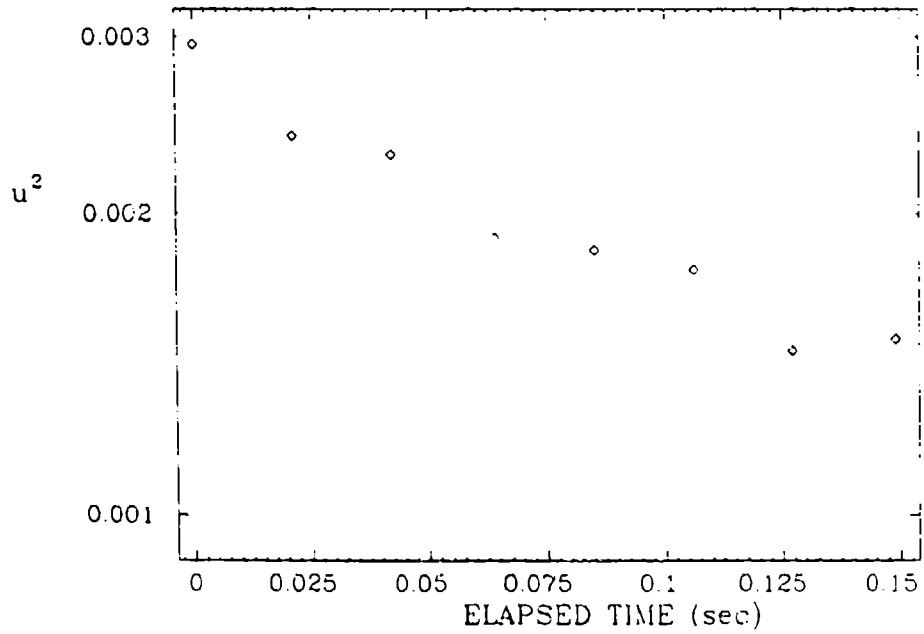
PLOT 1 CASE 0375B FILE 14

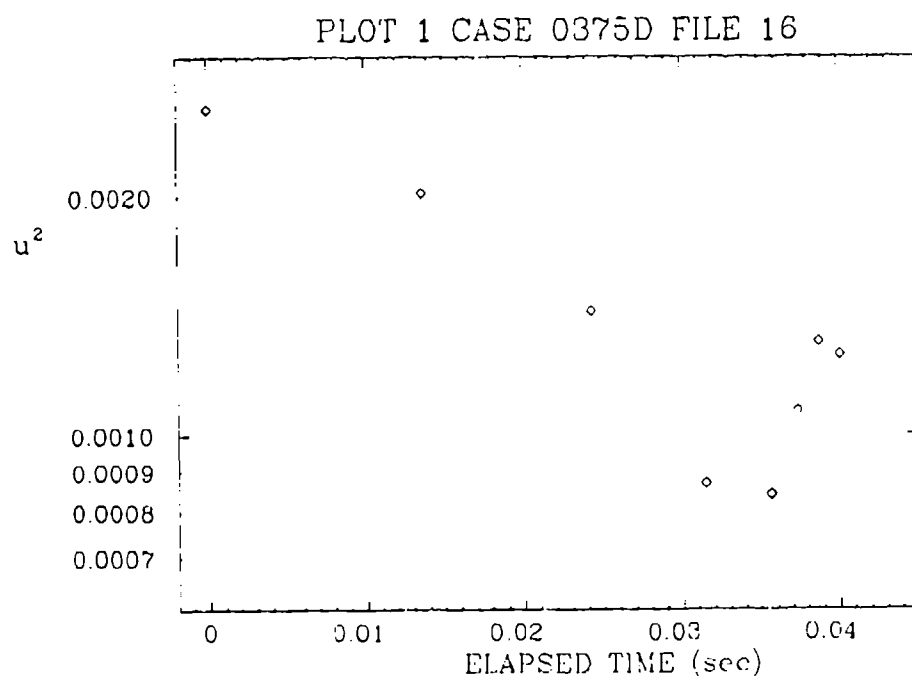
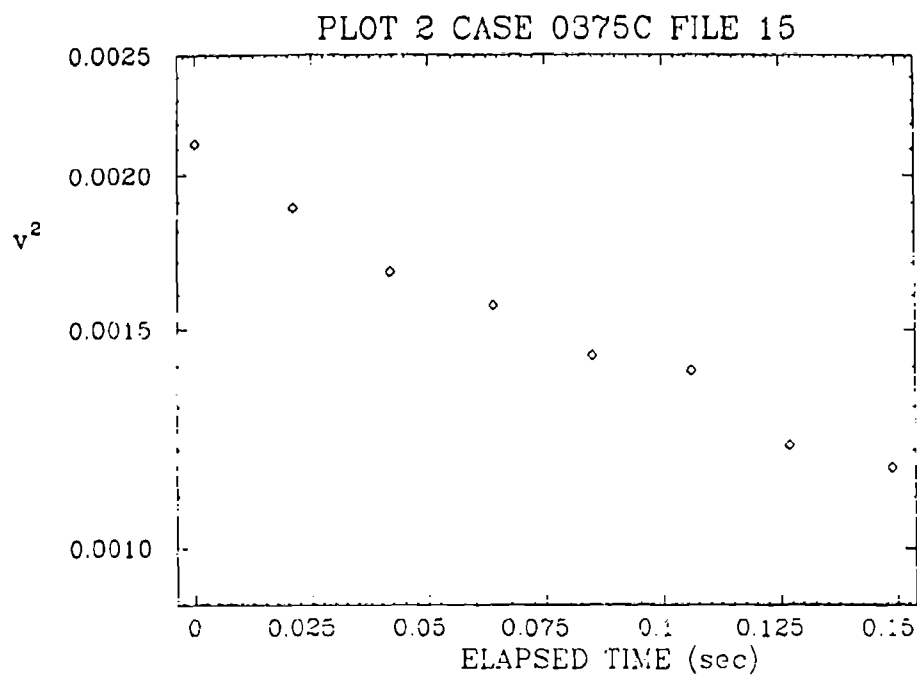


PLOT 2 CASE 0375B FILE 14

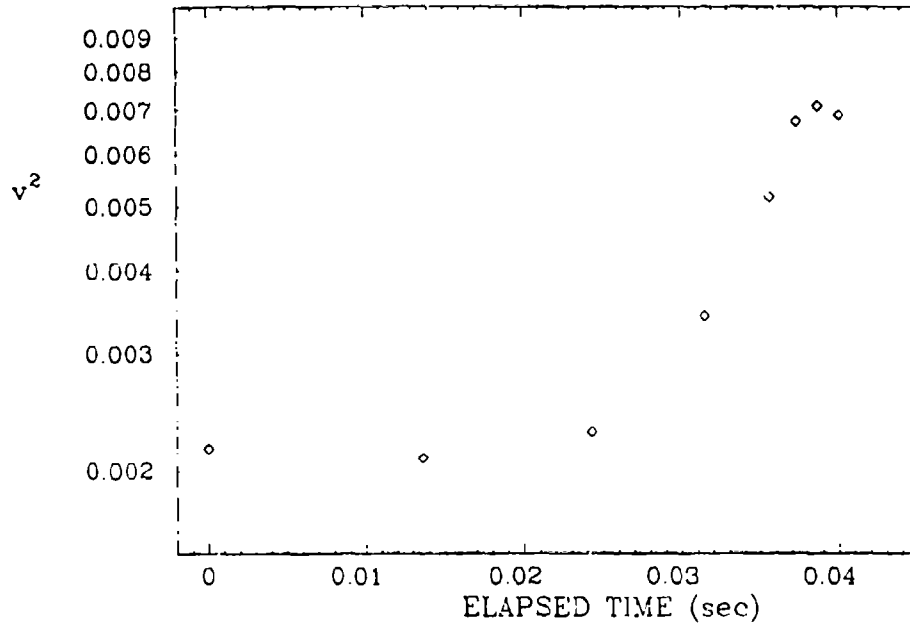


PLOT 1 CASE 0375C FILE 15

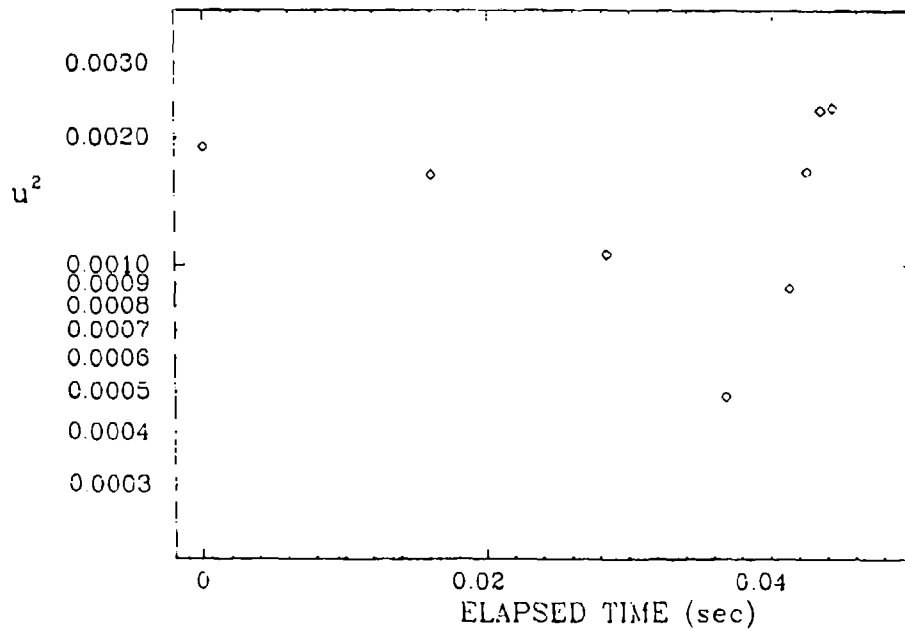




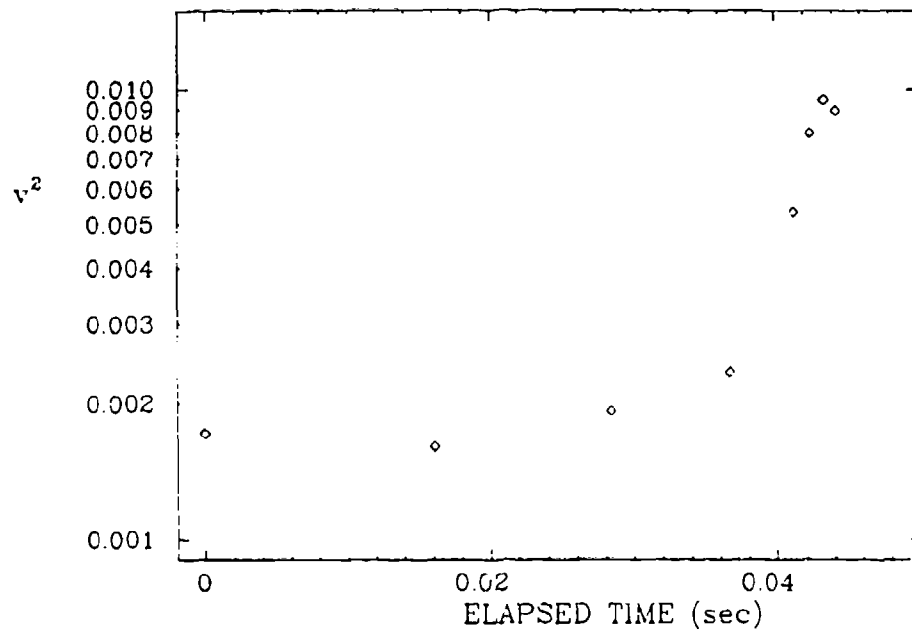
PLOT 2 CASE 0375D FILE 16



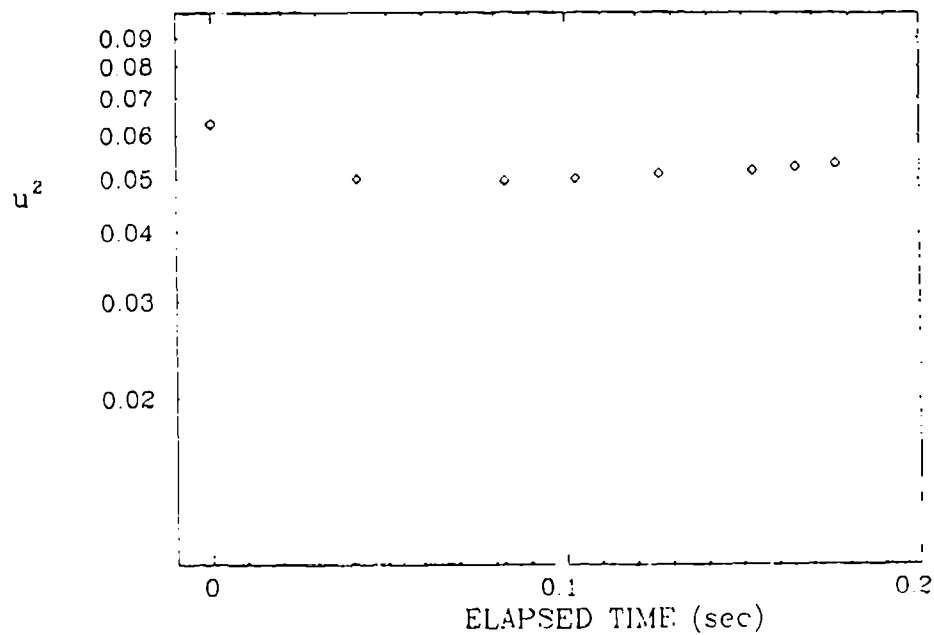
PLOT 1 CASE 0375E FILE 17



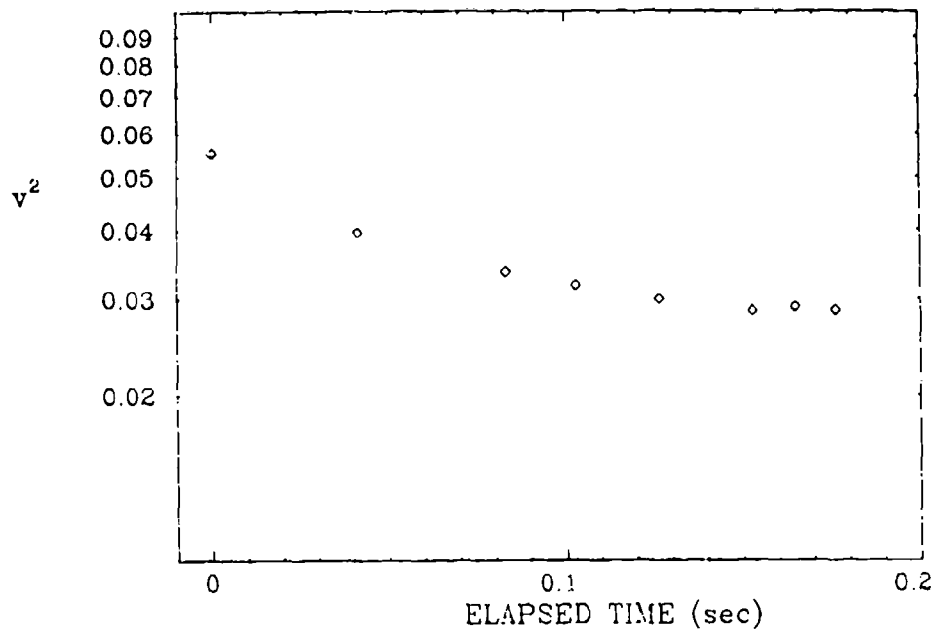
PLOT 2 CASE 0375E FILE 17



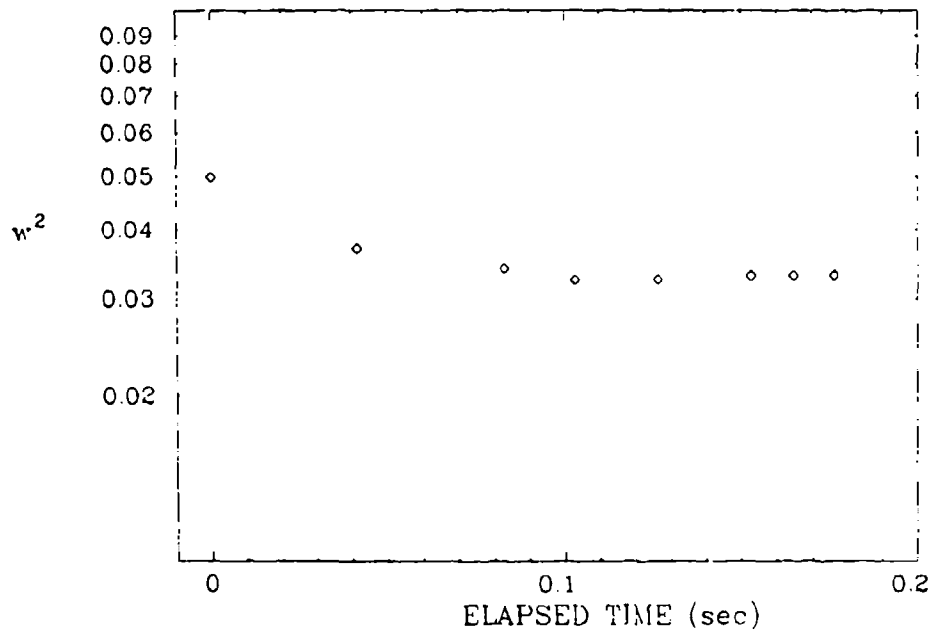
PLOT 1 CASE 0376A FILE 18



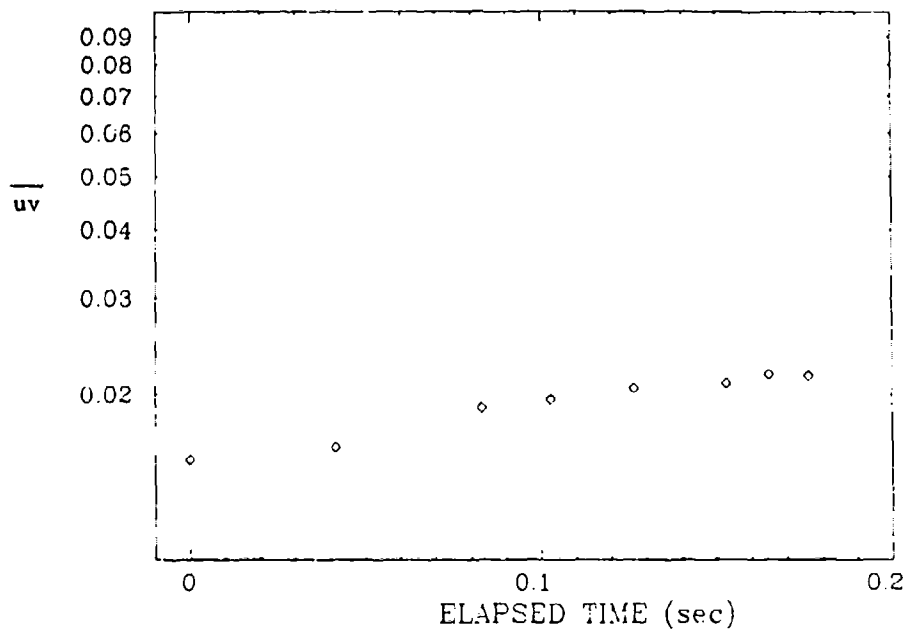
PLOT 2 CASE 0376A FILE 18



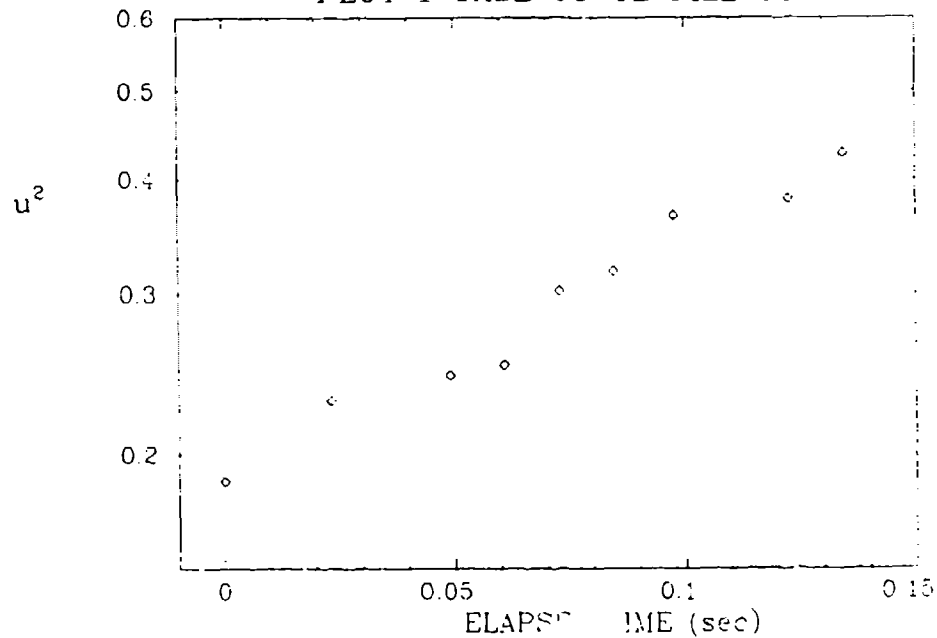
PLOT 3 CASE 0376A FILE 18



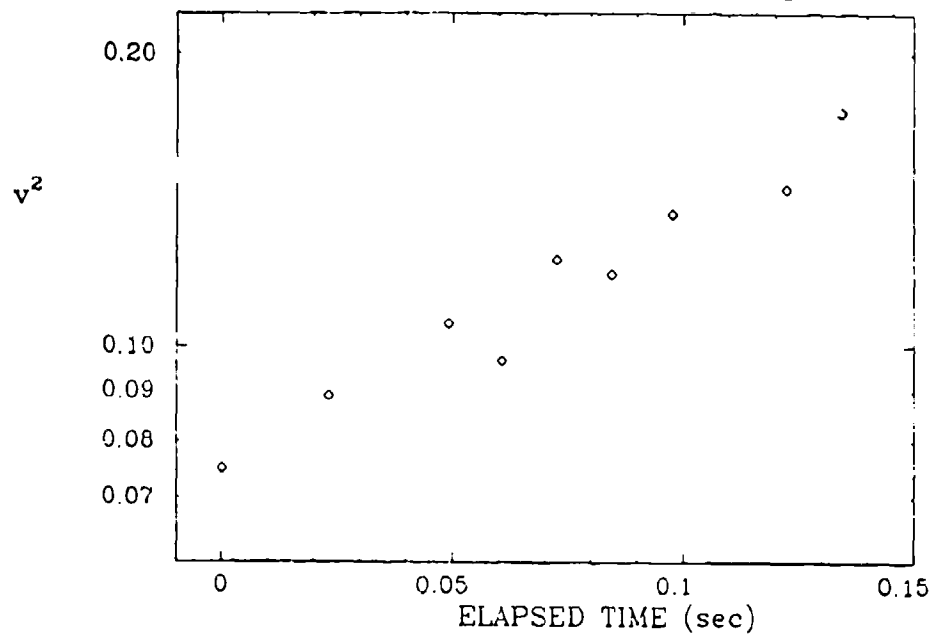
PLOT 4 CASE 0376A FILE 18



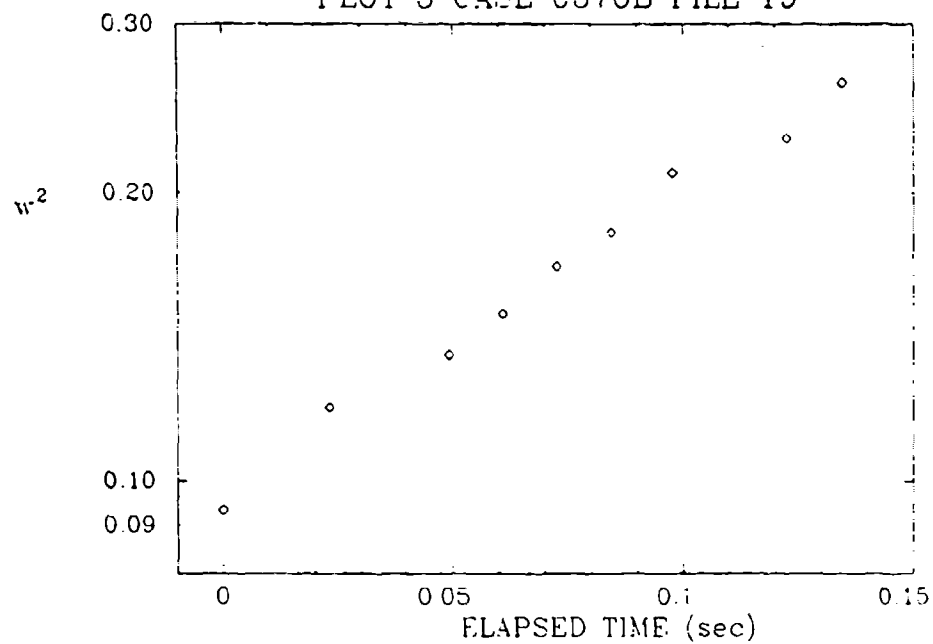
PLOT 1 CASE 0376B FILE 19



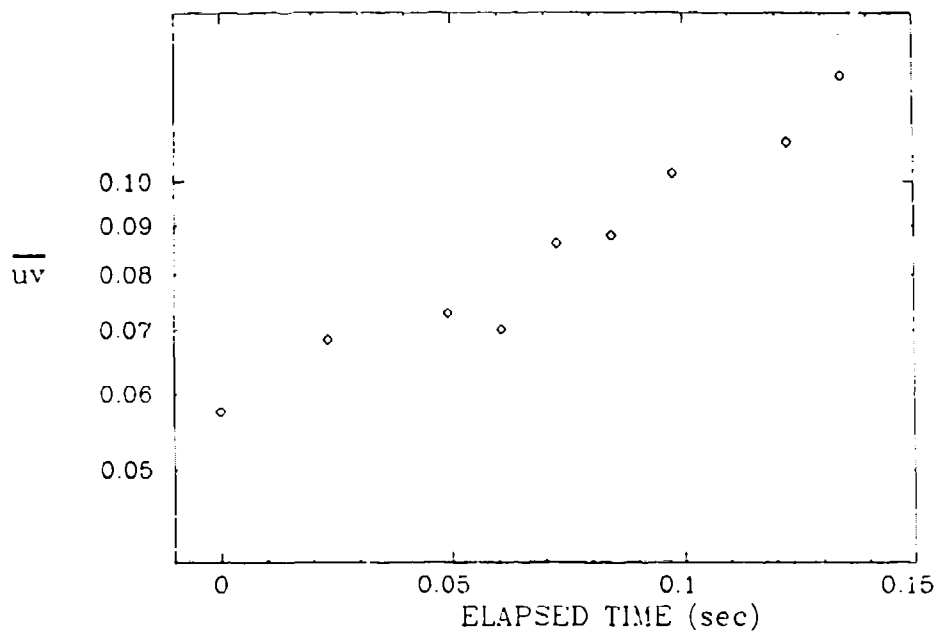
PLOT 2 CASE 0376B FILE 19



PLOT 3 CASE 0376B FILE 19



PLOT 4 CASE 0376B FILE 19



TURBULENT WALL JET

Flow 0260

Cases 0261, 0262, 0263, 0264

Evaluators: B. E. Launder* and W. Rodi†



SUMMARY

SELECTION CRITERIA

A wall jet may be defined as a thin shear flow directed along a wall where, by virtue of the initially supplied momentum, at any station, the streamwise velocity over some region within the shear flow exceeds that in the external stream. Within this broad definition, a very wide range of flows and phenomena has been examined. There have been well over two hundred experimental studies published on the turbulent wall jet. Of these about one half has been prompted by heat transfer considerations,[#] and in most of these cases the flow field has not been sufficiently well documented to merit close attention for the present purposes. Even where detailed data exist, these experiments have commonly employed sufficiently large temperature differences (or gases of different molecular weight) that one could not be certain that the flow field evolution was strictly independent of that of the thermal or species fields; our terms of reference precluded examination of such flows.

Among the remaining 100 or so "aerodynamic" studies, our attention has been given to those of relatively simple flow topography that allowed certain intrinsic and unambiguous truths about the turbulence structure to emerge--either by direct measurement or by inference from the mean-flow's evolution. Within each subclass of experiments, the following broad guidelines have shaped our recommendations:

(1) There should be strong direct or indirect evidence that the flow achieved good two-dimensionality. The principal criterion applied was the close satisfaction of the two-dimensional momentum integral equation. (For the three-dimensional wall jet, compliance with the corresponding three-dimensional form of the momentum equation was required.)

(2) The flow conditions should be well defined, and good experimental practice should be conveyed by the author's documentation of the work.

* Mech. Engr. Dept., University of Manchester, Inst. of Science and Technology, P. O. Box 88, Manchester, M60 1QD, England.

† Sonderforschungsbereich 80, Universität Karlsruhe, D75 Karlsruhe 1, West Germany.

[#] According to the initial angle of incidence between the wall and the jet and their respective temperatures, the wall jet provides a highly effective means of either promoting or inhibiting heat transfer rates from the wall.

(3) The experimental data should preferably include measurements of turbulence quantities as well as those for the mean flow.

(4) The experimental data should exhibit general credibility in comparison with established results in similar flows.

FLOWS SELECTED

A detailed evaluation of more than fifty experimental studies is provided in the writers' complete report (Launder and Rodi, 1980). The experiments have been analyzed in the following categories:

- (a) The self-preserving, two-dimensional wall jet on a plane surface with or without streamwise pressure gradient.
- (b) The two-dimensional wall jet on a plane surface with an external stream with zero or positive streamwise pressure gradient.
- (c) The two-dimensional wall jet developing around a circular cylinder.
- (d) The self-preserving, two-dimensional wall jet developing on a logarithmic spiral surface.
- (e) The three-dimensional wall jet developing in stagnant surroundings on a plane surface.

There follows a brief discussion of the experiments within each of these categories. Nomenclature relating to the two-dimensional wall jet is shown in Fig. 1 and to the three-dimensional wall jet in Fig. 2.

a. Case 0261. Self-Preserving 2D Wall Jet on Plane Surface

Within this flow category the great majority of studies have considered only the case where the streamwise pressure gradient is zero and thus the external fluid is at rest. Fifteen such studies have been scrutinized, and, of these, only the experiments of Bradshaw and Gee (1960), Patel (1962), Tailland (1967, 1970), Guitton (1970), Guitton and Newman (1977), and Verhoff (1970) show satisfactory compliance with the two-dimensional momentum integral equation. In the self-preserving region, which begins some 50 slot heights downstream of the exit slot, the rate of growth of the half-width is constant and given by

$$\frac{dy_{1/2}}{dx} = 0.073 \pm 0.002 \quad (1)$$

It is worth noting that the half-width grows over 30% less than in the plane, free-jet in still air (Rodi, 1975).

Wide variations exist in the values reported for the skin-friction coefficient. The direct force measurements of Alcaraz (1977) appear the most reliable and further display a variation that is in excellent accord with the earlier recommendation of Bradshaw and Gee (1960):

$$C_f = 0.0315 Re_m^{-0.182} \quad (2)$$

where

$$C_f \equiv \frac{2\tau_w}{\rho U_m^2} \quad \text{and} \quad Re_m \equiv \frac{U_m y_m}{\nu}$$

None of the turbulence data for this case of stagnant surroundings is entirely satisfactory, due principally to the very high percentage fluctuation levels near the outer edge and to the steep velocity gradients near the wall. Those of Guitton (1970) and Wilson (1970) show the best agreement between directly measured turbulent shear stress and those inferred from the momentum equation. There is reasonable agreement among the studies of Giles et al. (1966), Guitton (1970), Tailland and Mathieu (1967), and Wilson (1970) for the streamwise normal stress measured with a normal wire. Tailland also obtained this component from his slant wires, however, and the values for normal stress are substantially different. This discovery cannot help but raise doubts on the accuracy of all the data.

The case of an equilibrium wall jet in an adverse pressure gradient has been studied in three sequential studies at McGill University. Those of Gartshore and Newman (1969) and Irwin (1974) achieve satisfactory momentum balances and, while the former examines three different ratios of $U_m:U_E$, the latter provides a very detailed study for a velocity ratio of 2.65:1, including a complete and consistent set of directly measured Reynolds-stress profiles. (The presence of the moving external stream reduces the turbulence intensities and thus greatly improves the accuracy of the hot-wire data in comparison with the case of stagnant surroundings.) Collectively, therefore, these experiments provide a searching combination of breadth and detail against which to test the capabilities of flow calculation procedures.

b. Plane 2D Non-Similar Wall Jets on a Plane Surface (No test case)

We consider first the case of a uniform-velocity external stream. This flow is not a self-preserving one, for, as the jet develops downstream, the ratio of $U_m:U_E$ progressively diminishes. (Ultimately the velocity maximum would disappear and the shear flow eventually change into a normal turbulent boundary layer; usually the test sections are too short to allow this development to be documented, however.) Launder and Rodi (1980) examined some 15 studies of this class of flow. In most cases, initial conditions were not adequately reported. The most satisfactory cases from the point of view of momentum balance were those of Gartshore and Newman (1969), Nicoll (1967), and Kruka and Eskinazi (1964) (the last-named only for values of U_E/U_1 up to 0.263.) No formal test case is proposed for this problem. We feel that some of the other cases will test more searchingly and precisely the capabilities of any calculation procedure. Nevertheless, our survey (Launder and Rodi, 1980) has shown that the flows exhibiting reasonable conformity with the 2D momentum

integral equation display a nearly universal dependence of $(y_{1/2}/\theta)$ on $(x - x_0)/\theta$, where x_0 is the virtual origin of the flow and θ is the local momentum thickness of the wall jet.* For $(x - x_0)/\theta$ in the range 8-70, the variation is within experimental scatter, and $y_{1/2}/\theta$ is described by:

$$y_{1/2}/\theta = 0.03 + 0.033(x - x_0)/\theta$$

It is our view that the degree of compliance of computations with this line would provide a straightforward test which for large initial values of U_m/U_E would be insensitive to the details of the initial conditions.

The tangential injection of a high-velocity stream of fluid beneath a turbulent boundary layer developing in a positive (or "adverse") pressure gradient is important in several aeronautical flows. The aim is to prevent separation of the boundary layer, and the flows are sometimes referred to as "blown" boundary layers. In these flows, two-dimensionality is more difficult to maintain than in zero pressure gradient; moreover, several experimenters have failed to provide sufficient details of their flow conditions. Two of the five flow developments of this type examined by Irwin (1974) provide satisfactory and interestingly different cases for testing predictive schemes. For his Case B, the injected momentum flux of the wall jet is large enough to absorb entirely the initial boundary layer, while for Case C the shear flow develops a dangerously low velocity region midway between the wall and the edge of the boundary layer. Although competition from other flows precludes our nominating these experiments as a test case, they certainly provide a searchingly difficult test of any calculation procedure for turbulent boundary layers.

c. Case 0262. 2D Wall Jet on a Cylinder (not used in 1981 meeting)

The two-dimensional wall jet developing over a convex surface has proved to be a very difficult flow to establish, due to the tendency for small spanwise irregularities to amplify downstream and for streamwise vortices, driven by the imbalance of radial acceleration and pressure gradient in the vicinity of the end walls, to encroach on the whole flow. Of the six experimental studies analyzed, only that of Alcaraz (1977) and one of Fekete's configurations (1963) achieved demonstrably adequate two-dimensionality. Two crucial features of the apparatus design are carefully machined blunt exit slots and slot heights less than 1% of the cylinder radius. Alcaraz' experiment provides the most complete available documentation of any wall-jet study with generally consistent measurements of all non-zero Reynolds stresses and all but one of the active triple moments. As only the first 20 degrees of arc are

*This is an adaptation of a proposal of Patel (1970), who suggested that the momentum thickness at the slot exit should everywhere be used for the normalization.

considered, however, the effects of curvature are relatively mild. Fekete's experiments, in contrast, document the wall-jet development from discharge to separation (at about 220° of arc). The flow two-dimensionality steadily deteriorates with progress around the cylinder; however, for the smallest value of b/R^* (0.0074), the departure is not serious up to the 145° station. At this position the wall jet is about twice as thick as one developed for the same distance on a plane surface, which underlines the great sensitivity of this flow to the additional strain imposed by curvature.

The case of wall-jet development around the inside of a cylinder has formed the subject of two careful studies (Guitton, 1964; Spettel et al., 1972), though in neither case have the data been reported in sufficient detail to allow us to recommend their use as a test flow.

d. Case 0263. 2D Wall Jet on Logarithmic Spiral Surfaces

When a wall jet is developed over a logarithmic spiral surface where $x/R = K$, the jet thickness increases at the same rate as R . Thus, the non-dimensional strength of flow curvature remains the same from station to station, and the flow attains a self-preserving form. Sawyer (1962) appears to have been the first to recognize this fact, and, indeed, his Ph.D. thesis provided the first experimental data. Four careful studies have now been made of this flow for spirals of varying degrees of tightness. Each has included the plane surface as a limiting member of the class of flows examined, thus providing a valuable cross check. Guitton (1970; see also Guitton and Newman, 1977) has worked hardest at (and appears to have been the most successful in) reducing secondary flows; thus, although for a given value of K his two experiments exhibit a slightly smaller rate of spread than suggested by those of Sawyer (1962), Giles et al. (1966), and Kamemoto (1974), we judge them to be more reliable. The dependence of $y_{1/2}/x$ is well described by the formula:

$$y_{1/2}/x = 0.073 + 0.8y_{1/2}/R - 0.3(y_{1/2}/R)^2 \quad (3)$$

which reduces, in the case of $R \rightarrow \infty$, to the recommended plane-surface spreading rate. The mean velocity profile undergoes a small but consistently reproduced change of shape as the value of K is increased, becoming less pointed--more rounded--in the vicinity of the velocity maximum. A quantitative manifestation of this is that $y_m/y_{1/2}$ increases with K being well correlated by

$$y_m/y_{1/2} = 0.159 + 0.205 y_{1/2}/R \quad (4)$$

a relation proposed by Kamemoto (1974). There appears to be no firm evidence that the skin-friction coefficient is significantly affected by the level of K .

* R denotes radius of curvature of the surface (in this case the cylinder radius).

Guitton's (1970) experiments also provide a comprehensive set of Reynolds stresses measured by hot wire which generally exhibit (as they should) close similarity from station to station. A check of the agreement suggested by the momentum integral equation with the directly measured turbulent shear stress showed it to be within about 20% near the position of maximum stress.

f. Case 0264. Plane 3D Wall Jet in Stagnant Surroundings

Here, as elsewhere, we have not considered studies where the wall jet has been discharged other than tangentially to the test plate. Launder and Rodi (1980) provide a detailed examination of the five sets of investigations. At the nozzle exits the jets discharged variously from rectangular (or square), circular, and semi-circular holes, and the working medium has included both air and water. Only two studies (Newman et al., 1972; Rajaratnam and Pani, 1974) have reported their measurements sufficiently fully to allow a check on the momentum balance to be made; both exhibit satisfactory behavior in this respect. The shear flow exhibits a behavior in the near field that depends strongly on the shape of the nozzle and the exit flow conditions, and these have not been thoroughly defined in any of the studies considered. Beyond about 100 slot-exit widths, however, the exploration by Newman et al. (1972) indicates that the mean flow and turbulence quantities take on a self-preserving character in which the rate of spread is uniform and the velocity maximum decays as x^{-1} . The most striking feature about the flow is the highly unequal rates of spread in the y and z directions. There is good agreement among the various experiments about the stream-wise increase of $y_{1/2}$, all the data being bracketed by:

$$\frac{dy_{1/2}}{dx} = 0.048 \pm 0.003 \quad (5)$$

Greater variation exists in the reported lateral spreading rates, a feature we believe to be largely due to the slower approach of the lateral motion to fully developed conditions. The experiments of Newman et al. (1972) which extended to 200 nozzle diameters downstream are probably the most reliable; moreover, one of the two cases examined by Rajaratnam and Pani (1974) obtained effectively the same value. Having regard for the uncertainties of interpretation, the asymptotic lateral rate of growth very probably falls within the band:

$$\frac{dz_{1/2}}{dx} = 0.26 \pm 0.02 \quad (6)$$

No extensive sets of turbulence data are available in the far-field region, but Newman et al. (1972) have found that $\overline{u^2}/\overline{U_m^2}$ is similar for x/b greater than 110 and that on the symmetry plane this quantity shows levels about 50% greater than for Guitton's data of the plane two-dimensional wall jet.

RECOMMENDATIONS FOR FUTURE WORK

Under the general heading of "wall jet," a wide spectrum of flows has been studied. Despite the experimental difficulties, it is our view that several of these experiments will serve to provide difficult and incontrovertible tests of turbulence-closure proposals. Overall, the most successful studies have been those undertaken in laboratories that have made a large-scale effort evolving over a decade or more. This emphasizes how crucial design and experimental technique have been to obtaining really useful data. Certainly, before anyone embarks on further studies of the wall jet, he (or she) should read through the collected reports from Professor Newman's group at McGill (those of Fekete, Guitton, Gartshore, Irwin, etc.) to brief himself on the problems that may arise and the way that skill and patience can overcome them.

For the two-dimensional flows, perhaps the most irksome gap in our knowledge is that of the distributions of $\overline{v^2}$ and $\overline{w^2}$ in the "simplest" case--that of the plane wall jet in stagnant surroundings. Several data sets exist, but none can be called definitive. As part of a wider study, it might be possible to obtain a detailed documentation of these quantities using the now widely available laser-Doppler anemometer to lessen problems of high-intensity turbulence. Although the degree of two-dimensionality achieved in the study of Guitton (1970) of the wall jet on a logarithmic spiral surface was less than desirable, we feel that it would be very difficult for any further study to do better.

Future effort may, in our view, be most fruitfully directed to three-dimensional cases. The very rapid lateral rate of spread ($dz_{1/2}/dx$) found for the case of the jet developing on a plane surface in stagnant surroundings arises, in large measure, from the anisotropy of the Reynolds stresses acting in the plane normal to the stream direction which acts as a source of streamwise vorticity. It would be very worthwhile to obtain an accurate documentation of the profiles of these stresses. Further explorations should also include the way that the presence of an external stream affects the relative spreading rates in directions normal and parallel to the surface.

REFERENCES

- Alcaraz, E. (1977). "Contribution a l'étude d'un jet plan turbulent évoluant le long d'une paroi convexe à faible courbure," Thèse d'Etat, Université Claude Bernard, Lyon.
- Bradshaw, P., and M. T. Gee (1960). "Turbulent wall jets with and without an external stream," ARC Reports and Memoranda, No. 3252.
- Fekete, G. I. (1963). "Coanda flow in a 2-D wall jet on the outside of a circular cylinder," McGill University, Mech. Engr. Dept. Report No. 63-11.
- Gartshore, I., and B. G. Newman (1969). "The turbulent wall jet in an arbitrary pressure gradient," Aero. Quart., 20, 25.
- Giles, J. A., A. P. Hays, and R. A. Sawyer (1966). "Turbulent wall jets on logarithmic spiral surfaces," Aero. Quart., 17, 201.

- Guittou, D. E. (1964). "2-D turbulent wall jets over curved surfaces," McGill University, Mech. Engr. Report No. 64-7.
- Guittou, D. E. (1970). "Some contributions to the study of equilibrium and non-equilibrium wall jets over curved surfaces," Ph.D. thesis, McGill University, Montreal.
- Guittou, D. E., and B. G. Newman (1977). "Self-preserving turbulent wall jets over convex surfaces," J. Fluid Mech., 81, 155.
- Irwin, H. P. A. H. (1974). "Measurements in blown boundary layers and their prediction by Reynolds stress modelling," Ph.D. Thesis, McGill University, Montreal.
- Matsumoto, K. (1974). "Investigation of turbulent wall jets over logarithmic spiral surfaces. (1) Development of jets and similarity of velocity profile; (2) Properties of flow near the wall," Bulletin JSME, 17, 333.
- Kruka, V., and S. Eskinazi (1964). "The wall jet in a moving stream," J. Fluid Mech., 20, 555.
- Launder, B. E., and W. Rodi (1980). "The turbulent wall jet--a review of the experimental data," report commissioned for AFOSR/HTTM-Stanford Conference on Complex Turbulent Flows, September 1980 (to appear in Progress in the Aerospace Sciences, 1981).
- Newman, B. G., R. P. Patel, S. B. Savage, and H. K. Tjio (1972). "Three-dimensional wall jet originating from a circular orifice," Aero. Quart., 23, 187.
- Nicoll, W. B. (1967). "The turbulent wall jet: its development and film cooling effectiveness," Ph.D. Thesis, University of London.
- Patel, R. P. (1962). "Self-preserving, 2-D turbulent jets and wall jets in a moving stream," M.Eng. thesis, Dept. of Mech. Engr., McGill University, Montreal.
- Patel, R. P. (1970). "A study of two-dimensional symmetric and asymmetric turbulent shear flows," Ph.D. Thesis, McGill University, Montreal.
- Rajaratnam, N., and B. S. Pani (1974). "Three-dimensional turbulent wall jets," J. ASCE, Hydraulics Div. (HYI), 69.
- Rodi, W. (1975). "Free turbulent shear flows--a review of the experimental data," Studies in Convection, 1, 79.
- Sawyer, R. A. (1962). "Two-dimensional turbulent jets with adjacent boundaries," Ph.D. Thesis, Cambridge University.
- Sridhar, K., and P. K. C. Tu (1969). "Experimental investigation of curvature effects on turbulent wall jets," Aeronaut. Jou., 73, 977-981.
- Spettel, F., J. Mathieu, and J. Brison (1972). "Tensions de Reynolds et production d'énergie cinétique turbulente dans les jets pariétaux sur parois planes et concaves," Journal de Mécanique, 11, 403.
- Tailland, A., and J. Mathieu (1967). "Jet pariétal," Journal de Mécanique, 6, 103.
- Tailland, A. (1970). "Contribution à l'étude d'un jet plan dirigé tangentiellement à une paroi plane," Le Grade de Docteur des Sciences, Univ. de Lyon, No. 618.
- Verhoff, A. (1970). "Steady and pulsating 2-D turbulent wall jets in a uniform stream," Princeton University Rept. No. 273.
- Wilson, D. J. (1970). Ph.D. Thesis, Mech. Engr. Dept., University of Minnesota.

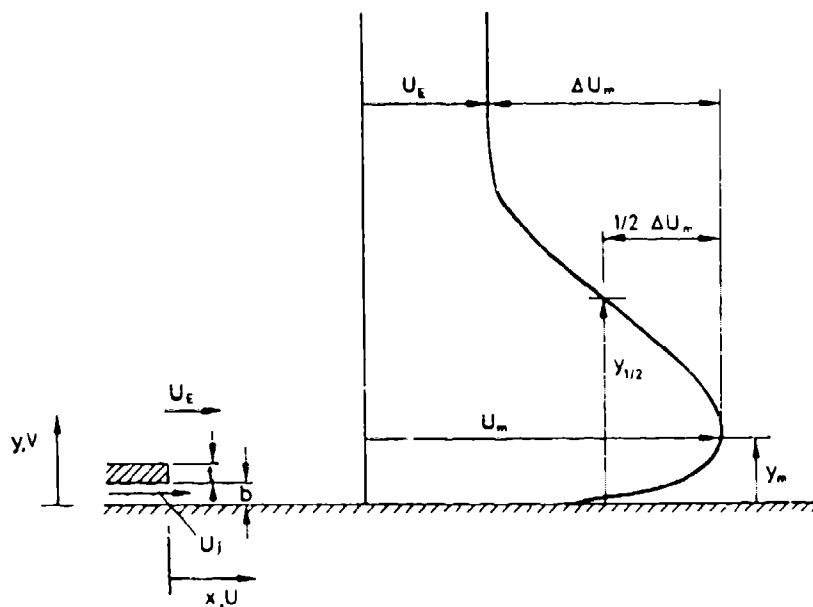


Figure 1. The plane wall jet: configuration and nomenclature for Cases 0261 and 0263.

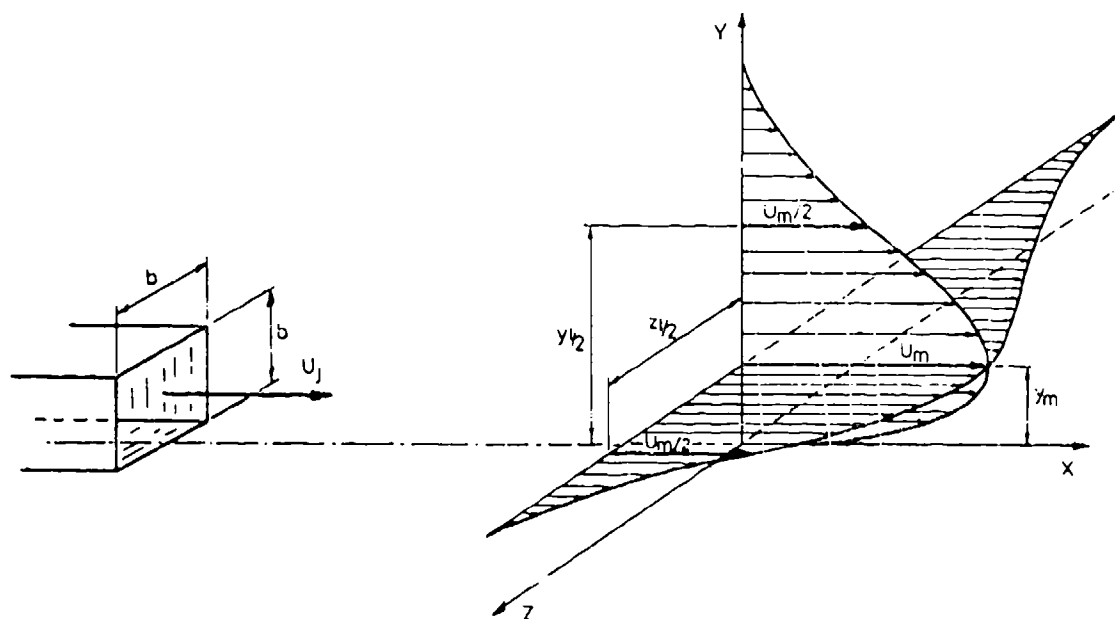


Figure 2. Flow configuration and nomenclature for the three-dimensional wall jet.

DISCUSSION

Flow 0260

1. It should be pointed out that the selection criteria used by Launder and Rodi were based on the check of the two-dimensionality of the flow and the satisfaction of the momentum balance. The cases meeting these criteria exhibited self-similarity within the experimental uncertainty, and are therefore insensitive to the initial conditions at the jet-nozzle exit.
2. Jets on curved surfaces are often sensitive to the initial conditions. When the jet-nozzle lip is sharp, wall experiments with a blunt trailing edge of the nozzle exhibit much less sensitivity.

SPECIFICATIONS FOR COMPUTATION

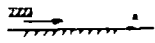
ENTRY CASE/INCOMPRESSIBLE

Case #0261; Data Evaluators: B. Launder and W. Rodi

Data Takers: Various--Correlations

PICTORIAL SUMMARY

Flow 0260. Data Evaluators: B. Launder and W. Rodi. "Turbulent Wall Jet."

Case Data Taker	Test Rig Geometry	dp/dx or C _p	Number of Stations Measured							C _f	Re	Ini- tial Cordi- tion	Other Notes
			Mean Velocity		Turbulence Profiles								
			U	V or W	$\overline{u^2}$	$\overline{v^2}$	$\overline{w^2}$	\overline{uv}	Others				
Case 0261 Various data takers		> 0	Yes	-	Yes	Yes	Yes	Yes	Inter- mit- tency, Triple, quad- ruple velocity corre- lations	Reactor blade	4×10 ³ to 5×10 ⁴		Equilibrium wall jet in adverse pressure gradient.

Plot	Ordinate	Abscissa	Range/Position	Comments
1	$dy_{1/2}/dx$	U_E/U_m	$0 \leq U_E/U_m \leq 0.8$	See Instruction 3 below.
2	dy_m/dx	U_E/U_m	$0 \leq U_E/U_m \leq 0.8$	See Instruction 3 below.
3	$\frac{U - U_E}{U_m - U_E}$	$y/y_{1/2}$	$0 \leq y/y_{1/2} \leq 2.0$	$U_E/U_m = 0.38.$
4	$uv/(U_m - U_E)^2$	$y/y_{1/2}$	$0 \leq y/y_{1/2} \leq 2.2$	$U_E/U_m = 0.38.$
5	$\frac{(\overline{u^2})^{1/2}}{U_m - U_E}$	$y/y_{1/2}$	$0 \leq y/y_{1/2} \leq 2.5$	$U_E/U_m = 0.38.$
6	$\frac{(\overline{v^2})^{1/2}}{U_m - U_E}$	$y/y_{1/2}$	$0 \leq y/y_{1/2} \leq 2.5$	$U_E/U_m = 0.38.$
7	$\frac{(\overline{w^2})^{1/2}}{U_m - U_E}$	$y/y_{1/2}$	$0 \leq y/y_{1/2} \leq 2.0$	$U_E/U_m = 0.38.$
8	$\frac{\overline{u^3}}{(U_m - U_E)^3}$	$y/y_{1/2}$	$0 \leq y/y_{1/2} \leq 2.0$	$U_E/U_m = 0.38.$
9	$\frac{\overline{uv^2}}{(U_m - U_E)^3}$	$y/y_{1/2}$	$0 \leq y/y_{1/2} \leq 2.0$	$U_E/U_m = 0.38.$
10	$\frac{\overline{v^3}}{(U_m - U_E)^3}$	$y/y_{1/2}$	$0 \leq y/y_{1/2} \leq 2.0$	$U_E/U_m = 0.38.$

Plot	Ordinate	Abscissa	Range/Position	Comments
11	$\log_{10} C_f$	$\log_{10} \left(\frac{U_m y_m}{\nu} \right)$	$3.5 \leq \log_{10} \left(\frac{U_m y_m}{\nu} \right) \leq 4.5$ $U_E = 0.$	See Instruction 4 below.

Special Instructions:

1. Nomenclature is defined on Fig. 1 of Summary, Flow 0260.
2. This test case considers the family of equilibrium wall jets on a plane surface in which the free-stream velocity is retarded by an adverse streamwise pressure gradient whose magnitude is adjusted to keep the ratio of free stream:maximum velocity invariant with x . Patel and Newman (1961) have demonstrated that the above conditions are met when

$$U_E = (x + x_0)^m \quad [1]$$

where x_0 is the effective origin of the flow and $-0.5 < m < -1/3$. The range of explorations is to include the wall jet in a stationary medium which is a limiting case of this family (for which $U_E/U_m = 0$ and $dp/dx = 0$).

3. Computers should calculate the wall-jet development for at least five values of U_E/U_m between zero and 0.8, including the values 0 and 0.38. There is a (very) weak effect of Reynolds number on the flow, and computers should ensure that the Reynolds number based upon the maximum velocity ($U_m y_m / \nu$) lies in the range 4×10^3 to 5×10^4 , which corresponds approximately to that of the experimental data.

For each set of flow conditions, start at the jet exit, $x = 0$, with an appropriate initial profile. Continue computations until self-similarity is achieved. Plot the computed linear growth of $y_{1/2}$ (Plot 1) and y_m (Plot 2) versus U_E/U_m on the accompanying figures. The figure already contains values by Irwin (1973), Gartshore and Newman (1969), and the value for the wall jet in stagnant surroundings recommended in the survey by Launder and Rodi (1960).

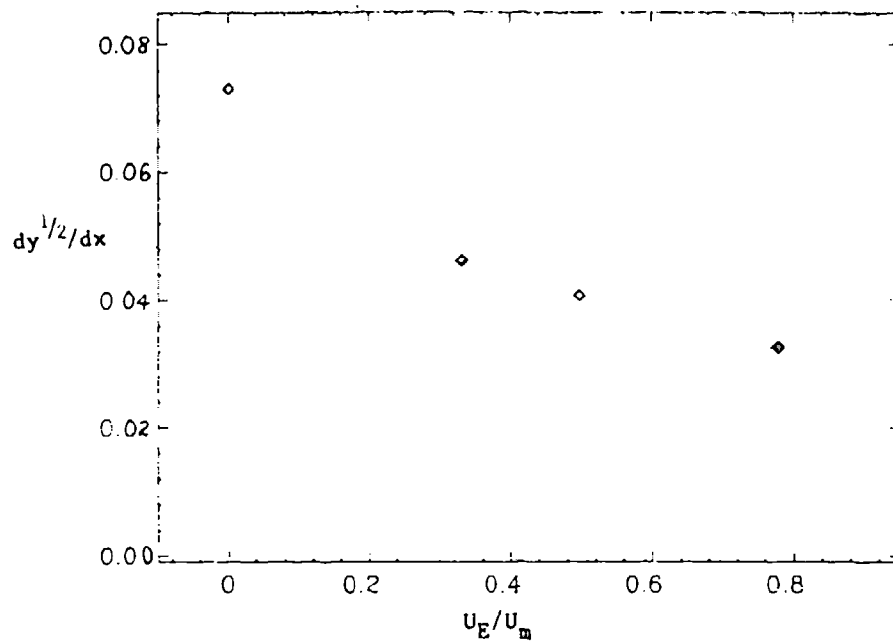
4. For the case where the external stream is at rest, calculated values of skin-friction coefficient $c_f (\equiv \tau_w / \frac{1}{2} \rho U_m^2)$ should be compared with the proposal of Bradshaw and Gee (1960):

$$c_f = 0.0315 \left(\frac{U_m y_m}{\nu} \right)^{-0.182} \quad [2]$$

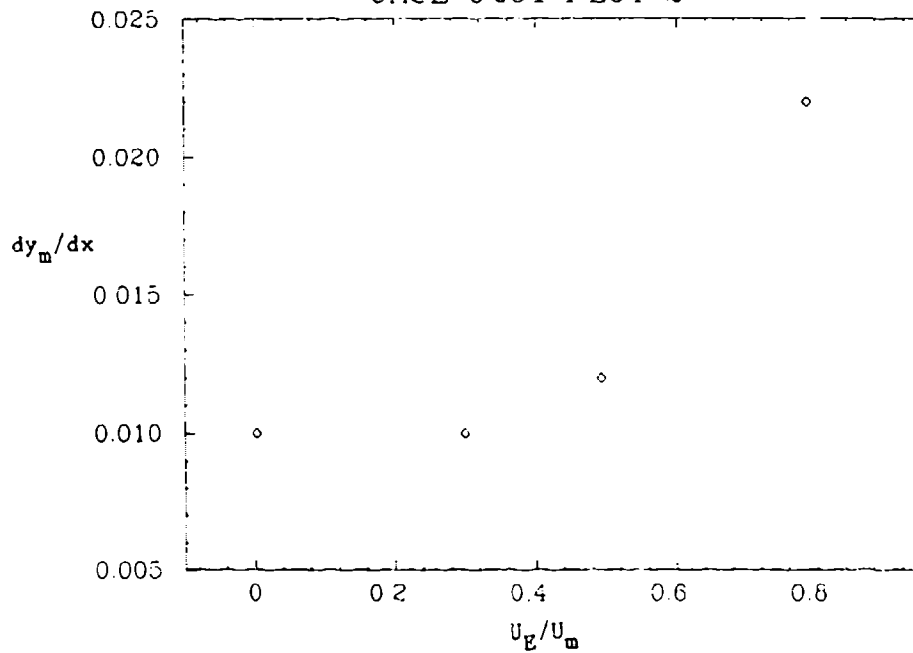
References (see also Summary)

- Irwin, H. P. A. H. (1973). "Measurement in a self-preserving plane wall jet in a positive gradient," J. Fluid Mech., 61, 33.
- Patel, R. P., and B. G. Newman (1961). "Self-preserving jets and wall jets in a moving stream," Report AE5, Mech. Engr. Dept., McGill University, Montreal.

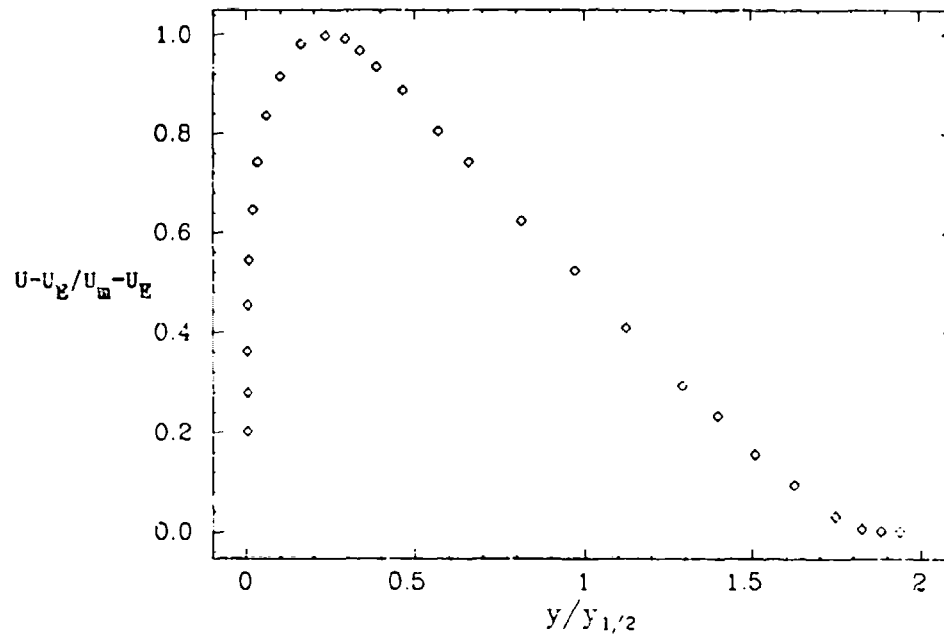
CASE 0261 PLOT 1



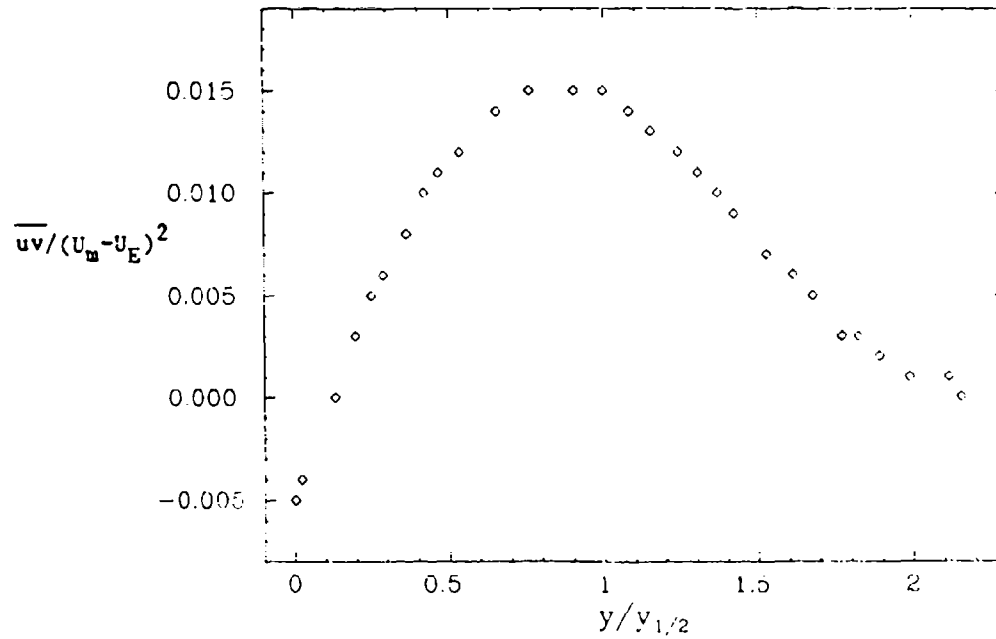
CASE 0261 PLOT 2



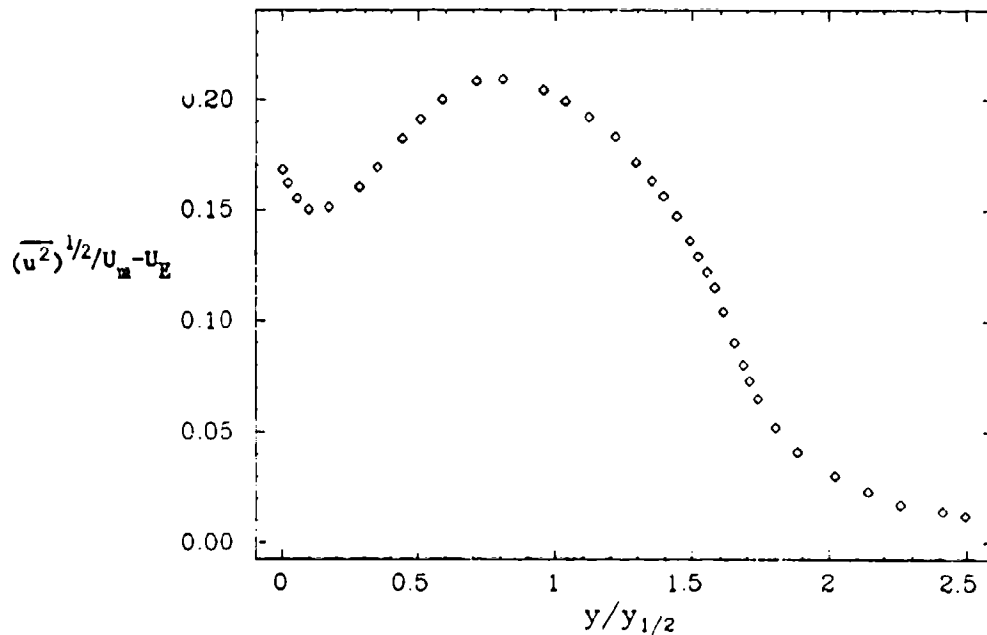
CASE 0261 PLOT 3



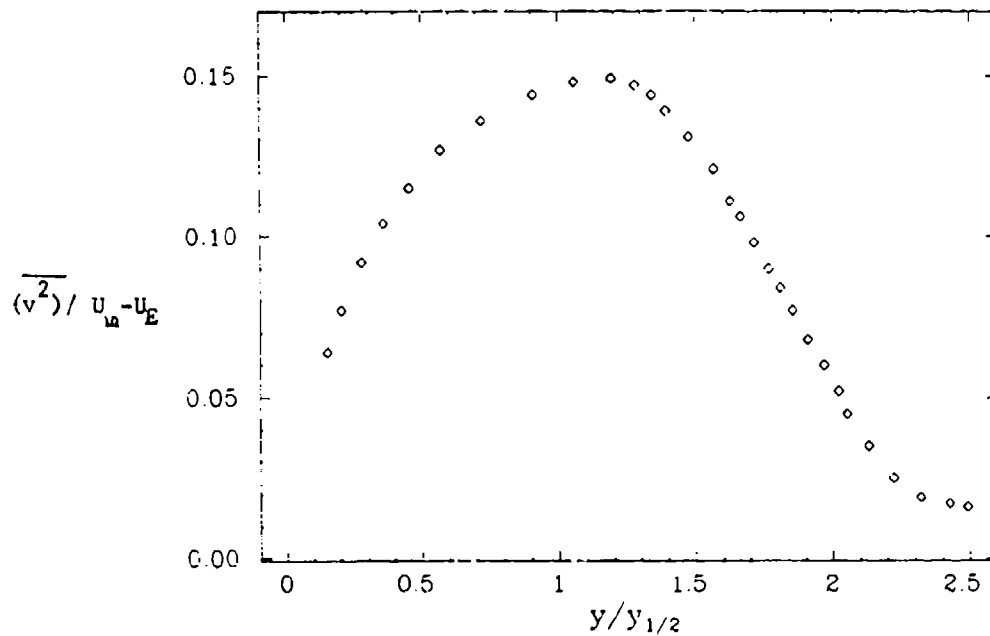
CASE 0261 PLOT 4



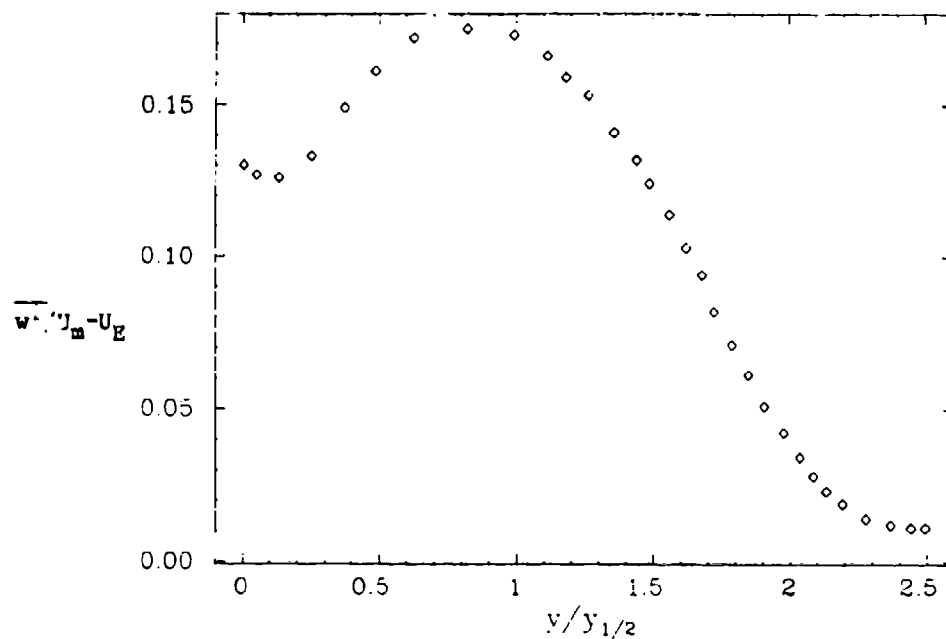
CASE 0261 PLOT 5



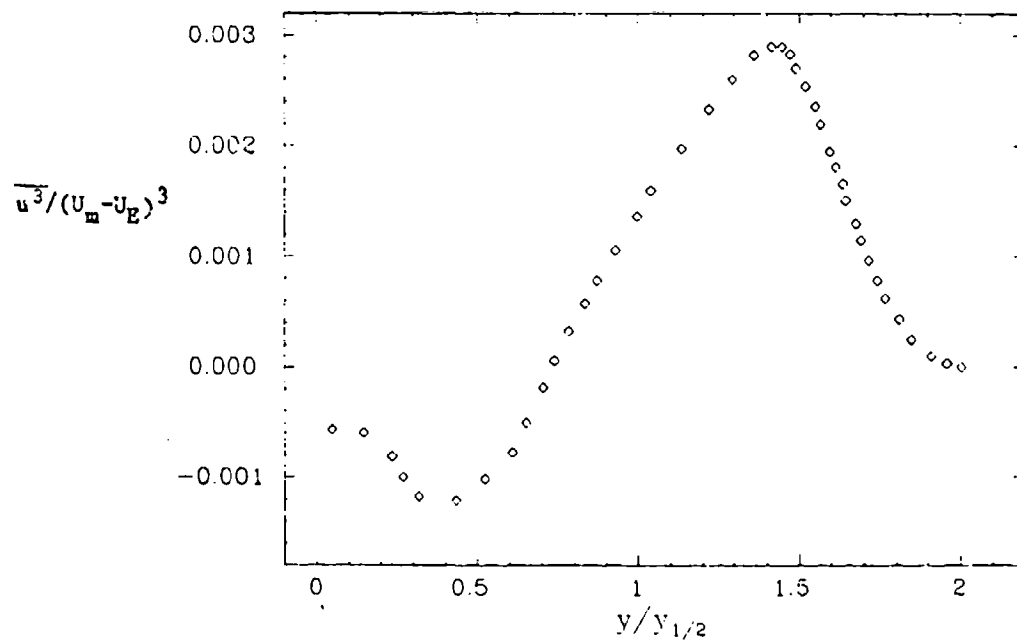
CASE 0261 PLOT 6



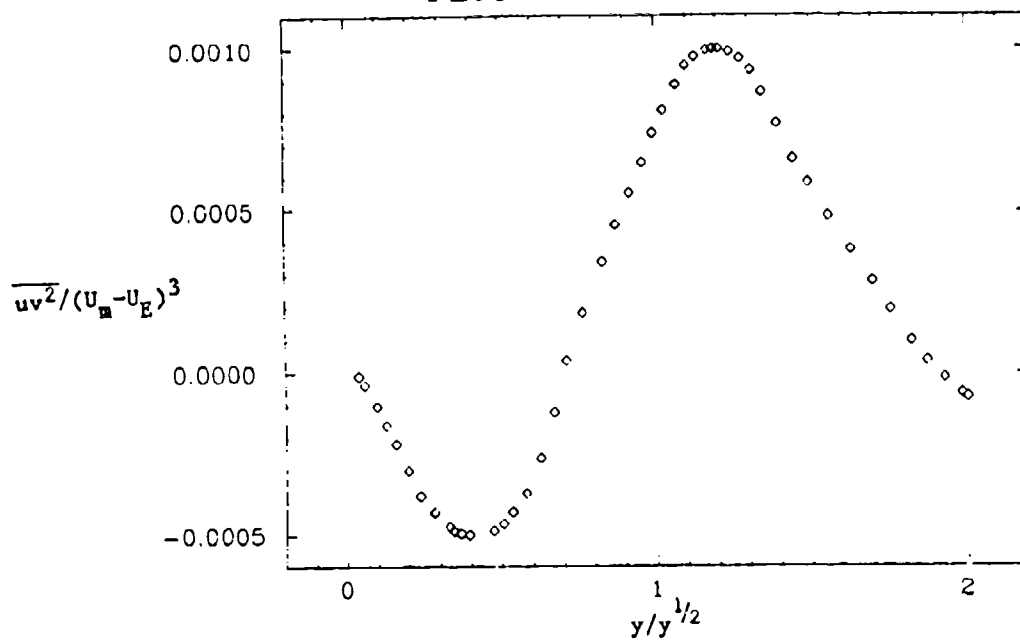
CASE 0261 PLOT 7



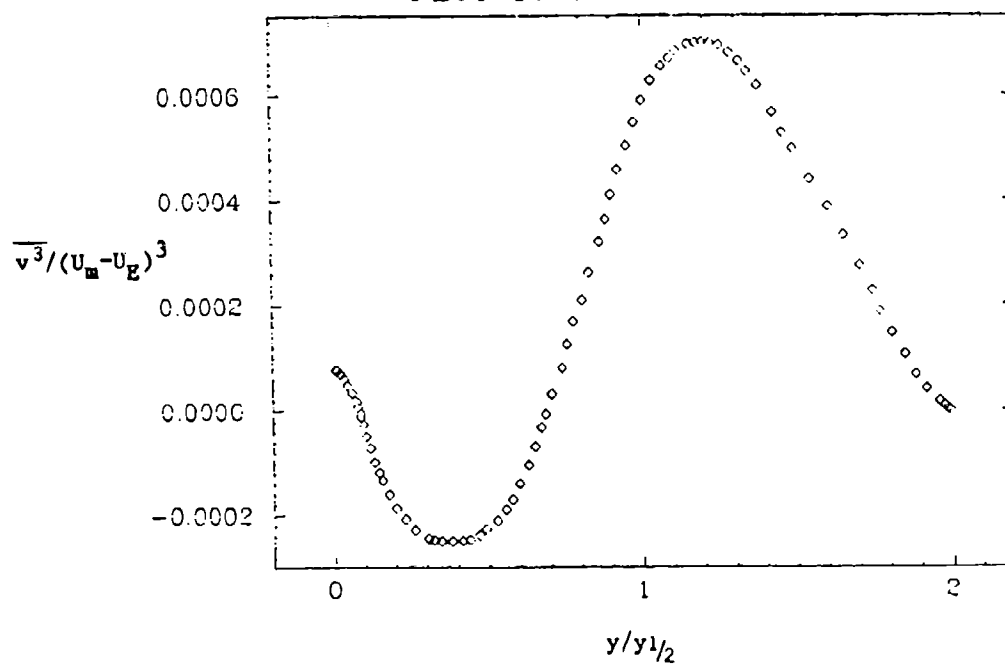
CASE 0261 PLOT 8



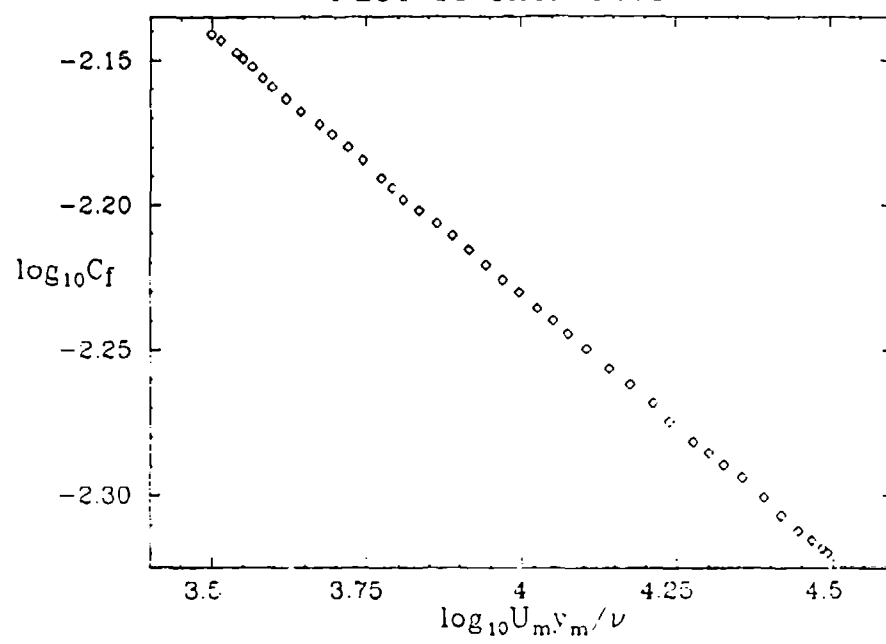
PLOT 9 CASE 0261



PLOT 10 CASE 0261



PLOT 11 CASE 0261



SPECIFICATIONS FOR COMPUTATION

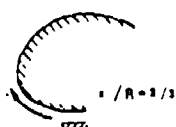
ENTRY CASE/INCOMPRESSIBLE

Case #0263; Data Evaluators: B. Launder and W. Rodi

Data Takers: D. Guitton and B. Newman

PICTORIAL SUMMARY

Flow 0260. Data Evaluators: B. Launder and W. Rodi. "Turbulent Wall Jet."

Case Date Taker	Test Rig Geometry	dp/dx or C _p	Number of Stations Measured								C _f	Re	Initial Condi- tion	Other Notes
			Mean Velocity		Turbulence Profiles									
			U	V or W	$\overline{u^2}$	$\overline{v^2}$	$\overline{w^2}$	\overline{uv}	Others					
Case 0263 D. Guitton B. Newman		-	Yes	-	Yes	Yes	-	Yes	K		7×10^3 to 5×10^4 (based on slot height)		Self-preserving wall jet on logarithmic spiral surface.	

Plot	Ordinate	Abscissa	Range/Position	Comments
1	$y_{1/2}/x$	$y_{1/2}/R$	$0 \leq y_{1/2}/R \leq 0.3$	See Instruction 2.
2	\overline{uv}/U_m^2	$y/y_{1/2}$	$0 \leq y/y_{1/2} \leq 2.0$	See Instruction 3; $K = 2/3$.
3	$\overline{u^2}/U_m^2$	$y/y_{1/2}$	$0 \leq y/y_{1/2} \leq 2.0$	See Instruction 3; $K = 2/3$.
4	$\overline{v^2}/U_m^2$	$y/y_{1/2}$	$0 \leq y/y_{1/2} \leq 1.2$	See Instruction 3; $K = 2/3$.
5	$2k/U_m^2$	$y/y_{1/2}$	$0 \leq y/y_{1/2} \leq 1.1$	See Instruction 3; $K = 2/3$. $2k = u^2 + v^2 + w^2$.

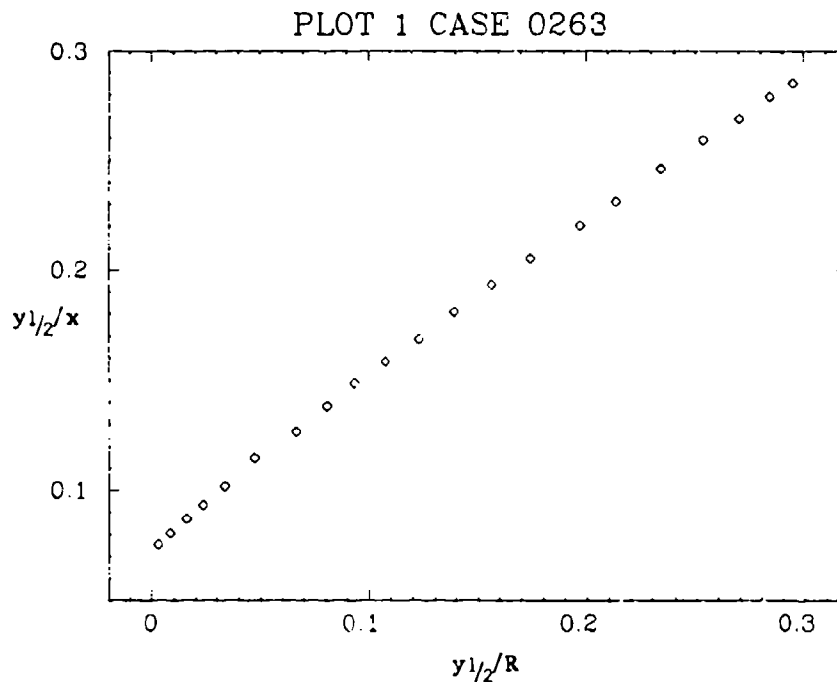
Special Instructions:

1. Nomenclature shown on Fig. 1 of Summary above, Flow 0260.
2. Computations should be made of the development of the two-dimensional wall jet over logarithmic spiral surfaces ($x/R = K$, a constant) for at least three values of K in the range 0-1.2, including the value 2/3. The coordinate x is measured along the wall surface from the virtual origin (i.e., where the radius of curvature R is zero). Interest is confined to the self-preserving state so that computations should extend until the normalized profiles of flow variables cease to change. The dependence of the growth rate of the wall jet should be displayed by plotting $y_{1/2}/x$ versus $y_{1/2}/R$ and comparing the calculated behavior with Plot 1; this plot displays the equation:

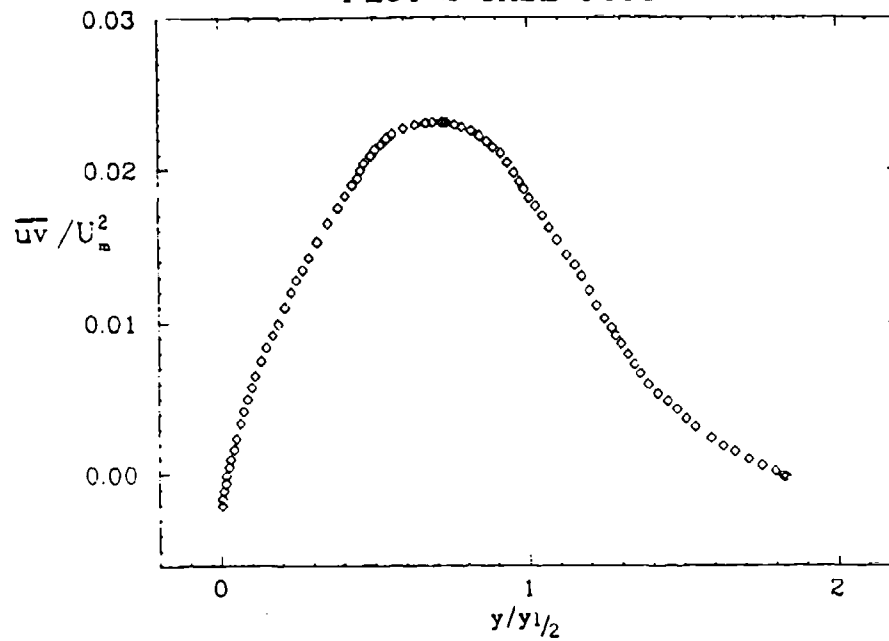
$$y_{1/2}/x = 0.073 + 0.8y_{1/2}/R - 0.3(y_{1/2}/R)^2$$

which fits the experimental data of Guitton and Newman (1977; see Summary). Although no Reynolds-number dependence is discernible in the data, computers should arrange that the Reynolds number, $U_m y_m / \nu$, in the asymptotic region lies in the range $7 \times 10^3 - 5 \times 10^4$.

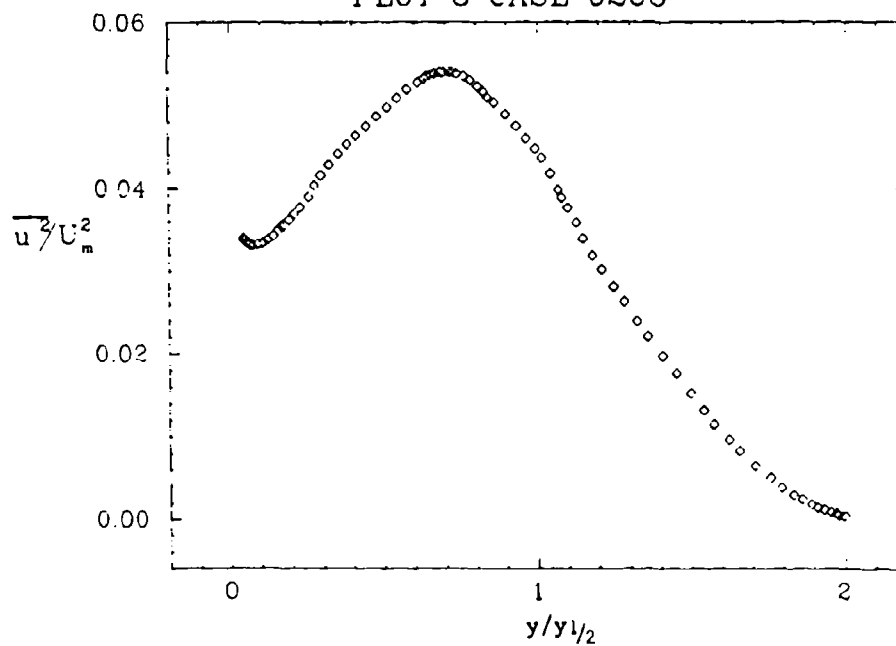
3. For $K = 2/3$, detailed comparisons should be made with the Guitton-Newman results, of which the profiles averaged over the final three measuring stations are provided on the accompanying graphs. Compare calculated and measured distributions of normalized Reynolds shear stress, UV/U_m^2 and, if provided by the calculation method, the normal stresses u^2/U_m^2 , v^2/U_m^2 , and $2k/U_m^2$. (k denoting the turbulence kinetic energy.)



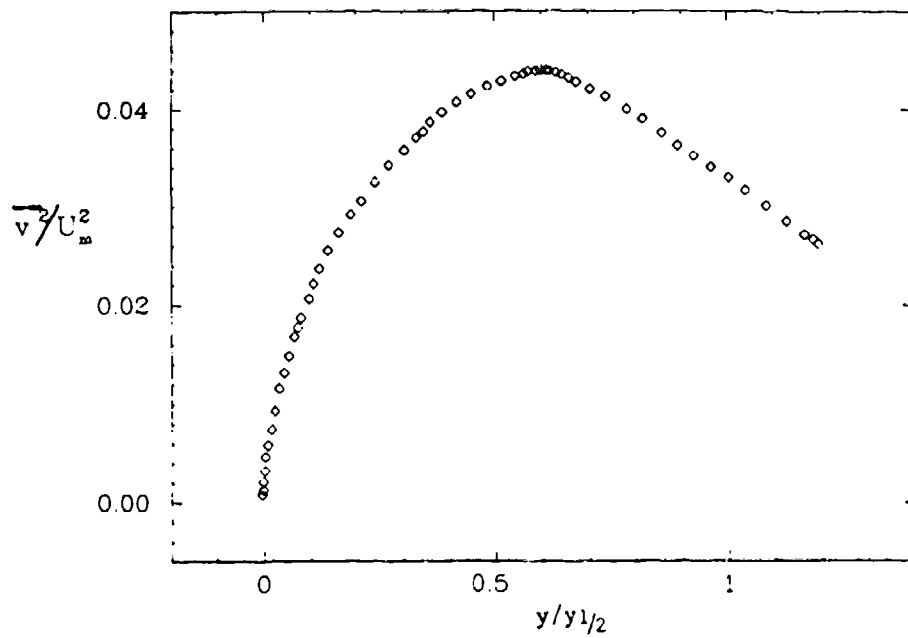
PLOT 2 CASE 0263



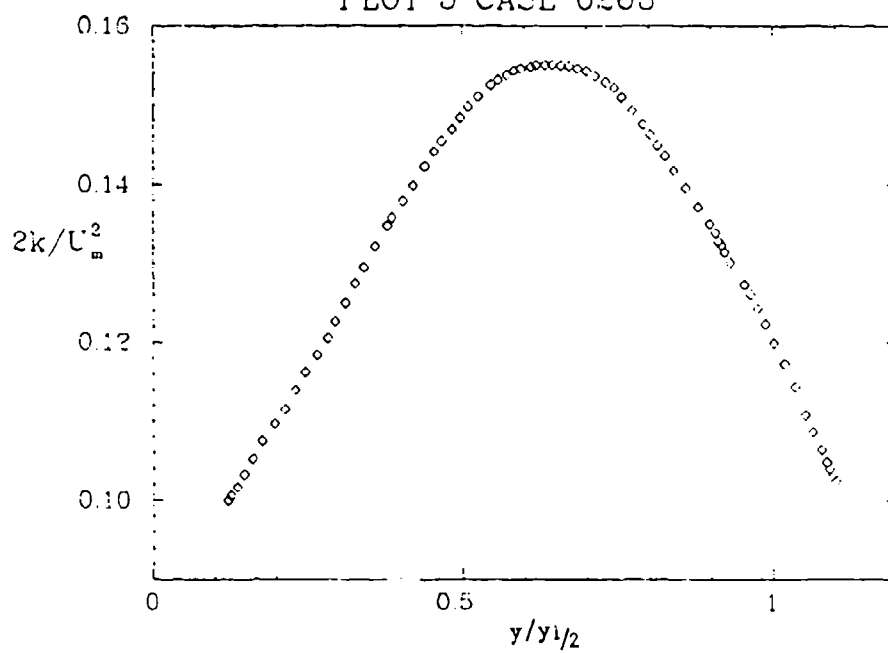
PLOT 3 CASE 0263



PLOT 4 CASE 0263



PLOT 5 CASE 0263



SPECIFICATIONS FOR COMPUTATION

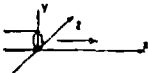
ENTRY CASE/INCOMPRESSIBLE

Case #0264; Data Evaluators: B. Launder and W. Rodi

Data Takers: Various

PICTORIAL SUMMARY

Flow 0260. Data Evaluators: B. Launder and W. Rodi. "Turbulent Wall Jet."

Case Data Taker	Test Rig Geometry	C_L/Lx or C_p	Number of Stations Measured								C_f	Re	Initial Condi- tion	Other Notes
			Mean Velocity		Turbulence Profiles									
			U	V or W	$\overline{u^2}$	$\overline{v^2}$	$\overline{w^2}$	\overline{uv}	Others					
Case 0264 Various Data Takers		-	Yes	-	-	-	-	-	-	-	$> 10^4$	Self-similar	3D wall jet in still air on plane surface. No output plots required.	

Plot	Ordinate	Abscissa	Range/Position	Comments
0				For this case, no plots are needed. Output consists of constants; see comments below.

Special Instructions:

- The flow configuration and the nomenclature are shown in Fig. 2 of the Summary, Flow 0260. Sufficiently far from the nozzle exit, the flow becomes self-similar and independent of the exact exit conditions. In this similarity region, the jet spreads linearly both normal to the wall and in the spanwise direction, so that $dy_{1/2}/dx$ and $dz_{1/2}/dx$ are constant; further U_m decays approximately as x^{-1} .

Computors should calculate the spreading rates $dy_{1/2}/dx$ and $dz_{1/2}/dx$ for the self-preserving state and compare them with the measured values recommended by the survey by Launder-Rodi (1980):

$$\frac{dy_{1/2}}{dx} = 0.248, \quad \frac{dz_{1/2}}{dx} = 0.26 \quad [1]$$

Equation [1] corresponds closely to the measurements of Newman et al. (1972). Although no clear Reynolds-number effect was discerned in the experiments, computors should make the calculations with a slot Reynolds number $U_m b/\nu$ of 10^4 or greater. The nozzle shape should have no influence on the self-preserving state, but the recommendation to computors is to consider the jet issuing from a square nozzle as shown in Fig. 2 of the Summary, Flow 0260. Computors may solve either the self-preserving form of the equations (in which properties are assumed to be functions only of (y/x) and (z/x) or march in the stream direction until a self-preserving state is reached.

SESSION IX

Chairman: S. Bogdonoff

Technical Recorders:

P. Eibeck
T. Morel



Flow 8610

Flow 8630

Flow 8640

Flow 8680

COMPRESSIBLE FLOWS OVER DEFLECTED SURFACES

Flows 8610, 8630, 8640

Cases 8611, 8612, 8631, 8632, 8641

Evaluators: M. W. Rubesin* and C. C. Horstman*

SUMMARY

SELECTION CRITERIA AND FLOWS SELECTED

The experiments treated in this summary are characterized by flow fields resulting from the interaction of fully turbulent boundary layers with shock or expansion waves generated by the shape of the test surface itself. The experiments selected as test cases are reported in detail in Dussauge and Gaviglio (1980); Bachalo and Johnson (1979); Delery and Le Dizet (1979); Settles et al. (1976); and Settles et al. (1980). In this summary each of these experiments will be described in view of the needs of a computer, and specifications will be given for presenting the output of the computations.

Even the best of these experiments cannot be used to guide improvements in turbulence-closure models. They do, however, provide a means of assessing the overall performance of particular computational methods and specific, pre-existing turbulence models. One reason these experiments are limited is that they are conducted within compressible flow facilities that are so small as to preclude measurements within the important sub- and buffer-layers of the boundary layers. Another reason is the greater inaccuracies of compressible-flow measurements. The reduction of hot-wire data requires additional assumptions to account for density fluctuations, and LDV systems suffer from small windows and from seeding nonuniformities. The high speeds of the air adds a burden on the frequency response of the sensing systems. It has been estimated that none of the experiments can provide measurement of local fluctuating quantities better than $\pm 5\%$ to $\pm 15\%$. Nonetheless, the technological importance of prediction for complex turbulent fields in compressible flows requires an assessment of the existing turbulence modeling and computational schemes; the data selected can serve this purpose.

Selection of each particular experiment was made on the basis of: uniqueness of the configuration studied; the largest range of variables over which the experiment was conducted; and the variety and number of quality data. To qualify, the experiment had to have a well-defined flow: e.g., if nominally a two-dimensional experiment, the two-dimensionality had to be well documented. The accuracy of the selected

*NASA-Ames Research Center, Moffett Field, CA 94035.

experiments was estimated from these sources: (1) comparing the results with data from similar experiments; (2) the experimenters' own estimates of accuracy; (3) a judgment of the accuracies of particular instrumentation based on the evaluator's experience with similar instrumentation.

Cases 8611, 8612. Transonic Flows Over an Axisymmetric Bump and Two-Dimensional Bump

A bump on the surface of a model, or on a wind-tunnel wall, in transonic flow produces an acceleration over the bump that terminates with a shock wave. At sufficiently high Mach numbers, the strength of this shock wave can be sufficient to separate the turbulent boundary layer flowing over the bump. Since the flow over a bump resembles a flow on an aircraft wing, understanding of such configurations are very important technologically. Of course, the flow fields on the bump and on the wing differ significantly in that reattachment occurs on the surface of the former and in the wake of the latter. "Reattachment" in a wake can be thought of as the location beyond which downstream motion occurs everywhere. The primary advantage of a bump over an airfoil as a test model for fluid mechanics is that the bump can usually be made to produce thicker, more-easily-probed boundary layers. These thicker boundary layers, however, accentuate streamline curvature effects, which may or may not be desired depending on the objectives of a particular experiment.

Case 8611 is an experiment by Bachalo and Johnson (1979). The experiment is described in Fig. 1. The axisymmetry of the model has the advantages that it avoids interactions of the generated shock wave with the boundary layers on the wind-tunnel walls at the sides of the test zone and at zero angle of attack assures two-dimensional flow.

Case 8612 is an experiment by Delery and Le Duizet (1979), who employ a two-dimensional bump placed on the bottom wall of a wind tunnel. The experiment is described in Fig. 2. Although the shock wave generated by the bump interacts with the side-wall boundary layers, the flow remains largely two-dimensional. The shock wave extends rather close to the top wall of the tunnel and may cause some choking. Computers may have to include the top wall in their computational domain for this case.

Both Cases 8611 and 8612 feature the use of LDV systems and provide mean- and turbulence-moment information in the x and y directions. It is urged that computers use both Cases 8611 and 8612 to determine if their turbulence model can accommodate transverse curvature in thick shear layers.

Case 8631. Attached and Separated Compression Corner (Settles et al., 1976, 1979).

This experiment deals with ramps placed on the bottom walls of a wind tunnel to create shock waves that interfere with the wall boundary layer. Increases in ramp angle strengthen the shock wave to the point where the boundary layer separates. Figure 3 shows the experimental configuration and indicates the measurements that were

made. The ramp did not extend to the side walls, and had fences at its sides. Oil flow showed the flow be mostly two-dimensional. Although the measurements indicated are confined to mean quantities only, it is understood that turbulence quantities are to be measured soon with hot wires.

Case 8632. Expansion Interaction at Supersonic Speed (Dussauge and Gaviglio, 1986).

The flow field investigated in this experiment occurs on the wall of a wind tunnel suddenly deflected outwardly by an angle of 12° . The pertinent geometric details, the flow conditions, and the quantities measured in this experiment are shown in Fig. 4. This experiment is particularly suited to assess the use of mass-weighted dependent variables in the turbulence-transport equations in that the boundary layer is rapidly changed between two Mach number states without introducing the complexities of separation. Rapid dilatation emphasizes terms of the mass-weighted turbulence-transport equations that have no counterpart in incompressible flow (Wilcox and Alber, 1972; Rubesin, 1976), but are usually neglected. Also, first-order boundary-layer methods may be severely tested by the static-pressure gradient that occurs normal to the deflected surface.

Case 8641. Reattaching Planar Free-Shear Layer (Supersonic) (Settles et al., 1980)

This flow field is similar to Flow 8631 except that the ramp is preceded by a cavity in the plate on which the turbulent boundary layer is generated. The experiment is described in Fig. 5. By carefully adjusting the length of the cavity, the experimenters achieved a separation at the upstream edge of the cavity that did not disturb the boundary layer ahead of the separation and created a free-shear layer with a dividing streamline that remained essentially in the free-stream direction. This eliminates streamline-curvature effects near the maximum shear region of the free-shear layer. Just upstream of reattachment, the free-shear layer achieved mean-velocity equilibrium, although preliminary tests of the turbulence do not show a corresponding equilibrium. The experiment emphasizes reattachment and the re-equilibration processes that occur downstream.

RECOMMENDATIONS FOR FUTURE DATA TAKERS

Of the five experiments recommended here for computation, only those dealing with transonic flow over a bump employ the nonintrusive LDV instrument systems. In separated regions, these systems do not suffer from directional ambiguities of hot wires or the questionable accuracy of reversed pitot tubes. It is important, however, that redundant measurements be made with other types of probes, where they are appropriate. One such experiment (Ardonceanu et al., 1979) found differences between velocities measured by pitot tubes and LDV so large as to bring into question the data of a carefully thought-out experiment. One recommendation, then, is that future data takers

should use redundant instrumentation and if possible resolve the differences that occur. Other recommendations are as given in the Summary on Shock-Wave Boundary-Layer Interaction Flows (Cases 8651, 8661, 8601, and 8691).

Editors' Note: For other important comments on data needs and instrument accuracy, see also the following in this volume: (i) "Experimental Data Needs for Computational Fluid Dynamics" by Bradshaw et al., a position paper; (ii) reports of ad-hoc committees on accuracy of hot-wire data and difficulties in compressible flow measurements; (iii) comments concerning difficulty in measuring reversing flows by J. K. Eaton and others in Flow 0420 and by R. Simpson for Flow 0430; (iv) the editor's comment by S. J. Kline on the general nature of accuracy control and uncertainty analysis in compressible flows--a footnote to general comment 1 in the discussion of Flows 8610, 8630, and 8640.

REFERENCES

- Ardonceanu, F., D. H. Lee, T. Alziary de Roquefort, and R. Goethals (1979). "Turbulence behavior in a shock wave/boundary layer interaction," AGARD Conference on Turbulent Boundary Layers - Experiments, Theory, and Modelling, AGARD-CP-271 (September).
- Bachalo, W. D., and D. G. Johnson (1979). "An investigation of transonic turbulent boundary layer separation generated on an axisymmetric flow model," AIAA Paper 79-1479, Williamsburg, VA (July).
- Delery, J., and P. Le Dizet (1979). "Découlement résultant d'une interaction onde de choc/couche limite turbulente," T.P. No. 1979-146, ONERA.
- Dussauge, J. P., and J. Gaviglio (1980). "Turbulent boundary layer/expansion interaction at supersonic speed," Travaux de l'I.M.S.T. LA, No. 130 au CNRS Contrats ONERA, Institute de Mécanique Statistique de la Turbulence, Université de Aix-Marseille II (June).
- Rubesin, M. W. (1976). "A one-equation model of turbulence for use with the compressible Navier-Stokes equations," NASA TMX-73 (April).
- Settles, G. S., S. M. Bogdonoff, and I. E. Vas (1976). "Incipient separation of a supersonic turbulent boundary layer at high Reynolds numbers," AIAA Jou., 14, 50-56 (January).
- Settles, G. S., T. J. Fitzpatrick, and S. M. Bogdonoff (1979). "Detailed study of attached and separated compression corner flow fields in high Reynolds number supersonic flow," AIAA Jou., 17, 579-585 (June).
- Settles, G. S., B. K. Baca, D. R. Williams, and S. M. Bogdonoff (1980). "A study of reattachment of a free shear layer in compressible turbulent flow," Princeton University, AIAA-80-1408, AIAA 13th Fluid & Plasma Dynamics Conference, July 14-16, 1980, Snowmass, CO.
- Wilcox, D. C., and I. E. Alber (1972). "A turbulence model for high speed flows," Proceedings of the 1972 Heat Transfer and Fluid Mechanics Institute, Stanford University Press, pp. 231-252.

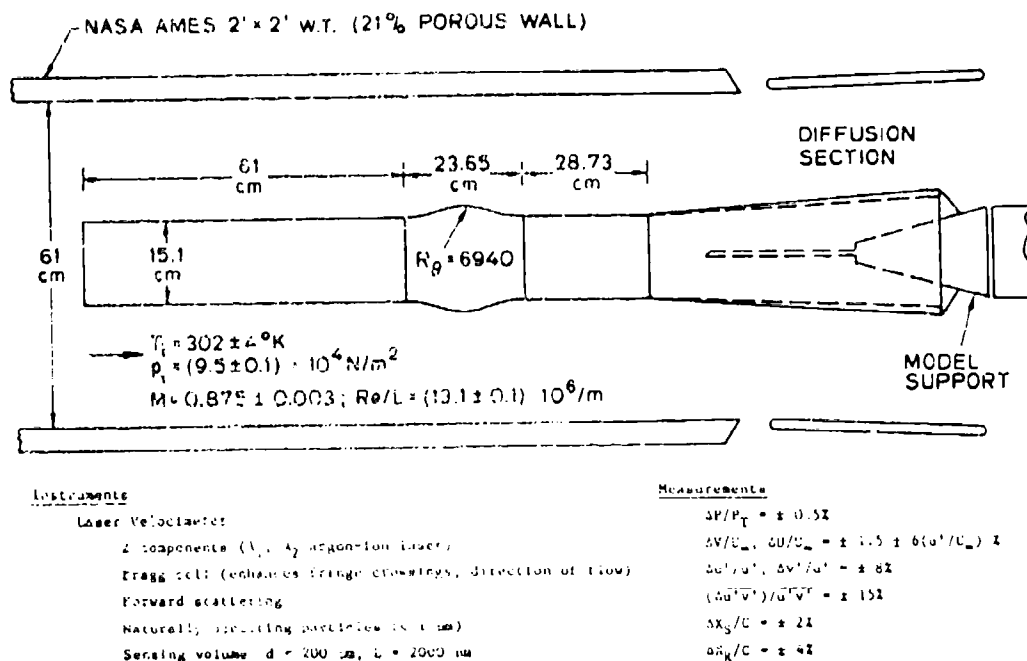


Figure 1. Test apparatus, Case 8611.

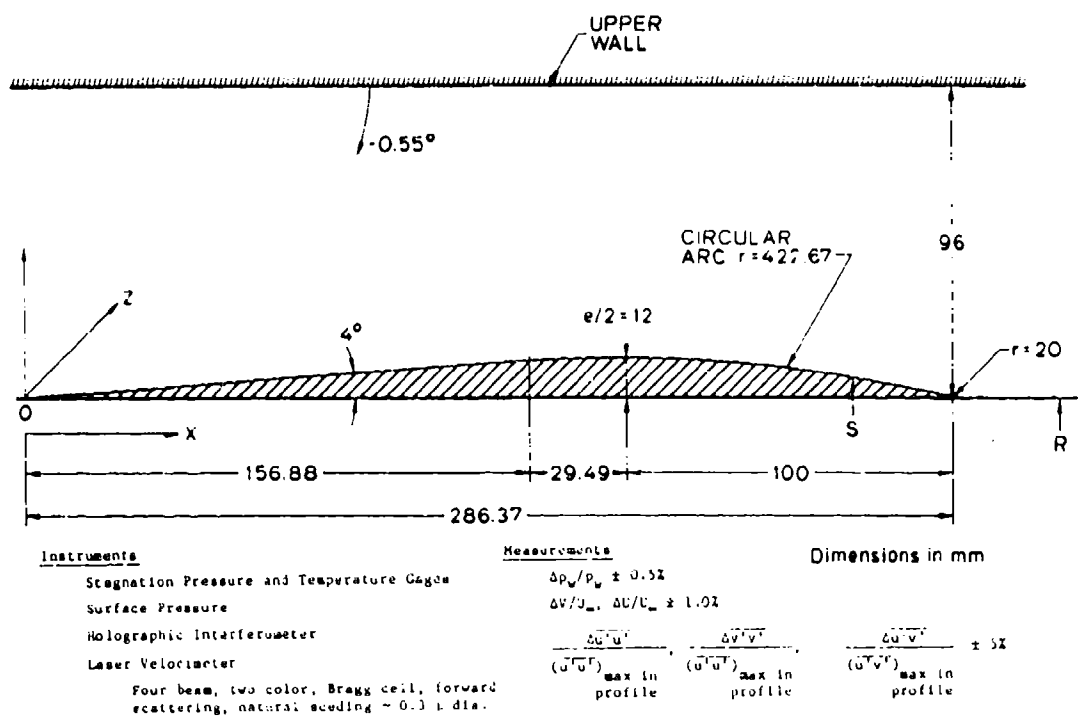
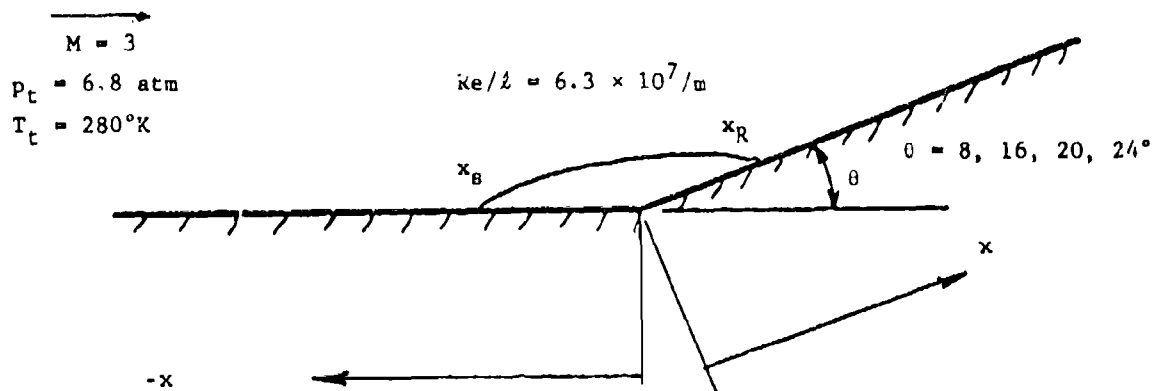


Figure 2. Test Configuration, Case 8612.



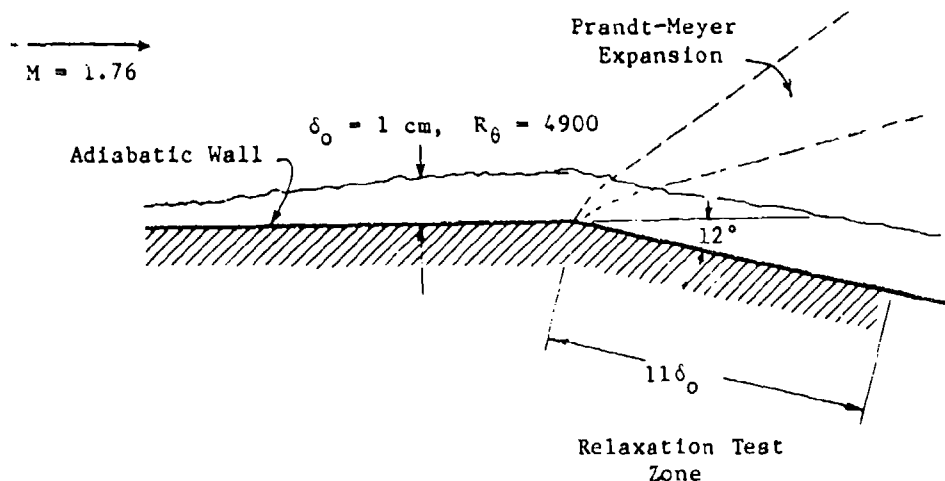
Instrumentation

Pitot tube, reverse Pitot tube
 Static pressure probe
 Total temperature hot-wire probe
 Shadowgraph, schlieren

Measurements

$\Delta P_{t2}/P_{t2} = \pm 2\%$
 $\Delta P/P = \pm 4\%$
 $\Delta T_t/T_t = 1.5\%$
 $\Delta U/U = \pm 5\%$

Figure 3. Case 8631 (Settles et al., 1979).



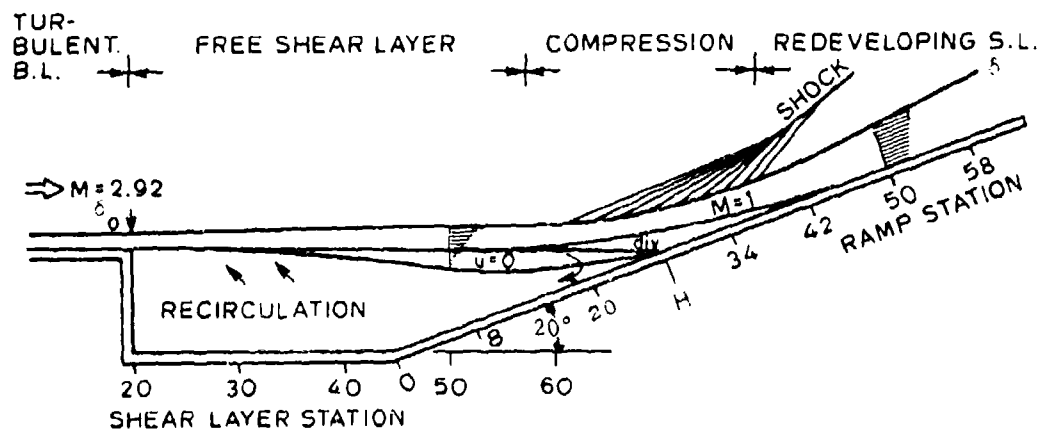
Instrumentation

Pitot pressure tube
 Static pressure probe (supplemented by method of characteristics)
 Hot-wire stagnation temperature probe, $0.5 \mu \text{ dia}, L/d = 300$
 Hot-wire $2.5 \mu \text{ dia}, L/d = 320$

Measurements

$\rho, U, V, T \pm 1\%$
 $\overline{u^2}, \overline{T'^2}, R_{TU} \pm 10\%$ along a streamline
 C_f van Driest transformed u , "law-of-the-wall" plot, $\kappa = 0.41$

Figure 4. Test configuration, Case 8632.



Instrumentation

Pitot Probe

Static Pressure Probe

Hot-Wire Total Temperature Probe

Hot-Wire (Normal) 5 μ dia, $L/d = 200$

Measurements

$\Delta p/p = \pm 4\%, \pm 10\% @ R$

$\Delta T_t/T_t = 0.5\%$

$\Delta(\rho u)' / (\rho u)' = ?$

Figure 5. Test configuration for Case 8641.

DISCUSSION

Flows 8610, 8630, 8640

Flow 8610--Transonic flow over a bump.

Case 8611--The Conference accepted this case as recommended by the evaluators.

Case 8612--The Conference accepted this case but recommended it be treated as a channel flow because the interaction with the top wall is considered an essential feature of this flow.*

Flow 8630--Compressible flow over deflected surfaces.

Case 8631/2--The Conference accepted these cases as recommended by the evaluators.

Flow 8640--Compressible flow over compression corner with reattaching planar shear layer.

Case 8641--The geometry of this flow case is similar to Case 8631 but is at a different Mach number. It was accepted by the Conference, although it was hoped that fluctuating measurements will be made and supplied to the data bank in the near future.

General Comments

1. H. V. Meier (DFVLR): How can you rely on an accuracy of 15% for skin-friction measurements if there are no independent checks on that value? In my experience the accuracy of skin-friction measurements made with a Preston tube is more like $\pm 100\%$.

Response: The view of the experimenters was that their C_f values, as measured, were within 15% of the local value. The Conference felt that further discussion of the problem of C_f measurement in compressible flows is needed to reach a consensus on the true state of affairs.[†]

2. Another topic was that concerning the specification of the upstream conditions. It was concluded that the preferred procedure was to let the computer pick his own starting conditions so that he matches reasonably well the data at the first station as provided from the data set.

*[Ed.: This comment has been incorporated into the specifications.]

[†]Comment added in editing by S. J. Kline: Dr. Meier's skepticism is not unfounded, in my view. The discussion during the meeting revealed the fact that the aeronautics community, unlike some others, has not normally reported uncertainty values in measured data. As a result, the uncertainties are sometimes higher than recognized. Also the uncertainties in this volume have been estimated by M. Rubesin and C. Horstman after the fact for most of the compressible flows. Such estimates are better than no values for uncertainty, but are less satisfactory than estimates made by the data takers, and far less satisfactory than initial control estimates followed by closing the loop to insure experimental control as recommended in the paper by R. J. Moffat in this volume. It is my opinion that if the desired goals of accuracy in data as a basis for modeling and for checking computational outputs for compressible flows, as set forth by M. Rubesin and C. Horstman at several places in this volume are to be achieved, it will be absolutely necessary to incorporate systematic use of uncertainty analysis including feedbacks to check experimental control as suggested by Moffat and also to use redundant instruments. This is clearly a topic that deserves much further careful attention by the research community concerned with compressible flows.

SPECIFICATIONS FOR COMPUTATION


ENTRY CASE/COMPRESSIBLE

Flow 8610, Case #8611; Data Evaluators: M. Rubesin and C. Horstman

Data Takers: W. Bachalo and D. Johnson

PICTORIAL SUMMARY

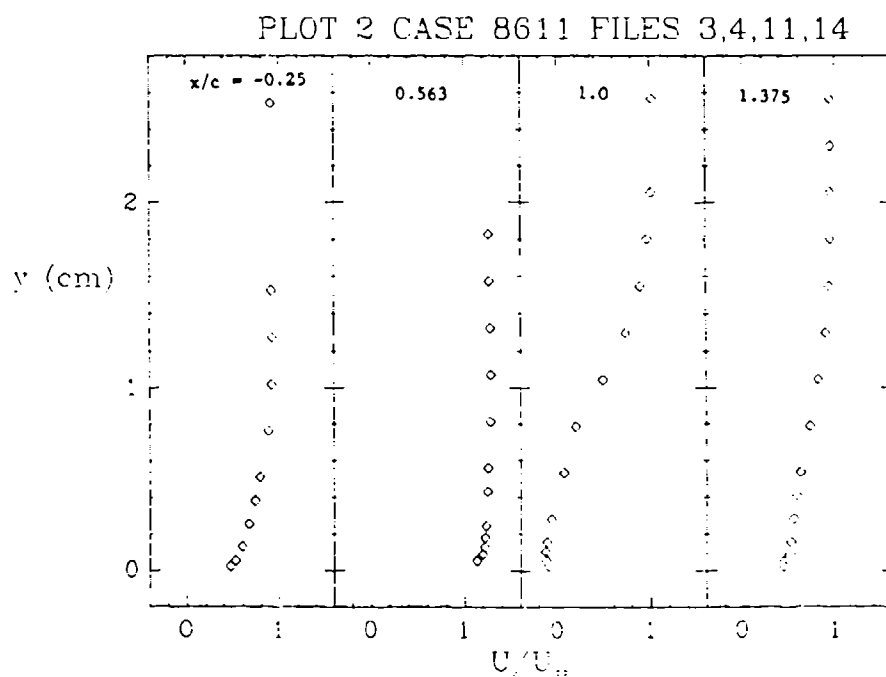
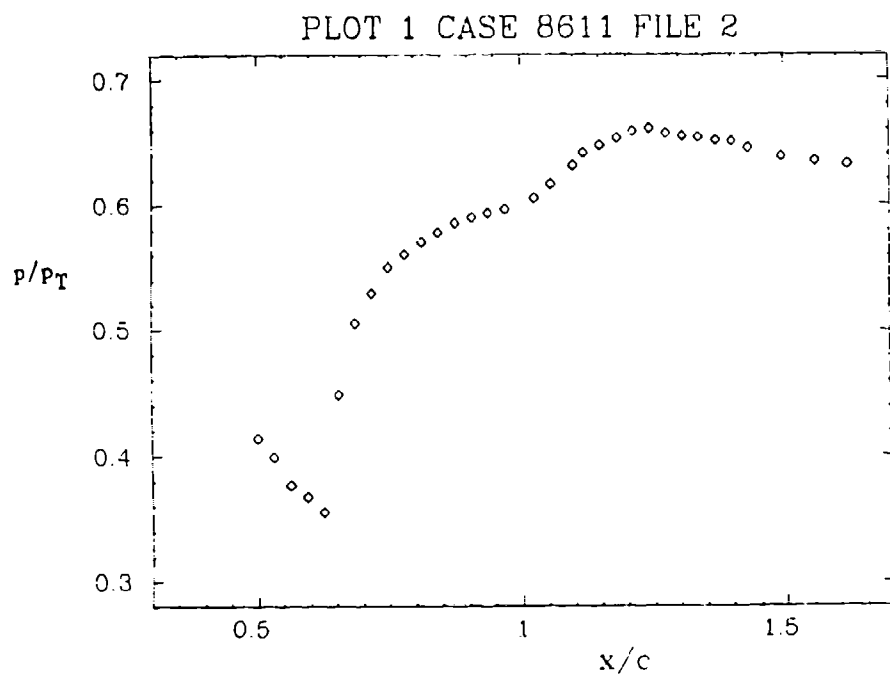
Flow 0610. Data Evaluators: M. Rubesin and C. Horstman. "Transonic Flow over a Bump."

Case Data Taker	Test Rig Geometry	dp/dx or C _p	Number of Stations Measured							C _f	Re	M _∞	Other Notes
			Mean Velocity		Turbulence Profiles								
			U	V or W	$\overline{u^2}$	$\overline{v^2}$	$\overline{w^2}$	\overline{uv}	Others				
Case 8611 W. Bachalo D. Johnson			12	12	12	12	-	12	-	-	1.4 × 10 ⁵ (based on δ ₀)	0.875	Axisymmetric. Complete LDV data.

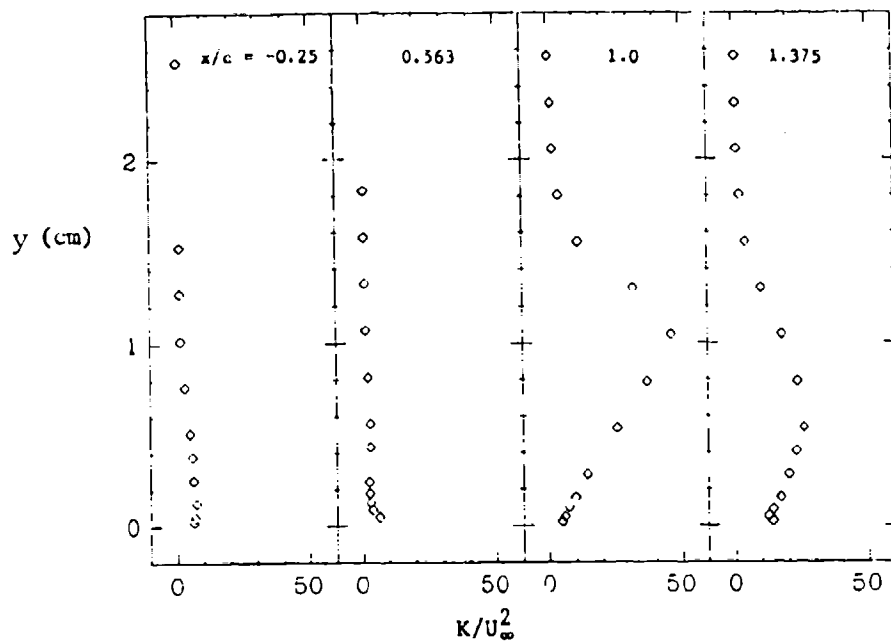
Plot	Ordinate	Abcissa	Range/Position	Comments
1	p/p _T	x/c	0.2 ≤ p/p _T ≤ 1.0 0.5 ≤ x/c ≤ 1.5	Wall-pressure distribution. p _T is tunnel total pressure.
2	y	U/U _∞	-0.5 ≤ U/U _∞ ≤ 1.5 0.0 ≤ y ≤ 0.025 m	4 curves at x/c = -0.25, 0.563, 1.0, and 1.375.
3	y	K/U _∞ ²	0 ≤ K/U _∞ ² ≤ 0.08 0.0 ≤ y ≤ 0.025 m	4 curves at x/c = -0.25, 0.563, 1.0, and 1.375.
4	y	$\overline{uv}/U_{\infty}^2$	0 ≤ $\overline{uv}/U_{\infty}^2$ ≤ 0.04 0.0 ≤ y ≤ 0.025 m	4 curves at x/c = -0.25, 0.563, 1.0, and 1.375.

Special Instructions:

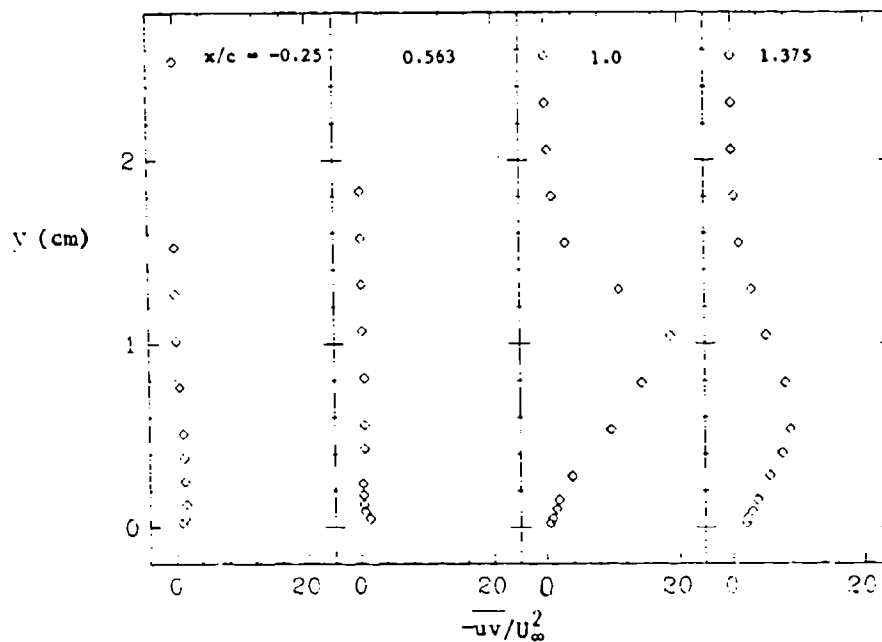
This test case considers the transonic flow over an axisymmetric bump model resulting in a shock-wave boundary-layer interaction with an extensive separated-flow region.



PLOT 3 CASE 8611 FILES 3,4,11,14



PLOT 4 CASE 8611 FILES 3,4,11,14



SPECIFICATIONS FOR COMPUTATION

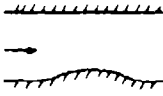
ENTRY CASE/COMPRESSIBLE

Flow 8610, Case #8612; Data Evaluators: M. Rubesin and C. Horstman

Data Takers: J. Delery and P. Le Diuzet

PICTORIAL SUMMARY

Flow 8610. Data Evaluators: M. Rubesin and C. Horstman. "Transonic Flow over a Bump."

Case Data Taker	Test Rig Geometry	dp/dx or C _p	Number of Stations Measured							C _f	Re	M _∞	Other Notes
			Mean Velocity		Turbulence Profiles								
			U	V or W	$\overline{u^2}$	$\overline{v^2}$	$\overline{w^2}$	\overline{uv}	Others				
Case 8612 J. Delery P. Le Diuzet			28	28	28	28	-	28	-	-	7·10 ⁴ (based on δ)	Mach 1.37	Complete LDV data. Top wall is important in solving problem.

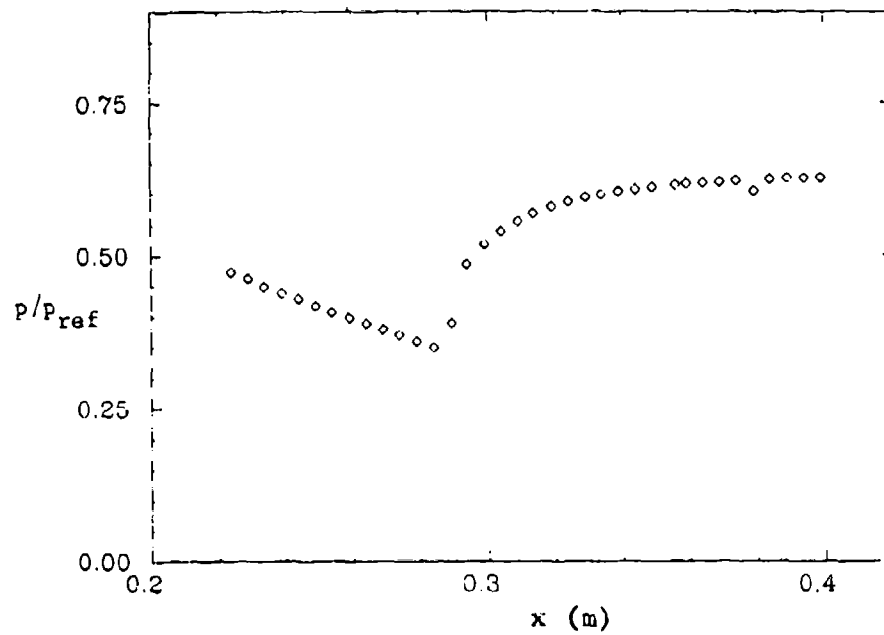
Plot	Ordinate	Abscissa	Range/Position	Comments
1	p/p _{ref}	x	0.2 ≤ p/p _{ref} ≤ 1.0 0.2 ≤ x ≤ 0.4 m	Wall-pressure distribution.
2	y	U/U _∞	-0.2 ≤ U/U _∞ ≤ 1.0 0.0 ≤ y ≤ 0.03 m	4 curves at x = 0.270, 0.280, 0.310, 0.350 m.
3	y	K/U _∞ ²	-0 ≤ K/U _∞ ² ≤ 0.1 0 ≤ y ≤ 0.03 m	4 curves at x = 0.280, 0.310, 0.350, 0.40 m.
4	y	uv/U _∞ ²	-0.02 ≤ uv/U _∞ ² ≤ 0.0 0 ≤ y ≤ 0.03 m	4 curves at x = 0.280, 0.310, 0.350, 0.40 m.

Special Instructions:

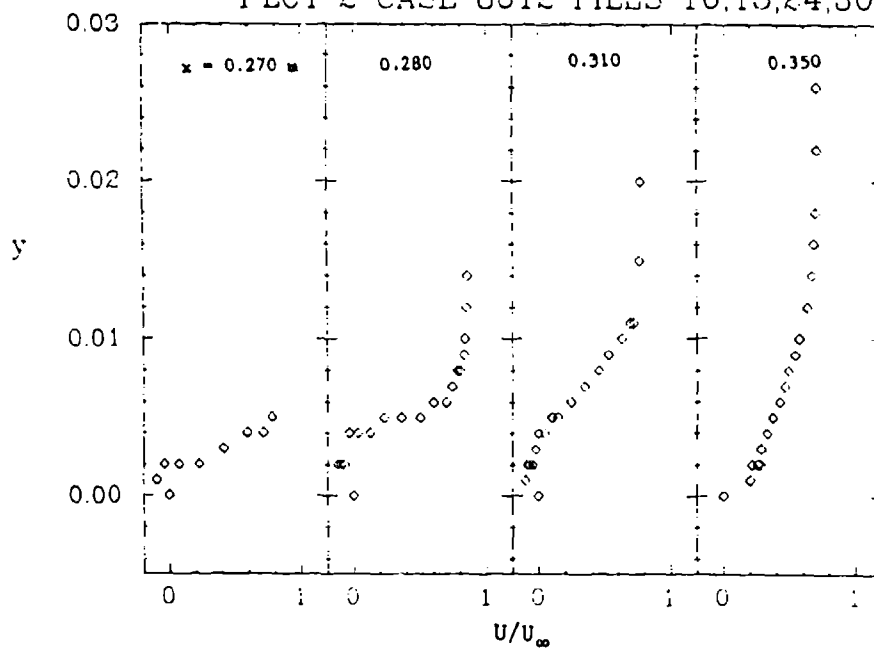
This test case considers the transonic flow over a two-dimensional bump mounted in a wind-tunnel side wall. The resulting flow field is a shock-wave boundary-layer interaction with an extensive separated-flow region. To compute the turbulent kinetic energy from the data set, assume $K = 0.75 \overline{u^2} + \overline{v^2}$. For normalizing the data, use $U_{\infty} = 382 \text{ m/s}$.

It is recommended that this flow be computed as a channel flow because the interaction with the top wall is considered essential.

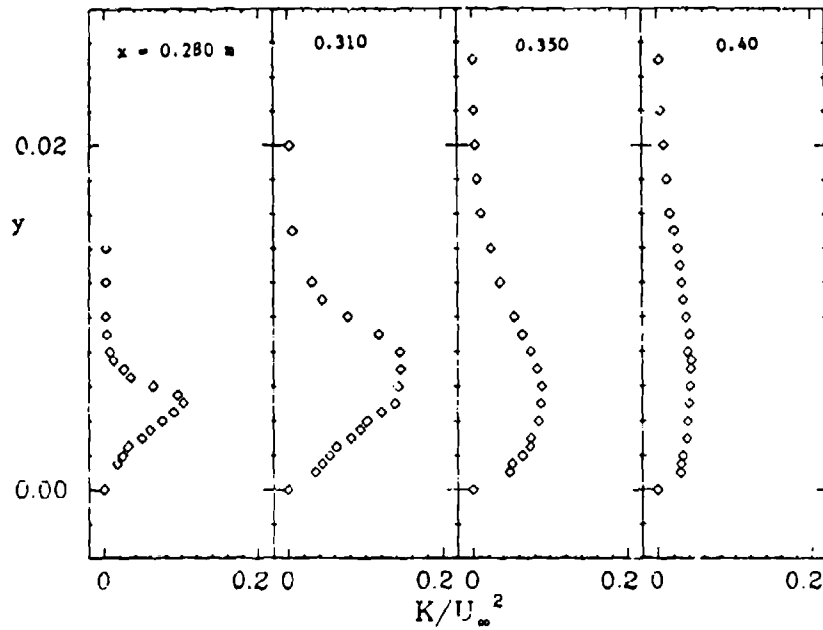
PLOT 1 CASE 8612 FILE 6



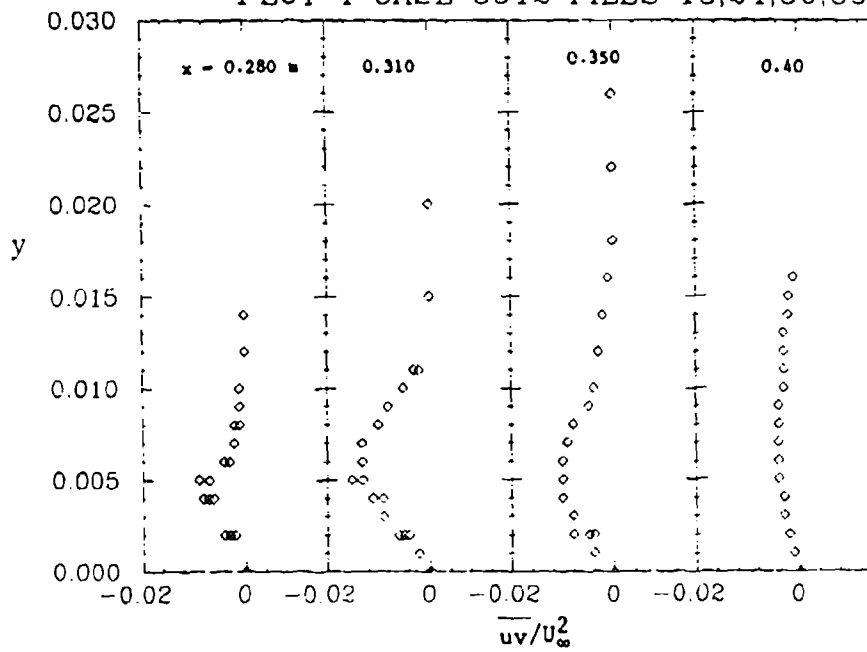
PLOT 2 CASE 8612 FILES 16,18,24,30



PLOT 3 CASE 8612 FILES 18,24,30,35



PLOT 4 CASE 8612 FILES 18,24,30,35



SPECIFICATIONS FOR COMPUTATION

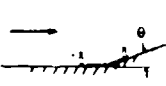
CENTRAL ENTRY CASE/COMPRESSIBLE

Flow 8630, Case #8631; Data Evaluators: M. Rubesin and C. Horstman

Data Takers: G. Settles, S. Bogdonoff, and T. Fitzpatrick

PICTORIAL SUMMARY

Flow 8630. Data Evaluators: M. Rubesin and C. Horstman. "Compressible Flow over Deflected Surfaces."

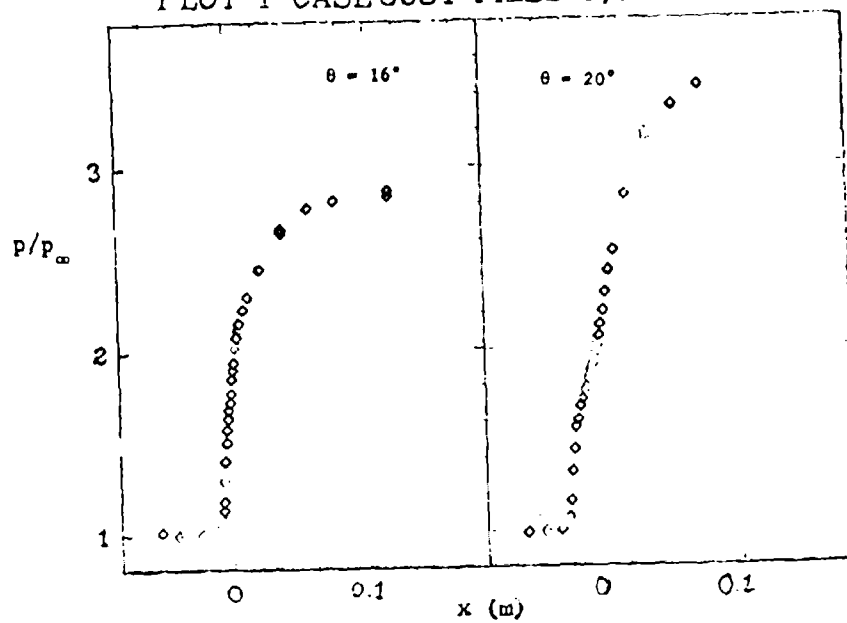
Case Data Taker	Test Rig Geometry	dp/dx or C _p	Number of Stations Measured							C _f	Re	M _∞	Other Notes
			Mean Velocity		Turbulence Profiles								
			U	V or W	$\overline{u^2}$	$\overline{v^2}$	$\overline{w^2}$	\overline{uv}	Others				
Case 8631 C. Settles T. Fitzpatrick S. Bogdanoff		> 0	9	-	-	-	-	-	M and p/p _∞	Pres- ton tube	8·10 ⁵ to 7.6 · 10 ⁶ (based on δ ₀)	2.83	θ = 8, 16, 20 and 24°. Wall pressure also available.

Plot	Ordinate	Abcissa	Range/Position	Comments
1	p/p _∞	x	-0.05 ≤ x ≤ 0.15 m 1 ≤ p/p _∞ ≤ 4	2 curves for θ = 16° and 20°.
2	C _{f∞}	x	-0.05 < x < 0.15 m. -0.001 ≤ C _{f∞} ≤ 0.002	2 curves for θ = 16° and 20°.
3	y	U/U _∞	0 ≤ y ≤ 0.03 m -0.1 ≤ U/U _∞ ≤ 1.0	4 curves for θ = 16° at x = -0.0381, 0, 0.0381, 0.0762 m.
4	y	U/U _∞	0 ≤ y ≤ 0.03 m -0.1 ≤ U/U _∞ ≤ 1.0	4 curves for θ = 20° at x = -0.0381, 0, 0.0381, 0.0762 m.
5	x _{sep} x _{reat}	Re _{δ_∞}	-0.02 ≤ x _{sep} ≤ 0.01 m -0.02 ≤ x _{reat} ≤ 0.01 m 0.5 × 10 ⁶ ≤ Re _{δ_∞} ≤ 8 × 10 ⁶	x separation vs Re _{δ_∞} and x reattachment vs Re _{δ_∞} -- (output only). 1 curve for θ = 20°.

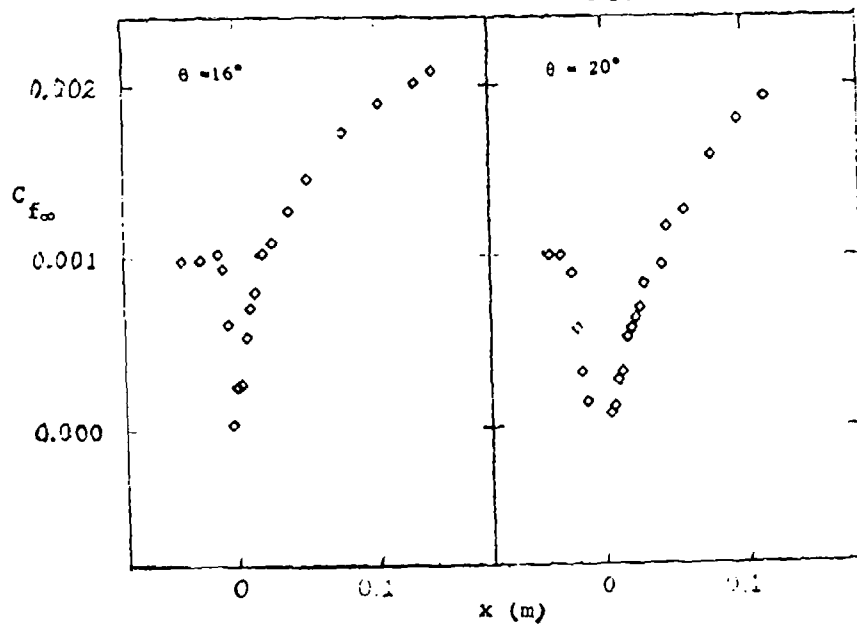
Special Instructions:

This test case considers a two-dimensional compression corner at supersonic speeds. There are four sets of data on the tape. Only two cases are to be calculated, corner angles of 16° and 20°. For these flows x is the distance along the surface measured from the corner and y is the distance normal to the wall (at x = 0, y is normal to the upstream wall).

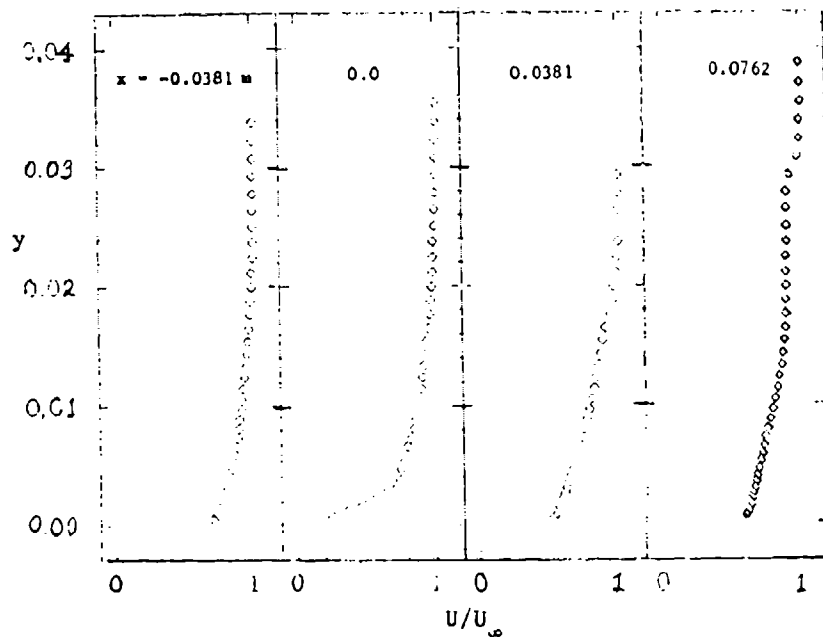
PLOT 1 CASE 8631 FILES 3,4



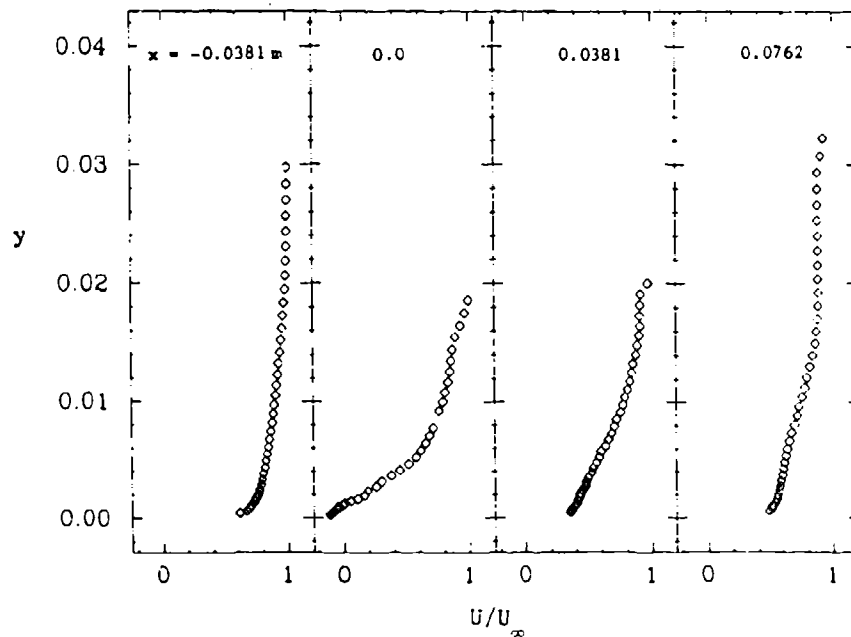
PLOT 2 CASE 8631 FILES 11,12

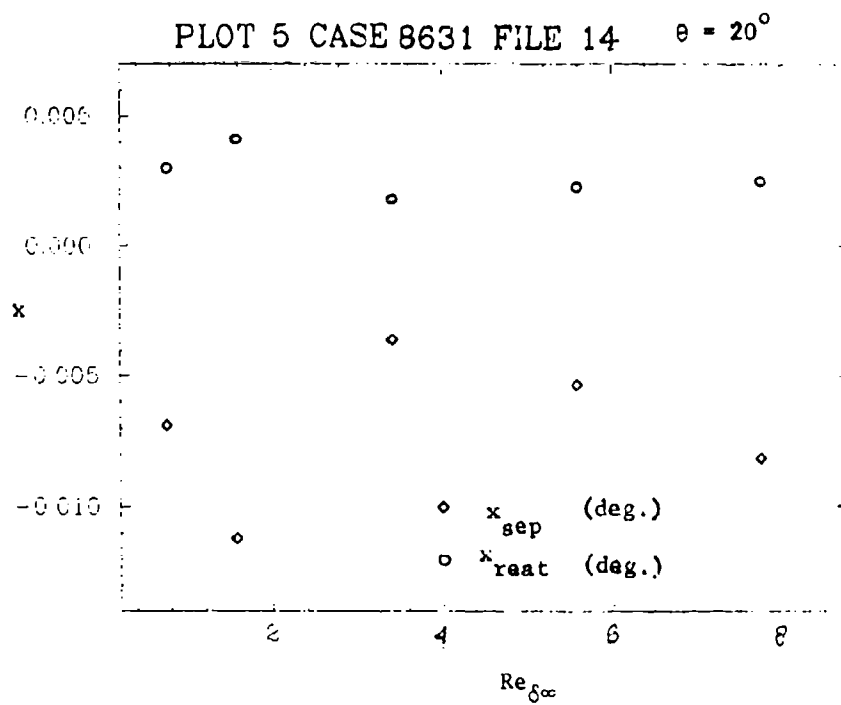


PLOT 3 CASE 8631 FILES 24,27,30,31 $\theta = 16^\circ$



PLOT 4 CASE 8631 FILES 33,35,38,40 $\theta = 20^\circ$





SPECIFICATIONS FOR COMPUTATION

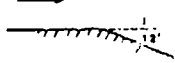
ENTRY CASE/COMPRESSIBLE

Flow 8630, Case #8632; Data Evaluators: M. Rubesin and C. Horstman

Data Taken: J. Dussauge and J. Gavigli

PICTORIAL SUMMARY

Flow 8630. Data Evaluators: M. Rubesin and C. Horstman. "Compressible Flow over Deflected Surfaces."

Case Data Taker	Test Fig Geometry	$\frac{dp}{dx}$ or C_p	Number of Stations Measured								Re	M_∞	Other Notes
			Mean Velocity		Turbulence Profiles								
			U	V or W	$\overline{u^2}$	$\overline{v^2}$	$\overline{w^2}$	\overline{uv}	Others	δ_f^+			
Case 8632 J. Dussauge J. Gavigli		< 0	22	-	2	-	-	-	\overline{Tu}	Law of wall	5×10^3 (based on δ_o)	1.76	Prandtl Meyer expansion. Wall pressure also available.

Plot	Ordinate	Abscissa	Range/Position	Comments
1	$P_w/P_{t,ref}$	x, s	$-0.0725 \leq x \leq 0 \text{ m}$ $0 \leq s \leq 0.115 \text{ m}$ $0.0 \leq P_w/P_{t,ref} \leq 0.20$	Wall-pressure distribution. x measured along upstream wall. s measured from corner along the deflected stream.
2	U	y	$0 \leq U \leq 500 \text{ m/s}$ $0 \leq y \leq 0.02 \text{ m}$	Mean velocity profiles at $x = -0.0325, 0.0061, 0.0313,$ and 0.098 m .
3	$\overline{u^2}/U_{ref}^2$	x	$0.0 \leq \overline{u^2}/U_{ref}^2 \leq 0.004$ $-0.005 \leq x \leq 0.006 \text{ m}$	Streamwise component of turbu- lent kinetic energy along the streamline $\frac{\int_0^{\delta} \rho U^n d\eta}{\rho_{t,ref}^n U_{t,ref}^n} = 0.063$

Special Instructions:

Instruments

Pitot pressure probe

Static pressure probe (supplemented by method of characteristics)

Hot-wire stagnation temperature probe, $5-\mu$ dia, $L/d = 300$

Hot wire $2.5-\mu$ dia, $L/d = 320$

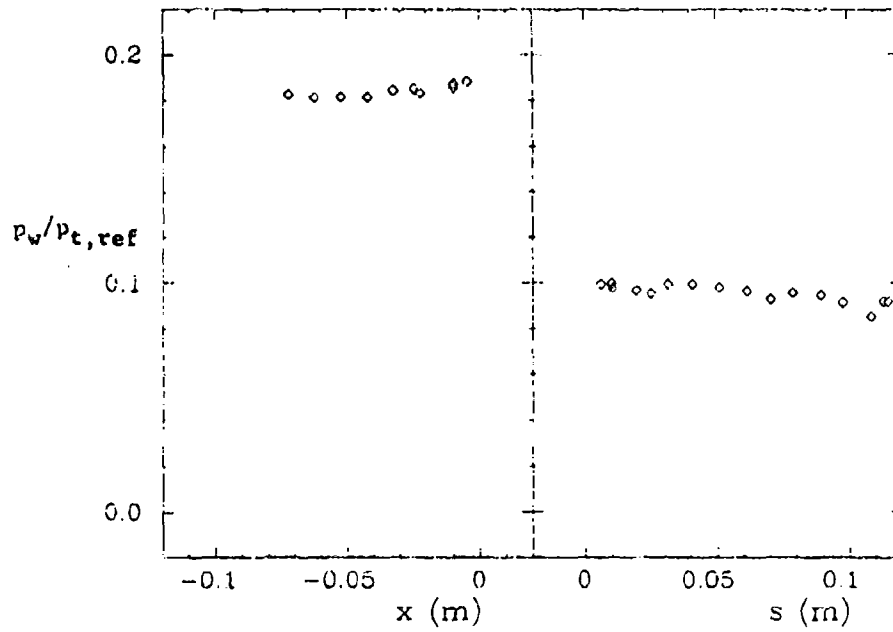
Measurement:

$\rho, U, V, T \pm 1\%$

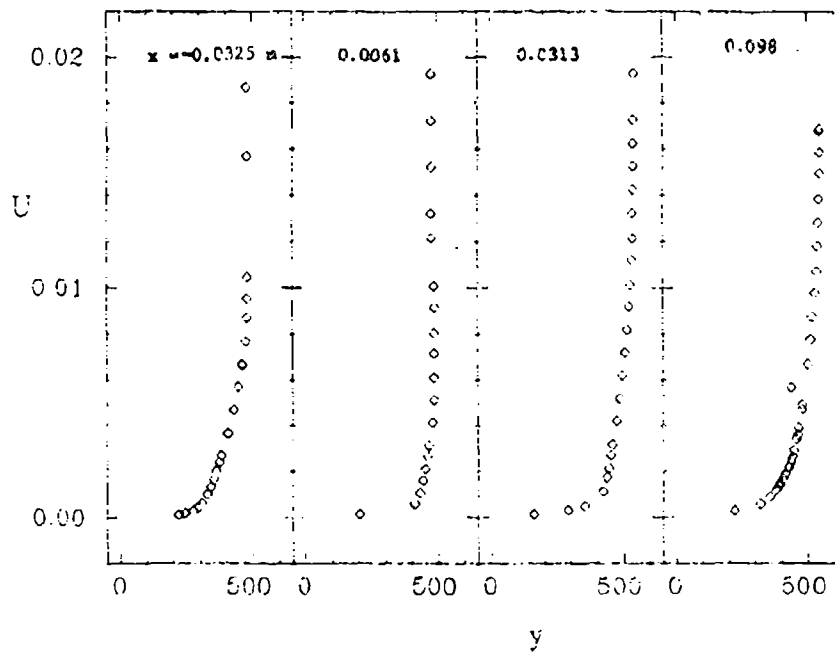
$\overline{u^2}, \overline{v^2}, R_{TU} \pm 10\%$ along a streamline

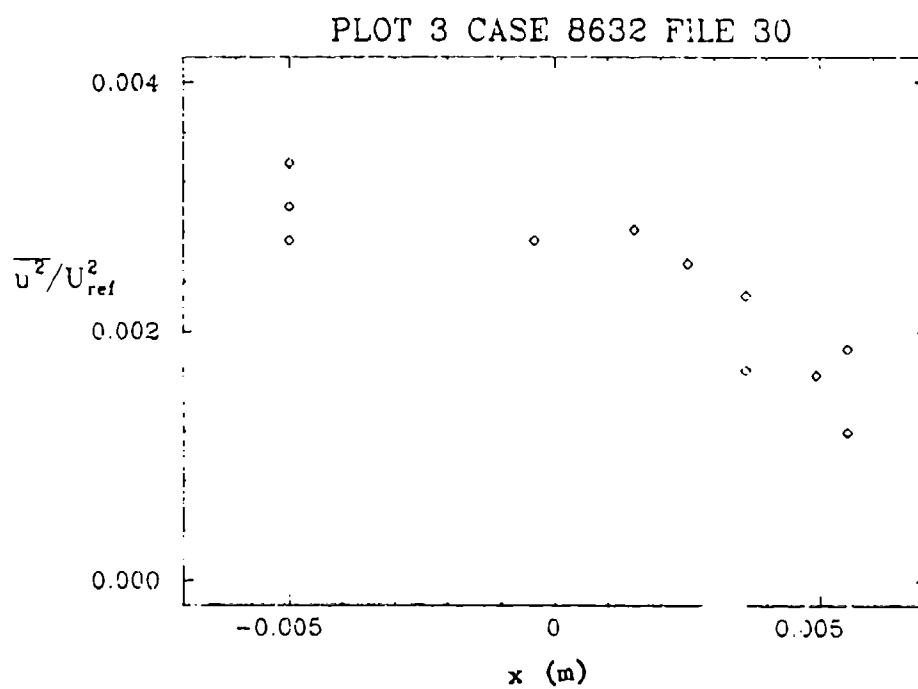
C_f van Driest transformed u , "law-of-the-wall" plot, $\kappa = 0.41$.

PLOT 1 CASE 8632 FILES 31,32



PLOT 2 CASE 8632 FILES 6 13,16,22





SPECIFICATIONS FOR COMPUTATION


ENTRY CASE/COMPRESSIBLE

Flow 8640, Case #3641; Data Evaluators: M. Rubesin and C. Horstman

Data Takers: G. Settles, B. Baca, D. Williams, and S. Bogdonoff

PICTORIAL SUMMARY

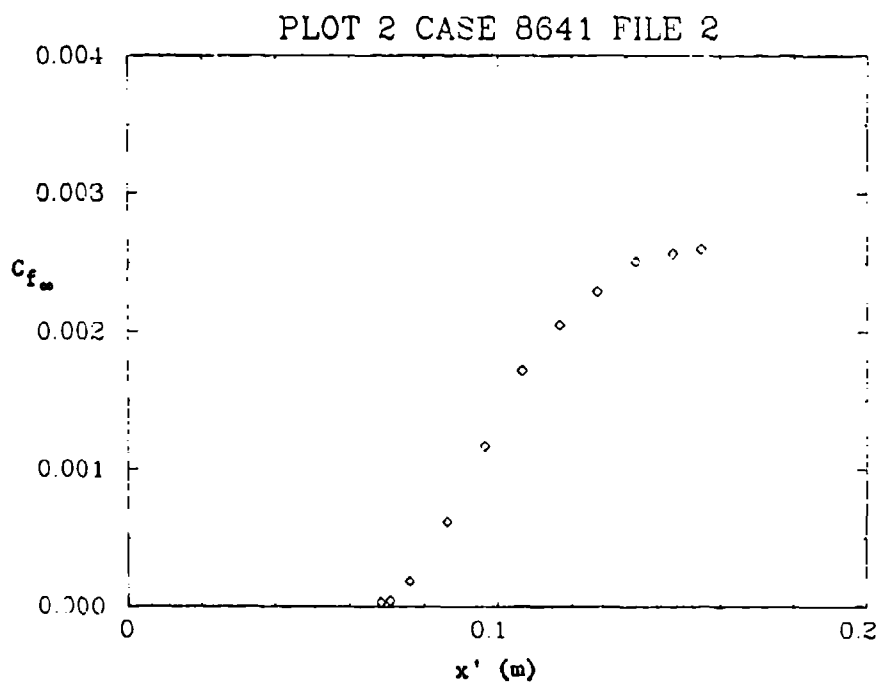
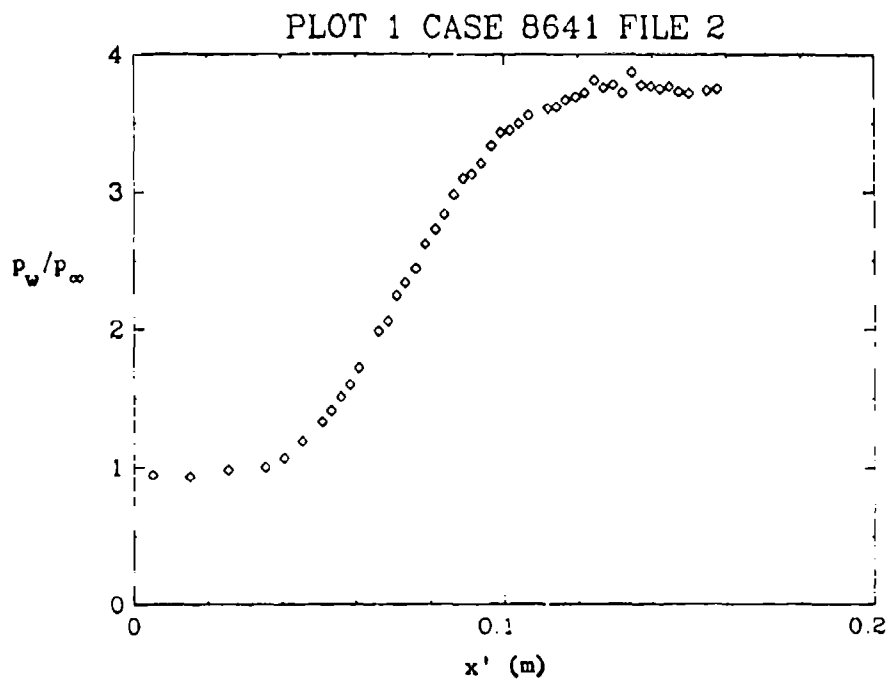
Flow 8640. Data Evaluators: M. Rubesin and C. Horstman. "Compressible Flow over Compression Corner with Reattaching Planar Shear Layer."

Case Data Taker	Test Rig Geometry	dp/dx or C _p	Number of Stations Measured								C _f	Re	M _∞	Other Notes
			Mean Velocity		Turbulence Profiles									
			U	V or W	$\overline{u^2}$	$\overline{v^2}$	$\overline{w^2}$	\overline{uv}	Others					
Case 8641 G. Settles B. Baca E. Williams S. Bogdonoff		> 0	11	-	-	-	-	-	M, ρ/p_∞ 11	Free- ton probe	2.2 x 10 ⁵ (based on d_0)	2.8	Combines three problems: Free-shear layer develop- ment, reattachment, and downstream development.	

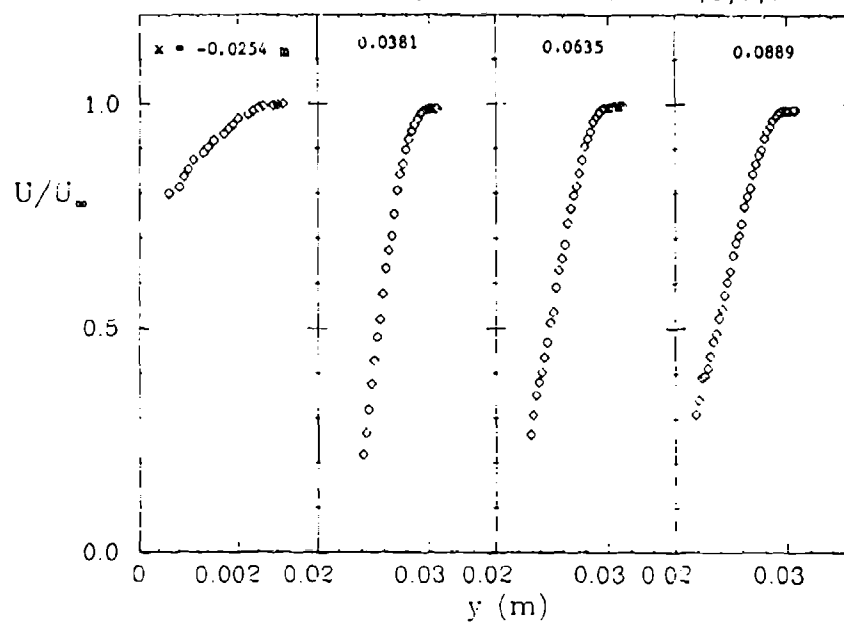
Plot	Ordinate	Abcissa	Range/Position	Comments
1	p_w/p_∞	x'	$0 \leq p_w/p_\infty \leq 4$ $0 \leq x' \leq 0.2 \text{ m}$	Wall-pressure distribution on the ramp.
2	C_{f_∞}	x'	$0 \leq C_{f_\infty} \leq 0.004$ $0 \leq x' \leq 0.2 \text{ m}$	Skin-friction distribution on the ramp. $C_{f_\infty} = \tau_w / \frac{1}{2} \rho_\infty U_\infty^2$.
3	U/U_∞	y	$0 \leq U/U_\infty \leq 1.0$ $0 \leq y \leq 0.03 \text{ m}$	Mean velocity in the free-shear layer at $x = -0.0254, 0.0381, 0.0635$, and 0.0889 m (4 curves).
4	U/U_∞	y	$0 \leq U/U_\infty \leq 1.0$ $0 \leq y \leq 0.02 \text{ m}$	Mean velocity on the ramp at $x' = 0.0686, 0.0965$, and 0.1549 m (3 curves).

Special Instructions:

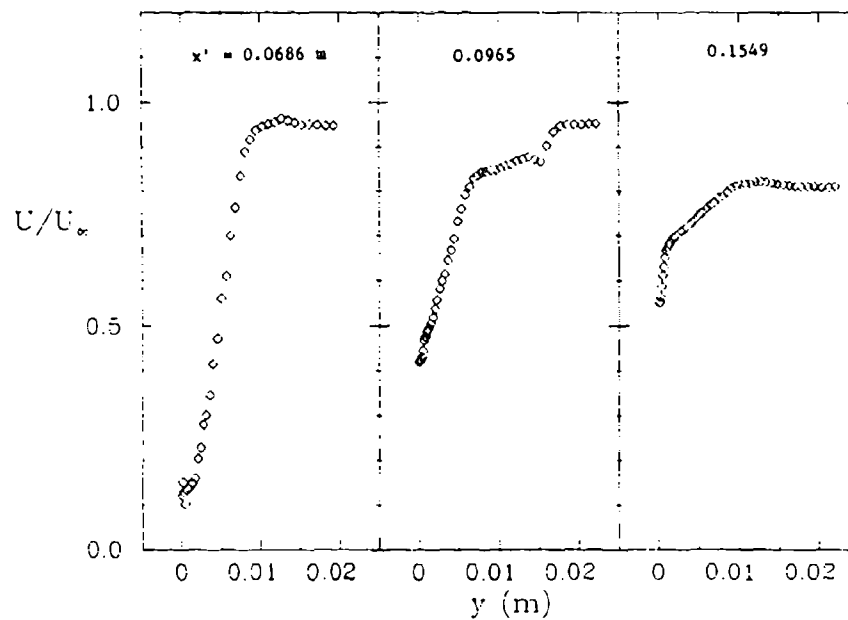
This test case considers a reattaching planar free-shear layer (generated by a backward-facing step) reattaching upon a 20° ramp at supersonic speed. Wall-pressure and skin-friction data comparisons are needed on the ramp. Mean-velocity profile comparisons are needed in the free-shear layer, the upstream boundary layer, and on the ramp. In the free-shear layer and upstream boundary layer, comparisons are to be made at $x = -2.54, 3.81, 6.35$, and 8.89 cm . On the ramp, comparisons are to be made at $x' = 6.86, 9.65$, and 15.49 cm . (x is the horizontal distance from the step, x' is the distance along the ramp measured from the corner and y is the distance normal to the model surface.)



PLOT 3 CASE 8641 FILES 3,5,6,7



PLOT 4 CASE 8641 FILES 8,10,13



AXISYMMETRIC NEAR-WAKE FLOW (SUPERSONIC)

Flow 8680

Evaluator: A. Favre*

(Prepared by D. J. Cockrell†)

SUMMARY

INTRODUCTION

Experimental data are reported in Gaviglio et al. (1977) and Dussauge et al. (1978) for steady flow developing in the near wake, downstream of a 40-mm-dia. body of revolution in a supersonic stream for which the free-stream Mach number was 2.3. The Reynolds numbers of the two tests described were 1.68×10^4 and 3.36×10^4 , based on boundary-layer thickness upstream of flow separation, or 1×10^3 and 2×10^3 , respectively, based on upstream momentum thickness. Large pressure and velocity gradients exist in the fully turbulent boundary layer, which is strongly out of equilibrium.

EXPERIMENTAL CONDITIONS

A 40-mm-dia. body of revolution with a streamlined nose section was set at zero angle of incidence in a supersonic nozzle. The nominal Mach number was 2.3. Two series of experiments were performed, at total pressures of 0.375 and 0.75 atmospheres. Reynolds numbers, determined in terms of boundary-layer thicknesses just upstream of flow separation near the base wedge, were 1.68×10^4 and 1×10^3 for the first series; 3.36×10^4 and 2×10^3 † for the second. In both cases, the first number is in terms of physical thickness, the second in terms of momentum thickness. To ensure fully turbulent boundary layers for the first series of tests, ridges were placed on the lateral surface of the model downstream of the nozzle.

The flow configuration is shown in Fig. 1. The boundary layer separates from the model near the base wedge, is accelerated through an expansion fan, forms a mixing layer which is subjected to a compression by turning and then transforms into a wake. The mixing layer encloses a recirculation zone in which no turbulence measurements were performed, thus only the properties of the expansion region and the compression region were considered. The recirculating zone is separated from the mixing layer by a randomly fluctuating interface or dividing surface, which in a radial plane becomes a dividing streamline.

*Institut de Mécanique Statistique de la Turbulence, Marseille, France.

†University of Leicester Engineering Department, England.

‡Note that here the momentum thicknesses have been reversed in order from that given in Gaviglio et al. (1977).

EXPERIMENTAL METHODS

Mean-velocity profiles and mean streamlines were deduced from pressure measurements made by probes that were moderately sensitive to yaw. Two approximations were made to the mean-streamline derivations in order to account for their obliqueness. Velocity and temperature fluctuations were determined using 0.9-mm-long platinum-plated tungsten hot-wire sensors having a diameter of 3.8 μm . Caviglio et al. (1977) discuss the errors which arise as a consequence of anemometer imperfections but show that there was good agreement between longitudinal turbulence intensity measured upstream of flow separation and corresponding results at a similar Mach number obtained by Kistler.

LATER EXPERIMENTAL WORK

Later experimental work performed at I.M.S.T. has been directed towards emphasizing the interactions which take place between the boundary layer and either the expansion wave or the shock wave. In two parallel test sections two-dimensional models of the flow configuration have been devised in which a wall replaces the dividing streamline between the mixing layer and the recirculating zone. In the first test section, the wall is deflected expansively through 12 degrees, in the second, it is deflected compressively through 6 degrees. The resulting flows are much steadier, accuracy in turbulence measurement has been improved, and experimental uncertainties are known. Further details of this later work are given in Dussauge and Caviglio (1981?) and Debieve and Caviglio (1981?); computational results through the 6-degree shock are compared with experimental data in Debieve (1981?); for further details concerning these three references, apply to the Institut de Mécanique Statistique de la Turbulence, 12, Avenue Général Leclerc, 13003 Marseille, France.

REFERENCES

- Debieve, J. F. (1981?). "Bilan de tensions de Reynolds dans une interaction onde de choc-turbulence," to be published by C. R. Acad. Sci., Paris.
- Debieve, J. F., and J. Caviglio (1981?). "Shock wave turbulent boundary layer interaction on a compression corner," to be published.
- Dussauge, J. P., J. Caviglio, and A. Favre (1978). "Density changes and turbulence production in the expansion or the compression of a turbulent flow, at supersonic speed," in Structure and Mechanics of Turbulence II, p. 385, Springer-Verlag.
- Dussauge, J. P., and J. Caviglio (1981?). "Interaction turbulent boundary layer expansion at supersonic speed," to be published.
- Caviglio, J., J.-P. Dussauge, J. F. Debieve, and A. Favre (1977). "Behavior of a turbulent flow, strongly out of equilibrium, at supersonic speeds," Phys. Fluids, 20, S179.

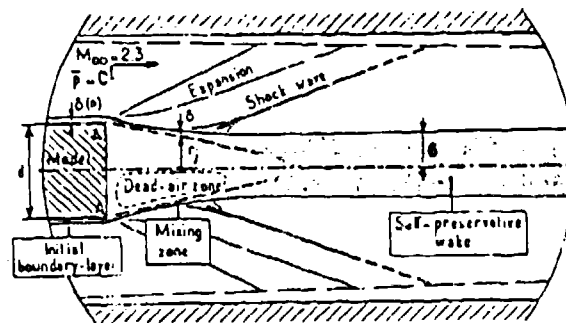


Figure 1. Sketch of the flow (8680).

DISCUSSION

Flow 8680

The Conference recommended that this flow be held in abeyance until the following data are received:*

1. Detailed information on the flow field upstream of the base of the model.
2. Base-pressure measurements.
3. Uncertainty analysis of data.
4. Details of how the pressure is measured along the wake centerline.
5. Optical pictures of the flow field.
6. Circumferential data at base of the model when these data are available.

The evaluators will examine this case for possible inclusion in the data bank.

A. Favre agreed to forward these data.

*[Ed.: This flow was not used in the 1981 meeting.]

SESSION X

Chairman: J. McCroskey

Technical Recorders:

R. Strawn
R. So



Flow 8650

Flow 8660

Flow 8600

Flow 8690

SHOCK WAVE - BOUNDARY-LAYER INTERACTION FLOWS

Flows 8650, 8660, 8600, 8690

Cases 8651, 8661, 8663, 8601, 8691

Evaluators: M. W. Rubesin* and C. C. Horstman*

SUMMARY

SELECTION CRITERIA

The existing experiments on the behavior of shock wave, turbulent boundary-layer interactions cover a rather wide range of flow-field configurations, Mach numbers and Reynolds numbers. To pick the experimental test cases for this conference all known experiments were grouped into several categories and within each category a particular experiment was chosen on the basis of the largest range of variables and variety of quality data. Each flow chosen had to be a well-defined flow. The upstream turbulent boundary layer had to be in equilibrium and the upper and downstream boundaries had to either not influence the flow field or be precisely defined. As a minimum the measurements had to include surface pressure and mean flow profiles throughout the flow field. Surface skin-friction measurements were also desired. If the experiment is two-dimensional, the two-dimensionality had to be quite well documented. Compatibility with other like experiments was also checked. Although not necessarily redundant, mean flow and fluctuating measurements throughout the flow field were also desired. Finally, variation of a parameter such as Mach or Reynolds number or the shock-wave strength was an important consideration.

Case 8651 - Axisymmetric Shock Impingement (Supersonic)

In this category a concentric shock-wave generator is used to produce a conical incident shock wave on the outer surface of a circular cylinder. The experiment by Kussoy and Horstman (1975) was chosen. The experimental geometry is shown in Fig. 1. The measurements included surface pressure, skin-friction and heat-transfer, and complete mean flow-field data for two shock-wave strengths resulting in attached and separated flows. Hot-wire data were also obtained, but the accuracy of these data were not sufficient to be used for comparison with computations.

Cases 8661, 8662[†] and 8663. Three-Dimensional Shock Impingement (Supersonic)

In this category three flow fields met the above criteria. Two of the three experiments were chosen for computation. The first case (Case 8661) is for an oblique

*NASA-Ames Research Center, Moffett Field, CA 94035.

[†]This case was not finally used for the 1980-81 Conference. It is, however, in the Data Library.

shock wave boundary-layer interaction by Peake (1976). [A similar experiment (Case 8662) at $M = 3$, has been done by Oskam et al., 1975; 1976.] The second case (Case 8663) chosen is for a conical shock wave boundary-layer interaction by Kussoy et al. (1980). The flow geometries for Case 8661 is shown in Fig. 2. The measurements for this case included: surface-pressure and skin-friction magnitude and direction; complete mean flow-field data planes. The flow geometry for Case 8663 is shown in Fig. 3. In addition to mean surface and flow-field data, the measurements also include fluctuating data on the windward and leeward data planes.

Cases 8601, 8602^{*}. Impinged Normal Shock Wave, Boundary-Layer Interaction at Transonic Speeds

In this category two flow fields were chosen, the axisymmetric experiment of Mateer et al. (1976); Mateer and Viegas (1979), and the two-dimensional experiment of Kooi (1978). The flow geometry for Case 8601 is shown in Fig. 4. The measurements for this case included mean surface-pressure and skin-friction, and both mean and fluctuating flow-field parameters. In addition several experimental data sets of mean surface and skin friction were obtained to investigate the effects of variations in free-stream Mach number at constant Reynolds number and variations in Reynolds number at constant Mach number. The flow geometry for Case 8602 is shown in Fig. 5. This is the two-dimensional experiment of Kooi (1978). Mean-surface and flow-field data were obtained at three free-stream Mach numbers resulting in flow fields with various degrees of separation.

Case 8691. Nonlifting, Transonic Airfoil with Shock Separation

The experiment by McDevitt et al. (1976)[†] was chosen as the most complete experiment of a transonic airfoil with a large shock-separated region. The measurements were extensive and include: surface-pressure, skin-friction, and complete mean and fluctuating flow-field data in the separated flow region. The flow geometry is shown in Fig. 6.

RECOMMENDATIONS FOR FUTURE DATA TAKERS

When an experiment is designed, care must be taken that the flow field is well defined. All boundary conditions must be specified, or shown not to be important; this is especially critical for transonic flows. The establishment of an upstream equilibrium boundary layer is also important. Experiments should also be designed to test a particular aspect of turbulence modeling when possible.

^{*}This case was not finally used for the 1980-81 Conference. It is, however in the Data Library.

[†]See also Seegmiller et al. (1978).

Improvements in the operation and interpretation of the data from laser-Doppler and hot-wire anemometers in recent years, makes it possible to consider these instruments for gathering data of turbulence parameters upon which turbulence-model improvements can be made. The relatively small models associated with supersonic wind tunnels utilized for studies of fluid mechanics suggests that measurement within boundary layers can be performed with greater spatial resolution when these boundary layers occur on the wind-tunnel walls. Redundant measurements of both mean and fluctuating quantities are also recommended. Pitot tubes should be used to obtain near-wall data where LDV measurements are suspect. Continuing efforts should be made to obtain more accurate surface skin-friction measurements.

The instruments should be applied to measure all the quantities they can. Measurements of all the components of the Reynolds stress tensor will be most useful in guiding modeling through two-equation modeling to models that account for the lack of equilibrium between mean strain and turbulent stress. Efforts should be expended to assess both the Morkovin hypothesis and Favre mass-weighting in a quantitative manner through the careful comparison of LDV and hot-wire measurements.

Of the equations utilized in second-order modeling, the scale equation, be it expressed as a length scale, frequency scale, or dissipation rate, has the weaker theoretical foundation. Two-point correlation-length measurements, or multipoint measurements, or other measurements directed toward defining better scale equations in compressible flow should be attempted.

Some thought should be given to experiments designed to guide the next generation of modeling, when some of the dynamics of the largest scales are calculated, and when the models account for the contribution of the remaining scales. These measurements will have to consider the phase relationship for, at least, the largest scales. This will modify data-recording techniques as it will require continuous recording of the raw data in time, with subsequent computer analysis. The use of rms meters or correlators will no longer be appropriate. Studies will have to be made to increase LDV seeding so that "continuous" data of the largest eddies can be achieved. Histograms will lose much of their meaning. The continuous, high-frequency-response characteristics of hot wires should lead to multi-sensor experiments. Again, multipoint measurements will be critical.

Finally, three-dimensional flow fields with and without separation must be investigated in more detail. At present our understanding of three-dimensional flow fields is limited. The available experimental data base is almost nonexistent.

REFERENCES

- Kooi, J. W. (1978). "Influence of freestream Mach number on transonic shock wave-boundary layer interaction," NLR-MP-78013-U.
- Kussoy, M. I., and C. C. Horstman (1975). "An experimental documentation of a hypersonic shock-wave turbulent boundary-layer interaction flow - with and without separation," NASA TM X62,412.
- Kussoy, M. I., C. C. Horstman, and J. R. Viegas (1980). "An experimental and numerical investigation of a 3-D shock separated turbulent boundary layer," Paper 80-0002, AIAA 18th Aerospace Science Meeting, Jan. 14-16, 1980, Pasadena, CA.
- Mateer, G. G., A. Brosh, and J. R. Viegas (1976). "A normal-shock-wave turbulent boundary-layer interaction at transonic speeds," AIAA Paper 76-161, Washington, D.C..
- Mateer, G. G., and J. R. Viegas (1979). "Effect of Mach and Reynolds numbers on a normal shock-wave/turbulent boundary-layer interaction," AIAA Paper 79-1502, Williamsburg, VA.
- McDevitt, J. B., L. L. Levy, Jr., and G. S. Deiwert (1976). "Transonic flow about a thick circular-arc airfoil," AIAA Jou., 14(5), 606-613.
- Oskam, B., S. M. Bogdonoff, and I. E. Vas (1975). "Study of three-dimensional flow fields generated by the interaction of a skewed shock wave with a turbulent boundary layer," AFFDL-TR-75-21.
- Oskam, B., I. E. Vas, and S. M. Bogdonoff (1976). "Oblique shock wave/turbulent boundary layer interactions in three dimensions at Mach 3," parts I and II, AFFDL-TR-76-48.
- Peake, D. J. (1976). "Three-dimensional swept shock/turbulent boundary-layer separations with control by air injection," Aeronautics Report LR-592, National Research Council, Canada.
- Rubsin, M., A. F. Okuno, L. L. Levy, Jr., J. B. McDevitt, and H. L. Seegmiller (1976). "An experimental computational investigation of the flow field about a transonic airfoil in super-critical flow with turbulent boundary layer separation," Tenth Congress of the International Council of the Aeronautical Sciences, Ottawa, Canada, October 3-8.
- Seegmiller, H. L., J. G. Marvin, and L. L. Levy, Jr. (1978). "Steady and unsteady transonic flow," AIAA Jou., 16(12), 1260-1270.

Table
Uncertainty Estimates for
Cases 8651, 8661, 8663, 8601, 8691

Case No.	Quantity	Uncertainty
8651	p_w	$\pm 10\%$
	τ_w	$\pm 15\% \cdot \tau_{w\infty}$
	q_w	$\pm 10\%$
	$U(y)$	$\pm 3\%$
	$U(y)$ reversed flow region	$\pm 35\%$
	$\rho(y)$	$\pm 12\%$
8661	p_w	$\pm 1\%$
	C_f	$\pm 10\%$
	$U(y)$	$\pm 2\%$
	$\alpha(y)$	$\pm 0.2^\circ$
8663	p_w	$\pm 5\%$
	τ_w	$\pm 15\% \cdot \tau_{w\infty}$
	$U(y)$	$\pm 3\%$
	$\alpha(y)$	$\pm 0.5^\circ$
	$\overline{u^2}^{1/2}, \overline{v^2}^{1/2}, \overline{w^2}^{1/2}$	$\pm 15\%$
	ρuv	$\pm 15\%$
8601	p_w	$\pm 5\%$
	τ_w	$\pm 15\%$
	$U(y)$	$\pm 3\%$
	ρuv	$\pm 15\%$
8691	C_p	$\pm 0.02\%$
	C_f	$\pm 15\%$
	$U(y)$	$\pm 4\%$
	$\overline{u^2} + \overline{v^2}$	$\pm 8\%$
	\overline{uv}	$\pm 8\%$

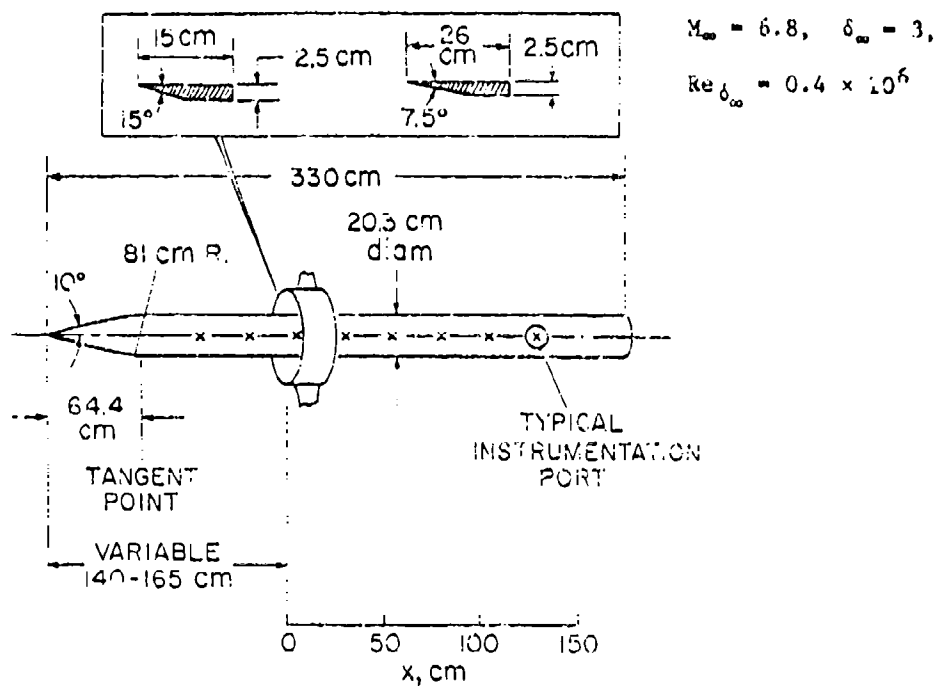


Figure 1. Test configuration, Case 8651.

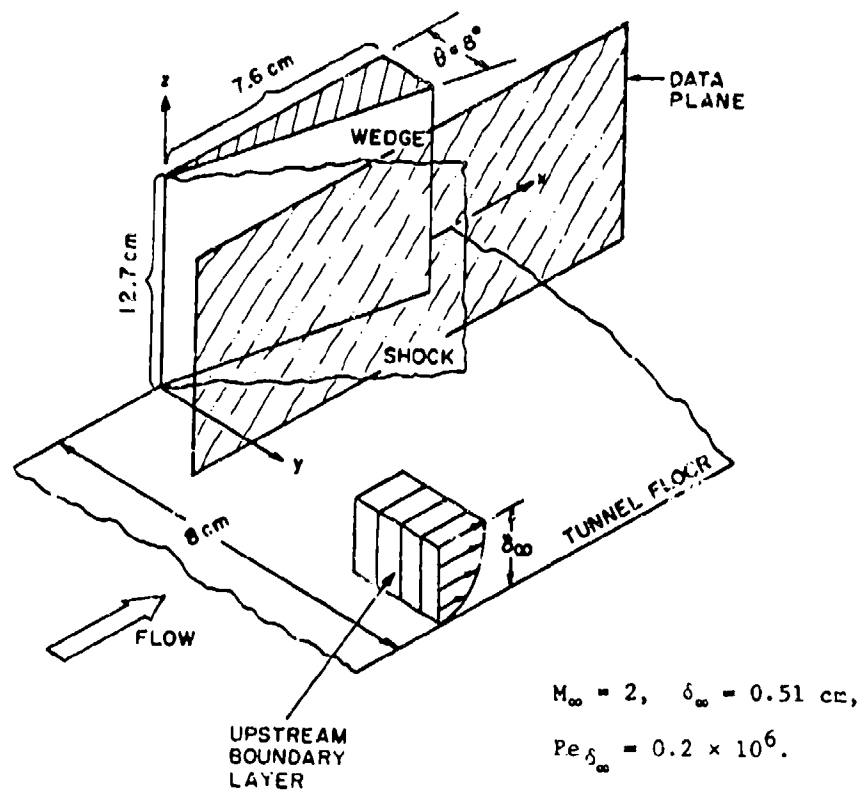


Figure 2. Case 8661, three-dimensional shock impingement.

$$M_\infty = 2.2, \quad Re = 36 \times 10^6, \quad \delta \approx 4.4 \text{ cm}, \quad Re_\delta = 1.0 \times 10^6$$

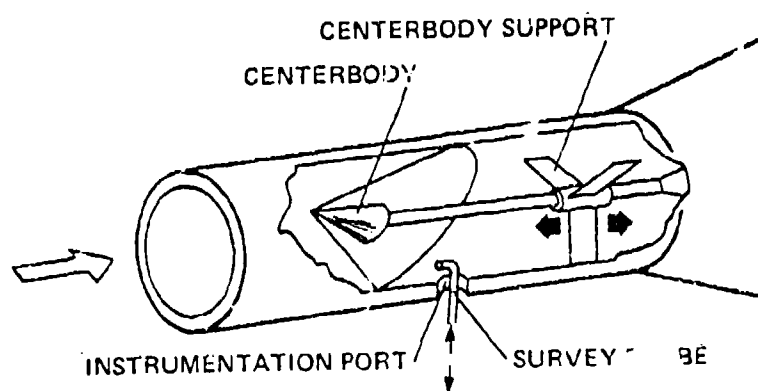


Figure 3a. Overall experimental test configuration, Case 8663.

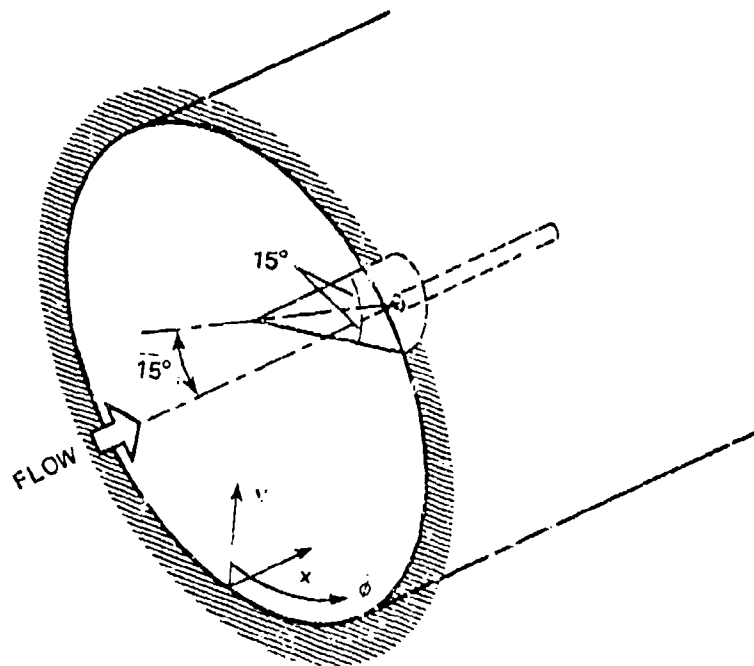


Figure 3b. Inset detail of test configuration, Case 8663.

$$M_\infty = 1.3-1.5, \quad \delta_\infty = 2.5 \text{ cm}, \quad Re_x = 8.5-225 \times 10^6, \quad Re_\delta = 0.3-6.0 \times 10^6$$

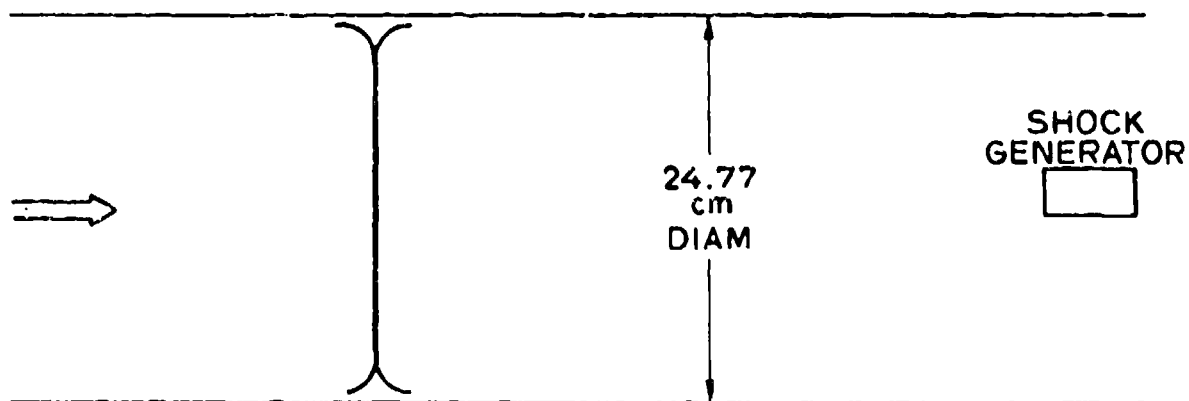
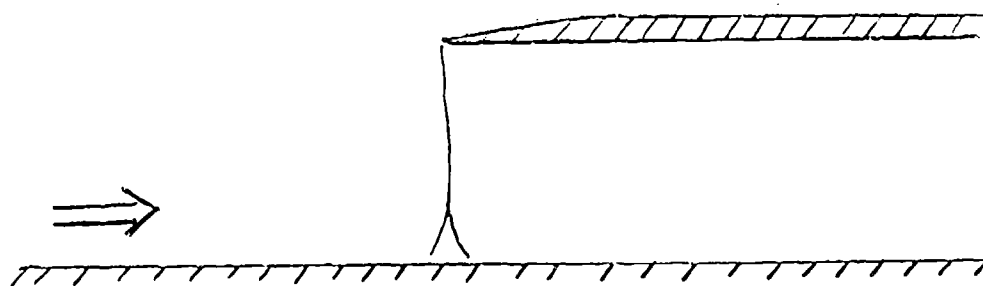
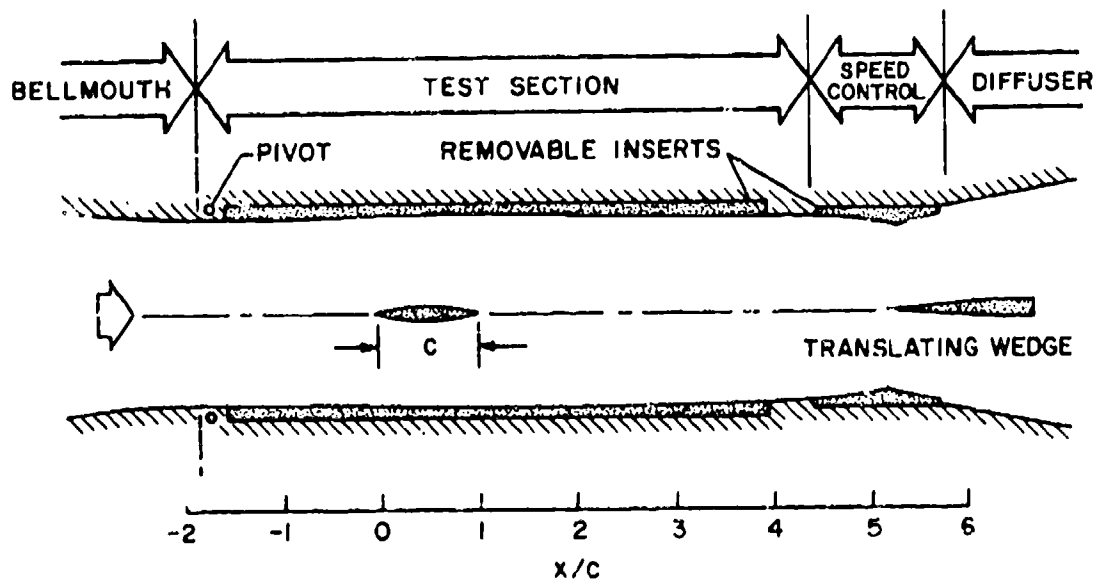


Figure 4. Experimental test configuration, Case 8601.



$$M_\infty = 1.4-1.46, \quad \delta_\infty = 1 \text{ cm}, \\ Re_{\delta_\infty} = 0.3 \times 10^6$$

Figure 5. Experimental test configuration, Case 8602.



$$M_{\infty} = 0.785, Re_c = 10 \times 10^6.$$

Figure 6. Case 8691, nonlifting transonic airfoil with shock separation.

DISCUSSION

Flows 8650 and 8660

Cases 8651 and 8661:

- M. Morkovin: I wish to comment on the necessity of specifying stagnation and static temperatures in the boundary layers. There are hidden uncertainties that arise from unknown thermal fields in flows of this kind.
- C. Horstman: The total temperature field was measured at each profile. This information is included in the data file.
- S. Kline: The data library will record all the data supplied by the experimenters, not only the information required for specifications.
- G. Settles: I am concerned about flow-field steadiness in boundary-layer shock interactions. We never see perfectly steady flows in the free stream. Is there some criterion by which we could judge the flow steadiness, and does Case 8651 meet this criterion?
- C. Horstman: Whenever separation and reattachment are not confined, one sees unsteadiness. However, although the separation is unsteady, the shock position is steady.
- K. Owen: There are large-scale motions for unconfined separation in almost all experiments. This large-scale unsteadiness will influence the measurement of turbulence quantities.
- A. Favre: How was the Reynolds-stress component measured? We measure it with cross wires.
- C. Horstman: The Reynolds stress was measured with a "V" wire. The uncertainty obtained was within 7-8% of the integrated velocity profiles upstream.

Flows 8600 and 8690

Cases 8601, 8602, and 8691.

- M. Firmin: What are the two-dimensionality checks on the airfoil experiment?
- M. Rubesin: Oil-streak flowgraphs were used. There was only a one-inch section on each end of the airfoil which was not two-dimensional.
- R. Melnik: One should really have a better test of two-dimensionality. Perhaps flow-field surveys could be made rather than oil flowgraphs. It is not enough for a flow to simply look two-dimensional. If a shock wave interacts with a wind-tunnel wall, the flow is no longer two-dimensional. This applies for both the airfoil and the Kooi experiment.

- M. Rubesin: Calculations were run for the Kooi experiment. The results did not quite agree, but the disagreement was consistent with other known two-dimensional experiments. It was concluded that three-dimensional effects are not too serious in this flow.
- R. Melnik: Was the pressure downstream assumed to be the pressure behind the shock wave? It shouldn't be if there are three-dimensional effects present.
- M. Rubesin: Yes, the downstream pressure was used.
- J. Viegas: I have used the downstream pressure in my experiments, and it has been satisfactory.
- H. McDonald: I question the use of the McDevitt flow for three reasons: 1. The geometry of the flow will require a special mesh generator in order to be computed. 2. Mesh definition in the vicinity of the leading edge seems to be particularly important for this flow. 3. Since this is not a practical airfoil design, it will be difficult to find funding for the computations.
- G. Lilley: In Case 8601, the calculation needs to be made in a circular duct. It is agreed that this interaction of a shock with a boundary layer should be considered as a tube flow or can it be represented by a two-dimensional flow?
- M. Rubesin: This is a tube-flow case.
- S. Bogdonoff: Is the shock really standing still in the tube flow of Kooi? It looks as though it should be an unstable (unsteady) configuration. Could this possibly explain the three-dimensional effects?
- J. Marvin: Data in the experiment were obtained by slowly moving the shock across the measuring instruments. Static-pressure measurements did not show any significant large-scale movements.
- M. Rubesin: I doubt that computations will be able to handle the high-frequency jitter of shock waves. It usually gets smeared out in these schemes.
- S. Bogdonoff: I am concerned with problems in stabilizing the position of the shock. In my experience, I've had trouble doing stabilizing normal shocks.

Further Discussion on Flows 8650, 8660, 8600, 8690

Case 8651

The Conference agreed to recommend Case 8651 as a test case. It was noted, however, that this is a special case relating to a high Mach number flow with relatively high uncertainties.

Cases 8661, 8662, and 8663

After lengthy discussions, all three of the above cases were recommended by the Conference without further comment.

Case 8601

The Conference agreed to recommend this flow as a test case. Based on questions that were raised in the morning session and the past experience of the committee members, there was considerable discussion concerning possible unsteadiness of the shock wave. When queried about this, however, the experimenter stated that information from high-frequency instrumentation (surface hot-wire signals) showed that the shock position was indeed steady.

Case 8602

The Conference agreed to accept this experiment. However, its summary and specifications need to provide a clearer description as to the exact nature and type of the flow.

Case 8691

This flow was recommended by the Conference. However, questions were raised, both in the morning session and at the evening committee meeting about the possibility of three-dimensional effects in this experiment. The available experimental evidence seems to indicate that the flow is sufficiently two-dimensional to make this a useful test of turbulence models and computational methods.

SPECIFICATIONS FOR COMPUTATION


ENTRY CASE/COMPRESSIBLE

Flow 8650, Case #8651; Data Evaluators: M. Rubesin and C. Horstman

Data Takers: M. Kussoy and C. Horstman

PICTORIAL SUMMARY

Flow 8650. Data Evaluators: M. Rubesin and C. Horstman. "Axisymmetric Shock Impingement (Supersonic)."

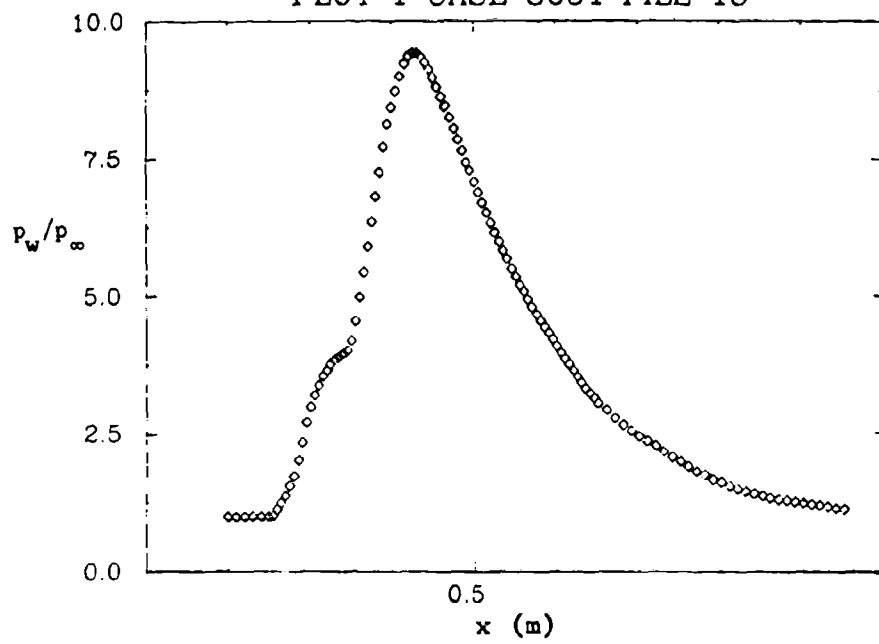
Case Data Taker	Test Rig Geometry	dp/dx or C _p	Number of Stations Measured								Re	M _∞	Other Notes
			Mean Velocity	Turbulence Profiles						C _f			
				U	V or W	$\overline{u^2}$	$\overline{v^2}$	$\overline{w^2}$	\overline{uv}				
Case 8651 H. Kussoy C. Horstman		various	10	-	-	4	-	-	PS 4	float- ing ele- ment	3.6 = 10 ⁵ (based on δ ₀)	7.2	Axisymmetric. Two cases - one attached and one separated. Heat transfer measure- ments included.

Plot	Ordinate	Abcissa	Range/Position	Comments
1	p_w/p_∞	x	$0.2 \leq x \leq 0.90$ m $0 \leq p_w/p_\infty \leq 10$	Wall-pressure distribution.
2	C_{f_∞}	x	$0.2 \leq x \leq 0.90$ m $-0.001 \leq C_{f_\infty} \leq 0.005$	Wall shear-stress distribution. $C_{f_\infty} = \tau_w / \frac{1}{2} \rho_\infty U_\infty^2$
3	y	U/U_∞	$0 \leq y \leq 0.035$ m $-0.3 \leq U/U_\infty \leq 1.0$	4 curves of velocity profile at x = 0.20, 0.33, 0.425, 0.70 m.
4	y	ρ/ρ_∞	$0 \leq y \leq 0.035$ m $0 \leq \rho/\rho_\infty \leq 5$	4 curves of density profile at x = 0.20, 0.33, 0.425, 0.70 m.

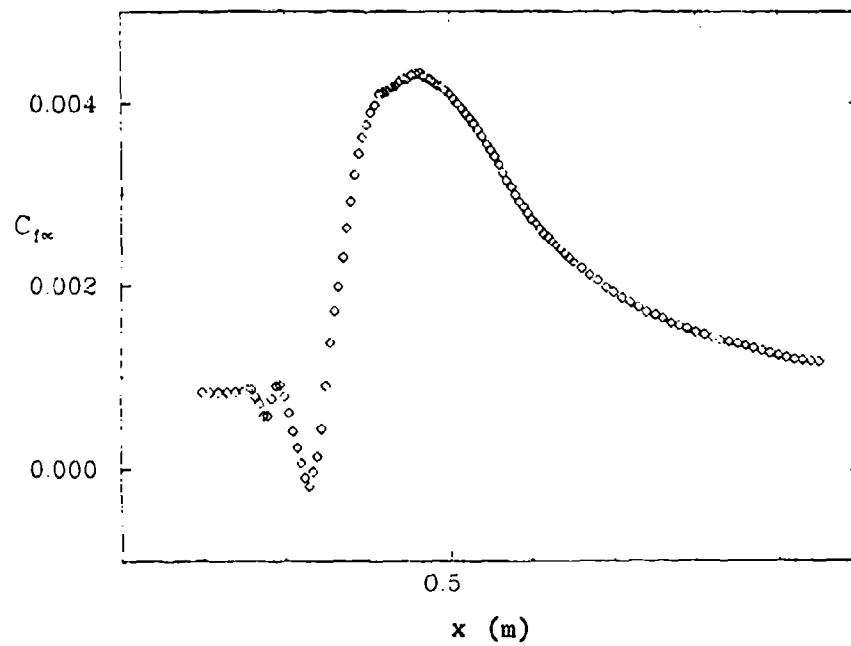
Special Instructions:

This test case considers the interaction of an axisymmetric shock wave with an axisymmetric boundary layer on the outside of a circular cylinder. Although two test cases are on the data tape, only one case (the separated case with a 15° shock generator) is to be calculated.

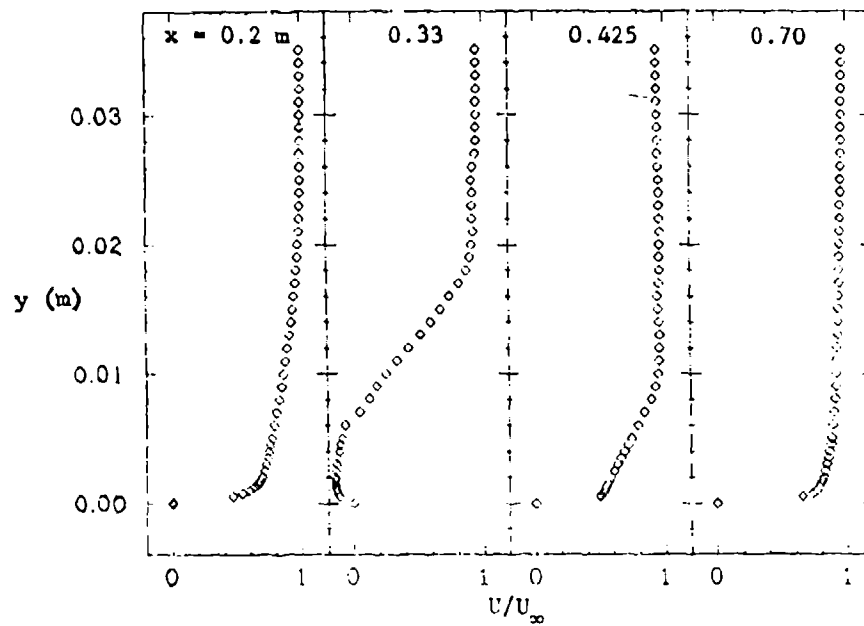
PLOT 1 CASE 8651 FILE 18



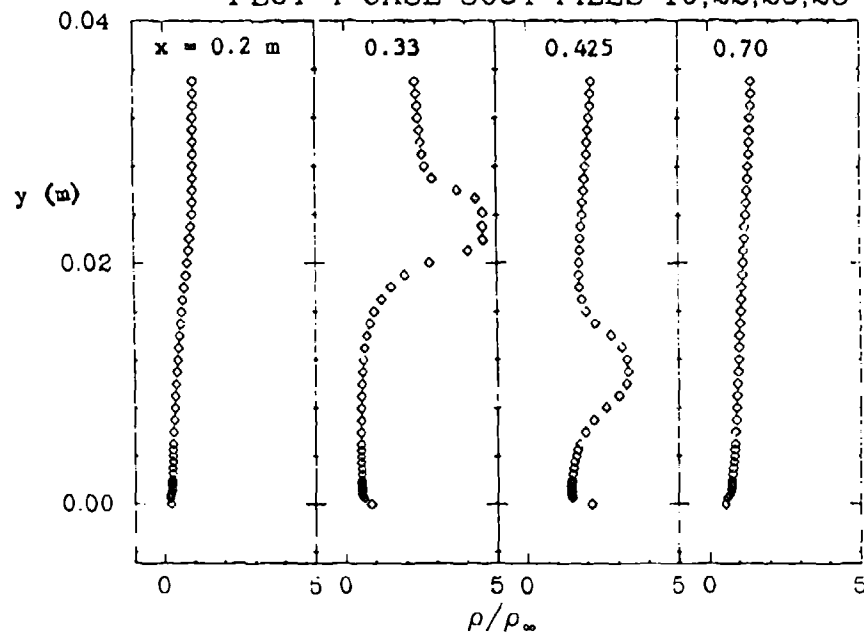
PLOT 2 CASE 8651 FILE 18



PLOT 3 CASE 8651 FILES 19,22,25,28



PLOT 4 CASE 8651 FILES 19,22,25,28



SPECIFICATIONS FOR COMPUTATION

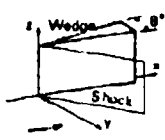
ENTRY CASE/COMPRESSIBLE

Flow 8660, Case #8661; Data Evaluators: M. Rubesin and C. Horstman

Data Taker: D. Peake

PICTORIAL SUMMARY

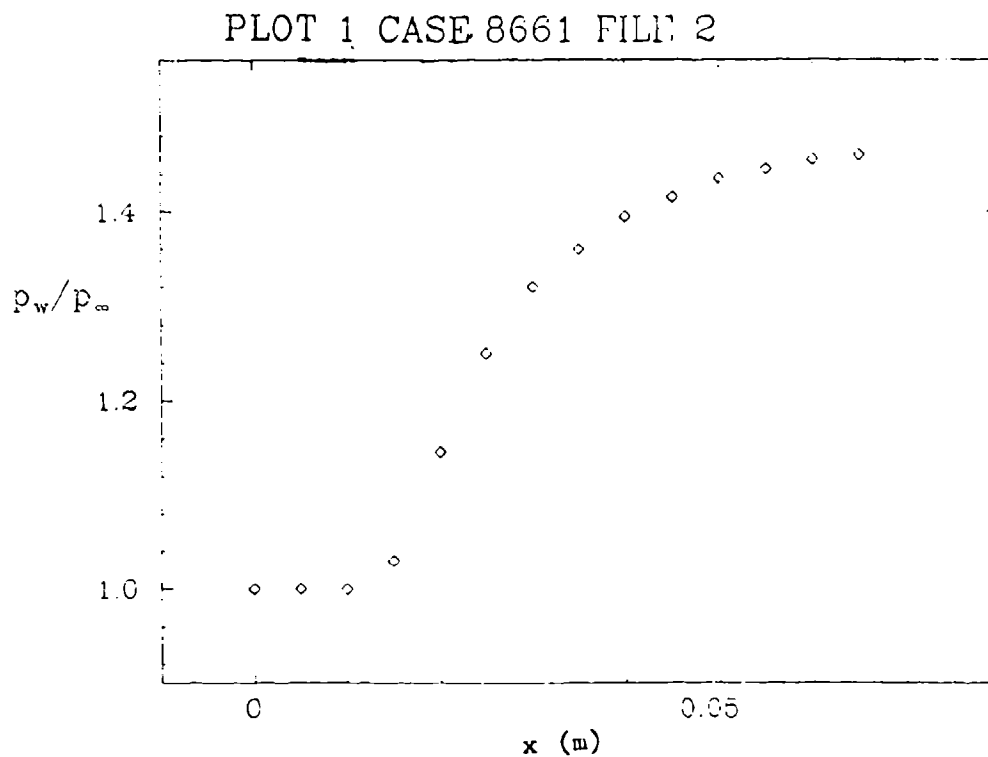
Flow 8660. Data Evaluators: M. Rubesin and C. Horstman. "Three-Dimensional Shock Impingement (Supersonic)."

Case Date Taker	Test Rig Geometry	dp/dx or C _p	Number of Stations Measured							C _f	Re	M _∞	Other Notes
			Mean Velocity		Turbulence Profiles								
			U	V or W	$\overline{u^2}$	$\overline{v^2}$	$\overline{w^2}$	\overline{uv}	Others				
Case 8661 D. Peake			5	5 ^a	-	-	-	-	Wall pres- sure	Pres- ton probe	1.5 × 10 ⁵ (based on δ ₀)	2	3D planar shock inter- section. ^a V known in terms of U and flow angle.

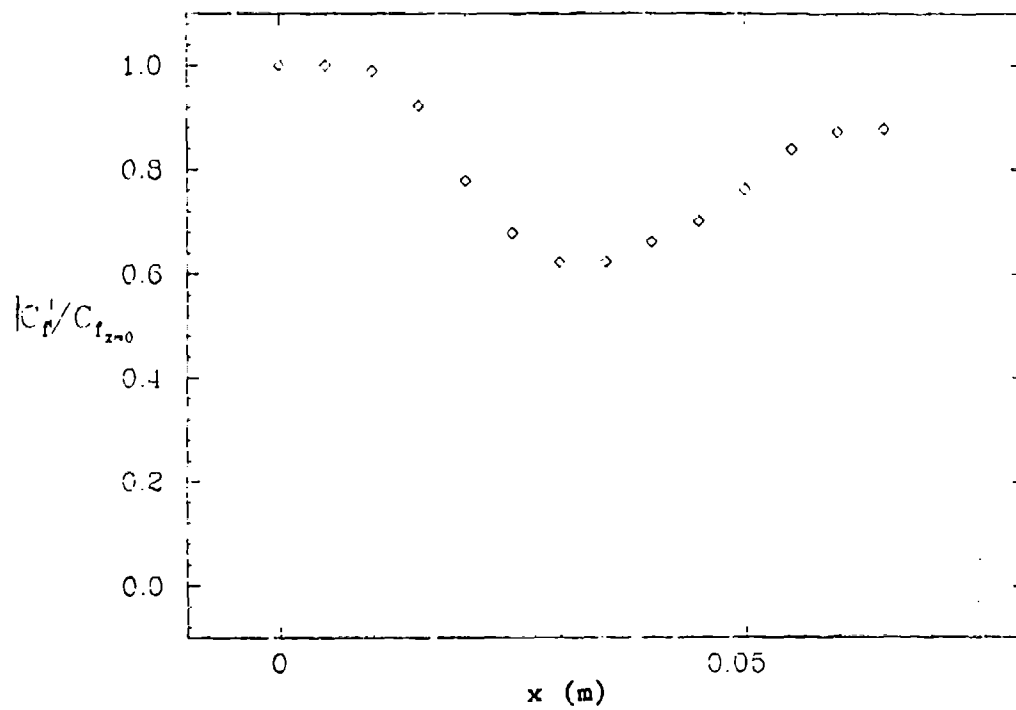
Plot	Ordinate	Abcissa	Range/Position	Comments
1	p_w/p_∞	x	$0 \leq x \leq 0.07 \text{ m}$ $1 \leq p_w/p_\infty \leq 1.6$	Wall-pressure distribution along $y = 0.0254 \text{ m}$.
2	$ C_f /C_{f_{x=0}}$	x	$0 \leq x \leq 0.07 \text{ m}$ $0 \leq C_f /C_{f_{x=0}} \leq 1.0$	Surface shear stress, $C_{f_{x=0}}$ is the surface skin-friction coef- ficient on the wind-tunnel floor at an x station corresponding to $x = 0$ (the leading edge of the wedge). Along $y = 0.0254 \text{ m}$.
3	$\alpha _{z=0}$ (deg.)	x	$0 \leq x \leq 0.07 \text{ m}$ $0 \leq \alpha _{z=0} \leq 40^\circ$	Surface shear direction along $y = 0.0254 \text{ m}$. $\alpha _{z=0} = \tan^{-1} \left\{ \left(\frac{\partial v}{\partial z} \right)_{z=0} / \left(\frac{\partial u}{\partial z} \right)_{z=0} \right\}$.
4	z	U/U_∞	$0 \leq z \leq 0.07 \text{ m}$ $0 \leq U/U_\infty \leq 1.0$	4 velocity profiles in the x-z plane at $y = 0.0254 \text{ m}$ at $x =$ 0.009, 0.0236, 0.0523, 0.0643 m.
5	z	α	$0 \leq z \leq 0.007 \text{ m}$ $0 \leq \alpha \leq 40^\circ$	4 curves of flow angle α for $y = 0.0254 \text{ m}$; $x = 0.009, 0.0236,$ 0.0523, 0.0643 m. $\alpha = \tan^{-1}(V/U)$.

Special Instructions:

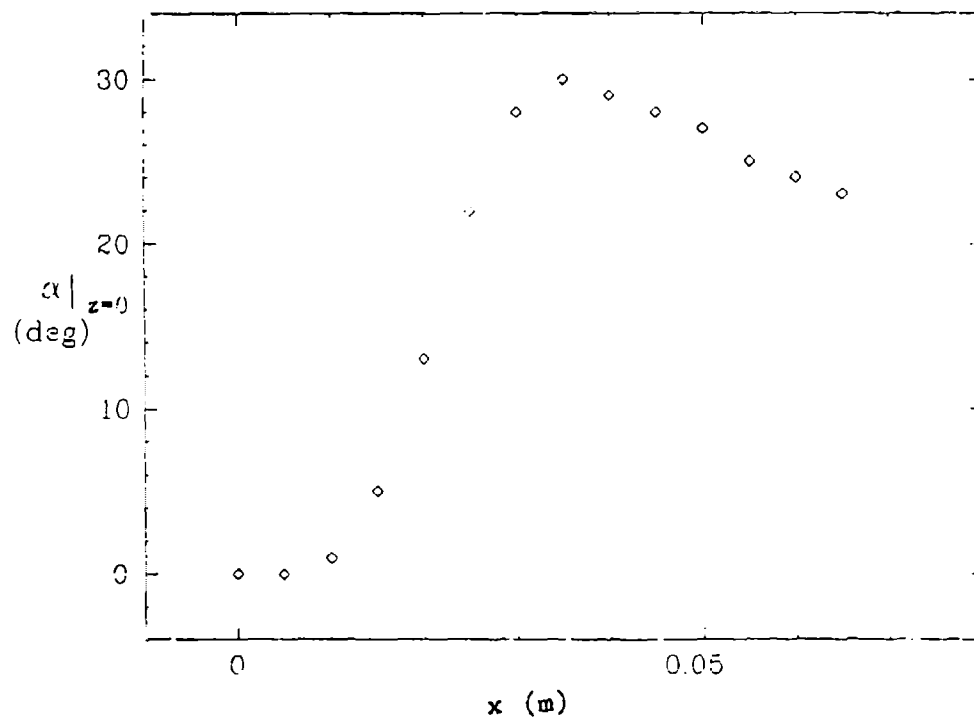
This test case considers the interaction of a skewed shock wave on a two-dimensional boundary layer. One test condition is to be computed. Upstream boundary conditions have been specified at $x = 0$, corresponding to the wedge leading edge.



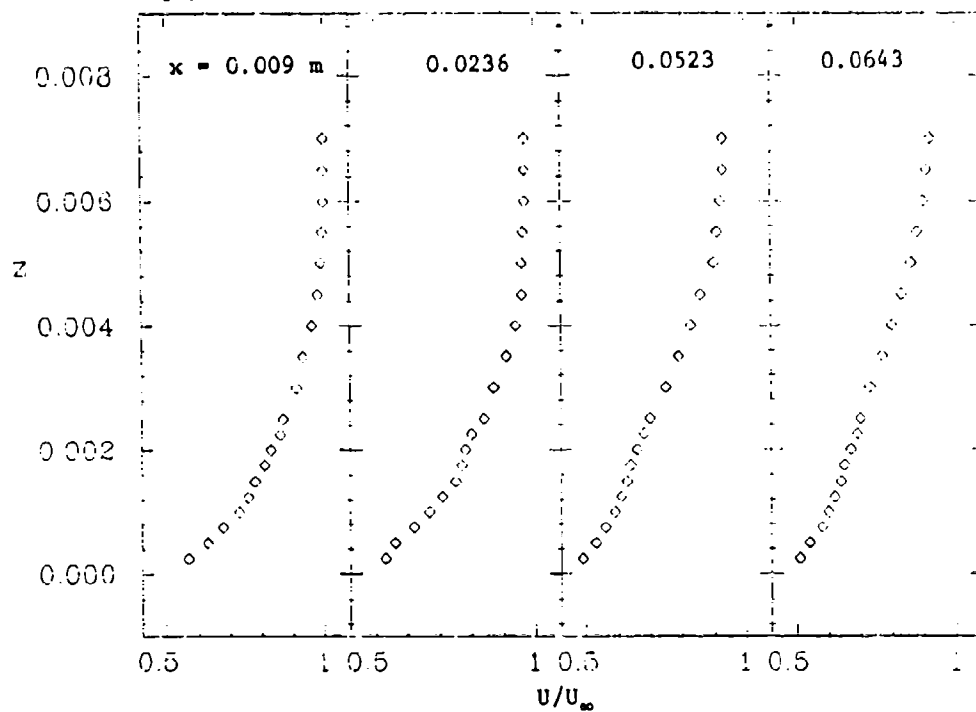
PLOT 2 CASE 8661 FILE 2



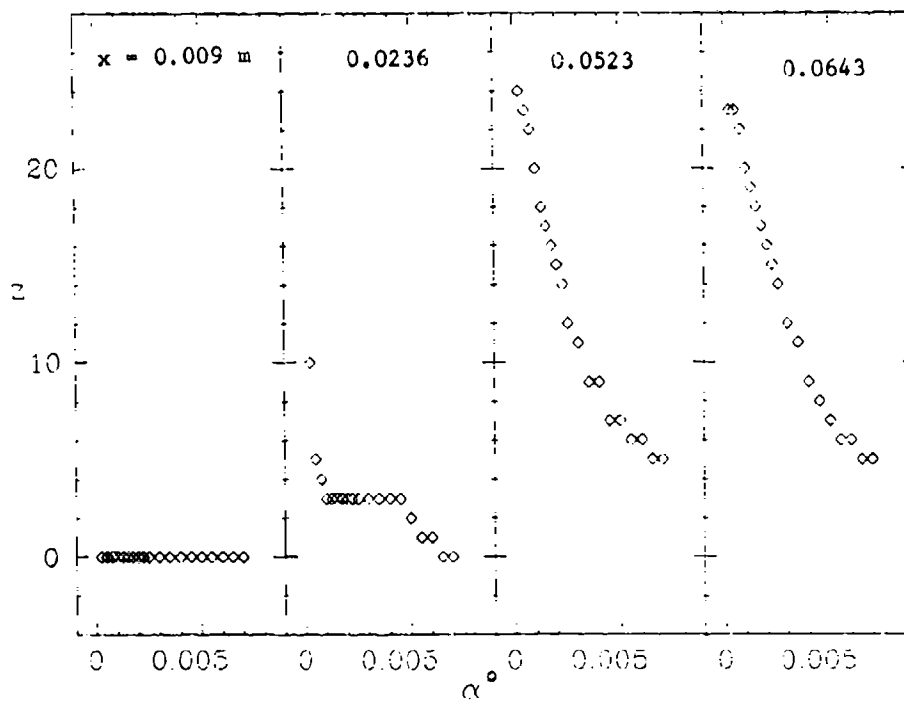
PLOT 3 CASE 8661 FILE 2



PLOT 4 CASE 8661 FILES 3,4,6,7



PLOT 5 CASE 8661 FILES 3,4,6,7



SPECIFICATIONS FOR COMPUTATION

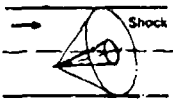
ENTRY CASE/COMPRESSIBLE

Flow 8660, Case #8663; Data Evaluators: M. Rubesin and C. Horstman

Data Takers: M. Kussoy, J. Viegas and C. Horstman

PICTORIAL SUMMARY

Flow 8660. Data Evaluators: M. Rubesin and C. Horstman. "Three-Dimensional Shock Impingement (Supersonic)." .

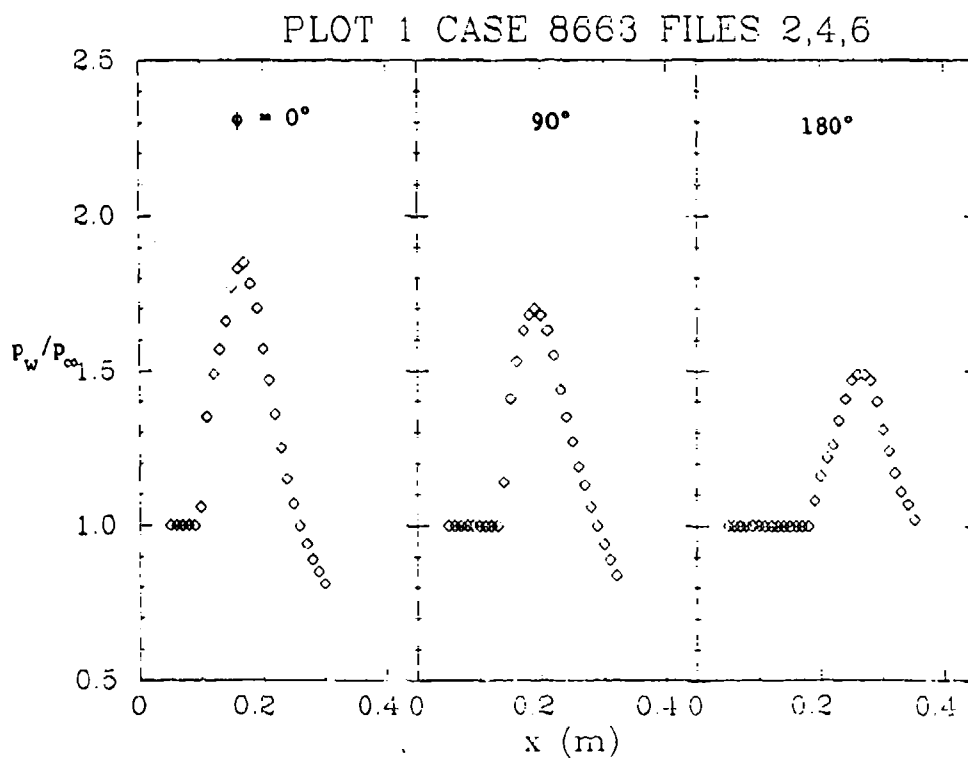
Case Data Taker	Test Rig Geometry	dp/dx or C _p	Number of Stations Measured								C _f	Re	M _∞	Other Notes
			Mean Velocity		Turbulence Profiles									
			U	v or W	$\overline{u^2}$	$\overline{v^2}$	$\overline{w^2}$	\overline{uv}	Others					
Case 8663 M. Kussoy J. Viegas C. Horstman			5	Flow angle at various sta- tions around cone	5	5	5	5	5	1.0 x 10 ⁶ (based on d _o)	2.17	1D curved shock inter- action. Turbulence measurements limited to windward and leeward planes.		

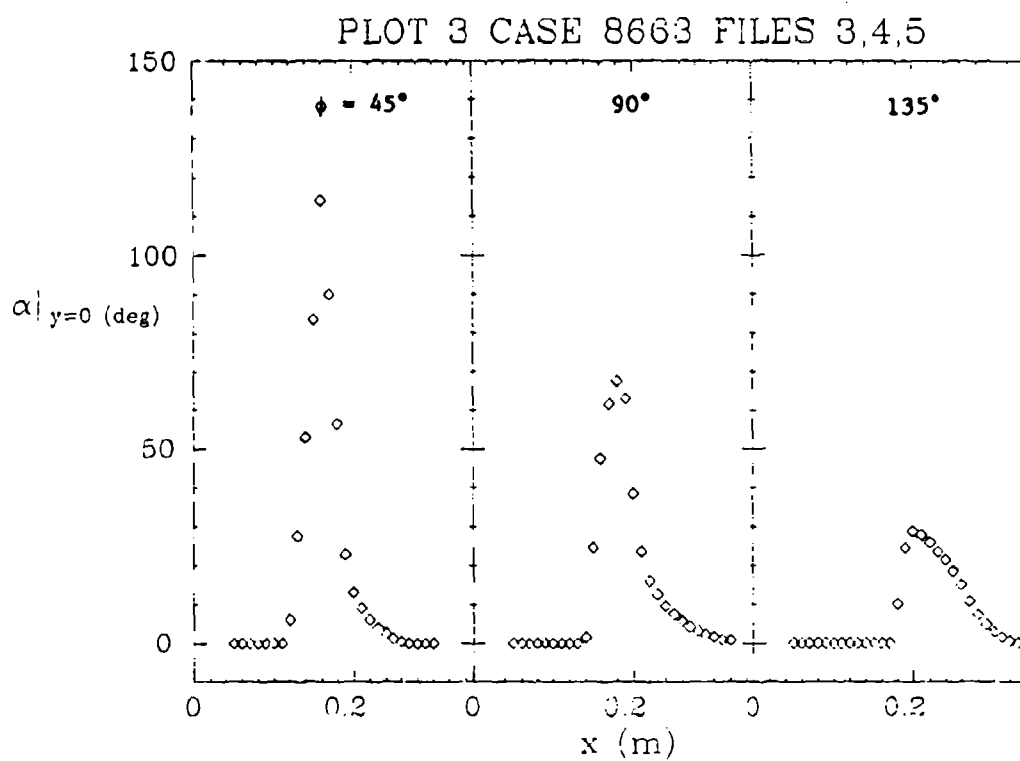
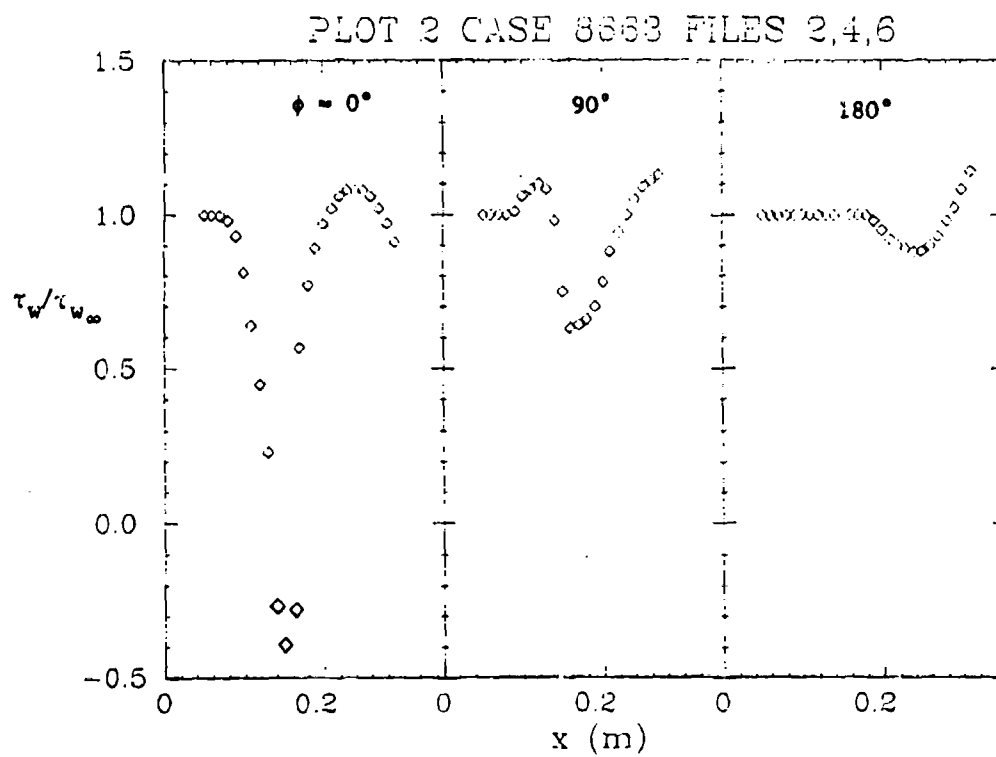
Plot	Ordinate	Abcissa	Range/Position	Comments
1	p_w/p_∞	x	$0.06 \leq x \leq 0.28$ m $0.5 \leq p_w/p_\infty \leq 2.5$	Wall-pressure distribution. 3 curves at $\phi = 0^\circ, 90^\circ, 180^\circ$.
2	τ_w/τ_{w_∞}	x	$0.06 \leq x \leq 0.28$ m $-0.5 \leq \tau_w/\tau_{w_\infty} \leq 1.5$	Wall shear-stress distribution. τ_{f_∞} evaluation at $x = 6$ cm. 3 curves at $\phi = 0^\circ, 90^\circ, 180^\circ$.
3	$\alpha _{y=0}$ (deg.)	x	$0.06 \leq x \leq 0.28$ m $0 \leq \alpha _{y=0} \leq 150^\circ$	Surface shear direction $\alpha _{y=0} = \tan^{-1} \left(\frac{\partial w}{\partial y} \right)_{y=0} / \left(\frac{\partial u}{\partial y} \right)_{y=0}$ 3 curves at $\phi = 45^\circ, 90^\circ, 135^\circ$.
4	y	U/U_∞	$0 \leq y \leq 0.04$ m $-0.1 \leq U/U_\infty \leq 1.0$	Velocity profile at $\phi = 0^\circ$. 4 curves at $x = 0.06, 0.12, 0.20, 0.26$ m.
5	y	\sqrt{K}/U_∞	$0 \leq y \leq 0.04$ m $0 \leq \sqrt{K}/U_\infty \leq 0.1$	Turbulence kinetic-energy profiles at $\phi = 0^\circ$. 4 curves at $x = 0.06, 0.12, 0.20, 0.26$ m.
6	y	$\tau/\rho_\infty U_\infty^2$	$0 \leq y \leq 0.04$ m $-0.0003 \leq \tau/\rho_\infty U_\infty^2 \leq 0.0008$	Turbulence shear-stress profiles at $\phi = 0^\circ$. 3 curves at $x = 0.06, 0.20, 0.26$ m.

Plot	Ordinate	Abscissa	Range/Position	Comments
7	y	α (deg.)	$0 \leq y \leq 0.04 \text{ m}$ $0 \leq \alpha \leq 40^\circ$	Flow-angle profiles at $\phi = 90^\circ$. 4 curves at $x = 0.12, 0.15,$ $0.20, 0.26 \text{ m}$. $\alpha = \tan^{-1}(W/U)$.

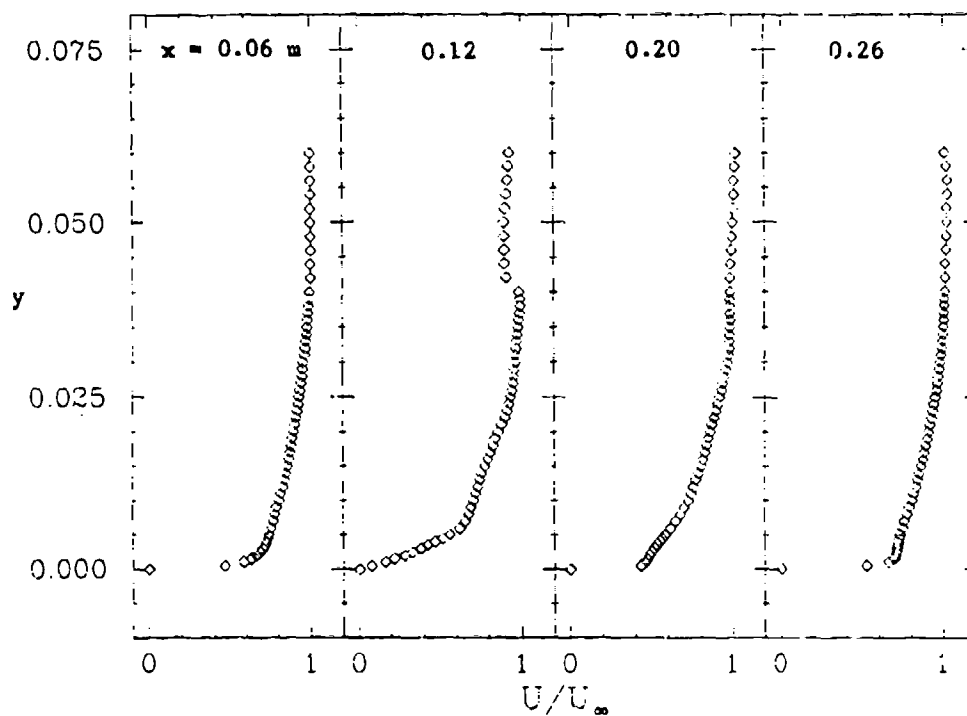
Special Instructions:

This test case considers the interaction of a skewed three-dimensional shock wave with an axisymmetric boundary layer inside a tube.

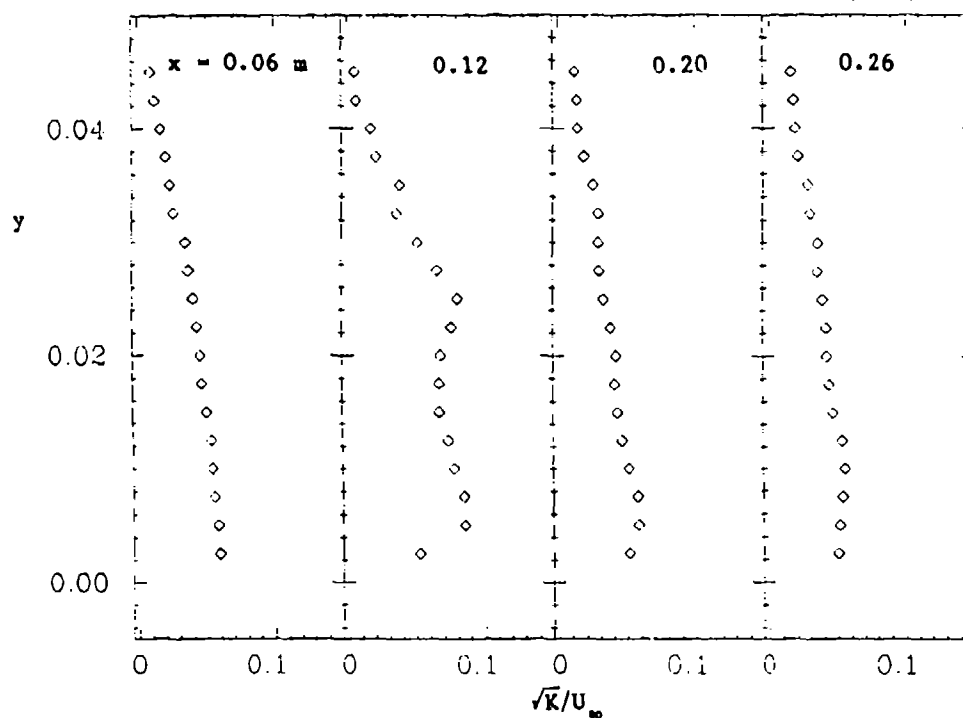




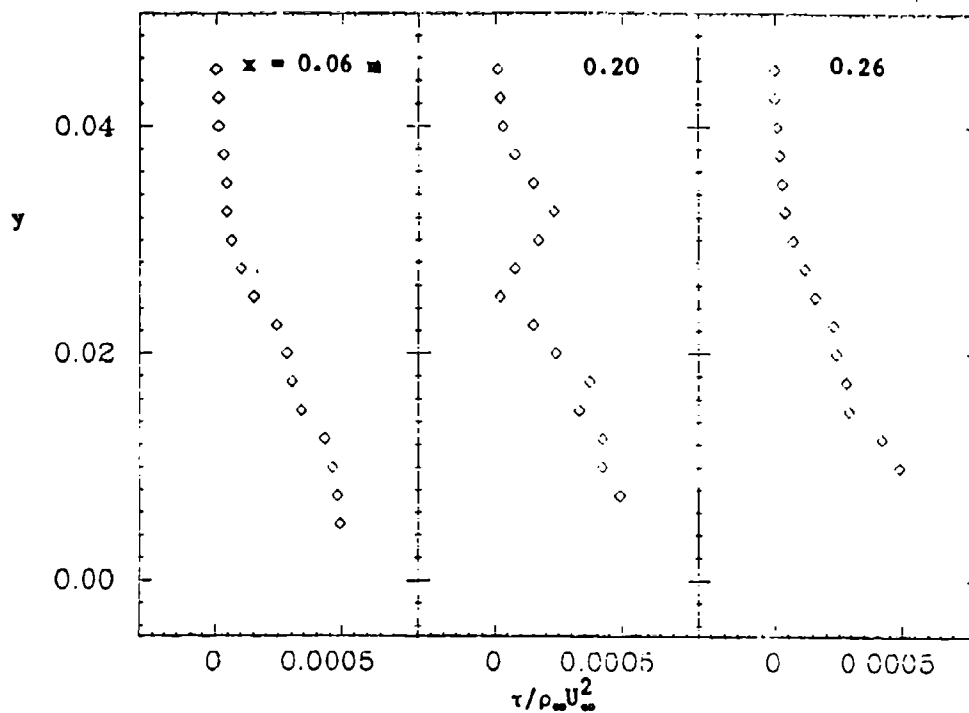
PLOT 4 CASE 8663 FILES 7,3,10,11



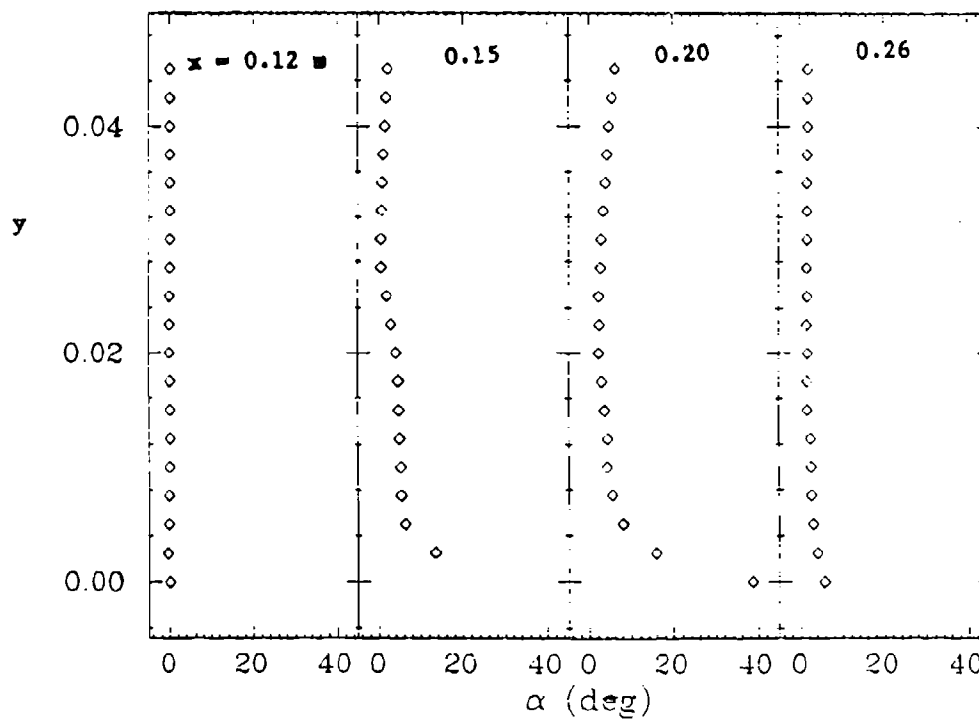
PLOT 5 CASE 8663 FILES 37,38,40,41



PLOT 6 CASE 8663 FILES 37, 10,41



PLOT 7 CASE 8663 FILES 25,26,27,28




SPECIFICATIONS FOR COMPUTATION

ENTRY CASE/COMPRESSIBLE

Flow 8600, Case #8601; Data Evaluators: M. Rubesin and C. Horstman
Data Takers: G. Mateer, A. Brosh and J. Viegas

PICTORIAL SUMMARY

Flow 8600. Data Evaluators: M. Rubesin and C. Horstman. "Impinged Normal Shock Wave-Boundary Layer Interaction at Transonic Speeds."

Case Data Taker	Test Rig Geometry	dp/dx or C _p	Number of Stations Measured										Re	M _∞	Other Notes
			Mean Velocity		Turbulence Profiles						C _f				
			U	V or W	$\overline{u^2}$	$\overline{v^2}$	$\overline{w^2}$	\overline{uv}	Others						
Case 8601 G. Mateer A. Brosh J. Viegas			8	-	-	-	-	8	pr -	Buried wire	3×10 ⁵ to 6×10 ⁶ (based on δ ₀)	1.3 - 1.5	Axisymmetric profile data for one test condition. Skin friction data for several test conditions varying M and Re.		

Plot	Ordinate	Abscissa	Range/Position	Comments
1-7	p/p_∞	x	$-2 \leq x \leq 20$ $1 \leq p/p_\infty \leq 2$	Wall pressure distribution for each of 7 test conditions; see instruction 1.
8-14	C_{f_∞}	x	$-2 \leq x \leq 20$ $0 \leq C_{f_\infty} \leq 0.0022$	Skin friction distribution $C_{f_\infty} =$ $\tau_w / \frac{1}{2} \rho_\infty U_\infty^2$ for each of 7 test conditions; see instruction 1.
15	y	U/U_∞	$0 \leq y \leq 0.10$ m $0 \leq U/U_\infty \leq 1.0$	Velocity profiles for test condition A at $x/\delta_\infty = 0, 4, 8,$ and 16; see instruction 2.
16	y	$-\rho \overline{uv} / \rho_\infty U_\infty^2$	$-0.002 \leq$ $-\rho \overline{uv} / \rho_\infty U_\infty^2$ ≤ 0.01	Shear-stress profiles for test condition A at $x/\delta_\infty = 4, 8,$ and 16; see instruction 2.

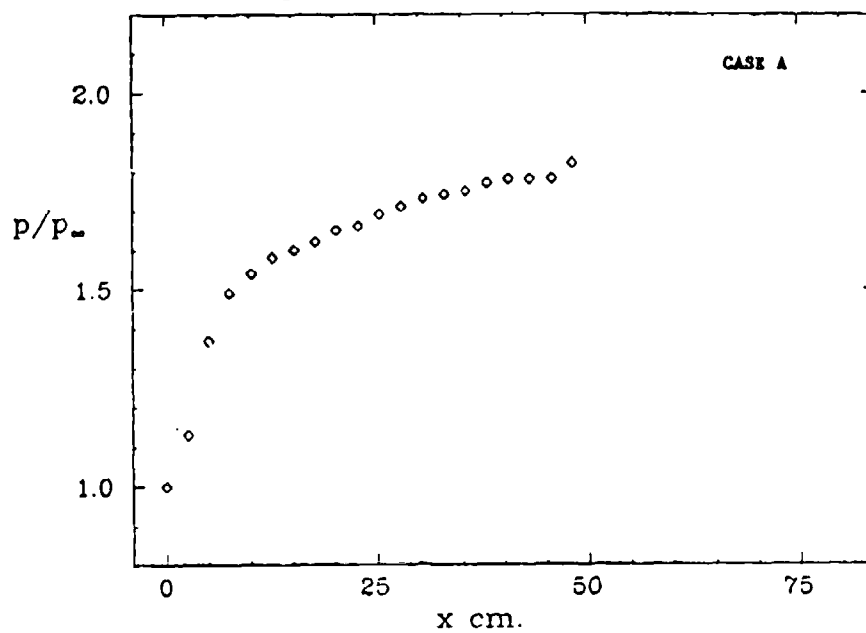
Special Instructions:

- Measurements were made for several Mach numbers and Reynolds numbers. Cases are designated as follows:

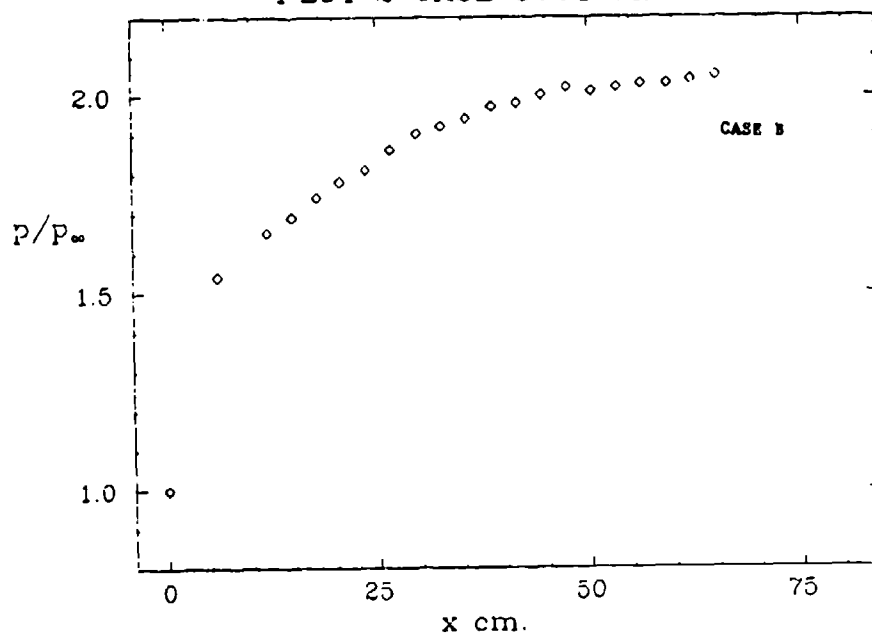
Case	M_∞	$\rho_\infty (\text{kg/m}^3)$	Plots
A	1.44	0.713	1, 8
B	1.42	0.182	2, 9
C	1.42	0.835	3, 10
D	1.42	2.908	4, 11
E	1.32	0.301	5, 12
F	1.41	0.368	6, 13
G	1.48	0.513	7, 14

- $\delta_\infty = 0.0254$ m for Case A.

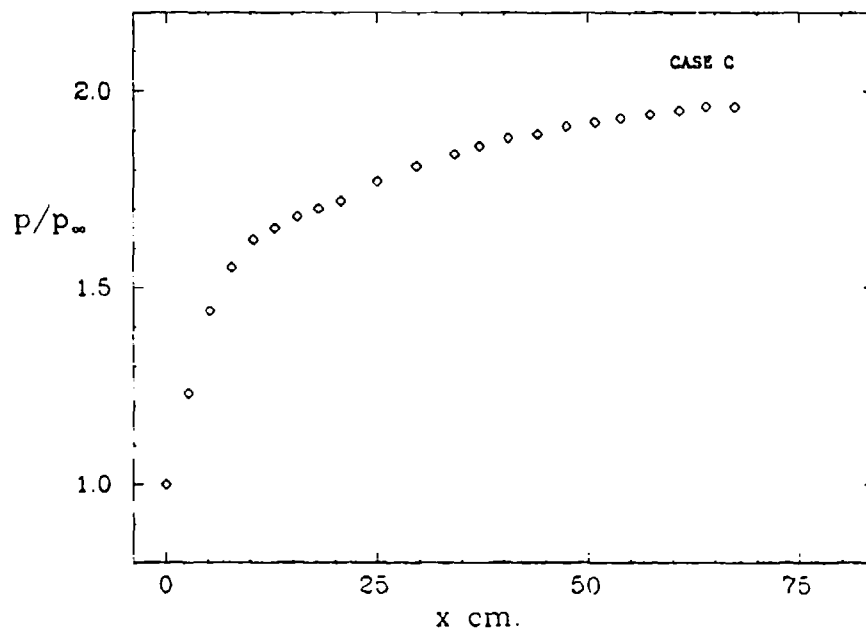
PLOT 1 CASE 8601 FILE 2



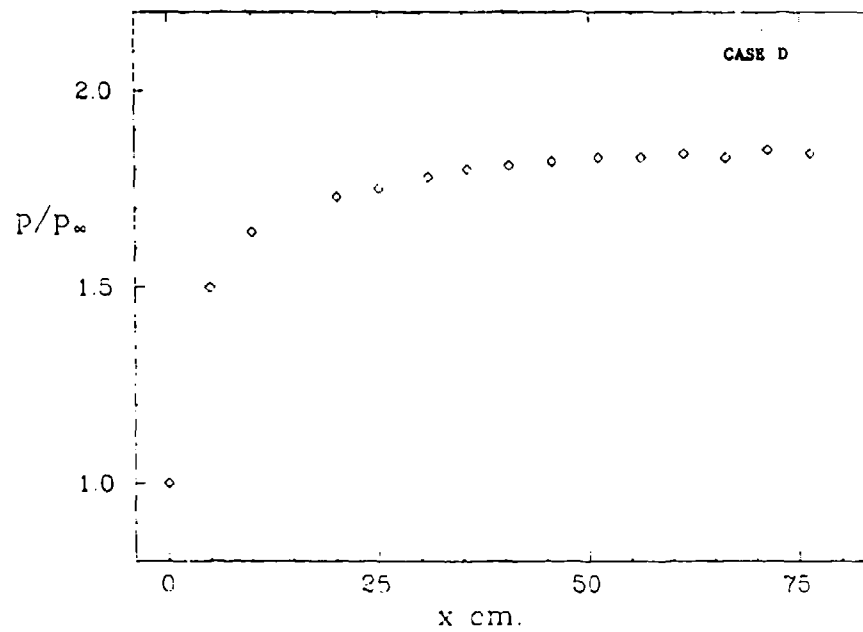
PLOT 2 CASE 8601 FILE 20



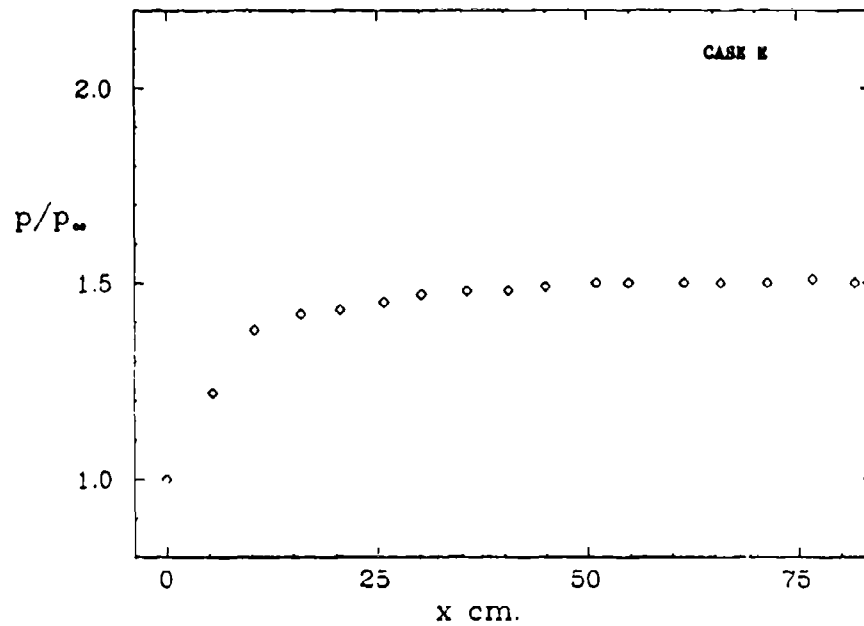
PLOT 3 CASE 8601 FILE 24



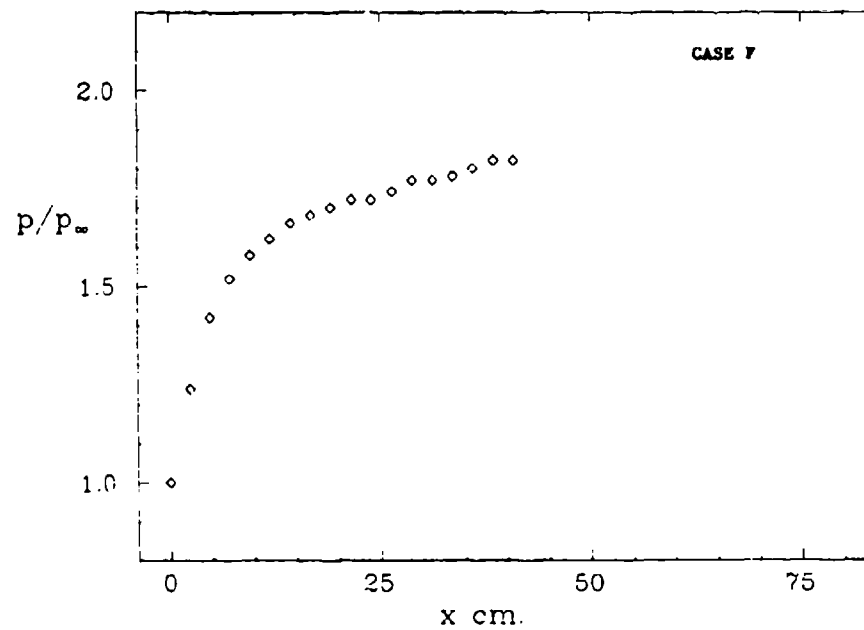
PLOT 4 CASE 8601 FILE 26



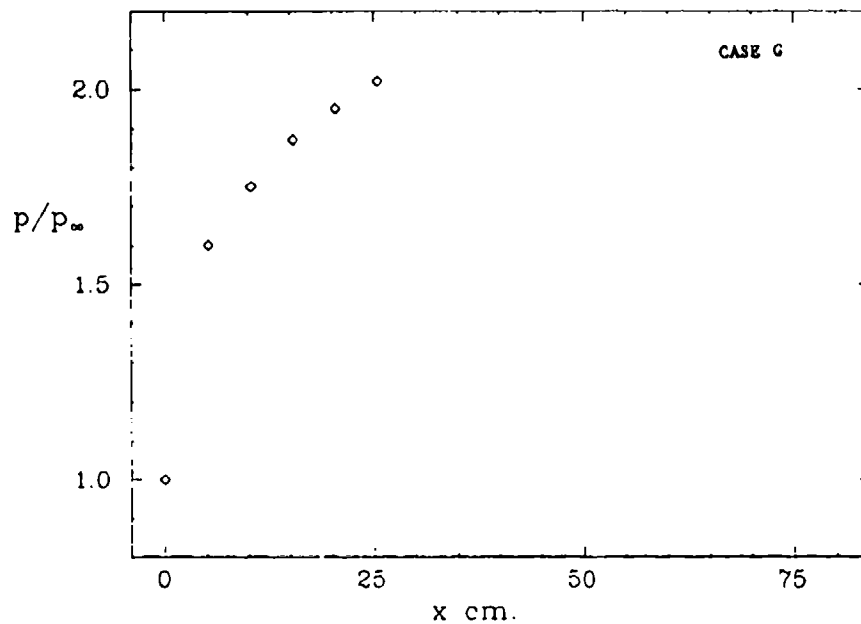
PLOT 5 CASE 8601 FILE 26



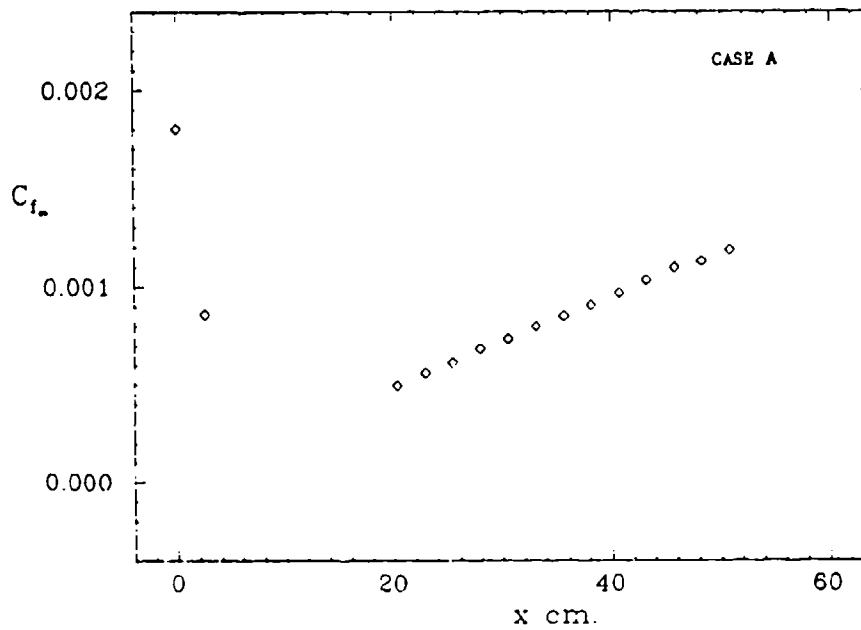
PLOT 6 CASE 8601 FILE 28



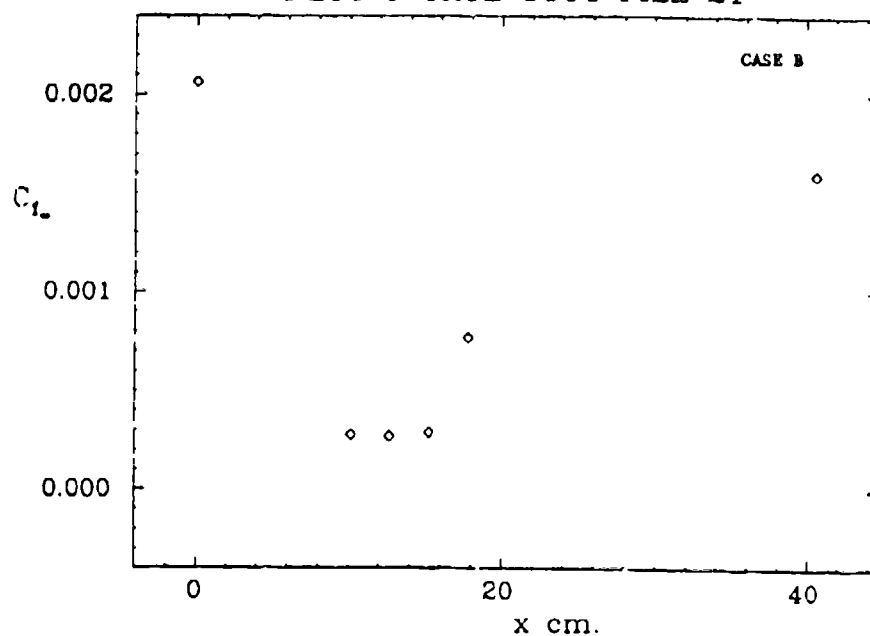
PLOT 7 CASE 8601 FILE 30



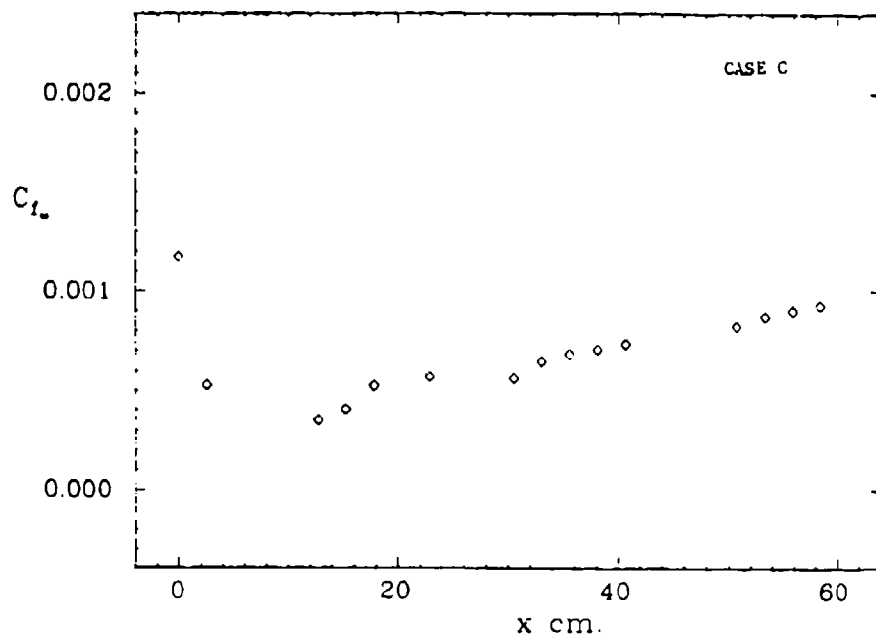
PLOT 8 CASE 8601 FILE 3



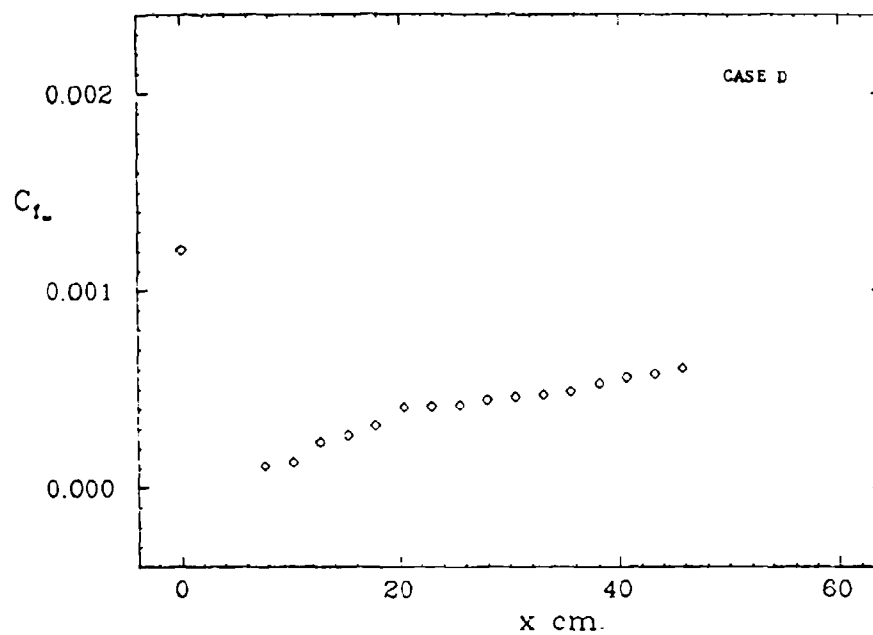
PLOT 9 CASE 8601 FILE 21



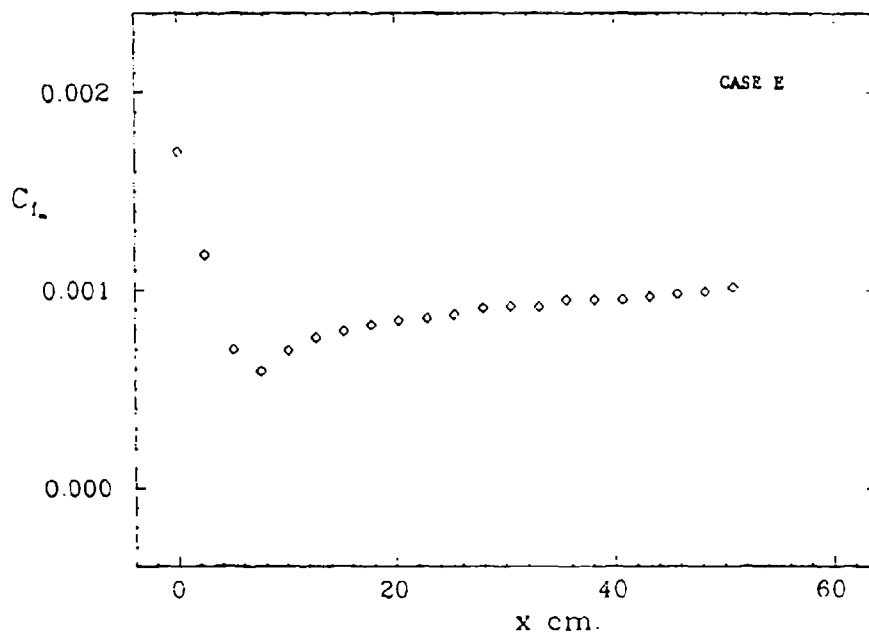
PLOT 10 CASE 8601 FILE 23



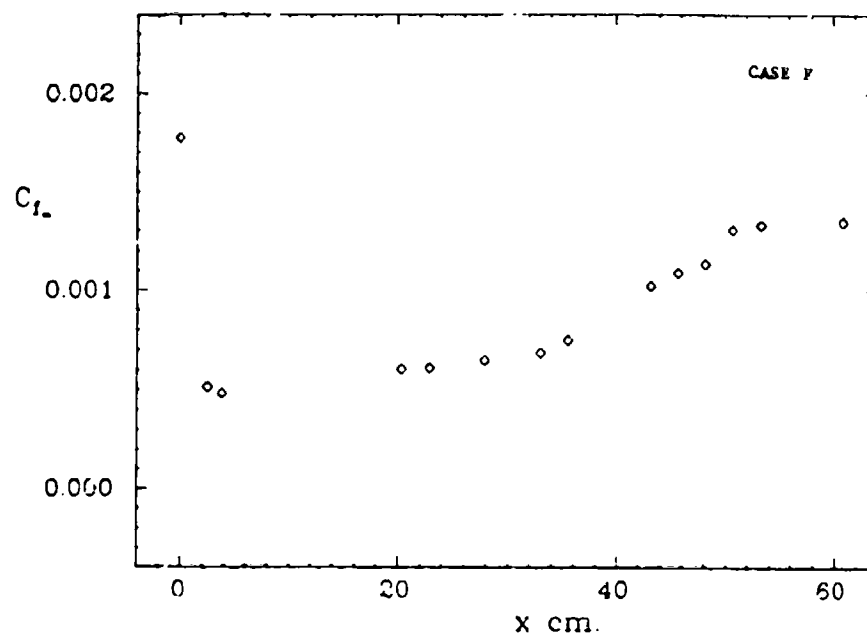
PLOT 11 CASE 8601 FILE 25



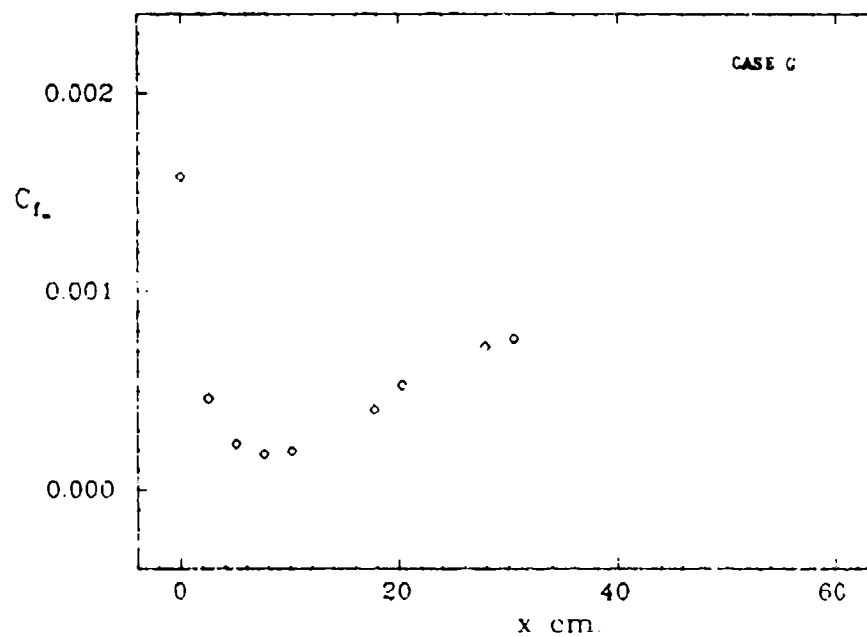
PLOT 12 CASE 8601 FILE 27



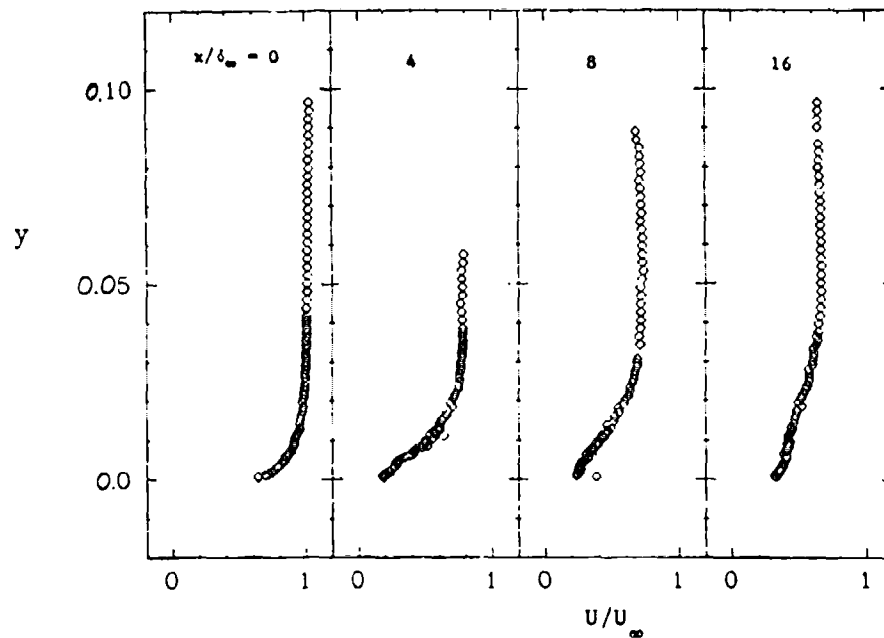
PLOT 13 CASE 8601 FILE 29



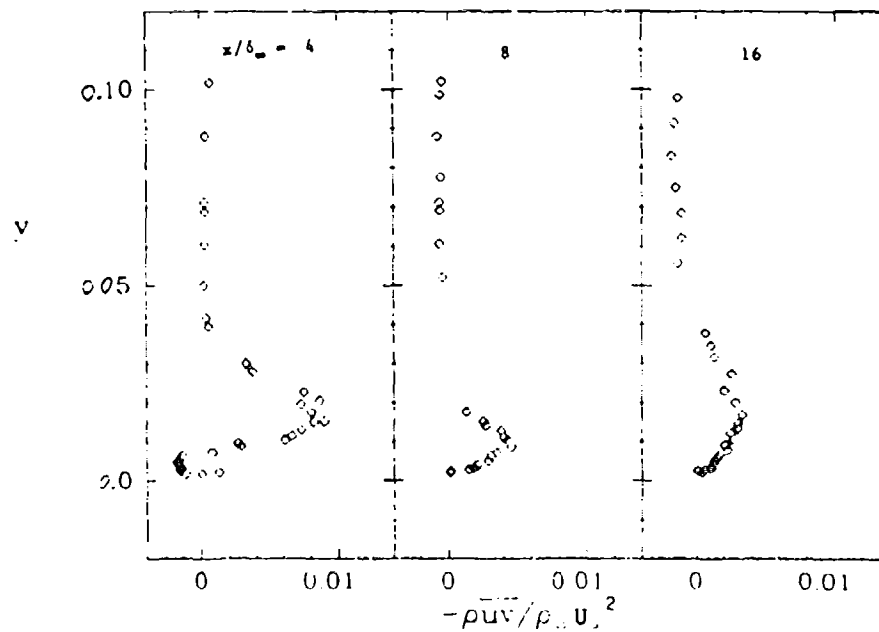
PLOT 14 CASE 8601 FILE 31



PLOT 15 CASE 8601 FILES 5,7,9,15



PLOT 16 CASE 8601 FILES 6,8,14



SPECIFICATIONS FOR COMPUTATION


ENTRY CASE/COMPRESSIBLE

Flow 8690, Case #8691; Data Evaluators: M. Rubesin and C. Horstman

Data Takers: J. McDevitt, H. Seegmiller, and A. Okuno

PICTORIAL SUMMARY

Flow 8690. Data Evaluators: M. Rubesin and C. Horstman. "Non-Lifting, Transonic Airfoil with Shock-Separation."

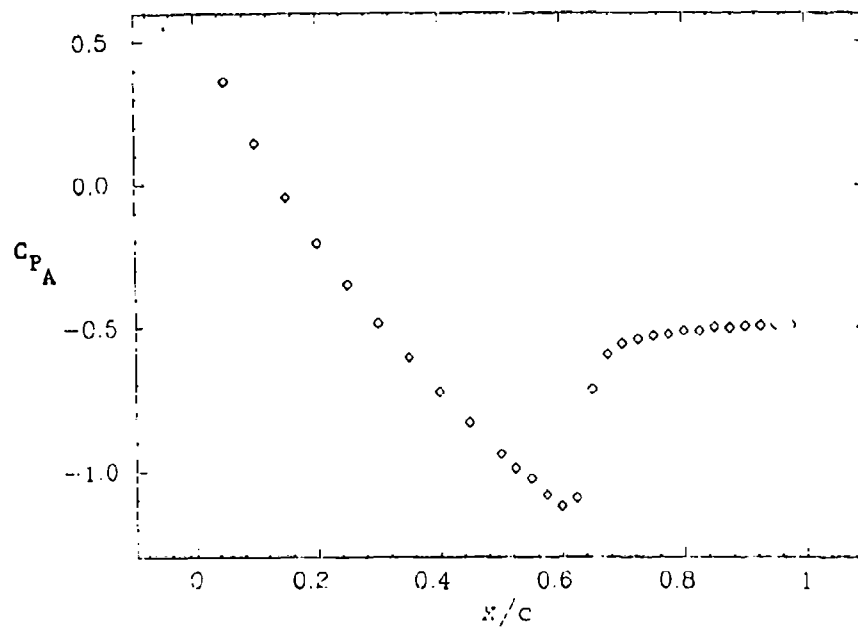
Case Data Taker	Test Rig Geometry	dp/dx or C _p	Number of Stations Measured							Re	M _∞	Other Notes
			Mean Velocity	Turbulence Profiles				C _f				
				U V W	u ²	v ²	w ²		uv			
Case 8691 J. McDevitt A. Okuno H. Seegmiller			7 7	7 7	-	7	Surface pres- sure	buried wire	1.1 x 10 ⁷ (based on chord)	0.785	Circular arc airfoil with large separation.	

Plot	Ordinate	Abscissa	Range/Position	Comments
1	C _{pA}	x/c	0 ≤ x/c ≤ 1.0 0.4 ≤ C _{pA} ≤ 1.2	Wall-pressure distribution, C _{pA} = (p - p _∞)/1/2 ρ _∞ U _∞ ² .
2	y/c	U/U _∞	0 ≤ y/c ≤ 0.16 -0.5 ≤ U/U _∞ ≤ 1.5	4 curves at x/c = 0.8, 0.9, 1.0, and 1.1.
3	y/c	K/U _∞ ²	0 ≤ y/c ≤ 0.16 0 ≤ K/U _∞ ² ≤ 0.20	4 curves at x/c = 0.8, 0.9, 1.0, and 1.1.
4	y/c	-uv/U _∞ ²	0 ≤ y/c ≤ 0.16 0 ≤ -uv/U _∞ ² ≤ 0.05	4 curves at x/c = 0.8, 0.9, 1.0, and 1.1.

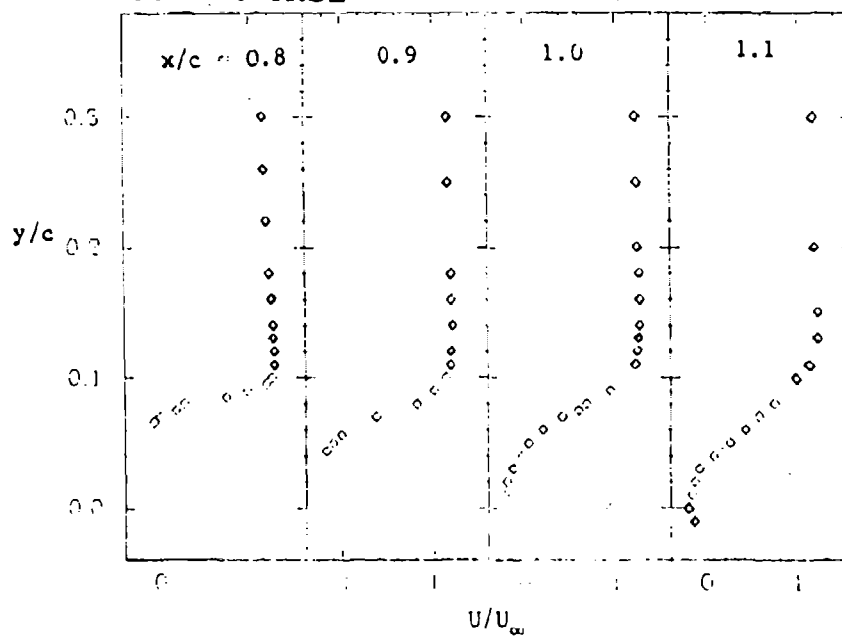
Special Instructions:

This test case considers the transonic flow over a circular-arc airfoil with a large region of shock-separated flow. To compute the turbulent kinetic energy from the data set, assume $K/U_{\infty}^2 = 0.75(u^2 + v^2)/U_{\infty}^2$.

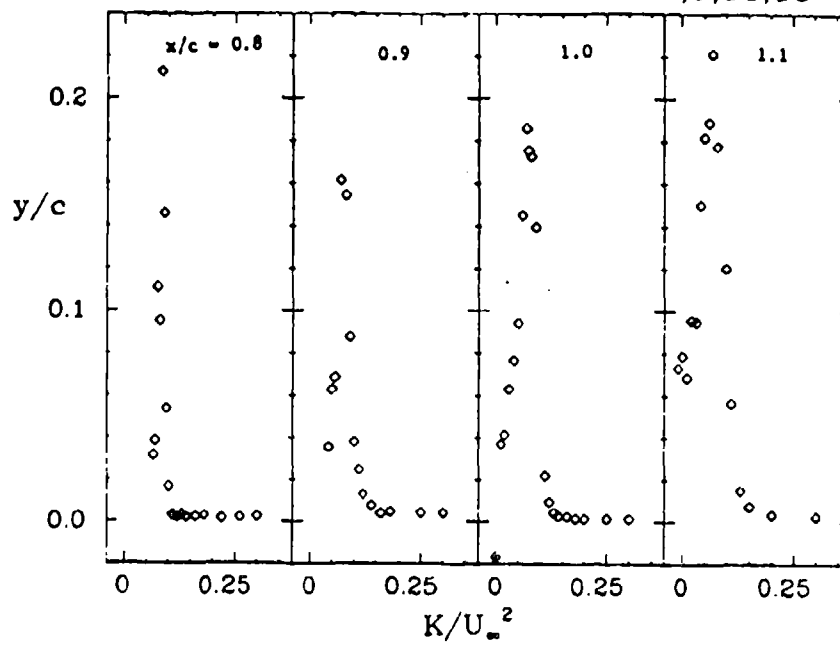
PLOT 1 CASE 8691 FILE 3



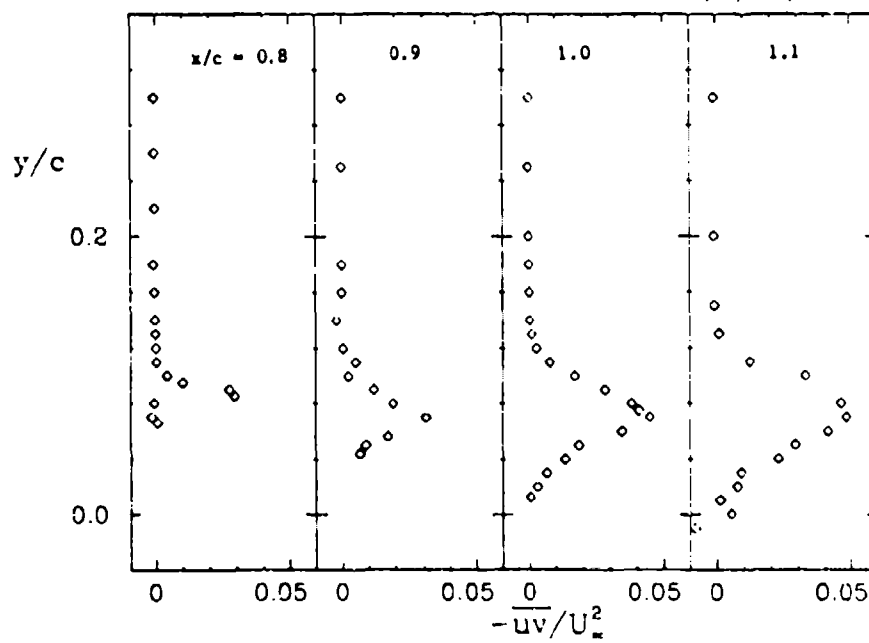
PLOT 2 CASE 8691 FILES 7,9,11,13



PLOT 3 CASE 8691 FILES 7,9,11,13



PLOT 4 CASE 8691 FILES 7,9,11,13



SESSION XI

Chairman: P. Bradshaw

Technical Recorders:

R. Carella
P. N. Joubert

Flow 8620

Flow 8670

Flow 8310

TRANSONIC AIRFOILS

Flow 8620

Cases 8621, 8623

Evaluator: R. E. Melnik*



SUMMARY

In this study we examined available wind-tunnel data for transonic flow over planar airfoils to assess their usefulness for validating theoretical methods for viscous transonic flow. Only wind-tunnel data that included measurements of boundary-layer-velocity profiles were considered in this study. Due to the scarcity of such data only very loose criteria could be applied in accepting data for the study. All of the proposed data sets have some shortcomings that make them not entirely satisfactory for the purposes of the Stanford Conference. However, it was felt that the chosen data sets were the best available for the purposes of the Conference and that comparisons of theory with these data would serve the useful purpose of focusing attention on possible shortcomings of both the theoretical methods and the available data base.

SELECTION CRITERIA

The main criteria we employed for selecting data for this study involved (1) airfoil geometry; (2) flow conditions; (3) type of measurements; and (4) documentation.

Airfoil Geometry

Only airfoil geometries with blunt leading edges and sharp trailing edges (with a possible small trailing-edge gap) were considered. It was thought desirable to include airfoils with significant rear camber, typical of the new generation of supercritical airfoils, as these lead to enhanced boundary-layer effects and to more definitive tests of theoretical methods. Experiments on airfoil-like shaped tunnel walls or airfoils with sharp leading edges were not considered representative of airfoil flows in free air and hence were not recommended for use in the study.

Flow Conditions

Only transonic data sets that included supercritical flows with extensive supersonic zones and shock waves were considered acceptable. We also felt it important to include cases with variations of shock strength and Reynolds number. We also restricted attention to cases with fully attached boundary layers as we felt separated cases involved complicating features that would best be addressed in the conference section

*Crumman Aerospace Corp., Research Dept., Bethpage, New York 11714.

dealing exclusively with separated flows. In addition, it was required that the position of transition be known and that it be demonstrated that a fully developed turbulent boundary layer was established upstream of all shock waves.

Measurements

Only data sets that included both surface-pressure measurements and boundary-layer velocity-profile surveys on the airfoil were considered. In addition we felt it highly desirable that the data include velocity-profile surveys just downstream of the transition point (and definitely upstream of any shock wave).

Documentation

It was judged important that data accepted for use at the Conference include complete documentation of the experimental environment in the wind tunnel and uncertainty estimates for the primary variables. However, due to the general lack of appropriate data, one data set (DSMA 523s airfoil) was recommended for use at the Conference with only minimal supporting uncertainty assessments.

PROPOSED DATA SETS

On the basis of this study two wind-tunnel data sets were finally recommended for use at the 1981 meeting. These are for the RAE 2822 and DSMA 523s airfoils documented in Cook et al. (1979) and Spaid and Stivers (1979), respectively. The data were obtained with rectangular wings of relatively high aspect ratio spanning a wind-tunnel test section of solid side walls and ventilated upper and lower walls. The height-to-chord ratio was 4 in both cases. The DSMA airfoil had an aspect ratio of 4; the RAE 2822 had an aspect ratio of 3. The airfoil sections were all rear-loaded supercritical types leading to substantial boundary-layer effects.

CASE 8621. RAE 2822 Airfoil (Cook et al., 1979)

The RAE 2822 airfoil is moderately rear-loaded, 12.1% thick supercritical section. The conditions for the test cases recommended for the Conference are given in the following table. All tests, except Test 1, involved supercritical flow with shock waves.

	RAE 2822				
	Test Number				
	1	6	7	9	12
M_∞	0.676	0.725	0.725	0.730	0.730
Geometric angle of attack α_g (degrees)	2.40	2.92	2.55	3.19	3.19
$Re \times 10^{-6}$	5.7	6.5	6.5	6.5	2.7
x/c transition	0.11	0.03	0.03	0.03	0.03

Boundary-layer velocity profiles determined from pitot-tube surveys are available only on the upper surface of the airfoil. Skin-friction and boundary-layer integral parameters were determined from the measured velocity profiles.

Significant features of these data are:

1. The data include a range of shock strengths and one case tested at two Reynolds numbers.
2. The velocity-profile data included a measuring station just downstream of transition that demonstrated the establishment of a fully developed turbulent flow.
3. The data appear useful as a free-air simulation with wall effects that are small and correctable. Blockage corrections are estimated (in the original documentation) to vanish and downwash corrections based on linear theory are provided in Cook et al. (1979).

CAST 7 (Stanewsky et al., 1979)

The CAST 7 airfoil is an 11.8% thick supercritical airfoil with a small trailing-edge thickness equal to $t_{TE}/c = 0.005$ and somewhat more rear-loading than the RAE 2822. The conditions for the two test cases recommended for the conference are given in the following table. Both cases involved supercritical flow with shock waves. Velocity profiles were determined on the upper surface from pitot-tube surveys. Skin-friction and boundary-layer integral parameters were determined from the velocity profiles.

Case Number	CAST 7		DSMA 523s		
	1	2	1	2	3
M_∞	0.766	0.785	0.60	0.80	0.80
α_g (Degrees)	2.5	2.5	2.6	1.8	2.4
$Re \times 10^{-6}$	2.4	2.4	4	2	3
x/c Transition (Upper)	0.075	0.075	0.05	0.35	0.35
x/c Transition (Lower)	0.075	0.075	0.18	0.18	0.18

Significant features of the CAST 7 data are:

1. The data are for two supercritical flows at the same Reynolds number and (geometric) incidence at two different Mach numbers $M = 0.765$ and 0.785 . These conditions resulted in strong shock wave ($M_{local} = 1.30$) but fully attached boundary layers in both cases.
2. The velocity-profile data included a measuring station downstream of transition that demonstrated the establishment of fully developed turbulent flow.
3. Fairly complete documentation is provided in Stanewsky et al. (1979).

CASE 8623. DSMA 523s (Spaid and Stivers, 1979)

The DSMA 523s airfoil is a modified Whitcomb 11.0% thick supercritical airfoil with significant rear-loading. The test conditions for the airfoil are given in the following table. The lower Mach number test (Test 1) was subcritical while the other two tests involved supercritical flow with relatively strong shock waves ($M_{local} = 1.25$). Boundary-layer profiles were determined on both the upper and lower surfaces with a traversing pitot tube. Skin-friction and boundary-layer integral parameters were determined from the velocity profiles.

DSMA 523s			
	Test Number		
	1	2	3
M_∞	0.60	0.80	0.80
Geometric angle of attack α_g (degrees)	2.6	1.8	2.4
$Re \times 10^{-6}$	4	2	3
x/c transition (upper)	0.05	0.35	0.35
x/c transition (lower)	0.18	0.18	0.18

Significant features of the DSMA 523s data are:

1. The data set include two difficult supercritical cases with large supersonic zones, strong shocks, and large viscous effects.
2. The velocity-profile data included a measuring station between the transition strip and the shock wave that demonstrated the establishment of fully developed turbulent boundary layer.
3. The velocity-profile surveys included measurements of the profile in the "cove" region on the lower surface of the airfoil.
4. The data analysis included a study of probe-interference effects.

RESERVATIONS/PROBLEMS WITH THE DATA

The main reservations in using the proposed data sets for the Conference are associated with uncertainties due to (1) wind-tunnel wall interference and (2) pitot-tube interference.

The main effect of wind-tunnel wall interference, if it is small, is to introduce (hopefully) small corrections to the free-stream Mach number and angle of attack. The magnitude of the wall corrections is most strongly affected by the ratio of tunnel height to model chord, h/c . In the tests reported here, large models were employed, with $h/c = 4$ in both data sets, in order to provide thick boundary layers that were suitable for velocity-profile measurements. Hence wall-interference effects can be expected to be significant in both data sets. Blockage and downwash corrections to

the free-stream Mach number and incidence were provided in both the RAE 2822 and DSMA 523s airfoil tests. The estimated corrections were based on empirical fits of linear-interference-theory solutions to wind-tunnel data on similar airfoils of different sizes. Unfortunately, the quantitative assessment of wind-tunnel wall effects at transonic speeds is beyond the state-of-the-art and the accuracy of the simple-linear-theory estimates are unknown. Preliminary comparisons of the data with theoretical results from an interacting boundary-layer method suggest that the interference effects in the RAE 2822 experiments are small and correctable. The magnitude of the estimated blockage and downwash corrections are consistent with the shifts in Mach number and incidence required to achieve agreement with data. Similar comparisons for the DSMA 523s airfoil suggest that the wall interference is much larger and probably not correctable. The comparisons with theory indicate that blockage corrections of the order of $\Delta M = 0.04$ are required. The relatively large correction in Mach number suggested by the comparisons indicates that the data for the DSMA 523s may not be correctable to free-air conditions. Thus it appears only the RAE 2822 data will be useful as a free-air simulation. The DSMA 523s data will likely only be useful for comparisons with boundary-layer-type methods that use the measured surface-pressure distributions in the computations. In this case, uncertainty in the effective free-stream Mach number and incidence can be expected to have only small influence on the computed results. Since these conclusions are based on comparison with only a single theoretical method, they should be regarded as tentative, to be re-examined as part of the work of the 1981 Meeting.

The other area of significant uncertainty in the data arises from the influence of probe interference on the boundary-layer-profile measurements. The presence of a pitot probe in the boundary layer induces an increased adverse-pressure gradient that significantly alters the measured velocity profiles and the inferred boundary-layer parameters. Although there have been attempts to develop rough estimates for the effects of probe interference such estimates are not reliable. Simple estimates based on two-dimensional flow approximations have been developed for the DSMA 523s test results (Spaid and Stivers, 1979), which indicate effects of the order of 5-10% on the skin-friction and boundary-layer integral parameters. However, the actual interference problem involves complex three-dimensional nonuniform flow-field effects which are definitely not accounted for in the simple theory. The effects of probe interference remains a significant source of uncertainty in the present data, a situation that is not likely to be improved in the foreseeable future.

Other potential problems with the data of a less serious nature are associated with side-wall boundary-layer effects and with the appearance of an anomalous pressure disturbance on the forward, upper surface of the RAE 2822 airfoil. The rapid growth

of the side-wall boundary layer in the vicinity of the airfoil introduces three-dimensional disturbances into the flow that can have a significant effect on the measured characteristics of the airfoil. The effects are not well understood, and cannot be corrected for with existing methods. The side-wall effects are controlled mainly by the ratio of the side-wall boundary-layer thickness to the span of the wing. Because of the large spans, ($S/c = 3,4$), employed in the tests considered in this study, this effect is not expected to be significant. Nevertheless, since the thicknesses of the side-wall boundary layers were not measured in the experiments, this effect will remain an area of uncertainty in the data sets.

All the supercritical cases of the RAE 2822 data show a very rapid expansion followed by rapid compression near the leading edge of the upper surface of the airfoil. A reason for concern is that this very noticeable feature in the experimental pressure distribution does not appear in theoretical solutions. The pressure overshoots occur near the upper-surface roughness band and one may speculate that they are caused by disturbances induced by the roughness strip. In the absence of more definitive information this effect will remain a source of uncertainty in the data.

SUGGESTIONS FOR FUTURE EXPERIMENTS

On the basis of the present study the following advice can be offered to experimentalists planning further airfoil tests:

1. There is a continuing need for a careful experiment on a planar airfoil at transonic speeds which includes measurements of both surface pressures and velocity profiles. Since it is known that the wake can have a significant effect on section characteristics, the boundary-layer measurements should include detailed surveys of the near wake and measurements of the pressure variation across the boundary layer and wake near the trailing edge.
2. In order to emphasize the boundary-layer effect, the airfoil geometry should be an aft-cambered, rear-loaded supercritical airfoil. The airfoil should be closed at the trailing edge to simplify the theoretical modeling of the flow.
3. The transition point should be fixed as in the experiments of this study and velocity-profile surveys should include stations just downstream of the transition strip.
4. The effects of wind-tunnel-wall interference is the main area of concern in the use of wind-tunnel data for validating theoretical methods. Small uncertainties in the effective free-stream Mach number and angle of attack are the main source of uncertainties that prevent a clear-cut evaluation of theoretical methods. If they are to be useful for code

validation, future tests must provide for a careful assessment of wind-tunnel wall interference and an unambiguous statement of the blockage and downwash corrections that should be employed in the theoretical computations. This can, perhaps, be achieved by carrying out repeated tests on similar airfoils with various chord-to-height ratios or by contouring the walls to eliminate the interference. The pressure on the upper and lower wind-tunnel walls should be measured for possible use in theoretical codes that can employ this information in the boundary conditions.

5. If feasible, the boundary-layer surveys should be with a laser velocimeter or other nonintrusive devices to avoid uncertainties due to probe interference.
6. The thickness of the side-wall boundary layers should be measured in the experiment and the effect on the flow from this source should be assessed.

It is, of course, realized that an experimental program along these lines would be very expensive. However, to be useful for code validation it is believed that all the above points are important and should be addressed in future airfoil tests aimed at filling this role.

REFERENCES

- Cook, P. H., M. A. McDonald, and M. C. P. Firmin (1979). "Airfoil RAE 2822 - pressure distributions, boundary layer and wake measurements," in Experimental Data Base for Computer Program Assessment, AGARD Advisory Report No. 138.
- Spaid, F. W., and L. S. Stivers, Jr. (1979). "Supercritical airfoil boundary layer measurements," AIAA Paper No. 79-1501.
- Stanewsky, E., W. Puffert, R. Muller, and T. E. B. Bateman (1979). "Supercritical airfoil CAST 7--surface pressure, wake and boundary layer measurements," Experimental Data for Computer Program Assessment AGARD Advisory Report No. 138.

DISCUSSION

Flow 8620

The definition of "sharp trailing edge" was queried (U. Mehta). The answer given by R. Melnik was that a "negligible trailing-edge thickness" is anything significantly less than the momentum thickness of the boundary layers at the trailing edge.

In the evening discussion, the main topics were tunnel interference, starting conditions, and numerical inaccuracy in the "inviscid" part of the calculation. Attendees were: P. Bradshaw (Chairman), G. Brune, R. Carella, F. Dvorak, M. C. P. Firmin, D. Humphreys, R. E. Melnik, E. P. Sutton.

It was resolved that the CAST 7 case should be deleted on grounds of excessive and uncertain interference (2-degree corrections to an α of 2.4 degrees). The RAE 2822 case has a much smaller interference.

Computers are recommended to run at the nominal Mach number and to adjust α to get the quoted lift coefficient; the actual α used should be quoted. Computers are encouraged to do further runs, varying M to optimize agreement with shock position or, perhaps better, with lower surface-pressure distributions.

Pressure distribution should be plotted as p/P_∞ , where P_∞ is the upstream total pressure, to simplify comparisons between these different cases.*

Drag should be evaluated (1) in terms of θ far downstream, and (2) as an integral of surface pressure and surface shear stress.

In boundary-layer calculations an increment in θ should be applied at the transition point (trip position) to give a match of θ at the first measured profile (in the turbulent region). Boundary-layer profiles for evaluation of integral parameters should be plotted as $(P-P_w)^{1/2}/(P_e-P_w)^{1/2}$, where the subscript w denotes wall conditions and subscript e denotes edge conditions (nearly independent of y but different upstream and downstream of any shock wave). In the wake plot $(P-p_\infty)^{1/2}/(P_\infty-p_\infty)^{1/2}$. This will reach unity only in the absence of a shock. Pressure should be plotted as a function of y in the form of the usual pressure coefficient $(p-p_\infty)/(1/2\rho_\infty U_\infty^2)$. Local skin-friction coefficient should be plotted.

To distinguish between errors due to the turbulence model (or shear-layer numerics) and numerical inaccuracy of compressible external-flow solutions we recommend that all computers, whose methods allow it, should calculate the inviscid flow around RAE 2822, using the same (measured) ordinates as for the full viscous flow. The usual Kutta condition of regular pressure near the trailing edge should be used, and a Mach number M_∞ should be used to give a shock Mach number equal to that occurring in the real flow for the highest Mach number case.

*[Ed.: This recommendation has not been followed; computations request $(p(x/c))$ as requested by the data evaluator.]

SPECIFICATIONS FOR COMPUTATION


CENTRAL ENTRY CASE/COMPRESSIBLE

Case #8621; Data Evaluator: R. Melnik

Data Takers: P. Cook, M. McDonald and M. Firmin (RAE 2822 Airfoil)

PICTORIAL SUMMARY

Flow 8620. Data Evaluator: R. E. Melnik: "Transonic Airfoils."

Case Data Taker	Test Rig Geometry	dp/dx or C _p	Number of Stations Measured								C _f	Re	M _∞	Other Notes
			Mean Velocity		Turbulence Profiles									
			U	V or W	$\overline{u^2}$	$\overline{v^2}$	$\overline{w^2}$	\overline{uv}	Others					
Case 8621 P. Cook M. McDonald M. Firmin	RAE 2822 Airfoil  Side View	Air- foil upper & lower surface pres- sure	9	-	-	-	-	-	-	Modi- fied Law of the Wall	5.7 to 6.5 × 10 ⁶ (based on chord)	0.676 to 0.730	RAE 8-6 ft. transonic tunnel. Data include computed values of boundary-layer integral parameters.	

Plot	Ordinate	Abcissa	Range/Position	Comments
1	θ/c	x/c	$0 \leq x/c \leq 1.0$ $0 \leq \theta/c \leq 0.02$	5 curves corresponding to Tests 1, 6, 7, 9, 12.
2	H	x/c	$0 \leq x/c \leq 1.0$ $0 \leq H \leq 5$	5 curves corresponding to Tests 1, 6, 7, 9, 12.
3	C_f	x/c	$0 \leq x/c \leq 1.0$ $0 \leq C_f \leq 0.006$	5 curves corresponding to Tests 1, 6, 7, 9, 12.
4	$-C_p$	x/c	$0 \leq x/c \leq 1.0$ $-1.8 \leq -C_p \leq 1.2$	1 curve of upper and lower surface pressure for Test 1. Negative C_p plotted up.
5	$-C_p$	x/c	$0 \leq x/c \leq 1.0$ $-1.8 \leq -C_p \leq 1.2$	1 curve of upper and lower surface pressure for Test 6. Negative C_p plotted up.
6	$-C_p$	x/c	$0 \leq x/c \leq 1.0$ $-1.8 \leq -C_p \leq 1.2$	1 curve of upper and lower surface pressure for Test 7. Negative C_p plotted up.
7	$-C_p$	x/c	$0 \leq x/c \leq 1.0$ $-1.8 \leq -C_p \leq 1.2$	1 curve of upper and lower surface pressure for Test 9. Negative C_p plotted up.
8	$-C_p$	x/c	$0 \leq x/c \leq 1.0$ $-1.8 \leq -C_p \leq 1.2$	1 curve of upper and lower surface pressure for Test 12. Negative C_p plotted up.

Special Instructions:

Participants are invited to submit computations in either of the following two categories; indicate which is used on output graphs:

Category I - A boundary-layer-type calculation employing the measured surface pressures.

Category II - A complete solution of the problem including the theoretical determination of the surface pressure.

Input Data

The input data for each test should be the airfoil coordinates, the experimental values of M_∞ , C_L , R_e , and the transition point locations. The lift coefficient is specified instead of the angle of attack in order to avoid the uncertainty in the angle of attack caused by wind-tunnel wall interference. The turbulent boundary layer should be initiated at the location of the transition strips in the experiment. In addition, in the Category I computations, the input pressure distribution should include all measured surface-pressure data.

A major deficiency of the data is the uncertainty in the effective Mach number caused by tunnel-wall interference. Therefore, Category II type computations at other than the experimental Mach number are acceptable as an attempt to allow for blockage corrections. Participants are encouraged to find the value of free-stream Mach number that results in best agreement in shock position on the upper surface of the airfoil. However in all cases, the results must also include computations at the experimental Mach number (or a clear statement of why this could not be done). If the free-stream Mach number is shifted, the experimental pressures and life coefficient must be corrected as follows:

$$C_{p_{corr}} = [A M_{exp}^2 / M_{corr}^2] C_{p_{exp}} + \frac{10(A-1)}{7 M_{corr}^2} \quad (1)$$

$$C_{L_{corr}} = [A M_{exp}^2 / M_{corr}^2] C_{L_{exp}} \quad (2)$$

where

$$A = \left[\frac{5 + M_{corr}^2}{5 + M_{exp}^2} \right]^{3.5} \quad (3)$$

These formulas were determined from the condition that the ratio of measured static to total pressure is unaffected by the Mach number correction. The theoretical computations should be carried out with the imposed lift coefficient equal to C_L .

Drag should be evaluated (1) in terms of θ far downstream, (2) as an integral of surface pressure and surface shear stress.

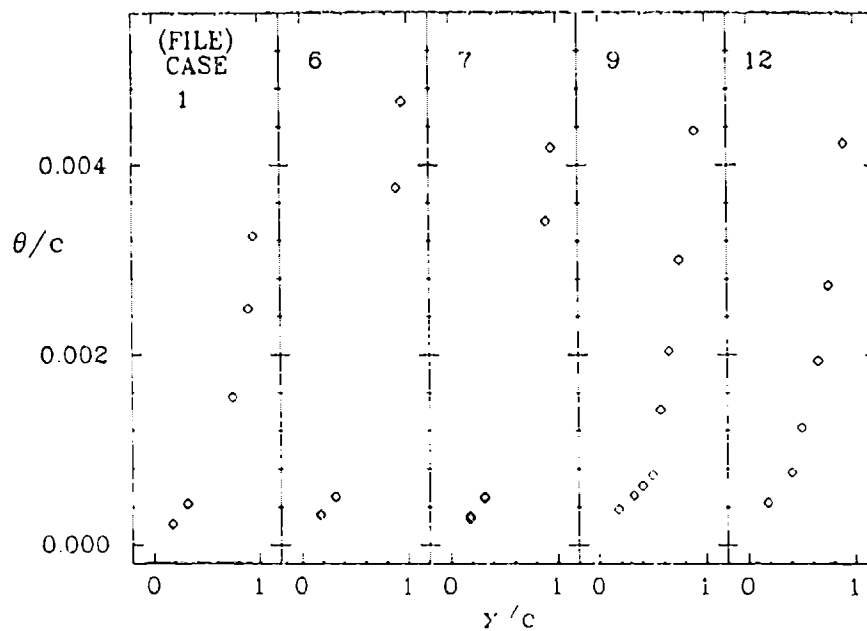
To distinguish between errors due to the turbulence model (or shear-layer numerics) and numerical accuracy of compressible external-flow solutions we recommend that when possible computers calculate the inviscid flow around RAE 2822 using the same airfoil coordinates as for the full viscous flow. The usual Kutta condition of regular pressure near the trailing edge should be used, and M_∞ should be taken to give a shock Mach number equal to that occurring in the highest Mach number case.

The theoretical surface-pressure distributions should be compared with the corrected experimental surface pressures. Results for upper and lower surface quantities should be plotted on the same figure.

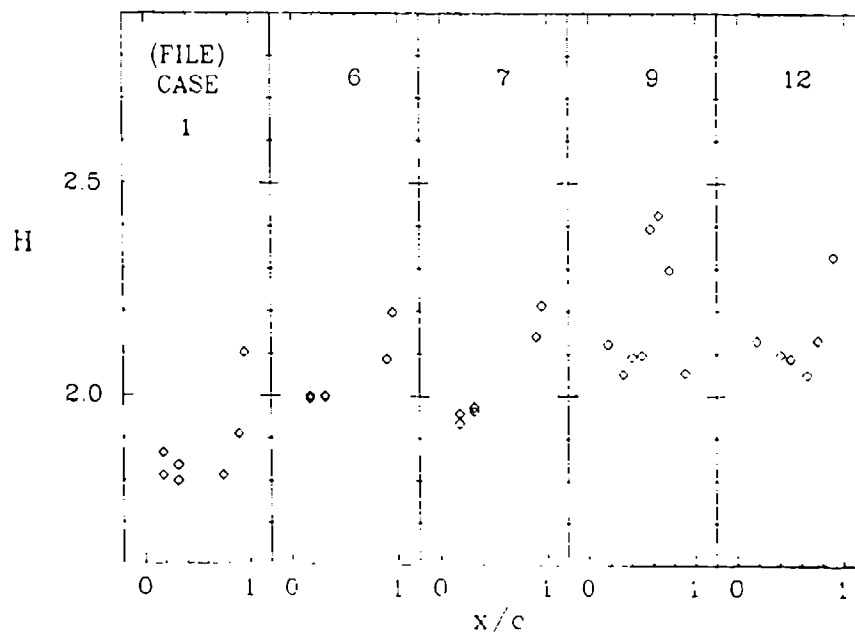
If Mach number corrections are employed in the calculations, the plotted experimental pressure distributions should be corrected using Eq. 1 above. In addition, the computed values of α (angle of attack), total drag, skin friction, and pressure drag should be included in a tabular output that also lists M_∞ , Re , C_L , and transition locations (x_t/c). The skin-friction and pressure drags are to be computed from an integration of the skin-friction and surface-pressure distributions.

A record of successive adjustments to the angle of attack, Mach number, and related shock location should be reported in tabular form.

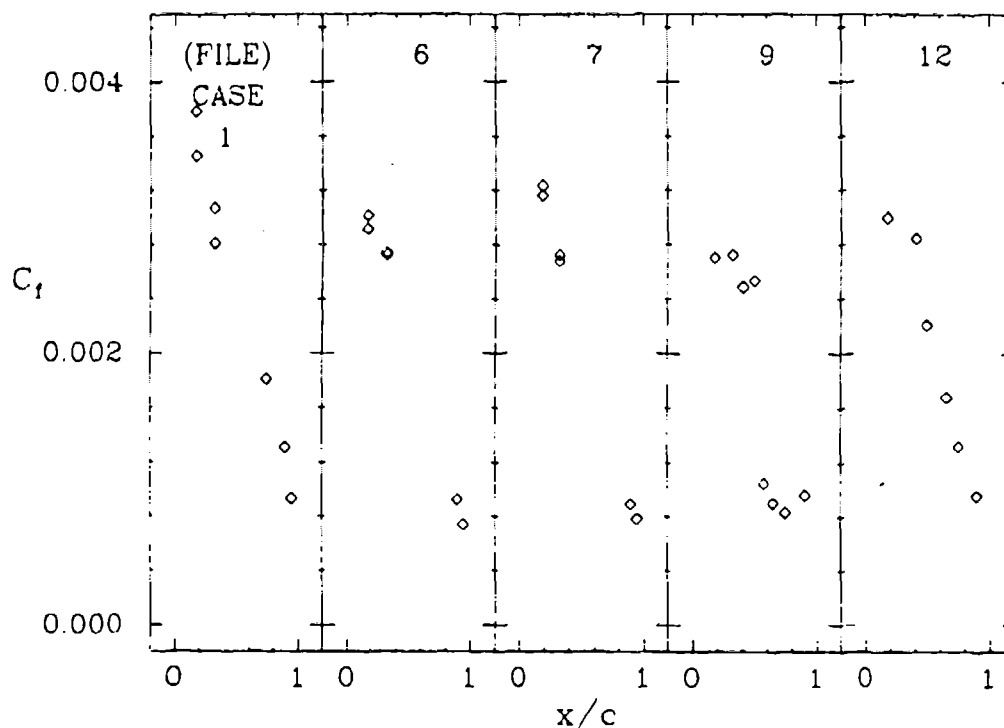
PLOT 1 CASE 8621 FILES 70-74



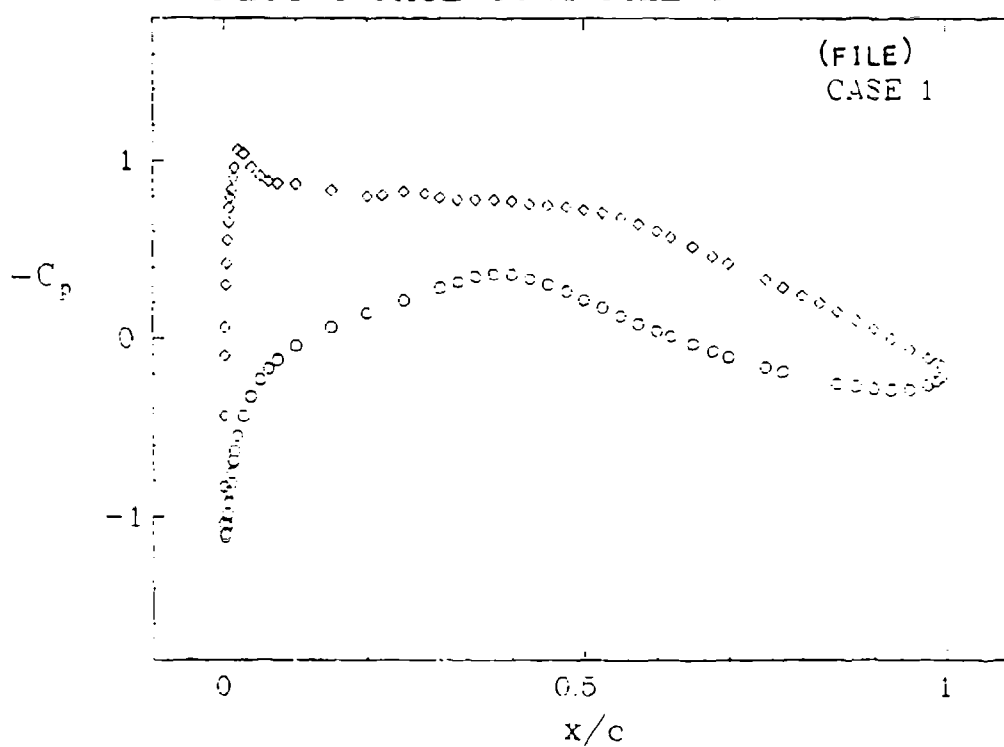
PLOT 2 CASE 8621 FILES 70-74



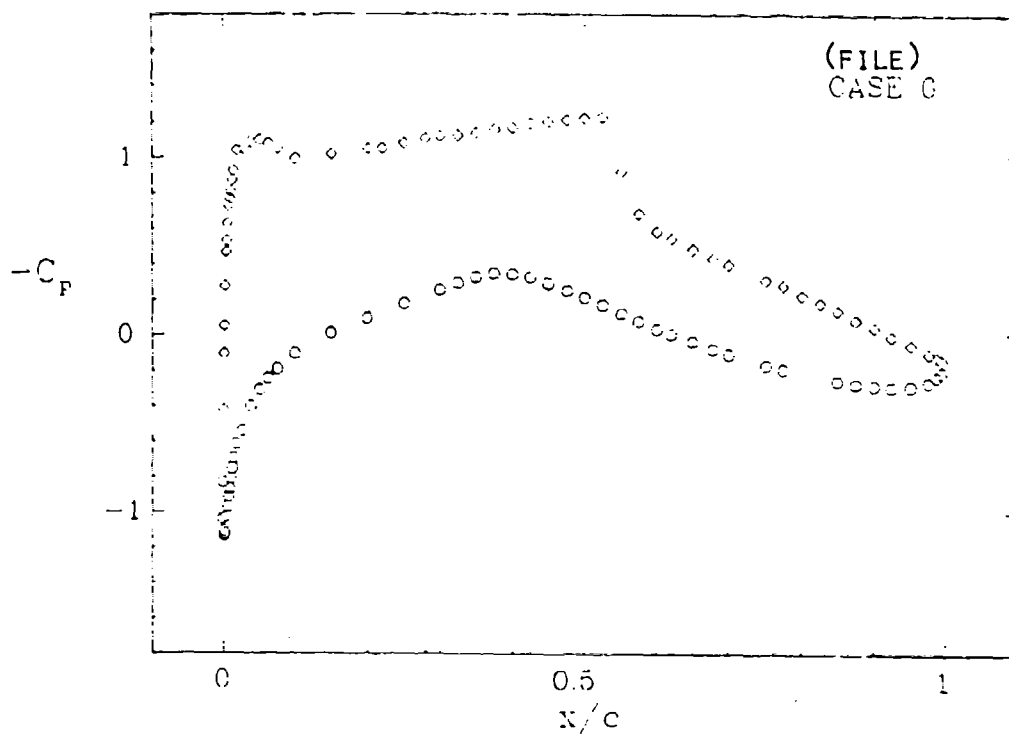
PLOT 3 CASE 8621 FILES 70-74



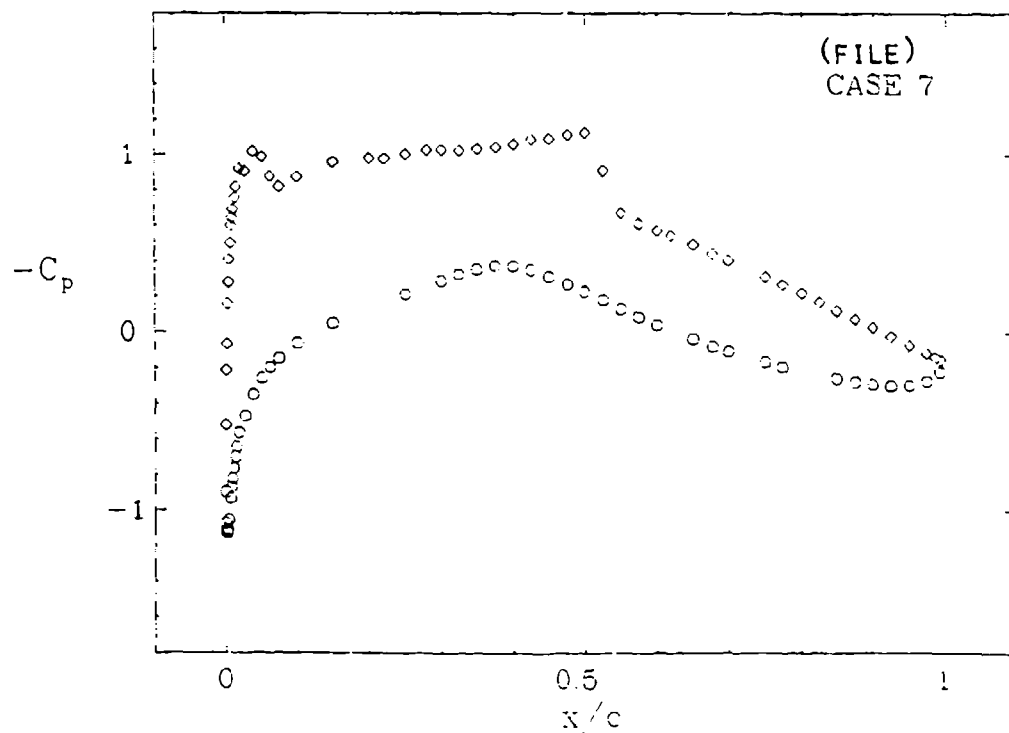
PLOT 4 CASE 8621 FILE 4



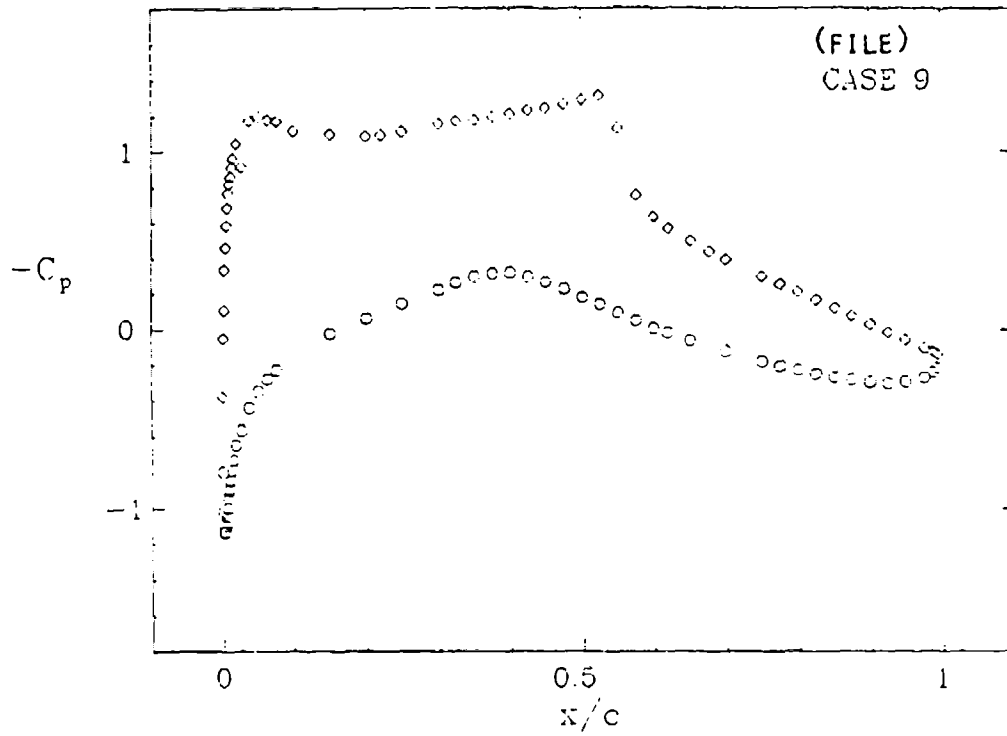
PLOT 5 CASE 8621 FILE 5



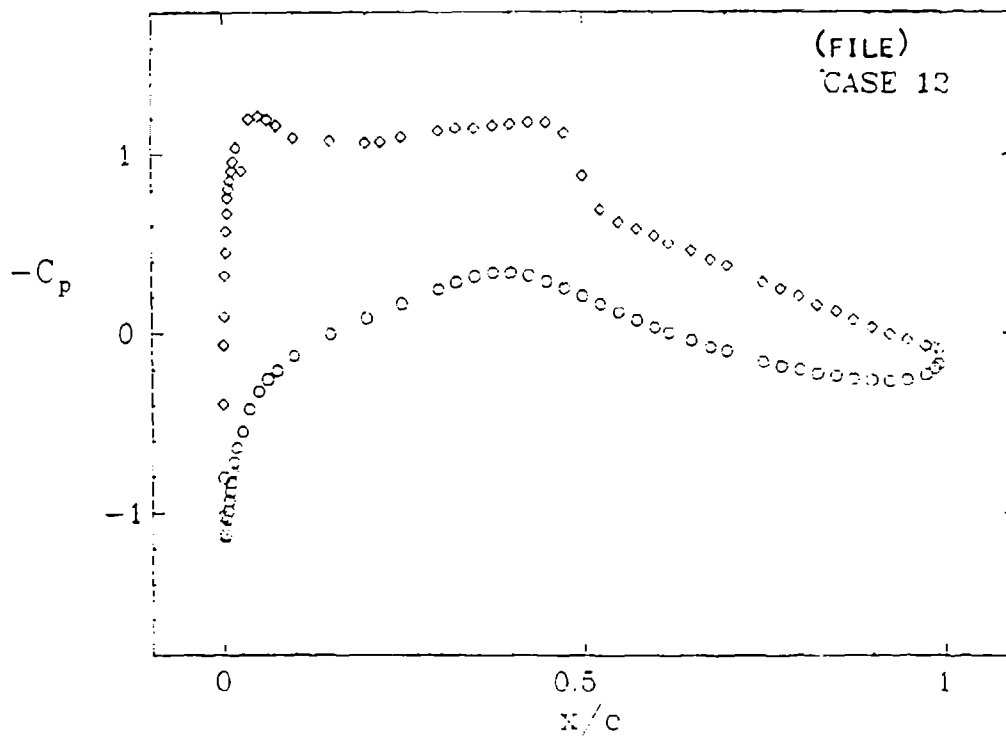
PLOT 6 CASE 8621 FILE 6



PLOT 7 CASE 8621 FILE 7



PLOT 8 CASE 8621 FILE 8



SPECIFICATIONS FOR COMPUTATION


ENTRY CASE/COMPRESSIBLE

Case #8623; Data Evaluator: R. Melnik

Data Takers: F. Spaid and L. Stivers, Jr. (DSMA 523s Airfoil)*

PICTORIAL SUMMARY

Flow 8620. Data Evaluator: R. E. Melnik: "Transonic Airfoils."

Case Data Taker	Test Rig Geometry	dp/dx or C _p	Number of Stations Measured							C _f	Re	M _∞	Other Notes
			Mean Velocity		Turbulence Profiles								
			U	V or W	$\overline{u^2}$	$\overline{v^2}$	$\overline{w^2}$	\overline{uv}	Others				
Case 8623 F. Spaid L. Stivers, Jr.	DSMA 523s Airfoil 	Air- foil upper & lower surface pressure	7	-	-	-	-	-	p/s	Law of Wall by trans- formed veloc- ity	2-4 = 10 ⁶ (based on chord)	3.6 to 0.8	NASA-Ames 2x2 ft. tran- sonic tunnel.

Plot	Ordinate	Abscissa	Range/Position	Comments
1	z/c	U/U _e	$0 \leq z/c \leq 0.04$ $0 \leq U/U_e \leq 1.0$	Profiles for Case 1, upper surface at x/c = 0.3, 0.5, 0.7, 0.8, 0.95. See instruction 1.
2	z/c	U/U _e	$0 \leq z/c \leq 0.04$ $0 \leq U/U_e \leq 1.0$	Profiles for Case 1, lower surface at x/c = 0.3, 0.5, 0.75, 0.91, 1.0.
3	z/c	U/U _e	$0 \leq z/c \leq 0.04$ $0 \leq U/U_e \leq 1.0$	Profiles for Case 2, upper surface at x/c = 0.3, 0.45, 0.75, 0.85, 0.95.
4	z/c	U/U _e	$0 \leq z/c \leq 0.04$ $0 \leq U/U_e \leq 1.0$	Profiles for Case 2, lower surface at x/c = 0.3, 0.5, 0.65, 0.75, 0.91.
5	z/c	U/U _e	$0 \leq z/c \leq 0.04$ $0 \leq U/U_e \leq 1.0$	Profiles for Case 3, upper surface at x/c = 0.3, 0.45, 0.65, 0.8, 0.9.

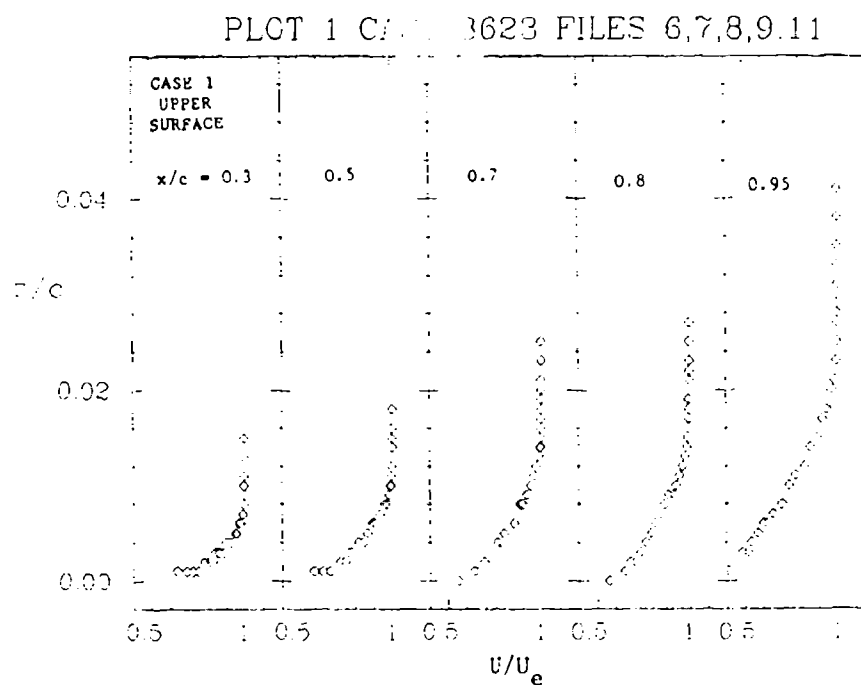
*In a review, R. S. Shevell indicated that the designation DSMA is an acronym for Douglas Santa Monica Airfoil, although the plant is no longer in that location, and the company name has been changed.

Plot	Ordinate	Abscissa	Range/Position	Comments
6	z/c	U/U_e	$0 \leq z/c \leq 0.04$ $0 \leq U/U_e \leq 1.0$	Profiles for Case 3, lower surface at $x/c = 0.3, 0.5, 0.75, 0.91, 1.0$.
7	C_p	x/c	$0 \leq x/c \leq 1$ $-1.8 \leq C_p \leq 1.2$	Surface-pressure coefficient $C_p = (P - P_\infty) / \frac{1}{2} \rho_\infty U_\infty^2$ for Case 2.

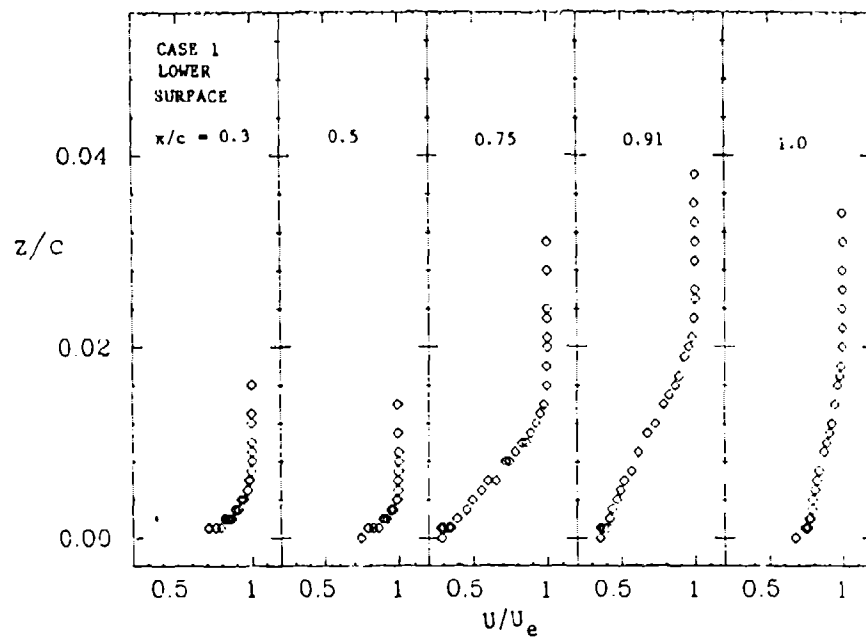
Special Instructions:

1. This flow is composed of three cases designated as follows:

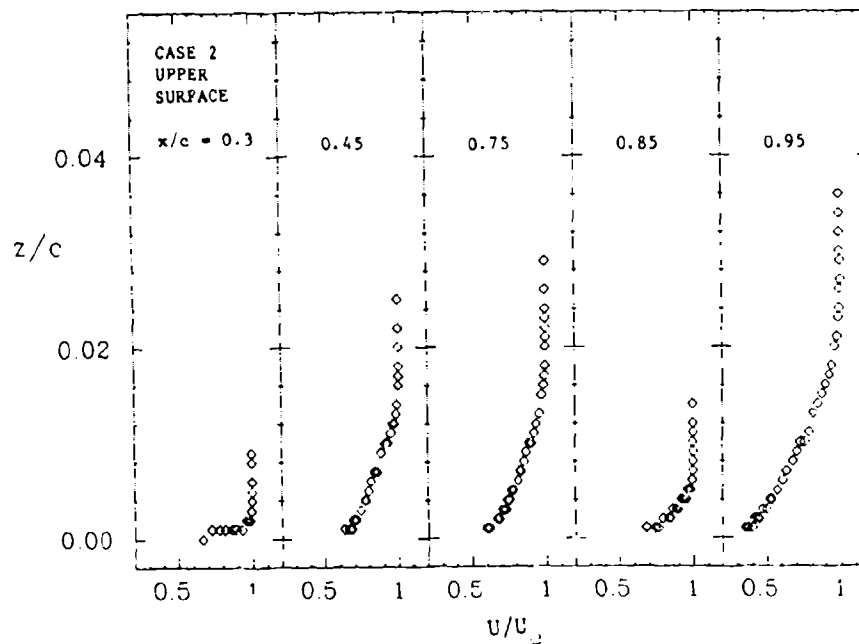
Case	1	2	3
M_∞	0.60	0.80	0.80
α°	2.60	1.80	2.40



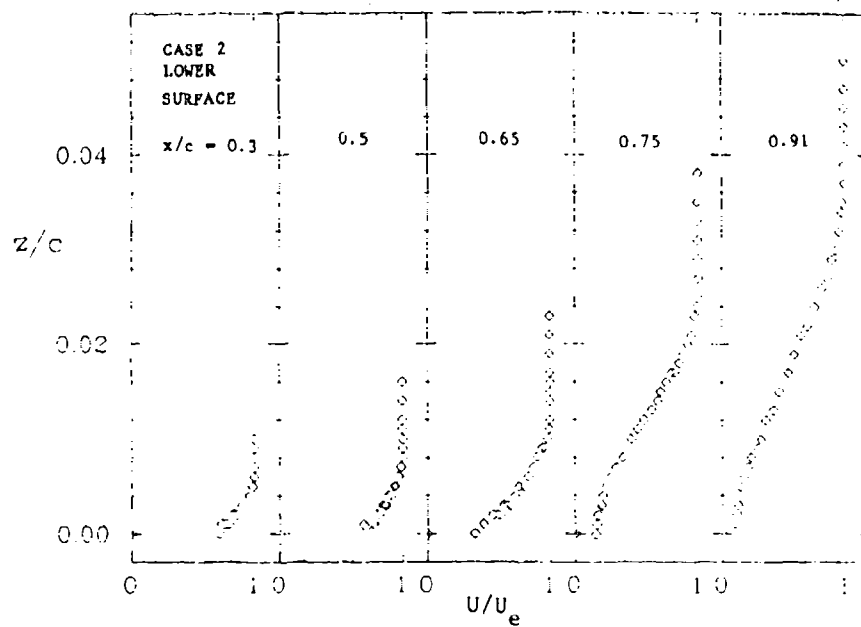
PLOT 2 CASE 8623 FILES 14,15,17,18,19



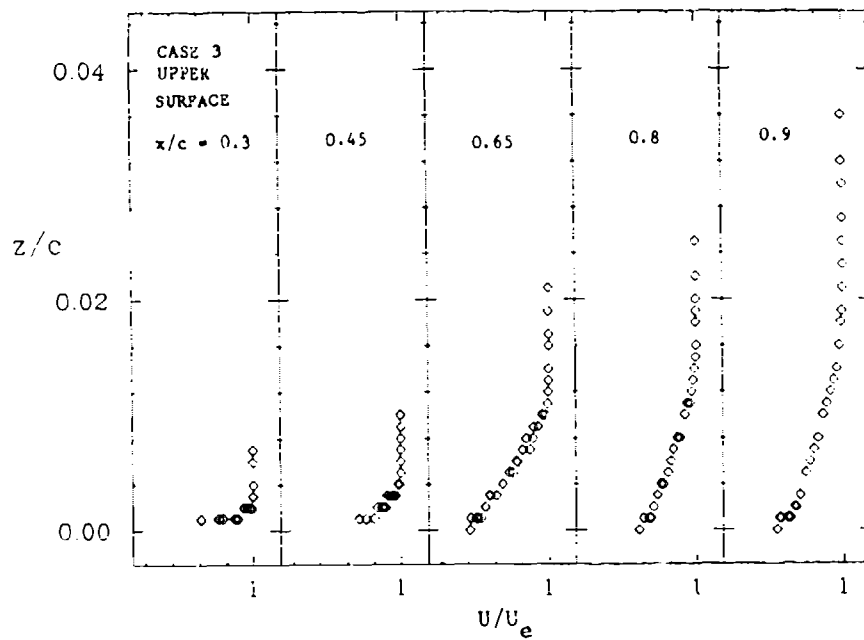
PLOT 3 CASE 8623 FILES 20,24,25,22,27



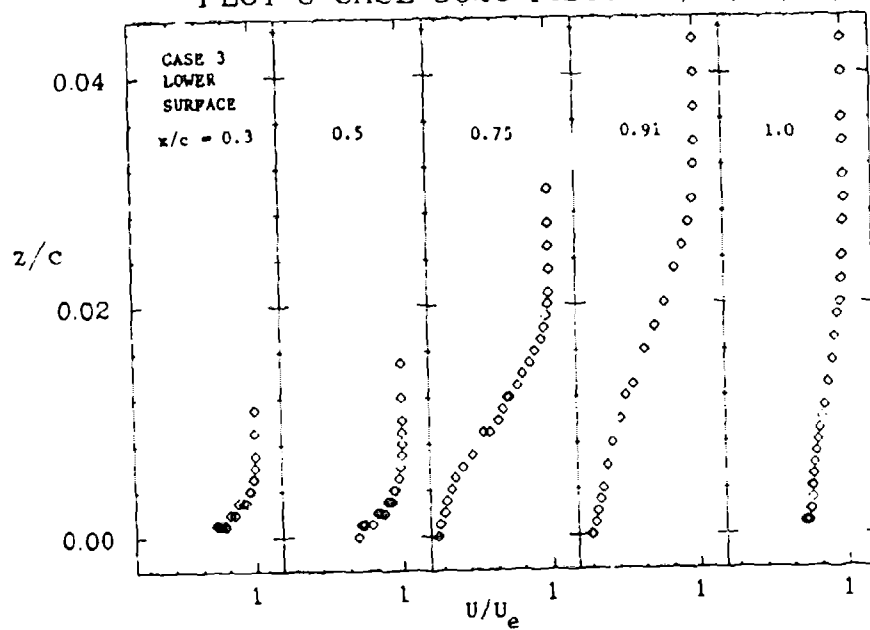
PLOT 4 CASE 8623 FILES 29,30,32,33,34



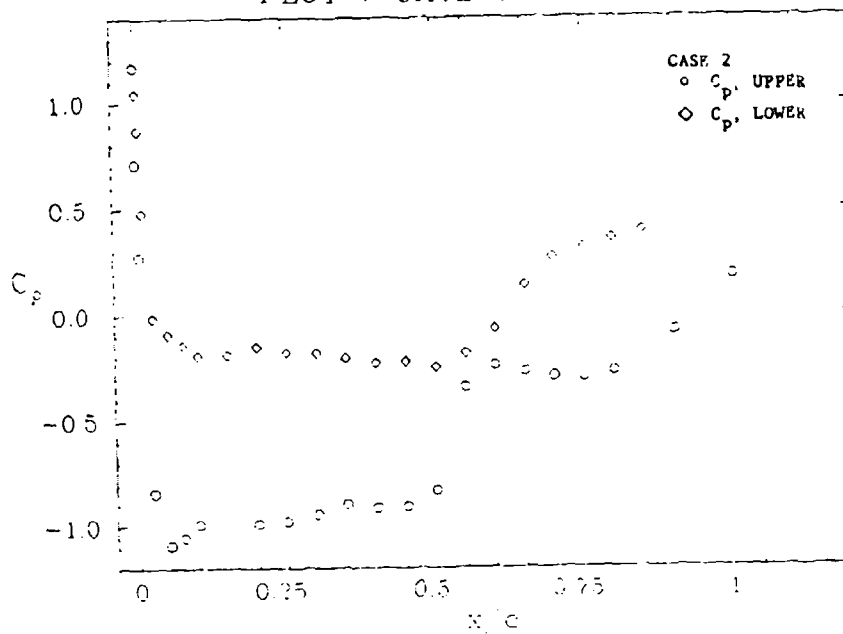
PLOT 5 CASE 8623 FILES 36,37,38,39,40



PLOT 6 CASE 8623 FILES 43,44,46,47,48



PLOT 7 CASE 8623 FILE 4



POINTED AXISYMMETRIC BODIES AT ANGLE OF ATTACK (SUPERSONIC)

Flow 8670

Case 8671

Evaluator: D. Peake*

(Prepared by D. J. Cockrell†)



SUMMARY

INTRODUCTION

Boundary-layer development and flow past a yawed cone at a free-stream Mach number of 1.8 and a Reynolds number based on cone length of 2.5 to 3.4×10^7 is reported by Rainbird (Rainbird, 1968a, b). Experimental data are given in these references and were included in the review by Peake and Tobak (1980). The flow field past a yawed cone is sketched in Fig. 1.

EXPERIMENTAL METHOD

Two sets of experiments are described. Both were conducted in the N.A.E. 1.5-m (5-ft) intermittent blowdown-wind-tunnel. In the first set, pressure distributions, surface shear stresses and boundary-layer traverses were obtained with a 0.457-m (18-inch) diameter, $12\frac{1}{2}^\circ$ semiangle (θ_c), 1.37-m (54-inch) long (L) cone. In the second set, pressure distributions, surface shear stresses, and external flow-field measurements were made with a 0.241-m (9-1/2-inch) diameter, 5° semiangle, 1.37-m (54-inch) long cone. Reynolds numbers for these tests, based on axial length, ranged from 2.5×10^7 to 3.4×10^7 . No boundary-layer trip was used, but, because the free stream was highly turbulent, transition was assumed to occur close to the cone apex ($x/L < 0.1$). Hence, boundary layers were taken to be fully turbulent but at the time of the tests no measurements of free-stream turbulence had been made. The shape of the separation lines made it evident that the flows over the cones were fully turbulent and measurements made later of free-stream-turbulence intensity in this wind-tunnel facility showed it to be about 0.2%.

Test results have been selected at which $M_\infty = 1.8$. For the first set, $\alpha/\theta_c = 1.82$, while for the second set $\alpha/\theta_c = 2.1$. At these normalized incidences both primary and secondary separation lines are on the leeward side of the body. At these conditions, evidence of conicity is given in the references.

*3-d Flowz, Inc., P. O. Box 244, Moffett Field, CA 94035.

†University of Leicester, Engineering Department, England.

During a run duration of 20 to 30 seconds, changes in the wall temperatures of the cones were less than 3°C , hence zero heat transfer was assumed. Detailed measurements were confined to a single axial station at $x/L = 0.85$ aft of the apex of the cones. Circumferential pressure distributions were measured using unbonded strain-gage pressure transducers closely coupled pneumatically to 0.5-mm (0.02-inch) diameter holes spaced 45° apart at the measurement station. The model was pitched to the desired angle of incidence, then slowly rolled during the wind tunnel run. The pressure distribution data were given at about $2\text{-}1/2^{\circ}$ circumferential intervals from a circumferential angle ϕ (measured from the windward generator) of -5° up to about 185° . Surface-shear-stress directions were measured from flow visualization traces taken with an oil-dot technique. Magnitude and direction of shear stresses were also determined in the first set of experiments by using a three-tube measuring head boundary-layer probe (see Rainbird, 1968a), touching the cone surface. As this probe was traversed out through the boundary layers, from an initial position in contact with the cone surface to a maximum extension of 20 mm (0.8 inch), it was kept turned in to the local mean stream direction by a yaw servosystem. The accuracy of measurement of probe height above the cone surface was 0.025 mm (0.001 inch) and of yaw angle, $\pm 0.2^{\circ}$.

In the second set of experiments magnitude was measured by the use of small Preston tubes (see Rainbird, 1968b) and local Mach numbers, pitot pressures and flow direction in the external flow above the cone were all measured using flow-field probes (Rainbird, 1968b). Overall force measurements were made with an internal strain-gage balance. The oil-dot technique was also used to provide evidence of flow separation.

The stagnation pressure was 1.8 atmospheres (25 psia). Because it was so high, good resolution in pressure-based measurements was facilitated, and although the accuracy of measurement is now not known, it was undoubtedly high. Repeatability of the measurement was excellent. As McRae et al. (1980) show, agreement is good between data which Rainbird obtained in these experiments and those later obtained at the same Mach number at Ames Research Center. Similar experimental results resulting from flight tests made at NASA Dryden are shortly to be presented.

Owing to increasing circumferential pressure gradients as α/θ_c increases, Rainbird (1968b) shows there to be substantial variation in the surface-shear-stress direction in the two tests.

REFERENCES

- McRae, D. S., D. J. Peake, and D. F. Fisher (1980). "A computational and experimental study of high Reynolds number viscous/inviscid interaction about a cone at high angle of attack," 13th Fluid and Plasma Dynamics Conference, AIAA-80-1422.
- Peake, D. J., and M., Tobak (1980). "Three-dimensional interactions and vortical flows with emphasis on high speeds," NASA TM 81169. Also AGARDograph currently in press.
- Rainbird, W. J. (1968a). "Turbulent boundary layer growth and separation on a yawed cone," AIAA Jou., 6, 2410.
- Rainbird, W. J. (1968b). "The external flow field about yawed circular cones," AGARD CP.30, p. 19.1.

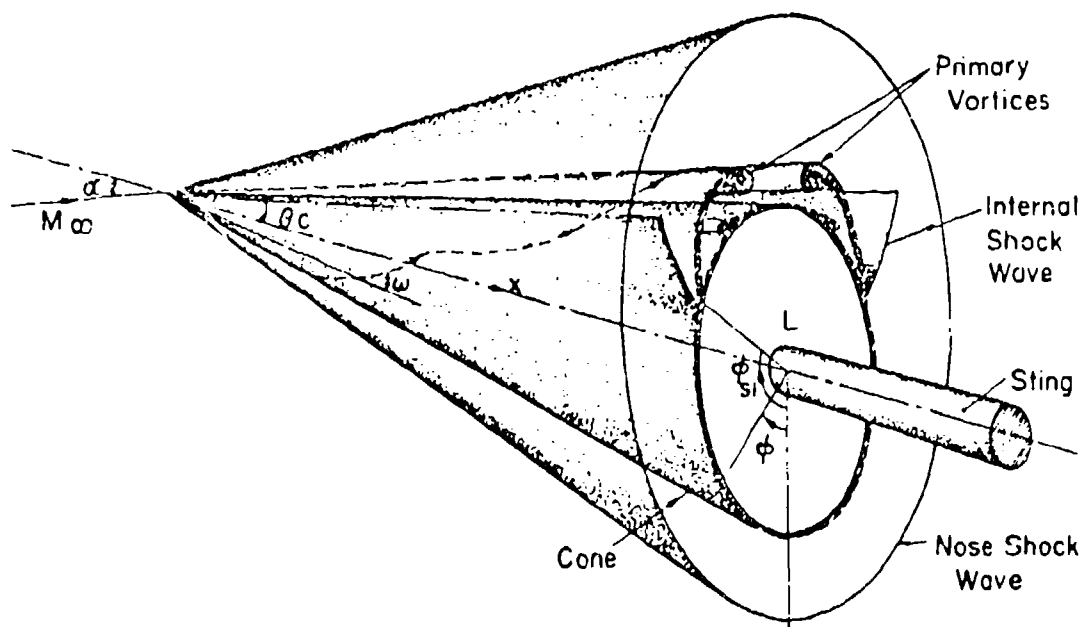


Figure 1. Test configuration, Case 8671. Flow past yawed cone.

DISCUSSION

Flow 8670

- S. Kline: Which of the 10 variables are most important?
- D. Peake: Skin friction and pressures.
- P. Bradshaw: How did you find the center of the vortex?
- D. Peake: From the point of minimum pressure.
- M. Morkovin: You assumed that you had a fully turbulent boundary layer at zero angle of attack, where in fact it was not.
- D. Peake: Our evidence from pressure probes and from the straightness of the asymptotic separation lines suggests that all transition effects were confined very close to the nose.
- G. Paynter: A secondary shock was induced on the cone surface; do you consider this the same kind of phenomenon as swept shock interactions?
- D. Peake: Yes! Although it was not well behaved for the lower Mach number cases. An imbedded shock existed for the $M = 4.2$ case.
- G. Lilley: Are the position and height of the vortices at $M = 1.4, 4.2$ similar to what you get in the incompressible case?
- D. Peake: Yes, very similar! The flow is dominated by the circumferential pressure field.
- J. McCroskey: What is the uncertainty of the data? Can you discriminate among the turbulence models for this flow which is so dominated by the pressure field?
- D. Peake: I think so! It is the same magnitude as in other cases; $\pm 2\%$ for wall static pressure, $\pm 12-15\%$ for skin friction. Experience to date shows sensitivity of the models to these variables.
- E. Reshotko: You had an adiabatic wall in the wind tunnel; how does this compare with your flight tests?
- D. Peake: Some heat transfer occurs in flight, but we don't expect these effects to be large.

SPECIFICATIONS FOR COMPUTATION

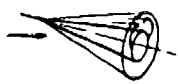
ENTRY CASE/COMPRESSIBLE

Case #8671; Data Evaluator: D. J. Peake

Data Taker: W. Rainbird

PICTORIAL SUMMARY

View 0470. Data Evaluator: D. Peake (D. J. Cockrell). "Pointed Axisymmetric Bodies at Angle of Attack (Supersonic)."

Case Data Taker	Test Rig Geometry	dp/ds or C _p	Number of Stations Measured								C _f	Re	M _∞	Other Notes
			Mean Velocity	V or W	Turbulence Profiles				Others					
					u ²	v ²	w ²	uv						
U														
Case 8671			1	-	-	-	-	-	-	Sur- face pres- sure	Pre- ton- tubes and oil flow visual- ization (cone length)	2.5 to 3.4 x 10 ⁷ (based on cone length)	1.8	Free-stream turbulence ~ 0.2%. Data at two angles of attack. Measurements at one axial station x/L = 0.85.
W. Rainbird														

Plot	Ordinate	Abscissa	Range/Position	Comments
1	C _p	φ	0 ≤ φ ≤ 180° -0.1 ≤ C _p ≤ 0.15	Circumferential pressure distribution at x/L = 0.85.
2	ω _B	φ	0 ≤ φ ≤ 180° -30° ≤ ω _B ≤ 50°	Surface shear stress direction at x/L = 0.85.
3	C _{fe}	φ	0 ≤ φ ≤ 180° 0 ≤ C _{fe} ≤ 0.003	Local skin-friction coefficient at x/L = 0.85.
4	θ _v /θ _c	φ	0 ≤ φ ≤ 180° 1.0 ≤ θ _v /θ _c ≤ 1.4	Vortex height at x/L = 0.85.
5	δ _{0.99}	φ	0 ≤ φ ≤ 180° 0 ≤ δ _{0.99} ≤ 0.005 m	Boundary-layer thickness at x/L = 0.85.
6	δ*	φ	0 ≤ φ ≤ 180° -0.0005 ≤ δ* ≤ 0.002 m	Displacement thickness at x/L = 0.85.
7	θ ₁₁ , θ ₂₁	φ	0 ≤ φ ≤ 180° -0.0005 ≤ θ ₁₁ , θ ₂₁ ≤ 0.00075 m	Boundary-layer thickness parameters at x/L = 0.85.
8	θ ₁₂ , θ ₂₂	φ	0 ≤ φ ≤ 180° -0.0005 ≤ θ ₁₂ , θ ₂₂ ≤ 0.00075 m	Boundary-layer thickness parameters at x/L = 0.85.

Special Instructions:

1. The flow field to be calculated is sketched in Fig. 1 and consists of a 12-1/2° semiangle sharply pointed cone set at an angle of incidence of 22-3/4° in a supersonic flow at $M = 1.8$ and a Reynolds number based on cone length, L , of 2.5×10^7 . In the experiment, the stagnation pressure and temperature were 1.8 atmospheres and 21°C, respectively.

Under these conditions, the flow field is not wholly conical. However, in some flow evaluation methods it may be necessary to assume conicality with little overall loss in accuracy. Assume that the boundary layer is fully turbulent downstream of the bow shock.

2. The x-coordinate is measured along, and the y-coordinate normal to, the cone axis.

Special Nomenclature

C_{fe} = local skin-friction coefficient, $\tau_w / 0.7 p_e M_e^2$

C_p = local surface-pressure coefficient, $(p_e - p_w) / 0.7 p_w M_w^2$

$\delta_{0.99}$ = boundary-layer thickness, where $U/U_o = 0.99$

δ_1^* = streamwise displacement thickness = $\int_0^{h_e} (1 - \frac{\rho U}{\rho_e U_e}) dh$

δ_2^* = crossflow displacement thickness = $-\int_0^{h_e} \frac{\rho v}{\rho_e U_e} dh$

θ_{11} = $\int_0^{h_e} \frac{\rho U}{\rho_e U_e} (1 - \frac{U}{U_e}) dh$

θ_{12} = $\int_0^{h_e} \frac{\rho v}{\rho_e U_e} (1 - \frac{U}{U_e}) dh$

θ_{21} = $-\int_0^{h_e} \frac{v}{U_e} \frac{\rho U}{\rho_e U_e} dh$

θ_{22} = $-\int_0^{h_e} \frac{\rho v^2}{\rho_e U_e^2} dh$

} Various momentum thickness
in streamline coordinates

h = distance normal to cone surface.

Editors' Note: Because the data were not received in time at Stanford, standard plots for this case were not prepared for the 1981 meeting. Computations were accepted for the 1981 meeting, however, and the data were later put on the tape.

VARIATION IN C_f/C_{f0} FOR BLOWING/SUCTION WITH MACH NUMBER

Flow 8310

Evaluator: L. C. Squire*

SUMMARY

(presented at the 1980 Conference by E. P. Sutton)

In an earlier letter to Professor S. J. Kline, L. C. Squire had explained why a test case "Variation in C_f for blowing/suction with Mach number" was impossible to be drawn up based on the experimental data presently available. E. P. Sutton presented L. C. Squire's conclusions to the Conference.

DISCUSSION

FLOW 8310

The conclusions of L. C. Squire were regretted but no contradictory evidence was offered to the Conference.

[Ed.: This case will be excluded from the library and the 1981 meeting.]

*Cambridge University, Trumpington Street, Cambridge, CB2 1PZ, ENGLAND.

SESSION XII

Chairman: P. S. Klebanoff

Technical Recorders:

M. Lee
J. Gerrard



Flow 0350

Flow 0290

Flow 0470

Flow 0280

TRANSIENT FLOWS

Evaluator: L. W. Carr

SUMMARY

Transient flows lie beyond the defined scope of the 1980-81 Conference. However, W. J. McCroskey and L. W. Carr of the Army Air Mobility Command, Moffett Field, CA, are planning a meeting in Toulouse early in 1981 on transient flows. They have been collecting data and sponsoring further experiments as possible trial cases. The data are being added to the data library established by the 1980-81 Conference.

Mr. Carr reported on the current state of the data in transient flows.

REFERENCES

- Acharya, M., and W. C. Reynolds (1975). "Measurements and predictions of a fully developed turbulent channel flow with imposed controlled oscillations," Tech. Rept. TF-8, Thermosciences Div., Dept. of Mech. Eng., Stanford University.
- Hussain, A. K. M. F., and W. C. Reynolds (1970). "The mechanics of an organized wave in turbulent shear flow," J. Fluid Mech., 41, 241.

DISCUSSION

The Conference agreed that the unsteady flow 0150 (Acharya and Reynolds, Case 0151; Hussain and Reynolds, Case 0152) should be kept in the data library, but not be considered as test cases in the 1981 meeting.

SHIP WAKES

Flow 0350

Evaluator: V. C. Patel*

SUMMARY

Although the three-dimensional boundary layer on the middle body of a ship is thin and the cross-flow within it is usually weak, the characteristic geometry of the stern leads to a rapid thickening of the boundary layer over a short distance. The stern flow is characterized by large and reversing cross-flows, leading to the formation of longitudinal vortices (which may remain buried within the thick boundary layer or leave the surface, giving rise to an open or free-vortex separation), and an interaction between the viscous and inviscid flows as well as the stern waves. An understanding of the flow over the stern is therefore a necessary prerequisite to the understanding of the wake since the wake originates in this environment. The velocity field in the wake is obviously three-dimensional and is dictated not only by the upstream stern flow but also by the local influence of propellers and the waves at the free surface. The wake of a surface ship is therefore an excellent example of a "complex" turbulent shear flow.

CRITERIA

If the various complexities are to be documented experimentally, it is obvious that quite extensive and detailed measurements are required. Naval architecture and related literature was examined to identify experimental data which met the following criteria:

- (a) The data should have well-documented upstream conditions, e.g., measurements in the thin three-dimensional boundary layer at some section on the hull.
- (b) Measurements should have been made at several streamwise stations over the stern and in the near wake.
- (c) It should be possible to extract the necessary boundary conditions required by modern calculation procedures, e.g., hull geometry and pressure distribution, velocity field outside the viscous flow, etc.
- (d) Since the primary goal of the Conference is to evaluate turbulence models, some turbulence measurements are essential.

AVAILABLE DATA

A quick search through the literature indicates that ship wakes have been extensively investigated. This observation must, however, be qualified since, in naval architecture, the word "wake" is used synonymously with a velocity survey or the

*Iowa Inst. of Hydraulic Res., Univ. of Iowa, Iowa City, Iowa 52240.

distribution of velocity defect at or near the propeller plane. Wake measurements with towing-tank models usually refer to a Pitot traverse across the wake at a single streamwise location and therefore there are literally thousands of wake data sets. However, if we interpret the wake in the more general sense, as implied by the above criteria, to refer to the viscous, turbulent flow over and downstream of the stern, there are no data sets which can qualify as a test case. This is borne out by a review of several experiments performed over the years on full-scale ships, on models in towing tanks and water tunnels, and on double or reflex models in wind tunnels. Some discussion of the limitations of the available data may be found in the Review Report (Patel, 1980) prepared for the Conference.

RECOMMENDATIONS

In view of the complexity of the flow and the associated difficulties of making reliable and detailed measurements in such a highly three-dimensional environment, it is not surprising to find that there is, at present, no data set that can be used to test the performance of calculation methods which claim to address this type of flow. There is, however, a glimmer of hope. The use of double models in wind tunnels offers the best near-term prospects for acquiring a complete set of data which may meet the suggested criteria. Progress is being made in this direction through the experiments under way at several laboratories, notably the British Ship Research Association and the National Maritime Institute in England, the Institut für Schiffbau der Universität Hamburg in Germany, and the Statens Skeppsprövningsanstalt in Sweden. The latter two investigations seek to extend the already completed hull boundary-layer measurements (Hoffman, 1976; Larsson, 1974) into the thick boundary layer over the stern and the near wake, with emphasis on the development of the stern vortices. A recent unpublished report by Kux and Wiegardt (1980) gives a preview of the complex mean velocity field over the stern and in the near wake. It is recommended that the results of the investigations in progress be monitored and evaluated as they become available, since they may provide suitable test cases.

REFERENCES

- Hoffman, H. P. (1976). "Untersuchung der 3-dimensionalen, turbulenten Grenzschicht an einem Schiffsdoppelmodell im Windkanal," Inst. Schiffbau, Univ. Hamburg, Report 343.
- Kux, J., and K. Wiegardt (1980). "Three-dimensional measurements near the stern of a double model of a ship," unpublished report, Inst. Schiffbau, Univ. Hamburg.
- Larsson, L. (1974). "Boundary layer of ships. Part III. An experimental investigation of the turbulent boundary layer on a ship model," Statens Skeppsprövningsanstalt, Report 46.
- Patel, V. C. (1980). "Ship wakes: an overview of experimental data," Review Report, 1980-81 AFOSR-HTTM-Stanford Conference on Complex Turbulent Flows: Comparison of Computation and Experiment.

LAMINAR-TURBULENT TRANSITION

Flow 0290

Evaluator: E. Reshotko^{*}

SUMMARY

E. Reshotko and M. Morkovin had reported earlier that no usable cases exist. E. Reshotko reported these conclusions to the Conference.

DISCUSSION

Flow 0290

The Conference agreed with the conclusion of E. Reshotko that there were no viable test cases at the present time.

^{*}Case-Western Reserve Univ., University Circle, Cleveland, OH 44106.

FLOW OVER THE TRAILING EDGE OF BLADES AND AIRFOILS

Flow 0470

Case 0471

Evaluator: P. Drescher*

SUMMARY

SELECTION CRITERIA

A survey of the literature indicates that a considerable amount of experimental work on the flow over sharp or blunt trailing edges of blades and airfoils has been done in the past. In selecting experiments which could provide the basis for a test case, the following criteria were used: (1) the flow is complex; (2) it is attached to the trailing edge; (3) the data contain streamwise distributions and/or cross-profiles of important flow quantities at several streamwise locations; (4) they include the near-wake region; (5) the experimental boundary conditions are known and reliable; and (6) if the flow is unsteady, it is accounted for correctly in the measurements. Thus, most of the experiments reported in the literature had to be rejected. Mainly, the data are not sufficiently detailed, and the boundary conditions are extensively unknown.

In a second step, the few remaining candidates were scrutinized in detail. The results can be summarized as follows (for details, see Drescher, 1979-80).:

- Sharp trailing edge: the experiment of Viswanath et al. (1979) on flow over a sharp trailing edge of an airfoil fits the requirements of accuracy and reliability imposed for a test case. There is no data set on flow over compressor or turbine blades with sharp trailing edges that is suitable for a test case.
- Blunt trailing edges: the common deficiency of all data sets considered is that the measurements in the reverse flow region are not sufficiently reliable. This is true for isolated bodies as well as for cascades.

FLOW SELECTED

The experiment of Viswanath et al. (1979) on compressible flow over a sharp trailing edge is proposed as a test case. The model configuration is shown in Fig. 1. The flat plate is 0.0254 m thick and the tunnel height is 0.381 m. The model provides a pressure gradient region upstream of the trailing edge similar to an airfoil. The boundary layer is thick and fully developed. Data were taken at

*Brown, Boveri Ltd., CH-5401, Baden, Switzerland.

- (a) $M = 0.4$, $Re = 24.3 \times 10^6$, $\alpha = 0^\circ$
- (b) $M = 0.7$, $Re = 36.6 \times 10^6$, $\alpha = 0^\circ$, and
- (c) $M = 0.4$, $Re = 24.3 \times 10^6$, $\alpha = 6.25^\circ$.

where M = nominal free-stream Mach number; Re is based on free-stream conditions and model length $L = 0.9289$ m; α = deflection angle of the aftbody flap (positive direction: clockwise); stagnation pressure, $p_T = 2.75 \times 10^5$ N/m²; and nominal total temperature = 266.7°K.

Flow-field measurements were made using a laser-Doppler velocimeter and also conventional pitot and static probes. Static-pressure orifices were provided on the model surface as well as on the tunnel top and bottom walls. The data include surface-pressure distributions and mean-velocity, turbulent-shear-stress, and kinetic-energy profiles across the boundary layer approaching the trailing edge and across the near-wake.

Several checks were performed to validate two-dimensionality and symmetry of the flow field, as well as to assess the uncertainty in the measured data (for details, see Drescher, 1979-80, and Viswanath et al., 1979). Essentially, the checks did not reveal any significant deficiency, except that the momentum balance showed poor agreement for the last downstream station at $M = 0.4$, $\alpha = 0^\circ$, where the balance is very sensitive to the accuracy in the evaluation of θ . According to the worst-case analysis done by the experimentalists, mean velocities are accurate within $\pm 4\%$, turbulent quantities within $\pm 8\%$, static pressures on model surface and tunnel walls within 0.25% of p_T , and static pressure on wake centerline within 3% of p_T . The uncertainty in the probe/measurement locations is 0.4×10^{-3} m in the x - and 0.25×10^{-3} m in the y -direction. Furthermore, the total values of the turbulent kinetic energy were calculated on the assumption that the contribution of the unknown spanwise component, $\overline{w^2}$, is equal to $1/2 (\overline{u^2} + \overline{v^2})$.

ADVICE TO FUTURE DATA TAKERS

There are numerous experiments in which a few flow quantities are measured in the trailing-edge region at varying flow conditions and model configurations. They are not adequate for reliably testing sophisticated computation methods. What is needed are detailed flow-field measurements at fixed flow conditions and model configurations. Therefore, future efforts should concentrate on that task. Sufficiently detailed and reliable data sets are lacking so far for:

- airfoils and isolated bodies with (a) a sharp trailing edge in supersonic flow and (b) a blunt trailing edge in subsonic and supersonic flow;
- compressor and turbine blades with sharp and blunt trailing edges in the entire Mach-number range.

Since the accurate specification of the complete initial flow conditions are a prerequisite for a credible comparison of computation and experiment, it is essential they should be measured. In particular, this refers to the flow approaching the trailing edge. In the case of a blunt base, the flow is already affected a considerable distance upstream of the base region. The measurements must therefore include the upstream region. The reverse flow at the base apparently provides the main difficulty in taking good data from flow over a blunt trailing edge. A further difficulty arises in subsonic flow because the wake is of the vortex street type and thus essentially unsteady. Therefore, instrumentation is required which permits instantaneous measurements.

Editor's Note: Important remarks concerning measurement in reversed-flow regions appear in the comments by Simpson (Flow 0430) and Eaton and Johnston (Flow 0420).

REFERENCES

- Drescher, P. (1979-80). "Flow over the trailing edge of blades: final report on the evaluation of data," submitted to the Organizing Committee, 1980-81 AFOSR-HTTM-Stanford Conference on Complex Turbulent Flows, Part I, February 1979; Part II, May 1979; Part III, April 1980.
- Viswanath, P. R., J. W. Cleary, H. L. Seegmiller, and C. C. Horstman (1979). "Trailing-edge flows at high Reynolds number," AIAA Paper 79-1503.

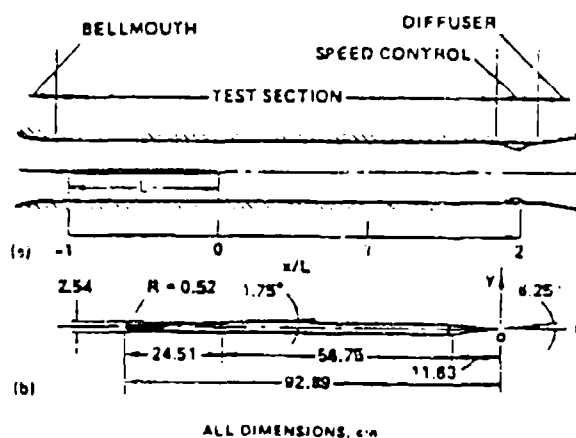


Figure 1. Schematic of test section and test model.

DISCUSSION

Flow 0470

The Conference recommended use of Case 0471, Viswanath et al. (1979). The attendants present believes the flow was well documented; there was no objection to its acceptance. A number of other two-dimensional wake flows exist and need to be evaluated (see in particular the reports of V. C. Patel concerning Flows 0350 and 0360).

SPECIFICATIONS FOR COMPUTATION


ENTRY CASE/INCOMPRESSIBLE

Case #0471; Data Evaluator: P. Drescher

Data Taker: P. R. Viswanath et al.

PICTORIAL SUMMARY

Flow 0470. Data Evaluator: P. Drescher. "Flow over the Trailing Edge of Blades and Airfoils."

Case Date Taker	Test Rig Geometry	dp/dx or C _p	Number of Stations Measured							C _f	Re	M _∞	Other Notes
			Mean Velocity		Turbulence Profiles								
			U	V or W	$\overline{u^2}$	$\overline{v^2}$	$\overline{w^2}$	\overline{uv}	Others				
Case 0471 P. Viswanath J. Cleary H. Boegmler C. Moreman		Sur- face and wake pres- sure	9	-	7	7	-	7	-	-	2.4 to 3.7 = 10 ⁷ (based on chord)	0.4 and 0.7	Subsonic trailing edge flow, variable flap angle Symmetric and unsymmetric cases.

Plot	Ordinate	Abcissa	Range/Position	Comments
1	y	U/U_{ref}	$0 \leq y \leq 0.015$ m M = 0.4, $\alpha = 0^\circ$	4 curves at $x/\theta_0 = -2.7, 4.3,$ 43.0, 94.5. See Instruction 1.
2	y	$-\tau/(\rho U^2)_{ref}$	$0 \leq y \leq 0.02$ m M = 0.4, $\alpha = 0^\circ$	4 curves at $x/\theta_0 = -2.7, 4.3,$ 43.0, 94.5.
3	y	K/U_{ref}^2	$0 \leq y \leq 0.02$ m M = 0.4, $\alpha = 0^\circ$	4 curves at $x/\theta_0 = -2.7, 4.3,$ 43.0, 94.5.
4	y	U/U_{ref}	$0 \leq y \leq 0.02$ m M = 0.7, $\alpha = 0^\circ$	4 curves at $x/\theta_0 = -2.0, 3.2,$ 32.5, 71.4. See Instruction 2.
5	y	$-\tau/(\rho U^2)_{ref}$	$0 \leq y \leq 0.02$ m M = 0.7, $\alpha = 0^\circ$	4 curves at $x/\theta_0 = -2.0, 3.2,$ 32.5, 71.4.
6	y	K/U_{ref}^2	$0 \leq y \leq 0.02$ m M = 0.7, $\alpha = 0^\circ$	4 curves at $x/\theta_0 = -2.0, 3.2,$ 32.5, 71.4.
7	y	U/U_{ref}	$-0.02 \leq y \leq 0.02$ m M = 0.4, $\alpha = 6.25^\circ$	4 curves at $x/\theta_0 = -2.3, 4.0,$ 36.2, 79.1. See Instruction 3.
8	y	$-\tau/(\rho U^2)_{ref}$	$-0.025 \leq y \leq 0.025$ m M = 0.4, $\alpha = 6.25^\circ$	4 curves at $x/\theta_0 = -2.3, 4.0,$ 36.2, 79.1.
9	y	K/U_{ref}^2	$-0.025 \leq y \leq 0.025$ m M = 0.4, $\alpha = 6.25^\circ$	4 curves at $x/\theta_0 = -2.3, 4.0,$ 36.2, 79.1.

Plot	Ordinate	Abscissa	Range/Position	Comments
10	p/p_T	x/L	$-0.24 \leq x/L \leq 0.2$ $M = 0.4, \alpha = 0^\circ$	Pressure distribution on surface and wake centerline (optional).
11	p/p_T	x/L	$-0.24 \leq x/L \leq 0.2$ $M = 0.7, \alpha = 0^\circ$	Pressure distribution on surface and wake centerline (optional).
12	p/p_T	x/L	$-0.24 \leq x/L \leq 0.2$ $M = 0.4, \alpha = 6.25^\circ$	Pressure distribution on surface and wake centerline (optional).

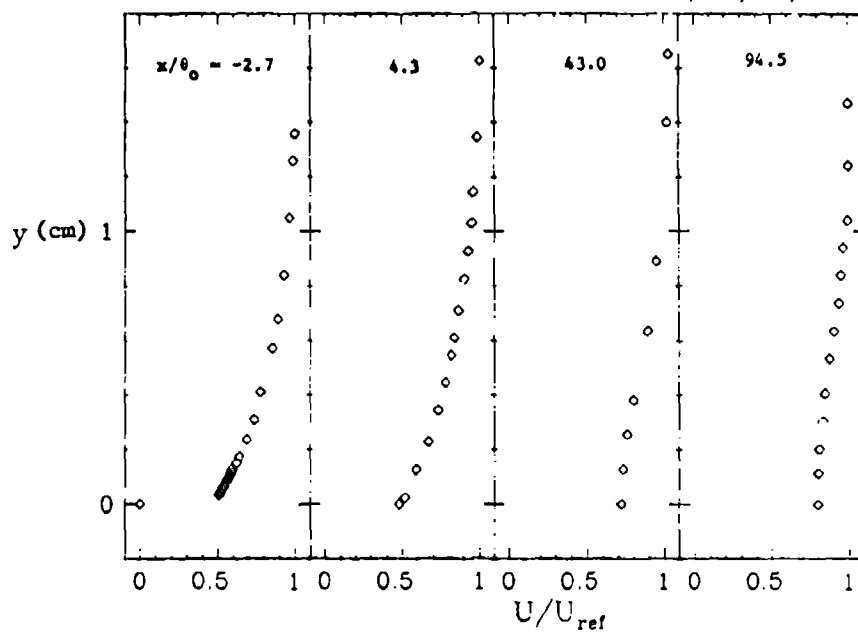
Special Instructions:

1. Reference values for Plots 1, 2, 3: $U_{ref} = 124.2$ m/s; $(\rho U^2)_{ref} = 5.163 \times 10^4$ N/m², $p_T = 2.75 \times 10^5$ N/m², $\theta_0 = 0.147$ cm.
2. Reference values for Plots 4, 5, 6: $U_{ref} = 215.8$ m/s, $(\rho U^2)_{ref} = 13.375 \times 10^4$ N/m², $p_T = 2.75 \times 10^5$ N/m², $\theta_0 = 0.195$ cm.
3. Reference values for Plots 8, 9: $U_{ref} = 153.6$ m/s, $(\rho U^2)_{ref} = 7.592 \times 10^4$ N/m², $p_T = 2.75 \times 10^5$ N/m², $\theta_0 = 0.177$ cm.
4. y/θ_0 is the vertical coordinate normal to the model centerline; it is measured from the model surface and the wake centerline.

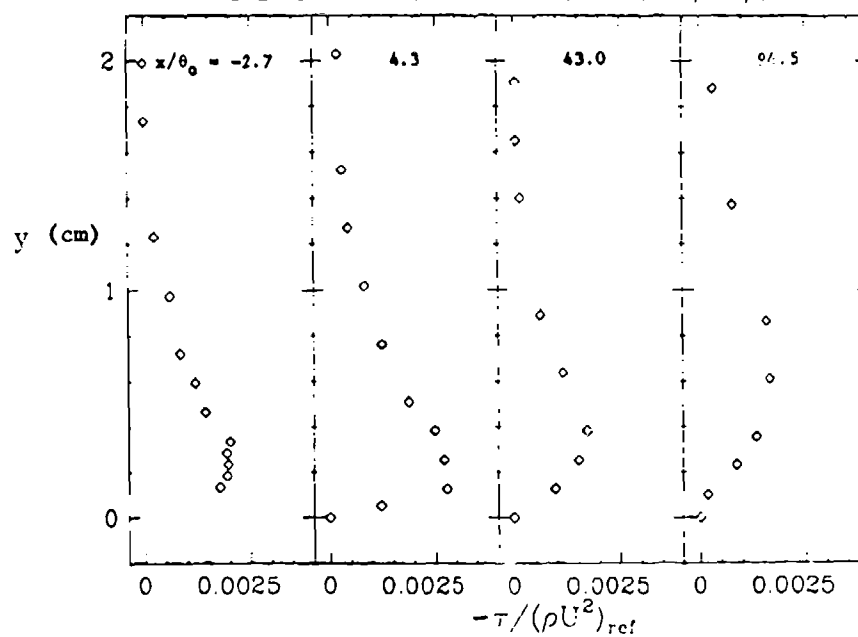
The flow to be calculated is shown in Fig. 1 and consists of a two-dimensional flat plate positioned symmetrically between parallel walls. It is essential to include the top and bottom walls in the flow calculation, since the model blockage of 6.6% is not small enough to assume negligible wall interference. For a boundary-layer method, the measured wall-pressure distribution can be used. Computations using Reynolds equations and Large Eddy Simulation can calculate the wall-pressure distributions.

Commence the computation sufficiently far upstream and match the measured data at the first measurement station ($x/L = -0.220$). Position the downstream boundary far enough behind the trailing edge that the streamwise gradients are asymptotically zero. The model can be assumed adiabatic.

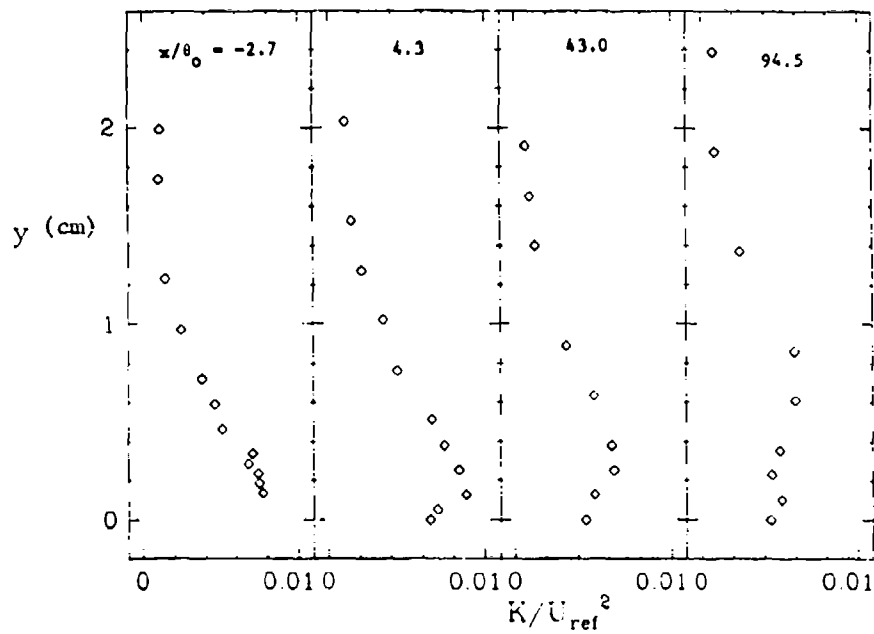
PLOT 1 CASE 0471 FILES 7,11,15,17



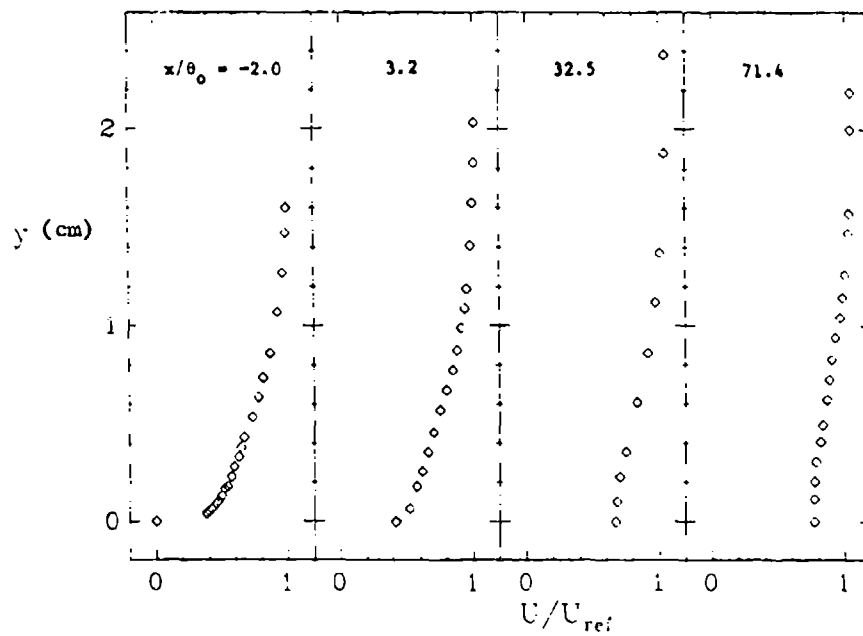
PLOT 2 CASE 0471 FILES 8,12,15,13



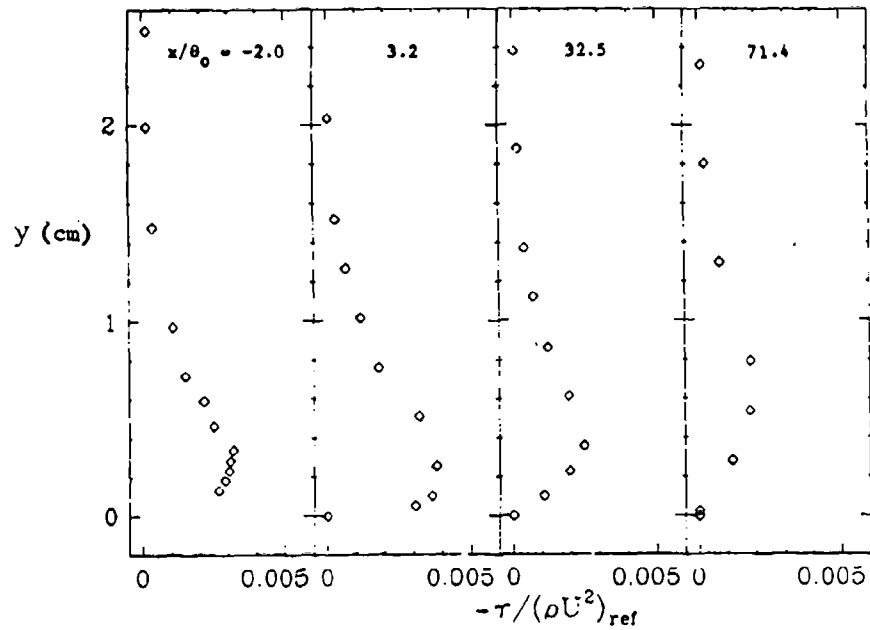
PLOT 3 CASE 0471 FILES 8,12,15,18.



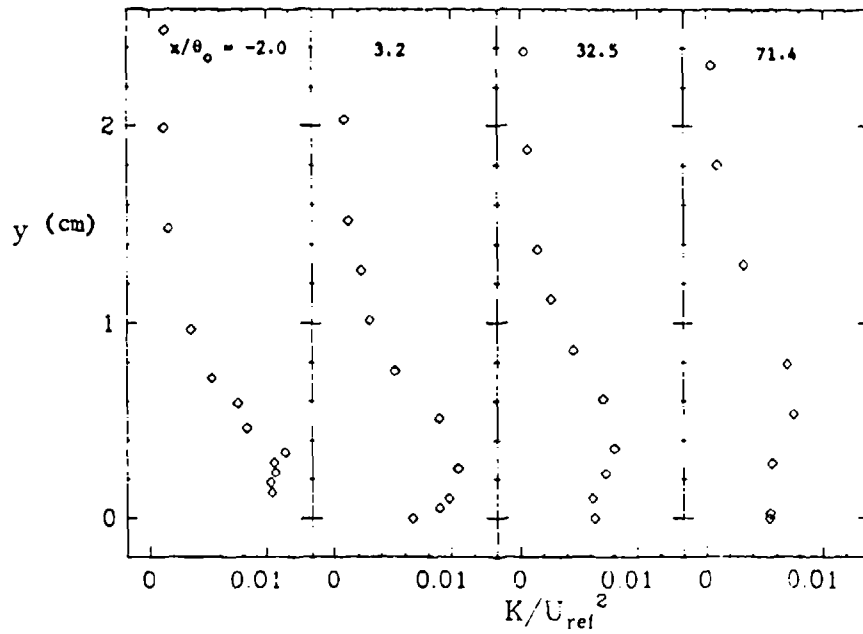
PLOT 4 CASE 0471 FILES 24,28,32,34



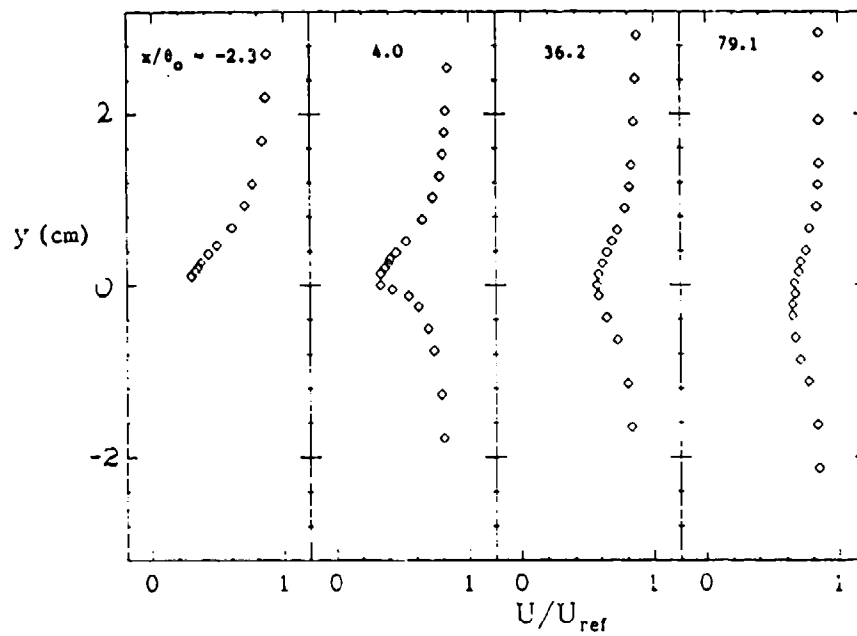
PLOT 5 CASE 0471 FILES 25,29,32,35



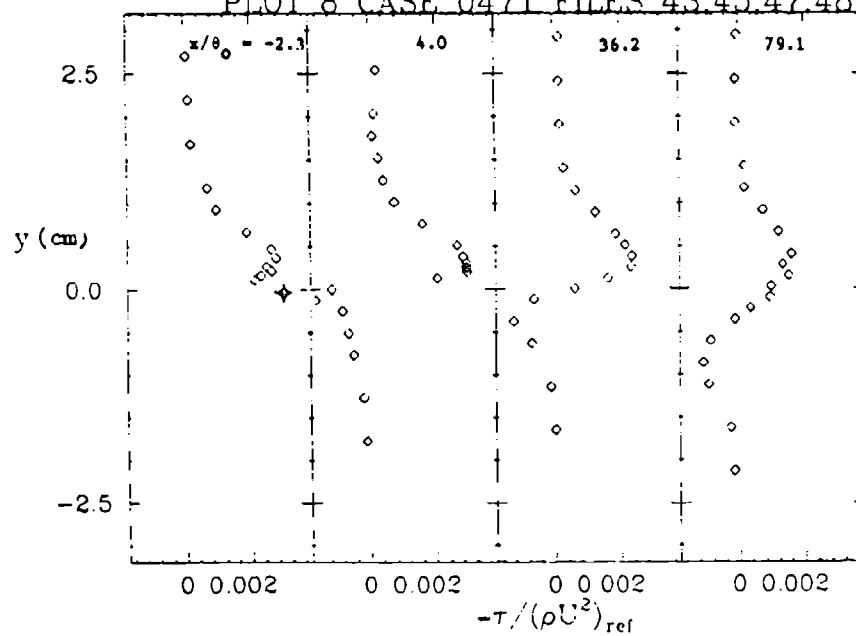
PLOT 6 CASE 0471 FILES 25,29,32,35

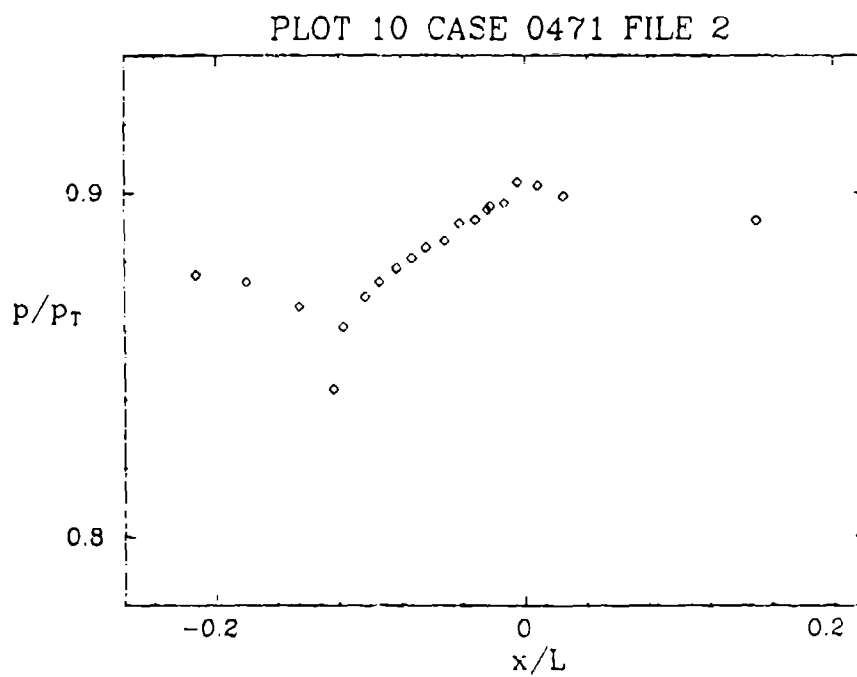
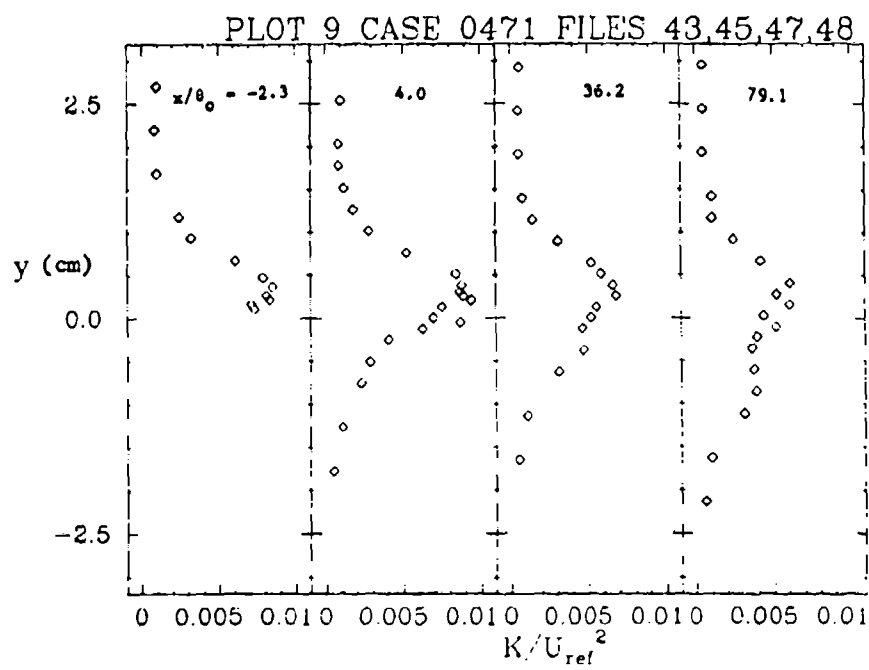


PLOT 7 CASE 0471 FILES 43,45,47,48

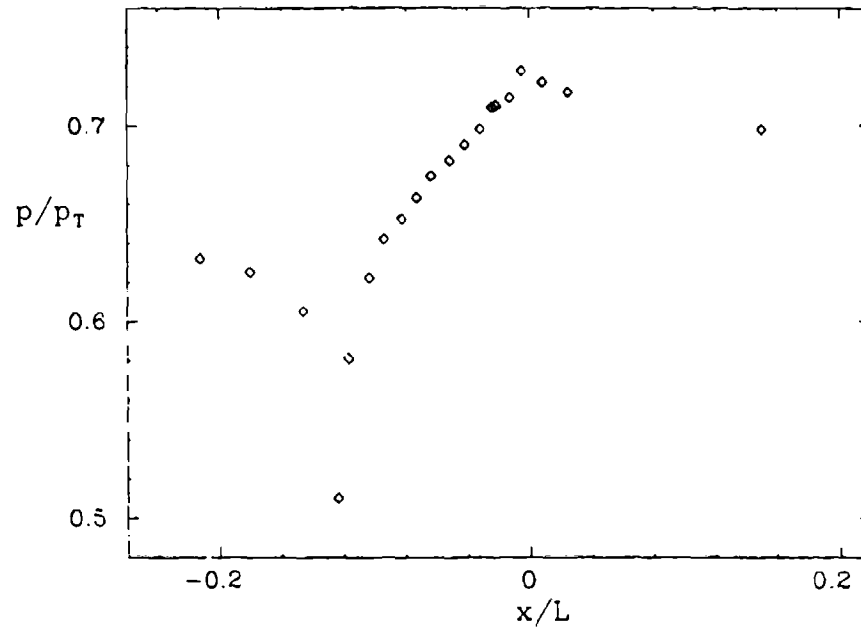


PLOT 8 CASE 0471 FILES 43,45,47,48

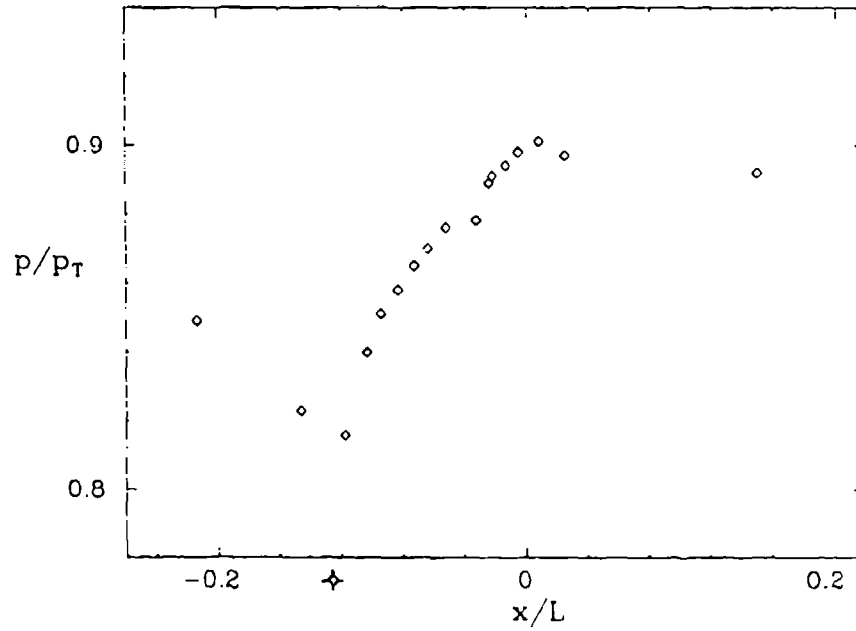




PLOT 11 CASE 0471 FILE 19



PLOT 12 CASE 0471 FILE 36



RELAMINARIZING FLOWS

Flow 0280

Cases 0281, 0282

Evaluator: K. R. Sreenivasan*

SUMMARY

INTRODUCTION

Relaminarization is a process by which an initially turbulent flow is rendered effectively laminar. An extreme test of whether a turbulence model incorporates the right physics is its capability for predicting accurately the succession of stages that occur in a relaminarizing flow.

Although relaminarization occurs in a wide variety of circumstances, only two classes of flows have been documented in sufficient detail; these classes of flows form the subject of discussion here.

CASE 0281. INCOMPRESSIBLE ACCELERATED TURBULENT BOUNDARY LAYER

A turbulent boundary layer developing at constant pressure (say, on one of the wind-tunnel walls) up to a point x_0 is subjected to a sustained steep, streamwise acceleration beyond x_0 . This can be accomplished, for example, by fixing a liner of desired shape on the opposite wall of the wind tunnel (Fig. 1). Experiments show that the boundary layer asymptotically tends to a laminar state. In the past, nearly thirty flows of this type have been studied (see Sreenivasan, 1980).

a. Selection Criteria

(i) Initial conditions: It is desirable that the initial state of the turbulent boundary layer be self-preserving in constant pressure; those initial functions needed in a calculation method, not directly measured, can then be prescribed with a relatively high degree of confidence. High initial Reynolds numbers (Re_0 of the order of a few thousands) are also desirable because this eliminates the possibility of identifying relaminarization in this class of flows with low-Reynolds-number effects.

(ii) Flow conditions: The flow must then be subjected to sustained steep acceleration so that a succession of states from the fully turbulent to the truly laminar occurs.

(iii) Measurements: At least all mean flow parameters (including the skin friction) and profiles of Reynolds stresses (both normal and shear) should be measured at close intervals during acceleration, especially in the region of maximum C_f , where a

*Dept. Engineering and Appl. Science, Yale University, New Haven, CT 06520.

lot of detailed changes occur. Generally, more care than is usual must be taken near the wall since the linear part of the velocity profile diminishes in extent.

(iv) Internal consistency: Momentum balance and other checks as appropriate must be applied to ensure internal consistency of measurements.

b. Flow Selected

Unfortunately, none of the available flows qualified as an ideal test case, but about half a dozen of them can serve as moderately good test cases. In these flows, although there is a general consistency and reproducibility of all essential features, different levels of confidence can be placed on different measured parameters, and a good substitute to having an ideal test case would be to compute all these moderately good flows with the purpose of predicting in each flow at least the most reliable of the measured parameters. Since this requires too many computations, we are forced to choose one set of data (Flow A from Simpson and Wallace, 1975) that appears to represent a reasonable compromise among these moderately good flows. Details of the evaluation can be found in Sreenivasan (1980).

A few words of caution for the computers, however: the boundary layer in this flow was developing under mild adverse pressure gradient upstream of where the acceleration set in, so that its initial state is somewhat (but not terribly) different from that of the standard constant-pressure boundary layer at the same Reynolds number.

CASE 0282. SUBCRITICAL PIPE OR DUCT FLOWS

The experimental situation involves a gradual enlargement of a pipe or channel from one diameter or width to another (Fig. 2). The Reynolds number goes down from, say, R_1 upstream of the divergence to R_2 downstream. If $R_1 > R_{cr}$ and $R_2 < R_{cr}$, where R_{cr} is an appropriate critical Reynolds number, an approaching turbulent flow will revert to the laminar state.

a. Selection Criteria

For similar reasons as cited in Case 0281, it is desirable that the turbulent flow upstream of expansion be fully developed. Narasimha and Sreenivasan (1979) have shown that the best estimate of R_{cr} (based on average section velocity and pipe radius or channel width) is 1500. Thus, the initial Reynolds numbers must be substantially greater than 1500; the larger the difference ($R_{cr} - R_2$), the faster (in terms of x/D) is the laminar state effectively attained.

The angle of divergence in the expanding section should be kept sufficiently small to ensure that no flow separation occurs. Other comments made on measurements in Case 0281 hold here too.

b. Flow Selected

Relaminarizing flows of this class have been reported by Laufer (1962) and Sibulkin (1962) in pipes and by Badri Narayanan (1968) in a channel. These investigations do not reveal any basic difference between relaminarizing channel and pipe flows. In terms of both thoroughness and accuracy (as judged by scatter in data and an examination of the instrumentation) Laufer's flow is chosen here as the best available test case.

ACCURACY OF MEASUREMENTS

Since the measurements of interest here concern only mean parameters and rms streamwise velocity, the accuracy of measurements must be generally good. The greatest uncertainty rests with skin-friction measurements (where made); note that in Case 0282, or in any comparable flow, no reliable skin-friction measurements are available. Typical accuracy estimates claimed by Simpson and Wallace (or estimated from other given information) are:

Mean velocity	$U = \pm 1/2\%$
Streamwise rms fluctuation	$(\overline{u^2})^{1/2} = \pm 1\%$
Skin-friction coefficient	$c_f = \pm 20\%$

REFERENCES

- Badri Narayanan, M. A. (1968). "An experimental study of reverse transition in two-dimensional channel flow," J. Fluid Mech., 31, 609.
- Laufer, J. (1962). "Decay of non-isotropic turbulent field," in Miszellaneen de angewandte Mechanik, Festschrift Walter Tollmien, Akademik-Verlag, Berlin.
- Narasimha, R., and K. R. Sreenivasan (1979). "Relaminarization of fluid flows," Advances in Applied Mechanics, 19, 221.
- Patel, V. C., and M. R. Head (1969). "Some observations on skin-friction and velocity profiles in fully developed pipe and channel flow," J. Fluid Mech., 38, 181.
- Sibulkin, M. (1962). "Transition from turbulent to laminar flow," Phys. Fluids, 5, 280.
- Simpson, R. L., and D. B. Wallace (1975). "Laminarizing turbulent boundary layers: experiments on sink flows," Project SQUID Report SMU-1-PU.
- Sreenivasan, K. R. (1980). "A guide to the data in relaminarizing flows," Report prepared for the Stanford 1980/1981 Conference.

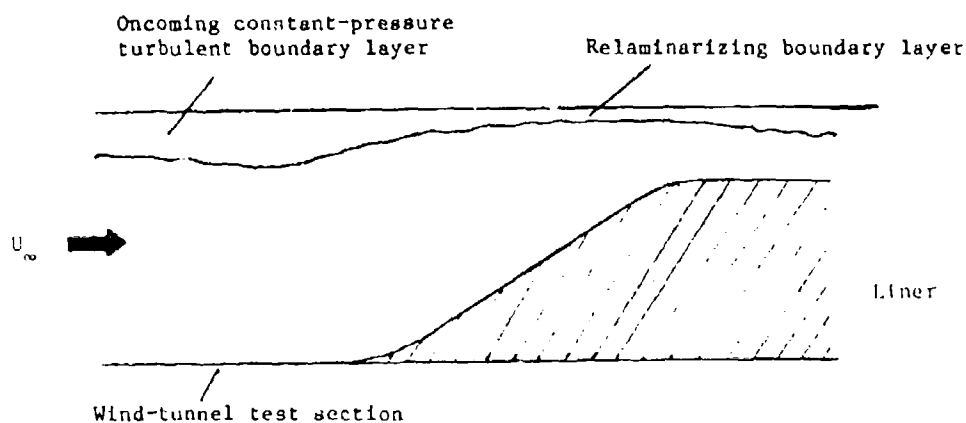


Figure 1. Schematic of experimental apparatus for producing relaminarization of incompressible turbulent boundary layers.

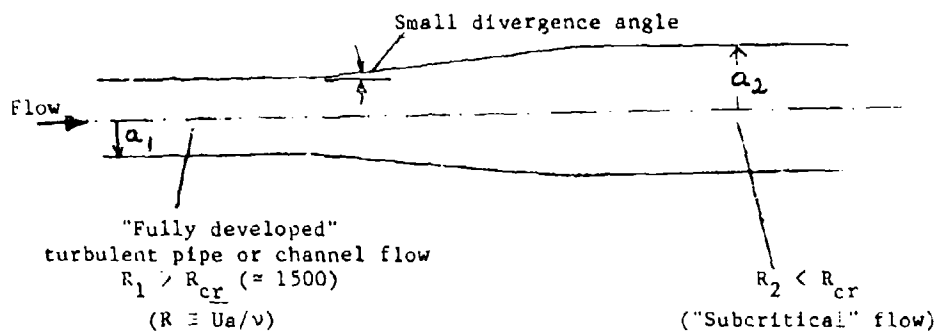


Figure 2. Schematic of experimental apparatus for producing relaminarizing subcritical pipe or channel flow.

DISCUSSION

Flow 0280

Consensus was reached by the Conference that of the two test cases recommended, namely Simpson and Wallace (1975) and Laufer (1962) were not documented as fully as desired; however, they are the best we have. Moreover, they are sufficient to establish "limits" for turbulent behavior and are thus important checks. Hence, the Conference recommended that the two different classes of flow involving relaminarizing be used as test cases.*

Certain written discussion on the data evaluation for relaminarizing boundary layers between Dr. P. N. Inman (Imperial College, London) and Dr. K. R. Sreenivasan regarding future experiments appears important to place on record:

P. N. Inman: I agree that the "pre-laminarizing" state should be represented, and the existing data sets constitute sufficient information to test the performance of turbulence models. The ability to predict the approach to relaminarization is an essential part of a relaminarization model, so that it is desirable that test cases should start in the fully turbulent regime. Although many of the existing data have shortcomings, in terms both of quantities measured and of flow quality (especially two-dimensionality), the report of Dr. Sreenivasan suggests new experiments which may be difficult to perform. At least in low-speed flow without body forces, relaminarization cannot be separated from low Reynolds number effects, since R_θ always falls well below the upper limit of low Reynolds number effects (say, $R_\theta = 5000$) before relaminarization occurs; in relaminarization induced by pressure gradients, R_θ usually falls to 300-400. The approach to relaminarization from high initial R_θ (> 2500 , say) is particularly difficult to reproduce in a conventional wind tunnel. To produce $R_\theta = 2500$ requires an initial length of order 1 m at $U_e = 15$ m/s.

Also in a "wedge flow" values of $K = \nu/U_e^2(dU_e/dx) \approx 3 \times 10^{-6}$ and a wedge angle, say, of 20° , implies a tunnel height of only 0.12 m and an effective wedge length of only 0.3 m. This length is unlikely to be long enough to give a reasonable range of $x/\delta_{\text{initial}}$. Dr. Sreenivasan's requirement that the boundary-layer thickness should be not more than 1% of the tunnel height also causes problems, for then the wedge angle must be greater than 55° .

Increasing the wedge angle (or more generally shortening the region of pressure drop) allows higher speeds and higher initial R_θ , but must be traded against the length of the relaminarization region and the possibility of curvature effects in the outer part of the boundary layer. Also, cross-flows in the tunnel side walls become increasingly violent leading to departures from two-dimensionality of the test boundary layer on the tunnel floor.

The constraints discussed above probably account for the lack of experiments with initial $R_\theta > 2500$. The existing data explore the readily attainable

*[Ed.: Reworded for clarity, hopefully, without change of emphasis.]

combinations and the envelope of test conditions is perhaps unlikely to be extended much in the near future. It would be unwise to argue that because the more extreme conditions cannot be easily obtained in wind tunnels, they will never occur in practice, but future experimenters should be encouraged on better exploration of the easily attainable range of relaminarizing flows than on attempts to produce flows with high R_0 and high K .

K. R. Sreenivasan: Firstly, I agree that computing the fully turbulent "pre-laminarizing" region provides a challenge to computers, but I want to emphasize that the ability to predict the "pre-laminarizing" flow is not a necessary prerequisite for a successful prediction of the later stages of relaminarization. In the latter case, it is enough to be able to, say, switch off the production of turbulent energy at the appropriate point and merely recognize that further downstream turbulent stresses play no significant role in determining the mean flow dynamics. Unless a model grossly violates the physics (see Narasimha and Sreenivasan (1973), J. Fluid Mech., 61, 417), it is unlikely that the outcome exhibits strong sensitivity to the details of the model. This simplicity (which is nevertheless complicated enough to be sufficiently challenging) is due to the fact that relaminarization is an asymptotic case. That is, of course, why we study asymptotic limits in general.

Secondly, it is not correct to say that relaminarization in accelerated turbulent boundary layers cannot be separated from low Reynolds number effects. It is not true that R_0 is always about 300-400 whenever relaminarization occurs. There are experiments that show the contrary (Patel and Head (1968), J. Fluid Mech., 34, 371; Blackwelder and Kovasznay (1972), J. Fluid Mech., 53, 61). I believe this will also be the outcome in future experiments with higher initial R_0 . We both agree these experiments will be difficult to perform. I believe we need to resort to experiments in a large enough wind-tunnel, capable of producing without acceleration-producing devices, such as a liner, a constant-pressure boundary layer with $R_0 \approx 10,000$. Hence when a liner is added, we may have a chance to obtain a relaminarizing boundary layer with an initial R_0 of the order of 3000-4000.

Lastly, I do believe smaller values of δ/h , than are usual, are essential to eliminate momentum imbalances due to possible normal pressure-gradient effects induced by flow curvature but I do not wish to stick to $\delta/h \approx 10^{-2}$ as a steady-fast rule. This rule calls for a large wind-tunnel height and therefore a large wind tunnel. Your calculations are useful but may be misleading in the context you use them. Large R_0 and moderate wedge angles are not incompatible, if we do not insist on large K . I do not care to stipulate the attainment of large K and high R_0 ; I believe large K is neither necessary nor sufficient for relaminarization. Incidentally, we can always produce large values of K by resorting to non-linear wedges. Locally large wedge angles do not produce important cross-flow effects as long as δ/h is small enough (see Badri Narayanan and Ramjee (1969), J. Fluid Mech., 35, 225-241).

SPECIFICATIONS FOR COMPUTATION


ENTRY CASE/INCOMPRESSIBLE

Case #0281; Data Evaluator: K. R. Sreenivasan

Data Takers: R. L. Simpson and D. B. Wallace

PICTORIAL SUMMARY

Flow 0280 Data Evaluator: K. R. Sreenivasan. "Semi-laminarizing Flows."

Case Data Taker	Test Rig Geometry	dp/dx or C _p	Number of Stations Measured							C _f	Re	Initial Condi- tion	Other Notes
			Mean Velocity		Turbulence Profiles								
			U	V or W	$\overline{u^2}$	$\overline{v^2}$	$\overline{w^2}$	\overline{uv}	Others				
Case 0281 R. Simpson D. Wallace		-	15	-	15	-	-	-	-	15	2342 (based on δ at inlet)		Boundary layer developing under mild adverse pres- sure gradient upstream of contraction.

Plot	Ordinate	Abscissa	Range/Position	Comments
1	θ	x	$2.235 \leq x \leq 4.846$ m	$R_\theta = \theta U_e / \nu$ $U_e = U_e(x)$ $U_{ref} = U_e$ at $x = 2.235$ m.
2	H	x	$2.235 \leq x \leq 4.846$ m	
3	C_f	x	$2.235 \leq x \leq 4.846$ m	
4	yU_e/ν	U/U_e	$0 \leq U/U_e \leq 1$ $0 \leq yU_e/\nu \leq 20,000$	x = 2.718, 2.992, 3.486, 3.785 m.
5	yU_e/ν	U/U_e	$0 \leq U/U_e \leq 1$ $0 \leq yU_e/\nu \leq 20,000$	x = 4.239, 4.604, 4.693, 4.846 m.
6	yU_e/ν	$(\overline{u^2})^{1/2}/U_e$	$0 \leq (\overline{u^2})^{1/2}/U_e \leq 0.1$ $0 \leq yU_e/\nu \leq 20,000$	x = 2.718, 3.486, 4.239, 4.693 m.

Special Instructions:

1. If possible, provide tabulated output for R_θ , H, C_f at stations of measurements.
2. The geometry of the test channel is shown in Fig. 3.
3. Range: The acceleration effects do not begin until after $x = 2.235$ m, which will thus be chosen as the initial station, x_0 . Computations should begin at x_0 and continue to $x = 4.846$ m.
4. Input: All measured conditions at x_0 , and the prescribed variation of the free-stream velocity U_∞ with x are given in Table 1.

TABLE 1

Known Initial Conditions and Variation of U_e , Case 0281

Reference: Simpson and Wallace (1975), Boundary Layer A

(a) Mean and rms profiles at x_0 (i.e., $x = 2.235m$)		(b) Prescribed variation of U_e with x	
$10^4 y, m$	$U, m \cdot sec^{-1}$	$10^2 (u'/U_0)$	x, m
0	0	0	
2.0	0.317	1.6	
3.8	0.410	3.7	
5.1	0.516	5.1	2.235
7.6	0.696	6.9	2.583
10.2	0.885	8.9	2.718
15.2	1.076	9.8	2.868
20.3	1.228	9.4	2.992
25.4	1.338	9.1	3.112
31.7	1.419	9.2	3.486
38.1	1.468	8.9	3.627
50.7	1.564	8.3	3.785
76.1	1.659	7.4	3.937
101.5	1.741	7.1	4.239
152.2	1.866	6.8	4.453
203.0	1.971	6.6	4.604
253.7	2.066	6.4	4.629
317.1	2.184	6.0	4.693
380.6	2.307	5.9	4.846
507.5	2.505	4.8	
634.3	2.644	2.3	
761.2	2.670	1.2	

 $U_e = U_e(x)$
 $U_{ref} = U_e$ at $x = 2.235 m$
 $\theta = 8.88 \times 10^{-3} m, \delta^* = 13.16 \times 10^{-3} m, C_f = 4.82 \times 10^{-3}.$

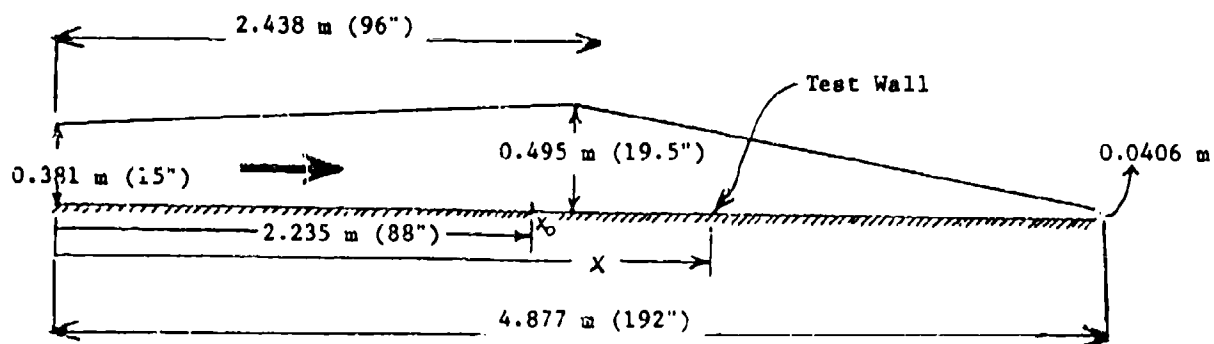
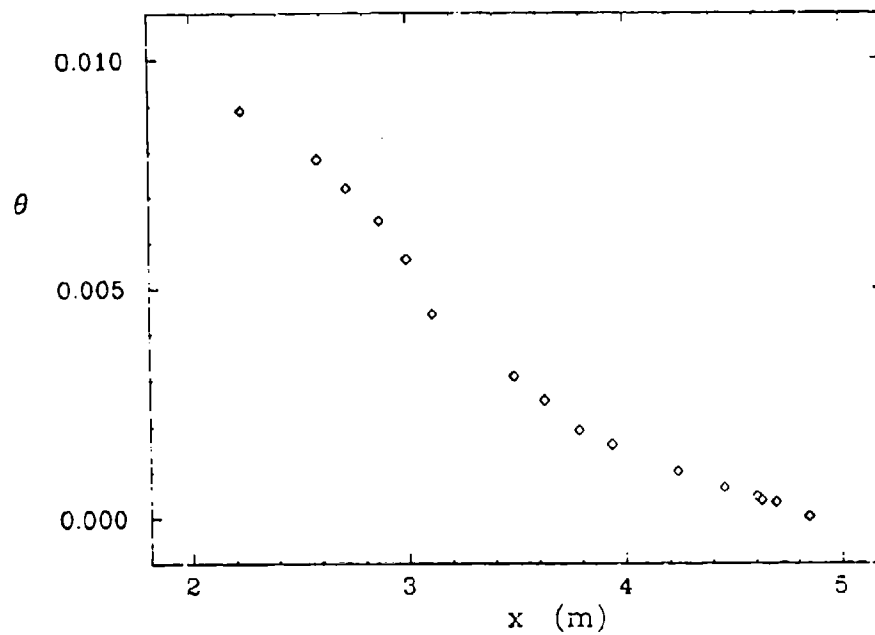
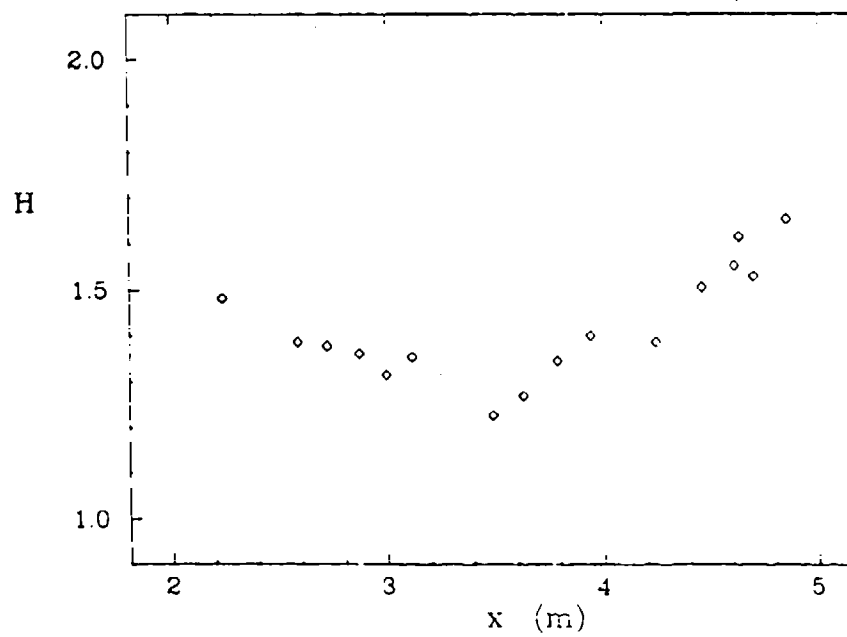


Figure 3. Test channel geometry for Flow A of Simpson and Wallace (1975), Case 0281.

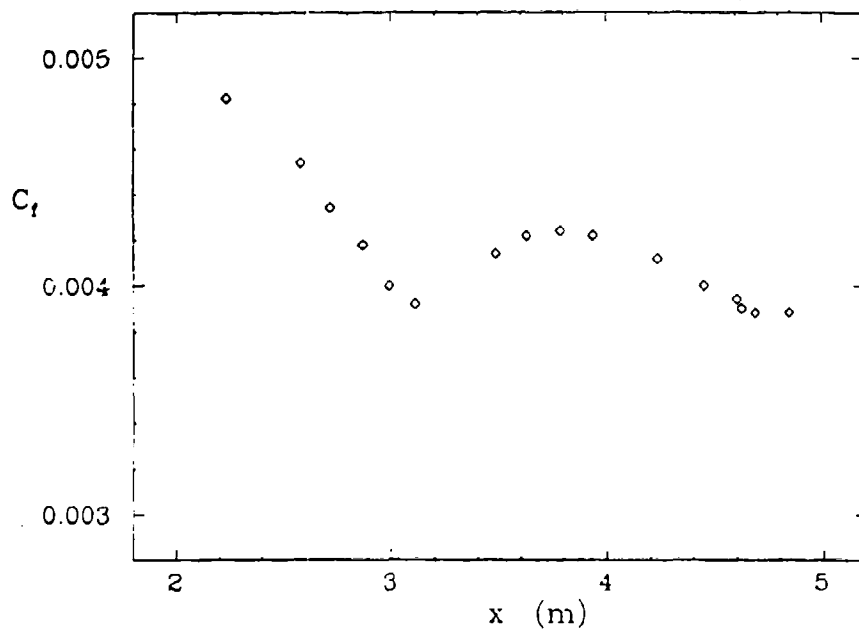
PLOT 1 CASE 0281 TABLES 1,2



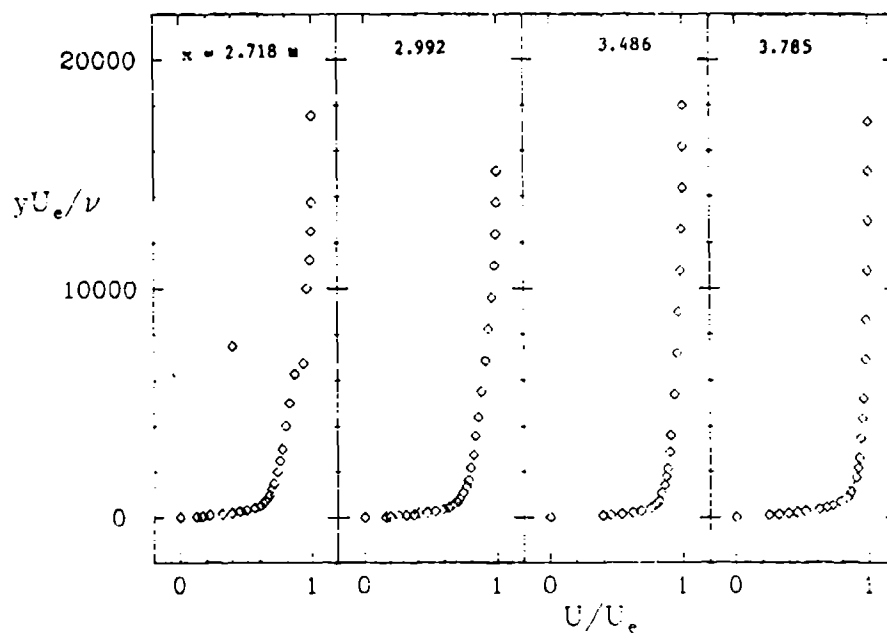
PLOT 2 CASE 0281 TABLES 1,2



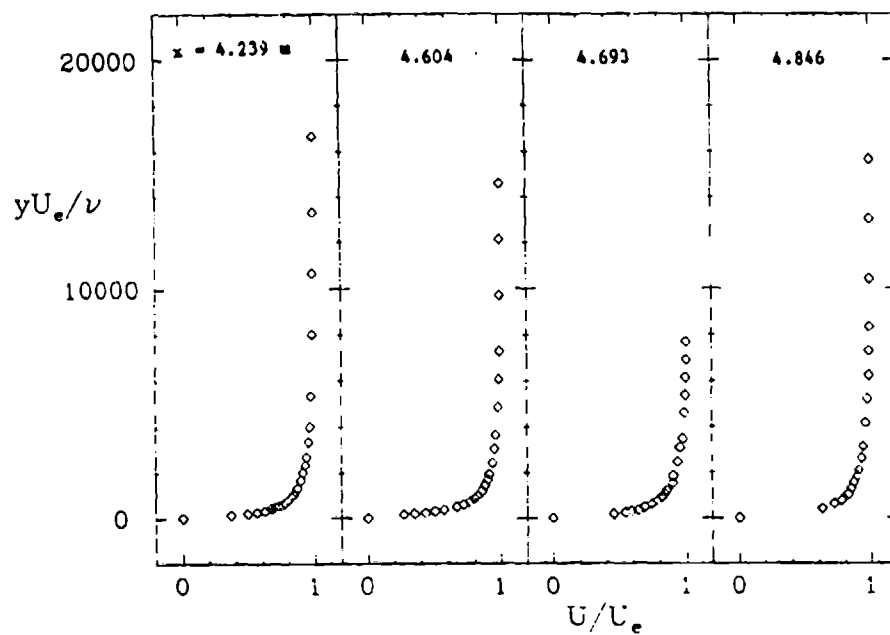
PLOT 3 CASE 0281 TABLES 1,2



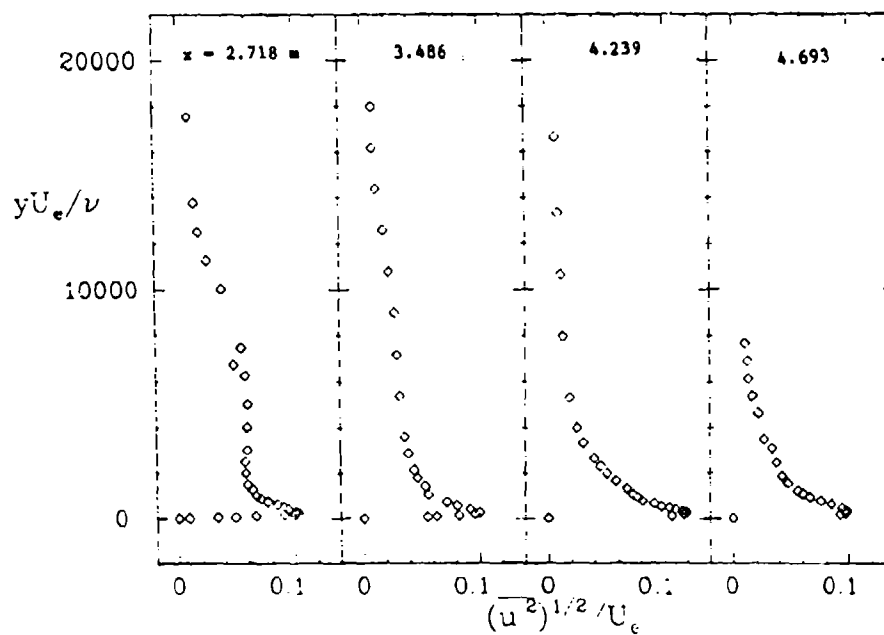
PLOT 4 CASE 0281 TABLE 2



PLOT 5 CASE 0281 TABLE 2



PLOT 6 CASE 0281 TABLE 2



SPECIFICATIONS FOR COMPUTATION


ENTRY CASE/INCOMPRESSIBLE

Case #0282; Data Evaluator: K. R. Sreenivasan

Data Takers: J. Laufer (V. C. Patel and M. R. Head)

PICTORIAL SUMMARY

Flow 0280. Data Evaluator: K. R. Sreenivasan. "Re laminarizing Flow."

Case Data Taker	Test Rig Geometry	dp/dx or C _p	Number of Stations Measured								Re	Ini- tial Condi- tion	Other Notes
			Mean Velocity		Turbulence Profiles					C _f			
			U	V or W	$\overline{u^2}$	$\overline{v^2}$	$\overline{w^2}$	\overline{uv}	Others				
Case 0282 J. Laufer (V. Patel & M. Head)		-	6	-	5	-	-	-	-	-	1725 (based on radius at inlet)	No con- ditions up- stream of di- vergence given	Initial mean velocity data taken from Patel and Head (1969).

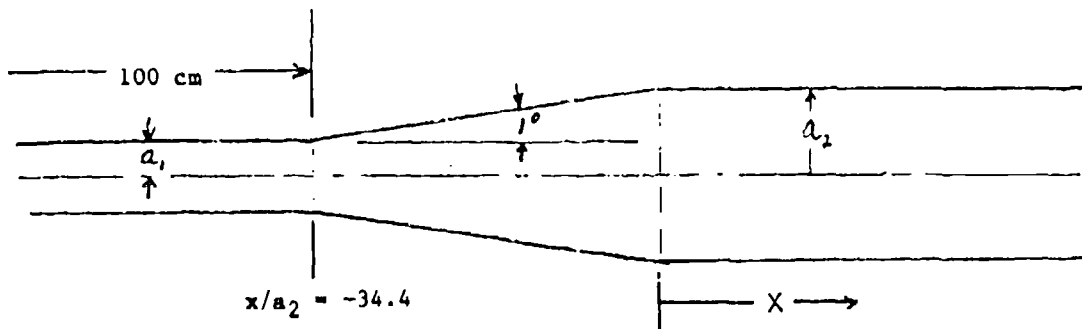
Plot	Ordinate	Abscissa	Range/Position	Comments
1	y/a_2	U/\overline{U}_2	$0 \leq y/a_2 \leq 1$ $0 \leq U/\overline{U}_2 \leq 2$	$x/a_2 = 20, 60, 80, 100, 120$ $\overline{U}_2 = 1.06 \text{ m/sec}, a_2 = 0.01 \text{ m}.$
2	y/a_2	$(\overline{u^2})^{1/2}/\overline{U}_2$	$0 \leq y/a_2 \leq 1$ $0 \leq (\overline{u^2})^{1/2}/\overline{U}_2 \leq 0.1$	$x/a_2 = 20, 60, 80, 100.$

Special Instructions:

1. Since no conditions upstream of divergence are given by Laufer, initial mean velocity data are taken from Patel and Head (1969) for appropriate $Re = U_1 a_1 / \nu = 1725$; see Table 2.
2. The specifics of the Laufer experimental set-up are given in Fig. 4.
3. Start calculation at $x/a_2 = -34.4$ and continue to $x/a_2 = 120$.

TABLE 2
Initial Mean Velocity Data, $x/a_2 = -34.4$
Reference: Patel and Head (1969)

$y/a_1 \bar{U}/\bar{U}_1$	
0	0
0.05	0.514
0.10	0.729
0.15	0.905
0.2	1.020
0.3	1.115
0.4	1.189
0.5	1.230
0.6	1.257
0.7	1.297
0.8	1.310
0.9	1.338
1.0	1.351



$$\bar{U}_1 = 6.62 \text{ m/sec}$$

$$a_1 = 0.4 \text{ cm}$$

$$R_1 = (\bar{U}_1 a_1)/\nu = 1725$$

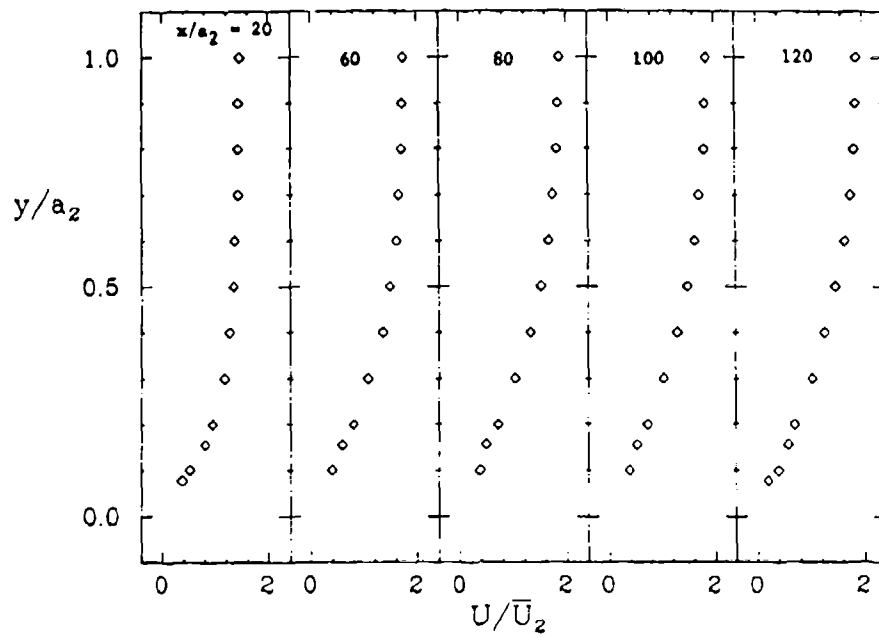
$$\bar{U}_2 = 1.06 \text{ m/sec}$$

$$a_2 = 1 \text{ cm}$$

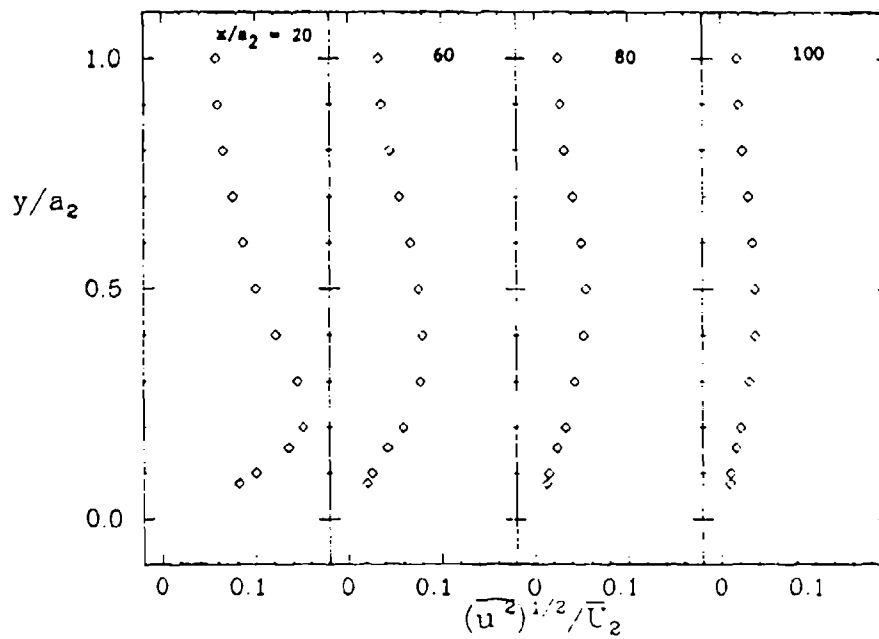
$$R_2 = (\bar{U}_2 a_2)/\nu = 690$$

Figure 4. Parameters of the Laufer (1962) experiment, Case 0282.

PLOT 1 CASE 0282 TABLE 4



PLOT 2 CASE 0282 TABLE 4



SESSION XIII

Chairman: J. B. Jones

Technical Recorders:

R. Westphal
P. Moin

REPORTS FROM AD-HOC COMMITTEES

1. Working Group on
Hot-Wire Anemometry at Low Mach Numbers
(Chairman: B. G. Newman)
2. Working Group on
Use of Hot-Wire Anemometers in Compressible Flows
(Chairman: E. Reshotko)
3. Working Group on
Free-Shear Layers
(Chairman: F. Champagne)
4. Working Group on
Turbulence Management and Control of Large-Eddy Structure
(Chairman: H. Nagib)

CLOSING DISCUSSION

on Ad-Hoc Committee Reports and Sessions I Through XII

REPORT OF EVALUATION COMMITTEE

(Chairman: H. W. Emmons)

AD-HOC COMMITTEE NO. 1

Report of the Working Group on Hot-Wire Anemometry at Low Mach Numbers

Chairman: B. G. Newman

Recorder: R. Westphal

Members: P. Bradshaw	A. E. Perry
I. P. Castro	F. J. Pierce
F. Durst	V. A. Sandborn
F. Gessner	H. C. Saetharam
J. B. Jones	R. L. Simpson
R. J. Moffat	B. van den Berg

We were asked to answer four questions.

- a) What is the first-order uncertainty of hot-wire anemometry considering the difficulties of drift? What steps are useful in controlling and measuring the effect of drift?

After due attention has been paid to the removal of dust (typically 1 μ m and above), the compensation for changes of ambient temperature and the provision of adequate time for averaging (typically 10 s for U; it is 100 s for the turbulence quantities) the drift in calibration for mean velocity $\Delta U/U$ is perhaps 2%/day. Members of the group, however, quoted values as low as 1%/month and as high as 3%/hour. Wire material appears to be important. Platinum-coated tungsten welded to the prongs and platinum-iridium Wollaston wire soldered to the prongs are preferred.

- b) Do the uncertainties in (a) vitiate meaningful measurements of turbulence dissipation?

Three ways of measuring dissipation ϵ were considered:

- i) Assume local isotropy and Taylor's hypothesis to measure

$$15\nu \overline{\left(\frac{\partial u}{\partial x}\right)^2} = 15\nu \frac{1}{U^2} \overline{\left(\frac{\partial u}{\partial t}\right)^2}.$$

(Variants of the method measure more individual components of

$$\frac{1}{2}\nu \overline{\left(\frac{\partial u}{\partial x_j} + \frac{\partial u}{\partial x_1}\right)^2},$$

but accuracies are usually similar). The wire should be shorter than the Kolmogoroff length scale $(\nu^3/\epsilon)^{1/4}$. Sandborn in a 1-m boundary layer claimed accuracies $\pm 10\%$, which was similar to the accuracy of Klebanoff who uses wires of various lengths and extrapolates to small length. Other members of the group were less sanguine and thought that accuracies of ± 25 to $\pm 50\%$ were typical.

- ii) If the microscale Reynolds number exceeds 100, a universal inertial range of the spectrum may be expected (Bradshaw). For that part

$\overline{u^2} \phi(k) = K\epsilon^{2/3} k^{-5/3}$, where k is the wave number and $K \approx 0.5$. ϵ can therefore be inferred from the frequency ω spectrum assuming $k = \omega/U$.

Accuracies of $\pm 20\%$ were suggested although this may be improved to perhaps $\pm 10\%$ by choosing K so that the turbulence-energy equation, when integrated across the flow, is balanced. The unknown turbulence diffusion terms are eliminated by this integration.

- iii) Simpson has used the k^{-1} portion of the spectrum to obtain ϵ near the wall, but the accuracy is somewhat less.

It was concluded that ϵ can usefully be measured. However, it was recommended that N^{th} -order uncertainty should be checked by measuring a standard flow of similar scale such as fully developed pipe flow or a thick boundary layer in zero pressure gradient.

- c) What is the N^{th} -order uncertainty for various fluctuation quantities assuming good practice. Can it be improved?

The following figures for uncertainty estimates are presented with considerable diffidence.* They are based on measurements in known flows and also on oscillating probe experiments (Perry). For a longitudinal turbulence $\sqrt{\overline{u^2}}/U = 10\%$ or less, linearized response equations may be used. Likely errors are: $U < 2\%$; $\overline{u^2}$ normal wire ± 5 to $\pm 8\%$; crossed wire $\pm 15\%$; \overline{vw} between $\pm 5\%$ and $\pm 15\%$; and $\overline{v^2}$, $\overline{w^2} \pm 15\%$.

Good practice for slanting wires involves careful measurement of the wire angle, and yawing the wire in a smooth flow to obtain the response to yaw.

R. Moffat had misgivings about quoting $\overline{v^2}$ uncertainties, in particular as a percentage of $\overline{v^2}$, because this quantity tends to zero rapidly near a wall.

For a higher turbulence of about 25% direct digital processing of the hot-wire signal was recommended. Then only the non-linearities associated with pitch and yaw of the wire relation to the instantaneous velocity vector need be accounted for. Castro referred to the paper by Tutu and Chevray (*J. Fluid Mech.*, 71, 785, 1975).

For turbulence greater than 35 to 40% some rectification of the signal due to backflow is encountered. The use of either a flying hot wire (Coles, Perry) or a pulsed wire (Bradbury, Castro) is then recommended.

- d) Will the hot wire be replaced by the laser? Everywhere? In some applications?

We had a lively discussion on this question. Hot wires have been used for about 50 years of turbulence measurement, lasers for less than 10 years. There is therefore

*[Ed.: The word error has been changed to uncertainty in editing to make usage consistent with that of R. J. Moffat's paper in this volume.]

enthusiasm for the latter technique without the thorough testing which the former has received.

Fortunately three members of our group (Durst, Sandborn, and Simpson) were experienced users, and indeed developers, of laser anemometry. Other members quizzed them, and, in general, were surprised at their claims for the new instrument. From turbulence of very low intensity, say 1%, to very high intensity with even mean back-flow, it was thought that mean velocity could be measured to an accuracy of 0.2%. A two-laser system could measure uv to accuracy similar to the very best which could be achieved with a hot wire. Measurements of ϵ and also two-point correlations were possible with special signal-processing techniques. The non-intrusive nature of the instrument was recognized as important in many applications.

In using laser anemometry some difficulties may be experienced from a paucity of reflecting particles very close to a wall. Air flow usually has to be seeded. It seems to take a graduate student at least one year to master the technique and to start making useful measurements. Traversing gears, particularly with forward scattering, may be physically difficult to arrange for large flows. The cost of the instrument is typically 2 to 4 times that of comparable hot-wire equipment.

We concluded that those who have hot-wire equipment are likely to continue to use it for many years. However, those purchasing new equipment to measure turbulence may find it desirable to invest in a laser anemometer.

AD-HOC COMMITTEE NO. 2

Report of the Working Group on Use of Hot-Wire Anemometers in Compressible Flows

Chairman: E. Meshotko
Technical Recorder: S. Fronchick

Members: A. Demetriades M. Morkovin
A. Favre A. Roshko
C. Horstman

The committee discussed the two questions:

- a) What is the zeroth-order and N^{th} -order uncertainty of hot-wire fluctuation measurements for various quantities in transonic and supersonic flow?
- b) Can they be improved?

Horstman described the calibration procedure used in obtaining his hot-wire data. Demetriades specifically questioned whether the assumption that the sensitivity of the output to total temperature fluctuations was small relative to its sensitivity to $(\rho u)^2$ had been verified. Horstman's method of calibration did not address this question. Rather, Horstman made measurements at two different overheats and concluded that his total temperature-fluctuation amplitudes were negligible. Accordingly, it was agreed that the data are acceptable on this score.

Favre raised the question of the bandpass width used in obtaining the data, which was 100 KHz. It was felt that this was probably too low to retain the high frequency components of the energy spectrum related to dissipation, but that it was probably sufficient to retain nearly all of the turbulent energy. The Horstman data are thus considered to be acceptable as a test case.

Morkovin and Demetriades noted that hot-wire calibrations in compressible flow must be verified using the mode equations,* and Morkovin further pointed out that the validity of the mode equations in flows with strong shear gradients may break down due to assumptions made in the underlying analysis.

In discussing requirements for future data which are to be considered suitable for use in modeling, it was initially agreed that hot-wire measurements will, in conjunction with LDV, remain an important method for obtaining turbulence data in compressible flows, and would not be rendered completely obsolete by the use of LDV in the near future. Demetriades then proposed 7 standards for compressible hot-wire anemometer applications, which are appended.

Some discussion of uncertainty estimates was also conducted. Horstman and Sandborn suggested that uncertainty estimates may be obtained by comparing suitably non-

*For a detailed discussion of the mode equations for hot-wire calibrations in compressible flow, see Morkovin, AGARDograph No. 24 (1956).

dimensionalized fluctuating velocity and Reynolds shear-stress measurements made in a compressible turbulent flat-plate boundary layer to results obtained in low-speed flow. This is in line with the "Morkovin hypothesis."

Appendix

PROPOSED STANDARDS FOR COMPRESSIBLE HOT-WIRE ANEMOMETRY APPLICATIONS

by A. Demetriades

1. Transonic/supersonic/hypersonic flow facilities should be turbulence-categorized, i.e., their stream-turbulence content should be measured and reported:

Minimum:

$$\left. \begin{array}{l} u' \\ T' \\ p' \end{array} \right\} \text{ as functions of } P_o, T_o, x_1$$

Desirable Additions:

$$\left. \begin{array}{l} v', w' \\ \text{Spectra} \\ \text{Correlations} \\ \text{Higher Moments} \end{array} \right\} \text{ as functions of } P_o, T_o, x_1$$

2. The neglect of pressure fluctuations in reducing shear-flow turbulence data should be justified.
3. Free-stream turbulence is distorted in flowing through shocks, expansions, etc.; therefore, it should be measured in the immediate vicinity (e.g., just beyond $y = \delta$) of the measured flow.
4. Since large T' , ρ' , p' can be triggered by moderate u' at high speeds, nonlinearities may be important--especially the effect of large fluctuations on the sensitivity coefficients, which are usually assumed constant.
5. There should be a rigorous, precise accounting of the frequency response of the entire measuring system at all times. Recommendations:
 - a. Use of constant-temperature anemometer (subject to assurance of adequate response, i.e., 0.5 MHz or higher)
and/or
 - b. Continual adjustments of compensating circuit at all times
and/or
 - c. Response restoration "a posteriori."
6. Heat-transfer calibrations of the hot wire used before and after the measurement is mandatory. Any approximations made in the reduction formulas should be explicitly stated and successfully defended (e.g., $\partial M / \partial Re = 0$, $e_u u' \gg e_T T'$, etc.).
7. (Long term) The quasi-steady Kovasznay-Morkovin hot-wire analysis requires revision for constant-current hot-wire anemometry in the context of the complete unsteady heat-transfer problem for arbitrary compressible flows.

AD-HOC COMMITTEE NO. 3

Report of the Working Group on Free-Shear Layers

Chairman: F. Champagne

Recorder: R. Childs

Members: S. Birch	H. Nagib
P. Bradshaw	V. C. Patel
A. Hussain	B. Quinn
R. Luxton	I. Wygnanski
	K. Yen

The committee discussed:

"What is needed to fully specify the initial conditions for the near zone of a free-shear layer in order to be sure we can compare data with computations?"

The free-shear layer or mixing layer will be classified into two categories: (1) planar and (2) axisymmetric.

1. Planar Case

a) Specification of Computational Box Required:

$U = U(x, y)$

x = streamwise coordinate

y = direction of mean shear; height of computational domain should be at least greater than 5 shear-layer thicknesses, or $x\lambda$, where $\lambda = (U_1 - U_2)/(U_1 + U_2)$ using Birch's nomenclature. This choice of height should be sufficient for the vertical velocity fluctuations to vanish and also may ease any transpirational boundary conditions introduced to avoid pressure gradients.

z = spanwise coordinate; at least $x\lambda$.

b) Initial Conditions:

- (1) A flat-plate, zero-pressure-gradient equilibrium turbulent boundary layer characterized by R_θ just upstream of the trailing edge. R_θ should be greater than 500, and possible Reynolds number effects on the outer layer may exist for $R_\theta < 5000$.
- (2) Laminar boundary layer--a good approximation to a Blasius profile at, say, 5δ upstream of the trailing edge.
- (3) Avoid disturbed boundary layer, except for well-documented, artificially induced disturbances which may conceivably be useful for time-dependent methods.

c) Free-Stream Turbulence:

- (1) If the initial boundary layer is turbulent, free-stream "turbulence" is not likely to be important if less than 0.5%, with the possible exception of coupling with acoustic modes and instabilities of mixing layer.
- (2) If the initial boundary layer is laminar, transition in the free-shear layer may be affected by free-stream turbulence.

d) Definition of Trailing Edge-Geometry:

- (1) For a one-stream case, there is no difference with or without an end plate.
- (2) For a two-stream case, a maximum included angle of 3° for a trailing edge with a resulting trailing-edge thickness being an order of magnitude less than the boundary-layer momentum thickness.

2. Axi-Symmetric Case

The computations should be limited to $x < 2D$, if the object is to simulate a planar mixing layer; D is the nozzle exit diameter. The initial boundary-layer momentum thickness should be at least two orders of magnitude less than the diameter of the jet nozzle to allow full development before the onset of "axisymmetry" effects at $x \approx 2D$.

AD-HOC COMMITTEE NO. 4

Report of the Working Group on
Turbulence Management and Control of Large-Eddy Structure

Chairman: H. Nagib
Recorder: R. Westphal

Members:	S. Bogdonoff	P. Klebanoff
	D. Bushnell	J. LaRue
	F. Champagne	T. Morel
	J. Eaton	V. Sandborn
	J. Ferziger	I. Wygnanski
	J. Gerrard	

In view of recent successful attempts at manipulation of the turbulence structure in flow fields of technological importance, the above group met to discuss the possible influence of the results of the 1980-81 Conference and these experiments on large-eddy structure control. Examples of this research in management and control of large-scale turbulence structures are found in free-shear layers, as well as in wall boundary layers; their possible applications range from enhanced mixing to augmentation of heat transfer to reduction in surface drag.

The group recommends that the advanced computer-prediction schemes be tested for their sensitivity to the initial conditions for some of the above cases, e.g., shear layers with controlled initial excitation or boundary layers with flow manipulators for removing the large-scale structures. In particular, it is suggested that the variability of the downstream evolution of the mean flow and the turbulence intensities be predicted for a range of initial conditions which depart from the equilibrium cases and are representative of some of the successful experiments. Since most of these flow-manipulation techniques depend on modifications of the spectral distribution of turbulent energy, a more detailed description of the initial conditions, including spectral data, will be required.



H. Nagib

CLOSING DISCUSSION

The Chairmen of the Ad-Hoc Committees and each Session Chairman presented their reports, and this was followed by the closing discussion on Ad-Hoc Committees and Sessions I through XII.

REPORTS FROM AD-HOC COMMITTEES

Ad-Hoc Committee No. 1--Hot-Wire Anemometry at Low Mach Numbers

B. Newman reported the results of the committee meeting on hot-wire uncertainties at low Mach numbers and a comparison of laser and hot-wire performance.

Questions:

P. Bradshaw: Why do we not use pure platinum wires?

B. Newman: They lack strength.

P. Bradshaw: Does the lack of a continuous signal in air with an LDV preclude some spectral measurements?

F. Durst: It depends on the frequencies of interest.

Ad-Hoc Committee No. 2--Use of Hot-Wire Anemometers in Compressible Flows

E. Reshotko reported on the discussion concerning the use of hot wires in transonic/supersonic flows. He noted the need for very high frequency response, and that the available calibration methods are questionable for sheared flows. An LDA gives little temperature/density information, so continued hot-wire use is recommended.

Questions:

M. Morkovin: Noted the existence of large scatter of hot-wire data at high Mach numbers, particularly in the transonic range. He also said the derivation of the calibration method involves assumptions which make these measurements very uncertain.

C. Horstman: 15% uncertainty would be good here for any hot wire data.

Ad-Hoc Committee No. 3--Free-Shear Layers

H. Nagib reported the discussions regarding the initial conditions for free-shear layer experiments and computation. The extreme sensitivity of free-shear layers to disturbances in the initial region was once again noted.*

Questions:

B. Cantwell: Could the channel be divergent to compensate for pressure effects?

P. Bradshaw: $\partial F/\partial x$ would be small for large channels anyway.

B. Ramaprian: How may a good future experiment be set up?

J. Eaton: How was $Re_\theta = 500$ chosen?

P. Bradshaw: From Coles' wake-parameter curve.

*[Ed.: See also the conclusions to this volume.]

S. Luxton: The Committee is trying to give a general guide, although the conclusions are not well documented.

S. Kline: A minimum R_θ of 1000 would be better!

P. Bradshaw: Low R_θ is needed for rapid development.

Ad-Hoc Committee No. 4--Turbulence Management and Control of Large-Eddy Structure

The report of this ad-hoc committee was received but there was no further discussion.

REPORTS FROM SESSION CHAIRMEN

Reports from Sessions I, II, III, VII, and XII were received but invoked no further comment from the Conference.

Session IV - W. C. Reynolds, Chairman

The laminar-flow numerical checks have been withdrawn; instead computers will be asked to demonstrate mesh-independence by using two different grids. Specifications for Case 0111 will be altered.

Questions:

J. Murphy: How should code set-up be documented?

S. Kline: The Evaluating Committee has yet to decide if more information than that in the Questionnaire will be needed. We will rely on feedback from the Evaluation Committee and the two teams on "numerics." See also discussion in Session IV.*

W. McNally: Computers may not be able to double their grid density.

W. Reynolds: Grid density can always be halved.

G. Lilley: Does Dr. Gessner propose changes to his specifications?

F. Gessner: Yes.

Session V - A. Roshko, Chairman

The circular cylinder has been recommended as an entry test case, for which a complete (non-elliptic) calculation will be requested. Ellipsoid data are high-quality but are limited in extent--only centerplane data are available. Also, pressure data and total drag are needed for the ellipsoid. Hence the ellipsoid should be retained in the data bank but is not emphasized for computation at this time. Diffuser flows might all be optionally computed as boundary-layer flow only if desired. The Samuel-Joubert data should be considered as a boundary layer.†

*[Ed.: This reply has been extended in editing for clarity.]

†[Ed.: The Samuel-Joubert flow is listed as a simple case (boundary-layer flow). Diffuser flows can be calculated as computers desire or their codes dictate; that is, as fields or as boundary layers. In no case is the method of computation (field or zonal) specified for the 1981 meeting. Indeed, we hope that both approaches will be used so that we can obtain direct comparisons for evaluation.]

Questions:

- G. Lilley: Was the Wadcock flow discussed?
- A. Roshko: Yes! A. Wadcock may improve the specification of wall conditions.
- P. Saffman: One should not distinguish steady and unsteady turbulent flows--computers can consider the flow as they wish.
- J. Hunt: Why do some data sets not have unsteady data?*
- G. Mellor: Unsteadiness may be unambiguously defined.*
- A. Perry: Phase-averaged flows are difficult to specify and must be operationally specified.
- J. Johnston: Simpson's case is not the only diffuser case; Ashjaee's data do not have turbulence but could be useful.
- S. Kline: I will not recommend Ashjaee's diffuser data since they are our own data, and the data evaluator has not included them.

Session VI - E. Reshotko, Chairman

Complete geometry and initial conditions will be provided, but no downstream conditions for the predictive cases. Technical oversight of predictive cases will be provided and is being arranged.

- J. Hunt: Complete hardware and geometry must be specified.
- J. Kim: Elliptic codes need downstream data for backstep.
- P. Bradshaw: There is no upstream influence in the backstep!
- W. Reynolds: A status report on each predictive case should be maintained.
- J. Eaton: Reports are planned, but even if some predictive data are not obtained computations may be compared.

Session VIII - H. Nagib, Chairman

- P. Saffman: The flows presented by J. Ferziger are not really homogeneous flows, so actual wind-tunnel conditions would be desired.
- J. Ferziger: The recent data are very nearly homogeneous, but many cases have actual conditions documented.
- R. Narasimha: Self-similarity should not be an input to the calculation for wall jets; this should come out of the computation.

*[Editor's note regarding unsteadiness: Many cases involve a request for computation of fluctuations; that is, turbulence and implicitly unsteadiness owing to shocks or flow detachment. As a means of defining a manageable domain for evaluation, flows with unsteady mainstreams have been omitted from this conference. As noted elsewhere, L. Carr and J. McCroskey are tabulating unsteady flows, and they might profitably be addressed in another meeting.]

Sessions IX, X - S. Bogdonoff and J. McCroskey, Chairmen

Measurements for high-speed flows, especially wall-skin friction, are highly uncertain. However, the trends are reliable and the data should be useful in judging computer results.

M. Morkovin: A clear distinction between the accuracy of data in low- and high-speed flow is necessary and should be flagged.

S. Bogdonoff: High-speed flows give a better test of turbulence models in some cases and are very important for this reason and also technologically.

S. Kline: Highly uncertain data will not provide a good test for turbulence models.

J. McCroskey: Skin-friction uncertainty in high-speed flows has been over-emphasized.

S. Kline: This may well be so. Nevertheless, the relatively large uncertainty of high-speed data should be flagged as Morkovin recommends.

Session XI - P. Bradshaw, Chairman

The CAST 7 case has been discarded.

MISCELLANEOUS TOPICS

Evaluation Committee - H. W. Emmons, Chairman

G. Lilley read H. W. Emmons' report (see below) and asked for comment.

Questions:

W. Reynolds: Model constants should be allowed to change via computer algorithm, as long as the computer himself does not subjectively modify constants.*

G. Lilley: The Evaluation Committee recommends that model constants must not be changed in different flow situations.

S. Kline: Evaluators should put priorities on flows of the same class to aid computers.

W. Reynolds: The timing of the meeting should be discussed.

*[Ed.: This point is covered by the existing Questionnaire which is to be filed by computers disclosing methods.]

REPORT OF THE EVALUATION COMMITTEE TO THE 1980 MEETING*

Chairman: H. W. Emmons

The problems presented by turbulent flows are numerous, as we have seen. It is questionable if many, if any, computing methods exist which are universal in the sense that one method can solve all problems (a change of anything, even a single constant, by the computer constitutes a change of method).

We do not expect to give a single rating for all methods because methods designed for different purposes will be difficult or impossible to compare.

We therefore expect to rate the methods in various classes and for various purposes. I hope that it will be possible for the Evaluation Committee to suggest which types of methods are the most promising approach to become a universal code some time in the (distant ?) future.

We request that the evaluators carefully review the number of plots they specify in their "Specifications." If these can be reduced in number to only those plots which bring out the essential features of the complex nature of the flows, this will help the Evaluation Committee enormously.

We hope to examine the numerical techniques and the physics of the submitted methods to help with our evaluations. It is clear that a method that is used on many cases will provide better information for evaluation than a method used on only one.

From the above plans, it is clear that we will be able to do a better job of evaluation if computations are submitted as soon as completed, rather than all coming in on July 15th 1981.

*[Ed.: This report is preliminary to the Final Report of the Evaluation Committee and is intended as input for the Organizing Committee and for computers. The Final Report will appear in the Proceedings of the 1981 Meeting.]

SESSION XIV

Chairman: G. Sovran

Technical Recorders:

R. Jayaraman
G. M. Lilley



(J. Lumley)

Plans for 1981 and Beyond

Minutes of Session XIV

The Chairman opened the meeting by stating that the purpose of the session was to receive opinions regarding the 1980 conference and suggestions regarding the 1981 conference for consideration by the Evaluation and Organizing Committees. He stated that the major problems for 1981 were the procedure for comparing computational results with the experimental data and the need for complete, effective disclosure of computing methods and programs. He posed the following questions as a start to this discussion:

I. Complete Disclosure of Computational Method

1. Are there any important pieces of information commonly missing from published descriptions of computational methods?
2. Are sufficient details (on initial and boundary conditions, etc.) usually given with respect to a particular calculation that it can be replicated by another computer?
3. What are some specific ideas for formalizing a procedure to achieve complete disclosure of the significant factors involved in a particular method and computation?

II. Questionnaire (for computers to file as disclosure of method)

1. What type of additional questions would you like to ask about someone else's method?
2. What computer-influences will not be identified by the present questionnaire, if any?
3. What specific suggestions do you have for improving the questionnaire?

III. Evaluation Process

1. How important are numerics in computational methods for complex turbulent flows?
2. What elements of computer technique (e.g., choice of mesh size, wall functions) are there that can influence the output from a code, and for what types of flows are they most significant?
3. What type(s) of evaluation is (are) possible/feasible for turbulent computational methods?

IV. System Checkout

1. For what flow will you volunteer to do a complete computation, using data from the magtape file, to check out the mechanics of the system?

Bradshaw: I wish to report a suggestion on a possible numerical accuracy check on behalf of Dennis Bushnell. It appears to be accepted that the numerical-accuracy and turbulence-modeling problems are interrelated, especially for elliptic flows. Simple partial checks such as mesh refinement are not necessarily definitive; for example, mesh refinement might not check the influence of boundary condition treatment.

Therefore, as a suggestion, predictors should all use the same turbulence model (and constants) for several test cases, mostly elliptic ones. The turbulence model specified might be the k- ϵ or the three-equation model, either with wall functions or computed directly to the wall. Grid-resolution and boundary-condition treatment, etc., would be required for each case and should be determined by the predictors for their individual numerical approaches. The intent is to provide empirical checks of the numerical approach as a whole, where some of the major influences of turbulence-model inclusion, such as steep wall gradients are included.

W. Reynolds: Is the suggestion that all computers use the same model for one problem, so that the differences in the results would be due to the numerical methods used?

G. Sovran: Yes.

J. Murphy: I suggest that the mixing-length model is the one to be used.

J. Johnston: I agree with Murphy that a model using a mixing-length distribution be used, since otherwise many computers using only these models will be excluded.

R. Melnik: We want to show that a method using given turbulence models is consistent in itself. The computer should demonstrate by refining the mesh that his numerics are independent of the mesh size, i.e., by using two grids. I suggest that the Organizing Committee clarify what is required from computers in the way of numerical checks.

D. Wilcox: Something like Bushnell's suggestion was raised at an earlier session by Saffman, but was discarded, since in many cases it would involve writing new codes.

G. Sovran: There are two questions: (a) would an inordinate amount of time be involved in making the checks, and (b) even if done, would they prove anything?

P. Bradshaw: Speaking for Bushnell, not all computers would be required to do these checks. If just some of them, representing a range of methods, do these checks, then our purposes will be served. I feel that it will be necessary to use a complicated model rather than a mixing-length model.

G. Lilley: I wish to present to the meeting some matters which arose out of the discussions in the Evaluation Committee. It is hoped these matters will receive comments from attendees at the meeting:

1. Did your method conserve mass, momentum, energy precisely or only approximately (some numerical methods introduce small errors)?
2. Give CPU time, total run time, bits of storage required, digits (bits) used (double-precision?), machine used for each case submitted.
3. Does your performance in some simple case look poor because your code is more general and powerful than required for this case?
4. Computers should rate the test cases they submit in the order of difficulty.

W. Reynolds: I hope that what is implied in the questions above is performance in terms of computer time rather than the physics.

G. Lilley: Yes.

G. Mellor: I wonder if CPU time is a relevant criterion in a scientific evaluation.

G. Sovran: This brings in the engineering versus the scientific aspects of computations, and there are developers of codes who intentionally sacrifice accuracy for shorter running times.

G. Mellor: It appears we need to carefully calibrate different computers in judging performance of codes in terms of CPU time.

T. Morel: CPU time comparisons may not be straightforward in elliptic computations where convergence depends upon how close to the final solution the initial trial is.

G. Sovran: In summarizing this part of the discussion, it appears that computers are not in agreement with the proposal of Bushnell.

W. Reynolds: I suggest that it might be possible to perform some useful numerical checks as course work at Stanford.

G. Sovran: I note there is agreement that such a proposal is very desirable and it is hoped that the Organizing Committee will make the necessary arrangements. Another aspect of numerics is that concerning the solution of elliptic flow problems. I understand that McDonald has prepared a statement on this matter.

The main points from a Prepared Report by H. McDonald are as follows: Turbulent Flow Predictions--Evaluation of State of the Art, 1980-81--Flow Predictions Involving Numerical Solution of Elliptic Partial Differential Equations

Background

- Advanced turbulence models for complex or recirculating flows have been and are being developed.
- Evaluation of the predictive capacity of such turbulence models eventually requires a mean flow prediction of the complex shear flow involved.
- In making this type of turbulence model evaluation, numerical error must be at a known, acceptable, unimportant level.

- In 1968 Stanford Conference solution of ODE systems used off-the-shelf numerics to produce accurate numerical solutions to posed problems with negligible computer resources. Numerical accuracy of the finite-difference schemes employed was unquestioned. Numerics were not an issue in 1968.
- In the 1980s, off-the-shelf numerics for complex shear flows are not yet available. Obtaining the desired (required?) numerically accurate solutions to the posed system of nonlinear partial differential equations may be a difficult problem, requiring significant research and development in itself. Hence numerics are an issue in the 80s, so that turbulence models will not be inappropriately maligned.
- A prediction constitutes a combination of governing equations (including boundary conditions)--turbulence model--and (numerical) solution procedure.
- Allocation of blame/credit to constitutive components for failure/achievement to predict flow field requires consideration of all three components (together with data uncertainty band).
- Numerical sources of error must be negligible or tolerable to remove this component from consideration.
- Governing equations and boundary conditions are often standard and noncontroversial, and in many cases the data not suspect; hence error can be ascribed to a turbulence model only after removal of numerical solution methodology (including approximations to boundary conditions) as a source of error.

Reservations

Experience has shown that

- User operational skill and familiarity (or lack of it) with numerical methods can significantly contribute to (or detract from) results obtained. Hence inappropriate inferences concerning turbulence models have sometimes been drawn.
- Non-standard numerical methodology has often been used and has often been inadequately described (or tested?) to permit evaluation. Hence an inability to allocate the source of discrepancy between prediction and measurement occurs.
- Potential and encountered numerical problems of major significance are not always apparent from predictions. Comparison with data are not necessarily the sole evaluation criterion.

Is It Important to Have a "Good" Numerical Algorithm?

- Traditional view--ends justify means. Approximations are introduced to permit a solution to a difficult problem. Algorithm is part of means--hence unimportant.
- Experience shows that inappropriate or misused numerical algorithms or approximations can result in an erroneous trend.

- As a result of inappropriate or misused algorithms, solutions contain significant numerical errors contributing either favorably or unfavorably to the predictive agreement and/or convergence rate. Thus the evaluation is contaminated.
- It may not be possible to reduce the numerical errors to insignificance with reasonable computer resources (how defined?) with the chosen algorithm for this particular problem or category of problems.
- The user community may not be interested in means--the research community ought to be. A knowledge and appreciation of the means would seem a prerequisite to any realistic assessment. In this way the user community will be alerted to probable limitations, and undue optimism and disappointments minimized.

"User Operational Skill with Numerical Methods Can Contribute to Results Obtained"

- However, problems with numerics might not be discernible in predictions because
 - Numerical error can masquerade as physics and be compensated out, but this may produce an incorrect parametric dependence.
 - Boundary and initial condition selection can hold solution "in place" but be unrealistic for user.
 - Good initial guess--limited iterations hold solution "in place." Poor convergence (divergence?) not noticed.
 - Coarse mesh makes calculation feasible yet solution may not be mesh-independent. Large error--slow decrease with mesh size--often mistaken for mesh independence.
- If numerical problems are not discernible in predictions, are they important?

Since the Quality of the Numerics Is Important, Can the Quality of the Numerics Be Assessed?

To a degree, yes, but ...

- Standard numerical tests on a model problem are necessary but not sufficient. Real problems might introduce sufficient differences to raise additional questions.
- Numerical algorithm often very complex, non-standard, and incompletely described. One cannot assess the algorithm without a very complete statement of what is done, what boundary conditions are applied, how implemented, and how sensitive the solution is to key numerical approximations.
- Danger of "I've tried that and it didn't work ..." due to a sensitivity to detail. Prior experience may or may not be relevant.

CONCLUDING REMARKS

- For these complex turbulent flow predictions numerical error levels must be known and acceptable to permit turbulence model and predictive accuracy to be correctly evaluated.
- Labor to make the assessment of the possible or probable level of numerical errors and to provide supporting evidence for Stanford '81 may be overwhelming.
- Even without such assurance Stanford '81 could result in a more widespread recognition and consequent exposure of the numerical methodology (with appropriate validation) in the technical literature (and a consequent reduction in the number of malignant turbulence models!)

P. Bradshaw: Is McDonald suggesting checks are unnecessary?

H. McDonald: What I am suggesting is that the numerical analyst will make his own checks. Even with full disclosure a computer may not know how sensitive his method is to some of the approximations. Hence there will be some constraints on what can be asked from computers for the 1981 Conference.

P. Bradshaw: We are developing codes for the engineering community and it is necessary for us to separate the effects of numerics from the inaccuracies of the turbulence models.

G. Mellor: Each computer will be making a large number of checks on his method to satisfy himself of its accuracy. (He added that these checks will take a long time, so is 1981 too soon for the next conference?)

S. Kline: The 1981 meeting is currently planned for September 14-18, 1981, but could be delayed until Christmas 1981 or June 1982.

B. Launder: I wish to remind the meeting that about 50 prospective computers have already replied to Professor Kline and expressed the desire to compute most flows and that they expect to complete these in time for the July deadline for the September 1981 Conference. Also, even if only half the cases are completed these will still present a difficult task for evaluation.

G. Sovran: (Asked for a show of hands. There were 16 who said they could meet the July 1981 deadline; none reported that they could not meet the July 1981 deadline; of the 16, 4 stated they would prefer a later date for the proposed September 1981 Conference).

Several discussors (Kline, Reynolds, Launder): Felt that just as the Data Library would be an ongoing program, the resulting evaluation might well be regarded similarly. That is, the 1981 meeting (unlike 1968) will not largely finish the task. It can and hopefully will provide a snapshot of the state of the art and thereby clarify both status for users and profitable avenues of further researches.

E. Reshotko: The numerical evaluation of codes is very similar to the evaluation of experiments. I wonder if they could be tested in a way analogous to that of Moffat's Uncertainty Analysis.

P. Saffman: I suggest that the codes be tested for different sensitivities.

W. Rodi: This is automatically done when the same code (like TEACH) is used for different problems.

Editor's Note:

As a result of this and other discussions during the meeting concerning checks on numerics, two actions have been planned regarding numerical checks for the 1981 meeting.

1. Computers will be asked to do a halving of mesh size or, if halving is not possible, to do a doubling, and in either case to report the results (if possible on central cases to give dense results for comparison).
2. Two groups of computers will specifically study problems of numerics: one group will be coordinated by B. E. Launder and W. Rodi at Manchester and Karlsruhe; the other group will be coordinated by J. Ferziger, J. Steger, and W. Reynolds at Stanford. The Launder/Rodi group will produce results for a common (probably $k-\epsilon$) model using various numerics. Ferziger et al. may do similar work, but will also study results and disclosures as received to generate further ideas re numerical checks if possible. B. E. Launder will coordinate overall for the Organizing Committee.

These steps on checking numerics are seen by the Organizing Committee as less than what is desired (needed?), but as the best that current knowledge can suggest. The problem of numerics is of great importance and will be given serious ongoing consideration as results are accumulated. As on other problems arising from the work of the Conference, we expect that considerable learning will occur before the end of the 1981 meeting. Suggestions on this topic will be welcome.

S. Birch and W. Reynolds: Computers will need to fully understand their codes so that they can fully disclose their methods during the coming year.

B. Launder: All details of wall matching must be completely reported.

S. Kline: Will Brian Launder please look carefully into this aspect of the Questionnaire and add specific questions on wall matching?

J. Hunt: The Questionnaire does not address methods other than Reynolds transport equation methods.

G. Sovran: Will Prof. Hunt propose some specific questions on these additional methods which can be incorporated in the Questionnaire?

G. Sovran: On another topic, we would appreciate volunteers who will try some of these flows at an early stage so any problems that arise can be clarified for the rest of the computers.

The following volunteered:

Bradshaw: All the boundary layer cases, Flows 0210, 0240, 0620, 0630.

Dvorak: Separated airfoil, Flow 0440.

Rodi: Boundary layers with wall curvature, Flow 0230. and wall jets, Flow 0260.

Wilcox: Boundary-layer cases, compressible C_f variation with Mach number and wall temperature, three-dimensional boundary layers, Flows 0250, 0810, 0820.

Murphy: Flows presented by Simpson, Flows 0140, 0430.

Cook/Firmin: Transonic airfoil, Flow 0862.

Rodi: Square duct (Gessner), Flow 0110.

S. Kline: Stated that the first package of flow cases will be dispatched in late November 1980. He expressed the hope that the volunteers would submit the results of these trials as soon as possible.

S. Kline closed the conference with a vote of thanks for the hard work of essentially all the attendees at the 1980 meeting.

CONCLUSIONS

- (1) The 1980 Meeting of the AFOSR-HTTM 1980-81 Stanford Conference was a cooperative effort of a large fraction of the experimental fluid mechanics research community aimed at reaching a consensus concerning:

"what currently available experimental data for turbulent flows are sufficiently trustworthy to be used as inputs to turbulence modeling, and/or a basis for standard 'trials' for checking outputs from computations?"

The Conference is best viewed as a learning process, a way of accelerating understanding and research progress.

- (2) The meeting demonstrated that increased interaction is needed between computers and experimentalists in fluid mechanics to close the loop iteratively between experiment and computation, and thereby speed progress. The framework provided by the paper on "Uncertainty Analysis" can inform this process, and is strongly recommended for use.
- (3) The Working Groups and general discussion at the 1980 Meeting highlighted many problems of present concern in experimental fluid mechanics. Among those discussed were
 - (i) the accuracy of hot-wire measurements in subsonic, transonic, and supersonic flows, and the need for redundancy checks for laser-doppler anemometers;
 - (ii) uncertainty analysis for skin-friction measurements with Preston tubes in complex turbulent flows;
 - (iii) whether shock waves are ever truly steady even in weakly turbulent interacting flows, or whether some high-speed jitter is always present. If high-speed jitter exists, what are the resulting effects on the turbulence structure and the overall characteristics of the flow?
- (4) Although the 1980 Meeting confirmed that many good data sets are available, more data sets of high quality are required particularly for very complex turbulent flows. Redundant data sets, redundant measurements, and improved checks on experimental control are also required.
- (5) The 1980 Meeting of the Conference made recommendations concerning:
 - (i) the planning of record experiments for turbulence modeling and checking of computations;
 - (ii) improved care needed in setting up the initial and boundary conditions of record experiments;

- (iii) the improved use of uncertainty analysis through appropriate feedback checks at various stages of experimental work.

This use of uncertainty analysis is particularly important in compressible flow experiments, not only because they are more expensive and difficult to perform, but also because there is less "clear consensus" on trustworthy instrumentation and the resulting data. This suggests careful preplanning and cross-checking of compressible flow data, as well as the use of uncertainty analysis in appropriate feedback modes. (See also comment by S. J. Kline on Discussion of Flows 8610, 8630, and 8640.)

- (6) All of us who were privileged to participate in the 1980 Meeting know that CFD is an active and expanding branch of fluid dynamics. The "state of the art" in 1981 will be out of date relatively soon. Nevertheless, we believe the 1980-81 Conference will delineate the state of the art in turbulence models and numerical procedures and thereby help in directing future research. This work again emphasizes that progress in complex turbulent flow analysis and prediction is vitally dependent on a sound and expanding Data Base. The data library created through the 1980 Meeting should provide a current data base and a mechanism for future expansion.

LIST OF PARTICIPANTS, 1980 MEETING ON DATA

<u>No. in Photo</u>	<u>Name</u>	<u>Affiliation or Address</u>	<u>Tasks</u>
B.41	Dr. Mukund Acharya	Fluid Mechanics Group Brown, Boveri & Company, Ltd. CH-5405 Baden-Dättwil SWITZERLAND	Data Eval.
B.2	Mr. Eric W. Adams	Mech. Eng. Department Stanford University Stanford, CA 94305	Aide; Tech. Rec.
A.30	Mr. Bahram Afshari	Mech. Eng. Department Stanford University Stanford, CA 94305	Aide; Tech. Rec.
R.40	Dr. W. T. Ashurst	Sandia Laboratories Livermore, CA 94550	Computer
	Mr. Harry Bailey	NASA-Ames Research Center Mail Stop 202 ¹ -1 Moffett Field, CA 94035	Computer
A.19	Mr. Jorge Bardina	Mech. Eng. Department Stanford University Stanford, CA 94305	Aide
A.13	Mr. Juan G. Bardina	Mech. Eng. Department Stanford University Stanford, CA 94305	Aide
	Dr. P. Bearman	Dept. of Aeronautics Imperial College Prince Consort Road London SW7 2BY, ENGLAND	Review Comm.
	Dr. Claude Beguier	Inst. de Mécanique Statistique de la Turbulence 13, avenue du Général Leclerc Marseille 13003, FRANCE	Computer; Data Taker
	Dr. Muriel Y. Bergman	NASA-Ames Research Center Mail Stop 229-1 Moffett Field, CA 94035	Computer
B.30	Dr. Claude Berner	Aerospace & Mech. Eng. Dept. The University of Arizona Tucson, AZ 85721	Discussor
A.50	Dr. Stanley F. Birch	Org. L-7150, Mail Stop 41-52 Boeing Military Airplane Co. P. O. Box 3999 Seattle, WA 98124	Data Eval.
B.23	Prof. S. M. Bogdonoff	Dept. of Aeronaut./Mech. Eng. Princeton University Princeton, NJ 08544	Chairman
A.78	Prof. Peter Bradshaw	Aeronautics Department Imperial College Prince Consort Road London, SW7 2BY, ENGLAND	Org. Comm.; Chairman; Rev. Comm. Chairman; Data Eval.; Data Taker

<u>No. in Photo</u>	<u>Name</u>	<u>Affiliation or Address</u>	<u>Tasks</u>
A.25	Mr. Guenter Brune	Boeing Military Airplane Co. P. O. Box 3707, Mail Stop 3N-29 Seattle, WA 98124	Discussor
A.39	Dr. Dennis Bushnell	NASA-Langley Research Center Hampton, VA 23665	Discussor
A.8	Prof. Brian Cantwell	Aero & Astro Department Stanford University Stanford, CA 94305	Org. Comm.; Supervisor Data Library; Data Eval.
A.31	Mr. Robert Carella	Aero & Astro Department Stanford University Stanford, CA 94305	Aide; Tech. Rec.; Data Entry
B.20	Dr. Lawrence W. Carr	U.S. Army Aeromechanics Lab. NASA-Ames Research Center Mail Stop 215-1 Moffett Field, CA 94035	Chairman; Discussor; Data Eval.
A.35	Dr. Ian P. Castro	Dept. of Mech. Eng. University of Surrey, Guildford Surrey, GU2 5XH, ENGLAND	Review Comm.; Tech. Rec.
B.28	Prof. F. H. Champagne	Aerosp. & Mech. Eng. Dept. University of Arizona Tucson, AZ 85721	Special Comm.
	Dr. Dean R. Chapman	NASA-Ames Research Center Mail Stop 200-4 Moffett Field, CA 94035	Eval. Comm.; Discussor
A.7	Prof. R. Chevray	Dept. of Mechanics State University of New York Stony Brook, NY 11790	Computer; Data Taker
A.4	Prof. M. Childs	Dept. of Mech. Eng. University of Washington Seattle, WA 98105	Discussor
A.16	Mr. Robert Childs	Mech. Eng. Department Stanford University Stanford, CA 94305	Aide; Tech. Rec.
A.27	Dr. Thomas J. Coakley	NASA-Ames Research Center Mail Stop 229-1 Moffett Field, CA 94035	Computer
B.25	Dr. David J. Cockrell	Department of Engineering The University Leicester, LE1 7RH, ENGLAND	Tech. Rec.; Tech. Reviews
A.2	Prof. Donald Coles	GALCIT 321 Guggenheim Laboratory Calif. Inst. of Technology Pasadena, CA 91125	Data Eval.;
A.82	Dr. J. Cousteix	CERT/DERAT 2, avenue Edouard Belin Complex Aerospatiale, B.P. 4025 31055 Toulouse, FRANCE	Review Comm.

<u>No. in Photo</u>	<u>Name</u>	<u>Affiliation or Address</u>	<u>Tasks</u>
B.5	Mr. Andrew D. Cutler	Mech. Eng. Department Stanford University Stanford, CA 94305	Aide; Tech. Rec.
A.58	Dr. R. B. Dean	Atkins Research & Development Woodcote Grove, Ashley Road Epsom, Surrey, KT18 5BW, ENGLAND	Data Eval.
B.42	Dr. Antony Demetriades	Dept. of Mech. Eng. 220 Roberts Montana State University Bozeman, MT 59717	Special Comm.
A.54	Mr. Pius Drescher	Brown Boveri & Company, Ltd. Dept. TX CH-5401, Baden-Dättwil SWITZERLAND	Data Eval.
B.48	Prof. Franz Durst	Sonderforschungsbereich 80 Universität Karlsruhe Kaiserstrasse 12 D 75 Karlsruhe 1, WEST GERMANY	Review Comm.
A.75	Dr. F. A. Dvorak	President & Dir. of Research Analytical Methods, Inc. 100-116th Avenue S. E. Bellevue, WA 98004	Tech. Rec.; Computer; Discussor
B.49	Prof. John Eaton	Mech. Eng. Department Stanford University Stanford, CA 94305	Host Comm.; Data Eval.; Coord: Aides
B.9	Ms. Pam Eibeck	Mech. Eng. Department Stanford University Stanford, CA 94305	Aide; Tech. Rec.
B.29	Prof. H. W. Emmons	Room 308, Pierce Hall Harvard University Cambridge, MA 02138	Chairman, Eval. Comm.
A.26	Prof. Torstein K. Fanneløp	Div. of Aero & Gas Dynamics Norges Tekniske Høgskole Høgskoleringen 1 N 7034 Trondheim, NORWAY	Data Taker
	Prof. A. Favre	Inst. de Mécanique Statistique de la Turbulence 13, avenue du Général Leclerc Marseille 13003, FRANCE	Computer; Data Taker
	Mr. Bill Feiereisen	Mech. Eng. Department Stanford University Stanford, CA 94305	Aide
A.11	Prof. H. Fernholz	Herman-Fottinger Institut für Thermo- und Fluidodynamik Technische Universität D-1000 Berlin 12, WEST GERMANY	Data Taker
B.26	Prof. Joel Ferziger	Mech. Eng. Department Stanford University Stanford, CA 94305	Host Comm.; Data Eval.

<u>No. in Photo</u>	<u>Name</u>	<u>Affiliation or Address</u>	<u>Tasks</u>
B.33	Dr. Anthony W. Fiore	AFWAL/FIMG Aeromech. Division Flight Dynamics Laboratory Wright-Patterson AFB, OH 45433	Discussor
B.11	Mr. M. C. P. Firmin	Aerodynamics Department Royal Aircraft Establishment Farnborough, Hampshire GU14 6TD, ENGLAND	Discussor
A.15	Mr. Mauricio N. Frota	Mech. Eng. Department Stanford University Stanford, CA 94305	Aide
A.6	Prof. Jack H. Gerrard	Dept. of Mechs. of Fluids University of Manchester Manchester M13 9PL, ENGLAND	Tech. Rec.; Rev. Comm.
A.9	Prof. Fred Gessner	Dept. of Mech. Eng., FU-10 University of Washington Seattle, WA 98195	Data Eval.; Rev. Comm.
A.3	Prof. Isaac Greber	Dept. of Mech. & Aerosp. Eng. Case Western Reserve University Cleveland, OH 44106	Discussor
A.40	Dr. K. Hanjalić	Masinski fakultet Omladinsko Setaliste 71000 Sarajevo, YUGOSLAVIA	Computer
A.59	Dr. Robert Hantman	Mech. Branch, G.E. Company Bldg. K-1, P. O. Box 8 Schenectady, NY 12301	Tech. Rec.
A.65	Dr. H. Higuchi	NASA-Ames Research Center Mail Stop 229-1 Moffett Field, CA 94035	Discussor
	Prof. Philip G. Hill	Head, Mech. Eng. Dept. The Univ. of British Columbia Vancouver, B.C., V6T 1W5, CANADA	Eval. Comm.
B.19	Prof. S. Honami	Science Univ. of Tokyo Kagurazaka, Sinju-ku Tokyo, 162, JAPAN	Data Eval.; Pictorial Summ.
B.12	Dr. C. C. Horstman	NASA-Ames Research Center Mail Stop 229-1 Moffett Field, CA 94035	Data Eval.
B.10	Dr. Thomas T. Huang	Code 1552 David Taylor Naval Ship R & D Bethesda, MD 20084	Discussor
A.1	Dr. J. A. C. Humphrey	Dept. of Mech. Eng. University of California Berkeley, CA 94720	Tech. Rec.; Data Taker
A.76	Mr. D. A. Humphreys	Aerodynamics Dept. Aeronaut. Res. Inst. of Sweden P. O. Box 11021 S-161 11 Bromma, SWEDEN	Data Eval.; Discussor

<u>No. in Photo</u>	<u>Name</u>	<u>Affiliation or Address</u>	<u>Tasks</u>
A.55	Dr. Ching Hung	NASA-Ames Research Center Mail Stop 202A-1 Moffett Field, CA 94035	Computer
A.47	Mr. Julian C. R. Hunt	CIRES University of Colorado Boulder, CO 80309	Discussor
B.31	Prof. A. K. M. F. Hussain	Dept. of Mech. Eng. University of Houston Houston, TX 77004	Tech. Rec.; Discussor
A.71	Dr. Kuneo Iribu	Mech. Eng. Dept. University of Ryukyus Tonokura-cho, Naha Okinawa, JAPAN	Discussor
A.34	M. Ramesh Jayaraman	Mech. Eng. Department Stanford University Stanford, CA 94305	Aide
A.33	Mr. Ranga Jayaraman	Mech. Eng. Department Stanford University Stanford, CA 94305	Aide; Tech. Rec.
	Dr. Charles E. Jobe	AFWAL/PIMM Wright-Patterson AFB, OH 45433	Review Comm.
A.69	Dr. Dennis Johnson	NASA-Ames Research Center Mail Stop 227-8 Moffett Field, 94035	Discussor
B.14	Prof. J. P. Johnston	Mech. Eng. Department Stanford University Stanford, CA 94305	Host Comm.; Chairman; Data Eval.; Rev. Comm. Chairman
A.53	Prof. J. B. Jones	Dept. of Mech. Eng. Virginia Polytechnic Inst. Blacksburg, VA 24061	Tech. Rec.
A.52	Prof. Peter N. Joubert	Dept. of Mech. Eng. The University of Melbourne Parkville, Victoria 3052 AUSTRALIA	Tech. Rec.
	Dean William M. Kays	School of Engineering Stanford University Stanford, CA 94305	Rev. Comm.
B.45	Dr. John Kim	NASA-Ames Research Center Mail Stop 229-1 Moffett Field, CA 94035	Discussor
A.67	Mr. P. S. Klebanoff	National Bureau of Standards Room 109, Building FM Gaithersburg, MD 20760	Chairman; Data Taker
	Dr.-Ing. Armin Klein	Motoren- und Turbinen Union München GmbH D-8000 München, WEST GERMANY	Review Comm.
A.83	Prof. S. J. Kline	Mech. Eng. Department Stanford University Stanford, CA 94305	Chairman, Org. Comm.; Host Comm.; Rev. Comm. Chairman

<u>No. in Photo</u>	<u>Name</u>	<u>Affiliation or Address</u>	<u>Tasks</u>
	Mr. D. M. Kuehn	NASA-Ames Research Center Mail Stop 229-1 Moffett Field, CA 94035	Data Taker
	Dr. John LaRue	Dept. of Appl. Mech. Sci. P. O. Box 109 Univ. of California, San Diego La Jolla, CA 92037	Data Taker
A.74	Prof. Brian Launder	University of Manchester Inst. of Sci. & Tech. Mech. Eng. Dept. Sackville Street, P. O. Box 88 Manchester M60 1QD, ENGLAND	Org. Comm.; Chairman; Data Eval.; Rev. Comm. Chairman
A.45	Mr. Mario Lee	Mech. Eng. Department Stanford University Stanford, CA 94305	Aide; Tech. Rec.
B.44	Dr. Anthony Leonard	NASA-Ames Research Center Mail Stop 202A-1 Moffett Field, CA 94035	Computer
A.42	Dr. Steve Lewellen	ARAP. Inc. P. O. Box 2229 Princeton, NJ 08540	Computer
B.22	Prof. G. M. Lilley	Dept. of Aero and Astronautics University of Southampton Southampton, ENGLAND	Eval. Comm.; Tech. Rec.; Tech. Reviews
A.18	Prof. John L. Lumley	Sibley Sch. of Mech/Aero Eng. 238 Upson Hall Cornell University Ithaca, NY 14853	Chairman; Rev. Comm. Chairman
A.12	Prof. R. E. Luxton	Dept. of Mech. Eng. University of Adelaide GPO Box 498, Adelaide S. Australia 5001, AUSTRALIA	Discussor
A.23	Mr. Aristoteles Lyrto	Mech. Eng. Department Stanford University Stanford, CA 94305	Aide
B.38	Mr. Joseph G. Marvin	NASA-Ames Research Center Mail Stop 229-1 Moffett Field, CA 94035	Rev. Comm.; Gov't Monitor
	Dr. J. Mathieu	Ecole Centrale de Lyon B. P. No. 17 69130 Ecully, FRANCE	Rev. Comm.; Computer
	Dr. W. J. McCroskey	U.S. Army Aeromechanics Lab NASA-Ames Research Center Mail Stop 215-1 Moffett Field, CA 94035	Chairman; Discussor
	Dr. H. McDonald	Scientific Research Assoc. P. O. Box 498 Glastonbury, CT 06033	Computer

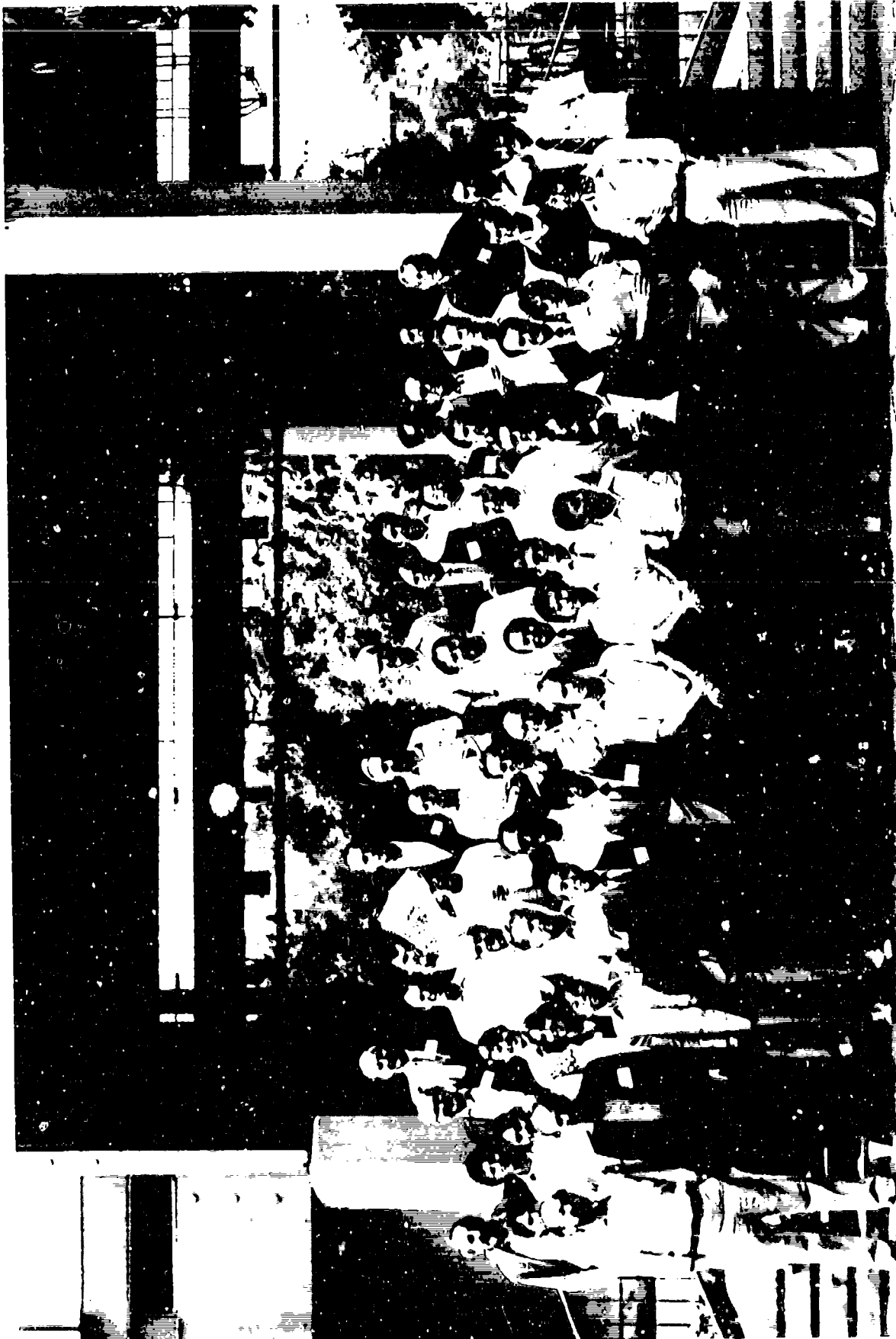
<u>No. in</u> <u>Photo</u>	<u>Name</u>	<u>Affiliation or Address</u>	<u>Tasks</u>
A.21	Dr. William D. McNally	Chief, Comp. Fluid Mech. Branch NASA-Lewis Research Center Mail Stop 5-9 Cleveland, OH 44135	Gov't Monitor
B.21	Dr. Unweel Mehta	NASA-Ames Research Center Mail Stop 202A-1 Moffett Field, CA 94035	Computer
B.13	Dr. Hans Ulrich Meier	DFVLR-AVA, Institut für Exp. Strömungsmechanik Bunsenstrasse 10 D-3400 Göttingen, WEST GERMANY	Computer; Tape Library Access
A.51	Prof. George Mellor	Geophys. Fluid Dyn. Lab. P. O. Box 308 Princeton University Princeton, NJ 08540	Rev. Comm.; Computer
B.7	Dr. R. E. Melnik	Research Dept., M/SA-08-35 Grumman Aerospace Corp. Bethpage, NY 11714	Data Eval.; Computer
B.37	Dr. H. Ha Minh	Inst. de Mécanique des Fluides 2, rue Camichel 31071 Toulouse Cedex, FRANCE	Computer
	Prof. R. J. Moffat	Mech. Eng. Department Stanford University Stanford, CA 94305	Host Comm.; Speaker
	Dr. Parviz Moin	Mech. Eng. Department Stanford University Stanford, CA 94305	Tech. Rec.
A.48	Dr. Thomas Morel	Fluid Dynamics Dept., Res. Labs. General Motors Tech. Center 12 Mile & Mound Roads Warren, MI 48090	Tech. Rec., Computer
A.14	Dr. Mark Morkovin	1104 Linden Avenue Oak Park, IL 60302	Eval. Comm.; Rev. Comm.
B.16	Mr. Alan Morse	Dept. of Mech. Eng. Imperial College London SW7 2BY, ENGLAND	Data Eval.
A.68	Prof. Hal L. Moses	Dept. of Mech. Eng. Virginia Polytechnic Inst. Blacksburg, VA 24061	Tech. Rec.; Rev. Comm.; Computer
A.38	Mr. John Murphy	NASA-Ames Research Center Mail Stop 227-8 Moffett Field, CA 94035	Computer
B.3	Prof. H. Nagib	Mech. & Aerospace Eng. Illinois Institute of Tech. Chicago, IL 60616	Tech. Rec.; Discussor
B.35	Prof. Roddam Narasimha	Dept. of Aeronautical Eng. Indian Institute of Science Bangalore 560 012 INDIA	Rev. Comm.; Computer

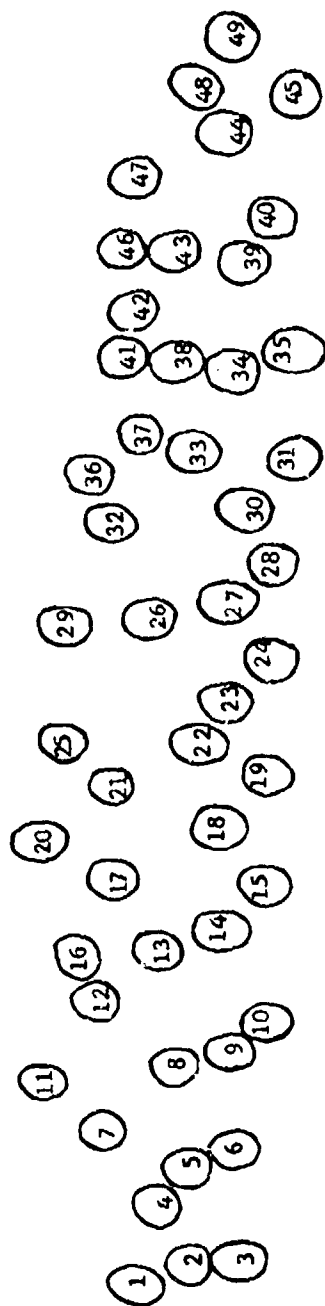
<u>No. in Photo</u>	<u>Name</u>	<u>Affiliation or Address</u>	<u>Tasks</u>
A.77	Dr. Barry G. Newman	Dept. of Mech. Eng. McGill University 817 Sherbrooke St. West Montreal, P.Q. H3A 2K6, CANADA	Rev. Comm.; Discussor
A.44	Dr. F. K. Owen	Consultant P. O. Box 1697 Palo Alto, CA 94302	Data Taker
	Prof. Pradip Parikh	Mech. Eng. Department Stanford University Stanford, CA 94305	Tech. Rec.
A.66	Prof. V. C. Patel	Iowa Inst. of Hydraulic Res. University of Iowa Iowa City, IA 52240	Chairman; Data Eval.; Rev. Comm.; Discussor
A.80	Dr. G. C. Paynter	Boeing Military Airplane Co. P. O. Box 3999, Mail Stop 4152 Seattle, WA 98124	Computer
A.79	Dr. David Peake	Sr. Research Associate NASA-Ames Research Center Mail Stop 227-8 Moffett Field, CA 94035	Data Taker
	Prof. A. E. Perry	Dept. of Mech. Eng. University of Melbourne Parkville, Victoria 3052 AUSTRALIA	Data Taker
B.34	Dr. Stuart L. Petrie	Professor and Chairman Dept. Aero. and Astronaut. Eng. The Ohio State University 2036 Neil Avenue Columbus, OH 43210	Data Taker
	Prof. Felix J. Pierce	Dept. of Mech. Eng. Virginia Polytechnic Institute Blacksburg, VA 24061	Rev. Comm.; Computer
A.41	Prof. R. H. Pletcher	Dept. of Mech. Eng. Iowa State University Ames, IA 50011	Computer
	Mr. L. G. Presley	NASA-Ames Research Center Mail Stop 227-8 Moffett Field, CA 94035	Rev. Comm.
A.22	Mr. Steve W. Pronchick	Mech. Eng. Department Stanford University Stanford, CA 94305	Aide; Tech. Rec.
A.60	Dr. Brian Quinn	ARAP, Inc. Princeton, NJ 08540	Computer
A.62	Prof. S. R. Ramaprian	Inst. of Hydraulic Res. The University of Iowa Iowa City, IA 52242	Rev. Comm.
B.47	Prof. Eli Reshotko	Dept. of Mech. & Aerosp. Eng. Case/Western Reserve Univ. Cleveland, OH 44106	Org. Comm.; Chairman; Data Eval.; Rev. Comm. Chairman

<u>No. in Photo</u>	<u>Name</u>	<u>Affiliation or Address</u>	<u>Tasks</u>
A.20	Prof. W. C. Reynolds	Mech. Eng. Department Stanford University Stanford, CA 94305	Eval. Comm.; Chairman; Host Comm.; Rev. Comm. Chairman
	Dr. P. J. Roache	4925 Kathryn Circle S.E. Albuquerque, NM 87108	Eval. Comm.; Computer
A.63	Dr. Wolfgang Rodi	Sonderforschungsbereich 80 Universität Karlsruhe Kaiserstrasse 12 D 75 Karlsruhe 1, WEST GERMANY	Data Eval.; Computer
B.6	Dr. Anatol Roshko	Guggenheim Lab. 105-50 Calif. Inst. of Technology Pasadena, CA 91125	Chairman; Rev. Comm. Chairman
A.56	Mr. Morris Rubesin	NASA-Ames Research Center Mail Stop 202A-1 Moffett Field, CA 94035	Org. Comm.; Data Eval.; Rev. Comm. Chairman
A.5	Dr. Philip G. Saffman	Appl. Math., Firestone 217-50 Calif. Inst. of Technology Pasadena, CA 91125	Discussor
B.13	Prof. V. A. Sandborn	Dept. of Civil Eng. Engineering Res. Center Colorado State University Fort Collins, CO 80521	Data Taker
A.81	Prof. Joe Schetz	Dept. of Aerosp. & Ocean Eng. Virginia Polytechnic Inst. & State University Blacksburg, VA 20461	Computer
	Dr. H. C. Seetharam	Boeing Military Airplane Co. P. O. Box 3999, Mail Stop 3N-43 Seattle, WA 98124	Data Taker
B.15	Prof. Y. Senoo	Res. Inst. of Ind. Science Kyushu University Hakozaki, Fukuoka-si 812 JAPAN	Computer
A.24	Dr. Gary S. Settles	Gas Dynamics Laboratory Forrestal Campus, Princeton Univ. Princeton, NJ 08544	Data Taker
	Mr. Terry Simon	Mech. Eng. Department Stanford University Stanford, CA 94305	Data Eval.
A.61	Prof. Roger L. Simpson	Civil & Mechanical Eng. Southern Methodist Univ. Dallas, TX 75275	Data Eval.; Rev. Comm.; Discussor
A.36	Dr. A. J. Smits	Dept. of Mech. Eng. University of Melbourne Parkville, Victoria 3052 AUSTRALIA	Discussor
A.64	Dr. Ronald M. C. So	Mechanics Branch General Electric Company Bldg. K-1, P. O. Box 8 Schenectady, NY 12301	Tech. Rec.; Data Taker

<u>No. in Photo</u>	<u>Name</u>	<u>Affiliation or Address</u>	<u>Tasks</u>
A.10	Dr. Peter M. Sockol	Research Eng. Comp. Fluid Mech. Branch NASA-Lewis Research Center, MS 5-9 Cleveland, OH 44135	Gov't. Monitor
	Dr. Gino Sovran	Fluid Dynamics Dept. Research Laboratories General Motors Technical Center 12 Mile & Mounds Roads Warren, MI 48090	Org. Comm.; Chairman; Rev. Comm. Chairman
A.57	Prof. K. R. Sreenivasan	Dept. of Eng. & Appl. Science Yale University P. O. Box 2159 New Haven, CT 21218	Data Eval.; Rev. Comm.
	Mr. Joseph Stegler	Flow Simulations, Inc. 298 S. Sunnyvale Avenue Sunnyvale, CA 94087	Eval. Comm.
A.43	Mr. Tony Strawa	Aero and Astro Department Stanford University Stanford, CA 94305	Aide; Tech. Rec.; Data Entry
B.4	Mr. Roger C. Strawn	Mech. Eng. Department Stanford University Stanford, CA 94305	Aide; Tech. Rec.
	Prof. Robert L. Street	Civil Eng. Department Stanford University Stanford, CA 94305	Discussor
A.32	Mr. Ram Subbarao	Mech. Eng. Department Stanford University Stanford, CA 94305	Aide; Tech. Rec.; Data Entry
A.17	Prof. E. P. Sutton	Univ. Eng. Dept. Trumpington Street Cambridge, CB2 1PZ, ENGLAND	Presentor
B.46	Dr. Y. Tassa	Lockheed Dept. 72-74, Zone 404 GEORGIA	Computer
B.43	Prof. H. Thomann	Institut für Aerodynamik ETH-Zentrum 8092 Zürich, SWITZERLAND	Data Taker
B.17	Mr. Murray Tobak	NASA-Ames Research Center Mail Stop N234-1 Moffett Field, CA 94035	Computer
B.24	Mr. Cam Tropea	Sonderforschungsbereich 80 Universität Karlsruhe Kaiserstrasse 12 D-75 Karlsruhe 1, WEST GERMANY	Data Taker
	Dr. T. J. Tyson	Energy and Env. Res. Corp. 2400 Michelson Drive Irvine, CA 92715	Computer
A.49	Dr. Hiromasa Ueda	Natl. Inst. for Env. Studies P. O. Yatabe, Tsukuba, Ibaraki 305 JAPAN	Data Taker

<u>No. in Photo</u>	<u>Name</u>	<u>Affiliation or Address</u>	<u>Tasks</u>
A.73	Dr. B. van den Berg	National Aerospace Lab NLR Anthony Fokkerweg 2 Amsterdam - 1017, NETHERLANDS	Data Eval.
A.28	Dr. John Viegas	NASA-Ames Research Center Mail Stop 229-1 Moffett Field, CA 94035	Computer
B.36	Dr. P. R. Viswanath	Aero & Astro Department Stanford University Stanford, CA 94305	Data Taker
A.29	Dr. Alan Wadcock	NASA-Ames Research Center Mail Stop 247-1 Moffett Field, CA 94035	Data Eval.; Data Taker
B.8	Mr. Russ V. Westphal	Mech. Eng. Department Stanford University Stanford, CA 94305	Aide; Tech. Rec.
	Prof. J. H. Whitelaw	Dept. of Mech. Eng. Imperial College Prince Consort Road London SW7 2BY, ENGLAND	Data Taker
A.70	Dr. D. C. Wilcox	DCW Industries 4367 Troost Avenue Studio City, CA 91604	Computer
B.1	Prof. I. Wignanski	School of Engineering Tel-Aviv University Ramat Aviv, ISRAEL	Rev. Comm.
B.27	Dr. Eisho Yamazato	Mechanical Eng. Dept. University of Ryukyus Tonokura-cho, Naha Okinawa, JAPAN	Data Taker
	Dr. K. T. Yen	Department of the Navy Naval Air Development Center Warminster, PA 18974	Computer
A.46	Mr. Paul Youssefmir	Mech. Eng. Department Stanford University Stanford, CA 94305	Aide



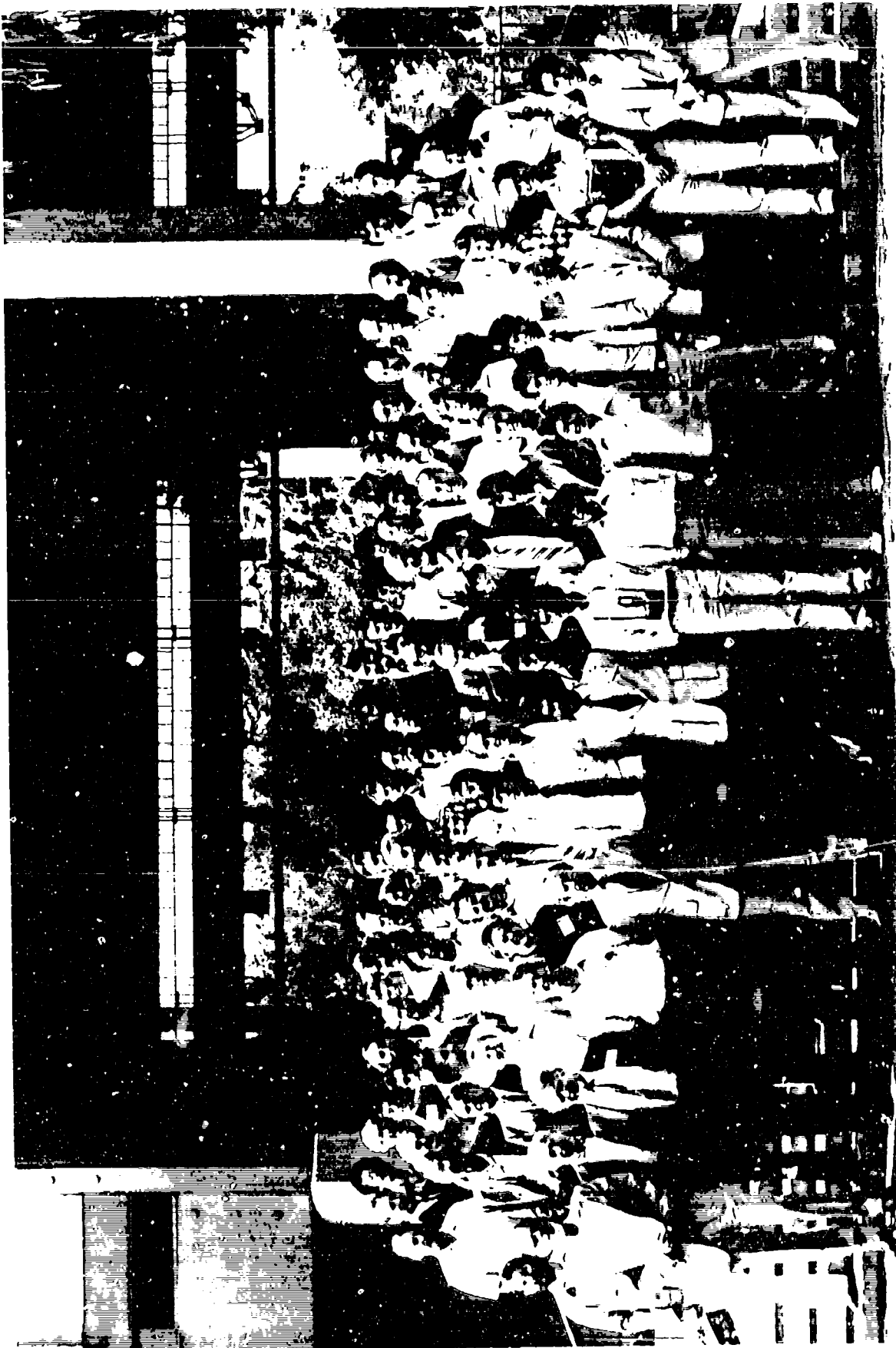


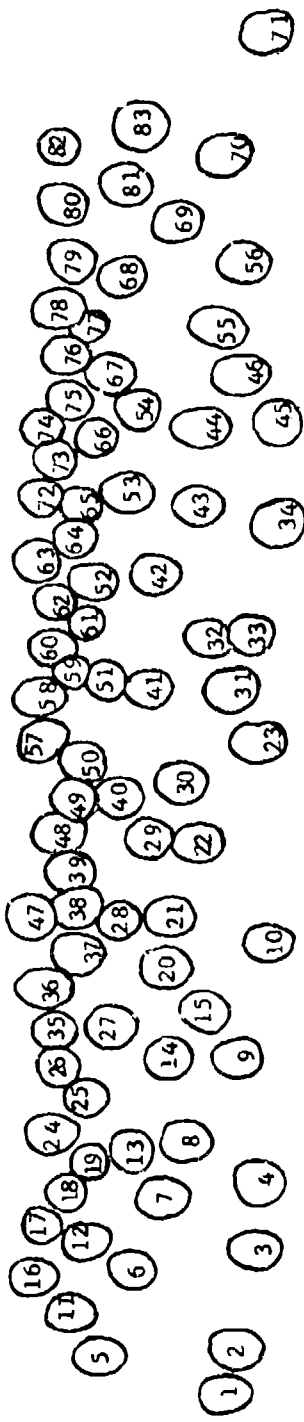
- | | | | | | |
|-----------------|-----------------|------------------|------------------|--------------------|-----------------|
| 1. I. Wygnanski | 7. R. Melnik | 16. A. Morse | 25. D. Cockrell | 36. P. Viswanath | 46. Y. Tassa |
| 2. E. Adams | 8. R. Westphal | 17. M. Tobak | 26. J. Ferziger | 37. H. Minh | 47. E. Reshotko |
| 3. H. Nagib | 9. P. Elbeck | 18. H. Meier | 27. E. Yamazato | 38. J. Marvin | 48. F. Durst |
| 4. R. Strawn | 10. T. Huang | 19. S. Honami | 28. Z. Champagne | 39. W. Ashurst | 49. J. Eaton |
| 5. A. Cutler | 11. M. Firmin | 20. L. Carr | 29. H. Emmons | 40. M. Acharya | |
| 6. A. Roshko | 12. C. Horstman | 21. U. Mehta | 30. C. Berner | 41. A. Demetriades | |
| | 13. V. Sandborn | 22. G. Lilley | 31. A. Hussain | 42. H. Thomann | |
| | 14. J. Johnston | 23. S. Bogdonoff | 32. R. Chevray | 43. A. Leonard | |
| | 15. Y. Senoo | 24. C. Tropea | 33. A. Flore | 44. J. Kim | |
| | | | 34. S. Petrie | | |
| | | | 35. R. Narasimha | | |

Participants at the 1980 Stanford Conference
on

Complex Turbulent Flows

PHOTOGRAPH A





- | | | | | |
|----------------|-------------------|-----------------------|--------------------|---------------------|
| 1. J. Humphrey | 11. H. Fernholz | 24. G. Settles | 47. J. Hunt | 72. B. van den Berg |
| 2. D. Coles | 12. R. Luxton | 25. G. Brune | 48. T. Morel | 73. B. Launder |
| 3. I. Greber | 13. Juan Bardina | 26. T. Fannelóp | 49. H. Ueda | 74. P. Dvorak |
| 4. M. Childs | 14. M. Morkovin | 27. T. Coakley | 50. S. Birch | 75. D. Humphreys |
| 5. P. Saffman | 15. M. Frota | 28. J. Viegas | 51. G. Mellor | 76. B. Newman |
| 6. J. Gerrard | 16. R. Childs | 29. A. Wadcock | 52. P. Joubert | 77. P. Bradshaw |
| 7. R. Grevray | 17. E. Sutton | 30. B. Afshari | 53. J. Jones | 78. D. Peake |
| 8. B. Cantwell | 18. J. Lumley | 31. R. Carella | 54. P. Drescher | 79. G. Paynter |
| 9. P. Gessner | 19. Jorge Bardina | 32. R. Subbarao | 55. C. Hung | 80. J. Schetz |
| 10. P. Sockol | 20. W. Reynolds | 33. Ranga Jayaraman | 56. M. Rubesin | 81. J. Cousteix |
| | 21. W. McNally | 34. Ramesh Jayaraman | 57. K. Sreenivasan | 82. S. Kline |
| | 22. S. Prorichick | 35. I. Castro | 58. R. Dean | |
| | 23. A. Lyrio | 36. A. Smits | 59. R. Hantman | |
| | | 37. D. Peschcke-Koedt | 60. B. Quinn | |
| | | 38. J. Murphy | 61. R. Simpson | |
| | | 39. D. Bushnell | 62. S. Ramaprian | |
| | | 40. K. Hanjalic | 63. W. Rodi | |
| | | 41. R. Fletcher | 64. R. So | |
| | | 42. S. Lewellen | 65. H. Higuchi | |
| | | 43. A. Strawa | 66. V. C. Patel | |
| | | 44. F. Owen | 67. P. Klebanoff | |
| | | 45. M. Lee | 68. H. Moses | |
| | | 46. P. Youssefmir | 69. D. Johnson | |
| | | | 70. D. Wilcox | |
| | | | 71. K. Irabu | |

Participants at the 1980 Stanford Conference

on

Complex Turbulent Flows

PHOTOGRAPH B

LIST OF DATA EVALUATORS

Name	Flow No.	Flow Category	Page
M. Acharya	0150	2-dimensional channel flow with periodic perturbations	178
S. Birch	0310	Planar mixing layer	170
P. Bradshaw	0210	Effect of free-stream turbulence on boundary layers	86
"	0330	Free shear layer with streamwise curvature	130
"	8500	Compressibility effects on free-shear layers	364
B. Cantwell	0410	Evaluation of bluff-body, near-wake flows	220
D.J. Cockrell	8670	Pointed axisymmetric bodies at angle of attack (supersonic)	543
D.E. Coles	0610	Attached boundary layers - ('68 Conference)	82
R.B. Dean	0510	Turbulent secondary flows of the first kind	139
P. Drescher	0470	Flow over the trailing edge of blades and airfoils	555
J.K. Eaton	0420	Backward-facing step flow	275
A. Favre	8680	Axisymmetric near wake flow (supersonic)	482
J.H. Ferziger	0370	Homogeneous turbulent flows	405
F.B. Gessner	0110	Corner flow (secondary flow of the second kind)	182
S. Honami	0230	Boundary layer flows with streamwise curvature	94
C.C. Horstman	8100	Supersonic flow over a flat plate (insulated wall)	369
"	8200	Supersonic flow over a flat plate (cooled wall)	369
"	8400	Boundary layers in an adverse pressure gradient in an axisymmetric internal flow	378
"	8410	Boundary layers in an adverse pressure gradient in two-dimensional flow	378
"	8600	Impinged normal shock wave-boundary layer interaction at transonic speeds	486
"	8610	Transonic flow over a bump	458
"	8630	Compressible flow over deflected surfaces	458
"	8640	Compressible flow over compression corner with reattaching planar shear layer	458
"	8650	Axisymmetric shock impingement (supersonic)	486
"	8660	Three-dimensional shock impingement (supersonic)	486
"	8690	Nonlifting, transonic airfoil with shock separation	486
D.A. Humphreys	0250	Three-dimensional turbulent boundary layers	162
J.P. Johnston	0420	Backward-facing step flow	275
J.B. Jones	0130	Entry zone of round tube	213
B.E. Launder	0260	Turbulent wall jet	434
R.E. Melnik	8620	Transonic airfoils	523
A.P. Morse	0340	Flows with swirl	317

Name	Flow No.	Flow Category	Page
V.C. Patel	0350	Ship wakes	552
"	0360	Wakes of round bodies	327
"	0380	Wakes of two-dimensional bodies	340
"	0390	Axisymmetric boundary layer with strong streamwise and transverse curvature	327
D. Peake	8670	Pointed axisymmetric bodies at angle of attack (supersonic)	543
E. Reshotko	0290	Laminar-turbulent transition	554
W. Rodi	0260	Turbulent wall jet	434
M.W. Rubesin	8100	Supersonic flow over a flat plate (insulated wall)	369
"	8200	Supersonic flow over a flat plate (cooled wall)	369
"	8400	Boundary layers in an adverse pressure gradient in an axisymmetric internal flow	378
"	8410	Boundary layers in an adverse pressure gradient in two-dimensional flow	378
"	8600	Impinged normal shock wave-boundary layer interaction at transonic speeds	486
"	8610	Transonic flow over a bump	458
"	8630	Compressible flow over deflected surfaces	458
"	8640	Compressible flow over compression corner with reattaching planar shear layer	458
"	8650	Axisymmetric shock impingement (supersonic)	486
"	8660	Three-dimensional shock impingement (supersonic)	486
"	8690	Nonlifting, transonic airfoil with shock separation	486
T.W. Simon	0230	Boundary layer flows with streamwise curvature	94
R. L. Simpson	0140	Diffuser flows (unseparated)	253
"	0430	Diffuser flows (separated)	253
L.C. Squire	0240	Turbulent boundary layers with suction or blowing	112
"	8300	Turbulent boundary layers with suction or blowing at supersonic speeds	112
"	8310	Variation in C_f/C_{f0} for blowing/suction with Mach Number	549
K.R. Sreenivasan	0280	Relaminarizing flows	567
B. van den Berg	0250	Three-dimensional turbulent boundary layers	162
A.J. Wadcock	0440	Two-dimensional stalled airfoil	234
J.C. Wyngaard	9000	Flows with buoyancy forces	314

NUMERICAL INDEX TO FLOW CASES AND DATA LIBRARY TAPE

Nomenclature:

Prefix 0 : Incompressible Flow
 8 : Compressible Flow

Flow number 0
 or } Two digits { 0
 8

Case number 0
 or } Two digits { 1
 8 2
 3
 4
 5
 6

(Evaluator)	Flow Category	(Flow No.)
-------------	---------------	------------

Case No.	Data Taker	Title	Index to the Tape		
			No. of Files	File Number	Page

Incompressible Flows

(F. Gessner)	Corner flow (secondary flow of the second kind) (0110)
--------------	--

0111	J. Po/E. Lund; F. Gessner	Developing flow in a square duct	28	2-29	182
0112	J. Hinze	Secondary currents in the turbulent flow through a straight conduit	4	30-33	182
0113	--	Asymmetric flow in a square duct	*		287

(J.B. Jones)	Entry zone of round tube (0130)
--------------	---------------------------------

0131	A. Barbin/J. Jones	Entry zone of round tube	†		213
0132	D. Miller	Entry zone of round tube	†		213

(R.L. Simpson)	Diffuser flows (unsepar.) (0140)
----------------	----------------------------------

0141	A. S muel/ P. Joubert	Increasingly adverse pressure gradient flow	30	34-63	254
0142	R. Pozzorini	Six-degree conical diffuser flow, low-core turb.	39	64-102	254
0143	R. Pozzorini	Six-degree conical diffuser flow, high-core turb.	39	64-102	254

* Predictive Case Pl.

† Not used for 1981 Conference.

(Evaluator)

Flow Category (Flow No.)

Case No.	Data Taker	Title	Index to the Tape		
			No. of Files	File Number	Page

Incompressible Flows (cont.)

(M. Acharya) Two-dimensional channel flow with periodic perturbations (0150)

0151	A. Hussain/ W. Reynolds	Perturbation wave in turbulent shear flow	†		178
0152	M. Acharya/ W. Reynolds	Fully developed turbulent channel flow with imposed controlled oscillations	†		179

(P. Bradshaw) Effect of free-stream turbulence on boundary layers (0210)

0211	P. Hancock/ P. Bradshaw	Effect of free-stream turbulence	2	103-104	86
------	----------------------------	----------------------------------	---	---------	----

(T.W. Simon/
S. Honami) Boundary layer flows with streamwise curvature (0230)

0231	P. Hoffmann/ P. Bradshaw	Turbulent boundary layers on surfaces of mild longitudinal curvature (convex)	26	105-130	95
0232	P. Hoffman/ P. Bradshaw	Turbulent boundary layers on surfaces of mild longitudinal curvature (concave)	26	105-130	95
0233	J. Gillis/ J. Johnston	Turbulent boundary layer on a convex, curved surface	26	131-156	95
0234	I. Hunt/ P. Joubert	Effects of small streamline curvature on turbulent duct flow	17†	157-173	96
0235	A. Smits/S. Young/ P. Bradshaw	The effects of short regions of high surface curvature on turbulent boundary layers (convex 30 deg.)	17†	174-190	96

(L.C. Squire) Turbulent boundary layers with suction or blowing (0240)

0241	P. Andersen/ W. Kays/R. Moffat	Zero pressure gradient, constant injection	11	191-201	114
0242	P. Andersen/ W. Kays/R. Moffat	Adverse pressure gradient with constant suction	13	202-214	114
0244	A. Favre et al.	Zero pressure gradient with constant (high) suction	11	215-225	114

† Not used for 1981 Conference.

(Evaluator)	Flow Category	(Flow No.)
-------------	---------------	------------

Case No.	Data Taker	Title	Index to the Tape		
			No. of Files	File Number	Page

Incompressible Flows (cont.)

(D.A. Humphreys/ B. van den Berg)	Three-dimensional turbulent boundary layers	(0250)
--------------------------------------	---	--------

0251	B. van den Berg/ A. Elsenaar	NLR infinite swept wing experiment	20 [†]	226-245	164
0252	L. Bissonnette	Part-rotating cylinder experiment	22 [†]	246-267	164
0253	R. Dechow	Cylinder on a flat test plate	26 [†]	268-293	164
0254	Lohmann, R.	Part-rotating cylinder	23 [†]	294-316	164

(B.E. Launder/ W. Rodi)	Turbulent Wall Jet	(0260)
----------------------------	--------------------	--------

0261	Various	Turbulent wall jet data (equilibrium wall jet)	17	317-333	435
0262	E. Alcaraz; C. Fekete	Turbulent wall jet data (2-dimensional, on a cylinder)	†		437
0263	D. Guitton/ B. Newman	Turbulent wall jet data (self-preserving on log-spiral)	17	317-333	438
0264	Various	Turbulent wall jet data (3-dimensional on plane surface)	17	317-333	439

(K. Sreenivasan)	Relaminarizing flows	(0280)
------------------	----------------------	--------

0281	R. Simpson/ D. Wallace	Relaminarizing boundary layer	*		567
0282	J. Laufer	Relaminarizing tube flow	*		568

(S. Birch)	Planar mixing layer	(0310)
------------	---------------------	--------

0311	Various	Planar mixing layer developing from turbulent wall boundary layers	6	334-339	170
------	---------	--	---	---------	-----

[†]Not used for 1981 Conference.

*This case is not on data tape for Library I; it will appear on future revisions.

(Evaluator)	Flow Category	(Flow No.)
-------------	---------------	------------

Case No.	Data Taker	Title	Index to the Tape		
			No. of Files	File Number	Page

Incompressible Flows (cont.)

(P. Bradshaw)	Free shear layer with streamwise curvature	(0330)
---------------	--	--------

033i	I. Castro/ P. Bradshaw	The turbulence structure of a highly curved mixing layer	36	340-375	130
------	---------------------------	--	----	---------	-----

(V.C. Patel)	Wakes of round bodies	(0360)
--------------	-----------------------	--------

036i	R. Chevray	The turbulent wake of a body of revolution	72	376-447	327
------	------------	--	----	---------	-----

(J.H. Ferziger)	Homogeneous turbulent flows	(0370)
-----------------	-----------------------------	--------

037i	G. Comte-Bellot/ S. Corrsin	Isotropic turbulence	19	448-466	406
0372	R. Wigeland/ H. Nagib	Rotating turbulence	"	"	406
0373	M. Uberoi; H. Tucker/A. Reynolds	Return to isotropy	"	"	406
0374	A. Townsend; H. Tucker/A. Reynolds	Plane strain	"	"	406
0375	J. Tan-atichat	Axisymmetric strain	"	"	407
0376	F. Champagne et al.; V. Harris et al.	Sheared turbulence	"	"	407

(V.C. Patel)	Wakes of two-dimensional bodies	(0380)
--------------	---------------------------------	--------

038i	J. Andreopoulos	Measurements of interacting turbulent shear layers in the near wake of an airfoil (symmetric)	52	467-518	346
0382	J. Andreopoulos	Measurements of interacting turbulent shear layers in the near wake of an airfoil (asymmetric)	"	"	350

(Evaluator)	Flow Category	(Flow No.)
-------------	---------------	------------

Case No.	Data Taker	Title	Index to the Tape		
			No. of Files	File Number	Page

Incompressible Flows (cont.)

(B. Cantwell)	Evaluation of bluff-body, near-wake flows	(0410)
---------------	---	--------

0411	B. Cantwell/ D. Coles	A flying hot-wire study of the turbulent near-wake of a circular cylinder at a Reynolds number of 140,000	19	519-537	221
0412	A. Perry/ J. Watmuff	Phase-averaged large-scale structures in 3-dimensional wakes	+		223

(J.K. Eaton/ J.P. Johnston)	Backward-facing step flow	(0420)
--------------------------------	---------------------------	--------

0421	J. Kim/S. Kline/ J. Johnston	Flow over a backward-facing step	32	538-569	275
0422	--	Backward-facing step; variable opposite wall angle	*		297
0423	--	Backward-facing step; turned flow passage	†		301
0424	--	Backward-facing step; variable area ratio	#		304

(R.L. Simpson)	Diffuser flows (sep.)	(0430)
----------------	-----------------------	--------

0431	R. Simpson et al.	Separating adverse pressure gradient flow	36	570-605	255
------	-------------------	---	----	---------	-----

(A.J. Wadcock)	Two-dimensional stalled airfoil	(0440)
----------------	---------------------------------	--------

0441	A. Wadcock/ D. Coles	Flying hot-wire study of 2-dimensional turbulent separation of an NACA 4412 airfoil at maximum lift	4	606-609	234
------	-------------------------	---	---	---------	-----

† Not used for 1981 Conference.

* Predictive Case P2. # Predictive Case P3. # Predictive Case P4.

(Evaluator)	Flow Category (Flow No.)
-------------	--------------------------

Case No.	Data Taker	Title	Index to the Tape		
			No. of Files	File Number	Page

Incompressible Flows (cont.)

(P. Drescher)	Flow over the trailing edge of blades and airfoils (0470)
---------------	---

0471	P. Viswanath et al.	Trailing edge flows at high Reynolds number	48	610-657	555
------	---------------------	---	----	---------	-----

(R.B. Dean)	Turbulent secondary flows of the first kind (0510)
-------------	--

0511	I. Shabaka	Turbulent flow in an idealized wing-body junction	135	658-792	140
------	------------	---	-----	---------	-----

0512	J. Humphrey	Turbulent flow in a curved duct of square cross-section	21	793-813	141
------	-------------	---	----	---------	-----

(D.E. Coles)	Attached boundary layers (1968 Conference) (0610)
--------------	---

0612	K. Wieghardt	On the turbulent friction layer for rising pressure	25	814-838	82
------	--------------	---	----	---------	----

Compressible Flows

(M.W. Rubesin/ C.C. Horstman)	Supersonic flow over a flat plate (insulated wall) (8100)
----------------------------------	---

8101	Various	Correlation: C_f/C_{f0} versus M --insulated plate	*		369
------	---------	--	---	--	-----

(M.W. Rubesin/ C.C. Horstman)	Supersonic flow over a flat plate (cooled wall) (8200)
----------------------------------	--

8201	Various	Correlation: C_f/C_{f0} versus T_w/T_{aw} --constant M	*		369
------	---------	--	---	--	-----

(L.C. Squire)	Turbulent boundary layers with suction or blowing at supersonic speeds (8300)
---------------	---

8301	G. Thomas	Favorable pressure gradient at supersonic speeds with injection	3	839-841	115
------	-----------	---	---	---------	-----

* Single curve--not shown on data tape.

(Evaluator)	Flow Category	(Flow No.)
-------------	---------------	------------

Case No.	Data Taker	Title	Index to the Tape		
			No. of Files	File Number	Page

Compressible Flows (cont.)

(M.W. Rubesin/ C.C. Horstman/ G.M. Lilley)	Boundary layers in an adverse pressure gradient in an axisymmetric internal flow (8400)
--	---

8401	D. Peake et al.	Boundary layer in adverse pressure gradient	4 [†]	842-845	378
8402	J. Lewis et al.	Boundary layer in adverse pressure gradient	9 [†]	846-854	379
8403	M. Kussoy et al.	Pressure gradient and Reynolds number effects on compressible turbulent boundary layers in supersonic flow	47	855-901	380, 388

(M.W. Rubesin/ C.C. Horstman/ G.M. Lilley)	Boundary layers in an adverse pressure gradient in two-dimensional flow (8410)
--	--

8411	F. Zwarts	Boundary layer in adverse pressure gradient	8	902-909	381, 390
------	-----------	---	---	---------	-------------

(P. Bradshaw)	Compressibility effects on free-shear layers (8500)
---------------	---

8501	Various	Compressibility effects on free-shear layers	2	910-911	364
------	---------	--	---	---------	-----

(M.W. Rubesin/ C.C. Horstman)	Impinged normal shock wave-boundary layer interaction at transonic speeds (8600)
----------------------------------	--

8601	G. Mateer et al.	Normal shock wave/turbulent boundary-layer interaction at transonic speeds	31	912-942	487
8602	J. Kooi	Influence of free-stream Mach number on transonic shock wave-boundary layer interaction	119 [†]	943-1061	487

[†]Not used for 1981 Conference.

(Evaluator) Flow Category (Flow No.)

Case No.	Data Taker	Title	Index to the Tape		
			No. of Files	File Number	Page

Compressible Flows (cont.)

(M.W. Rubesin/ C.C. Horstman) Transonic flow over a bump (8610)

8611	W. Bachalo/ D. Johnson	Transonic turbulent boundary layer separation on an axisymmetric bump	14	1062-1075	459
8612	J. Delery/ P. Le Duzet	Transonic flow over two-dimensional bump, $M = 1.37$	44	1076-1119	459

(R.E. Melnik) Transonic airfoils (8620)

8621	P. Cook et al.	Aerofoil RAE 2822--pressure distribution, boundary layer and wake measurements	74	1120-1193	524
8623	F. Spaid/ L. Stivers	Supercritical airfoil boundary layer measurements	48	1194-1241	526

(M.W. Rubesin/ C.C. Horstman) Compressible flow over deflected surfaces (8630)

8631	G. Settles et al.	Attached and separated compression corner flow fields in high Reynolds number supersonic flow	50	1242-1291	459
8632	J. Dussauge/ J. Gaviglio	Turbulent boundary-layer/expansion interaction at supersonic speed	32	1292-1323	460

(M.W. Rubesin/ C.C. Horstman) Compressible flow over compression corner with reattaching planar shear layer (8640)

8641	G. Settles et al.	Reattaching planar free-shear layer (supersonic)	13	1324-1336	460
------	-------------------	--	----	-----------	-----

(M.W. Rubesin/ C.C. Horstman) Axisymmetric shock impingement (supersonic) (8650)

8651	M. Kussoy/ C. Horstman	Hypersonic shock wave turbulent boundary-layer interaction-- with and without separation	34	1337-1370	486
------	---------------------------	--	----	-----------	-----

(Evaluator)

Flow Category (Flow No.)

Case No.	Data Taker	Title	Index to the Tape		
			No. of Files	File Number	Page
<u>Compressible Flows (cont.)</u>					
<div>(M.W. Rubesin/ Three-dimensional shock C.C. Horstman) impingement (supersonic) (8660)</div>					
8661	D. Peake	Three-dimensional swept shock/turbulent boundary layer interaction	7	1371-1377	486
8663	M. Kussoy et al.	Investigation of three-dimensional shock separated turbulent boundary layer	47	1378-1424	486
<div>(D.J. Peake/ Pointed axisymmetric bodies at D.J. Cockrell) angle of attack (supersonic) (8670)</div>					
8671	W. Rainbird	Pointed axisymmetric bodies at angle of attack (supersonic)	30	1425-1454	543
<div>(M.W. Rubesin/ Nonlifting, transonic airfoil C.C. Horstman) with shock separation (8690)</div>					
8691	J. McDevitt et al.	Non-lifting transonic airfoil, shock-separated flow	13	1455-1467	487